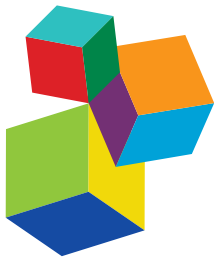


ANAEROBIC DIGESTION

EDITED BY: **Gavin Collins, Eric D. van Hullebusch, Giovanni Esposito,
Cynthia Carliell-Marquet and Fernando G. Fermoso**

PUBLISHED IN: **Frontiers in Microbiology, Frontiers in Bioengineering and
Biotechnology and Frontiers in Environmental Science**





Frontiers Copyright Statement

© Copyright 2007-2018 Frontiers Media SA. All rights reserved.

All content included on this site, such as text, graphics, logos, button icons, images, video/audio clips, downloads, data compilations and software, is the property of or is licensed to Frontiers Media SA ("Frontiers") or its licensees and/or subcontractors. The copyright in the text of individual articles is the property of their respective authors, subject to a license granted to Frontiers.

The compilation of articles constituting this e-book, wherever published, as well as the compilation of all other content on this site, is the exclusive property of Frontiers. For the conditions for downloading and copying of e-books from Frontiers' website, please see the Terms for Website Use. If purchasing Frontiers e-books from other websites or sources, the conditions of the website concerned apply.

Images and graphics not forming part of user-contributed materials may not be downloaded or copied without permission.

Individual articles may be downloaded and reproduced in accordance with the principles of the CC-BY licence subject to any copyright or other notices. They may not be re-sold as an e-book.

As author or other contributor you grant a CC-BY licence to others to reproduce your articles, including any graphics and third-party materials supplied by you, in accordance with the Conditions for Website Use and subject to any copyright notices which you include in connection with your articles and materials.

All copyright, and all rights therein, are protected by national and international copyright laws.

The above represents a summary only. For the full conditions see the Conditions for Authors and the Conditions for Website Use.

ISSN 1664-8714
ISBN 978-2-88945-679-6
DOI 10.3389/978-2-88945-679-6

About Frontiers

Frontiers is more than just an open-access publisher of scholarly articles: it is a pioneering approach to the world of academia, radically improving the way scholarly research is managed. The grand vision of Frontiers is a world where all people have an equal opportunity to seek, share and generate knowledge. Frontiers provides immediate and permanent online open access to all its publications, but this alone is not enough to realize our grand goals.

Frontiers Journal Series

The Frontiers Journal Series is a multi-tier and interdisciplinary set of open-access, online journals, promising a paradigm shift from the current review, selection and dissemination processes in academic publishing. All Frontiers journals are driven by researchers for researchers; therefore, they constitute a service to the scholarly community. At the same time, the Frontiers Journal Series operates on a revolutionary invention, the tiered publishing system, initially addressing specific communities of scholars, and gradually climbing up to broader public understanding, thus serving the interests of the lay society, too.

Dedication to Quality

Each Frontiers article is a landmark of the highest quality, thanks to genuinely collaborative interactions between authors and review editors, who include some of the world's best academicians. Research must be certified by peers before entering a stream of knowledge that may eventually reach the public - and shape society; therefore, Frontiers only applies the most rigorous and unbiased reviews.

Frontiers revolutionizes research publishing by freely delivering the most outstanding research, evaluated with no bias from both the academic and social point of view. By applying the most advanced information technologies, Frontiers is catapulting scholarly publishing into a new generation.

What are Frontiers Research Topics?

Frontiers Research Topics are very popular trademarks of the Frontiers Journals Series: they are collections of at least ten articles, all centered on a particular subject. With their unique mix of varied contributions from Original Research to Review Articles, Frontiers Research Topics unify the most influential researchers, the latest key findings and historical advances in a hot research area! Find out more on how to host your own Frontiers Research Topic or contribute to one as an author by contacting the Frontiers Editorial Office: researchtopics@frontiersin.org

ANAEROBIC DIGESTION

Topic Editors:

Gavin Collins, NUI Galway, Ireland

Eric D. van Hullebusch, UNESCO-IHE Institute for Water Education, Netherlands

Giovanni Esposito, University of Cassino and Southern Lazio, Italy

Cynthia Carliell-Marquet, University of Birmingham, United Kingdom

Fernando G. Fermoso, Consejo Superior de Investigaciones Científicas (CSIC), Spain

Anaerobic digestion (AD) is a naturally-occurring biological process in soils, sediments, ruminants, and several other anoxic environments, that cycles carbon and other nutrients, and converts organic matter into a methane-rich gas. As a biotechnology, AD is now well-established for the treatment of the organic fraction of various waste materials, including wastewaters, but is also increasingly applied for an expanding range of organic feedstocks suitable for biological conversion to biogas. AD applications are classified in various ways, including on the basis of bioreactor design; and operating parameters, such as retention time, temperature, pH, total solids (TS) and volatile solids (VS) contents, and biodegradability of substrates.

AD is an attractive bioenergy and waste / wastewater treatment technology. The advantages of AD for waste treatment include: production of a useable fuel (biogas/ methane); possibility of high organic loading; reduced carbon footprint; and suitability for integration into a wide variety of process configurations and scales. Specifically, two important, and developing, applications exemplify the potential of AD technologies: (1) the integration of AD as the basis of the core technologies underpinning municipal wastewater, and sewage, treatment, to displace less sustainable, and more energy-intensive, aerobic biological treatment systems in urban water infrastructures; and (2) technical innovations for higher-rate conversions of high-solids wastestreams, and feedstocks, for the production of energy carriers (i.e. methane-biogas, but possibly also biohydrogen) and other industrially-relevant intermediates, such as organic acids.

Internationally, the research effort to maximize AD biogas yield has increased ten-fold over the past decade. Depending on the feedstocks, bioreactor design and process parameters, fundamental and applied knowledge are still required to improve conversion rates and biogas yields.

This Research Topic cover aspects related to AD processes, such as the effect of feedstock composition, as well as the effect of feedstock pre-treatment, bioreactor design and operating modes, on process efficiency; microbial community dynamics and systems biology; influence of macro- and micro-nutrient concentrations and availability; process control; upgrading and calibration of anaerobic digestion models (e.g. ADM1) considering the biochemical routes as well as the hydrodynamics in such ecosystems; and novel approaches to process monitoring, such as the development, and application, of novel, and rapid diagnostic assays, including those based on molecular microbiology. Detailed full-scale application studies were also particularly welcomed.

Citation: Collins, G., van Hullebusch, E. D., Esposito, G., Carliell-Marquet, C., Fermoso, F. G., eds (2018). Anaerobic digestion. Lausanne: Frontiers Media.
doi: 10.3389/978-2-88945-679-6

Table of Contents

- 05 Bioreactor Scalability: Laboratory-Scale Bioreactor Design Influences Performance, Ecology, and Community Physiology in Expanded Granular Sludge Bed Bioreactors**
Stephanie Connelly, Seung G. Shin, Robert J. Dillon, Umer Z. Ijaz, Christopher Quince, William T. Sloan and Gavin Collins
- 20 Trace Elements Induce Predominance Among Methanogenic Activity in Anaerobic Digestion**
Babett Wintsche, Karin Glaser, Heike Sträuber, Florian Centler, Jan Liebetrau, Hauke Harms and Sabine Kleinstreuer
- 32 Mass Loss Controlled Thermal Pretreatment System to Assess the Effects of Pretreatment Temperature on Organic Matter Solubilization and Methane Yield From Food Waste**
Martha M. Yeshanew, Luigi Frunzo, Piet N. L. Lens, Francesco Pirozzi and Giovanni Esposito
- 45 Significance of Vivianite Precipitation on the Mobility of Iron in Anaerobically Digested Sludge**
Jimmy Roussel and Cynthia Carliell-Marquet
- 57 Metagenomic Reconstruction of Key Anaerobic Digestion Pathways in Municipal Sludge and Industrial Wastewater Biogas-Producing Systems**
Mingwei Cai, David Wilkins, Jiapeng Chen, Siu-Kin Ng, Hongyuan Lu, Yangyang Jia and Patrick K. H. Lee
- 69 Formate-Dependent Microbial Conversion of CO₂ and the Dominant Pathways of Methanogenesis in Production Water of High-temperature Oil Reservoirs Amended With Bicarbonate**
Guang-Chao Yang, Lei Zhou, Serge M. Mbadinga, Jin-Feng Liu, Shi-Zhong Yang, Ji-Dong Gu and Bo-Zhong Mu
- 80 Iron, Cobalt, and Gadolinium Transport in Methanogenic Granules Measured by 3D Magnetic Resonance Imaging**
Jan Bartacek, Frank J. Vergeldt, Josef Maca, Edo Gerkenma, Henk Van As and Piet N. L. Lens
- 88 Life Cycle Environmental Impacts of Electricity From Biogas Produced by Anaerobic Digestion**
Alessandra Fusi, Jacopo Bacenetti, Marco Fiala and Adisa Azapagic
- 105 Biological Phosphorus Removal During High-Rate, Low-Temperature, Anaerobic Digestion of Wastewater**
Ciara Keating, Jason P. Chin, Dermot Hughes, Panagiotis Manesiotis, Denise Cysneiros, Therese Mahony, Cindy J. Smith, John W. McGrath and Vincent O'Flaherty
- 119 Enhanced Anaerobic Digestion of Food Waste by Supplementing Trace Elements: Role of Selenium (VI) and Iron (II)**
Ariunbaatar, Giovanni Esposito, Daniel H. Yeh and Piet N. L. Lens

130 Substrate Type and Free Ammonia Determine Bacterial Community Structure in Full-Scale Mesophilic Anaerobic Digesters Treating Cattle or Swine Manure

Jiabao Li, Junpeng Rui, Minjie Yao, Shiheng Zhang, Xuefeng Yan, Yuanpeng Wang, Zhiying Yan and Xiangzhen Li

140 Effects of Sludge Inoculum and Organic Feedstock on Active Microbial Communities and Methane Yield During Anaerobic Digestion

David Wilkins, Subramanya Rao, Xiaoying Lu and Patrick K. H. Lee



Bioreactor Scalability: Laboratory-Scale Bioreactor Design Influences Performance, Ecology, and Community Physiology in Expanded Granular Sludge Bed Bioreactors

Stephanie Connelly^{1†}, Seung G. Shin^{2†}, Robert J. Dillon³, Umer Z. Ijaz¹, Christopher Quince⁴, William T. Sloan¹ and Gavin Collins^{1,3*}

¹ Infrastructure and Environment, School of Engineering, University of Glasgow, Glasgow, UK, ² School of Environmental Science and Engineering, Pohang University of Science and Technology, Pohang, South Korea, ³ Microbial Communities Laboratory, National University of Ireland Galway, Galway, Ireland, ⁴ Microbiology and Infection, University of Warwick, Warwick, UK

OPEN ACCESS

Edited by:

Peter Neubauer,
Technische Universität Berlin,
Germany

Reviewed by:

Daniel Puyol,
Universidad Rey Juan Carlos, Spain
Jose Antonio Morillo Perez,
University of Granada, Spain

*Correspondence:

Gavin Collins
gavin.collins@nuigalway.ie

[†]Joint first authors.

Specialty section:

This article was submitted to
Microbiotechnology, Ecotoxicology
and Bioremediation,
a section of the journal
Frontiers in Microbiology

Received: 17 June 2016

Accepted: 31 March 2017

Published: 01 May 2017

Citation:

Connelly S, Shin SG, Dillon RJ, Ijaz UZ, Quince C, Sloan WT and Collins G (2017) Bioreactor Scalability: Laboratory-Scale Bioreactor Design Influences Performance, Ecology, and Community Physiology in Expanded Granular Sludge Bed Bioreactors. *Front. Microbiol.* 8:664.
doi: 10.3389/fmicb.2017.00664

Studies investigating the feasibility of new, or improved, biotechnologies, such as wastewater treatment digesters, inevitably start with laboratory-scale trials. However, it is rarely determined whether laboratory-scale results reflect full-scale performance or microbial ecology. The Expanded Granular Sludge Bed (EGSB) bioreactor, which is a high-rate anaerobic digester configuration, was used as a model to address that knowledge gap in this study. Two laboratory-scale idealizations of the EGSB—a one-dimensional and a three-dimensional scale-down of a full-scale design—were built and operated in triplicate under near-identical conditions to a full-scale EGSB. The laboratory-scale bioreactors were seeded using biomass obtained from the full-scale bioreactor, and, spent water from the distillation of whisky from maize was applied as substrate at both scales. Over 70 days, bioreactor performance, microbial ecology, and microbial community physiology were monitored at various depths in the sludge-beds using 16S rRNA gene sequencing (V4 region), specific methanogenic activity (SMA) assays, and a range of physical and chemical monitoring methods. SMA assays indicated dominance of the hydrogenotrophic pathway at full-scale whilst a more balanced activity profile developed during the laboratory-scale trials. At each scale, *Methanobacterium* was the dominant methanogenic genus present. Bioreactor performance overall was better at laboratory-scale than full-scale. We observed that bioreactor design at laboratory-scale significantly influenced spatial distribution of microbial community physiology and taxonomy in the bioreactor sludge-bed, with 1-D bioreactor types promoting stratification of each. In the 1-D laboratory bioreactors, increased abundance of *Firmicutes* was associated with both granule position in the sludge bed and increased activity against acetate and ethanol as substrates. We further observed that stratification in the sludge-bed in 1-D laboratory-scale bioreactors was associated with increased richness in the underlying microbial community at species (OTU) level and improved overall performance.

Keywords: 16S rRNA gene, anaerobic digestion, EGSB, Illumina MiSeq, laboratory-scale, full-scale, industrial wastewater, specific methanogenic activity

INTRODUCTION

Anaerobic digestion (AD) is a microbially-driven wastewater treatment process enabling energy, nutrient and water recovery from wastes. The development of new biotechnologies such as those used for the AD of wastes, has historically followed the empirical route from laboratory-scale through to pilot- and full-scale trials (Switzenbaum, 1995; Tchobanoglous et al., 2004; O'Flaherty et al., 2006; Shida et al., 2012). Advantages of testing and development at laboratory-scale prior to scale-up include greatly reduced capital and construction costs, rapid project turnaround and minimal effluent generation, which collectively provide flexibility to test hypotheses and optimize processes. However, whilst many parameters may be readily reproduced across scales, e.g., operating temperature and hydraulic retention times, others, such as bioreactor geometry or hydrodynamics, may not. Compounding this, published research rarely, if ever, tracks the success of environmental biotechnology trials across each of the laboratory-, pilot-, and full-scale development stages, and so the applicability of laboratory-scale results to full-scale design and operation is therefore limited and poorly understood. We aimed to circumvent this knowledge gap and to inform the design and interpretation of future laboratory trials using *scale-down* of an existing biotechnology, as opposed to scale-up, to investigate the impact of scale and geometry on bioreactor performance, ecology, and microbial community physiology.

A full-scale expanded granular sludge bed (EGSB) bioreactor operated at a Scottish whisky distillery was selected as the full-scale bioreactor for this study. The EGSB is an anaerobic digester type utilizing retained granular biomass for high-rate treatment of high-strength, low-solids industrial wastes. EGSB bioreactors have previously been used in many laboratory-scale trials investigating adaptation of the EGSB to the treatment of a growing range of wastes (Pereira et al., 2002; Fang et al., 2011), contaminants (Collins et al., 2005; Enright et al., 2005; Scully et al., 2006; Londoño and Peñuela, 2015), and operating conditions (Syutsubo et al., 2008; O'Reilly et al., 2010) which, if applicable at full-scale, have the potential to revolutionize the way we treat wastewater. Hence, this bioreactor design represents an ideal reactor type in which to investigate the effects of scale. A broad range of EGSB reactor designs (Arcand et al., 1994; Kato et al., 1994; Karnchanawong and Wachara, 2009) are commonly used in laboratory-scale studies. Recognizing that laboratory-scale reactor design is likely to influence both performance and underlying physiology and ecology, we designed two laboratory-scale bioreactor idealizations, described here as "1-D" and "3-D" bioreactors (**Figure 1**), to mimic the full-scale EGSB in the laboratory and to enable evaluation of scale effects. Where possible the 1-D and 3-D laboratory-scale EGSBs were operated under near-identical conditions to the full-scale bioreactor, including the use of a common inoculum and maintaining common substrate (distillery wastewater), organic loading rate (OLR), hydraulic retention time, operating temperature, and upflow velocity between scales and idealizations. We applied a range of physical and chemical monitoring techniques coupled with specific methanogenic activity assays and high-throughput

16S rRNA gene sequencing (V4 region) to evaluate differences in performance, physiology, and ecology between:

- i. The full- and laboratory-scale bioreactors.
- ii. The laboratory-scale idealizations.

MATERIALS AND METHODS

Full-Scale Bioreactor Design and Operation

The full-scale bioreactor (FSB) is one of a set of three anaerobic digesters operated at a Scottish whisky distillery to treat spent water from the distillation of alcohol from maize. FSB is a second-generation EGSB described as the External Circulation Sludge Bed (ECSB) bioreactor (Meyer and Edwards, 2014). The primary variant between the EGSB and the ECSB is the inclusion of two gas-solid-liquid separators in the bioreactor to improve process stability and biomass retention under high OLR. Additionally, the ECSB design includes sampling ports distributed with depth in the reactor vessel enabling spatial, as well as temporal, sampling of granules from the sludge bed. The ECSB maintains the defining features of the EGSB however i.e., it is an anaerobic, upflow, retained-biomass system using liquor recycling to promote bed expansion and mixing, and treatment is underpinned by the microbial activity of the granular sludge bed. FSB has a total working volume of 425 m³, geometric diameter-to-height ratio of 7:12, and is operated semi-continuously at 37°C and a mean OLR of 9 g COD/L-reactor.d (s.d. 2 g COD/L-reactor.d). Operational data from FSB, obtained for a 6-month period prior to design of the laboratory-scale trials, were used to determine operating parameters for the laboratory bioreactors (**Table 1**). In addition to defining operating parameters, FSB served as the source of seed sludge for the laboratory-scale bioreactors, which was obtained 31 days (D-31) prior to commencement of the laboratory trial. Distillery wastewater was used as substrate at both scales. Additional biomass samples were drawn from FSB at days D-21 and D-14 to determine the structure of the microbial community at full-scale with depth and time (**Figure 2**). Operating and performance data reported for FSB were recorded for an 85-day period (D-85 to D0) during which FSB was temporarily shut down for a 5-day interval (D-59 to D-54) for routine maintenance of upstream reactors and was also subject to temporary shutdown immediately before and after the period of study.

Laboratory-Scale Bioreactor Design

Two laboratory-scale bioreactor types were designed, described here as 1-D and 3-D bioreactors (**Figure 1**). Each type was built and operated in triplicate: the 1-D reactor set, R1-3; and the 3-D reactor set, R4-6 (**Figure 2**). The laboratory-scale bioreactor designs used are intended to reflect the wide range of geometries across which the EGSB is interpreted at laboratory-scale. The 1-D bioreactor type is proportionately exaggerated in the vertical direction and may be idealized as a "core" through a full-scale bioreactor. The 3-D bioreactor, by contrast, is a more direct scaling of the volumetric dimensions of a typical

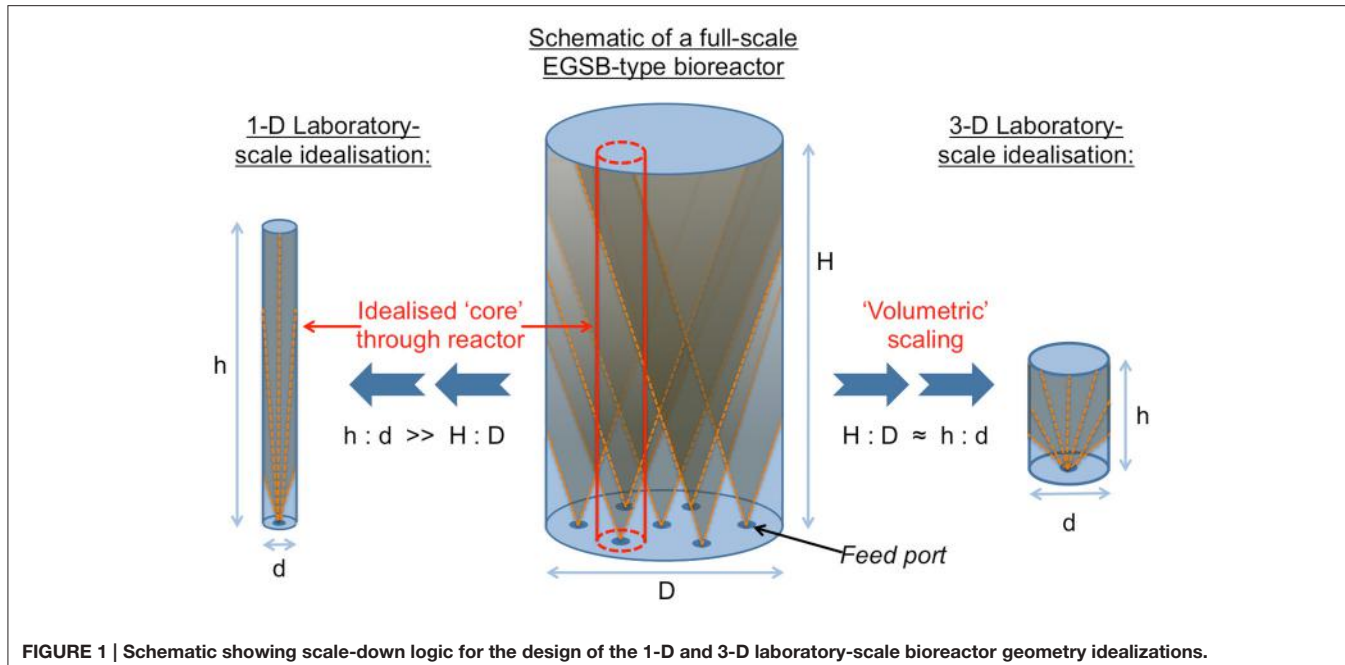


FIGURE 1 | Schematic showing scale-down logic for the design of the 1-D and 3-D laboratory-scale bioreactor geometry idealizations.

TABLE 1 | Design operating parameters at laboratory-scale.

Parameter	Design value or condition
Temperature (°C)	37
Feed type	Distillery waste transported to laboratory on weekly basis.
HRT (hours)	16
Upflow velocity (m/h)	3.5
Influent pH	6
OLR	Governed by COD of distillery waste during the trial.

full-scale bioreactor but, due to practicality of scaling, the design is simplified to include only a single feed port. The diameter-to-height aspect ratios employed were 1:15 and 1:4 for the 1-D and 3-D bioreactor types, respectively and both types were of 20-L total working volume. To facilitate spatial as well temporal biomass sampling, eight sampling ports were distributed along the length of each laboratory-scale bioreactor (from P1 at the bottom to P8 at the top), which was similar to the full-scale FSB. A single solid-liquid separator was employed in each of the 1-D and 3-D bioreactors. The separators were positioned above the sludge-bed to avoid stratification of the biomass by physical separation but below the recycle line to avoid forcible mixing of the sludge-bed by passage of granules through the recycle line.

Operation of the laboratory-scale bioreactors targeted the same mean temperature, influent, upflow velocity, hydraulic retention time (HRT), and OLR as FSB (Table 1). Each of the 20-L laboratory-scale bioreactors was seeded similarly to FSB to an initial volatile suspended solids (VSS) concentration of 12 g/L. After seeding the bioreactors and commencing feeding, biogas production was monitored over 16 days until stable rates were observed. The sampling and monitoring schedule

at laboratory-scale is provided in Figure 2. The operating temperature (37°C) was controlled using external water jackets. Recirculation and feeding was applied using peristaltic pumps (Watson and Marlow 300-series). Distillery wastewater served as substrate and was transferred from the distillery to the laboratory in two 640-L intermediate bulk containers (IBCs) on a weekly basis and stored at room temperature until used. All six of the laboratory-scale bioreactors were fed from a single tank utilizing in-tank mixing to promote homogenous solids delivery to the bioreactors and to ensure replicated feeding conditions. Dissimilarly to full-scale, no shut down period was applied at laboratory-scale i.e., operation was continuous for the duration of the trial.

Physical and Chemical Monitoring

At laboratory-scale, bioreactor influent and effluent was sampled twice per week for analysis of pH, total and soluble chemical oxygen demand (COD, sCOD) and volatile fatty acids (VFA). COD and sCOD was measured using the closed reflux colorimetric method (Standard Methods 5220D; APHA, 2005). Particulate COD (pCOD) was calculated as the difference between the two (COD-sCOD) to indicate solids loading. VFA (C_2-C_6 , including iso-forms of C_4-C_6) and ethanol concentrations were measured using a gas chromatograph (7890A, Agilent, Palo Alto, CA) equipped with a DB-FFAP capillary column and a flame ionization detector. Biogas production was recorded on a daily basis using 10-L rubber gasbags attached to each bioreactor to collect the biogas produced for timed periods of ~2 h. Biogas volumes were measured using a graduated gas-tight syringe to empty gasbags and biogas production rates (BPR) were calculated. Methane content in the biogas was determined on a biweekly basis, to coincide with influent and effluent monitoring, using a gas chromatograph

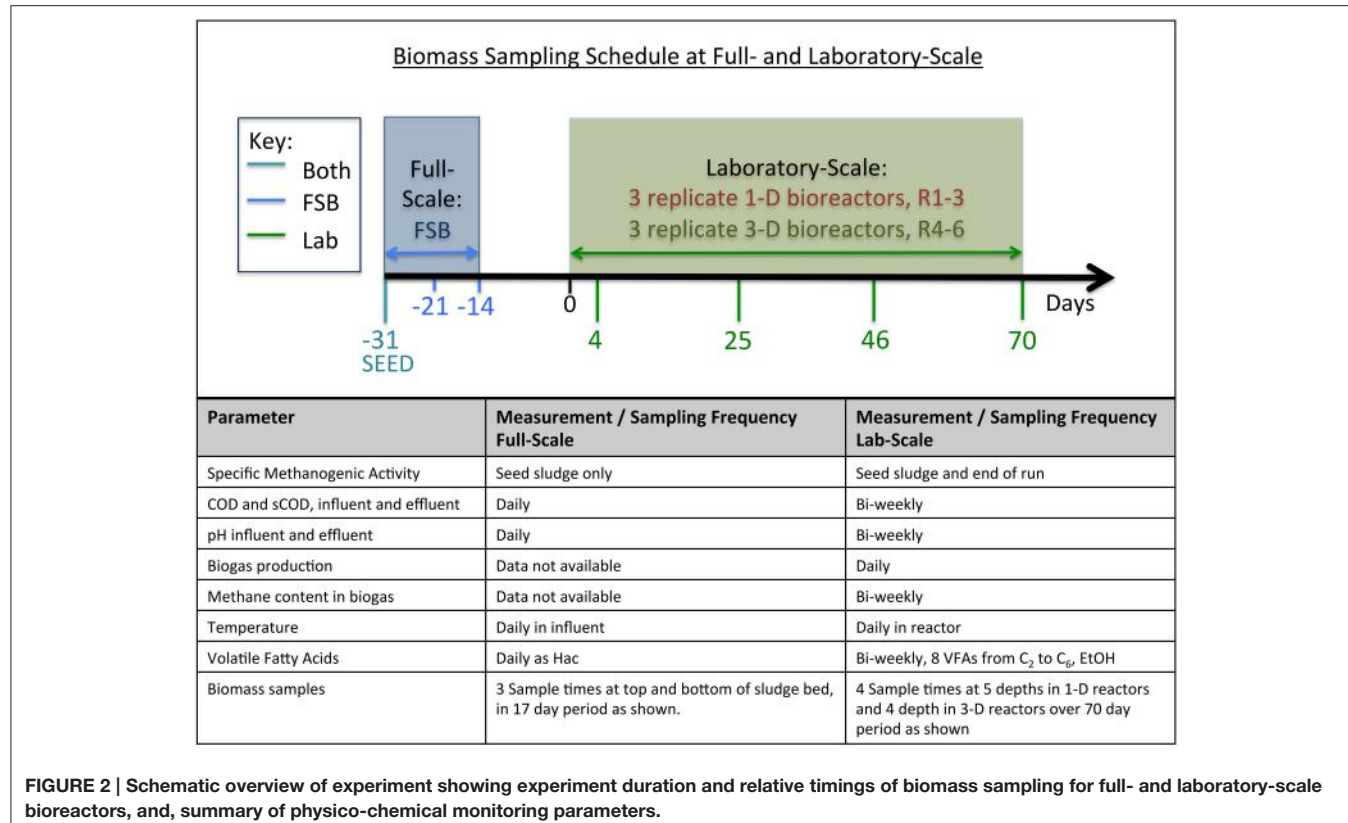


FIGURE 2 | Schematic overview of experiment showing experiment duration and relative timings of biomass sampling for full- and laboratory-scale bioreactors, and, summary of physico-chemical monitoring parameters.

(7890A, Agilent, Palo Alto, CA) equipped with a GS-Carbon Plot capillary column and a flame ionization detector.

At full-scale, operation and monitoring data were provided by the distillery. Parameters measured were common with laboratory-scale monitoring with two exceptions. First, at full-scale, BPR and methane content in the biogas were measured for the collective output for the three on-site digesters i.e., collected data is not specific solely to the performance of FSB. By contrast at laboratory-scale monitoring was specific to individual bioreactors and a mean for each bioreactor type is reported. Second, at full-scale a single measurement was made for total VFAs (TVFA). As such, laboratory-scale VFA data were used to calculate TVFA as an acetate-equivalent based on measurements of individual VFAs for improved comparison of data between scales.

Specific Methanogenic Activity Testing

Specific methanogenic activity (SMA) testing was conducted using the pressure transducer method (Colleran et al., 1992). Substrates tested were acetate, propionate, butyrate, ethanol, and hydrogen/CO₂ and each test was conducted in triplicate at 37°C. Assays using the seed sludge at D-31 represented both the activity at full-scale and activity at laboratory-scale at the beginning of the laboratory-scale trial. SMA testing was additionally conducted on samples taken from the top and bottom of the sludge beds in the 1-D and 3-D bioreactor types at the end of the trials i.e., after microbial adaptation to reduced scale and the alternative bioreactor geometries.

16S rRNA Library Preparation

Microbial community composition in the biomass was monitored by preparation of amplicon libraries targeting the V4 hyper variable region of the 16S rRNA gene using next generation sequencing (NGS) methods and a multiplexed barcoded sample preparation approach. At laboratory-scale, biomass samples (2 ml) were drawn from each port in the sludge bed and then centrifuged to remove liquor and transferred to -20°C storage within 2 h. At full-scale, sludge samples (50 ml) taken from each port in the sludge bed were drawn to sterile, air-tight containers from which 2-ml sub-samples were taken, centrifuged and then stored at -20°C until further processing. At each scale, ports were flushed of biomass prior to capturing samples to ensure that any depth-associated effects determined were not sampling artifacts. Frozen biomass samples were thawed and subject to homogenization prior to extraction. Each DNA extraction used 0.1 g (wet weight) of biomass. DNA extraction and purification was done using the FastDNA® Spin Kit for Soils (MP Biomedical) and the FastPrep® Instrument (MP Biomedicals, Santa Ana, CA) according to the manufacturer's instructions. Extracted DNA was quantified using the Broad-Range Qubit Assay (Life Technologies) and stored at -20°C until used in NGS library preparation. NGS libraries were prepared by PCR amplification of the V4 region of the 16S rRNA gene using Golay barcoded primers (Caporaso et al., 2012), with an adaptation on the forward primer, and the KAPA HiFi HotStart PCR Kit. Our forward primer (F515: GTGNCAAGCMGCCGCGGTAA) included an additional

degeneracy for improved detection of Archaea, whilst the reverse primer, R806 (GGACTTACHVGGGTWTCTAAT), was as per the Caporaso design. Efficacy of our adapted primer pair was tested *in-silico* using the Ribosomal Database Project's (RDP) Probe Match tool and indicated detection of 87.59 and 90.95% of good quality bacterial and archaeal sequences, respectively (search conditions: no mismatches, sequences should lie with the region 465–866 on the *E. coli* genome i.e., limiting the search to sequences that might contain the V4 region). By contrast the original Caporaso primer pair detected 87.53 and 54.81% of bacterial and archaeal sequences in the database, respectively using the same search conditions. Thus, our primer pair offered significant improvement for the detection of Archaea and should return a relatively representative microbial community composition with respect to relative abundance of bacterial and archaeal sequences. PCR conditions applied were: 95°C for 5 min initial denaturation; with amplification proceeding for 25 cycles of 98°C for 20 s denaturation, 60°C for 15 s annealing and 72°C for 40 s extension; followed by 72°C for 1 min final extension. Each sample was assigned a unique barcode pair and PCR was conducted in triplicate to enable a high concentration of PCR product to be obtained using a reduced number of PCR cycles. Triplicate PCR products were gel-purified and quantified prior to pooling for sequencing using the High-Sensitivity Qubit Assay (Life Technologies). Positive and negative controls for sequencing were generated using triplicate blank DNA extractions for the negative control and both skewed and evenly distributed mock communities for the positive controls. The controls were each assigned three barcode pairs to enable replicate sequencing, which was used in quality control checking. The purified barcoded PCR products were normalized to 5 ng/uL DNA and pooled for sequencing. The final pool sequenced contained samples not reported here but prepared from DNA from a similar source (laboratory-scale EGSSBs treating low-strength waste) and barcoded and normalized same using the same protocol as outlined above. The concentration of the final pool was 5.6 ng/uL and comprised 249 uniquely barcoded sample libraries, of which 107 sample libraries pertain to this study. The pool was sequenced using the Illumina MiSeq bench-top sequencer and V2 chemistry. Sample libraries returning fewer than 5,000 raw reads (40 samples) after sequencing were re-sequenced in a further sequencing run following the same preparation protocol but with alternative sequencing barcodes assigned to the sample. This process was repeated a third time to improve coverage of 11 of the sample libraries reported here.

Bioinformatics

The forward and reverse reads were obtained from the sequencing center in FastQ format. Each sample library across the three sequencing runs was assigned a unique identifier and the data merged for processing as a single data set comprising 730 samples libraries of which 107 are included in this study. The positive and negative control samples were sequenced in each run. The negative control, prepared as a “blank” DNA extraction and subject to PCR as other samples, yielded no reads in any of the three runs indicating that no contamination was introduced

to samples by the DNA extraction procedure used. The positive controls were processed, along with all other samples, according to the *Illumina Amplicons Processing Workflow* (<http://userweb.eng.gla.ac.uk/umer.ijaz#bioinformatics>), which is outlined as follows. Raw forward and reverse reads were trimmed using a sliding window approach to a minimum quality score of 20 and minimum length of 10 bp using Sickle Version 1.33 (Joshi and Fass, 2011). Trimmed paired-end reads were overlapped using PANDAseq (Masella et al., 2012) with a maximum search radius of 50 bp to form single sequences covering the V4 region. Any paired-end reads that failed to overlap were discarded. The UPARSE pipeline (Edgar, 2013) was then used to construct operational taxonomic units (OTUs, used as a proxy for species) as described in <https://bitbucket.org/umerijaz/amplimock/src>. The overlapped sequences from each sample were multiplexed, pooled and dereplicated, and singletons were discarded. Sequences were clustered at 97% similarity and the default setting in USEARCH, in which sequences of <32 bp are discarded, was applied. Chimeras from abundant reads were removed *de-novo* within the UPARSE pipeline as is inherent in the “cluster_OTU” command in USEARCH. Additionally, a reference-based approach was applied to remove chimeras with lower relative abundances using a gold database (http://drive5.com/uchime/uchime_download.html) and UCHIME (Edgar et al., 2011). An OTU abundance table was then generated by matching the original barcoded overlapped reads against the cleaned consensus sequences at 97% similarity. The resultant OTU table contained re-sequenced samples as individual sample libraries e.g., the sample library for sample “S1” was represented as three “repeat” libraries S1_run1, S1_run2, S1_run3. Prior to analysis and downstream processing of the OTU table, one-way subject ANOVA (<http://ww2.coastal.edu/kingw/statistics/R-tutorials/repeated.html>) was used to confirm abundance profiles within these repeats were similar. Where so, the samples were collated by addition e.g., reads for OTU1 in S1_run1 were added cumulatively to reads for OTU1 in S1_run2 and to reads for OTU1 in S1_run3 to produce a single sample library “S1” containing Σ OTU1 etc. Where abundance profiles were dissimilar, the library with the highest read count of the re-run libraries was used to represent that sample. Thus, after collation of repeats, the OTU table contained a single library for each sample sequenced. At this stage a final quality check on our library preparation process, across the PCR, sequencing, and OTU clustering stages collectively, was enabled by comparison of the positive control samples against known sequences. It was determined that 95.1% (s.d. 0.6%) and 97.0% (s.d. 0.4%) of OTUs in the even and skewed mock community samples matched the predicted sequences thus confirming our procedure returned high quality data.

All OTUs (4,272 at this stage) were then taxonomically classified against the RDP database at phylum, class, order, family, and genus level, using the RDPClassifier V2.6 (Wang et al., 2007) to obtain abundance tables at each taxonomic level. To determine phylogenetic distances between the OTUs, mafft V7.040 (Katoh and Standley, 2013) was used for multi-sequence alignment of the OTUs within the dataset enabling generation of an approximately-maximum-likelihood tree using FastTree

v2.1.7 (Price et al., 2010). Finally, the OTU and taxonomic abundance tables and FastTree were reduced to include only the 107 sample libraries pertaining to this study, herein referred to as “the OTU table,” “taxa tables,” and the “FastTree.”

Qualitative and Statistical Data Analysis Methods

Statistical evaluation of difference in operation and performance data with scale and bioreactor type was conducted using one-way analysis of variance [ANOVA, *aov()*, R] and stated *p*-values for significance were as calculated within that function. For qualitative assessment of taxonomy across the full sample set, mean relative abundance, and standard deviation at phylum level was calculated directly from count data in the RDP classified phylum level taxa table using R-Software. To enable visualization of phylogeny amongst dominant OTUs, the FastTree was trimmed to represent the 100 most abundant OTUs using the Phyloseq package in R (McMurdie and Holmes, 2013) and the trimmed tree plotted using the web application Evolview v2 (He et al., 2016). The plotted tree was annotated in Evolview using heatmaps showing the mean relative abundance of the 100 most abundant OTUs in each reactor type (FSB, 1-D, 3-D), alongside the log transform of mean relative abundance for enhanced visualization of difference in abundance between reactor types. Non-metric multidimensional scaling (NMDS) plots were used to visualize clustering of all OTUs in samples by bioreactor type, by sampling day and by sampling depth using the Phyloseq package in R. Distances used to plot NMDS were Bray-Curtis dissimilarity calculated from OTU count data and GUniFrac distances (Chen, 2012) calculated using the FastTree and enabling inspection of grouping by abundance and phylogeny, respectively. Trends identified in the NMDS plots were assessed statistically using PERMANOVA [Adonis(), R-Vegan; Oksanen et al., 2014] and the respective distance measures (Bray-Curtis, GUniFrac), and *p*-values reported were computed within that function. Statistical difference in relative abundance with reactor type, and by sampling depth at laboratory-scale was determined by the Kruskall-Wallis test in R using log-transformed relative abundance data at phylum level. Benamini-Hochberg correction for multiple testing was applied and adjusted *p*-values were reported. Ecology indices calculated were rarefied richness, Simpson’s index of diversity and Pielou’s evenness index. In each case, rarefaction was applied to the full sample set to a common minimum (that of the lowest read count sample) using the rrarefy() function in R-Vegan. Variation of ecology indices with time and depth in the laboratory scale sample sets was assessed by fitting a linear model, lm() in R, and significance values reported were computed within that function. All R scripts used are maintained by the authors and all sequence data will be deposited with the European Nucleotide Archive (PRJEB18489).

RESULTS AND DISCUSSION

Operation at Full- and Laboratory-Scales

Qualitatively, operation of FSB (Table 2) was variable with respect to OLR and temperature but relatively stable with respect to both total COD content and the relative proportions of

soluble, and particulate, components. The variability in operation arose from a 5-day shut down period (D-59 to D-54) in which both volumetric loading rate (VLR) and temperature fluctuated. The maximum and minimum values for VLR (2.82 and 0.67 L/L_{reactor.d}) and the minimum recorded temperature (30.0°C) were recorded during the re-start of operations. Neither extreme of loading rate was sustained for more than two HRTs, nor repeated during the period of interest, and temperature fluctuation was maintained for <2 HRTs.

Operation at laboratory-scale (Table 2) was comparatively stable yet significant difference was determined in bioreactor influent characteristics between scales. Total COD, TVFA, pH, and the proportion of pCOD in the influent were significantly lower (*p* < 0.001, ANOVA) at laboratory-scale than that at full-scale. These physico-chemical differences, each of which may impact the underlying microbial community, arose from the influence of seasonal variation in productivity at the distillery on wastewater strength and composition. Further difference in operation between scales was that no disruption to operation was applied at laboratory-scale. Together, seasonal variation of wastes and semi-continuous feeding indicate that scalability of biotechnologies must be considered in the broadest sense and not only in relation to bioreactor volume and design. Operating data at laboratory scale indicated that no significant difference (ANOVA) in operation occurred between either the 1-D and 3-D bioreactor types, nor within triplicate bioreactor sets such that the laboratory reactors may be described as true replicates in terms of operating conditions applied.

Performance Indicators at Full- and Laboratory-Scales

The performance indicators at full-scale (Table 3) qualitatively indicate stable performance. Whilst VFA accumulation was observed in the effluent, mean COD and sCOD removal efficiencies were both high and stable. By contrast, pCOD removal was stable but low, however low pCOD removal is consistent with EGSBs reported elsewhere (Chan et al., 2009). Biogas production at full-scale was recorded for the plant as

TABLE 2 | Temperature, loading, and influent characteristics of FSB (D-85 to D-0) and laboratory-scale bioreactors (D0-D70).

Parameter	Digester	FSB ^a	Laboratory-scale ^a	
			1-D	3-D
Temperature (°C)		36.1 ± 1.0	37.1 ± 0.5	37.0 ± 1.6
VLR (L/L _{reactor.d})		1.6 ± 0.3	1.6 ± 0.1 ^b	
OLR (gCOD/L _{reactor.d})		9.9 ± 3.0	9.4 ± 1.4	
pH		7.0 ± 0.2	6.2 ± 0.4	
COD (mg/L)		6530 ± 950	4710 ± 730	
sCOD (% COD)		67.2 ± 4.2	75.0 ± 10.5	
pCOD (% COD)		32.8 ± 4.2	25.0 ± 10.5	
TVFA (mg as acetate/L)		1424 ± 298	766 ± 157	
Ethanol (mg/L)		Not determined	54 ± 109	

^aMean ± standard deviation.

^bBoth types of laboratory-scale bioreactors were fed with the same feedstock.

a whole i.e., a single biogas production rate was measured collectively for the three digesters on-site. It is noted however that for the period of study, mean methane content in the biogas was 70.0% (*s.d.* 2.9%) across the three on-site digesters and was relatively stable. Mean biogas production rate for FSB inferred as a proportion of the total was produced across the plant was approximately $2.5 \text{ m}^3/\text{m}^3_{\text{reactor}} \cdot \text{d}$. Although, ethanol was not monitored for FSB, ethanol accounted for about 2% of the influent COD in the laboratory-scale bioreactors (Table 2) and was almost completely degraded (>94% on average) in the effluent (Table 3).

At laboratory-scale, a high degree of reproducibility was found between bioreactors in the 1-D and 3-D replicate sets with no significant difference in performance found for any indicator except for TVFA in the 1-D bioreactors ($p < 0.05$, ANOVA). As such, performance indicators at laboratory-scale are presented as a mean by bioreactor type rather than for individual bioreactors (Table 3). For each of pH, COD removal efficiency, sCOD removal efficiency, BPR and methane content in the biogas, the 1-D and 3-D bioreactor types both demonstrate stable performance throughout the trial. As with the full-scale bioreactor, pCOD removal efficiency was lower than sCOD removal efficiency but dissimilarly, pCOD removal efficiency at laboratory-scale was somewhat unstable. It was observed that the higher pCOD efficiency recorded at laboratory-scale, particularly in the 1-D bioreactors, declined over the duration of the trial suggesting that increased efficiencies recorded may be a temporal phenomenon related to the age of the bioreactors. For each of COD, sCOD, and pCOD removal, the laboratory-scale bioreactors significantly out-performed ($p < 0.01$, ANOVA) the full-scale bioreactor. Tentatively, this suggests that tightly controlled laboratory studies have the potential to exaggerate treatment efficiency as compared to more variable full-scale operation; however as influent characteristics varied between scales this is not conclusive.

No significant difference was found between the two laboratory-scale bioreactor idealizations with respect to bioreactor pH, pCOD removal efficiency, or biogas production. However, significant differences were found between each of

TABLE 3 | Effluent characteristics and performance indicators of the full- and the laboratory-scale bioreactors.

Digester parameter	Full-scale	Laboratory-scale	
		1-D	3-D
pH	$6.9 \pm 1.3^{\text{a}}$	7.2 ± 0.2	7.3 ± 0.2
TVFA (mg as acetate/L)	282 ± 117	12.2 ± 13.4	30 ± 58
Ethanol (mg/L)	Not determined	3.1 ± 2.7	0.0 ± 0.0
COD removal (%)	70.7 ± 11.7	91.1 ± 5.1	88.1 ± 4.8
sCOD removal (%)	80.1 ± 12.6	93.7 ± 2.3	92.0 ± 4.9
pCOD removal (%)	49.8 ± 13.0	77.9 ± 28.3	69.3 ± 26.0
BPR (L/L d)	- ^b	2.95 ± 0.91	3.01 ± 0.61
CH ₄ ratio (%)	-	74.5 ± 3.5	72.8 ± 6.4

^aMean \pm standard deviation.

^bBiogas production in the full-scale bioreactor was monitored only collectively with two other bioreactors in parallel.

total VFA accumulation, COD and sCOD removal efficiencies and methane content in the biogas ($p < 0.05$, ANOVA), with the 1-D bioreactors marginally out-performing the 3-D systems. As laboratory-scale operating conditions were identical, this observation indicates that laboratory idealization does influence performance.

Community Physiology at Full- and Laboratory-Scales

Community physiology was investigated using SMA testing of biomass samples from the full-scale bioreactor (Port 2 on D-31, also used as seed-sludge for laboratory-scale bioreactors) and biomass samples from the top and bottom of the sludge bed in each of the 1-D and 3-D laboratory-scale bioreactor sets at the end of the trial (D70). At full-scale and in the seed sludge used at laboratory-scale (FSB/SEED Figure 3), hydrogenotrophic methanogenic activity was dominant. This was unexpected as acetoclastic methanogenesis is commonly assumed to be the dominant metabolic pathway in engineered AD systems (O'Flaherty et al., 2006). The literature has several reports of low-temperature laboratory-scale EGSB systems dominated by hydrogenotrophic methanogenesis (McKeown et al., 2009; O'Reilly et al., 2010). As the temperature in this study (37°C) was not low, it may be inferred that variable loading of higher solids wastes may induce similar stresses on acetoclastic methanogens by, for example, ammonia inhibition arising from protein degradation (Westerholm et al., 2011). By the conclusion of the laboratory trials where solids delivery was lower than at full-scale and loading was more stable, a significant decline ($p < 0.001$, ANOVA) in hydrogenotrophic activity was recorded at laboratory-scale, which in real terms was most pronounced in the 1-D bioreactor types.

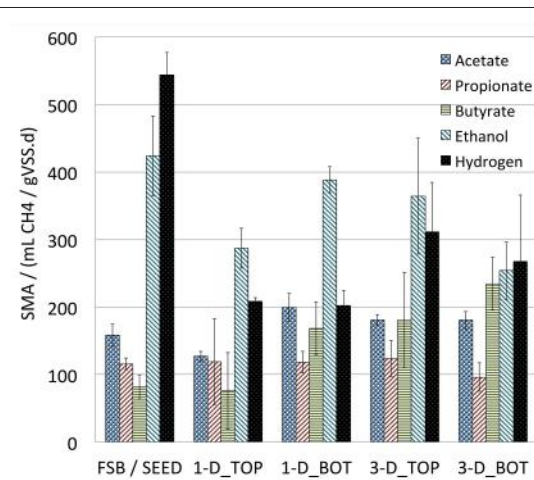


FIGURE 3 | Grouped bar plot showing SMA recorded in biomass from full-scale (SEED) and laboratory-scale bioreactors at the beginning (SEED) and end of the trial at the top (TOP) and bottom (BOT) of the sludge beds against specific substrates: acetate, propionate, butyrate, Ethanol, and hydrogen. Bars show blank-adjusted mean and error bars show standard deviation of triplicate measurements.

Comparison of physiological profiles between biomass adapted to the 1-D and 3-D laboratory-scale bioreactor types (i.e., at D70) indicated that no significant difference in activity was found using acetate, propionate, butyrate or ethanol as specific methanogenic substrates. However, a significant difference ($p < 0.05$) was found in activity against hydrogen with biomass from the 3-D bioreactor type exhibiting a more strongly hydrogenotrophic profile than the 1-D bioreactors. As such, laboratory-scale bioreactor idealization may influence not only performance but the inferred route to methanogenesis in laboratory studies, an important finding for studies of new biotechnologies intended to inform full-scale process design.

Comparison of the spatial distribution of activity in the biomass from the two laboratory-scale reactor types indicated that the 1-D bioreactors exhibited zoned community physiology whilst the 3-D bioreactors did not. In the 1-D bioreactors, activity was significantly higher in sludge from the bottom, than from the top, of the sludge bed against both acetate and ethanol ($p < 0.001$, ANOVA). By contrast, no significant difference in activity with depth was found in the 3-D type bioreactors for any substrate tested. Whilst the precise mechanisms promoting stratification of activity were not elucidated here, our data demonstrates that the depth at which biomass is sampled from 1-D type EGSB bioreactors at laboratory-scale might influence both the inferred dominant methanogenic pathway in the biomass and loading capacity of such bioreactors.

Microbial Community Composition and Structure at Full- and Laboratory-Scale Qualitative Overview of Microbial Community at Full- and Laboratory-Scales

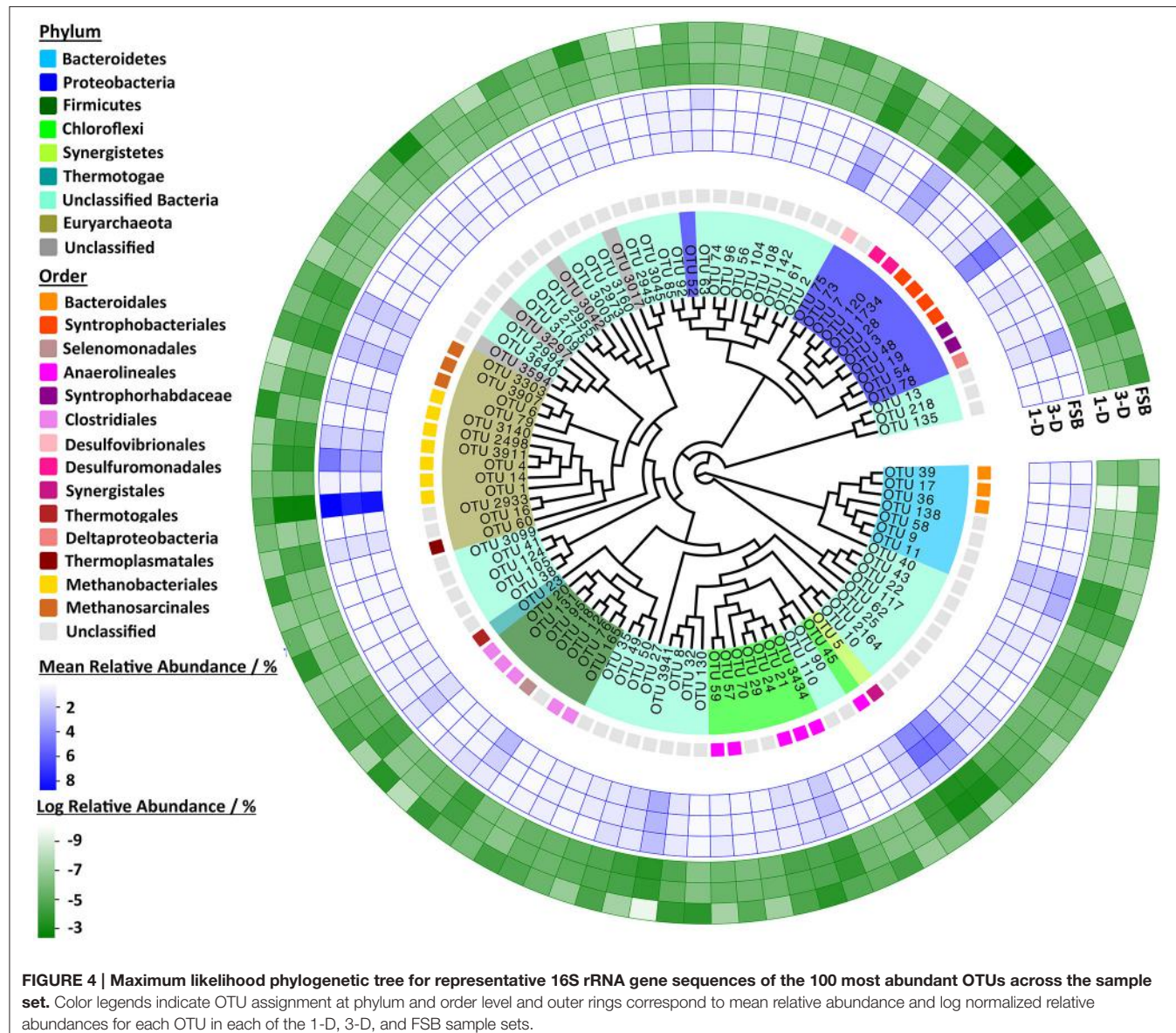
The OTU table containing the quality filtered, chimera and singleton free reads clustered into a total of 2,929 OTUs at 97% sequence similarity for the complete data set across 107 sample libraries. Two sample libraries returned fewer than 5,000 sequences per library (both on the 1-D bioreactor R3: at port P1 on day D25 and at port P2 on day D46) and were excluded from the remaining analyses such that the lowest read count for any library was 5,232 reads. The final distribution of sample libraries per bioreactor type was: 5 samples for FSB; 53 samples across the 1-D triplicate set; and 47 samples across the 3-D triplicate set. The mean number of reads per sample library was 74,034 ($s.d. 89,192$). Rarefaction curves plotted for all samples (**Figure S1**) indicate that saturation was not reached for any sample sequenced. Taxonomically, OTUs identified across all samples were assigned across 24 known phyla with a mean of only 1.33% of OTUs per sample assigned as “unknown phyla” ($s.d. 1.55\%$) however a mean of 36.08% of OTUs per sample were assigned as “unclassified bacteria” ($s.d. 7.88\%$) and 0.75% as “unclassified archaea” ($s.d. 0.04\%$). The most dominant phyla (mean relative abundance greater than 0.5%) in the sample set were *Euryarchaeota*, *Proteobacteria*, *Chloroflexi*, *Firmicutes*, *Bacteroidetes*, *Synergistetes*, and *Thermotogae* representing a mean relative abundance of 19.99 ($s.d. 8.70$), 13.22 ($s.d. 3.28$), 8.45 ($s.d. 2.24$), 7.70 ($s.d. 3.63$), 5.72 ($s.d. 3.21$), 4.76 ($s.d. 2.11$), and 0.50 ($s.d. 0.19$), respectively. Collectively, the remaining

17 phyla were attributed <0.5% of mean relative abundance thus the data appears skewed at phylum level. At lower taxonomic levels, the OTUs were classified across 62 classes, 92 orders, 180 families, and 378 genera. Ecology indices for the sample set were calculated using the OTU table by rarefying all samples in the sample set to a common read count of 5,232 (minimum in the set). Mean rarefied richness across all samples was 460 ($s.d. 55$) OTUs, Simpson’s index of diversity was 0.975 ($s.d. 0.01$) and Pielou’s evenness index was 0.763 ($s.d. 0.02$). Qualitatively then the data describes a phylogenetically rich and diverse community with relatively even distribution of abundance in the microbial population across the sample set at species (OTU) level.

Each of the 100 most abundant OTUs across the sample set (**Figure 4**) was present in each of the full-scale and laboratory-scale bioreactor communities indicating strong phylogenetic similarity between the communities at both scales and in each laboratory idealization. The relatively most abundant order identified was *Methanobacteriales*, accounting for seven of the 100 most abundant OTUs. Of those, six were identified at genus level as *Methanobacterium* including the most dominant OTU present (OTU_1). *Methanobacterium* are H₂/CO₂ and formate-utilizing methanogens (Madigan et al., 2009), so the finding was somewhat unexpected as acetate-utilizing methanogens typically dominate EGSBs. Nonetheless, this finding supports SMA data, which indicated dominance of the hydrogenotrophic pathway. The archaeal order *Methanosaetales* was also relatively highly abundant at both scales, comprising three OTUs amongst the 100 most abundant, each of which classified as *Methanosaeta* at genus level. *Methanosaeta* are filamentous, acetoclastic methanogens associated with granule formation and maintenance and thought to form the core of anaerobic granular biofilms (Hulshoff Pol et al., 2004). Whilst inspection of mean relative abundances of the 100 most abundant OTUs in the sample set indicates that phylogeny is maintained between scales, inspection of log relative abundances indicates that there are stronger similarities between the 1-D and 3-D laboratory-scale communities than between laboratory and full-scale communities. This may reflect the differences in operating conditions applied between scales.

Variability in Community Structure and Phylogeny between Scales, Replicate Bioreactors, and with Depth

Ordination plots were coupled with PERMANOVA using two alternative distance metrics; Bray-Curtis and GUniFrac alpha = 0.5 to determine variability in community structure and phylogeny across all OTUs in the sample set between scales. Across all time points sampled, the laboratory-scale bioreactor communities cluster more closely to each other than to the full-scale bioreactor from which the seed sludge was drawn (**Figure 5**). The plot using count data (**Figure 5A**) clusters less distinctly than that using phylogenetic distances (**Figure 5B**), suggesting variability in community structure but more stable community membership at both scales. PERMANOVA was applied and determined that no significant difference in structure was found between communities from the full-scale, 3-D, or 1-D bioreactors but that significant difference was found using GUniFrac distances [$p < 0.021$, adonis()]. Thus, phylogeny



appears relatively stable, yet distinct with scale, suggesting community adaptation at reduced scale did occur. The precise driver for change lacks certainty however as scale was not the only difference between the full- and laboratory bioreactors, differences in operating conditions also occurred.

A similar approach was applied to determine replication between bioreactors within 1-D and 3-D laboratory-scale test sets. No significant difference was found in species relative abundance or phylogeny across replicate 1-D bioreactors. Thus, replicated 1-D communities underpinned replicated performance metrics. However, a significant difference [$p < 0.001$ adonis(), Bray-Curtis] was found between the 3-D bioreactors estimated to account for 16% of variance across the samples despite the fact that the 3-D bioreactors appeared highly replicated with respect to operation and performance,

demonstrating the importance of running replicate bioreactors during laboratory trials.

Differences in microbial community structure with time (Figure 6) and depth (Figure 7) in the laboratory-scale bioreactor sets was also investigated. The full-scale digester was omitted from this analysis due to lack of replicate sampling. With time, the 1-D microbial community structure appeared to evolve more than the 3-D community. Further, with depth in the 1-D bioreactors, the microbial community at the bottom of the sludge bed (P1) clusters distinctly from those samples from higher in the sludge bed whilst little distinction with depth was observed in the 3-D bioreactors. This supports the SMA data that indicated stratification of community physiology with depth occurred in the 1-D bioreactors but not in the 3-D bioreactor type. Thus, stratified community physiology is linked with stratified

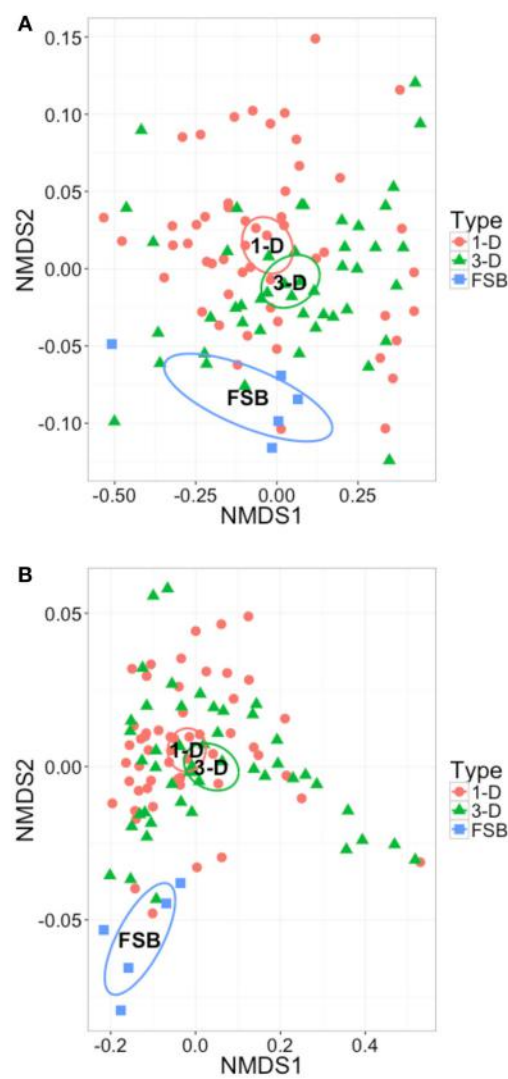


FIGURE 5 | Two-dimensional NMDS ordination plots of all OTUs in the sample set, grouped by reactor type, and plotted using (A) structure based Bray-Curtis similarity, stress = 0.044, (B) phylogeny based GUniFrac distance and alpha = 0.5, stress = 0.062. In each case ellipses show 95% confidence interval of the standard error of the samples in each group around the population mean.

community structure in the 1-D bioreactors. PERMANOVA confirmed that the trend was statistically significant, with depth estimated to account for 11.8% of variation across samples in the 1-D bioreactors [$p < 0.01$, adonis()] whilst no significant trend was found with depth in the 3-D bioreactors. This points to the importance of (i) the influence of laboratory-scale idealization on spatial and temporal community structure, and (ii) appropriate sampling strategies in AD bioreactors to adequately capture microbial community composition.

Key Taxa Associated with Scale, Bioreactor Idealization, and Depth

The relative abundance of 5 phyla varied significantly with bioreactor type [$p < 0.05$, kruskal.test()] of which *Bacteroidetes*

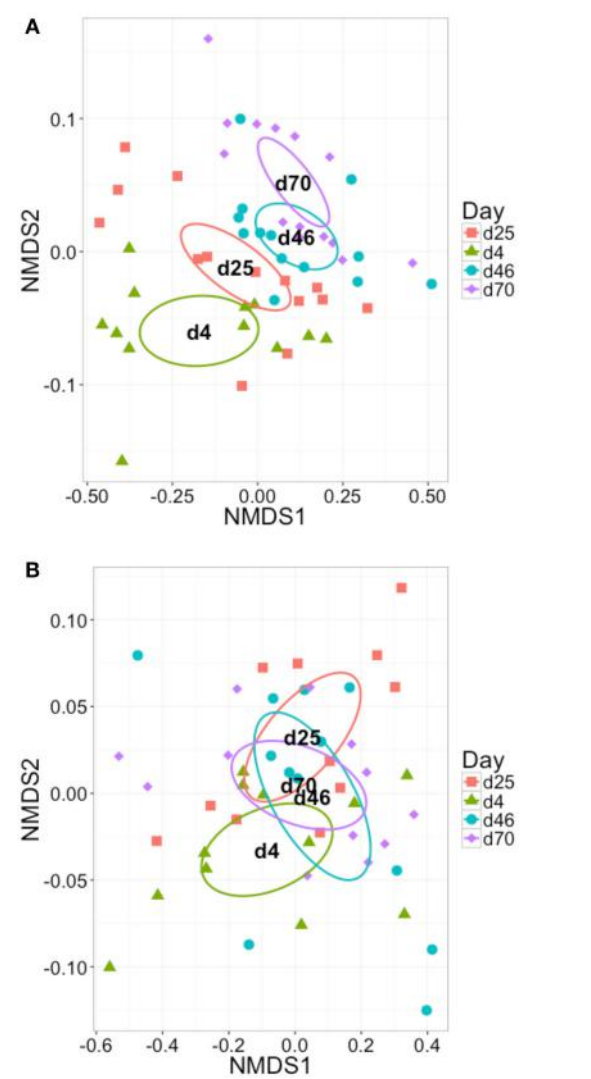


FIGURE 6 | Two-dimensional NMDS ordination plots of all OTUs in the sample set grouped by sampling day and plotted using Bray-Curtis similarity for (A) 1-D laboratory-scale samples, stress = 0.127, and (B) 3-D laboratory-scale samples, stress = 0.169. In each case ellipses show 95% confidence interval of the standard error of the samples in each group around the population mean.

(Figure 8) and *Armatimonadetes* were relatively more abundant at full-scale whilst *SR1*, *OD1*, and *Verrucomicrobia* were relatively more abundant at laboratory-scale. Of these, only *Bacteroidetes* contributed more than 1% of the total community relative abundance at any scale. The mean relative abundance of *Bacteroidetes* in the full-scale bioreactor FSB was 13.2% (*s.d.* 5.2%) compared to a mean of only 5.34% (*s.d.* 2.59%) at laboratory-scale thus the difference is not only significant but sizeable in real terms. Organisms of the phylum *Bacteroidetes* have been identified as core to the microbial communities in full-scale anaerobic digesters (Chouari et al., 2005; Lee et al., 2008; Rivière et al., 2009) and may be associated with degradation of long chain organics such as proteins and carbohydrates

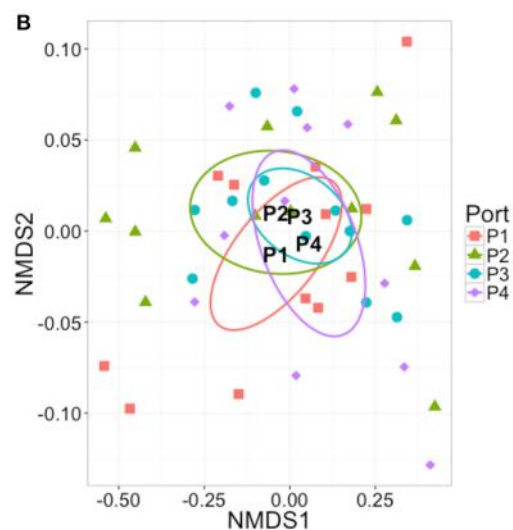
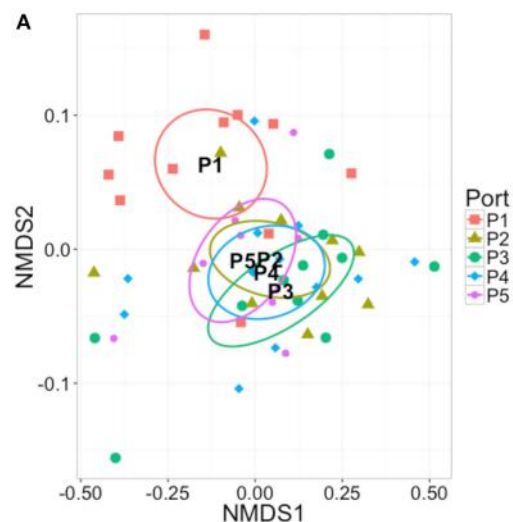


FIGURE 7 | Two-dimensional NMDS ordination plots of all OTUs in the sample set grouped by sampling depth and plotted using Bray-Curtis similarity for (A) 1-D laboratory-scale samples, stress = 0.118, and (B) 3-D laboratory-scale samples, stress = 0.129. In each case ellipses show 95% confidence interval of the standard error of the samples in each group around the population mean.

(Hernon et al., 2006; Klocke et al., 2007; Thomas et al., 2011). Increased abundance at full-scale here then may reflect the higher proportion of particulate COD in the influent to FSB rather than the scale of the reactor *per se*.

Difference in relative abundance of taxa with sampling position was assessed similarly at phylum level in the laboratory-scale bioreactors however FSB was omitted from the analysis due to lack of replicate samples. In the 3-D laboratory-scale bioreactors, no significant difference in relative abundance with depth in the sludge bed was found for any phyla. By contrast in the 1-D bioreactor type, in which stratified community physiology was observed, significant difference [$p < 0.05$, `kruskal.test()`] in mean relative abundance with depth was

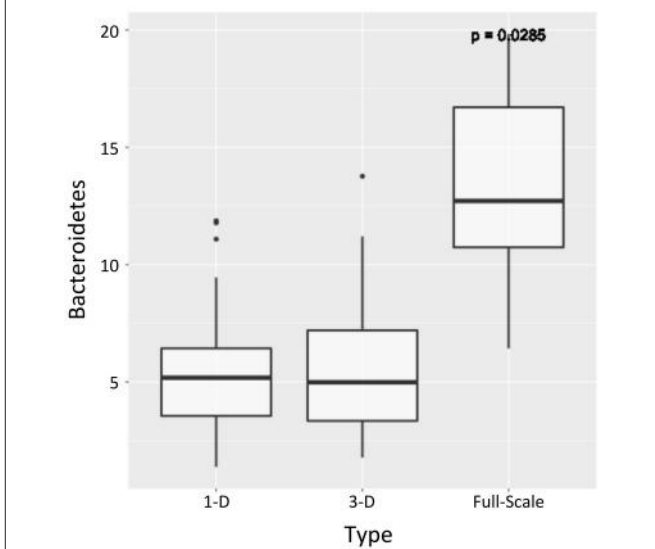


FIGURE 8 | Boxplot showing relative abundance (%) across each sample set for the phylum Bacteroidetes, the relative abundance of which was significantly greater at full-scale than at laboratory -scale (Kruskal-Wallis with Benjamini-Hochberg correction on p -value, $p < 0.05$). The bands show the median value for each group; bottom and top of boxes show the first and third quartiles; and whiskers show maximum and minimum values with 1.5 of IQR of upper and lower quartiles.

observed in two dominant phyla: *Firmicutes* whose relative abundance increased with depth (Figure 9A), and *Synergistetes* whose relative abundance decreased with depth (Figure 9B). Thus, we observe that bioreactor design significantly influenced the distribution of both microbial community physiology and taxonomy in laboratory-scale EGSB type bioreactors, with 1-D bioreactors promoting stratification of each. In each case, the difference in abundance was both significant and marked in real terms. Both *Firmicutes* and *Synergistetes* are widely reported as relatively highly abundant in engineered anaerobic systems (Satoh et al., 2007; Rivière et al., 2009; Milton et al., 2015; Chen et al., 2016) and as such significant stratification observed here demonstrates the importance of spatial, as well as temporal, sampling of bioreactors at laboratory-scale when aiming to characterize microbial community composition in such systems.

Ecology Indices with Scale, Bioreactor Type, and Depth

Ecology indices with time and depth for each of the full-scale and laboratory-scale bioreactor sets indicate species-rich communities that are highly diverse and distributed evenly (Figure 10). Linear regression [$\ln(\cdot)$, R] determined that rarefied richness increased significantly with time in each of the 1-D and 3-D bioreactor sets ($p < 0.001$ in 1-D, $p < 0.01$ in 3-D). Increasing community richness with reduced scale was unexpected as ecological theory suggests increasing scale tends to increase richness (Brown et al., 2001). Here however scale, as in reactor volume or geometry, was not the sole difference between the laboratory- and full-scale bioreactors. Operational differences occurred too including semi-continuous feeding at

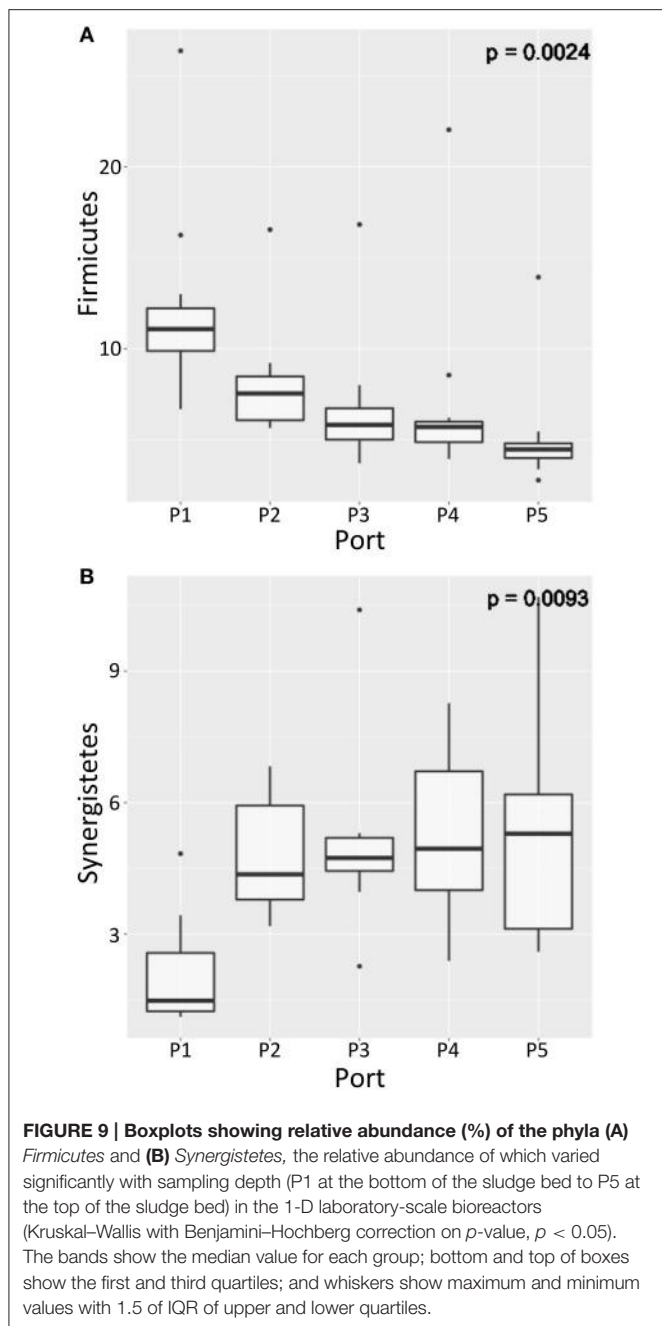


FIGURE 9 | Boxplots showing relative abundance (%) of the phyla (A) Firmicutes and (B) Synergistetes, the relative abundance of which varied significantly with sampling depth (P1 at the bottom of the sludge bed to P5 at the top of the sludge bed) in the 1-D laboratory-scale bioreactors (Kruskal–Wallis with Benjamini–Hochberg correction on p -value, $p < 0.05$). The bands show the median value for each group; bottom and top of boxes show the first and third quartiles; and whiskers show maximum and minimum values with 1.5 of IQR of upper and lower quartiles.

full-scale and differences in physico-chemical parameters of the bioreactor influent, each of which may impact the underlying microbial community. Thus, direct attribution of the increase in richness with scale in the purest sense was not possible. Tentatively however, it could be implied that steady loading of bioreactors at reduced loading rates for both particulate COD and TVFA positively influences richness of the underlying microbial community in EGSB-type bioreactors.

The increase in richness with time in the 1-D bioreactors was more marked in real terms than in the 3-D bioreactors such that mean rarefied richness in the 1-D bioreactor set across all time points was significantly greater ($p < 0.001$, ANOVA) than that of

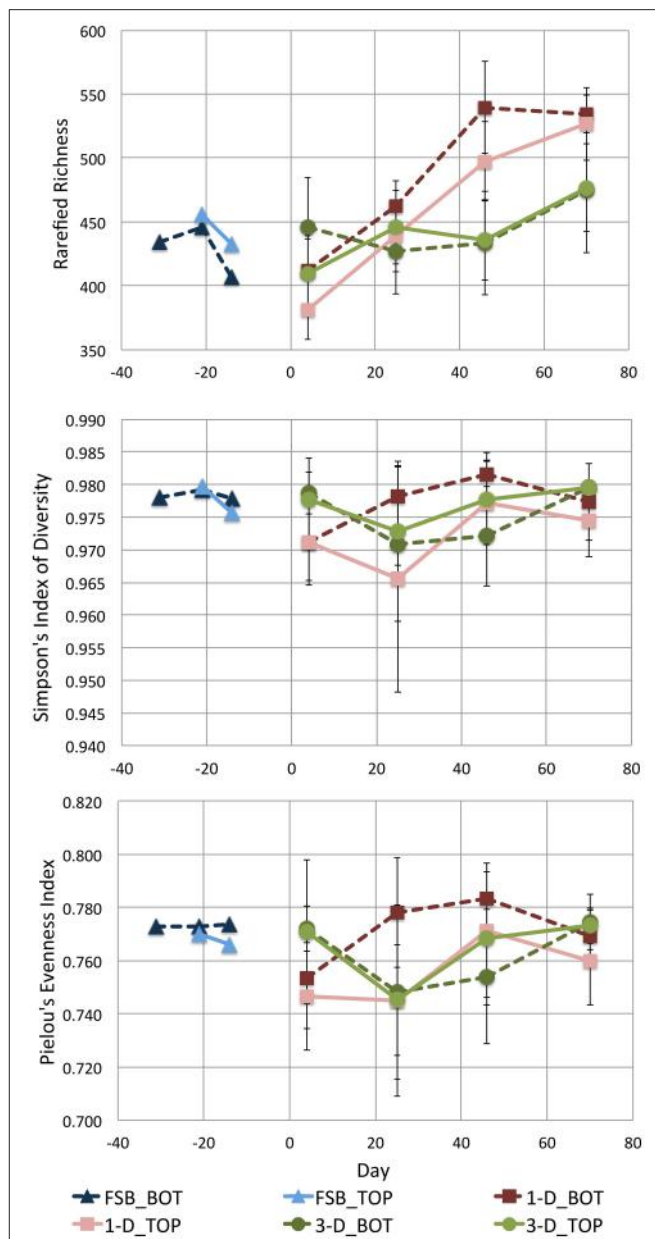


FIGURE 10 | Scatter plots showing time-series for mean rarefied richness, diversity, and evenness in each of the full-scale (FSB) and laboratory-scale (1-D and 3-D) sample sets; error bars show standard deviation. In each case, indices are calculated using samples grouped to represent the microbial community at the top (.TOP) and bottom (.BOT) of the sludge bed in each reactor type.

either the 3-D bioreactors or the full-scale bioreactor FSB. Whilst direct comparison between scales was difficult, good replication of the feeding regime and influent applied between the 1-D and 3-D bioreactor types enables more direct conclusions regarding the influence of bioreactor geometry on the underlying community to be inferred at laboratory-scale. The 1-D bioreactors, in which stratification of both microbial community composition and physiology was observed, supported a more rich community in real terms than the 3-D bioreactors in which no such stratification

was observed. Thus, we propose that 1-D type laboratory-scale bioreactors can support increased richness at laboratory scale by enabling a gradient of niches and microbial communities within a single reactor vessel.

GENERAL DISCUSSION

Disparities of Scale

SMA assays indicated hydrogenotrophic methanogenesis was dominant at full-scale, which was supported by NGS data showing *Methanobacterium* was relatively the most abundant order present in the full-scale bioreactor. By contrast, hydrogenotrophic activity was diminished at laboratory-scale. We suggest that the contrast was not attributable directly to bioreactor scale but likely to the semi-continuous operation and increased solids loading applied at full-scale promoting the development of a predominantly hydrogenotrophic methanogenic system. Indeed, hydrogenotrophic methanogenesis is reported elsewhere in anaerobic digester systems treating high- and very-high solids wastes (Song et al., 2010; Garcia-Peña et al., 2011; Cardinali-Rezende et al., 2012). Thus, we propose that the dominance of acetoclastic methanogenesis, as is widely reported in laboratory-scale EGSB studies, may in fact be an artifact of artificially regular feeding regimes and readily biodegradable wastes applied in laboratory trials. If laboratory-scale studies are to reflect full-scale results, laboratory operation should better reflect the variable modes of waste production, composition, and bioreactor operation likely at full-scale.

Whilst mean pCOD removal was lower at full-scale—49.8% efficiency compared with 77.9 and 69.3% in the 1-D and 3-D bioreactors, respectively—the data indicate a decreasing trend in pCOD removal efficiency at laboratory-scale. This suggests that solids gradually accumulate in “young” digesters, only to be released as the bioreactor matures. Additionally, whilst pCOD removal was lower in the full-scale digester, solids removal was more stable than in the laboratory-scale digesters as evidenced by a smaller standard deviation of pCOD removal efficiency. This suggests a better-adapted community for stable solids treatment may develop with higher solids loading, as was applied at full-scale. That *Bacteroidetes*, a bacterial phylum associated with degradation of complex organics was significantly more abundant in the full-scale digester than at laboratory-scale, appears to support this. The response of microbial communities to high-solids loading requires further study to ascertain upper limits of solids loading in EGSB type bioreactors and to better understand community adaptation.

Influence of Laboratory Idealization

The design of bioreactors adopted in laboratory-scale EGSB trials is highly varied. A key aim of this study was to ascertain the influence of two distinct laboratory-scale idealizations on both bioreactor performance and the microbial community. We demonstrated that the 1-D bioreactors significantly out-performed the 3-D bioreactors with higher COD and sCOD removal efficiencies, less VFA accumulation and higher concentration of methane in the biogas produced. Further, we demonstrated that laboratory-scale idealization significantly influences both microbial community function

and distribution inside bioreactors. SMA assays established that zoned community physiology developed in the 1-D bioreactors whereby biomass at the bottom of the sludge-bed was significantly more active against both acetate and ethanol than biomass from the top of the bed. Zoned physiology in the 1-D bioreactor types was underpinned zoned microbial community composition. We found distinct clustering of OTUs with depth in the 1-D digesters and 11.8% of variance in the 1-D digester community was attributed to sampling depth. Further, the relative abundance of dominant phyla *Firmicutes* and *Synergistetes* varied significantly with depth in the 1-D digester. Of those, *Firmicutes* appeared most abundant at the bottom of the 1-D type bioreactors where growth could be linked to the acetotrophic metabolism observed there. Nothing similar was found in the 3-D bioreactors. Whilst the observation that activity in 1-D type EGSB bioreactors may be zoned has been reported previously (Arcand et al., 1994), this study is novel in demonstrating that this is underpinned by stratified microbial community composition and that bioreactor geometry appears to act as a driver for stratification. Further, the study is novel in identifying that stratification in the underlying microbial community in 1-D type bioreactors appears to support increased species richness that may be associated with improved treatment observed in this bioreactor type. Whilst the precise mechanism promoting stratification in 1-D bioreactors was not elucidated here, tentatively we propose that the stratification may be driven by a confining effect of the 1-D reactor geometry on the granular sludge bed, enabling establishment of niche environments in the bioreactor.

CONCLUSIONS AND RECOMMENDATIONS

Laboratory-scale trials typically strive to attain “steady-state” operation, but full-scale bioreactor operation may be highly variable with respect to substrate composition, strength and loading rate, and feeding and heating regimes and schedules. Here it is proposed that variable operation was the key driver accounting for differing performance and ecology between scales. Hydrogenotrophic methanogenesis dominated the full-scale bioreactor, whereas balanced acetotrophic and hydrogenotrophic methanogenesis developed in more stably operated laboratory-scale bioreactors. As such it is recommended that the variable modes of waste generation, and of bioreactor operation, should be incorporated into controlled laboratory-scale trials where subsequent scale-up is intended. Demonstrating that the apparent dominance of the acetoclastic pathway in anaerobic digestion may, in fact, be an artifact of experimental design at laboratory-scale, could lead to great opportunities for improving full-scale digester design and operation.

Laboratory-scale idealization strongly influenced each of bioreactor performance, and microbial community structure, and spatial distribution. Thus, the influence of laboratory-scale bioreactor design on the success of scale-up must be better understood. The findings underscore the importance of sufficient biomass sampling to develop time series studies and to determine

spatial distribution in communities that might be wrongly assumed to be homogeneous.

AUTHOR CONTRIBUTIONS

SC, SS, GC, and WS designed the study. SC, SS, and RD operated and monitored the laboratory-scale bioreactors. SC and SS prepared the sequencing libraries. CQ designed the primer adaptation. SC, CQ, and UI wrote the scripts for data analysis. Data analysis was conducted by SC. The results were interpreted by SC, SS, GC, and WS. SC drafted the paper and SS, GC, WS, UI, RD, and CQ revised the document. All authors approve the paper and agree for accountability of the work therein.

ACKNOWLEDGMENTS

The authors thank Carole Jude and North British Distillery for providing support throughout the sampling of the full-scale

bioreactor, and for making available performance data from full-scale. The study was funded by the Engineering and Physical Sciences Research Council, UK (EP/J00538X/1; EP/K038885/1). GC was supported by a European Research Council Starting Grant (3C-BIOTECH 261330). UI was funded by NERC IRF NE/L011956/1. CQ was funded by an MRC fellowship MR/M50161X/1 as part of the CLoud Infrastructure for Microbial Genomics (CLIMB) consortium MR/L015080/1.

SUPPLEMENTARY MATERIAL

The Supplementary Material for this article can be found online at: <http://journal.frontiersin.org/article/10.3389/fmicb.2017.00664/full#supplementary-material>

Figure S1 | Rarefaction curves [rarefy(), R Vegan] for all samples in the sample set grouped by bioreactor type: 1-D laboratory-scale (red), 3-D laboratory-scale (green), and full-scale FSB (blue). Curves show saturation is not reached for any sample sequenced.

REFERENCES

- APHA (2005). *Standard Methods for the Examination of Water and Wastewater, 21st Edn.* Washington, DC: American Public Health Association.
- Arcand, Y., Guiot, S. R., Desrochers, M., and Chavarie, C. (1994). Impact of the reactor hydrodynamics and organic loading on the size and activity of anaerobic granules. *Chem. Eng. J. Biochem. Eng. J.* 56, B23–B35. doi: 10.1016/0923-0467(94)87028-4
- Brown, R. L., Jacobs, L. A., and Peet, R. K. (2001). *Species Richness: Small Scale*. New Jersey, NJ: eLS, John Wiley & Sons, Ltd.
- Caporaso, J. G., Lauber, C. L., Walters, W. A., Berg-Lyons, D., Huntley, J., Fierer, N., et al. (2012). Ultra-high-throughput microbial community analysis on the Illumina HiSeq and MiSeq platforms. *ISME J.* 6, 1621–1624. doi: 10.1038/ismej.2012.8
- Cardinali-Rezende, J., Colturato, L. F., Colturato, T. D., Chartone-Souza, E., Nascimento, A. M., and Sanz, J. L. (2012). Prokaryotic diversity and dynamics in a full-scale municipal solid waste anaerobic reactor from start-up to steady-state conditions. *Bioresour. Technol.* 119, 373–383. doi: 10.1016/j.biortech.2012.05.136
- Chan, Y. J., Chong, M. F., Law, C. L., and Hassell, D. (2009). A review on anaerobic-aerobic treatment of industrial and municipal wastewater. *Chem. Eng. J.* 155, 1–18. doi: 10.1016/j.cej.2009.06.041
- Chen, J. (2012). *GUniFrac: Generalized UniFrac Distances*. R package version 1.0. Available online at: <http://CRAN.R-project.org/package=GUniFrac>
- Chen, S., Cheng, H., Wyckoff, K. N., and He, Q. (2016). Linkages of Firmicutes and Bacteroidetes populations to methanogenic process performance. *J. Ind. Microbiol. Biotechnol.* 43, 771–781. doi: 10.1007/s10295-016-1760-8
- Chouari, R., Le Paslier, D., Daegelen, P., Ginestet, P., Weissenbach, J., and Sghir, A. (2005). Novel predominant archaeal and bacterial groups revealed by molecular analysis of an anaerobic sludge digester. *Environ. Microbiol.* 7, 1104–1115. doi: 10.1111/j.1462-2920.2005.00795.x
- Colleran, E., Concannon, F., Golden, T., Geoghegan, F., Crumlish, B., Killilea, E., et al. (1992). Use of methanogenic activity tests to characterize anaerobic sludges, screen for anaerobic biodegradability and determine toxicity thresholds against individual anaerobic trophic groups and species. *Water Sci. Technol.* 25, 31–40.
- Collins, G., Foy, C., McHugh, S., and O'Flaherty, V. (2005). Anaerobic treatment of 2,4,6-trichlorophenol in an expanded granular sludge bed-anaerobic filter (EGSB-AF) bioreactor at 15 °C. *FEMS Microbiol. Ecol.* 53, 167–178. doi: 10.1016/j.femsec.2004.10.008
- Edgar, R. C. (2013). UPARSE: highly accurate OTU sequences from microbial amplicon reads. *Nat. Methods* 10, 996–998. doi: 10.1038/nmeth.2604
- Edgar, R. C., Haas, B. J., Clemente, J. C., Quince, C., and Knight, R. (2011). UCHIME improves sensitivity and speed of chimer detection. *Bioinformatics* 27, 2194–2200. doi: 10.1093/bioinformatics/btr381
- Enright, A.-M., McHugh, S., Collins, G., and O'Flaherty, V. (2005). Low-temperature anaerobic biological treatment of solvent-containing pharmaceutical wastewater. *Water Res.* 39, 4587–4596. doi: 10.1016/j.watres.2005.08.037
- Fang, C., Sompong, O., Boe, K., and Angelidaki, I. (2011). Comparison of UASB and EGSB reactors performance, for treatment of raw and deoiled palm oil mill effluent (POME). *J. Hazard. Mater.* 189, 229–234. doi: 10.1016/j.jhazmat.2011.02.025
- Garcia-Peña, E. I., Parameswaran, P., Kang, D. W., Canul-Chan, M., and Krajmnik-Brown, R. (2011). Anaerobic digestion and co-digestion processes of vegetable and fruit residues: process and microbial ecology. *Bioresour. Technol.* 102, 9447–9455. doi: 10.1016/j.biortech.2011.07.068
- He, Z., Zhang, H., Gao, S., Lercher, M. J., Chen, W.-H., and Hu, S. (2016). Evolvview v2: an online visualization and management tool for customized and annotated phylogenetic trees. *Nucleic Acids Res.* 44, W236–W241. doi: 10.1093/nar/gkw370
- Hernon, F., Forbes, C., and Colleran, E. (2006). Identification of mesophilic and thermophilic fermentative species in anaerobic granular sludge. *Water Sci. Technol.* 54:19. doi: 10.2166/wst.2006.481
- Hulshoff Pol, L. W., de Castro Lopes, S. I., Lettinga, G., and Lens, P. N. (2004). Anaerobic sludge granulation. *Water Res.* 38, 1376–1389. doi: 10.1016/j.watres.2003.12.002
- Joshi, N. A., and Fass, J. N. (2011). Sickle: A Sliding-Window, Adaptive, Quality-Based Trimming Tool for FastQ Files (Version 1.33). Available online at: <https://github.com/najoshi/sickle>
- Karnchanawong, S., and Wachara, P. (2009). Effects of upflow liquid velocity on performance of Expanded Granular Sludge Bed (EGSB) system. *Int. J. Civil Environ. Eng.* 1, 141–144. Available online at: <http://waset.org/publications/1138>
- Kato, M. T., Field, J. A., Versteeg, P., and Lettinga, G. (1994). Feasibility of expanded granular sludge bed reactors for the anaerobic treatment of low-strength soluble wastewaters. *Biotechnol. Bioeng.* 44, 469–479. doi: 10.1002/bit.260440410
- Katoh, K., and Standley, D. M. (2013). MAFFT multiple sequence alignment software version 7: improvements in performance and usability. *Mol. Biol. Evol.* 30, 772–780. doi: 10.1093/molbev/mst010
- Klocke, M., Mähnert, P., Mundt, K., Souidi, K., and Linke, B. (2007). Microbial community analysis of a biogas-producing completely stirred tank reactor fed

- continuously with fodder beet silage as mono-substrate. *Syst. Appl. Microbiol.* 30, 139–151. doi: 10.1016/j.syapm.2006.03.007
- Lee, C., Kim, J., Shin, S. G., and Hwang, S. (2008). Monitoring bacterial and archaeal community shifts in a mesophilic anaerobic batch reactor treating a high-strength organic wastewater. *FEMS Microbiol. Ecol.* 65, 544–554. doi: 10.1111/j.1574-6941.2008.00530.x
- Londoño, Y. A., and Peñuela, G. A. (2015). Anaerobic biological treatment of methylparaben in an expanded granular sludge bed (EGSB). *Water Sci. Technol.* 71, 1604–1610. doi: 10.2166/wst.2015.118
- Madigan, M. T., Martinko, J. M., Dunlap, P. V., and Clark, D. C. (2009). *Brock Biology of Microorganisms*. San Francisco, CA: Pearson Benjamin Cummings.
- Masella, A. P., Bartram, A. K., Truszkowski, J. M., Brown, D. G., and Neufeld, J. D. (2012). PANDAseq: paired-end assembler for illumina sequences. *BMC Bioinformatics* 13:31. doi: 10.1186/1471-2105-13-31
- McKeown, R. M., Scully, C., Enright, A.-M., Chinalia, F. A., Lee, C., Mahony, T., et al. (2009). Psychrophilic methanogenic community development during long-term cultivation of anaerobic granular biofilms. *ISME J.* 3, 1231–1242. doi: 10.1038/ismej.2009.67
- McMurdie, P. J., and Holmes, S. (2013). phyloseq: an R package for reproducible interactive analysis and graphics of microbiome census data. *PLoS ONE* 8:e61217. doi: 10.1371/journal.pone.0061217
- Meyer, T., and Edwards, E. A. (2014). Anaerobic digestion of pulp and paper mill wastewater and sludge. *Water Res.* 65, 321–349. doi: 10.1016/j.watres.2014.07.022
- Militon, C., Hamdi, O., Michotey, V., Fardeau, M.-L., Ollivier, B., Bouallagui, H., et al. (2015). Ecological significance of *Synergistetes* in the biological treatment of tuna cooking wastewater by an anaerobic sequencing batch reactor. *Environ. Sci. Pollut. Res.* 22, 18230–18238. doi: 10.1007/s11356-015-4973-x
- O'Flaherty, V., Collins, G., and Mahony, T. (2006). The microbiology and biochemistry of anaerobic bioreactors with relevance to domestic sewage treatment. *Rev. Environ. Sci. Bio/Technol.* 5, 39–55. doi: 10.1007/s11157-005-5478-8
- Oksanen, J., Blanchet, F. G., Kindt, R., Legendre, P., Minchin, P. R., O'Hara, R. B., et al. (2014). *Vegan: Community Ecology Package. R Package Version 2.1-41/r2867*. Available online at: <https://CRAN.R-project.org/package=vegan>
- O'Reilly, J., Lee, C., Chinalia, F., Collins, G., Mahony, T., and O'Flaherty, V. (2010). Microbial community dynamics associated with biomass granulation in low-temperature (15 degrees C) anaerobic wastewater treatment bioreactors. *Bioresour. Technol.* 101, 6336–6344. doi: 10.1016/j.biortech.2010.03.049
- Pereira, M. A., Roest, K., Stams, A. J., Mota, M., Alves, M., and Akkermans, A. D. (2002). Molecular monitoring of microbial diversity in expanded granular sludge bed (EGSB) reactors treating oleic acid. *FEMS Microbiol. Ecol.* 41, 95–103. doi: 10.1111/j.1574-6941.2002.tb00970.x
- Price, M. N., Dehal, P. S., and Arkin, A. P. (2010). FastTree 2—approximately maximum-likelihood trees for large alignments. *PLoS ONE* 5:e9490. doi: 10.1371/journal.pone.0009490
- Rivièvre, D., Desvignes, V., Pelletier, E., Chaussonnerie, S., Guermazi, S., Weissenbach, J., et al. (2009). Towards the definition of a core of microorganisms involved in anaerobic digestion of sludge. *ISME J.* 3, 700–714. doi: 10.1038/ismej.2009.2
- Satoh, H., Miura, Y., Tsushima, I., and Okabe, S. (2007). Layered structure of bacterial and archaeal communities and their *in situ* activities in anaerobic granules. *Appl. Environ. Microbiol.* 73, 7300–7307. doi: 10.1128/AEM.01426-07
- Scully, C., Collins, G., and O'Flaherty, V. (2006). Anaerobic biological treatment of phenol at 9.5–15 degrees C in an expanded granular sludge bed (EGSB)-based bioreactor. *Water Res.* 40, 3737–3744. doi: 10.1016/j.watres.2006.08.023
- Shida, G. M., Sader, L. T., Cavalcante de Amorim, E. L., Sakamoto, I. K., Maintinguier, S. I., Saavedra, N. K., et al. (2012). Performance and composition of bacterial communities in anaerobic fluidized bed reactors for hydrogen production: effects of organic loading rate and alkalinity. *Int. J. Hydrogen Energy* 37, 16925–16934. doi: 10.1016/j.ijhydene.2012.08.140
- Song, M., Shin, S. G., and Hwang, S. (2010). Methanogenic population dynamics assessed by real-time quantitative PCR in sludge granule in upflow anaerobic sludge blanket treating swine wastewater. *Bioresour. Technol.* 101(Suppl. 1), S23–S28. doi: 10.1016/j.biortech.2009.03.054
- Switzenbaum, M. S. (1995). Obstacles in the implementation of anaerobic treatment technology. *Bioresour. Technol.* 53, 255–262. doi: 10.1016/0960-8524(95)00093-T
- Syutsubo, K., Yoochatchaval, W., Yoshida, H., Nishiyama, K., Okawara, M., Sumino, H., et al. (2008). Changes of microbial characteristics of retained sludge during low-temperature operation of an EGSB reactor for low-strength wastewater treatment. *Water Sci. Technol.* 57, 277–282. doi: 10.2166/wst.2008.077
- Tchobanoglou, G., Burton, F. L., and Stensel, D. H. (2004). *Wastewater Engineering Treatment and Reuse*. New York, NY: McGraw-Hill.
- Thomas, F., Hehemann, J.-H., Rebuffet, E., Czjzek, M., and Michel, G. (2011). Environmental and gut bacteroides: the food connection. *Front. Microbiol.* 2:93. doi: 10.3389/fmicb.2011.00093
- Wang, Q., Garrity, G. M., Tiedje, J. M., and Cole, J. R. (2007). Naive Bayesian classifier for rapid assignment of rRNA sequences into the new bacterial taxonomy. *Appl. Environ. Microbiol.* 73, 5261–5267. doi: 10.1128/AEM.00062-07
- Westerholm, M., Dolfig, J., Sherry, A., Gray, N. D., Head, I. M., and Schnürer, A. (2011). Quantification of syntrophic acetate-oxidizing microbial communities in biogas processes. *Environ. Microbiol. Rep.* 3, 500–505. doi: 10.1111/j.1758-2229.2011.00249.x

Conflict of Interest Statement: The authors declare that the research was conducted in the absence of any commercial or financial relationships that could be construed as a potential conflict of interest.

Copyright © 2017 Connelly, Shin, Dillon, Ijaz, Quince, Sloan and Collins. This is an open-access article distributed under the terms of the Creative Commons Attribution License (CC BY). The use, distribution or reproduction in other forums is permitted, provided the original author(s) or licensor are credited and that the original publication in this journal is cited, in accordance with accepted academic practice. No use, distribution or reproduction is permitted which does not comply with these terms.



Trace Elements Induce Predominance among Methanogenic Activity in Anaerobic Digestion

Babett Wintsche¹, Karin Glaser², Heike Sträuber¹, Florian Centler¹, Jan Liebetrau³, Hauke Harms^{1,4} and Sabine Kleinsteuber^{1*}

¹ Department of Environmental Microbiology, Helmholtz Centre for Environmental Research – UFZ, Leipzig, Germany,

² Department of Applied Ecology and Phycology, University of Rostock, Rostock, Germany, ³ Department of Biochemical Conversion, Deutsches Biomasseforschungszentrum – DBFZ, Leipzig, Germany, ⁴ German Centre for Integrative Biodiversity Research (iDiv), Leipzig, Germany

OPEN ACCESS

Edited by:

Regina-Michaela Wittich,
Spanish High Council for Scientific
Research, Spain

Reviewed by:

Maulin P. Shah,
Enviro Technology Limited, India
David Campbell Stuckey,
Imperial College London, UK

*Correspondence:

Sabine Kleinsteuber
sabine.kleinsteuber@ufz.de

Specialty section:

This article was submitted to
Microbiotechnology, Ecotoxicology
and Bioremediation,
a section of the journal
Frontiers in Microbiology

Received: 18 December 2015

Accepted: 02 December 2016

Published: 16 December 2016

Citation:

Wintsche B, Glaser K, Sträuber H, Centler F, Liebetrau J, Harms H and Kleinsteuber S (2016) Trace Elements Induce Predominance among Methanogenic Activity in Anaerobic Digestion. *Front. Microbiol.* 7:2034.
doi: 10.3389/fmicb.2016.02034

Trace elements (TE) play an essential role in all organisms due to their functions in enzyme complexes. In anaerobic digesters, control, and supplementation of TE lead to stable and more efficient methane production processes while TE deficits cause process imbalances. However, the underlying metabolic mechanisms and the adaptation of the affected microbial communities to such deficits are not yet fully understood. Here, we investigated the microbial community dynamics and resulting process changes induced by TE deprivation. Two identical lab-scale continuous stirred tank reactors fed with distiller's grains and supplemented with TE (cobalt, molybdenum, nickel, tungsten) and a commercial iron additive were operated in parallel. After 72 weeks of identical operation, the feeding regime of one reactor was changed by omitting TE supplements and reducing the amount of iron additive. Both reactors were operated for further 21 weeks. Various process parameters (biogas production and composition, total solids and volatile solids, TE concentration, volatile fatty acids, total ammonium nitrogen, total organic acids/alkalinity ratio, and pH) and the composition and activity of the microbial communities were monitored over the total experimental time. While the methane yield remained stable, the concentrations of hydrogen sulfide, total ammonia nitrogen, and acetate increased in the TE-depleted reactor compared to the well-supplied control reactor. *Methanosarcina* and *Methanoculleus* dominated the methanogenic communities in both reactors. However, the activity ratio of these two genera was shown to depend on TE supplementation explainable by different TE requirements of their energy conservation systems. *Methanosarcina* dominated the well-supplied anaerobic digester, pointing to acetoclastic methanogenesis as the dominant methanogenic pathway. Under TE deprivation, *Methanoculleus* and thus hydrogenotrophic methanogenesis was favored although *Methanosarcina* was not overgrown by *Methanoculleus*. Multivariate statistics revealed that the decline of nickel, cobalt, molybdenum, tungsten, and manganese most strongly influenced the balance of *mcrA* transcripts from both genera. Hydrogenotrophic methanogens seem to be

favored under nickel- and cobalt-deficient conditions as their metabolism requires less nickel-dependent enzymes and corrinoid cofactors than the acetoclastic and methylotrophic pathways. Thus, TE supply is critical to sustain the activity of the versatile high-performance methanogen *Methanosarcina*.

Keywords: biogas reactor, methanogenesis, *mcrA*, *Methanosarcina*, *Methanoculleus*, amplicon sequencing, T-RFLP

INTRODUCTION

Anaerobic digestion (AD) of organic waste and residues is an important component of renewable energy systems, advanced biorefineries, and sustainable waste management strategies. The biogas produced can be used to generate electricity and heat or can be upgraded to biomethane which is used as vehicle fuel or injected into the gas grid.

Anaerobic digestion is a complex multi-stage process relying on the activity of highly diverse microbial communities. Next to the macronutrients carbon, nitrogen, phosphorus and sulfur, trace elements (TE) are crucial for an effective biogas process due to the microbial demand for TE in the anaerobic environment (Demirel and Scherer, 2011). These demands are as diverse as the involved microorganisms and their functions. Many industrial biogas reactors in Germany are operated with energy crops such as maize silage as substrate. For maize silage it is known that its content of macro- and microelements is insufficient for the demands of anaerobic microorganisms. For instance, Lebuhn et al. (2008) showed that long-term mono-digestion of maize silage led to acidification and process failure even at low organic loading rates but the process recovered after TE supplementation. The authors concluded that cobalt was the most limiting element. In another study, both cobalt and nickel limitations caused process instability and decreased biogas production during AD of a model substrate for maize silage (Pobeheim et al., 2011). Stability of AD processes and efficient methane production are also impaired by deficiencies of other TE, for example molybdenum, tungsten or selenium (Plugge et al., 2009; Worm et al., 2009; Banks et al., 2012; Munk and Lebuhn, 2014).

To avoid a possible undersupply of TE, commercial TE supplements are added to biogas reactors based on the operator's experience (Lemmer et al., 2010; Schmidt, 2011; Lindorfer et al., 2012; Schmidt et al., 2013; Evranos and Demirel, 2015). Correct dosing of TE supplements is very important, since undersupply can cause process instability or low methane yield, whereas overdosage may have toxic effects on the microorganisms and impairs the compliance of the digestate with the requirements for fertilizer (Thanh et al., 2016). To achieve an optimal TE supplementation and raise the efficiency of the AD process, detailed knowledge about essential and beneficial TE and their role in AD would be instrumental.

TE play integral roles in enzymatic complexes, for example as central ions conferring catalytic functions. Microorganisms involved in AD have specific TE requirements. Molybdenum, tungsten and selenium are essential TE for syntrophic bacteria (Vorholt and Thauer, 2002; Plugge et al., 2009; Worm et al.,

2009) involved in the acetogenesis, i.e., converting volatile fatty acids (VFA) and alcohols to precursors of methanogenesis. The methane producing steps of AD also depend on several TE. For instance, the acetyl-CoA decarbonylase/synthase complex, the cofactor F430 and different hydrogenases – all key enzymes of methanogenic archaea – incorporate nickel (Deppenmeier et al., 1999; Thauer et al., 2008). Further essential TE in methanogenesis include cobalt and molybdenum or tungsten, which are the central ions of S-methyl-tetrahydrosarcinapterine and 5-methyl-tetrahydromethanopterine or the formylmethanofuran dehydrogenase, respectively (Vorholt and Thauer, 2002).

The methane-producing step in the AD process is exclusively performed by methanogenic archaea. Methanogenic communities are characterized by a lower diversity and lower functional redundancy than the highly diverse bacterial communities. Consequently, process conditions, which are adverse for methanogens can compromise process stability (Demirel, 2014). Methanogens are metabolically versatile and produce biogas by acetoclastic, methylotrophic or hydrogenotrophic methanogenesis (Costa and Leigh, 2014). During acetoclastic methanogenesis, methane is directly produced from acetate. All acetoclastic methanogens belong to the order *Methanosarcinales*. Particularly species of the genus *Methanosarcina* are considered as robust and effective methane producers occurring in high performance AD processes (Conklin et al., 2006; De Vrieze et al., 2012). They show high growth rates on diverse substrates (acetate, methanol, methylamines, or CO₂ and H₂) and are tolerant to fluctuating pH values and high ammonia concentrations (Liu and Whitman, 2008; Schnürer and Nordberg, 2008). *Methanosarcina* sp. are further capable of conducting hydrogenotrophic methanogenesis meaning that they can act as syntrophic partners of VFA degraders (Hao et al., 2011; Shimada et al., 2011; Karlsson et al., 2012). Thus, members of the genus *Methanosarcina* are usually regarded as 'robust workhorses' of AD (Willy Verstraete in his plenary lecture at the 13th World Congress on Anaerobic Digestion, Santiago de Compostela, June 25, 2013).

In the course of hydrogenotrophic methanogenesis, methane is formed from CO₂ and H₂ or formate. These substrates are products of the bacterial degradation processes acidogenesis and acetogenesis (Demirel and Scherer, 2008). Concentrations of formate and H₂ in the system determine the activity of syntrophic bacteria degrading VFA, alcohols, etc., because these processes become thermodynamically feasible only when methanogenesis maintains low concentrations of formate and H₂ (McInerney et al., 2009; Sieber et al., 2014). Hence, the presence of hydrogenotrophic methanogens is essential to keep the AD process running. However, the abundance and activity

of hydrogenotrophic methanogens as well as their share of the total methane production depend on the process conditions (Karakashev et al., 2005).

The impact of different TE on the AD process and reactor performance has been addressed by numerous studies. Furthermore, biochemical backgrounds of the requirements of several TE have been studied closely in pure cultures. However, little is known about how TE deficiencies in AD influence the microbial community and which metabolic pathways are impacted in a way that community changes and process instabilities occur.

The aim of the present study was to investigate the effect of a slowly increasing TE deficit on reactor performance and the microbial communities in a semi-continuous AD process. After parallel operation of two lab-scale reactors, which were well supplied with TE, the TE supply of one reactor was stopped. Besides various process parameters, the dynamics of bacterial and methanogenic communities were monitored by T-RFLP (terminal restriction fragment length polymorphism) fingerprinting and sequencing of phylogenetic marker genes and their transcripts. The community dynamics were correlated to process parameters and TE concentrations to unravel the role of TE in AD along with their impact on bacterial and methanogenic communities.

MATERIALS AND METHODS

Lab-Scale Biogas Reactors and Operation Conditions

Two identical lab-scale continuous stirred tank reactors designated R1 and R2 (total volume: 15 L; working volume: 10 L) were operated for 93 weeks with continuous stirring at 50 rpm using an anchor agitator propelled by an overhead stirrer RZR 2102 control (Heidolph, Germany). The temperature was kept constant at 37°C (± 1 K) controlled by a water bath. A construction scheme of the lab-scale reactors used was given by Schmidt (2011). The inoculum was obtained from a running lab-scale biogas reactor operated with dried distiller's grains with solubles (DDGS; CropEnergies AG, Germany). A mixture of 53.1 g DDGS, 2.57 g of a commercial iron additive for sulfide precipitation, and 2 mL of a TE stock solution containing cobalt, nickel, molybdenum and tungsten was dissolved in 345 mL water and fed daily as described by Schmidt et al. (2013) who found that efficient AD of DDGS requires supplementation of these TE. The TE mixture was composed of 2.13 g L⁻¹ Ni(II)Cl₂ × 6H₂O (AppliChem, Germany), 0.531 g L⁻¹ Co(II)Cl₂ × 6H₂O (AppliChem, Germany), 0.332 g L⁻¹ NaMoO₄ × 2H₂O (Merck KGaA, Germany), and 4.268 g L⁻¹ (NH₄)₄H₂W₁₂O₄₀ × H₂O (Sigma-Aldrich, USA). All TE salts were analytically pure.

The reactors were operated at an organic loading rate of 5 gVS L⁻¹ d⁻¹ (VS: volatile solids) resulting in a hydraulic retention time of 25 days. Both reactors were operated in parallel for 72 weeks before starting the experimental period, during which R2 was subjected to TE decline by omitting the TE solution and reducing the supply of iron additive from 2.57 to 0.86 g per day.

Analysis of Process Parameters and Analytical Techniques

Gas production, gas composition, and pH value were measured daily. The biogas volume was measured using drum-type gas meters TG 05 (Ritter, Germany) and normalized to dry gas at standard pressure (101.325 kPa) and standard temperature (273.15 K). The biogas composition (CH₄, CO₂, H₂, H₂S, and O₂) was analyzed by an AWIFLEX gas analyzer (AWITE Bioenergie, Germany).

The total organic acids/alkalinity ratio and VFA concentrations were measured twice per week. Total ammonium nitrogen (TAN) concentrations were generally determined twice per week with a few exceptions when only one sample per week was measured. The total organic acids/alkalinity ratio and VFA concentrations were measured in triplicates and TAN concentrations in single measurements as described by Ziganshin et al. (2011). Total solids and volatile solids contents of substrates and digestates were determined weekly in duplicates as described by Sträuber et al. (2012).

TE concentrations were analyzed in duplicates at four sampling times (weeks 65, 77, 80, 84). Total element concentrations of TE and major elements were determined according to Schmidt et al. (2013). Daily concentrations of cobalt, manganese, molybdenum, nickel, and zinc between sampling times were estimated by a mass-conservative reactor model with daily feeding according to

$$c_t = c_{t-1} + \frac{1}{\tau} \times (c_{\text{Inflow}} - c_{t-1})$$

with concentration c_t of the respective TE at day t , concentration at the preceding day c_{t-1} , total TE concentration in the inflow c_{Inflow} (summing over substrate, iron additive, and TE mixture), and retention factor τ given by the volume of the fluid reactor content divided by the daily exchanged fluid volume $V_{\text{Reactor}}/V_{\text{Exchange}}$. Goodness of model fit for one TE was evaluated as the mean deviation of model predictions f_i from n measurements y_i , relative to the measurement mean \bar{y} : $GF_{\text{TE}} = \frac{1}{n} \sum_{i=1}^n |f_i - y_i|/\bar{y}$. A retention factor of 25 as calculated from the applied feeding regimen led to a reasonable fit with experimental data obtained before TE deprivation (mean GF over all TE of 0.09), but not for those obtained after TE deprivation (mean GF of 0.14). This is likely due to the limitation of the analysis method for very low TE concentrations, which were reached at the end of the experiments. Hence, we used the modeled TE concentrations (Supplementary Data Sheet 2) for further statistical analysis.

Extraction of Nucleic Acids and PCR

Samples for the extraction of nucleic acids were taken twice per week (three replicates of 2 mL reactor content) and stored at -80°C until DNA/RNA extraction. For DNA extraction, the PowerSoil DNA Isolation Kit (MoBio Laboratories Inc., USA) was used and DNA was finally eluted in 50 μL elution buffer. For RNA extraction, the ZR Soil/Fecal RNA Microprep Kit (Zymo Research, Germany) was used and the RNA was eluted in 40 μL elution buffer. The quality of the nucleic acids was checked by agarose gel electrophoresis.

DNA was quantified with a NanoDrop® ND-1000 UV-Vis spectrophotometer (ThermoFisher Scientific, Germany) and RNA was quantified after staining with RiboGreen (Invitrogen, USA) using a NanoDrop 3300 fluorimeter (ThermoFisher Scientific, Germany). Total RNA was converted to cDNA using the RevertAid™ H Minus First Strand cDNA Synthesis Kits (Fermentas, Germany) and applying random hexamer primers. Aliquoted DNA and cDNA samples were kept at -20°C until further analysis. For PCR amplification of bacterial 16S rRNA gene fragments, the primers UniBac27F (5'-GAG TTT GAT CMT GGC TCA G-3') and Univ1492R (5'-TAC GGY TAC CTT GTT ACG ACT T-3') were used (according to Lane, 1991). The cycling program included an initial denaturation step of 4 min at 94°C , 30 cycles of 45 s at 94°C , 1 min at 58°C , 2 min at 72°C , and a final elongation step of 20 min at 72°C . For the amplification of *mcrA* gene fragments, the primer set (mlas/mcrA_rev) and the cycling program described by Steinberg and Regan (2008) were applied. PCR was carried out in 12.5- μL reaction mixtures. The reaction mixtures for both genes contained 1.0 μL (5 ng) genomic DNA or cDNA, respectively, 0.5 μL (2.5 pmol) of each primer (Eurofins Genomics, Ebersberg, Germany), 0.5 μl DMSO and 6.25 μL of *Taq* Master Mix (Qiagen, Hilden, Germany).

T-RFLP Analysis of 16S rRNA and *mcrA* Amplicons

The T-RFLP analysis of bacterial and methanogenic communities using FAM-labeled PCR products was done as described previously (Sträuber et al., 2012; Lucas et al., 2015). PCR product quality was checked by agarose gel electrophoresis and amplicons were purified with SureClean (Bioline, Luckenwalde, Germany). Purified PCR products were quantified after electrophoresis in 1.5% agarose gels with ethidium bromide staining using the GeneTools program (Syngene, Cambridge, UK). The purified PCR products were digested with restriction endonucleases purchased from New England Biolabs (Schwalbach, Germany). The *mcrA* amplicons were digested with *MwoI* and the 16S rRNA amplicons with *RsaI*, using 2 units of the respective enzyme for digesting 10 ng of PCR product at 37°C overnight. The subsequent T-RFLP analysis was done for the *mcrA* amplicons with the GeneScan™-500Rox™ (Applied Biosystems, USA) as fragment size standard and for the 16S rRNA amplicons with the MapMarker1000 (BioVentures Inc., USA). Resulting electropherograms were analyzed by using the GeneMapper 5 software (Applied Biosystems) and processed according to Abdo et al. (2006). To differentiate between peaks and background, signals with low peak areas were removed according to eight times the standard deviation.

Sequencing of *mcrA* and 16S rRNA Amplicons

Cloning, sequencing, and identification of the *mcrA* amplicons were conducted as described by Lucas et al. (2015). The obtained partial *mcrA* sequences were deposited in GenBank under accession numbers KU179685–KU179691.

The bacterial communities of both reactors at two sampling times (week 76, 80) were analyzed by amplicon sequencing of

the bacterial 16S rRNA genes using the 454 pyrosequencing platform GS Junior (Roche) as described previously (Ziganshin et al., 2013). Raw sequence data were processed with MOTHUR (Schloss et al., 2009). The workflow was based on 454 SOP¹. After extracting FASTA and quality files out of the SFF file, the trim.seqs command was run by defining barcodes and primers (maxambig = 0, maxhomop = 8, bdiffs = 1, pdiffs = 2, minlength = 150, qwindowaverage = 35, qwindowsize = 50), producing a trimmed FASTA file. After running unique.seqs and aligning the sequences (reference = silva.bacteria.fasta), these sequences were screened (start = 1044, optimize = end) and filtered (vertical = T, trump=.). Chimeras were deleted using the chimera.uchime (dereplicate = T) command based on the UCHIME algorithm (Edgar et al., 2011) and phylogenetic classification of the sequences was done based on the SILVA database (Quast et al., 2013) (cutoff = 50). Operational taxonomic units (OTU) were defined using the dist.seqs command with a cutoff of 0.03. Finally, the OTUs were classified, a list of representative sequences for each OTU was compiled, and rarefaction curves were calculated with the rarefaction.single command. De-multiplexed sequences from each sample were deposited under the EMBL-EBI accession number PRJEB11824².

Statistical Analyses

Multivariate statistical analysis of normalized T-RFLP peak tables was executed using the R package “vegan” (Oksanen et al., 2011). Clustering and non-metric multidimensional scaling (nMDS) analyses were performed based on the Bray–Curtis dissimilarity index (Bray and Curtis, 1957). The function “envfit” was used to identify the abiotic parameters and the terminal restriction fragments (T-RF) which shaped the community most. The significance was assessed by 1000 permutations.

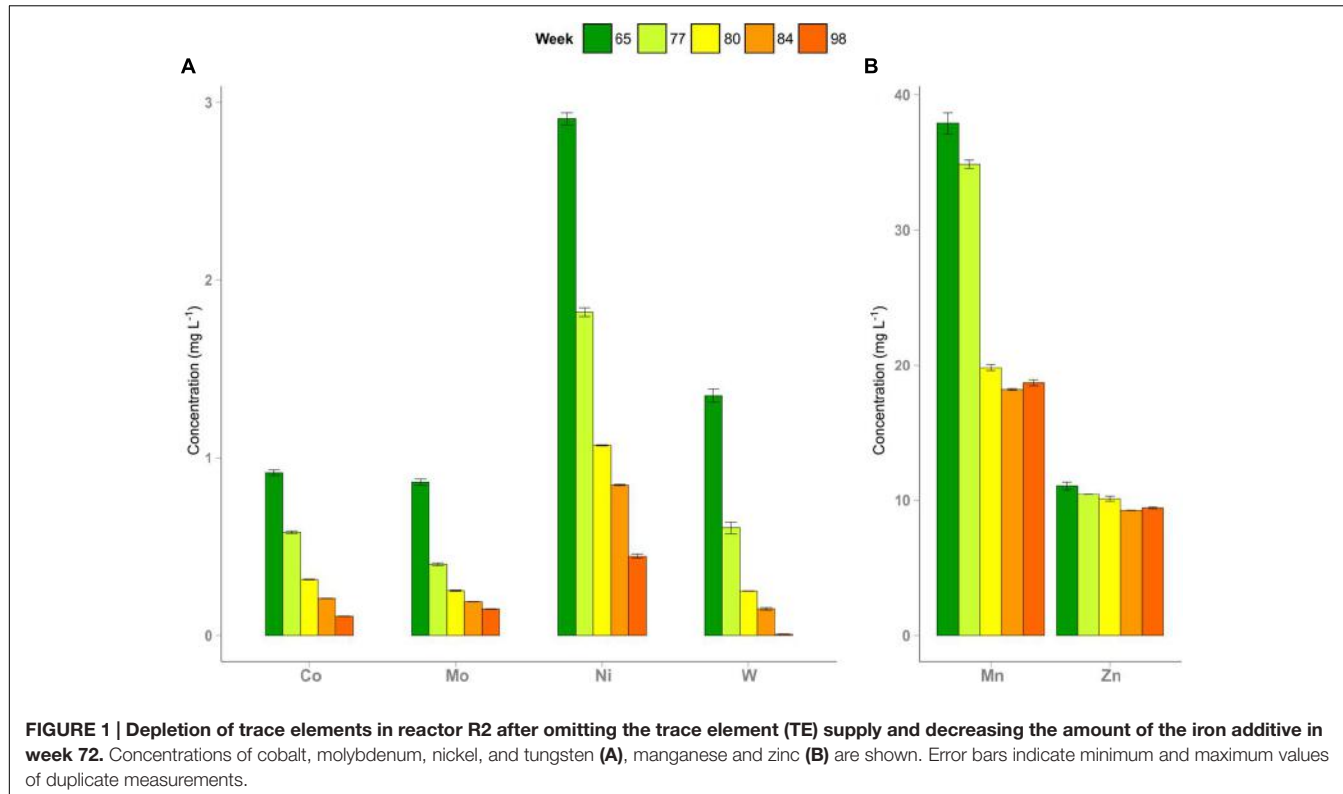
RESULTS

Decline of TE Concentrations and the Effect on Reactor Performance

In week 72, TE deprivation in R2 was started and continued until week 93. After omitting the TE solution and reducing the amount of the iron additive in R2, total concentrations of most TE decreased (**Figure 1**) depending on whether their main sources were the TE solution, the iron additive or the substrate. Average TE concentrations (week 50 till week 93) in R1 were as follows (in mg L⁻¹): cobalt 0.92 (± 0.04), iron 987.00 (± 62.96), manganese 38.75 (± 6.62), molybdenum 0.81 (± 0.04), nickel 3.15 (± 0.14), tungsten 1.23 (± 0.06), and zinc 10.53 (± 0.68). These average concentrations resembled those in R2 during the period with full TE supply. These TE were supplied to the reactors as components of the substrate (mainly zinc), the iron additive (mainly iron and manganese), and the TE solution (mainly cobalt, molybdenum, nickel, and tungsten). Most TE (cobalt, molybdenum, nickel, tungsten) concentrations declined over time. Cobalt, molybdenum, nickel, and tungsten were

¹http://www.mothur.org/wiki/454_SOP

²<http://www.ebi.ac.uk/ena/data/view/PRJEB11824>



present at concentrations of 1–3 mg L⁻¹ before the start, which then dropped below 1 mg L⁻¹ in R2 during the experiment. Manganese (40 mg L⁻¹) was present at a higher concentration at the beginning and declined to 20 mg L⁻¹. Zinc dropped from a concentration of 11 to 9 mg L⁻¹. Concentrations of the latter two elements decreased until week 84 and remained stable thereafter. The TE concentrations in R1 showed no significant changes during the experiment.

The process parameters of both reactors are shown in **Figure 2** and Supplementary Figures S1–S15. Initially, R1 and R2 were operated in parallel with DDGS as substrate and adequately supplied with TE for 72 weeks. Due to the iron amendment, no hydrogen sulfide was detected in the gas produced in both reactors. During the period of identical operation, the average methane yields of R1 with 315 (± 20) mL gvs⁻¹ and R2 with 314 (± 20) mL gvs⁻¹ (standard deviation in parentheses) showed no significant shifts as well as the pH values in both reactors with 7.74 (± 0.04) for R1 and 7.72 (± 0.02) for R2. The biogas of both reactors contained 57% ($\pm 2\%$) methane and 43% ($\pm 2\%$) carbon dioxide, the average organic acids/alkalinity ratio was 0.14 (± 0.01) in both reactors and the TAN concentrations were 3.4 (± 0.2) mg L⁻¹ and 3.3 (± 0.2) mg L⁻¹ in R1 and R2, respectively. Acetate concentrations were very low with 50 (± 14) mg L⁻¹ in R1 and 40 (± 14) mg L⁻¹ in R2. The sum concentrations of propionate and *n*-butyrate were mostly below 10 mg L⁻¹. For R1 without TE deprivation, these process parameters did not change during the entire experimental period.

Four weeks after the TE solution was omitted in R2 and the supply of the iron additive was decreased, a brighter color

of the digestate and a stronger sulfidic odor of the biogas were noticed. The formation of hydrogen sulfide reached a concentration of 1700 ppm in the gas phase of R2 after eight weeks of TE deprivation (week 80; **Figure 2C**). The hydrogen concentration in the gas phase increased from 70 to 110 ppm on average where it remained until the end of the experiment in R1 whereas it increased to more than 400 ppm in R2 after week 87 (Supplementary Figure S7). Although the biogas yield of R2 did not change (Supplementary Figure S2), the methane content of the biogas produced in R2 decreased over time (Supplementary Figure S5). However, the slight decrease of the methane content in R2 did not significantly affect the methane yield (**Figure 2A**). The unchanged pH value (Supplementary Figure S3) indicated that there was no strong process imbalance. In contrast, the total organic acid concentration increased from 1.3 to 1.6 g L⁻¹ (Supplementary Figure S4). This change seemed to originate from the increase of the acetate concentration up to 200 mg L⁻¹ (**Figure 2D**). Concentrations of propionic, butyric, valeric, and caproic acids did not differ significantly between both reactors (Supplementary Figures S8–S13). After TE deprivation, the final TAN concentration in R2 reached 4.5 g L⁻¹ (**Figure 2B**). For the sake of clarity, the experimental time starting from week 72 was divided into a period without visible effects (I – until week 78) and a period with visible effects (II – from week 79 on).

Effect of the TE Deprivation on the Microbial Community Composition

The community composition and dynamics were determined by T-RFLP fingerprinting of *mcrA* and bacterial 16S rRNA

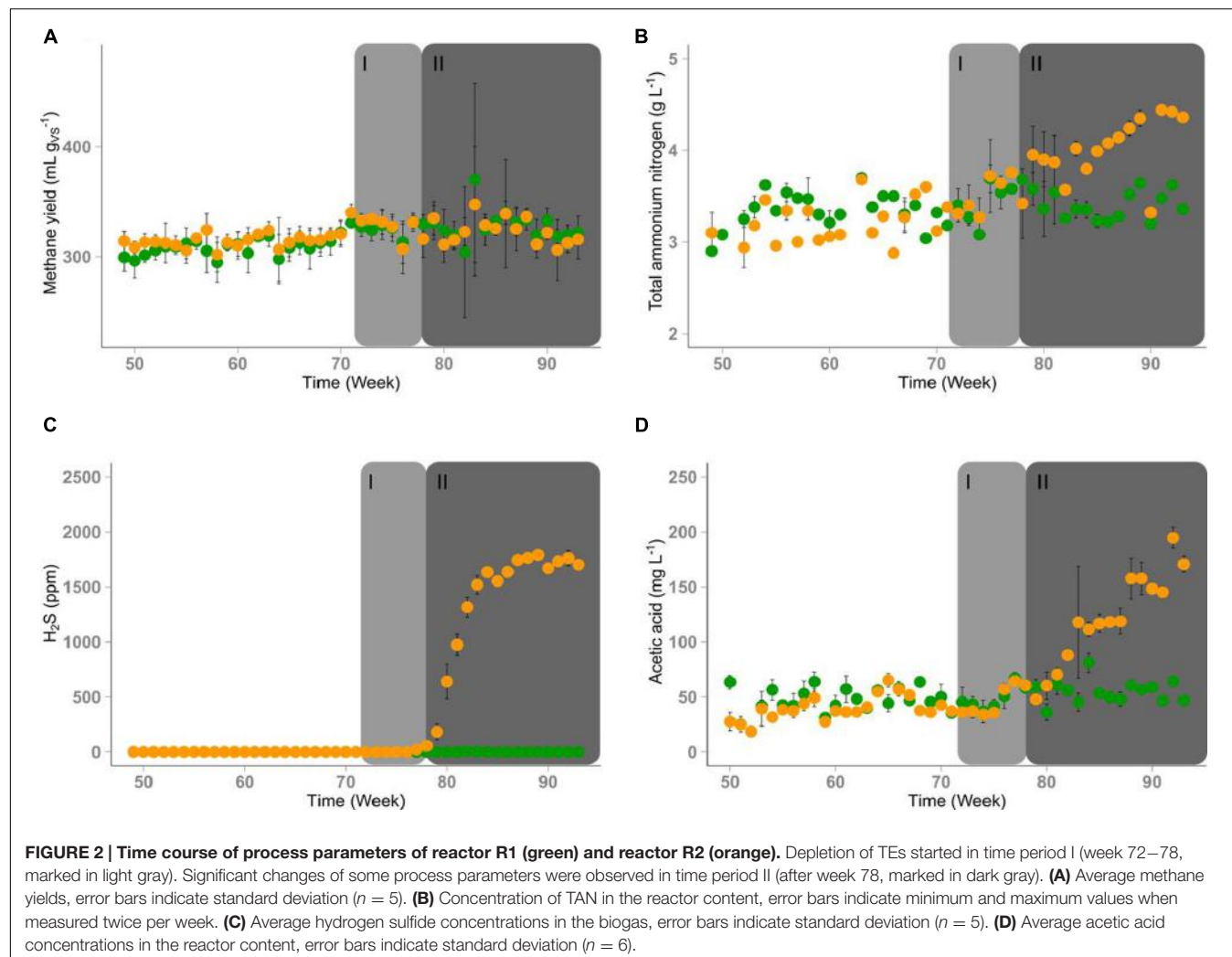


FIGURE 2 | Time course of process parameters of reactor R1 (green) and reactor R2 (orange). Depletion of TEs started in time period I (week 72–78, marked in light gray). Significant changes of some process parameters were observed in time period II (after week 78, marked in dark gray). **(A)** Average methane yields, error bars indicate standard deviation ($n = 5$). **(B)** Concentration of TAN in the reactor content, error bars indicate minimum and maximum values when measured twice per week. **(C)** Average hydrogen sulfide concentrations in the biogas, error bars indicate standard deviation ($n = 5$). **(D)** Average acetic acid concentrations in the reactor content, error bars indicate standard deviation ($n = 6$).

amplicons. The resulting *mcrA* T-RF profiles indicated changes in the methanogenic community composition (DNA-based profiles) and microbial activity (cDNA-based profiles). **Figure 3** shows nMDS plots for *mcrA* on cDNA and DNA level along with process parameters significantly associated with community shifts. The underlying T-RFLP profiles are shown in the Supplementary Figures S18–S23. The active methanogenic community based on *mcrA* transcripts was similar in R1 and R2 during the first six weeks after starting the TE depletion (period I). After week 78, the composition of *mcrA* transcripts in R2 was remarkably different. The effect of TE deprivation was more distinct on the cDNA level compared to the DNA level. The methanogenic communities of R1 and R2 were clearly dominated by two sequence types seen as major T-RF assigned to *Methanosarcina* sp. (T-RF 122) and *Methanoculleus* sp. (T-RF 113). The relative abundances of these T-RF in R1 and R2 were similar until week 72 indicating a high stability of the methanogenic communities in both reactors. In period II, proportions of *mcrA* transcripts of *Methanoculleus* sp. rose up to 70% whereas *mcrA* transcripts of *Methanosarcina* sp. dropped to

17% in R2. The relative abundance of *mcrA* transcripts from *Methanosarcina* sp. was positively correlated with the concentrations of cobalt, manganese, molybdenum, nickel and tungsten, whereas *mcrA* transcription of *Methanoculleus* sp. rose in parallel with rising acetate, TAN and hydrogen sulfide concentrations (**Figure 3A**). Similar dependencies were found for the methanogenic community composition based on DNA data (**Figure 3B**).

The bacterial community composition based on 16S rRNA genes was stable in R1 during the whole experiment and in R2 until week 78 (period I – **Figure 4**). The community profiles showed some dominant T-RF including T-RF 166, 310, 461, 470, and 570 (Supplementary Figures S22 and S23). The bacterial community in R2 changed after week 78. Changes of various bacterial T-RF were found with reduced concentrations of the same TE that influenced the methanogenic community and with rising concentrations of acetate and hydrogen sulfide (**Figure 4**). For instance, the relative abundance of T-RF 310 dropped from 30 to 8% and T-RF 474 disappeared in R2 during TE deprivation. In contrast, the proportion of T-RF 461 was stable in R2 whereas it dropped in R1.

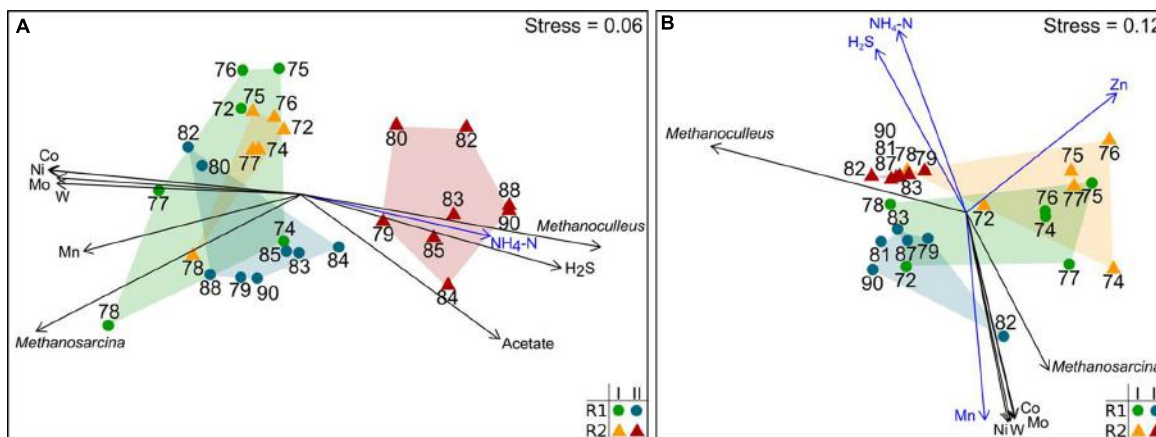


FIGURE 3 | Non-metric multidimensional scaling (nMDS) plots of T-RFLP profiles of *mcrA* transcripts (A) and *mcrA* genes (B). Data from reactor R1 (green dots: period I, week 72–78; blue dots: period II, after week 78) and reactor R2 (orange triangles: period I, week 72–78; red triangles: period II, after week 78) are shown. Data points are labeled by week of sampling. Plots are based on the Bray–Curtis dissimilarity index. Environmental factors and T-RF shaping the community profiles most are shown as vectors (blue: $p < 0.01$; black: $p < 0.001$).

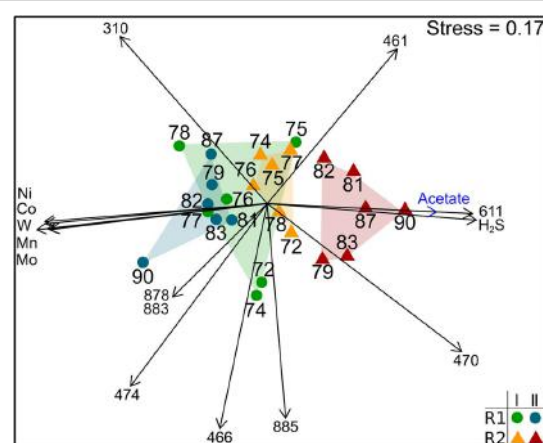


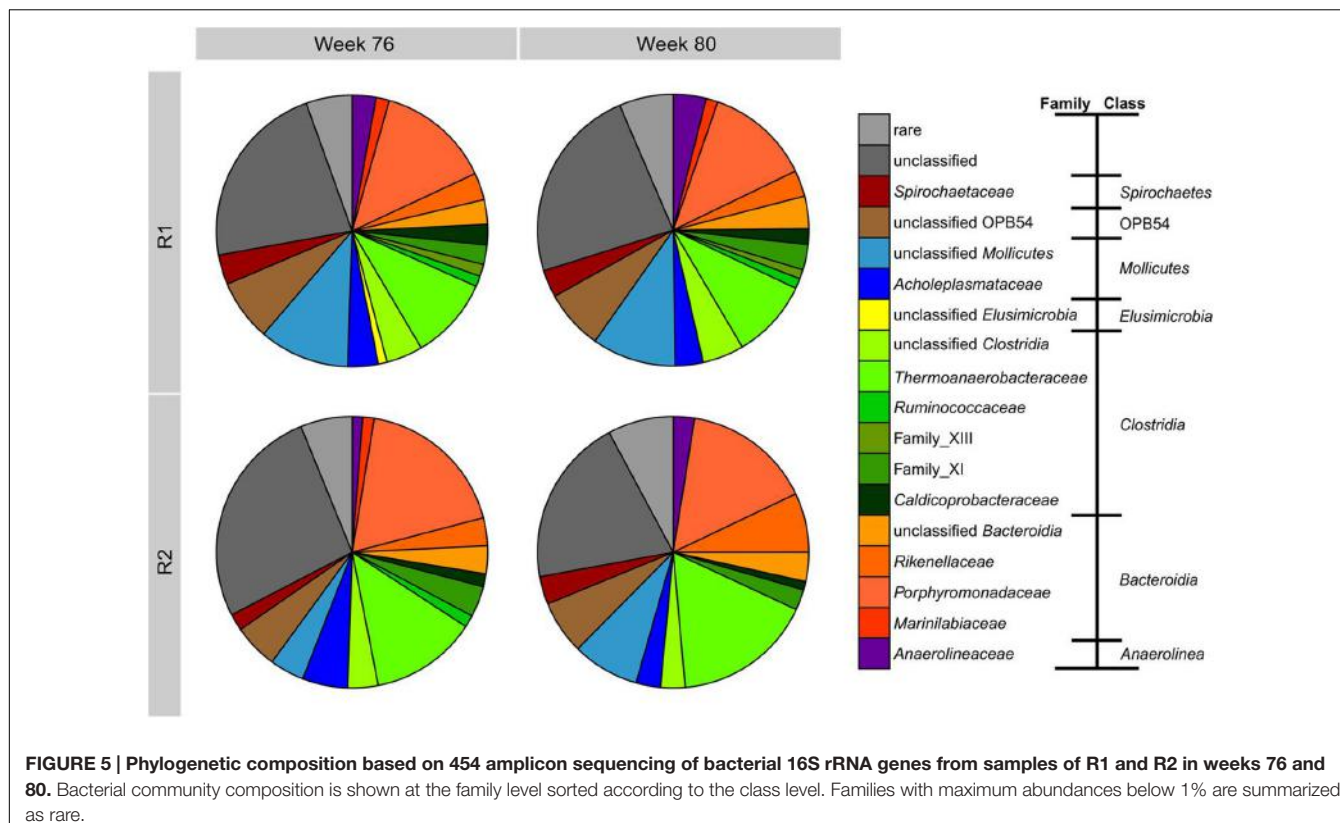
FIGURE 4 | Non-metric multidimensional scaling plot of T-RFLP profiles of bacterial 16S rRNA genes of reactor R1 (green dots: period I, week 72–78; blue dots: period II, after week 78) and reactor R2 (orange triangles: period I week 72–78; red triangles: period II after week 78). Data points are labeled by week of sampling. Plots are based on the Bray–Curtis dissimilarity index. Environmental factors and T-RF shaping the community composition most are shown as vectors (blue: $p < 0.01$; black: $p < 0.001$).

The bacterial community composition was determined by amplicon sequencing resulting in 55165 high quality reads, which were assigned to 1661 OTUs (97% similarity cutoff). Approximately 14000 reads were obtained per sample. All samples had 317 OTUs in common and each sample included on average 150 unique OTUs. These commonalities and differences are illustrated in a Venn diagram (Supplementary Figure S17). The respective rarefaction curves (Supplementary Figure S16) and the OTU list with representative sequences and their phylogenetic affiliations are given in the Supplementary Material (Data Sheet 3). The phylogenetic composition of the bacterial

communities on the family level is shown in Figure 5. The bacterial community composition of both reactors was stable between weeks 76 and 80 sharing the same major bacterial families. Coverage and diversity indices (Inverse Simpson Index, Shannon Index, Shannon Evenness Index) are given in Supplementary Table S1 showing a comparable diversity and evenness between the samples. The predominant class was *Clostridia* with *Thermoanaerobacteraceae* as the main family comprising at least 10% of the total bacterial community. All OTUs assigned to this family belonged to the genus *Gelria*. *Bacteroidia* represented by the families *Porphyromonadaceae* (88% of which were assigned to the genus *Proteiniphilum*) and *Rikenellaceae*, were the second dominant class followed by representatives of the class *Mollicutes*. During TE deprivation, the proportion of *Thermoanaerobacteraceae* in R2 increased up to 16% of the bacterial community. *Rikenellaceae* increased their relative abundance from 3 to 10% between week 76 and 80. The proportions of family_XIII (*Clostridia*), *Marinilabiaceae* (*Bacteroidia*), and *Ruminococcaceae* (*Clostridia*) decreased in R2 relative to R1.

DISCUSSION

Our study has shown that TE deprivation has a remarkable effect on the methanogenic community in anaerobic digesters treating DDGS. The decline of nickel, cobalt, molybdenum, tungsten, and manganese most strongly influenced the activity ratio of the dominant methanogens *Methanosaerina* and *Methanoculleus*. This observation is based on the total TE concentrations, which do not provide information on the bioavailable fraction of the respective TE. The bioavailability of trace metals depends on their chemical speciation which is influenced by the reactor configuration and operating conditions such as pH value, redox potential, temperature and hydraulic retention time (Thanh et al., 2016). Soluble TE supplied with the feedstock can be converted



to less bioavailable forms by adsorption, chelation/complexation or precipitation. Among the chemical processes affecting TE bioavailability, the precipitation of metal sulfides is the most critical one (Thanh et al., 2016). Thus, sulfide formed during the AD process can affect process performance not only due to the toxicity of hydrogen sulfide but also by impairing the bioavailability of essential trace metals. DDGS is a protein-rich substrate from which a high amount of sulfide is generated during AD (Gustavsson et al., 2011). Gustavsson et al. (2013) showed that only 10–20% of cobalt, an element that is in general easily accessible for microorganisms in AD, remained in a dissolved form when elevated sulfide concentrations were present. Nickel was entirely associated with organic matter or present as sulfide and had to be added regularly to remain bioavailable (Gustavsson et al., 2013).

In our experiment, most of the factors which determine trace metal speciation did not change except of TE supply and iron amendment. When we reduced the iron amendment in R2, the iron concentration and that of other TE contained in the iron additive decreased, while simultaneously the free sulfide concentration increased, indicated by a brighter color of the reactor sludge (i.e., less iron sulfide), a strong sulfidic odor and increasing H₂S concentrations in the biogas. Consequently, we assume that the intensified precipitation of TE caused by the low solubility of metal sulfides reduced the TE bioavailability (Rickard and Luther, 2006), although we did not apply analytical methods which can determine different TE speciations such as sequential extraction (Thanh et al., 2016). Our results underline

the importance of counter-measures against sulfide release and compensation of TE loss due to sulfide precipitation when protein-rich feedstock is treated in AD.

Besides sulfide, ammonia is readily generated during anaerobic degradation of protein-rich substrates such as DDGS. During TE deprivation, the TAN concentration in R2 increased, indicating stronger degradation of proteins. However, it is unlikely that the DDGS degradation was intensified under these conditions. It may be that due to the increasingly constrained TE situation, a considerable amount of microorganisms died and the emerging microbial biomass was degraded by the surviving bacteria. This assumption is supported by unpublished results in our lab showing increasing TAN concentrations under changing feeding conditions and a return to initial TAN concentrations after process adaptation. High ammonia concentrations are known to inhibit acetoclastic methanogens which are outcompeted by syntrophic acetate oxidizing bacteria (SAOB) under such conditions (Schnürer and Nordberg, 2008; Westerholm et al., 2015). Within the bacterial community, VFA degrading syntrophic bacteria are very important for the process equilibrium. High concentrations of VFA like butyrate, propionate, or acetate are detrimental for the biogas process and indicators of process imbalances, emphasizing the crucial role of syntrophic bacteria (Ahring et al., 1995; Nielsen et al., 2007). During our experiment, the acetate concentration in R2 increased from 50 to 170 mg L⁻¹, whereas butyrate and propionate did not accumulate. This indicates that syntrophic propionate or butyrate degraders remained unaffected by declining TE

concentrations. In contrast, acetoclastic methanogenesis as a direct acetate sink seemed to be inhibited. Acetate degradation by SAOB as a possible alternative did not compensate for this, resulting in increasing acetate concentrations. SAOB have low growth rates (Hattori, 2008) and therefore adapt only slowly to altered conditions. At the end of the experiment, the acetate concentration was still rising and we can only speculate if the community adaptation was still in progress.

The dominance shift from *Methanosarcina* to *Methanoculleus* was the main response of the methanogenic community to TE deprivation in our study. This shift occurred between 4 and 6 weeks after the start of the TE omission leading to a shortage of cobalt, manganese, nickel, tungsten, and zinc. Whereas *Methanosarcina* is a direct degrader of acetate and methylamine (Liu and Whitman, 2008), *Methanoculleus* utilizes CO₂ and H₂ or formate and acts as a syntrophic partner for VFA degraders and SAOB. Without TE deprivation, the relative proportion of *mcrA* transcripts indicated that both methanogens were similarly active. After starting the TE deprivation, a shift of the methanogenic community was observed on the activity level (*mcrA* transcripts), which was accompanied by only a minor shift in community composition (*mcrA* genes). Six weeks after starting the TE deprivation, the transcription rates of *mcrA* changed. *Methanoculleus* contributed a higher proportion of the overall *mcrA* transcripts than *Methanosarcina* sp. However, the overall methane yield did not change, suggesting that *Methanoculleus* increased its *mcrA* expression while *mcrA* expression in *Methanosarcina* decreased simultaneously.

All methanogenesis pathways rely on the methyl-CoM reductase, which depends on the nickel-containing cofactor F430 (Dey et al., 2010). Likewise, many hydrogenases possess a nickel–iron center (Thauer et al., 2010). Acetoclastic and methylotrophic pathways contain corrinoid iron–sulfur proteins (Burke and Krzycki, 1997; Ferguson et al., 2000; Svetlichnaia et al., 2006) and accordingly require cobalt. Several other enzymes involved in acetoclastic methanogenesis depend on specific TE. Acetate kinase requires magnesium, which, however, can be replaced by manganese, cobalt or calcium (Aceti and Ferry, 1988; Miles et al., 2001), and the acetyl-CoA decarbonylase/synthase complex (ACDS) contains cobalt and nickel (Jablonski et al., 1993). Hydrogenotrophic methanogenesis is independent of corrinoid iron-sulfur proteins, suggesting a lower demand of cobalt. On the other hand, hydrogenotrophic methanogenesis has other specific TE demands. The formylmethanofuran dehydrogenase uses molybdenum or tungsten as central atom (Bertram et al., 1994; Vorholt et al., 1996) and tetrahydromethanopterin-S-methyltransferase contains cobalt (Lienard et al., 1996). These diverse demands explain the TE dependency of methanogens.

We hypothesize that *Methanosarcina* and *Methanoculleus* adapt differently to TE deprivation in order to cover their energy demands. Deprivation of cobalt should lead to shortage of corrinoid iron–sulfur proteins required for methane production from acetate and methyl compounds. Furthermore, these pathways need approximately three times more nickel than hydrogenotrophic methanogenesis, based on the number of nickel-dependent enzymes involved

in the respective methanogenic pathways. Therefore, we assume that *Methanosarcina* switched to hydrogenotrophic methanogenesis to save cobalt and nickel and thus became a competitor of *Methanoculleus* for formate and hydrogen. However, the prevailing hydrogen concentrations in AD usually match the requirements of *Methanoculleus* more than those of *Methanosarcina*. *Methanosarcina* requires higher H₂ concentrations than *Methanoculleus* (Thauer et al., 2008), which is able to consume H₂ at partial pressure of as low as <10 Pa (Garcia et al., 2000) occurring in most AD processes. The weaker performance of *Methanosarcina* after TE deprivation can also be explained by the different energy conservation mechanisms occurring in methanogenesis by electron transport phosphorylation and flavin-based electron bifurcation (Thauer et al., 2008). Nickel plays an essential role as central atom of the hydrogenases involved. Hydrogenotrophic methanogens are able to replace their [NiFe] hydrogenases by nickel-free [Fe] hydrogenases (HMD), which are unique for methanogens (Thauer et al., 2010). It has been shown that a nickel-responsive transcriptional regulator upregulates HMD under nickel-limiting conditions (Afting et al., 2000). Thus, the activity of *Methanosarcina* depends on nickel bioavailability more strongly as there is no alternative to [NiFe] hydrogenases. Although *Methanosarcina* should have been particularly affected by TE deprivation due to its higher cobalt and nickel demands and as its *mcrA* expression was indeed downregulated compared to *Methanoculleus*, its abundance decreased only slightly. In contrast, *Methanoculleus* sp. showed relatively higher *mcrA* expression, which can be taken as a sign of higher activity. However, *Methanoculleus* did not outcompete *Methanosarcina*.

We speculate that the ability of *Methanosarcina* to switch between methanogenic pathways enabled it to enter the niche of the strictly hydrogenotrophic methanogen *Methanoculleus*. We assume that the activity of SAOB increases at higher acetate concentrations as they prevail after inhibition of the acetoclastic methanogenesis. Additionally to acidogenic and acetogenic bacteria, SAOB provide formate and H₂, which requires an increased metabolic activity of hydrogenotrophic methanogens such as *Methanoculleus*. As we have no information on hydrogen or formate concentrations in the liquid phase it was not possible to prove this hypothesis. One can speculate that *Methanoculleus* has to invest more energy to cope with TE limitation, for instance by increasing the production of TE transporters. This might explain why *Methanoculleus* did not overgrow *Methanosarcina* although it showed higher methanogenic activity.

CONCLUSION

Slowly increasing TE deficits did not change the reactor efficiency as indicated by stable biogas and methane yields. Nevertheless, increasing TAN and acetate concentrations pointed at microbial community shifts which might affect reactor performance on the long run. Shifts within the methanogenic community were less visible in composition (*mcrA* genes) than in activity (*mcrA* transcripts), particularly with the two

most abundant genera *Methanosarcina* and *Methanoculleus*. The bacterial composition changed only slightly suggesting a higher stress tolerance of the bacterial community due to a higher metabolic versatility. Our results confirm the importance of sufficient TE supply to keep the activity of the “heavy duty” methanogen *Methanosarcina* (De Vrieze et al., 2012). In contrast, *Methanoculleus* can cope better with limiting TE concentrations and keep the AD process stable under sub-optimal TE supply. However, whether the process efficiency can be kept in the long term cannot be predicted from this experiment.

AUTHOR CONTRIBUTIONS

BW, HS, JL, and SK designed the study and the experiments; BW and KG performed the experiments; BW, KG, HS and SK analyzed the data; FC designed and modeled the interpolation of trace element concentrations; BW, HS, JL, HH, and SK interpreted the data. BW and SK drafted the manuscript and HS, KG, FC, JL, and HH critically revised it. All authors approved the final version of the manuscript.

REFERENCES

- Abdo, Z., Schütte, U. M. E., Bent, S. J., Williams, C. J., Forney, L. J., and Joyce, P. (2006). Statistical methods for characterizing diversity of microbial communities by analysis of terminal restriction fragment polymorphisms of 16S rRNA genes. *Environ. Microbiol.* 8, 929–938. doi: 10.1111/j.1462-2920.2005.00959.x
- Aceti, D. J., and Ferry, J. G. (1988). Purification and characterization of acetate kinase from acetate-grown *Methanosarcina thermophila*. Evidence for regulation of synthesis. *J. Biol. Chem.* 263, 15444–15448.
- Afting, C., Kremmer, E., Brucker, C., Hochheimer, A., and Thauer, R. K. (2000). Regulation of the synthesis of H₂ forming methylenetetrahydromethanopterin dehydrogenase (Hmd) and of HmdII and HmdIII in *Methanothermobacter marburgensis*. *Arch. Microbiol.* 174, 225–232. doi: 10.1007/s002030000221
- Ahring, B. K., Sandberg, M., and Angelidaki, I. (1995). Volatile fatty acids as indicators of process imbalance in anaerobic digesters. *Appl. Microbiol. Biotechnol.* 43, 559–565. doi: 10.1007/BF00218466
- Banks, C. J., Zhang, Y., Jiang, Y., and Heaven, S. (2012). Trace element requirements for stable food waste digestion at elevated ammonia concentrations. *Bioresour. Technol.* 104, 127–135. doi: 10.1016/j.biortech.2011.10.068
- Bertram, P. A., Karrasch, M., Schmitz, R. A., Böcher, R., Albracht, S. P., and Thauer, R. K. (1994). Formylmethanofuran dehydrogenases from methanogenic Archaea. Substrate specificity, EPR properties and reversible inactivation by cyanide of the molybdenum or tungsten iron-sulfur proteins. *Eur. J. Biochem.* 220, 477–484.
- Bray, J. R., and Curtis, J. T. (1957). An ordination of the upland forest communities of southern Wisconsin. *Ecol. Monogr.* 27, 326–349. doi: 10.2307/1942268
- Burke, S. A., and Krzycki, J. A. (1997). Reconstitution of monomethylamine: coenzyme M methyl transfer with a corrinoid protein and two methyltransferases purified from *Methanosarcina barkeri*. *J. Biol. Chem.* 272, 16570–16577. doi: 10.1074/jbc.272.26.16570
- Conklin, A., Stensel, H. D., and Ferguson, J. (2006). Growth kinetics and competition between *Methanosarcina* and *Methanosaeta* in mesophilic anaerobic digestion. *Water Environ. Res.* 78, 486–496. doi: 10.2175/106143006X95393
- Costa, K. C., and Leigh, J. A. (2014). Metabolic versatility in methanogens. *Curr. Opin. Biotechnol.* 29, 70–75. doi: 10.1016/j.copbio.2014.02.012
- De Vrieze, J., Hennebel, T., Boon, N., and Verstraete, W. (2012). Methanosarcina: the rediscovered methanogen for heavy duty biomethanation. *Bioresour. Technol.* 122, 1–9. doi: 10.1016/j.biortech.2012.02.079
- Demirel, B. (2014). Major pathway of methane formation from energy crops in agricultural biogas digesters. *Crit. Rev. Environ. Sci. Technol.* 44, 199–222. doi: 10.1016/j.anaerobe.2013.11.009
- Demirel, B., and Scherer, P. (2008). The roles of acetotrophic and hydrogenotrophic methanogens during anaerobic conversion of biomass to methane: a review. *Rev. Environ. Sci. Biol. Technol.* 7, 173–190. doi: 10.1007/s11157-008-9131-1
- Demirel, B., and Scherer, P. (2011). Trace element requirements of agricultural biogas digesters during biological conversion of renewable biomass to methane. *Biomass Bioenergy* 35, 992–998. doi: 10.1016/j.biombioe.2010.12.022
- Deppenmeier, U., Lienard, T., and Gottschalk, G. (1999). Novel reactions involved in energy conservation by methanogenic archaea. *FEBS Lett.* 457, 291–297. doi: 10.1016/S0014-5793(99)01026-1
- Dey, M., Li, X., Kunz, R. C., and Ragsdale, S. W. (2010). Detection of organometallic and radical intermediates in the catalytic mechanism of methyl-coenzyme M reductase using the natural substrate methyl-coenzyme M a coenzyme B substrate analogue. *Biochemistry* 49, 10902–10911. doi: 10.1021/bi101562m
- Edgar, R. C., Haas, B. J., Clemente, J. C., Quince, C., and Knight, R. (2011). UCHIME improves sensitivity and speed of chimer detection. *Bioinformatics* 27, 2194–2200. doi: 10.1093/bioinformatics/btr381
- Evranos, B., and Demirel, B. (2015). The impact of Ni, Co and Mo supplementation on methane yield from anaerobic mono-digestion of maize silage. *Environ. Technol.* 36, 1556–1562. doi: 10.1080/09593330.2014.997297
- Ferguson, D. J. Jr., Gorlatova, N., Grahame, D. A., and Krzycki, J. A. (2000). Reconstitution of dimethylamine:coenzyme M methyl transfer with a discrete corrinoid protein and two methyltransferases purified from *Methanosarcina barkeri*. *J. Biol. Chem.* 275, 29053–29060. doi: 10.1074/jbc.M910218199
- Garcia, J. L., Patel, B. K., and Ollivier, B. (2000). Taxonomic, phylogenetic, and ecological diversity of methanogenic Archaea. *Anaerobe* 6, 205–226. doi: 10.1006/anae.2000.0345
- Gustavsson, J., Svensson, B. H., and Karlsson, A. (2011). The feasibility of trace element supplementation for stable operation of wheat stillage fed biogas tank reactors. *Water Sci. Technol.* 64, 320–325. doi: 10.2166/wst.2011.633
- Gustavsson, J., Yekta, S. S., Sundberg, C., Karlsson, A., Ejlersson, J., Skjellberg, U., et al. (2013). Bioavailability of cobalt and nickel during anaerobic digestion of sulfur-rich stillage for biogas formation. *Appl. Energy* 122, 473–477. doi: 10.1016/j.apenergy.2013.02.009
- Hao, L. P., Lü, F., He, P. J., Li, L., and Shao, L. M. (2011). Predominant contribution of syntrophic acetate oxidation to thermophilic methane formation at high

FUNDING

BW was funded by the German Environmental Foundation (Deutsche Bundesstiftung Umwelt – DBU, grant number 20011/165) and by the Graduate School HIGRADE.

ACKNOWLEDGMENTS

We thank the colleagues from the DBFZ Department of Biochemical Conversion for support in chemical analysis of trace elements and reactor parameters. Ute Lohse (UFZ Department of Environmental Microbiology) is acknowledged for her skilled technical assistance in amplicon pyrosequencing.

SUPPLEMENTARY MATERIAL

The Supplementary Material for this article can be found online at: <http://journal.frontiersin.org/article/10.3389/fmicb.2016.02034/full#supplementary-material>

- acetate concentrations. *Environ. Sci. Technol.* 45, 508–513. doi: 10.1021/es102228v
- Hattori, S. (2008). Syntrophic acetate-oxidizing microbes in methanogenic environments. *Microbes Environ.* 23, 118–127. doi: 10.1264/jsme2.23.118
- Jablonski, P. E., Lug, W., Ragsdale, S. W., and Ferry, J. G. (1993). Characterization of the metal centers of the corrinoid/iron-sulfur component of the CO dehydrogenase enzyme complex from *Methanosarcina thermophila* by EPR spectroscopy and spectroelectrochemistry. *J. Biol. Chem.* 268, 325–329.
- Karakashev, D., Batstone, D. J., and Angelidaki, I. (2005). Influence of environmental conditions on methanogenic compositions in anaerobic biogas reactors. *Appl. Environ. Microbiol.* 71, 331–338. doi: 10.1128/AEM.71.1.331–338.2005
- Karlsson, A., Einarsson, P., Schnürer, A., Sundberg, C., Ejlersson, J., and Svensson, B. H. (2012). Impact of trace element addition on degradation efficiency of volatile fatty acids, oleic acid and phenyl acetate and on microbial populations in a biogas digester. *J. Biosci. Bioeng.* 114, 446–452. doi: 10.1016/j.jbiosc.2012.05.010
- Lane, D. J. (1991). “16S/23S rRNA sequencing,” in *Nucleic Acid Techniques in Bacterial Systematics*, eds E. Stackebrandt and M. Goodfellow (Chichester: John Wiley & Sons), 177–203.
- Lebuhn, M., Liu, F., Heuwinkel, H., and Gronauer, A. (2008). Biogas production from mono-digestion of maize silage – long-term process stability and requirements. *Water Sci. Technol.* 58, 1645–1651. doi: 10.2166/wst.2008.495
- Lemmer, A., Vintiloiu, A., Preißler, D., Bastam, C., Bäuerle, L., and Oechsner, H. (2010). Untersuchungen zum Einsatz von mineralstoffen in biogasanlagen – bedeutung der mineralstoffe für die anaeroben mikroorganismen und ursachen für konzentrationsunterschiede in biogasfermentern. *Gültzower Fachgespräche* 35, 45–77.
- Lienard, T., Becher, B., Marshall, M., Bowien, S., and Gottschalk, G. (1996). Sodium ion translocation by N5-methyltetrahydromethanopterin: coenzyme M methyltransferase from *Methanosarcina mazei* Gö1 reconstituted in ether lipid liposomes. *Eur. J. Biochem.* 239, 857–864. doi: 10.1111/j.1432-1033.1996.0857u.x
- Lindorfer, H., Ramhold, D., and Frauz, B. (2012). Nutrient and trace element supply in anaerobic digestion plants and effect of trace element application. *Water Sci. Technol.* 66, 1923–1929. doi: 10.2166/wst.2012.399
- Liu, Y., and Whitman, W. B. (2008). Metabolic, phylogenetic, and ecological diversity of the methanogenic archaea. *Ann. N. Y. Acad. Sci.* 1125, 171–189. doi: 10.1196/annals.1419.019
- Lucas, R., Kuchenbuch, A., Fetzer, I., Harms, H., and Kleinsteuber, S. (2015). Long-term monitoring reveals stable and remarkably similar microbial communities in parallel full-scale biogas reactors digesting energy crops. *FEMS Microbiol. Ecol.* 91:fiv004. doi: 10.1093/femsec/fiv004
- McInerney, M. J., Sieber, J. R., and Gunsalus, R. P. (2009). Syntrophy in anaerobic global carbon cycles. *Curr. Opin. Biotechnol.* 20, 623–632. doi: 10.1016/j.copbio.2009.10.001
- Miles, R. D., Iyer, P. P., and Ferry, J. G. (2001). Site-directed mutational analysis of active site residues in the acetate kinase from *Methanosarcina thermophila*. *J. Biol. Chem.* 276, 45059–45064. doi: 10.1074/jbc.M108355200
- Munk, B., and Lebuhn, M. (2014). Process diagnosis using methanogenic Archaea in maize-fed, trace element depleted fermenters. *Anaerobe* 29, 22–28. doi: 10.1016/j.anabio.2014.04.002
- Nielsen, H., Uellendahl, H., and Ahring, B. (2007). Regulation and optimization of the biogas process: propionate as a key parameter. *Biomass Bioenergy* 31, 820–830. doi: 10.1016/j.biombioe.2007.04.004
- Oksanen, J., Blanchet, F. G., Kindt, R., Legendre, P., O’Hara, R. B., Simpson, G. L., et al. (2011). *The Vegan Package: Community Ecology Package. R Package Version 1.17–12*. Available at: <http://CRAN.R-project.org/package=vegan>
- Plugge, C. M., Jiang, B., de Bok, F. A., Tsai, C., and Stams, A. J. (2009). Effect of tungsten and molybdenum on growth of a syntrophic coculture of *Syntrophobacter fumaroxidans* and *Methanospirillum hungatei*. *Arch. Microbiol.* 191, 55–61. doi: 10.1007/s00203-008-0428-9
- Pobeheim, H., Munk, B., Lindorfer, H., and Guebitz, G. M. (2011). Impact of nickel and cobalt on biogas production and process stability during semi-continuous anaerobic fermentation of a model substrate for maize silage. *Water Res.* 45, 781–787. doi: 10.1016/j.watres.2010.09.001
- Quast, C., Pruesse, E., Yilmaz, P., Gerken, J., Schweer, T., Yarza, P., et al. (2013). The SILVA ribosomal RNA gene database project: improved data processing and web-based tools. *Nucleic Acids Res.* 41, 590–595. doi: 10.1093/nar/gks1219
- Rickard, D., and Luther, G. W. (2006). Metal sulfide complexes and clusters. *Rev. Mineral. Geochem.* 61, 421–501. doi: 10.2138/rmg.2006.61.8
- Schloss, P. D., Westcott, S. L., Ryabin, T., Hall, J. R., Hartmann, M., Hollister, E. B., et al. (2009). Introducing mothur: open-source, platform-independent, community-supported software for describing and comparing microbial communities. *Appl. Environ. Microbiol.* 75, 7537–7541. doi: 10.1128/AEM.01541–09
- Schmidt, T. (2011). Anaerobic digestion of *Jatropha curcas* L. press cake and effects of an iron-additive. *Waste Manag. Res.* 29, 1171–1176. doi: 10.1177/0734242X11425566
- Schmidt, T., Pröter, J., Scholwin, F., and Nelles, M. (2013). Anaerobic digestion of grain stillage at high organic loading rates in three different reactor systems. *Biomass Bioenergy* 55, 285–290. doi: 10.1016/j.biombioe.2013.02.010
- Schnürer, A., and Nordberg, A. (2008). Ammonia, a selective agent for methane production by syntrophic acetate oxidation at mesophilic temperature. *Water Sci. Technol.* 57, 735–740. doi: 10.2166/wst.2008.097
- Shimada, T., Morgenroth, E., Tandukar, M., Pavlostathis, S. G., Smith, A., Raskin, L., et al. (2011). Syntrophic acetate oxidation in two-phase (acid-methane) anaerobic digesters. *Water Sci. Technol.* 64, 1812–1820. doi: 10.2166/wst.2011.748
- Sieber, J. R., Le, H. M., and McInerney, M. J. (2014). The importance of hydrogen and formate transfer for syntrophic fatty, aromatic and alicyclic metabolism. *Environ. Microbiol.* 16, 177–188. doi: 10.1111/1462-2920.12269
- Steinberg, L. M., and Regan, J. M. (2008). Phylogenetic comparison of the methanogenic communities from an acidic, oligotrophic fen and an anaerobic digester treating municipal wastewater sludge. *Appl. Environ. Microbiol.* 74, 6663–6671. doi: 10.1128/AEM.00553-08
- Sträuber, H., Schröder, M., and Kleinsteuber, S. (2012). Metabolic and microbial community dynamics during the hydrolytic and acidogenic fermentation in a leach-bed process. *Energy Sustain. Soc.* 2:13. doi: 10.1186/2192-0567-2-13
- Svetlichnaya, T., Svetlichnyi, V., Meyer, O., and Dobbek, H. (2006). Structural insights into methyltransfer reactions of a corrinoid iron-sulfur protein involved in acetyl-CoA synthesis. *Proc. Natl. Acad. Sci. U.S.A.* 103, 14331–14336. doi: 10.1073/pnas.0601420103
- Thanh, P. M., Ketheesan, B., Yan, Z., and Stuckey, D. (2016). Trace metal speciation and bioavailability in anaerobic digestion: A review. *Biotechnol. Adv.* 34, 122–136. doi: 10.1016/j.biotechadv.2015.12.006
- Thauer, R. K., Kaster, A. K., Goenrich, M., Schick, M., Hiromoto, T., and Shima, S. (2010). Hydrogenases from methanogenic archaea, nickel, a novel cofactor, and H2 storage. *Annu. Rev. Biochem.* 79, 507–536. doi: 10.1146/annurev.biochem.030508.152103
- Thauer, R. K., Kaster, A. K., Seedorf, H., Buckel, W., and Hedderich, R. (2008). Methanogenic archaea: ecologically relevant differences in energy conservation. *Nat. Rev. Microbiol.* 6, 579–591. doi: 10.1038/nrmicro1931
- Vorholt, J. A., and Thauer, R. K. (2002). “Molybdenum and tungsten enzymes in C1 metabolism,” in *Metal Ions in Biological Systems*, Vol. 39, eds A. Sigel and H. Sigel (Boca Raton, FL: CRC Press), 571–619.
- Vorholt, J. A., Vaupel, M., and Thauer, R. K. (1996). A polyferredoxin with eight [4Fe-4S] clusters as a subunit of molybdenum formylmethanofuran dehydrogenase from *Methanosaarcina barkeri*. *Eur. J. Biochem.* 236, 309–317. doi: 10.1111/j.1432-1033.1996.t01-1-00309.x
- Westerholm, M., Müller, B., Isaksson, S., and Schnürer, A. (2015). Trace element and temperature effects on microbial communities and links to biogas digester performance at high ammonia levels. *Biotechnol. Biofuels* 8:154. doi: 10.1186/s13068-015-0328-6
- Worm, P., Fermoso, F. G., Lens, P. N. L., and Plugge, C. M. (2009). Decreased activity of a propionate-degrading community in a UASB reactor fed with synthetic medium without tungsten, molybdenum and selenium. *Enzyme Microb. Technol.* 45, 139–145. doi: 10.1016/j.enzmictec.2009.02.001
- Ziganshin, A. M., Liebetrau, J., Pröter, J., and Kleinsteuber, S. (2013). Microbial community structure and dynamics during anaerobic digestion of various agricultural waste materials. *Appl. Microbiol. Biotechnol.* 97, 5161–5174. doi: 10.1007/s00253-013-4867-0

Ziganshin, A. M., Schmidt, T., Scholwin, F., Il'inskaya, O. N., Harms, H., and Kleinstüber, S. (2011). Bacteria and archaea involved in anaerobic digestion of distillers grains with solubles. *Appl. Microbiol. Biotechnol.* 89, 2039–2052. doi: 10.1007/s00253-010-2981-9

Conflict of Interest Statement: The authors declare that the research was conducted in the absence of any commercial or financial relationships that could be construed as a potential conflict of interest.

Copyright © 2016 Wintsche, Glaser, Sträuber, Centler, Liebetrau, Harms and Kleinstüber. This is an open-access article distributed under the terms of the Creative Commons Attribution License (CC BY). The use, distribution or reproduction in other forums is permitted, provided the original author(s) or licensor are credited and that the original publication in this journal is cited, in accordance with accepted academic practice. No use, distribution or reproduction is permitted which does not comply with these terms.



Mass Loss Controlled Thermal Pretreatment System to Assess the Effects of Pretreatment Temperature on Organic Matter Solubilization and Methane Yield from Food Waste

Martha M. Yeshanew^{1,2*}, Luigi Frunzo³, Piet N. L. Lens⁴, Francesco Pirozzi² and Giovanni Esposito¹

¹ Department of Civil and Mechanical Engineering, University of Cassino and Southern Lazio, Cassino, Italy, ² Department of Civil, Architectural and Environmental Engineering, University of Naples Federico II, Naples, Italy, ³ Department of Mathematics and Applications Renato Caccioppoli, University of Naples Federico II, Naples, Italy, ⁴ UNESCO-IHE Institute for Water Education, Delft, Netherlands

OPEN ACCESS

Edited by:

Kartik Chandran,
Columbia University, USA

Reviewed by:

Hojeong Kang,
Yonsei University, South Korea
Seung Gu Shin,
Pohang University of Science and
Technology, South Korea

*Correspondence:

Martha M. Yeshanew
martaminale@gmail.com

Specialty section:

This article was submitted to
Microbiotechnology, Ecotoxicology
and Bioremediation,
a section of the journal
Frontiers in Environmental Science

Received: 15 February 2016

Accepted: 05 September 2016

Published: 23 September 2016

Citation:

Yeshanew MM, Frunzo L, Lens PN, Pirozzi F and Esposito G (2016) Mass Loss Controlled Thermal Pretreatment System to Assess the Effects of Pretreatment Temperature on Organic Matter Solubilization and Methane Yield from Food Waste. *Front. Environ. Sci.* 4:62.
doi: 10.3389/fenvs.2016.00062

HIGHLIGHTS

- Direct correlation between substrate composition and TP effect was identified.
- The new experimental TP set-up minimized organic compound loss during TP of FW.
- The solubilization of carbohydrate and protein determined the optimal temperature of FW TP.
- Low temperature (80°C) TP attained the highest carbohydrate solubilization and methane yield.

The effects of thermal pretreatment (TP) on the main characteristics of food waste (FW) and its biochemical methane potential (BMP) and distribution of volatile fatty acids (VFAs) under mesophilic condition (35°C) were investigated. The TP experiments were carried out at 80, 100, 120°C for 2 h and 140°C for 1 h. The designed TP set-up was able to minimize the organic matter loss during the course of the pretreatment. Soluble organic fractions evaluated in terms of chemical oxygen demand (COD) and soluble protein increased linearly with pretreatment temperature. In contrast, the carbohydrate solubilization was more enhanced (30% higher solubilization) by the TP at lower temperature (80°C). A slight increment of soluble phenols was found, particularly for temperatures exceeding 100°C. Thermally pretreated FW under all conditions exhibited an improved methane yield compared to the untreated FW, due to the increased organic matter solubilization. The highest cumulative methane yield of 442 (± 8.6) mL/gVS_{added}, corresponding to a 28.1% enhancement compared to the untreated FW, was obtained with a TP at 80°C. No significant variation in the VFAs trends were observed during the BMP tests under all investigated conditions.

Keywords: anaerobic digestion, thermal pretreatment, food waste, substrate composition, solubilization, methane production potential

INTRODUCTION

With the worldwide economic development and population growth, food waste (FW) production is alarmingly increasing and imposes a great challenge in waste management for most countries (Zhang et al., 2014; Li and Jin, 2015). Today, anaerobic digestion (AD) is one of the most consolidated technologies for waste treatment and valorization, compared to other possible treatment routes (Ferreira et al., 2013; Wagner et al., 2014; Zhang et al., 2014). The process allows to achieve a two-fold advantage of obtaining continuous power generation, whilst reducing the amount of waste to be disposed and thus alleviating environmental pollution (Elbeshbishi et al., 2012). Moreover, different directives such as the Renewable Energy directive (2009/28/EC, EU, 2009) and the Landfill directive (1999/31/EC, EU, 1999) were enacted by European countries. These laws stimulated further research and encouraged the intensive practice of AD for organic waste treatment (Bougrier et al., 2007; Marin et al., 2011; Wang et al., 2014).

The AD process is an integrated biochemical conversion of organic matter into biogas, through a sequence of four basic steps: hydrolysis, acidogenesis, acetogenesis and methanogenesis (Minale and Worku, 2014; Zhang et al., 2014). More in details, during the AD of FW, the first step of hydrolysis involves solubilization of particulate matter and bioconversion of organic polymers to monomers/dimers, making it the rate-limiting step for the overall process, and thus resulting in the necessity of larger reactor volumes for this specific type of organic waste (Bougrier et al., 2008; Kondusamy and Kalamdhad, 2014; Tampio et al., 2014; Ariunbaatar et al., 2014a). This is due to the nature of the substrate, which is mainly constituted of complex organic matter in particulate form (carbohydrate, protein, lipid and fat, lignocellulosic material) and a smaller inorganic part (Marin et al., 2010; Vavouraki et al., 2013; Wang et al., 2014). Therefore, through accelerating the FW solubilization, the whole process as well as reactor efficiency can greatly improve (Jiang et al., 2014; Wang et al., 2014). In these aspects, substrate pretreatments are effective methods for enhancing the methane yield from FW AD (Ferreira et al., 2013; Ariunbaatar et al., 2014b).

Several methods for the pretreatment of organic substrates have been proposed. The most common methods include mechanical grinding (Izumi et al., 2010), ultrasound (Elbeshbishi et al., 2011; Jiang et al., 2014), microwave (Marin et al., 2010, 2011), thermal (Liu et al., 2012; Tampio et al., 2014; Ariunbaatar et al., 2014b), chemical (Elbeshbishi et al., 2011; Ma et al., 2011), biological (Vavouraki et al., 2014) pretreatments or their combination (Strong and Gapes, 2012; Vavouraki et al., 2013). Among these methods, thermal pretreatment (TP) is considered as an economically viable and environmentally friendly alternative, as reported by different authors (Strong et al., 2011; Gianico et al., 2013; Zhou et al., 2013; Ariunbaatar et al., 2014a).

TP methods have been applied to several types of organic wastes in order to modify their structure by breaking the intermolecular bonds and thus aid in the release of soluble organic monomers/dimers, that are more accessible and readily biodegradable by anaerobic bacteria (Vavouraki et al., 2013).

Therefore, the kinetics of the AD process are improved, leading to a higher reactor efficiency (Bougrier et al., 2007; Wang et al., 2010; Zhou et al., 2013; Kondusamy and Kalamdhad, 2014; Li and Jin, 2015). Heating temperature and pretreatment time have been found as the key factors in determining the effectiveness of TP (Carrère et al., 2009; Rincón et al., 2013). Accordingly, wide ranges of temperature (50–250°C) and treatment time (0.5–12 h) have been adopted and tested based on the ultimate methane yield from FW (Elbeshbishi et al., 2011; Liu et al., 2012; Zhou et al., 2013; Prabhudesai et al., 2014; Tampio et al., 2014; Ariunbaatar et al., 2014a). In particular, these two parameters influence (i) the hydrolysis of organic matter in particulate form and the subsequent biodegradation enhancement, (ii) the loss of volatile organic matter, and (iii) the formation of refractory/inhibitory compounds (Carlsson et al., 2012). The latter two represent the main negative effects of TP on AD processes, and both processes usually occur at higher TP temperatures (Kondusamy and Kalamdhad, 2014). Loss of organic compounds can occur due to evaporation by the applied heat during TP, and hence induce a net decrease of available organic matter for methane production (Carlsson et al., 2012). Formation of inhibitory compounds during the course of TP can occur by two main phenomena: the release of soluble refractory compounds, e.g., phenolic compounds (Marin et al., 2010) or through chemical reactions of different soluble monomers, named as Maillard reactions (Liu et al., 2012). The reactions involve the non-enzymatic transformation of sugars and soluble protein and cause the formation of melanoidin compounds (Ariunbaatar et al., 2014a).

Despite of the large number of studies on this specific topic, no systematic research that relates the aforementioned effects of TP on the solubilization of FW organic matter and the subsequent biodegradation enhancement, and the correlation with the substrate organic composition has been conducted. In addition, conflicting results about the TP effects on FW have been reported in the literature. For instance, Liu et al. (2012) reported that TP of kitchen waste at 175°C for 60 min induced an increase in solubilization of particulate matter from 96.6 to 116.5 g/kg in terms of volatile dissolved solid concentration and a decrease (7.9%) of methane production as a result of melanoidin compound formation. In contrast, Wang et al. (2010) obtained a 13.6% higher cumulative methane yield due to the higher dissolved organic solid concentration achieved (greater than 30% hydrolysis ratio) after TP of municipal biowaste at 175°C for 60 min. In general, studies affirmed that the best temperature for TP of FW is in the range of 80–100°C (Ariunbaatar et al., 2014b). Other studies, instead, reported the proper temperature range for FW TP as 120–160°C (Ma et al., 2011; Yin et al., 2014) or even 170–175°C (Wang et al., 2010; Zhou et al., 2013).

In the present work, the effect of TP on FW characteristics at different temperatures was studied in order to better understand and fill the existing knowledge gaps on the topic. Deep investigations on solubilization of FW during TP and methane yield enhancement were performed using a newly proposed TP system. The release of soluble compounds, i.e., carbohydrate, protein, soluble chemical oxygen demand (COD) and inhibitory compounds were monitored, and their impacts

on AD biodegradability were evaluated for each TP condition. In particular, the relationship between soluble carbohydrate and soluble protein with the methane production was assessed. Biochemical methane potential (BMP) tests were used for evaluating the improvement of the methane yield and individual VFAs production after each TP condition.

MATERIALS AND METHODS

Substrate and Inoculum

FW synthetically prepared according to the method described by Ariunbaatar et al. (2014b) was used as the substrate. The FW composition was based on the actual characteristics of the food waste of most EU countries. The use of synthetic waste allows the repeatability of experimental results and their comparison with previous research. The following composition was used: 79% of vegetables and fruits; 5% of cooked pasta and rice; 6.0% of bread and bakery; 8.0% of meat and fish; and 2.0% dairy products (on wet basis). The synthetic FW was blended and stored in a refrigerator at -20°C until use. The anaerobic inoculum used in BMP tests was obtained from a full scale AD plant located in Capaccio-Salerno (Italy). The plant treats buffalo manure and dairy wastes at mesophilic conditions. The main physico-chemical characteristics of both the FW and inoculum are reported in **Table 1**.

Thermal Pretreatment (TP) Set-Up

Lab-scale TP experiments are mostly conducted in open systems using either an autoclave (Laurent et al., 2011; Gianico et al., 2013), oven or thermal baths (Rincón et al., 2013; Xue et al., 2015), which usually lead to high loss of organic compounds and odor emission during pretreatment of substrates. In this study, a new experimental TP set-up was developed (**Figure 1**). This set-up consisted of a thermostat oil bath equipped with a magnetic stirrer bar and temperature control unit, 500 mL pyrex glass bottle, two 50 mL trapping columns and water displacing gas measuring systems. The treatment bottle was connected with an inert plastic tube to the trapping column and gas measuring systems. The system operated in closed and airtight conditions. The trapping columns were placed in series (**Figure 1**) and filled with high pH sodium phosphate buffer solution (Na_3PO_3 and Na_2HPO_3 at a pH of 12), intended to trap volatile organic compounds released during the course of the TP. Phosphate buffers have been widely used in many biological and pharmaceutical applications in order to maintain organic

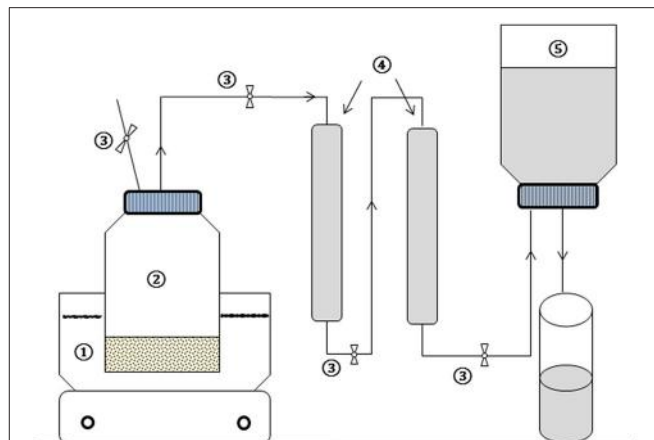


FIGURE 1 | Schematic diagram of the TP experimental set-up: (1) Oil bath heater with stirrer, (2) treatment bottle, (3) controlling valves, (4) trapping columns, and (5) water displacement gas measuring system.

compounds in their original forms (Soliman et al., 2015). In addition, as phosphoric acid has multiple dissociation constants, the buffer can be prepared near to three pHs, i.e., 2.15, 6.86, and 12.32. The trapping potential of the buffer solution as well as experimental replicability of the TP using the developed set-up was preliminary evaluated at each TP condition. This was performed using known concentrations of a synthetic organic acid solution containing a mixture of acetic acid, propionic acid and butyric acid (data not shown). The concentrations of the mixture before and after each TP and the amount trapped in the buffer were quantified and balanced.

Afterwards, 100 g of raw FW was placed in the treatment bottle for each TP condition. The gaseous mixture released during TP passed through the buffer trap solution and was volumetrically quantified by means of a water displacement system. After TP, the treatment bottle was cooled to ambient temperature prior to opening to avoid evaporation/volatilization and further organic matter loss. The gases were taken from the headspace of the displacement water system and analyzed for gaseous composition. Buffer samples were taken for COD analysis.

Four different temperatures 80 , 100 , 120°C for 2 h and 140°C for 1 h , were tested with regard to their effectiveness in terms of organic matter solubilization and enhancing methane production. These temperature ranges and pretreatment times were chosen based on the EU regulation (EC 1774/2002), which states that catering waste should be sterilized at a temperature of $\geq 70^{\circ}\text{C}$ for at least 60 min, or at a temperature $> 133^{\circ}\text{C}$ for at least 30 min. Moreover, these TP temperatures were shown to improve the AD process of various organic wastes (Carrère et al., 2009; Rincón et al., 2013; Ariunbaatar et al., 2014b). Each TP condition was performed in triplicate and results are presented as average values.

The proposed system provides operational advantages such as reduction of odor during TP experiments, simplicity of construction, easy operation and, in particular, the system allows not only to reduce the loss of organic matter during TP, but to

TABLE 1 | Main characteristic of FW and inoculum used in this study.

Parameters	Unit	FW	Inoculum
TS	% wet basis	22.7 ± 1.2	3.2 ± 0.3
VS	% wet basis	21.9 ± 0.9	2.2 ± 0.2
Total COD	g/kg	400 ± 3.4	107 ± 3.7
TKN	g/kg	6.7 ± 1.4	2.3 ± 0.3
Total carbohydrate	g/kg	134 ± 3.39	1.7 ± 0.1
Total protein	g/kg	30.4 ± 2.1	14.5 ± 0.6
Total lipid	g/kg	19.4 ± 0.29	3.1 ± 0.4

capture and quantify the loss of volatile organic compounds in the buffer solutions.

Sample Preparation and Calculations

Each sample of the raw and thermally pretreated FW was diluted with ultrapure water (1 g/50 mL) to properly measure the soluble fractions. The diluted samples were centrifuged at 4000 rpm for 15 min and filtered through a 0.45 μm microfiber filter prior to analysis. The following parameters of the solid and soluble fraction for raw and pretreated FW were analyzed: COD, protein, carbohydrate, phenols and VFAs. The effect of TP on the FW characteristics was mainly quantified by the extent of solubilization (Laurent et al., 2011). As defined in the work of Rincón et al. (2013) and Kim et al. (2003), solubilization is the transformation of the particulate fraction of FW to the soluble fraction and estimated by the following equation:

$$\text{S}_{\text{solubilization}}(\%) = (\text{S}_s/\text{S}_t) \times 100 \quad (1)$$

Where S refers to COD, carbohydrate or protein; S_s and S_t represent the soluble and total fraction of each parameter.

Biochemical Methane Potential Tests

BMP tests were carried out in 1 L glass bottles at mesophilic ($35 \pm 2^\circ\text{C}$) conditions, with a substrate to inoculum ratio (S/I) of 0.5 gVS/gVS, following the protocol described by Esposito et al. (2012). The temperature was maintained constant by a water bath connected with a thermostatically controlled flow heater. BMP tests of the untreated FW were carried out in order to quantify the effect of pretreatment on the substrate. BMP tests of the inoculum were also conducted in order to determine the net biogas production rate for each pretreated and untreated FW. Prior to the start of BMP experiments, the headspace of each bottle was flushed with argon gas to provide anaerobic conditions. Mixing was done manually daily. Biogas produced was measured daily by the displacement of acidified water to reduce CO_2 solubility. Subsequently, gas samples were collected from the headspace with an air tight syringe for methane (CH_4) and carbon dioxide (CO_2) determination. The BMP tests were followed until no gas was produced anymore. All tests were carried out in duplicate and results are given as average values of the tests. The cumulative methane production was normalized to standard temperature and pressure (STP).

Analytical Methods

Total solids (TS), volatile solids (VS), total and soluble COD, total Kjeldahl Nitrogen (TKN) and phenols (total and soluble) were determined according to standard methods for examination of water and wastewater (APHA, 1998). Total main elemental content, i.e., Carbon (TEC), Hydrogen (TEH) and Sulfur (TES) of FW was measured simultaneously by catalytic oxidation using an elemental analyzer (PerkinElmer® 2400 Series II). The temperature of the combustion and reduction zones were set at 970°C and 500°C , respectively, and argon gas was used as a purging gas.

Total and soluble protein were quantified by the Lowry-Folin method using bovine serum albumin (BSA) as the standard (Lowry et al., 1951). Total and soluble carbohydrate

were analyzed using the phenol-sulfuric acid method with glucose as the standard (Herbert et al., 1971). Both the protein and carbohydrate were measured through spectrophotometry (PhotoLab® 6600 UV-VIS SERIUS). Liquid-liquid extraction with chloroform and methanol as solvent was used to quantify total lipid (Phillips et al., 1997). To analyse individual VFAs, 1.5 mL samples were collected from each BMP bottle during the BMP tests. Subsequently, samples were centrifuged at a speed of 5000 rpm for 7 min and filtered through a 0.2 μm microfiber filter. The filtrate samples were analyzed with High Pressure Liquid Chromatography (HPLC) (Dionex LC 25 Chromatography Oven) equipped with Synergi 4u Hydro RP 80A (size 250 × 4.60 mm) column and UV detector (Dionex AD25 Absorbance Detector).

The biogas composition was determined using gas chromatography (GC, Varian STAR 3400), equipped with a ShinCarbon ST 80/100 column and thermal conductivity detector. The temperatures of injector port, detector and oven temperature were 50, 120, and 120°C , respectively, with argon as the carrier gas.

Statistical Analysis

Statistical analysis was carried out using *anova1* MATLAB tool. Data were analyzed by one-way ANOVA. The level of significance was set at $p < 0.05$. The significance of differences in the average methane yields, soluble and total COD, soluble and total carbohydrates, soluble and total proteins were determined.

RESULTS

Characteristics of FW before and after Each TP

Table 3 presents the main characteristics of FW before and after each TP. A general decreasing trend of the total COD and total elemental carbon (TEC) concentrations were observed with increasing TP temperature. The total COD was reduced by 3.6, 4.6, 5.4, and 7.4% for TP at 80, 100, 120, and 140°C , respectively, compared to the untreated FW. Similarly, the TEC concentration with respect to the untreated FW was decreased by 1.1, 3.1, 5.3, and 9.1% at 80, 100, 120, and 140°C , respectively. In contrast, the soluble COD concentration shows an increasing trend with TP temperature. **Figure 2** illustrates the solubilization of COD, carbohydrate and protein of FW before and after each TP. The carbohydrate and protein solubilization have different trends, while the concentration of soluble COD increased linearly with TP temperature. The highest carbohydrate solubilization of around 30% was obtained at 80°C , followed by 28.4% at 100°C , 27.8% at 120°C , 26.5% at 140°C and 18.4% for untreated FW (**Figure 2**). Protein solubilization increased linearly with pretreatment temperature and reached its maximum value (around 20%) at 140°C . The protein solubilization had a similar trend as the COD solubilization (**Figure 2**). A one-way ANOVA analysis showed a large statistical difference between the data sets (**Table 2**).

The lactic acid and VFAs concentrations (i.e., acetic, propionic and butyric acid) of thermally pretreated FW were lower than

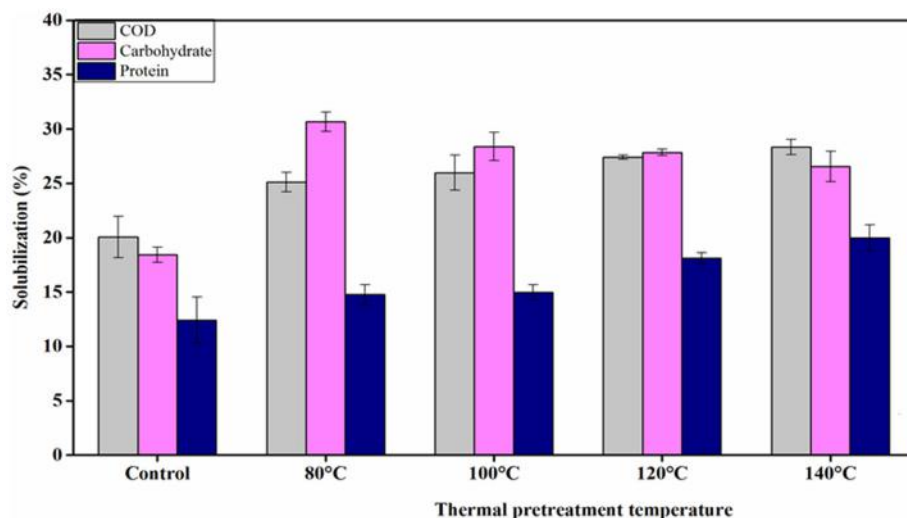


FIGURE 2 | Solubilization of COD, carbohydrate and protein of FW before and after each TP.

TABLE 2 | Summary table of the one-way ANOVA for experiment data.

Parameters	Methane yield	COD _T	COD _S	Total carbohydrate	Soluble carbohydrate	Total protein	Soluble protein
p-value	0.02058	4.1×10^{-8}	5.8×10^{-9}	0.0018	0.014	0.0094	0.033

the control and this reduction was more significant at higher temperature TPs (**Table 3**). The reason was that some of the VFAs were evaporated during the course of the TP. This was supported by the gas analysis in the headspace after each TP, in which neither CO₂ nor H₂ gas was detected (data not shown), which indicates that evaporation of organic compounds was the main cause for the decrease of VFAs concentration and thus TEC during the TPs of FW.

Total and soluble phenol before and after TP were determined to assess the possible release of soluble phenols due to the increased temperature exposure (**Table 4**). The presence of soluble phenols is an important parameter as they can inhibit the AD process (Rincón et al., 2013). A slight increase of the soluble phenol concentration was observed for pretreatment temperatures higher than 100°C.

Cumulative Biogas and Methane Yields

Figure 3 shows the cumulative biogas and methane production from the BMP tests of thermally pretreated and untreated FW. The specific cumulative methane yields of each thermally pretreated and untreated FW are illustrated in **Figure 4**. All the pretreated FW achieved a higher volumetric biogas and methane production than the control. The highest volumetric methane production was obtained for FW treated at 80°C (**Figure 3B**). The cumulative specific methane yield was 442 (± 8.6), 374 (± 10.9), 390 (± 12.4), 414 (± 8.9), and 345 (± 12.7) mL/gVS_{added} for 80, 100, 120, 140°C and the control, respectively (**Figure 4**). The one-way ANOVA showed that there was a significant difference among the methane yields of the pretreated FW (**Table 2**). The corresponding enhancement of

the specific methane yield with respect to the control was 28.1, 8.3, 12.9, and 20% at 80, 100, 120, and 140°C, respectively. Furthermore, the specific methane yields in terms of mL/gCOD before and after TP are given in **Table 5**. It should be noted that the higher specific methane yield of all thermally treated FW compared to the untreated (**Table 5**) coupled with the minor COD loss in the new TP system (**Table 3**) might have a positive energy balance and thus lead to increased economic profits of the AD process.

Figure 5 presents the percentage of methane gas in the produced biogas during each BMP test. The methane percentage increased from around 20 to 80% during the first 10 days of the digestion period for all tested conditions and afterwards remained around 58–69% until the end of the digestion period. A higher methane percentage in the produced biogas was observed for all thermally treated FW compared to the control, while no significant variations of the methane percentage were noticed between the TP conditions.

VFAs Distribution during BMP Tests

The VFAs distribution trends were followed during the BMP tests in order to observe any possible impact of TP on their production rate in the digestion process. The concentration profiles of the VFAs with respect to the digestion time in each BMP test are shown in **Figure 5**. Higher values of VFAs were obtained for all pretreated FWs compared to the control, though the concentration of some of the acids, i.e., lactic acid and VFAs (acetic and propionic acids), was reduced during the course of the TP (**Table 3**). Acetic, propionic and butyric acids were the major VFAs produced during the early experimental

TABLE 3 | Chemical composition of FW before and after each TP.

Parameter	Unit	Control*	Thermal pretreatment temperature			
			80°C	100°C	120°C	140°C
COD _T	g/kg	400.0 ± 3.4	385.2 ± 0.3	381.8 ± 1.9	379.1 ± 3.4	371.3 ± 1.1
COD _S	g/kg	80.2 ± 0.5	96.7 ± 1.3	99.2 ± 0.7	103.8 ± 1.1	105.3 ± 0.8
TEC ^a	% dry wt.	45.2 ± 1.6	44.7 ± 2.1	43.8 ± 1.1	42.8 ± 2.5	41.1 ± 1.2
TEH ^b	% dry wt.	7.01 ± 0.3	6.91 ± 0.5	6.87 ± 0.5	6.5 ± 0.4	6.3 ± 0.7
TES ^c	% dry wt.	0.87 ± 0.01	0.92 ± 0.05	0.86 ± 0.13	0.84 ± 0.09	0.85 ± 0.13
Total carbohydrate	g/kg	134 ± 3.39	127.8 ± 1.4	118.4 ± 2.2	117.8 ± 1.9	113.4 ± 1.2
Soluble carbohydrate	g/kg	24.7 ± 0.21	39.2 ± 0.8	33.6 ± 0.4	32.8 ± 0.9	30.1 ± 0.7
Total protein	g/kg	30.4 ± 2.1	27.1 ± 0.9	27.4 ± 1.4	24.6 ± 1.8	23.4 ± 1.5
Soluble protein	g/kg	3.8 ± 0.18	4.0 ± 0.02	4.1 ± 0.07	4.45 ± 0.24	4.67 ± 0.12
Lactic acid	mg/L	30.8 ± 0.2	17.0 ± 0.6	5.4 ± 1.5	3.0 ± 0.9	2.1 ± 0.3
Acetic acid	mg/L	79.0 ± 1.2	50.1 ± 0.9	42.0 ± 2.1	48.6 ± 0.7	46.5 ± 2.1
Propionic acid	mg/L	103.5 ± 2.4	40.1 ± 1.3	33.6 ± 1.7	45.9 ± 1.6	34.8 ± 1.2
Butyric acid	mg/L	0.35 ± 0.01	0.25 ± 0.7	0.18 ± 0.02	0.12 ± 0.3	0.09 ± 0.02

^aTotal elemental carbon.^bTotal elemental hydrogen.^cTotal elemental sulfur.

*Without TP.

TABLE 4 | Total and soluble phenol concentration before and after each TP.

Parameters	Unit	Control*	Thermally treated FW			
			80°C	100°C	120°C	140°C
Total phenol	g/kg	2.8 ± 0.14	2.7 ± 0.1	2.3 ± 0.18	2.26 ± 0.02	2.17 ± 0.007
Soluble phenol	g/kg	0.338 ± 0.03	0.348 ± 0.01	0.384 ± 0.03	0.441 ± 0.11	0.527 ± 0.12

*Without TP.

period, with acetic acid being the dominant VFA under all tested conditions. After 3 day of digestion, the highest total acetate concentration achieved was 2681.5 mg/L for the 80°C TP, followed by 2520.0 mg/L in 140°C TP, 2457.5 mg/L in 120°C TP, 2403.5 mg/L in 100°C TP and 2227.5 mg/L in the control BMP test bottle. The respective concentrations of propionic and butyric acids in these experimental days were 2282.0 and 1526 mg/L for TP at 80°C, 2152.0 and 1504.5 mg/L for TP at 100°C, 2322.0 and 1406.0 mg/L for TP at 120°C, 2328.5 and 1527.0 mg/L for TP at 140°C and 1729.0 and 1607.0 mg/L for the control. Valeric and iso-valeric acid concentrations were found higher for all thermally treated FW compared to the control and were more significant at higher temperatures (**Figure 5**).

In contrast, the pattern of VFAs production and consumption during the BMP tests appeared similar regardless of a thermal pretreatment. The higher concentrations of VFAs in the initial days (days 1–5) were due to the faster hydrolysis and acidification of FW (Li and Jin, 2015). Nonetheless, the concentration of the VFAs did not inhibit the methanogenic activity, as evidenced by the increased methane concentration during these operational days (days 1–5). From day 6 onwards, the VFAs concentration showed a descending trend in all BMP tests (**Figure 5**).

Analysis of the Carbon Balance

Carbon balances for each TP condition were estimated (**Figure 6**) in order to better understand the phenomena occurring during TP of FW. The carbon balance estimations were determined by considering the total elemental carbon (TEC) before and after each TP (**Table 3**) as well as the total COD concentration of the buffer solutions after each TP, according to the following equation:

$$\text{TEC}_{\text{initial}} = \text{TEC}_{\text{after TP}} + \text{TotalCOD}_{\text{buffer}} + \text{others} \quad (2)$$

Where: $\text{TEC}_{\text{initial}}$ = the total elemental carbon concentration of untreated FW $\text{TEC}_{\text{after TP}}$ = the total elemental carbon concentration after TP $\text{Total COD}_{\text{buffer}}$ = the total COD concentration trapped at each TP others = the organic compounds that were lost during the course of TP

The TEC content linearly declined with increasing pretreatment temperatures (**Figure 6** and **Table 3**). The amount of organic compounds trapped in the buffer solution was 1.1, 2.7, 4.5, and 7.4% for TP at 80, 100, 120, and 140°C, respectively. At the TP temperature of 120 and 140°C, relatively higher amounts of organics were lost compared to the lower temperature TPs. This was due to the observed high pressure in the TP bottles at these temperatures.

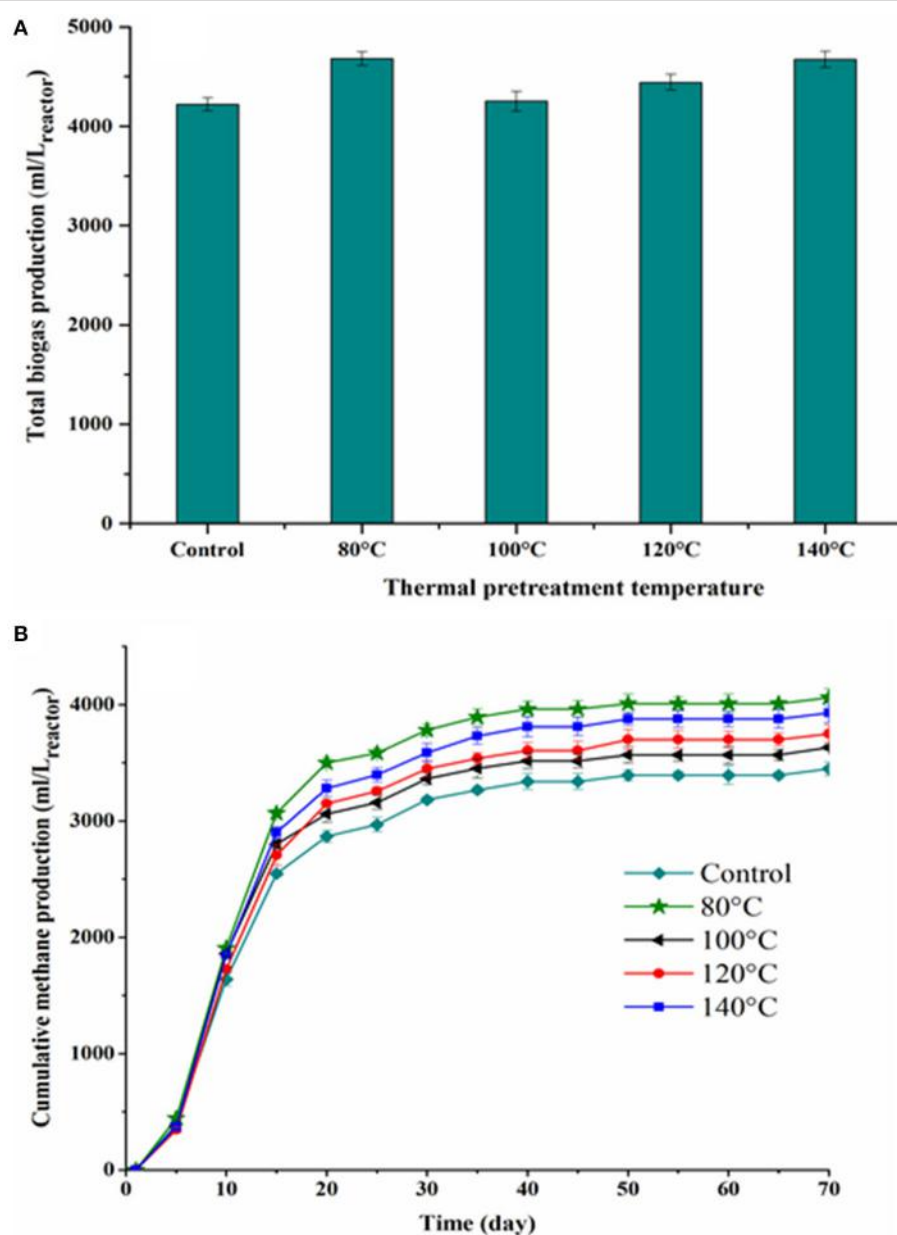


FIGURE 3 | Total biogas production (A) and cumulative methane production as a function of digestion time (B) for each TP.

DISCUSSION

Influence of TP on FW Characteristics

This study demonstrated the influence of TP on the main characteristics of FW. The higher COD solubilization after each TP compared to the control indicates that the TP significantly improved the FW characteristics by promoting the breakdown of complex organic particulates into soluble compounds. The carbohydrate and protein solubilization were also remarkably increased for all TP conditions, achieving a maximum value of 30 and 20% solubilization of the carbohydrate and protein, respectively (Figure 2). These results are also comparable with

previous studies. Marin et al. (2010) obtained an improvement of starch hydrolysis at a temperature of 60–70°C for kitchen waste. Yin et al. (2014) observed an increase of soluble COD from 73.3 to 121.3 g/kg and soluble protein from 1.33 to 21.38 g/kg after hydrothermal pretreatment of FW at 100–200°C. Thermal pretreatment temperatures around 120–121°C have also been found to increase COD solubilization of FW by 19% (Ma et al., 2011) and from 0.86 to 2.6 g/L of soluble COD of cottage cheese waste (Prabhudessai et al., 2014).

The increased solubilization of these compounds compared to the untreated FW could be due to thermal disintegration of the bonds that link the polysaccharides and amino acid strands,

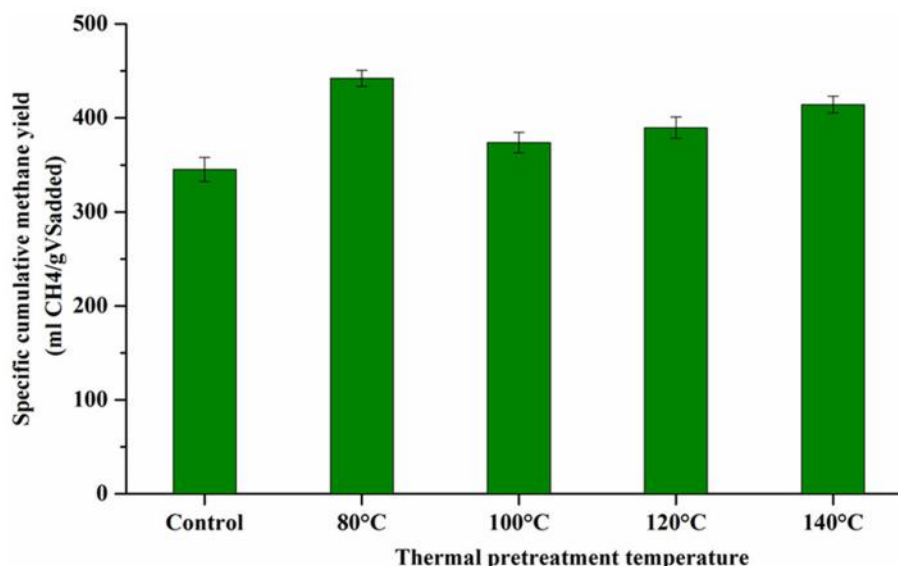


FIGURE 4 | Specific cumulative methane yields for the untreated and thermally pretreated FW.

TABLE 5 | Specific methane yield before and after each TP.

TP temperature	Unit	Before treatment	After treatment
Control	mL/gCOD	256.9 ± 8.9	-
80°C	mL/gCOD	-	316.4 ± 11.4
100°C	mL/gCOD	-	286.7 ± 9.2
120°C	mL/gCOD	-	295.9 ± 12.3
140°C	mL/gCOD	-	314.3 ± 7.7

thus aiding the release of soluble monomers/dimers from the bulk complex structure of FW. Vavouraki et al. (2013) reported that during pretreatment of FW, cleaving of glycoside bonds of carbohydrate polymers occurred and resulted in an increase of the concentration of mono sugars (glucose and fructose).

The carbohydrate solubilization was more favored at lower temperature pretreatments, i.e., 80°C, in contrast to poor protein solubilization at this particular temperature. Indeed, at higher temperatures it could be hypothesized to have a larger amount of soluble monomers of carbohydrates. However, the decrease of the soluble carbohydrate concentration at higher temperatures might be attributed to the formation of complex melanoidin compounds. The production of these compounds was confirmed by the observed turning of color to light brown (data not shown) and scorched flavor during the TP of FW at higher temperatures. Indeed, during higher temperature TPs, soluble monomers of carbohydrates might be involved in Maillard and caramelization reactions, which result in the formation of various flavoring and coloring compounds (Bougrier et al., 2008; Liu et al., 2012). In addition, the formation of these less biodegradable compounds was confirmed by the decrease of methane production at higher TP temperatures. These compounds are heterogeneous polymers characterized by a high-molecular weight that are not only difficult to degrade, but can also inhibit the degradation of other

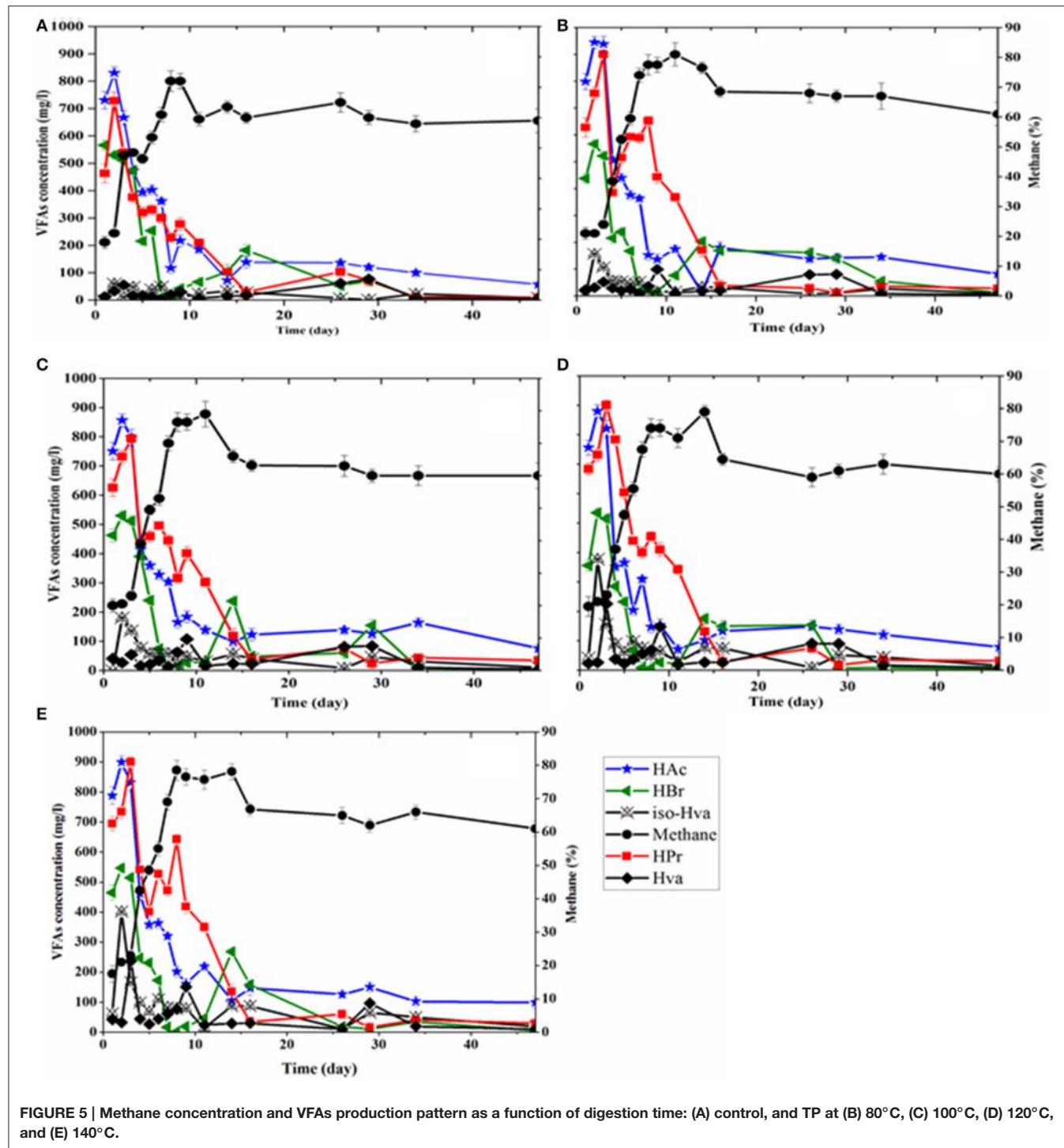
organics by suppressing the methanogenic activity (Tampio et al., 2014).

The loss of organic carbon was smaller (Figure 6) compared to the work of Elbeshbishi et al. (2011), who obtained a decrease of around 12% of the particulate organic fraction after TP of FW at 70°C for 30 min. For all TP investigated, indeed, the proposed new TP set-up succeeded in trapping the evaporated organics in the buffer solution (Figure 6). These results confirmed the feasibility of counteracting one of the negative effects of high temperature TP, i.e., the loss of organics during TP. Considering the scale up of the TP system, the captured organics such as lactic acid and VFAs can be further extracted and valorized for other applications, e.g., in the chemical industry (Wang et al., 2014; Yin et al., 2014), for biopolymer production such as polyhydroxyalkanoates (PHAs) via bacterial strains (Kumar et al., 2016), or biohydrogen production via photofermentation (Ghimire et al., 2015).

Enhancement of Methane and VFA Yields in the BMP Tests

The production of biogas and methane gas from FW was highly facilitated by the TP under all conditions (Figure 4). The highest specific methane yield for the pretreatment temperature of 80°C highlighted the impact of low temperature TP on enhancing the biodegradability of FW. A similar higher methane yield was obtained by Ariunbaatar et al. (2014b) after thermal pretreatment of FW at 80°C for 1.5 h compared to other pretreatment temperatures and times. In another study, Elbeshbishi et al. (2011) observed an improvement of the biogas yield after TP of FW at 70°C for 30 min.

The methane yield with pretreatment temperatures of 120 and 140°C was found higher than with a TP at 100°C, though at these temperatures a decrease of soluble carbohydrate and total COD were observed (Figure 2 and Table 3). However, it should



be noted that the solubilization of other organic molecules, in particular protein, was higher at these temperatures. The results indicate that despite the soluble carbohydrate concentration was lower at these temperatures, there is a positive effect due to the solubilization of protein, resulting in an increase of methane yield. It has been reported in the literature that for substrates containing a high amount of protein, a maximum solubilization

was achieved at higher TP temperatures (Bougrier et al., 2007). Raju et al. (2013) compared thermal pretreatment of pig manure from 100 to 225°C and found a lower methane yield at 100°C and an increasing trend with temperature from 125 until 200°C. Prabhudessai et al. (2014) found around 15% increment in methane yield from thermally treated cottage cheese solid waste at 120°C for 20 min. Strong and Gapes (2012) reported that

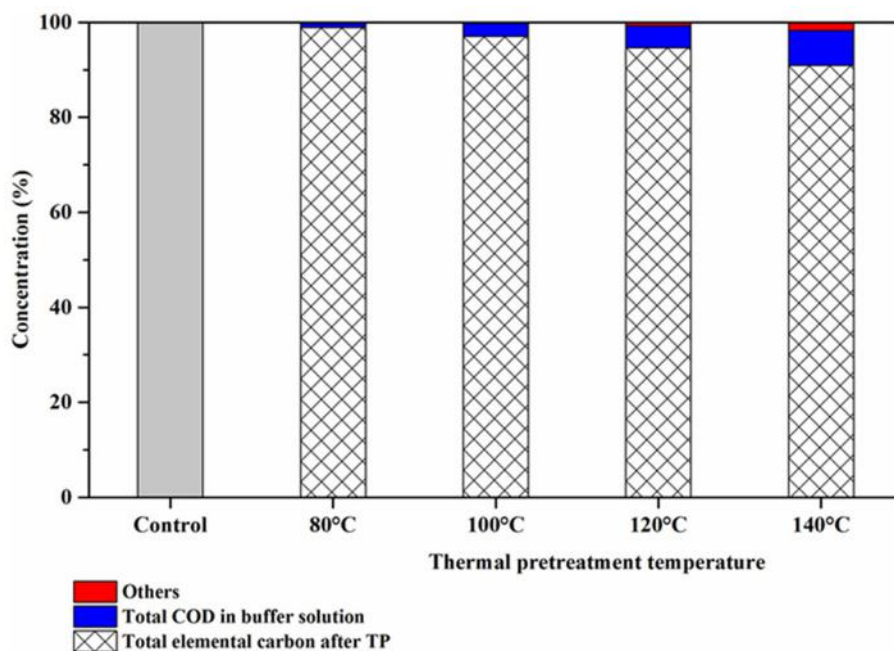


FIGURE 6 | Carbon balance of FW for each TP investigated.

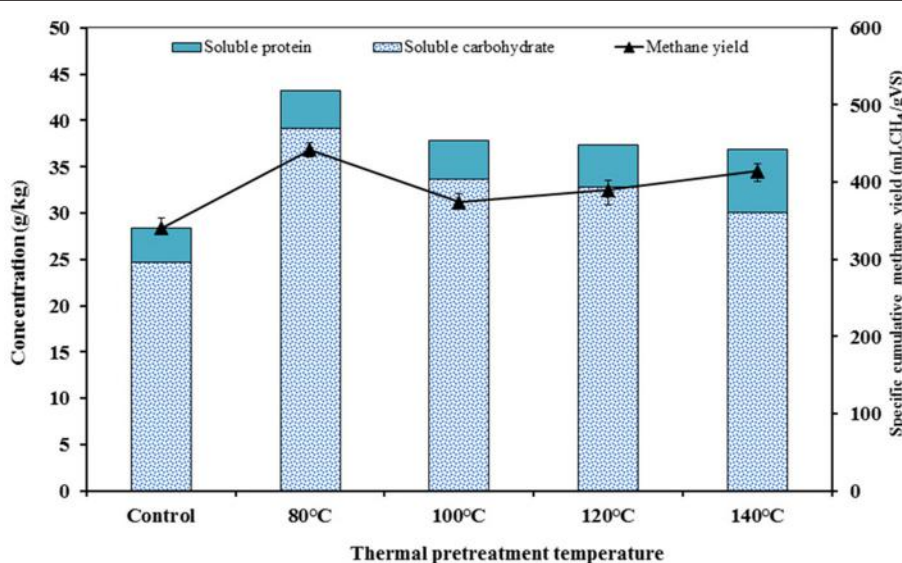


FIGURE 7 | Correlation between the concentration of soluble carbohydrate and soluble protein with the methane yield for each TP investigated.

thermal pretreatment of chicken feathers at 140°C led to a 3.5-fold higher methane yield compared to heating at 70°C.

The formation of inhibitory compounds, i.e., the formation of melanoidin and slight increment of the soluble phenol concentration at higher temperature TP (**Table 4**), did not completely alter the methanogenic activity as confirmed by the higher methane yield compared to the control (**Figures 3, 4**). According to literature data, the inhibitory concentrations of

such compounds are obtained at pretreatment temperatures higher than 150°C (Marin et al., 2010; Liu et al., 2012; Ariunbaatar et al., 2014a). A lower methane yield was achieved after autoclaving FW at 160°C, due to the occurrence of Maillard reactions as evidenced by a dark color and caramelized odor (Tampio et al., 2014).

Considering the VFAs profile during the BMP tests, the higher production of lower molecular weight VFAs (acetic,

propionic and butyric acid, **Figure 5**), could be ascribed to the larger proportion of carbohydrate concentrations present in the FW and its enhanced solubilization after TP (Lim et al., 2008; Wang et al., 2014). The results are consistent with the reports of Li and Jin (2015), who obtained higher concentrations of acetic, propionic and n-butyric acid for thermally treated kitchen waste compared to untreated kitchen waste during the anaerobic fermentation process. The rapid decrease of acetic acid corresponded to the increased methane percentage in the produced biogas in all BMP tests (**Figure 5**), which reflected the dominant activities of acetoclastic methanogens during the BMP tests (Luo et al., 2011). These results in turn suggest the wellbeing and stable operation of the AD process, since 70% of the methane gas in the AD process is derived from acetate that is mainly consumed by acetoclastic methanogens (Wagner et al., 2014; Aydin et al., 2015). The increase of valeric and iso-valeric acid for TP temperatures exceeding 100°C might be due to the higher solubilization of protein after the TPs, as the formation of these VFAs has been associated with degradation of protein compounds (Parawira et al., 2004).

Correlation between Soluble Carbohydrate and Protein Concentration with Methane Yield

The correlation between the concentration of soluble carbohydrate and soluble protein with cumulative methane yield was performed for each TP (**Figure 7**). A direct relationship between soluble carbohydrate/soluble protein and methane yields was obtained in this study. The low temperature TP (80°C) attained the highest methane yield. This was mainly attributed to the increased soluble carbohydrate at this specific temperature coupled to the high amount of carbohydrate in the FW (**Table 3**). However, higher temperature TP (>100°C) had positive effects on solubilization of protein, which also improves the methane yields. Based on this relationship, it is possible to reason out the apparent conflicting results reported in previous studies (Wang et al., 2010; Liu et al., 2012). The efficiency of a TP is the combinatory effect of pretreatment temperature and substrate composition (Carrère et al., 2009; Rincón et al., 2013). The TP of substrates rich in carbohydrate, e.g., FW, was more effective at lower temperature, accelerating the breakdown of complex compounds and increasing the release of soluble monomers. In addition, the lower temperature TP maintained the bioavailability of these soluble monomers for the subsequent enzymatic and biochemical reactions by avoiding the formation of less biodegradable melanoidin compounds. Conversely, when the substrates are characterized by a high protein content, higher temperature TP favored their solubilization and thus improved the methane yields. Similarly, Kondusamy and Kalamdhad

(2014) highlighted that the positive effects of TP were strongly dependent on both pretreatment temperature and substrate composition, and hence a TP should be properly designed to induce the desired positive effects on the AD of FW (Kondusamy and Kalamdhad, 2014).

CONCLUSION

- In this study, a remarkable improvement of organic matter solubilization and methane production of FW was obtained after TP.
- A direct correlation between soluble carbohydrate, soluble protein and methane yields with pretreatment temperature was observed. Lower temperature TP (80°C) was better suited for substrates owing a high carbohydrate content, resulting in the highest soluble carbohydrate concentration and enhanced methane yield.
- This study showed that the loss of organic compounds through evaporation was significantly reduced at lower TP temperature.
- At higher TP temperatures, the solubilization of protein from FW was more favored and melanoidin compounds were formed. However, the amounts of these less biodegradable compounds did not alter the digestion process and methane yields.
- The new proposed TP set-up is promising with several advantages: minimized negative effects of TP (loss of organics and odor emission), simple to implement and able to evaluate the main effects of TP on FW.

AUTHOR CONTRIBUTIONS

MY designed the study, performed the experiments as well as interpreted the data, wrote the manuscript and revised it until its final version. LF participated in designing the study as well as in analyzing the output data and in writing the manuscript. GE, PL, and FP participated in writing the manuscript and revising it critically.

ACKNOWLEDGMENTS

The authors acknowledge the financial support from the European Union (EACEA) under the Erasmus Mundus program of Environmental Technologies for Contaminated Solids, Soils and Sediments (ETeCoS³, grant agreement of FPA No. 2010-0009) and the project of “Modular photo—biologic reactor for bio—hydrogen: application to dairy waste—RE—MIDA” from the Agriculture department of the Campania Region (programme of rural development 2007–2013, Measure 124).

REFERENCES

APHA (1998). *Standard Methods for the Examination of Water and Wastewater, 20th Edn.* Washington, DC: American Public Health Association/American Water Works Association/Water Environment Federation.

- Ariunbaatar, J., Panico, A., Esposito, G., Pirozzi, F., and Lens, P. N. L. (2014a). Pretreatment methods to enhance anaerobic digestion of organic solid waste. *Appl. Energy* 123, 143–156. doi: 10.1016/j.apenergy.2014.02.035
- Ariunbaatar, J., Panico, A., Frunzo, L., Esposito, G., Lens, P. N. L., and Pirozzi, F. (2014b). Enhanced anaerobic digestion of food waste by thermal and

- ozonation pretreatment methods. *J. Environ. Manage.* 146, 142–149. doi: 10.1016/j.jenvman.2014.07.042
- Aydin, S., Ince, B., and Ince, O. (2015). Application of real-time PCR to determination of combined effect of antibiotics on *Bacteria*, *Methanogenic Archaea*, *Archaea* in anaerobic sequencing batch reactors. *Water Res.* 76, 88–98. doi: 10.1016/j.watres.2015.02.043
- Bougrier, C., Delgenès, J. P., and Carrère, H. (2007). Impacts of thermal pre-treatments on the semi-continuous anaerobic digestion of waste activated sludge. *Biochem. Eng. J.* 34, 20–27. doi: 10.1016/j.bej.2006.11.013
- Bougrier, C., Delgenès, J. P., and Carrère, H. (2008). Effects of thermal treatments on five different waste activated sludge samples solubilisation, physical properties and anaerobic digestion. *Chem. Eng. J.* 139, 236–244. doi: 10.1016/j.cej.2007.07.099
- Carlsson, M., Lagerkvist, A., and Morgan-Sagastume, F. (2012). The effects of substrate pre-treatment on anaerobic digestion systems: a review. *Waste Manag.* 32, 1634–1650. doi: 10.1016/j.wasman.2012.04.016
- Carrère, H., Sialve, B., and Bernet, N. (2009). Improving pig manure conversion into biogas by thermal and thermo-chemical pretreatments. *Bioresour. Technol.* 100, 3690–3694. doi: 10.1016/j.biortech.2009.01.015
- Elbeshbishi, E., Hafez, H., Dhar, B. R., and Nakhla, G. (2011). Single and combined effect of various pretreatment methods for biohydrogen production from food waste. *Int. J. Hydrogen Energy* 36, 11379–11387. doi: 10.1016/j.ijhydene.2011.02.067
- Elbeshbishi, E., Nakhla, G., and Hafez, H. (2012). Biochemical methane potential (BMP) of food waste and primary sludge: influence of inoculum pre-incubation and inoculum source. *Bioresour. Technol.* 110, 18–25. doi: 10.1016/j.biortech.2012.01.025
- Esposito, G., Frunzo, L., Liotta, F., Panico, A., and Pirozzi, F. (2012). Bio-methane potential tests to measure the biogas production from the digestion and co-digestion of complex organic substrates. *Open Environ. Eng. J.* 5, 1–8. doi: 10.2174/1874829501205010001
- Ferreira, L. C., Donoso-Bravo, A., Nilsen, P. J., Fdz-Polanco, F., and Pérez-Elvira, S. I. (2013). Influence of thermal pretreatment on the biochemical methane potential of wheat straw. *Bioresour. Technol.* 143, 251–257. doi: 10.1016/j.biortech.2013.05.065
- Ghimire, A., Frunzo, L., Pirozzi, F., Trably, E., Escudie, R., Lens, P. N. L., et al. (2015). A review on dark fermentative biohydrogen production from organic biomass: process parameters and use of by-products. *Appl. Energy* 144, 73–95. doi: 10.1016/j.apenergy.2015.01.045
- Gianico, A., Bruguglia, C. M., Mescia, D., and Mininni, G. (2013). Ultrasonic and thermal pretreatments to enhance the anaerobic bioconversion of olive husks. *Bioresour. Technol.* 147, 623–626. doi: 10.1016/j.biortech.2013.08.054
- Herbert, D., Philippss, P. J., and Strange, R. E. (1971). Carbohydrate analysis. *Meth. Enzymol.* 5B, 265–277.
- Izumi, K., Okishio, Y.-K., Nagao, N., Niwa, C., Yamamoto, S., and Toda, T. (2010). Effects of particle size on anaerobic digestion of food waste. *Int. Biodeterior. Biodegradation* 64, 601–608. doi: 10.1016/j.ibiod.2010.06.013
- Jiang, J., Gong, C., Wang, J., Tian, S., and Zhang, Y. (2014). Effects of ultrasound pre-treatment on the amount of dissolved organic matter extracted from food waste. *Bioresour. Technol.* 155, 266–271. doi: 10.1016/j.biortech.2013.12.064
- Kim, J., Park, C., Kim, T.-H., Lee, M., Kim, S., Kim, S.-W., et al. (2003). Effects of various pretreatments for enhanced anaerobic digestion with waste activated sludge. *J. Biosci. Bioeng.* 95, 271–275. doi: 10.1016/S1389-1723(03)80028-2
- Kondusamy, D., and Kalamdhad, A. S. (2014). Pre-treatment and anaerobic digestion of food waste for high rate methane production- a review. *J. Environ. Chem. Eng.* 2, 1821–1830. doi: 10.1016/j.jece.2014.07.024
- Kumar, P., Ray, S., and Kalia, V. C. (2016). Production of co-polymers of polyhydroxyalkanoates by regulating the hydrolysis of biowastes. *Bioresour. Technol.* 200, 413–419. doi: 10.1016/j.biortech.2015.10.045
- Laurent, J., Casellas, M., Carrère, H., and Dagot, C. (2011). Effects of thermal hydrolysis on activated sludge solubilization, surface properties and heavy metals biosorption. *Chem. Eng. J.* 166, 841–849. doi: 10.1016/j.cej.2010.11.054
- Li, Y., and Jin, Y. (2015). Effects of thermal pretreatment on acidification phase during two-phase batch anaerobic digestion of kitchen waste. *Renewable Energy* 77, 550–557. doi: 10.1016/j.renene.2014.12.056
- Lim, S.-J., Kim, B. J., Jeong, C.-M., Choi, J.-D.-R., Ahn, Y. H., and Chang, H. N. (2008). Anaerobic organic acid production of food waste in once-a-day feeding and drawing-off bioreactor. *Bioresour. Technol.* 99, 7866–7874. doi: 10.1016/j.biortech.2007.06.028
- Liu, X., Wang, W., Gao, X., Zhou, Y., and Shen, R. (2012). Effect of thermal pretreatment on the physical and chemical properties of municipal biomass waste. *Waste Manag.* 32, 249–255. doi: 10.1016/j.wasman.2011.09.027
- Lowry, O. H., Rosebrough, N. J., Farr, A. L., and Randall, R. J. (1951). Protein measurement with the Folin phenol reagent. *J. Biol. Chem.* 193, 265–275.
- Luo, G., Xie, L., Zhou, Q., and Angelidaki, I. (2011). Enhancement of bioenergy production from organic wastes by two-stage anaerobic hydrogen and methane production process. *Bioresour. Technol.* 102, 8700–8706. doi: 10.1016/j.biortech.2011.02.012
- Ma, J., Duong, T. H., Smits, M., Verstraete, W., and Carballa, M. (2011). Enhanced biomethanation of kitchen waste by different pre-treatments. *Bioresour. Technol.* 102, 592–599. doi: 10.1016/j.biortech.2010.07.122
- Marin, J., Kennedy, K. J., and Eskicioglu, C. (2010). Effect of microwave irradiation on anaerobic degradability of model kitchen waste. *Waste Manag.* 30, 1772–1779. doi: 10.1016/j.wasman.2010.01.033
- Marin, J., Kennedy, K. J., and Eskicioglu, C. (2011). Enhanced solubilization and anaerobic biodegradability of source-separated kitchen waste by microwave pre-treatment. *Waste Manag. Resour.* 29, 208–218. doi: 10.1177/0734242X10362705
- Minale, M., and Worku, T. (2014). Anaerobic co-digestion of sanitary wastewater and kitchen solid waste for biogas and fertilizer production under ambient temperature: waste generated from condominium house. *Int. J. Environ. Sci. Technol.* 11, 509–516. doi: 10.1007/s13762-013-0255-7
- Parawira, W., Murto, M., Read, J. S., and Mattiasson, B. (2004). Volatile fatty acid production during anaerobic mesophilic digestion of solid potato waste. *J. Chem. Technol. Biotechnol.* 79, 673–677. doi: 10.1002/jctb.1012
- Phillips, K. M., Tarrago-Trani, M. T., Grove, T. M., Grün, I., Luggogo, R., Harris, R. F., et al. (1997). Simplified gravimetric determination of total fat in food composites after chloroform-methanol extraction. *J. Am. Oil Chemist. Soc.* 74, 137–142. doi: 10.1007/s11746-997-0158-1
- Prabhudessai, V., Salgaonkar, B., Braganca, J., and Mutnuri, S. (2014). Pretreatment of cottage cheese to enhance biogas production. *Biomed. Res. Int.* 2014:374562. doi: 10.1155/2014/374562
- Raju, C. S., Sutaryo, S., Ward, A. J., and Möller, H. B. (2013). Effects of high-temperature isochoric pre-treatment on the methane yields of cattle, pig and chicken manure. *Environ. Technol.* 34, 239–244. doi: 10.1080/09593330.2012.689482
- Rincón, B., Bujalance, L., Fermoso, F. G., Martín, A., and Borja, R. (2013). Biochemical methane potential of two-phase olive mill solid waste: influence of thermal pretreatment on the process kinetics. *Bioresour. Technol.* 140, 249–255. doi: 10.1016/j.biortech.2013.04.090
- Soliman, M. G., Pelaz, B., Parak, W. J., and del Pino, P. (2015). Phase transfer and polymer coating methods toward improving the stability of metallic nanoparticles for biological applications. *Chem. Mater.* 27, 990–997. doi: 10.1021/cm5043167
- Strong, P. J., and Gapes, D. J. (2012). Thermal and thermo-chemical pre-treatment of four waste residues and the effect on acetic acid production and methane synthesis. *Waste Manag.* 32, 1669–1677. doi: 10.1016/j.wasman.2012.04.004
- Strong, P. J., McDonald, B., and Gapes, D. J. (2011). Combined thermochemical and fermentative destruction of municipal biosolids: a comparison between thermal hydrolysis and wet oxidative pre-treatment. *Bioresour. Technol.* 102, 5520–5527. doi: 10.1016/j.biortech.2010.12.027
- Tampio, E., Ervasti, S., Paavola, T., Heaven, S., Banks, C., and Rintala, J. (2014). Anaerobic digestion of autoclaved and untreated food waste. *Waste Manag.* 34, 370–377. doi: 10.1016/j.wasman.2013.10.024
- Vavouraki, A. I., Angelis, E. M., and Kornaros, M. (2013). Optimization of thermo-chemical hydrolysis of kitchen wastes. *Waste Manag.* 33, 740–745. doi: 10.1016/j.wasman.2012.07.012
- Vavouraki, A. I., Volioti, V., and Kornaros, M. E. (2014). Optimization of thermo-chemical pretreatment and enzymatic hydrolysis of kitchen wastes. *Waste Manag.* 34, 167–173. doi: 10.1016/j.wasman.2013.09.027

- Wagner, A. O., Reitschuler, C., and Illmer, P. (2014). Effect of different acetate:propionate ratios on the methanogenic community during thermophilic anaerobic digestion in batch experiments. *Biochem. Eng. J.* 90, 154–161. doi: 10.1016/j.bej.2014.05.014
- Wang, K., Yin, J., Shen, D., and Li, N. (2014). Anaerobic digestion of food waste for volatile fatty acids (VFAs) production with different types of inoculum: effect of pH. *Bioresour. Technol.* 161, 395–401. doi: 10.1016/j.biortech.2014.03.088
- Wang, W., Hou, H., Hu, S., and Gao, X. (2010). Performance and stability improvements in anaerobic digestion of thermally hydrolyzed municipal biowaste by a biofilm system. *Bioresour. Technol.* 101, 1715–1721. doi: 10.1016/j.biortech.2009.10.010
- Xue, Y., Liu, H., Chen, S., Dichtl, N., Dai, X., and Li, N. (2015). Effects of thermal hydrolysis on organic matter solubilization and anaerobic digestion of high solid sludge. *Chem. Eng. J.* 264, 174–180. doi: 10.1016/j.cej.2014.11.005
- Yin, J., Wang, K., Yang, Y., Shen, D., Wang, M., and Mo, H. (2014). Improving production of volatile fatty acids from food waste fermentation by hydrothermal pretreatment. *Bioresour. Technol.* 171, 323–329. doi: 10.1016/j.biortech.2014.08.062
- Zhang, C., Su, H., Baeyens, J., and Tan, T. (2014). Reviewing the anaerobic digestion of food waste for biogas production. *Renewable Sustainable Energy Rev.* 38, 383–392. doi: 10.1016/j.rser.2014.05.038
- Zhou, Y., Takaoka, M., Wang, W., Liu, X., and Oshita, K. (2013). Effect of thermal hydrolysis pre-treatment on anaerobic digestion of municipal biowaste: a pilot scale study in China. *J. Biosci. Bioeng.* 116, 101–105. doi: 10.1016/j.jbiosc.2013.01.014

Conflict of Interest Statement: The authors declare that the research was conducted in the absence of any commercial or financial relationships that could be construed as a potential conflict of interest.

Copyright © 2016 Yeshanew, Frunzo, Lens, Pirozzi and Esposito. This is an open-access article distributed under the terms of the Creative Commons Attribution License (CC BY). The use, distribution or reproduction in other forums is permitted, provided the original author(s) or licensor are credited and that the original publication in this journal is cited, in accordance with accepted academic practice. No use, distribution or reproduction is permitted which does not comply with these terms.



Significance of Vivianite Precipitation on the Mobility of Iron in Anaerobically Digested Sludge

Jimmy Roussel * and Cynthia Carliell-Marquet

Civil Engineering, School of Engineering, College of Engineering and Physical Sciences, University of Birmingham, Birmingham, UK

OPEN ACCESS

Edited by:

Kartik Chandran,
Columbia University, USA

Reviewed by:

Bharath Prithiviraj,
MetaSUB Consortium, USA
Seung Gu Shin,
Pohang University of Science and
Technology, South Korea

***Correspondence:**

Jimmy Roussel
j.roussel@bham.ac.uk

Specialty section:

This article was submitted to
Microbiotechnology, Ecotoxicology
and Bioremediation,
a section of the journal
Frontiers in Environmental Science

Received: 22 December 2015

Accepted: 29 August 2016

Published: 13 September 2016

Citation:

Roussel J and Carliell-Marquet C
(2016) Significance of Vivianite
Precipitation on the Mobility of Iron in
Anaerobically Digested Sludge.
Front. Environ. Sci. 4:60.
doi: 10.3389/fenvs.2016.00060

Anaerobic digestion requires a balanced availability of micro-nutrients with ideal growth conditions to reach optimal organic degradation and biogas production. Iron is the most abundant of the essential metals in an anaerobic digester and its mobility has a strong impact on microorganisms through its own bioavailability, but also through its influence on the bioavailability of other metals. Most previous research on iron mobility in anaerobic digestion has focused on sulfide as the controlling anion because digesters traditionally are sulfide rich and phosphate poor. However, chemical phosphorus removal (CPR) at wastewater treatment works (WWTW) can elevate phosphate concentrations in the digester 10-fold or more. The goal of this research was hence to examine the accepted wisdom of iron-sulfide dominance prevailing in all anaerobic digesters and by evaluating the potential for iron phosphate formation in municipal digesters treating CPR sludge. To fulfill this aim, iron compounds were identified experimentally from full-scale digesters at WWTW with CPR and the most likely iron species identified through modeling according to their thermodynamic probability of formation under the specific environmental conditions experienced in each anaerobic digester. Experimental and modeling data were then combined to identify the main chemical reactions controlling iron mobility in those anaerobic digesters. Results show that speciation of iron in the sampled anaerobic digesters was controlled by the solid phase through a primary reaction (sulfide precipitation to form pyrite and ferrous sulfide) and secondary reaction (phosphate precipitation to form vivianite). However, iron-sulfide precipitates represented only 10–30% of the total iron in the sampled digesters, while iron-phosphate precipitates represented more than 70%. The significance of the high quantity of vivianite in these digesters is that phosphate-rich anaerobic digesters will be more iron-mobile environments than sulfide-rich digesters, with iron being more readily exchanged between the solid and liquid phases during digestion, implying a higher level of bioavailability and the tendency to interact more readily with organic and inorganic counterparts.

Keywords: iron bioavailability, vivianite, anaerobic digestion, chemical phosphorus removal, sulfide, phosphate, equilibrium speciation modeling

INTRODUCTION

In the development of self-sustainable wastewater treatment plants, anaerobic digestion (AD) is a key process to reduce waste and produce renewable energy. The balanced availability of macro- and micro-nutrients, coupled with ideal growth conditions, is essential for a healthy anaerobic digester (Gustavsson, 2012). Any disruption of one of those factors can disturb the activity of micro-organisms and lead to the failure of the system. Some metals (such as iron, manganese, copper, cobalt, nickel, and zinc) are part of the essential micro-nutrients required for the well-being of the anaerobic digester and their presence, in a bioavailable form, are indispensable to reach the optimal performance of the anaerobic digester (Schattauer et al., 2011).

The bioavailability of metals is still the subject of considerable investigation both in natural and engineered ecosystems, but research to date generally agrees that most of the dissolved metals and a portion of weakly-bound metals (for example, biosorption) could be considered as available for microorganisms (Worms et al., 2006; Fuentes et al., 2008; Marcato et al., 2009). In the AD, metals undergo a complex series of reactions in the sludge matrix including sorption, complexation, or precipitation processes, influencing their speciation. Most of the metals are bound in the solid phase as precipitates or chelates (Oleszkiewicz and Sharma, 1990) and strongly bound compounds are unavailable for micro-organisms. However, weakly bound compounds can break down and release metals into the liquid phase, establishing a reserve of available metals. Any study of metal bioavailability must then consider the potential of a metals reserve moving from the solid phase to the liquid phase as the more readily bioavailable metals are removed by microbial activity and the equilibrium of the system shifts (Hassler et al., 2004; Jansen et al., 2007).

Iron is the most abundant of the essential metals in an anaerobic digester and hence, by virtue of its high concentration, may influence the speciation of other trace metals present in the digester by competing for the primary chemical reactions. Metcalf & Eddy Inc. (2003) report that the median concentration of iron in wastewater sludge is 17 g/kg Dried Solid (DS), 10 times higher than the median concentration of the second highest heavy metal, zinc, at 1.7 g/kg DS. Moreover, the iron concentration in anaerobic sludge digesters at municipal wastewater treatment works (WWTW) is often increased further by iron dosing for chemical phosphorus removal (CPR) and/or hydrogen sulfide control (Carliell-Marquet et al., 2010; Zhang et al., 2010). The establishment of a phosphorus limit discharge by Urban Wastewater Treatment Directive encouraged the development of CPR in the main WWTW in the UK. Carliell-Marquet et al. (2010) estimated that 300 WWTWs were removing phosphorus chemically in 2010 and this number was projected to increase to over 600 WWTWs by 2015 (Vale, 2012).

Iron, as most other metals in an anaerobic digester, should principally react with sulfide to form insoluble salts; sulfide precipitates being commonly accepted as the main thermodynamically stable compounds formed under anaerobic conditions (Callander and Barford, 1983; Morse and Luther, 1999; Zhang et al., 2010; Shakeri Yekta et al., 2014a). The

two main iron sulfide compounds observed are pyrite (FeS_2) and amorphous FeS (Kaksonen et al., 2003; van der Veen et al., 2007). Under anaerobic digestion conditions, pyrite is predicted to be the most stable inorganic precipitate when following the Pourbaix diagram (Pourbaix, 1963; Nielsen et al., 2005). However, pyritisation is a slow process and needs a reduction potential below -200 mV , so the formation of metastable amorphous FeS is likely to occur as a precursor to the transformation to pyrite (Nielsen et al., 2005). Other iron-sulfide precipitates have been detected in anaerobic digesters such as greigite (Fe_3S_4), mackinawite (monocrystalline FeS), and pyrrhotite (Fe_{1-x}S) (Jong and Parry, 2004; Dewil et al., 2009; Gustavsson, 2012).

Anaerobic digesters are traditionally sulfide rich and phosphate poor, but phosphorus recovery processes at WWTW can elevate phosphate concentrations in a digester 10-fold or more (Carliell-Marquet et al., 2010). When iron is dosed to co-precipitate phosphorus in activated sludge plants prior to AD, it results in ion-rich feed sludge entering the digester. Once in the digester, reduction of ferric ions to ferrous ions under anaerobic condition disturbs all the Fe(III) binding. The change from trivalent to divalent iron species implies the formation of new thermodynamically stable compounds for iron such as pyrite (FeS_2) or vivianite ($\text{Fe}_3(\text{PO}_4)_2 \cdot 8\text{H}_2\text{O}$). Researchers that have studied the fate of iron in anaerobic digesters treating such iron-rich CPR sludge have indeed speculated that a not negligible quantity of iron would continue to be bound with phosphate in the anaerobic digester to form ferrous phosphate precipitates (Miot et al., 2009; Carliell-Marquet et al., 2010), with phosphate effectively competing with sulfide to precipitate iron. The formation of the proposed iron-phosphate precipitates goes against theories of thermodynamic evolution, but can be hypothesized from an availability/kinetic point of view. Zhang et al. (2009) and Miot et al. (2009) suggested that the phosphate creates a bulk phase around the iron (II) which limits sulfide's availability for precipitation of iron and favors the formation of ferrous phosphate.

As the bioavailability of metals is not only dependent on their concentration in the sludge but on their speciation, the potential of phosphate to compete with sulfide for iron precipitation, could have an important impact on the bioavailability of iron in anaerobic digesters. The presence of vivianite or other iron-phosphate precipitates (weaker compounds than sulfide precipitates) in significant quantities, will change the overall speciation of iron in an anaerobic digester and so its behavior, potentially increasing iron mobility/availability for the microbial community.

The primary goal of this research was hence to examine the accepted wisdom of iron-sulfide dominance prevailing in all anaerobic digesters, by evaluating the potential for iron phosphate formation in municipal anaerobic digesters treating CPR sludge. To fulfill this aim, iron compounds were identified from full-scale digesters at WWTW to determine the main iron species according to their thermodynamic probability of formation under the specific environmental conditions experienced in each anaerobic digester. Experimental and modeling data were then combined to identify the main

chemical reactions controlling iron mobility in those anaerobic digesters.

MATERIALS AND METHODS

Sludge Collection

Seven UK WWTW were chosen for this experiment to obtain a wide range of iron concentrations in anaerobically digested sludge. Three types of sites were chosen; non-iron dosed sludge (NID), mixed sludge (MS), and iron dosed sludge (ID). The ratio primary:secondary sludge was around 60:40 across the seven anaerobically digested sludge and some digesters parameter are shown in **Table 1**. The three mixed sludge were taken from a digester receiving CPR sludge from the WWTW and imported no-iron dosed sludge from other WWTWs. The percentage of imported sludge for MS1-3 varied from 9 to 25%. The CPR was mostly accomplished by the dosage of iron chloride (FeCl_3).

Sludge samples were collected directly from anaerobic digesters and kept sealed in a hermetic container during transport, after which the liquid and solid phases were separated by centrifugation (6000 rpm for 10 min). The solid phase was stored in polyethylene bottles at 4°C . The liquid phase was filtered at $0.45 \mu\text{m}$ and stored in polyethylene bottles at 4°C .

Metals Extraction

The total acid digestion method used an Aqua Regia solution ($\text{HCl}:\text{HNO}_3$ 3:1, 50% dilution, Heated 110 – 115°C) to dissolve all the metal compounds present in the sludge; as per Standard Methods (3030F, APHA-AWWA-WEF, 1985) and modified by Roussel (2013). Sequential extraction methods used in this

research followed the modified BCR procedure described by Chao et al. (2006). The extractions were carried out with analytical grade reagents over a period of 4 days, in triplicate. The order of applied reagents in the BCR sequential extraction is: (1) weak acids, (2) reducing agent, (3) oxidizing agent, and (4) strong acid and so the four fractions produced from the BCR sequential extraction are classified as: (1) exchangeable, (2) reducible, (3) oxidisable, and (4) residual (**Figure 1**).

Metals Analysis

Flame atomic absorption spectroscopy (FAAS; Perkin Elmer AAS 800) was used to measure the concentration of iron at the absorption wavelength 248.3 nm. The calibration curves were calculated before any sample analysis and standard solutions were freshly made and diluted from a 1000 ppm standard iron solution provided by Fisher®. Calibration curves were only accepted with a correlation coefficient of 0.999 and standard solutions were used as control (10% error) for every 10 samples.

Scanning electron microscopy coupled with energy dispersive X-ray spectroscopy (SEM-EDS) requires dry compounds for analysis and so a fraction of the solid phase was dried at 105°C before being ground. The powdered compound was applied on an analytical disc and fixed with a carbon spray (carbon coated).

The microscope, XL-30 (with LaB6 filament) provided by Philips®, was fitted with a HKL EBSD system with NordlysS camera to obtain electron backscattering pictures to observe elements with high atomic number in the samples. The microscope was also fitted with INCA EDS system provided by Oxford Instrument to do microanalysis on the sample using

TABLE 1 | Sludge elemental composition and chemical model input values.

Iron dosing	Non-Iron Dosed (NID)		Mixed Sludge (MS)			Iron Dosed (ID)	
	1	2	1	2	3	1	2
Sludge							
Sludge conditions	pH	7.4	7.3	7.2	7.2	7.1	7.3
	ORP (mV)	-345	-330	-290	-280	-330	-260
	Digester capacity (m^3)	7000	9000	83,000	6000	11,000	11,000
	Biogas (m^3/h)	185	490	3900	155	465	300
	TS/VS (g/l)	18/13	22/15	23/16	23/15	21/15	20/14
	Alkalinity (g CaCO_3/l)	3.5	4.8	5.2	4.2	5.6	3.9
Metals (mmol/l)	Co	0.024	0.024	0.023	0.021	0.029	0.025
	Cu	0.16	0.090	0.11	0.17	0.085	0.13
	Fe	3.5	3.6	6.8	7.1	8	8.5
	Mn	0.13	0.13	0.26	0.079	0.087	0.11
	Ni	0.38	0.40	0.43	0.44	0.36	0.45
	Zn	0.22	0.18	0.50	0.19	0.27	0.25
Cations/Anions (mmol/l)	Ca	8.8	9.6	10.5	10.5	11.9	9.7
	K	2.6	2.3	2.3	2.7	2.5	2.8
	Mg	4.2	4.4	4.8	5.1	5.3	4.7
	Na	9.7	9.9	9.1	9.3	9.4	9.5
	P	13.9	13.2	14.1	15.6	15.8	15.1
	S	5.9	5.5	5.5	4.4	4.2	5.5

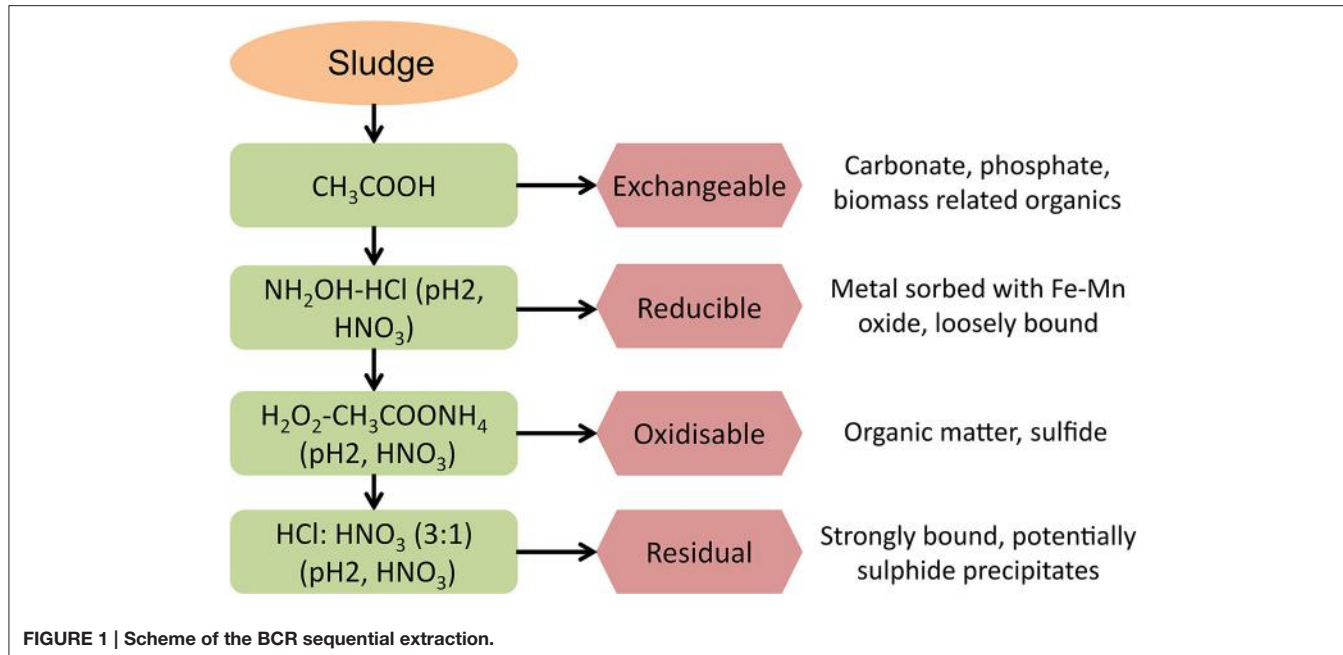


FIGURE 1 | Scheme of the BCR sequential extraction.

X-ray spectroscopy. The spectrum of energy analyzed during the scan was 0–9.5 keV.

Chemical Modeling

The chemical environments of the seven anaerobic digesters were simulated using Phreeqc with the database minteq.v4 (USGS). Experimental values (element concentrations and sludge conditions) used as input values are detailed in **Table 1**. Each element was entered in the liquid phase in its atomic form; its speciation then being predicted based on the environmental input values and the exchanges/reactions allowed in the simulation, as detailed below.

The parameters described in the Phreeqc, which represented the anaerobic digester conditions, were limited to temperature, electric potential (pe) and pH. The input pH was 8–8.2 to allow a potential charge balance during the simulation and produced an output pH value agreeing with the measured pH of each sludge (7.1–7.4). The input potential electric (pe) was −6.7 to ensure anaerobic condition and avoid any oxidation during the simulation.

Phreeqc was limited to simulating inorganic reactions, with no organic complexation or biomass adsorption. The only exchange between phases allowed in this simulation was solid-liquid and no consideration of the gas composition or potential H₂S exchange was considered. The exchange between solid-liquid phases was controlled by the saturation index of each precipitate (Roussel, 2013).

RESULTS

BCR Sequential Extraction

Iron concentrations in the solid phase of the seven anaerobic digesters sampled were in the range 9.7–28.8 g/kg DS using the

sum of the sequential extraction fractions and from 12.6 to 33 g/kg DS using total acid digestion (**Table 2**). An increase in total iron concentration of the digested sludge was observed when CPR processes influenced the digester sludge composition either through imported iron-dosed sludge being fed to the digester (MS), or when CPR was directly integrated into the WWTW (ID).

It should also be noted that in all cases a loss of material was observed during the BCR sequential extraction; the recovery of iron (measured as the sum of the extracted fractions) ranged from 77 to 89% of the total iron concentration measured by the acid digestion procedure. This has also been reported by other researchers using the BCR sequential extraction procedure; 87% recovery was reported by Fuentes et al. (2008) in their research, which is comparable to the 85% average recovery found in this research. Finally, the concentration of iron in the liquid phase increased with the concentration of total iron in the solid phase from 0.3 mg/l for NID sludge to 0.6 mg/l for ID sludge (**Table 2**). The amount of iron present in the liquid phase represents around 0.1% of the total iron and the results were lower than the range of 0.5–4% suggested by Oleszkiewicz and Sharma (1990). The Pearson product-moment correlation coefficient was calculated between the concentration of iron in the liquid phase and the total iron concentration to statically confirm any linear correlation. The Pearson coefficient was 0.928 ($p = 0.003$) confirming a positive linear correlation between the variables, meaning that the concentration of soluble iron increases with the total concentration.

The BCR exchangeable fraction (first extracted fraction) represented the main iron fraction in all digested sludge samples, with more than 50% of the total iron extracted in this fraction and a maximum of 76% obtained for the sludge ID2 (**Figure 2** and **Table 2**). This is in contrast to (last) fraction of sequential

TABLE 2 | Concentrations of iron in each BCR sequential extraction fraction and total acid digestion (T.A.D.) for the 7 anaerobically digested sludge.

Sludge	Soluble mg/l	Exchangeable	Reducible	Oxidisable	Residual	Σ fractions g/kg DS	T.A.D
		g/kg DS					
NID1	0.35 ± 0.21	5.2 ± 0.8	2.0 ± 0.6	<d.l.	2.4 ± 0.1	9.7 ± 1.2	12.6 ± 0.3
NID2	0.34 ± 0.06	6.2 ± 0.6	1.6 ± 0.1	<d.l.	2.4 ± 0.2	10.2 ± 0.7	13.1 ± 1.0
MS1	0.47 ± 0.19	11.9 ± 0.7	3.5 ± 0.4	<d.l.	3.5 ± 0.6	18.9 ± 1.3	21.3 ± 2.6
MS2	0.49 ± 0.25	13.4 ± 0.6	4.2 ± 0.5	<d.l.	2.2 ± 0.2	19.8 ± 0.8	22.6 ± 0.8
MS3	0.57 ± 0.37	15.0 ± 0.6	5.3 ± 1.0	<d.l.	2.2 ± 0.3	22.5 ± 1.9	26.4 ± 1.1
ID1	0.64 ± 0.06	15.8 ± 0.5	3.8 ± 0.8	<d.l.	4.3 ± 0.3	24.0 ± 0.9	27.3 ± 2.4
ID2	0.58 ± 0.02	23.5 ± 0.8	2.6 ± 0.3	<d.l.	2.7 ± 0.1	28.8 ± 0.9	33.0 ± 1.5

The concentrations are expressed as mean ± standard deviation ($n = 6$).

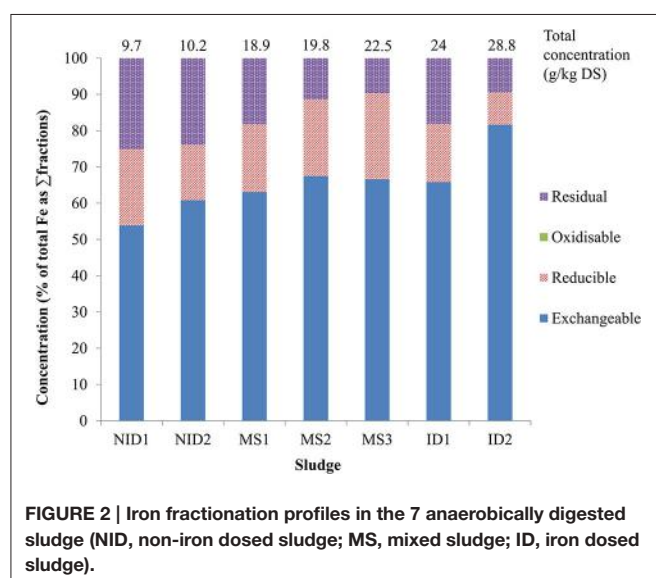


FIGURE 2 | Iron fractionation profiles in the 7 anaerobically digested sludge (NID, non-iron dosed sludge; MS, mixed sludge; ID, iron dosed sludge).

extraction schemes (Alvarez et al., 2002; van der Veen et al., 2007; Fuentes et al., 2008). However, Carliell-Marquet et al. (2010) and Dodd et al. (2000) found comparable results to those obtained during this research, with a high percentage of iron reported to be recovered in the first steps of the sequential extraction procedures (exchangeable and reducible fractions). The variation in iron extractability being reported by different researchers sampling different anaerobic digesters supports the argument that iron mobility can change markedly depending on the particular environmental conditions of each anaerobic digester. Notably, the concentration of iron extracted in the early fractions is heavily influenced by the presence of iron-phosphate rich CPR sludge in a digester. NID 1&2 sludge had 5.2 and 6.2 g/kg DS of iron extracted in the exchangeable fraction whereas 11.9–15.0 g/kg DS of iron was extracted in the same fraction in MS sludge and kept increasing to 23.5 g/kg DS for ID2. This linear correlation was statically confirmed by a Pearson coefficient between the iron extracted in the exchangeable fraction and the total iron (as sum of BCR fractions) of 0.984 ($p = 0.000$).

The BCR sequential extraction procedure cannot be used to determine the exact metal species extracted in each fraction;

so the presence of iron in the exchangeable fraction could result from dissolution of iron-carbonate or iron-phosphate precipitates or even the exchange of weakly bound iron from organic sites on the sludge matrix. In this research, vivianite was identified as one of the main compounds dissolved in the BCR exchangeable fraction, through the use of: SEM-EDS analysis, chemical equilibrium speciation modeling of the different AD environments, previous published research, and thermodynamic constants (Ofverstrom et al., 2011; Cheng et al., 2015).

Iron was also extracted in two other BCR sequential extraction fractions: the reducible and residual fractions, which represented each between 9 and 25% of the total iron. The concentration of iron in the BCR reducible fraction was between 2.0 g/kg DS (NID1) and 5.3 g/kg DS (MS3). No specific pattern was observed in the variation of iron extracted in the reducible fraction when compared with either the total iron concentration or the anaerobic digester environmental conditions (Pearson coefficient of 0.539; $p = 0.211$). Cheng et al. (2015) suggested that trivalent iron entering a digester in the feed sludge would not necessarily be reduced during the anaerobic digestion period in spite of the low oxidation-reduction potential of the anaerobic environment, if Fe(III) entered the digester as a well-ordered crystalline structure. This might occur, for example, when iron is dosed into an activated sludge process with a long sludge age, giving ample time for maturation of the crystalline ferric structure. Hence, the presence of ferric precipitates in the digested sludge should not be discounted as a possible contributing factor to the iron extracted during the reducible BCR fraction. Another hypothesis is that most Fe (III) entering an anaerobic digester is indeed reduced to Fe (II), leading to the rapid formation of ferrous phosphate or ferrous-hydroxyl-phosphate compounds (possibly amorphous; as suggested by Smith and Carliell-Marquet, 2009) that would then be readily dissolved by the low pH 2 of the reagent used in the second BCR extraction.

The iron concentration in the BCR residual fraction varied between 2.4 g/kg DS (NID1 and NID2) and 4.3 g/kg DS (ID1). As for the reducible fraction, no pattern was established between the concentration of iron extracted in the residual fraction and the total iron concentration of the digested sludge (Pearson coefficient of 0.298; $p = 0.516$). The iron extracted in the residual fraction was identified to be bound with sulfide and precipitated as pyrite or ferrous sulfide (SEM-EDS analysis).

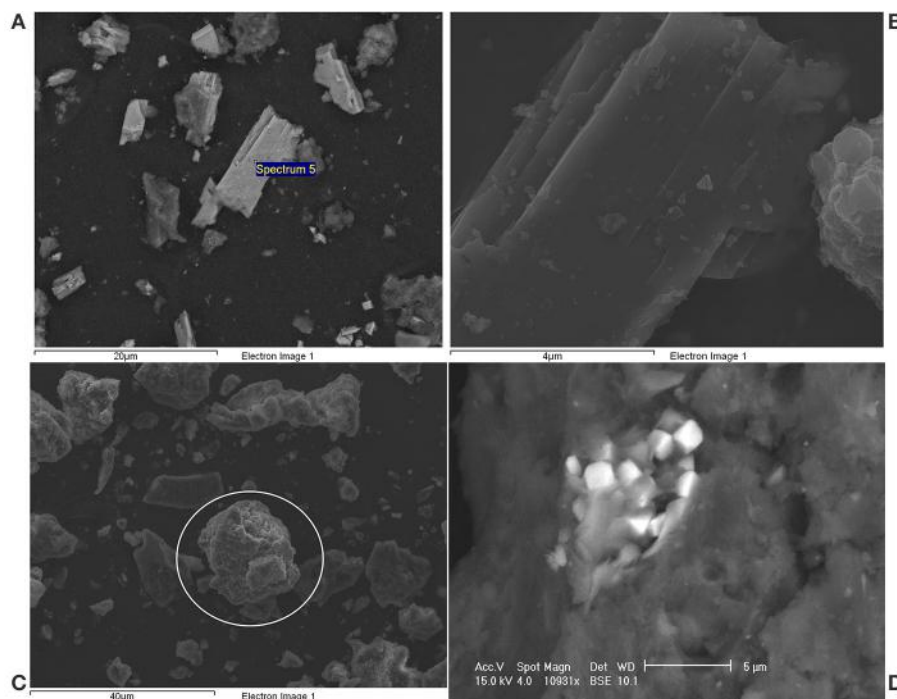


FIGURE 3 | Pictures of iron precipitates detected in anaerobically digested sludge by SEM-EDS. (A,B) Vivianite, (C) Ferrous sulphide, (D) Pyrite.

Sulfide precipitates are expected to be extracted in the oxidisable BCR fraction (Chao et al., 2006) but van der Veen et al. (2007) demonstrated that those precipitates were not systematically extracted in the oxidisable fraction and could be carried over to the residual fraction. In this research, measurement of the sulfur concentration in the different BCR sequential extraction fractions showed the presence of a high sulfur concentration in the residual fraction; suggesting that iron sulfide precipitates in the digested sludge were indeed being dissolved in this fraction, rather than the oxidisable fraction (Roussel, 2013); with concentrations of iron in the oxidisable BCR fractions below the detection limit and recorded as nil (Table 2).

SEM-EDS Analysis

SEM-EDS analysis was performed on the solid phase of each sludge to obtain information on the iron species present in it. Ferrous phosphate and ferrous sulfide were the two main types of precipitates observed during the analysis and are described below (Figure 3 and their corresponding elemental compositions are given in Table 3). Several ferrous phosphate compounds were detected (Roussel, 2013) but the main compound was vivianite and it was observed in every AD sludge studied (compounds A and B, Figure 3). Vivianite was identified by stoichiometric analysis and corroborated by crystallographic analysis (Roussel, 2013). Three main elements (Fe, O, and P) were detected in compound A and B (Table 3) with a respective atomic percent of 13, 72, and 12 while Mg and Ca were also detected at low concentrations (1%). In order to simplify the stoichiometric analysis, Mg and Ca were included with the iron percentage

TABLE 3 | Elemental analysis of the iron precipitates observed in the Figure 3.

Compound (Figure 3)	Element concentration (as atomic percent)						
	Ca	Fe	Mg	O	P	S	Si
A	1	16	1	70	12		
B	1	13	1	74	11		
C		43		14		43	
D		31				68	1

as interchangeability between those cations and iron has been suggested by Nriagu (1972) and De Vrieze et al. (2013) for phosphate precipitation. Then three modified ratios Fe /P: 1.5, O/Fe: 5, and O/P: 7 gave the formula $\text{Fe}_3\text{P}_2\text{O}_{14.5}$ written as $\text{Fe}_3(\text{PO}_4)_2 \cdot 6.5\text{H}_2\text{O}$. Loss of water in the molecule in comparison with the vivianite formula ($\text{Fe}_3(\text{PO}_4)_2 \cdot 8\text{H}_2\text{O}$) was likely to have occurred during the drying phase of the sample preparation for SEM-EDS. Frost et al. (2003) showed that natural vivianite is dehydrated in the temperature range 105–420°C and the dehydration occurs in five steps. The first step of dehydration incurs a loss of one water molecule and occurs at 105°C; this is the temperature that was used for drying the digested sludge samples prior to SEM-EDS and hence is likely to have affected the water content of vivianite detected by SEM-EDS.

The compounds C and D were identified as ferrous sulfide and pyrite, respectively. The identification was also done using stoichiometric analysis and crystallographic investigation. Both compounds contained mainly iron and sulfur but in different

ratios (**Table 3**). The ratio Fe:S for the compound C was 1 and did not exhibit any specific crystalline structure (in comparison to compound D). It was identified as ferrous sulfide a metastable amorphous compound (Nielsen et al., 2005). The presence of oxygen in compound C was likely to be to surface oxidation during the SEM sample preparation as the percentage was too low to demonstrate the presence of sulfate precipitate. Finally, the ratio Fe:S for the compound D was 0.5 and the chemical formula was calculated as FeS_2 , pyrite. One of the pyrite crystal habits is cubic and this was clearly observed in the digested sludge, as shown in the **Figure 3D** (Halder, 2014).

Chemical Modeling

The results from the predicted iron speciation are shown in the **Table 4** for the seven types of anaerobically digested sludge under study. The input values for the simulation have been obtained from the total concentration (liquid and solid phases) measured in each sludge (**Table 1**). Phreeqc predicted that iron would be precipitated as pyrite and vivianite. The concentration of pyrite varied between 4.8 and 9.8 g/kg DS (**Table 4**). The amount of pyrite precipitated in the sludge was not dependent on the total iron concentration but was related to the total sulfide concentration. MS2 and MS3 were the two sludge with the lowest sulfide concentration and both had the lowest pyrite concentrations with 5.0 and 4.8 g/kg DS. By contrast, NID1 and ID2 were the two sulfide-rich sludge types and had the highest pyrite concentration with, respectively 7.2 and 9.8 g/kg DS. Vivianite precipitation was primarily related to the total iron concentration in the digested sludge, increasing from 2.7 g/kg DS for NID1 to 19.3 g/kg DS for ID2.

A relationship was observed between the predicted concentration of iron as vivianite or pyrite and experimental concentrations of iron in two BCR sequential extraction fractions (**Figure 4**). The iron concentrations in the exchangeable fraction and the concentrations of iron as vivianite presented comparable concentrations with the different sludges and both were dependent on the total iron concentration. The concentration of pyrite predicted by the model was also comparable with the concentration of iron extracted in the residual fraction and both were dependent on the total sulfur concentration.

TABLE 4 | Predicted iron speciation from Phreeqc's simulation.

Sample	Initial	Predicted concentration					
		Total Fe mmol/l	mmol/l		g/kg DS		
			Fe as vivianite	Fe as pyrite	Fe as vivianite	Fe as pyrite	
NID1		3.5	0.0025	0.96	2.57	2.7	7.2
NID2		3.6	0.0027	1.2	2.4	3.4	6.7
MS1		6.8	0.0031	4.5	2.2	12.6	6.2
MS2		7.1	0.0031	5.3	1.8	14.9	5.0
MS3		8.0	0.0033	6.3	1.7	17.6	4.8
ID1		8.5	0.0036	6.5	2.1	18.2	5.9
ID2		10.4	0.0033	6.9	3.5	19.3	9.8

The modeling is limited to calculations based on thermodynamic equilibrium, which cannot entirely capture the complexity of a living reactor. Specifically, equilibrium speciation modeling does not take into account the effect of kinetics, potential local reactions and co-precipitations, or the impact of micro-organisms on metal speciation. As an example, greigite (Fe_3S_4) and ferrous sulfide were only predicted by Phreeqc to precipitate for iron and sulfur if the model was set so that pyrite was not allowed to precipitate. Those two compounds have been found to be pyrite's precursor (Nielsen et al., 2005; Gustavsson, 2012) and SEM-EDS in this research showed that ferrous sulfide and pyrite were indeed both present in the digested sludge sampled, indicating that the sludge retention time was not long enough to obtain a complete transformation from ferrous sulfide to pyrite. Unless the model parameters are specifically altered by the user, it should be noted that pyrite will be the main predicted output. The kinetics can also modify the balance between predicted vivianite and pyrite. It is hypothesized that, following the dissolution of ferric phosphate (originally present in the feed sludge) in the low redox environment of an anaerobic digester, a high concentration of phosphate subsequently surrounds the iron, creating a bulk limitation of sulfide availability for iron (Zhang et al., 2009). This potential disturbance of the thermodynamic equilibrium was not taken into account by the equilibrium speciation model; hence it is likely that phosphorus-rich digesters will contain more vivianite than predicted by equilibrium speciation modeling, which will reduce pyrite formation. Finally, the presence of iron extracted in the second fraction (reducible) of the BCR sequential extraction was not clearly characterized and could be from non-reduced Fe(III) or undissolved ferrous phosphate from the first extraction or even co-precipitates. The amount of iron extracted in the reducible fraction was bound as pyrite or vivianite by the model.

A series of theoretical simulations were done to represent a range of iron, phosphate, and sulfide concentrations in each digester. The iron concentration was simulated from 0 to 30 g/kg DS and the average (across the seven types of sludge) concentration of iron predicted as vivianite and as pyrite are

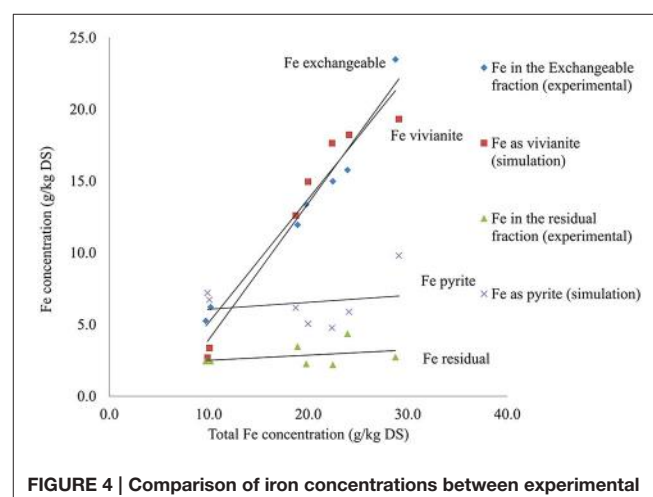


FIGURE 4 | Comparison of iron concentrations between experimental and predicted values.

shown in **Figure 5**. In the model simulation the first compound to be precipitated was pyrite, iron being converted into pyrite until sulfide became the limiting factor, after which the concentration of pyrite stayed constant and the iron precipitated as vivianite. Varying the sulfide concentration (0–40 g/kg DS, **Figure 6**) showed that, in the absence of sulfide, all the iron was precipitated as vivianite. Sulfide precipitates preferentially with copper, nickel, zinc and cobalt prior to the formation of pyrite, hence it is only when the sulfide concentration in a digester increases to 1 g/kg DS that pyrite formation is initiated in competition with vivianite formation. Varying the simulated phosphate content of the digested sludge (0–40 g/kg DS, results not shown) showed that, in absence of phosphate, iron was precipitated as pyrite and siderite (FeCO_3). The concentration of pyrite stayed constant as phosphate content increased, however the siderite concentration decreased as phosphate competed with carbonate for iron, with iron precipitating increasingly as vivianite, until no siderite remained. This series of simulation demonstrates that, based on thermodynamic calculations alone iron speciation in a digester would be primarily controlled by sulfide, then phosphate and finally carbonate.

DISCUSSION

Iron Speciation in Anaerobically Digested Sludge

Previous research has shown that sulfur plays an important role in the speciation of iron in many anaerobic digesters, but phosphate interaction with iron has traditionally been considered negligible, being dominated by full sulfide precipitation or by other binding such as carbonate, thiol, or organic material (Shakeri Yekta et al., 2014a). This research demonstrated that iron precipitates with both sulfide and phosphate in

sewage sludge anaerobic digesters, which are becoming more phosphate-rich environments due to the increasing legislative drive to remove phosphorus from wastewater. In these digesters, iron bonded with phosphate to form vivianite; agreeing with previous results demonstrating its thermodynamic stability under anaerobic condition (Miot et al., 2009). Indeed, the solubility product of vivianite ($\text{pK}_{\text{sp}} = 35.8$, Al-Borno and Tomson, 1994) agreed on the potential formation in anaerobically digested sludge from a thermodynamic approach. Rothe et al. (2016) found that vivianite is stable at pH conditions from 6 to 9 and its formation is detected in organic rich environment in presence of ferrous and orthophosphate ion. The pH range of vivianite stability agreed with its dissolution in the first BCR fraction (exchangeable, pH 4).

The precipitation of iron with phosphate has been previously qualitatively observed in anaerobically digested sludge (Miot et al., 2009; Carliell-Marquet et al., 2010). However, this study demonstrated that vivianite precipitation accounted for at least 50% of the total iron in non-sulfide rich AD and, when CPR was included in upstream wastewater treatment, vivianite could represent more than 90% of the total iron in an anaerobic digester. These results challenge the outputs from thermodynamic calculations (Callander and Barford, 1983) or previous experimental results (Morse and Luther, 1999; Zhang et al., 2010) who concluded that the majority of iron in anaerobic digesters would be present as sulfide precipitates. Previously, anaerobic digesters were often considered to be operating under sulfidic conditions with a threshold of 1 for S:Fe, however, a threshold of 2 is actually required for pyrite formation.

Concerning sulfide reacting with iron, SEM-EDS analysis showed the presence of two iron-sulfide compounds: amorphous ferrous sulfide and pyrite. Nielsen et al. (2005) demonstrated that pyrite is expected to be the most stable inorganic iron-sulfide precipitate. However, the relatively short time period for crystal

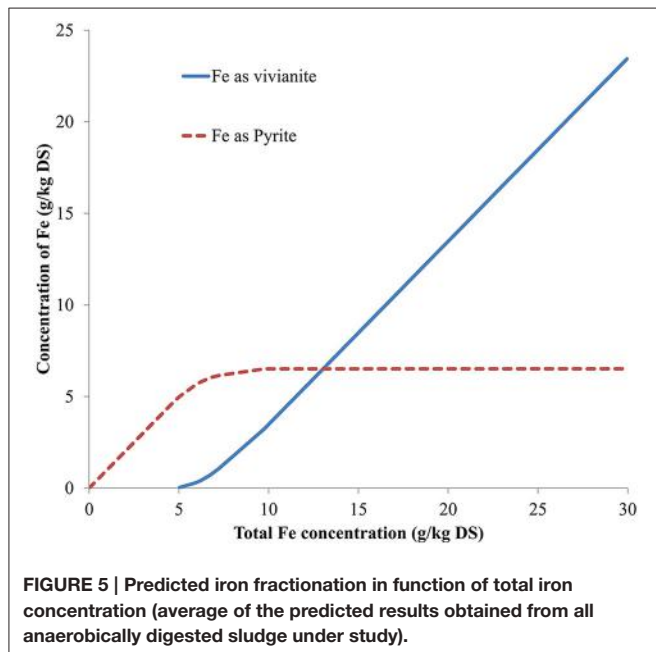


FIGURE 5 | Predicted iron fractionation in function of total iron concentration (average of the predicted results obtained from all anaerobically digested sludge under study).

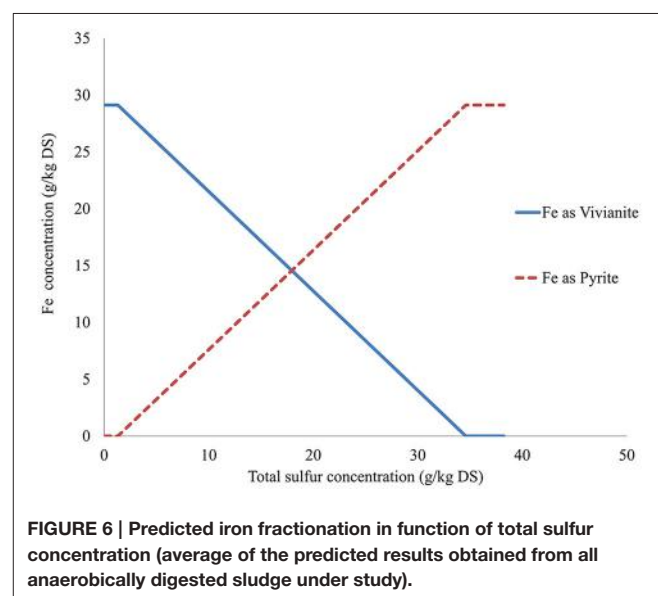


FIGURE 6 | Predicted iron fractionation in function of total sulfur concentration (average of the predicted results obtained from all anaerobically digested sludge under study).

formation and maturation in an anaerobic digester, coupled with redox potential variation (caused by the periodic addition of feed sludge) is likely to encourage ferrous sulfide formation over pyrite formation, as noted by Miot et al. (2009).

Concentration of different ferrous sulfide compounds varied from 10 to 25% of the total iron concentration in the seven studied digested sludge; no clear relationship could be seen between an increase of iron concentration in the digesters (resulting from CPR dosing) and the concentration of iron bound with sulfide (Table 2 and Figure 2). A relationship between total iron-sulfide precipitates and total sulfur concentration was demonstrated in this research through the BCR sequential extraction analysis, and had been suggested previously by Mosey and Hughes (1975). However, additional factors must also have been involved in controlling the precipitation of iron with sulfide in the digesters, as three sludges had the same amount of sulfur measured (NID2, MS1, and ID1) but demonstrated a variation in the concentration of iron extracted in the residual fraction, from 2.4 to 4.3 g/kg DS (Tables 1, 2). Moreover, the ID2 sludge represented the highest sulfur content but only 2.7 g/kg DS of iron was extracted as sulfide precipitates. Shakeri Yekta et al. (2014b) demonstrated that sulfur speciation in an anaerobic digester is an important factor determining the capacity of sulfur for iron precipitation, as each sulfur species possess a different binding capacity for iron. Sulfur species compete with each other for iron, and also with other anions such as phosphate. Moreover, kinetic effects can also enhance the preferential binding of iron with molecules other than sulfur in an anaerobic digester,

due to a local unavailability of sulfide anions (Zhang et al., 2009).

Reactions Controlling the Iron Behavior in Anaerobically Digested Sludge

The results of this study have been used to obtain a better understanding of iron speciation in municipal anaerobic digesters and also, importantly, to determine the most probable order of the sulfide and phosphate precipitation reactions (Figure 7). Results have shown that the first reaction controlling the behavior of iron in the solid phase is precipitation with sulfide to form ferrous sulfide first and then pyrite, regardless of the higher iron or phosphate concentrations in the digesters we studied. Iron sulfide precipitation is, however, strictly constrained by the iron/sulfur ratio in the anaerobic digester and is likely to be limited (Shakeri Yekta et al., 2014a). Following precipitation with sulfide, iron reacts with phosphate to precipitate as vivianite and various ferrous-(hydroxyl)-phosphate compounds. Vivianite represented the largest fraction of iron in all the digesters studied, without being the primary reaction.

These results hence agree with traditional thermodynamic calculations in predicting sulfide as the primary factor controlling iron speciation (Pourbaix, 1963; Callander and Barford, 1983) even if 90% of the total iron was found to be present as vivianite in the digesters studied. However, thermodynamic calculations do seem to overestimate the precipitation of iron

Iron present in AD feed (concentration and form depending on WWTP process (CPR))

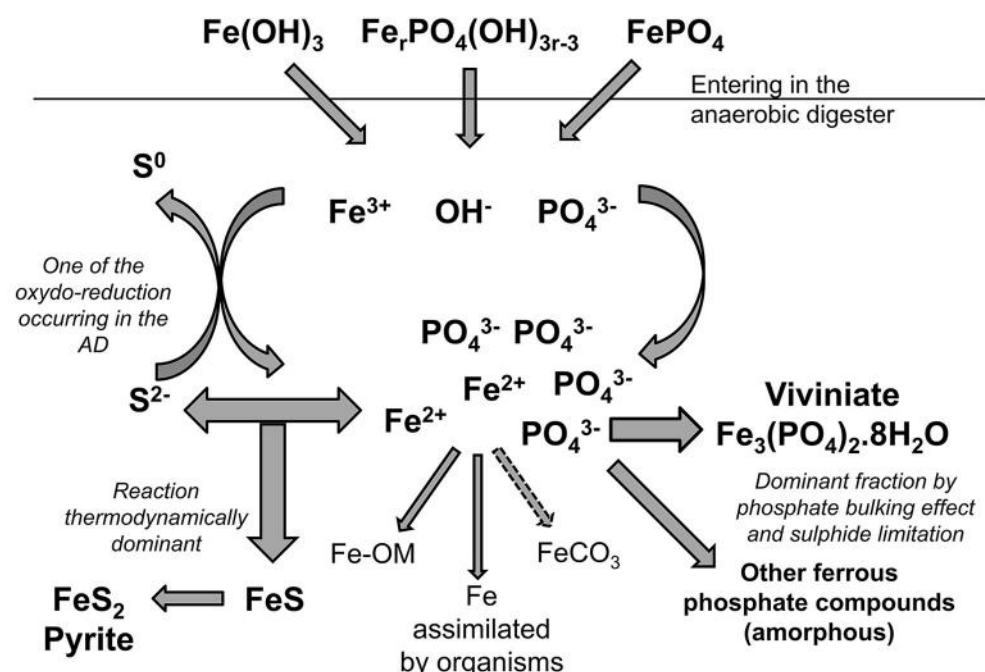


FIGURE 7 | Illustration of iron behavior in anaerobically digested sludge.

with sulfide when compared to experimental data. Shakeri Yekta et al. (2014a) controlled this overestimation in their model by including ligands in the liquid phase and thiols in the solid phase for sulfidic sludge; when sulfide became limiting in their simulated anaerobic digesters, carbonate was used to precipitate iron as siderite. This study has shown that phosphate can also compete kinetically with sulfide to react with iron, especially through the formation of stable iron-phosphate compounds such as vivianite. CPR at a WWTW enhances the ability of phosphate to compete for iron in an anaerobic digester by introducing iron as ferric phosphate in the digester feed sludge, effectively limiting the access of sulfide to iron (Miot et al., 2009; Zhang et al., 2009).

More research is required to complete the overall picture of iron mobility in phosphorus enriched anaerobic digesters, by understanding the speciation of iron in the liquid phase, particularly in terms of bioavailability. Quantitative determination of different iron species in the liquid phase is complicated by low detectable concentrations of individual species (Fermoso et al., 2009). Shakeri Yekta et al. (2014a) approached this subject by creating a model simulation from two sub-models developed by Rickard (2006) and Davison et al. (1999). Their results showed that the iron concentration in the liquid phase of an anaerobic digester, and its speciation, depended primarily on the ratio of sulfur to iron in their digester. Iron solubility was observed to increase when secondary iron precipitates were recorded alongside sulfide precipitation.

In this study, increased total iron concentration in the digested sludge also increased the concentration of iron measured in the liquid and could be linked with the solubility product constant of vivianite formation. Hence, the speciation of iron in the solid phase impacts directly on the reactions controlling the behavior of iron in the liquid phase and, ultimately, on the concentration of iron in the liquid phase.

Impact of Vivianite Precipitation on the Anaerobic Digestion Process

The presence of more than 50% and up to 80% of iron precipitated as vivianite in an anaerobic digester, instead of precipitated with sulfide as traditionally expected, means that iron in these digesters is likely to be more mobile and hence more bioavailable; this is likely to have a secondary effect on other metals speciation.

The optimal balance for metals bioavailability is a fragile equilibrium and any change in their speciation might tip a digester into the deficiency or toxicity zone (Zandvoort et al., 2006). The presence of CPR at a WWTW increases the total concentration of iron and phosphorus in the feed sludge, leading to an increase of vivianite precipitation and solubility of iron in the anaerobic digester. Previous results showed that CPR had negative impact on biogas production (Smith and Carliell-Marquet, 2009; Ofverstrom et al., 2011) that could be correlated to a concentration of iron in the liquid phase coupled with a higher mobility of iron in the solid phase. By contrast, De Vrieze et al. (2013) found that the addition of iron-rich activated

sludge stabilized kitchen waste anaerobic digesters, primarily because iron was a rate-limiting element and secondarily by reducing the high concentration of soluble phosphate in these digesters.

Previous research on metal solubility and bioavailability in digesters used the sulfide element to estimate metal solubility in sewage sludge digesters, assuming sulfide as the dominant anion (Mosey et al., 1971; Mosey and Hughes, 1975). Specifically, Mosey et al. (1971) used sulfide solubility (threshold at $pS = 17.2$) as a measure of the potential bioavailability and hence, toxicity, of heavy metals in anaerobic digestion. This hypothesis could still be used for sulfidic digesters, but sewage sludge today generally has a higher amount of iron than sulfur, due primarily to the prevalence of CPR. Under these new phosphate-rich conditions, phosphate availability must also be taken into consideration in order to calculate iron solubility. Vivianite is defined by the BCR sequential extraction analysis as a weakly bound compound; this weak binding capacity of vivianite enhances the transfer of iron between solid and liquid phase creating a reserved pool of iron able to quickly shift depending on the AD condition. This means that the overall mobility of iron in sewage sludge anaerobic digesters has changed over time as upstream wastewater treatment processes have changed to include phosphorus removal, in response to increasingly strict discharge requirements.

The large amount of iron bound with phosphate in sewage sludge digesters today, also reduces phosphate availability for other cations such as calcium or magnesium. Struvite is a high value end product from anaerobic digestion that can be precipitated through magnesium addition, post anaerobic digestion; struvite precipitation relying on phosphate having been released into the liquid phase during digestion. Phosphate entering an anaerobic digester from CPR is bound with iron and even though it is likely to be released temporarily as a result of Fe(III) reduction, this research showed that most phosphate is reprecipitated as vivianite and will remain in this form, preventing post-digestion struvite recovery.

Finally, the speciation of iron also has an impact on the other metals behavior in the anaerobic digester. Cobalt and nickel are both metals that kinetically precipitate with sulfide after iron and can potentially be absorbed onto ferrous sulfide compounds (Morse and Luther, 1999). Shakeri Yekta et al. (2014b) demonstrated that nickel solubility was controlled by three reactions, including interaction with ferrous sulfide. Hence, reduction of ferrous sulfide precipitates as a result of vivianite formation might reduce the effect of co-precipitation for nickel and cobalt, enhancing secondary reactions and consequently impacting on their solubility. Finally, increased iron mobility could also influence the kinetics of essential trace metals being supplemented to anaerobic digesters to boost biogas production. Roussel (2013) observed a quicker dissolution of supplemented cobalt bound to EDTA in iron-rich sludge than in iron-poor sludge. It was demonstrated that the acceleration of cobalt dissolution was due to higher availability of iron to react with EDTA and release the cobalt, which in turn made cobalt more bioavailable and increased the rate of biogas production from those digesters.

CONCLUSION

- Municipal sewage sludge digesters are today more phosphorus-rich environments than in the past, due to the increasing legislative requirements for WWTW to remove phosphorus from wastewater, which they achieve with iron dosing, resulting in an iron and phosphorus rich sludge being fed to the anaerobic digesters.
- Increasing iron concentrations in municipal sewage sludge digesters was linked to increasing concentrations of vivianite precipitated in the digested sludge.
- The first reaction controlling the behavior of iron in the solid phase is precipitation with sulfide to form ferrous sulfide initially and then pyrite, regardless of the higher iron or phosphate concentrations in the digesters we studied.
- Following precipitation with sulfide, iron reacts with phosphate to precipitate as vivianite and various ferrous-(hydroxyl)-phosphate compounds. Vivianite represented the largest fraction of iron in all the digesters studied, without being the primary reaction.

REFERENCES

- Al-Borno, A., and Tomson, M. B. (1994). The temperature dependence of the solubility product constant of vivianite. *Geochim. Cosmochim. Acta* 58, 5373–5378.
- Alvarez, E. A., Mochón, M. C., Jiménez Sánchez, J. C., and Ternero Rodríguez, M. (2002). Heavy metal extractable forms in sludge from wastewater treatment plants. *Chemosphere* 47, 765–775. doi: 10.1016/S0045-6535(02)00021-8
- APHA-AWWA-WEF (1985). *Standard Methods for the Examination of Water and Wastewater*, 16th Edn. Washington, DC: APHA.
- Callander, I. J., and Barford, J. P. (1983). Precipitation, chelation, and the availability of metals as nutrients in anaerobic-digestion 1. *Methodology* 25, 1947–1957.
- Carliell-Marquet, C. M., Smith, J., Oikonomidis, I., and Wheatley, A. (2010). Inorganic profiles of chemical phosphorus removal sludge. *Water Manag.* 163, 65–77. doi: 10.1680/wama.2010.163.2.65
- Chao, W., Li, X. C., Wang, P. F., Zou, L. M., and Ma, H. T. (2006). Extractable fractions of metals in sewage sludges from five typical urban wastewater treatment plants of China. *Pedosphere* 16, 756–761. doi: 10.1016/S1002-0160(06)60111-2
- Cheng, X., Chen, B., Cui, Y., Sun, D., and Wang, X. (2015). Iron(III) reduction-induced phosphate precipitation during anaerobic digestion of waste activated sludge. *Sep. Purif. Tech.* 140, 6–11. doi: 10.1016/j.seppur.2015.01.002
- Davison, W., Phillips, N., and Tabner, B. J. (1999). Soluble iron sulfide species in natural waters: reappraisal of their stoichiometry and stability constants. *Aquat. Sci.* 61, 23–43.
- De Vrieze, J., De Lathouwer, L., Verstraete, W., and Boon, N. (2013). High-rate iron-rich activated sludge as stabilizing agent for the anaerobic digestion of kitchen waste. *Water Res.* 47, 3732–3741. doi: 10.1016/j.watres.2013.04.020
- Dewil, R., Baeyens, J., Roels, J., and Steene, D. (2009). Evolution of the total sulphur content in full-scale wastewater sludge treatment. *Environ. Eng. Sci.* 26, 867–872. doi: 10.1089/ees.2007.0335
- Dodd, J., Large, D. J., Fortey, N. J., Milodowski, A. E., and Kemp, S. (2000). A petrographic investigation of two sequential extraction techniques applied to anaerobic canal bed mud. *Environ. Geochem. Health* 22, 281–296. doi: 10.1023/A:1006743630918
- Fermoso, F. G., Bartacek, J., Jansen, S., and Lens, P. N. (2009). Metal supplementation to UASB bioreactors: from cell-metal interactions to full-scale application. *Sci. Tot. Environ.* 407, 3652–3667. doi: 10.1016/j.scitotenv.2008.10.043
- Frost, R. L., Weier, M. L., Martens, W., Kloprogge, J. T., and Ding, Z. (2003). Dehydration of synthetic and natural vivianite. *Thermochim. Acta* 401, 121–130. doi: 10.1016/S0040-6031(02)00505-1
- Fuentes, A., Lloréns, M., Sáez, J., Isabel Aguilar, M. A., Ortúñoz, J. F., and Meseguer, V. F. (2008). Comparative study of six different sludges by sequential speciation of heavy metals. *Bioresour. Technol.* 99, 517–525. doi: 10.1016/j.biortech.2007.01.025
- Gustavsson, J. (2012). *Cobalt and Nickel Bioavailability for Biogas Formation*. Ph.D. thesis, Linköping University, Linköping Studies in Arts and Science, 549.
- Haldar, S. K. (2014). “Basic mineralogy,” in *Introduction to Mineralogy and Petrology* (Oxford, UK: Elsevier), 39–79.
- Hassler, C. S., Slaveykova, V. I., and Wilkinson, K. J. (2004). Some fundamental (and often overlooked) considerations underlying the free ion activity and biotic ligand models. *Environ. Toxicol. Chem.* 23, 283–291. doi: 10.1897/03-149
- Jansen, S., Gonzalez-Gil, G., and van Leeuwen, H. P. (2007). The impact of Co and Ni speciation on methanogenesis in sulfidic media - Biuptake versus metal dissolution. *Enzyme Microb. Technol.* 40, 823–830. doi: 10.1016/j.enzmotec.2006.06.019
- Jong, T., and Parry, D. L. (2004). Adsorption of Pb(II), Cu(II), Cd(II), Zn(II), Ni(II), Fe(II), and As(V) on bacterially produced metal sulfides. *J. Colloid Interface Sci.* 275, 61–71. doi: 10.1016/j.jcis.2004.01.046
- Kaksonen, A. H., Riekkola-Vanhainen, M. L., and Puhakka, J. A. (2003). Optimization of metal sulphide precipitation in fluidized-bed treatment of acidic wastewater. *Water Res.* 37, 255–266. doi: 10.1016/S0043-1354(02)00267-1
- Marcato, C.-E., Pinelli, E., Cecchi, M., Silvestre, J., Winterton, P., and Guiresse, M. (2009). Ecotoxicology and environmental safety bioavailability of Cu and Zn in raw and anaerobically digested pig slurry. *Ecotoxicol. Environ. Saf.* 72, 1538–1544. doi: 10.1016/j.ecoenv.2008.12.010
- Metcalf & Eddy Inc. (2003). *Wastewater Engineering: Treatment and Reuse*, 4th Edn. Boston, MA: McGraw-Hill.
- Miot, J., Benzerara, K., Morin, G., Bernard, S., Beyssac, O., Larquet, E., et al. (2009). Transformation of vivianite by anaerobic nitrate-reducing iron-oxidizing bacteria. *Geobiology* 7, 373–384. doi: 10.1111/j.1472-4669.2009.00203.x
- Morse, J. W., and Luther, G. W. (1999). Chemical influences on trace metal-sulfide interactions in anoxic sediments. *Geochim. Cosmochim. Acta* 63, 3373–3378.

- Vivianite is defined by the BCR sequential extraction analysis as a weakly bound compound; this weak binding capacity of vivianite enhances the transfer of iron between solid and liquid phase creating a reserved pool of iron able to quickly shift depending on the AD condition.

AUTHOR CONTRIBUTIONS

JR performed the doctoral research from which this paper was written. CC was the primary supervisor for that research. Both JR and CC have been involved in preparing, writing, and editing this manuscript.

FUNDING

The research in this paper was supported by the Engineering and Physical Sciences Research Council (UK) through a Doctoral Industrial CASE Studentship award (Voucher number: 07001986) “Increasing biogas quantity and quality from anaerobic digestion of wastewater sludge, using nutrient supplementation”; with industrial funding provided by Severn Trent Water Ltd.

- Mosey, F. E., and Hughes, D. A. (1975). The toxicity of heavy metal ions to anaerobic digestion. *Water Pollut. Control* 74, 18–39.
- Mosey, F. E., Swanwick, J. D., and Hughes, D. A. (1971). Factors affecting the availability of heavy metals to inhibit anaerobic digestion. *Water Pollut. Control* 70, 668–679.
- Nielsen, A. H., Lens, P. N. L., Vollersten, J., and Hvitved-Jacobsen, T. (2005). Sulfide-iron interactions in domestic wastewater from a gravity sewer. *Water Res.* 39, 2747–2755. doi: 10.1016/j.watres.2005.04.048
- Nriagu, J. O. (1972). Stability of vivianite and ion-pair formation in the system Fe₃(PO₄)₂-H₃PO₄-H₂O. *Geochim. Cosmochim. Acta* 36, 459–470.
- Ofverstrom, S., Regimantas, D., and Sapkaite, I. (2011). The effect of iron salt on anaerobic digestion and phosphate release to sludge liquor. *Science* 3, 123–126. doi: 10.3846/mla.2011.97
- Oleszkiewicz, J. A., and Sharma, V. K. (1990). Stimulation and inhibition of anaerobic processes by heavy-metals - a review. *Biol. Wastes* 31, 45–67.
- Pourbaix, M. (1963). *Atlas D'équilibres Electrochimiques*. Paris: Gauthier-Villars & Cie.
- Rickard, D. (2006). The solubility of FeS. *Geochim. Cosmochim. Acta* 70, 5779–5789. doi: 10.1016/j.gca.2006.02.029
- Rothe, M., Kleeberg, A., and Hupfer, M. (2016). The occurrence, identification and environmental relevance of vivianite in waterlogged soils and aquatic sediments. *Earth-Sci. Rev.* 158, 51–64. doi: 10.1016/j.earscirev.2016.04.008
- Roussel, J. (2013). *Metal Behaviour in Anaerobic Sludge Digesters Supplemented with Trace Nutrients*. Ph.D. thesis, University of Birmingham.
- Schattauer, A., Abdoun, E., Weiland, P., Plöchl, M., and Heiermann, M. (2011). Abundance of trace elements in demonstration biogas plant. *Biosyst. Eng.* 108, 57–65. doi: 10.1016/j.biosystemseng.2010.10.010
- Shakeri Yekta, S., Lindmark, A., and Skjellberg, U. (2014b). Importance of reduced sulfur for the equilibrium chemistry and kinetics of Fe(II), Co(II) and Ni(II) supplemented to semi-continuous stirred tank biogas reactors fed with stillage. *J. Hazard. Mater.* 269, 83–88. doi: 10.1016/j.jhazmat.2014.01.051
- Shakeri Yekta, S., Svensson, B., Bjorn, A., and Skjellberg, U. (2014a). Thermodynamic modeling of iron and trace metal solubility and speciation under sulfidic and ferruginous conditions in full scale continuous stirred tank biogas reactors. *Appl. Geochem.* 47, 61–73. doi: 10.1016/j.apgeochem.2014.05.001
- Smith, J. A., and Carliell-Marquet, C. M. (2009). A novel laboratory method to determine the biogas potential of iron-dosed activated sludge. *Bioresour. Technol.* 100, 1767–1774. doi: 10.1016/j.biortech.2008.10.004
- Vale, P. (2012). “Preparing for the 2nd cycle of the WFD - the twin challenge of phosphorus and iron,” in *Wastewater Forum*. Available online at: http://www.fwr.org/wastewat/2012%200702%20Preparing%20for%20the%202nd%20cycle%20of%20the%20WFD_P&Fe%20-%20Vale-SevernTrent-FWR.pdf (Accessed 6 June, 2016).
- van der Veen, A., Fermoso, F. G., and Lens, P. N. L. (2007). Bonding form analysis of metals and sulfur fractionation in methanol-grown anaerobic granular sludge. *Eng. Life Sci.* 7, 480–489. doi: 10.1002/elsc.200720208
- Worms, I., Simon, D. F., Hassler, C. S., and Wilkinson, K. J. (2006). Bioavailability of trace metals to aquatic microorganisms: importance of chemical, biological and physical processes on biouptake. *Biochimie* 88, 1721–1731. doi: 10.1016/j.biochi.2006.09.008
- Zandvoort, M. H., van Hullebusch, E. D., Fermoso, F. G., and Lens, P. N. L. (2006). Trace metals in anaerobic granular sludge reactors: bioavailability and dosing strategies. *Eng. Life Sci.* 6, 293–301. doi: 10.1002/elsc.200620129
- Zhang, L., Keller, J., and Yuang, Z. (2009). Inhibition of sulfate-reducing and methanogenic activities of anaerobic sewer biofilms by ferric iron dosing. *Water Res.* 43, 4123–4132. doi: 10.1016/j.watres.2009.06.013
- Zhang, L. S., Keller, J., and Yuang, Z. (2010). Ferrous salt demand for sulfide control in rising main sewers: tests on a laboratory-scale sewer system. *J. Environ. Eng.* 136, 1180–1187. doi: 10.1061/(ASCE)EE.1943-7870.0000258

Conflict of Interest Statement: The authors declare that the research was conducted in the absence of any commercial or financial relationships that could be construed as a potential conflict of interest.

Copyright © 2016 Roussel and Carliell-Marquet. This is an open-access article distributed under the terms of the Creative Commons Attribution License (CC BY). The use, distribution or reproduction in other forums is permitted, provided the original author(s) or licensor are credited and that the original publication in this journal is cited, in accordance with accepted academic practice. No use, distribution or reproduction is permitted which does not comply with these terms.



Metagenomic Reconstruction of Key Anaerobic Digestion Pathways in Municipal Sludge and Industrial Wastewater Biogas-Producing Systems

Mingwei Cai, David Wilkins, Jiapeng Chen, Siu-Kin Ng, Hongyuan Lu, Yangyang Jia and Patrick K. H. Lee*

School of Energy and Environment, City University of Hong Kong, Hong Kong, China

OPEN ACCESS

Edited by:

Giovanni Esposito,
University of Cassino and Southern Lazio, Italy

Reviewed by:

Stefan Schmidt,
University of KwaZulu-Natal,
South Africa
Seung Gu Shin,
Pohang University of Science and Technology, South Korea

*Correspondence:

Patrick K. H. Lee
patrick.kh.lee@cityu.edu.hk

Specialty section:

This article was submitted to
Microbiotechnology, Ecotoxicology and Bioremediation,
a section of the journal
Frontiers in Microbiology

Received: 29 February 2016

Accepted: 09 May 2016

Published: 24 May 2016

Citation:

Cai M, Wilkins D, Chen J, Ng S-K, Lu H, Jia Y and Lee PKH (2016) Metagenomic Reconstruction of Key Anaerobic Digestion Pathways in Municipal Sludge and Industrial Wastewater Biogas-Producing Systems. *Front. Microbiol.* 7:778.
doi: 10.3389/fmicb.2016.00778

Anaerobic digestion (AD) is a microbial process widely used to treat organic wastes. While the microbes involved in digestion of municipal sludge are increasingly well characterized, the taxonomic and functional compositions of AD digesters treating industrial wastewater have been understudied. This study examined metagenomes from a biogas-producing digester treating municipal sludge in Shek Wu Hui (SWH), Hong Kong and an industrial wastewater digester in Guangzhou (GZ), China, and compared their taxonomic composition and reconstructed biochemical pathways. Genes encoding carbohydrate metabolism and protein metabolism functions were overrepresented in GZ, while genes encoding functions related to fatty acids, lipids and isoprenoids were overrepresented in SWH, reflecting the plants' feedstocks. Mapping of genera to functions in each community indicated that both digesters had a high level of functional redundancy, and a more even distribution of genera in GZ suggested that it was more functionally stable. While fermentation in both samples was dominated by *Clostridia*, SWH had an overrepresentation of *Proteobacteria*, including syntrophic acetogens, reflecting its more complex substrate. Considering the growing importance of biogas as an alternative fuel source, a detailed mechanistic understanding of AD is important and this report will be a basis for further study of industrial wastewater AD.

Keywords: biogas, anaerobic digestion, metagenomes, municipal sludge, industrial wastewater

INTRODUCTION

Anaerobic digestion (AD) is a biological decomposition process widely used in municipal wastewater treatment plants (WWTPs). Globally, biogas-producing AD processes are gaining attention because they can not only degrade organic waste, which reduces water quality and poses a danger to public health if not properly treated (Sahlstrom, 2003; Bibby and Peccia, 2013), but also provide a renewable source of energy in the form of methane (biogas; Angelidaki and Ellegaard, 2003; Weiland, 2003; Luo et al., 2013). Despite its widespread use worldwide, the biological mechanisms of AD are still poorly understood, mostly due to the complexity of the microbial communities involved (Wagner and Loy, 2002; Nelson et al., 2011). Thus, detailed studies of the composition of AD microbial consortia and their metabolic functions are required.

An improved understanding of AD could enhance the efficiency of carbon recovery from waste streams, contributing to the global goal of turning WWTPs into sustainable systems (Jetten et al., 1997).

Identifying the microorganisms in AD systems has traditionally been accomplished by the construction of 16S rRNA gene clone libraries followed by Sanger sequencing (Riviere et al., 2009), which in recent years has been replaced by high-throughput next-generation sequencing of 16S rRNA gene amplicons (Schluter et al., 2008; Werner et al., 2011). However, both these methods focus on taxonomic identification, and the metabolic pathways present can be determined only indirectly. Moreover, these methods can introduce biases as a PCR amplification step is required. Shotgun metagenomic sequencing, which directly sequences the extracted DNA, can provide more detailed information on the identity of the microbes and their metabolisms as well as other biological information including novel genes (Ferrer et al., 2005a,b). In addition to these advantages, metagenomic sequencing is gaining importance in the study of microbial communities because the decreasing cost and increasing sequencing depth have enabled high-resolution analysis of complex environmental samples (Qin et al., 2010; Fierer et al., 2012) such as sea water (Tang et al., 2013), soils (Fierer et al., 2012), human gut (Qin et al., 2010), and freshwater (Breitbart et al., 2009). Metagenomics was first applied to AD in 2008 with the analysis of a German full-scale biogas plant treating farm waste (Schluter et al., 2008). Several further studies have since examined AD metagenomes, with the focus mainly on taxonomy and gene-centric functional analyses (Wirth et al., 2012; Wang et al., 2013; Wong et al., 2013; Yang et al., 2014). Recently, metagenomic analysis has shifted toward reconstructing important metabolic pathways and genomes present in AD systems (Li et al., 2013).

Of the AD metagenomes analyzed to date, samples have been obtained from full-scale biogas plants treating farm waste (Schluter et al., 2008), industrial (Wang et al., 2013) and municipal (Wong et al., 2013; Yang et al., 2014) sludge digesters, and lab-scale reactors (Wirth et al., 2012; Li et al., 2013). However, little analysis has yet been conducted of full-scale AD systems treating high-strength industrial wastewater. While municipal sludge digesters are important, AD systems treating high-strength wastewater should not be neglected because a substantial volume of industrial wastewater is generated every year. In China alone, the discharge of industrial wastewater was 6.9×10^{10} metric tons in 2012 and estimated to be 7.8×10^{10} metric tons in 2015, accounting for as high as 35% of total national wastewater discharge (Feng et al., 2015). This study aimed to determine whether and how the major AD processes and the taxonomic groups performing them differ in a high-strength industrial wastewater system compared to better-studied municipal sludge systems. We obtained metagenomes from one system of each type and reconstructed and compared their key AD metabolic pathways. The major taxonomic groups performing these processes were determined and compared between the two systems, and pathways with particular functional significance analyzed. The redundancy of organisms in the major pathways of the multi-step AD process was also examined.

MATERIALS AND METHODS

Sample Descriptions

Anaerobic digestion samples were collected from a full-scale industrial digester treating high-strength wastewater located in Guangzhou, China (hereafter abbreviated 'GZ'), and a municipal digester treating sludge located in Shek Wu Hui, Hong Kong ('SWH'). Detailed descriptions of the digester systems and sample collection procedures have previously been reported (Wilkins et al., 2015a). Briefly, GZ treats 0.7 million liters per day of high-strength industrial wastewater from beverage manufacturing with a retention time of 0.5 days. SWH treats 0.45 million liters per day of municipal sewerage sludge with a retention time of 23 days. The daily methane production and operating temperature are higher for SWH. Operating conditions and measured parameters are provided in Supplementary Table S1.

DNA Extraction and Illumina Sequencing

Genomic DNA was extracted using the PowerSoil DNA Isolation Kit (Mo Bio Laboratories, Carlsbad, CA, USA) as described previously (Lu et al., 2013). 6 µg of extracted DNA for each sample was used for library construction using the Illumina paired-end DNA sample preparation kit according to the manufacturer's instructions. The prepared libraries were sequenced using paired-end 100 bp reads on an Illumina HiSeq 2000 according to manufacturer's recommendations by BGI-Hong Kong. After removing reads containing 'N' and adapters, a total of ~16 Gb of paired-end reads (90 bp in length) were generated for both samples (~8 Gb for each sample). Sequencing reads from this study have been deposited in Metagenome Rapid Annotation using Subsystem Technology (MG-RAST¹) with accession numbers 4560350.3 (GZ) and 4560351.3 (SWH).

Taxonomic and Functional Annotation of Metagenomes

As recommended by the online metagenome analysis tool MG-RAST version 3.0 (Mason et al., 2014; Wilbanks et al., 2014), the reads were not assembled or filtered before submission for taxonomic and functional analyses. Read paired ends were merged prior to analysis according to the instructions provided by MG-RAST. Artificial replicate sequences and irrelevant sequences (e.g., plant, human, or mouse) were removed automatically by MG-RAST and low-quality sequences were filtered out using default settings. The read sets were normalized by random subsampling to 3.9 Gb, and rarefaction curves constructed to assess whether sequencing effort was sufficient to capture the majority of taxonomic diversity.

Reads were taxonomically annotated by comparison with the M5NR database using sBLAT (Kent, 2002). M5NR is a non-redundant (nr) protein database (Meyer et al., 2008) comprising the NCBI GenBank (Benson et al., 2008), SEED (Overbeek et al., 2005), KEGG (Kanehisa and Goto, 2000), IMG terms (Markowitz et al., 2008), eggNOGs (Jensen et al.,

¹<http://metagenomics.anl.gov>

2008), and Uniprot (Magrane and UniProt Consortium, 2011) databases. To identify genes and their functions, the reads were additionally annotated via sBLAT (Kent, 2002) searches against the COG and SEED gene databases, both of which organize genes into nested hierarchies of groups (COG categories and SEED subsystems) with related functional roles. For both the taxonomic and functional annotations, the best hit was accepted as the annotation for that read, and only read alignments ≥ 25 nucleotides with similarity to the reference database $\geq 60\%$ and $E\text{-value} \leq 1 \times 10^{-5}$ were retained (Tang et al., 2013; Wong et al., 2013; Mason et al., 2014). Taxon, COG category and SEED subsystem counts were normalized by dividing by the total number of hits in each metagenome (Mackelprang et al., 2011; Tang et al., 2013).

Reconstruction of Metabolic Pathways

Anaerobic digestion of organic compounds has four major steps: hydrolysis, acidogenesis, acetogenesis, and methanogenesis (Wirth et al., 2012). Representative pathways for the acidogenesis, acetogenesis, and methanogenesis steps of AD and for denitrification were constructed according to recently published articles (Francis et al., 2007; Agler et al., 2011) with reference to databases including KEGG, MetaCyc (Caspi et al., 2014), and BRENDa (Scheer et al., 2011). These pathways included the reaction steps producing major intermediate compounds and the enzymes that catalyze these steps. The relative abundances of the top five genera from each metagenome associated with the last step in the formation of major intermediates in acidogenesis, acetogenesis, and methanogenesis, and the top five genera from each metagenome associated with the major enzymes in the methanogenesis and denitrification pathways were mapped to the respective pathways. The Pielou evenness index was calculated for the top genera associated with major intermediates and for all genera in each digester using the R package vegan².

To gain insight into the functions and organisms involved in hydrolysis and to examine the samples' taxonomic and functional profiles more generally (Smith et al., 2012; Luo et al., 2013; Tang et al., 2013), Statistical Analysis of Metagenomic Profiles (STAMP, version 2.0; Parks and Beiko, 2010) was used to compare the abundances of taxa, COG categories and SEED subsystems between the samples. Detailed information regarding the method can be found in the manual³. Significant differences were identified with the two-sided Fisher's exact test (Fisher, 1958), with 0.95 confidence intervals determined by the Newcombe-Wilson method (Newcombe, 1998). Storey's False Discovery Rate (FDR; Storey and Tibshirani, 2003) was used to correct for multiple comparisons, and results with a $q\text{-value}$ (corrected $p\text{-value}$) <0.05 retained.

Assembly and Analyses of Contigs

Although the primary taxonomic and functional annotation was performed with unassembled reads as recommended by MG-RAST, contigs were assembled from each metagenome to identify longer sequences present in both samples and to perform

thorough searches for key marker genes. Raw sequence reads were filtered and trimmed using Fastq-Mcf⁴ with default settings. The filtered reads were merged and converted to FASTA format using 'fqwfa' (Ruby et al., 2013) followed by *de novo* assembly with IDBA_UD version 1.1.1 using the options '-step 10', '-mink 20', '-maxk 100', and '-min_contig 800' (Peng et al., 2012). Contigs >1200 bp in length were retained.

To identify long sequences shared between the samples, contigs from both samples were compared pairwise with BLASTN. Pairwise hits with an alignment length $\geq 3,000$ bp and sequence identity $\geq 95\%$ were retained and annotated via a BLAST search against the NCBI nr nucleotide database. The assembled contigs were also annotated in MG-RAST by searching against the M5NR, COG, and SEED databases as described above. Custom databases of protein sequences for all enzymes involved in methanogenesis were constructed from the KEGG database and contigs were compared with these databases to detect key methanogenesis genes.

Comparisons with Other Metagenomes

Metagenomes representing other AD systems (Supplementary Table S2) were submitted to MG-RAST for comparison with this study's metagenomes. Reads from the other metagenomes that matched reads from this study with an $E\text{-value} \leq 1 \times 10^{-3}$ were retained (Smith et al., 2012; Tang et al., 2013). To examine changes in the SWH community over time, functional and taxonomic profiles of two metagenomes obtained from SWH as part of a different study (Yang et al., 2014) were obtained. The operating conditions of the digester did not change significantly between the two studies. All taxon and function abundances were proportionally normalized as described above.

RESULTS

Overview of the Metagenomes

Following read quality control, a total of 14,949,014 and 20,124,753 reads with average lengths of 152 ± 24 bp and 152 ± 21 bp in GZ and SWH, respectively, were retained (Supplementary Table S3). After annotation, 32.3% of GZ and 48.3% of SWH reads attracted matches to the M5NR database, and 4,280,812 and 5,774,507 reads containing functional genes were identified in GZ and SWH, respectively (Supplementary Table S3). A wide range of sequencing depths, from 600 Mb (Wilbanks et al., 2014) to 3 Gb (Yang et al., 2014), have previously been used in metagenomic analyses. Rarefaction curves were asymptotic for both metagenomes at the 3.9 Gb subsampling depth (Supplementary Figure S1), showing this depth is sufficient to cover the majority of species richness.

Taxonomic Composition of the Metagenomes

The taxonomic composition of the metagenomes was determined from the annotation of reads against the M5NR database in MG-RAST (Meyer et al., 2008). At the domain level, the

²<http://CRAN.R-project.org/package=vegan>

³<http://kiwi.cs.dal.ca/Software/STAMP>

⁴<http://code.google.com/p/ea-utils/wiki/FastqMcf>

majority of reads were assigned to *Bacteria* (79.5% for GZ; 83.0% SWH), followed by *Archaea* (7.4% GZ; 4.0% SWH), and *Eukaryota* (1.0% GZ; 0.7% SWH). Within the *Bacteria*, the most abundant phyla were *Proteobacteria*, *Firmicutes*, *Actinobacteria*, and *Bacteroidetes* in both samples. STAMP analysis identified a significant overrepresentation of *Firmicutes*, *Actinobacteria*, and *Euryarchaeota* in GZ while *Proteobacteria* and *Bacteroidetes* were overrepresented in SWH (**Figure 1A**).

Class abundances were highly correlated between the two samples ($R^2 = 0.88$). In both samples, *Actinobacteria* (class) were highly abundant, followed by *Clostridia*, *Bacilli*, and classes of the *Proteobacteria*. The *alpha*-, *beta*-, and *gamma*-*Proteobacteria* were significantly overrepresented in SWH, while *delta-Proteobacteria*, which contains acetogenic bacteria that interact syntrophically with methanogens (Lopez-Garcia and Moreira, 2006; Sousa et al., 2009), were overrepresented in GZ (**Figure 1B**). These differences are likely due to differences in the feedstocks and/or operating conditions (e.g., retention time and temperature, Supplementary Table S1).

One thousand nine hundred thirty-nine genera were identified in GZ and 2,554 genera in SWH, of which 1,612 were shared between the metagenomes. Apart from high representations of *Streptomyces* in GZ and *Mycobacterium* in SWH (Supplementary Figure S2), the major genus in both metagenomes was *Clostridium* which formed a similar proportion of both samples (GZ 2.7%; SWH 2.6%). The abundance of minor genera varied greatly between the two metagenomes. Pathogens including *Mycobacterium* and *Burkholderia* were significantly more abundant in SWH, whereas bacterial genera associated with acetogenesis (e.g., *Syntrophobacter*) were overrepresented in GZ (Supplementary Figure S2).

Euryarchaeota, which includes all known methanogens (Li et al., 2013), was the most abundant archaeal phylum in both samples, followed by *Crenarchaeota*, *Thaumarchaeota*, *Korarchaeota*, and *Nanoarchaeota* (Supplementary Table S4). Within the *Euryarchaeota*, the methanogenic classes *Methanomicrobia* and *Methanobacteria* dominated both metagenomes, while at the order level *Methanomicrobiales* was most abundant followed by *Methanosarcinales* and *Methanobacteriales* (Supplementary Table S4). At the genus level, *Methanosarcina* was prevalent in both samples (GZ 9.3% of all *Archaea*; SWH 8.4%) while *Methanothermobacter* were abundant in GZ (GZ 4.9%; SWH 3.6%) and *Methanospirillum* (GZ 3.7%; SWH 6.8%), *Methanobrevibacter* (GZ 4.2%; SWH 5.4%), and *Thermococcus* (GZ 4.9%; SWH 5.4%) in SWH. *Methanosaeta* (GZ 2.7%; SWH 2.6%) were present in low abundance in both samples.

Functional Composition of the Metagenomes

To obtain metabolic function profiles for the two metagenomes, all reads were annotated via sBLAT search against the COG and SEED databases. In both samples, genes encoding functions from metabolism-related COG categories were dominant, representing more than 45% of the total hits within each sample. Within the metabolism COG category, more than 65% of reads in

both samples were annotated with sequences in the categories carbohydrate transport and metabolism, lipid transport and metabolism, energy production and conversion, and amino acid transport and metabolism. A high proportion of genes related to these functions has been previously reported in metagenomes (Li et al., 2013) and metaproteomes (Wilmes et al., 2008) from AD systems and may indicate a metabolism suitable for anaerobic microbial reactions. STAMP analysis indicated that genes related to carbohydrate transport and metabolism were overrepresented in GZ, while lipid transport and metabolism genes were overrepresented in SWH (Supplementary Figure S3).

Level 1 (broadest level) SEED subsystems such as clustering-based systems and carbohydrates metabolism were relatively abundant in both samples, accounting for almost 15% of each. The amino acids and derivatives metabolism and protein metabolism subsystems were also prevalent. As with the COG results, most of these abundant subsystems were related to the degradation of organic matter. Genes from carbohydrates metabolism and protein metabolism subsystems were overrepresented in GZ, whereas genes from fatty acids, lipids and isoprenoids subsystems were more abundant in SWH (**Figure 2**). In both anaerobic wastewater and sludge metagenomes, a number of genes related to nitrogen metabolism and to respiration were also detected, corroborating a previous finding (Ye et al., 2012).

Among level 4 (gene product) SEED subsystems, the most prevalent genes in both samples were those encoding glycosyltransferase, followed by decarboxylase. Glycosyltransferase had the largest difference between proportions in the two samples of all level 4 subsystems, being highly and significantly overrepresented in GZ (Supplementary Figure S4).

Reconstruction of Functional Pathways

To determine the major genera involved in AD in each sample, the abundances of genera associated with the last step in the formation of major intermediate products were examined. Genera contributing to the formation of acetate were dominant in both samples at the acidogenesis stage (**Figure 3**). A high abundance of genera capable of ethanol fermentation (e.g., *Bradyrhizobium*) was found in the sludge metagenome (SWH), while a high proportion of genes were assigned to the genera responsible for formate formation (e.g., *Clostridium* and *Bacteroides*) in the wastewater metagenome (GZ). In addition, genes from *Clostridium* were most frequently detected in the acidogenesis process in both samples, consistent with the high abundance of *Clostridium* in GZ and SWH (**Figure 3**).

Unlike acidogenesis, acetogenesis is a rate-limiting step as the conversion of long-chain volatile fatty acids (VFAs) to acetate, formate, CO_2 , and H_2 is endothermic under standard conditions and limited by factors including H_2 partial pressure and substrate concentration (Müller et al., 2010). Changes in these metabolite concentrations therefore have a large effect on the overall AD rate (McInerney et al., 2009). Acetogenesis was dominated in both metagenomes by the *delta*-proteobacterial genus *Syntrophobacter*, members of which can convert butyrate/propionate to acetate (Müller et al., 2010).

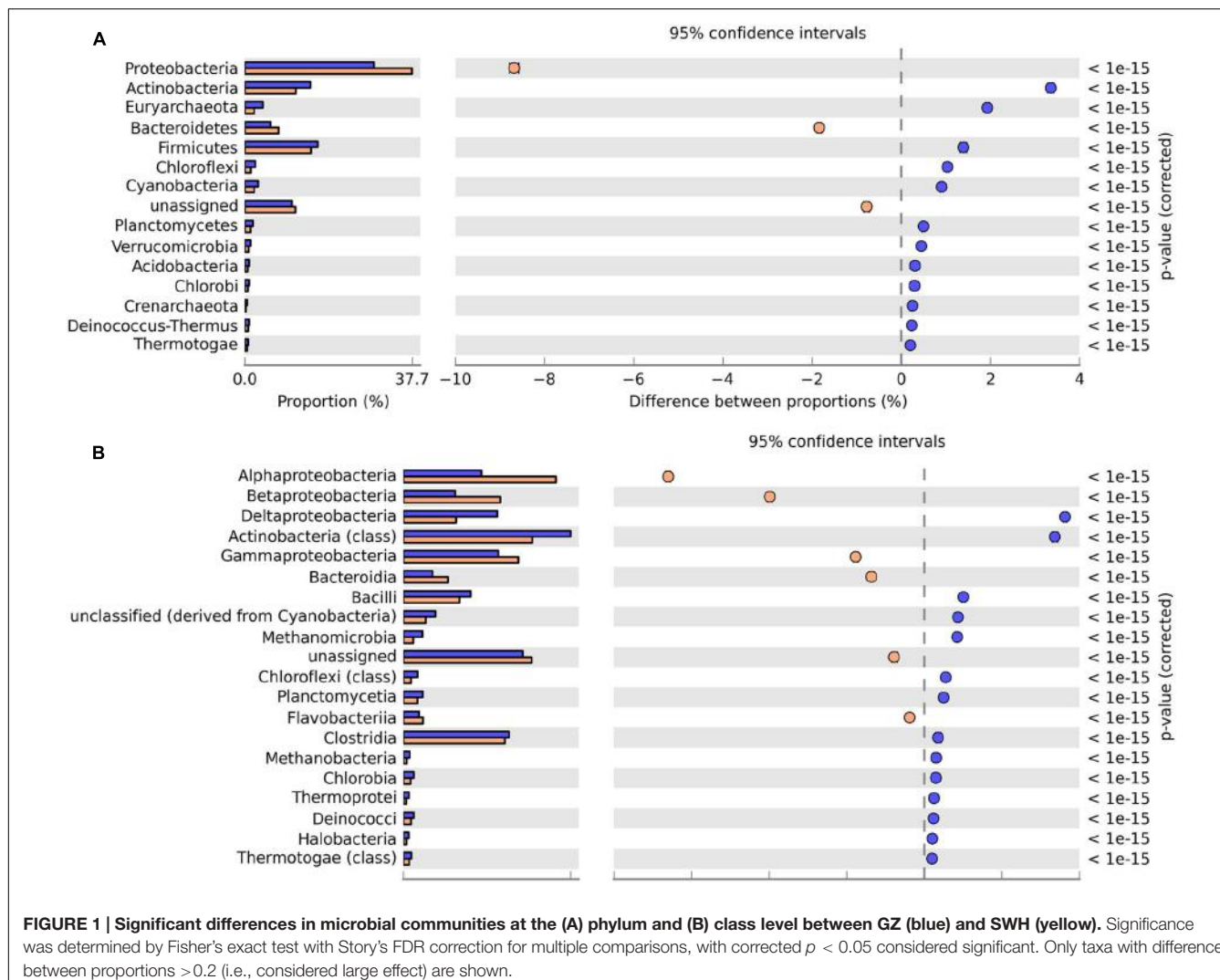


FIGURE 1 | Significant differences in microbial communities at the (A) phylum and (B) class level between GZ (blue) and SWH (yellow). Significance was determined by Fisher's exact test with Story's FDR correction for multiple comparisons, with corrected $p < 0.05$ considered significant. Only taxa with difference between proportions >0.2 (i.e., considered large effect) are shown.

Methanogenesis in both samples was likely contributed by the dominant genus *Methanosarcina*.

Overall, acidogenesis genera were less abundant than acetogenesis and methanogenesis genera in both digesters (Supplementary Table S5). However, for the formation of acetate as an intermediate product of acidogenesis, the relative abundances of the top genera were similar in both samples (**Figure 3**). Furthermore, the relative abundances of the single major acetogenic [e.g., *Syntrophobacter* (1.4%)] and methanogenic [e.g., *Methanosarcina* (1.1%)] genera were similar to those of the less evenly distributed major acidogenic genera [e.g., *Clostridium* (1.3–2.7%) and *Geobacter* (0.9–2.0%)] in GZ. Meanwhile, genera were overall more evenly distributed in GZ (Supplementary Table S5).

The methanogenesis and denitrification pathways were selected for more detailed pathway reconstructions in which all major enzymes were considered. Compounds including H₂/CO₂, acetate, and some C1 compounds (e.g., formate, methanol, dimethylamine, and methanethiol) can serve as substrates for methanogenesis (Francis et al., 2007; Li et al.,

2013). Both the hydrogenotrophic (H₂/CO₂ to methane) and acetoclastic (acetate to methane) pathways were detected in both metagenomes, though genes encoding enzymes in the acetoclastic pathway (EC 2.7.2.1, EC 2.3.1.8, EC 6.2.1.1, and EC 2.3.1.-) were more abundant than those in the hydrogenotrophic pathway (EC 1.2.99.5, EC 2.3.1.101, EC 3.5.4.27, EC 1.5.98.1, and EC 1.5.98.2) in both samples (Supplementary Figure S5). Within the acetoclastic pathway, genes encoding enzyme EC 6.2.1.1 (responsible for the formation of acetyl-CoA from acetate) were more abundant than EC 2.7.2.1 (acetate kinase) and EC 2.7.1.8 (phosphate acetyltransferase) in both metagenomes (Supplementary Figure S5). Although methanol-utilizing methanogens (e.g., *Methanospaera stadtmanae* and *Methanosarcina barkeri*) were found in both metagenomes, no sequence encoding enzymes *mtaA* (coenzyme M-binding methyltransferase) or *mtaB* (methanol-binding methyltransferase) was detected in reads or contigs from either metagenome, possibly due to incomplete sequencing.

As expected under anaerobic conditions, genes encoding enzymes involved in nitrification (e.g., ammonia monooxy-

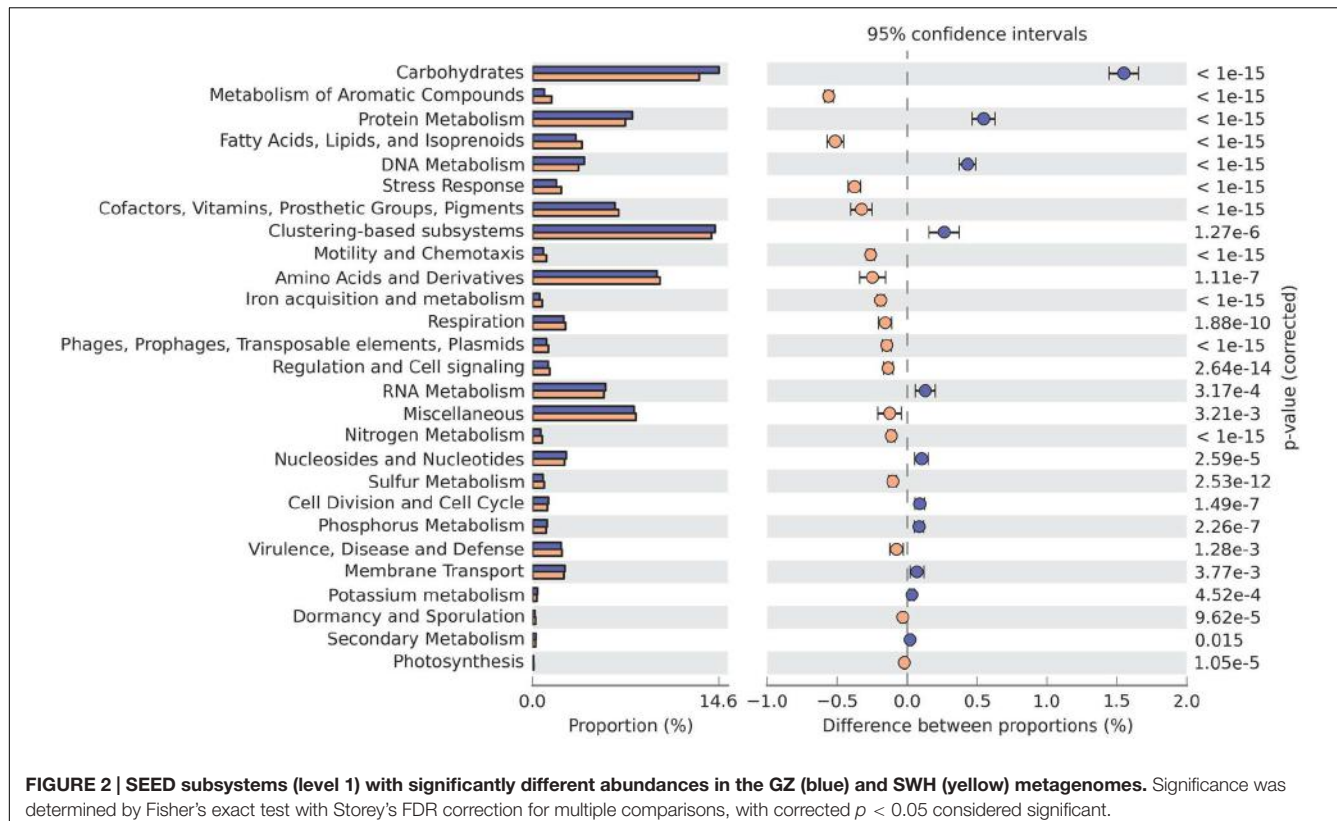


FIGURE 2 | SEED subsystems (level 1) with significantly different abundances in the GZ (blue) and SWH (yellow) metagenomes. Significance was determined by Fisher's exact test with Storey's FDR correction for multiple comparisons, with corrected $p < 0.05$ considered significant.

genase, EC 1.14.99.39 and EC 1.7.2.6) were either undetected or at low abundance in both GZ and SWH (Supplementary Figure S6). In contrast, a high abundance of enzymes related to denitrification (nitrate reductases, EC 1.7.99.4, EC 1.7.2.4, and EC 1.7.2.1; nitrous oxide reductase, EC 1.7.2.5) was detected (Supplementary Figure S6). In addition, a high proportion of reads in both samples were assigned to nitrite reductase (EC 1.7.1.4) and nitrogenase (EC 1.18.6.1) genes (Supplementary Figure S6). Genes for hydrazine oxidoreductase (EC 1.7.99.8), an enzyme involved in anaerobic ammonia oxidation (anammox), were searched for by BLASTP in contigs from both samples but not found. As previously reported (Francis et al., 2007), both bacteria and archaea contributed enzymes to the denitrification pathway.

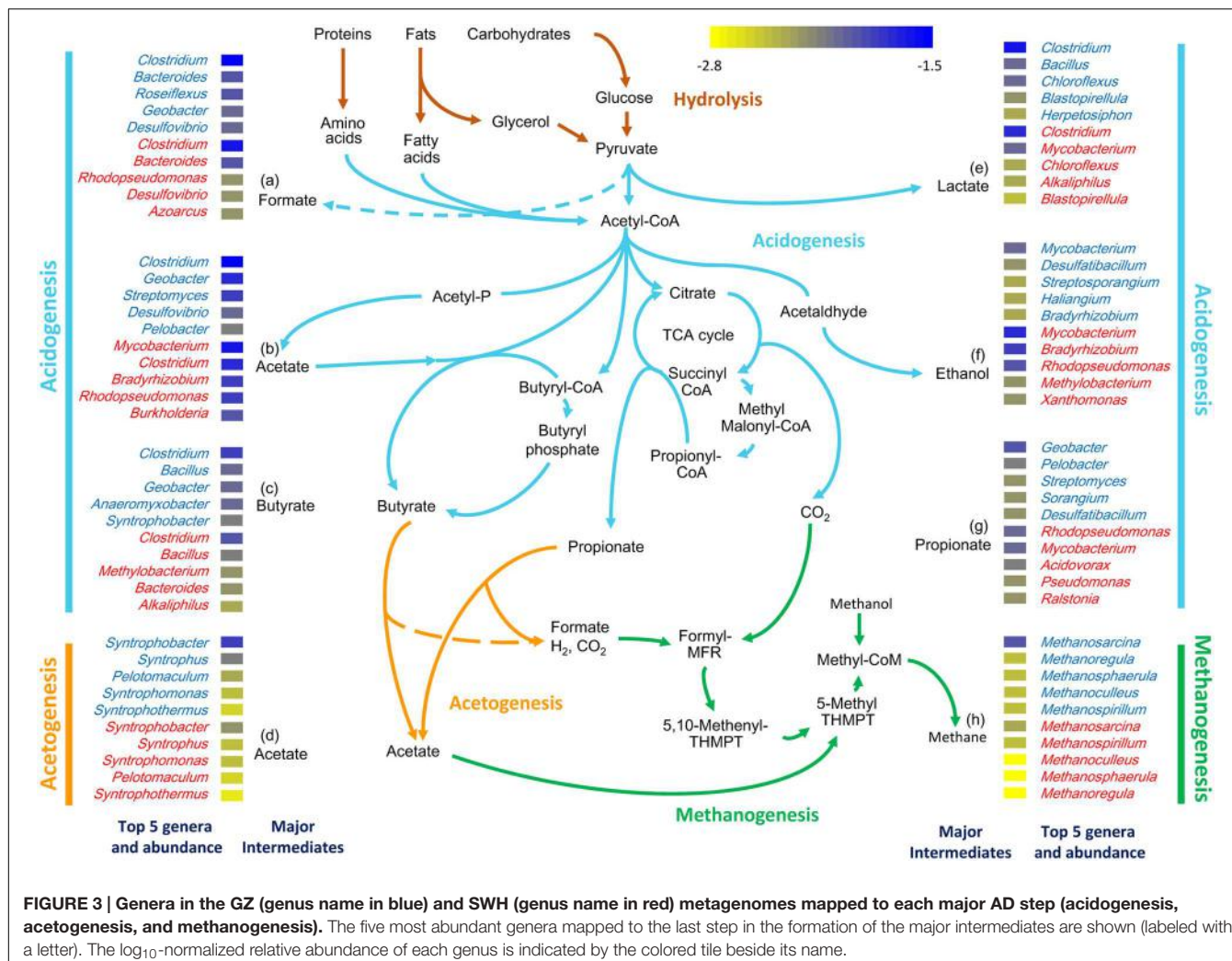
Comparison with Other Metagenomes

Four additional AD metagenomes were selected for comparison with GZ and SWH (Supplementary Table S2). The GZ metagenome was taxonomically and functionally most similar to that of a German production-scale biogas plant fed with a mixture of crops (~98%) and chicken manure (~2%), but was distinct from those treating cellulose sludge and lab-scale municipal sludge (**Figure 4**). SWH shared a high degree of similarity, especially among functional genes (similarity >95%), with a metagenome from a lab-scale anaerobic sludge reactor (**Figure 4**; Lv et al., 2014). Two metagenomes from AD systems treating paper mill wastewater and cellulolytic sludge were very dissimilar from the metagenomes in this study.

To investigate temporal variability in taxa and functions, we examined two additional metagenomes also from SWH but collected at different times for a different study (Yang et al., 2014). The two samples used for comparison were collected in September 2011 and March 2012, while the sample in this study was collected in November 2011. A comparison of the taxonomic and functional profiles indicated shifts in the dominant microbial community members present (Supplementary Figure S7), even between the two samples from the previous study that were sequenced using the same method. Smaller changes were observed in the functional gene profiles, especially for essential functions (e.g., transcription and DNA replication).

DISCUSSION

Anaerobic digestion has been widely applied in the treatment of municipal sludge (Riviere et al., 2009; Yang et al., 2014) and industrial wastewater (Rajeshwari et al., 2000) as this technology decomposes organic waste while simultaneously producing biogas (Angelidaki and Ellegaard, 2003; Weiland, 2003; Luo et al., 2013). However, previous AD studies have mainly focused on the phylogenetic diversity of municipal digesters treating waste sludge from secondary treatment (Yang et al., 2014) or farm waste (Schluter et al., 2008). The taxonomic and functional composition of AD digesters treating high-strength industrial wastewater have not been extensively studied, especially those taxa and functions involved with

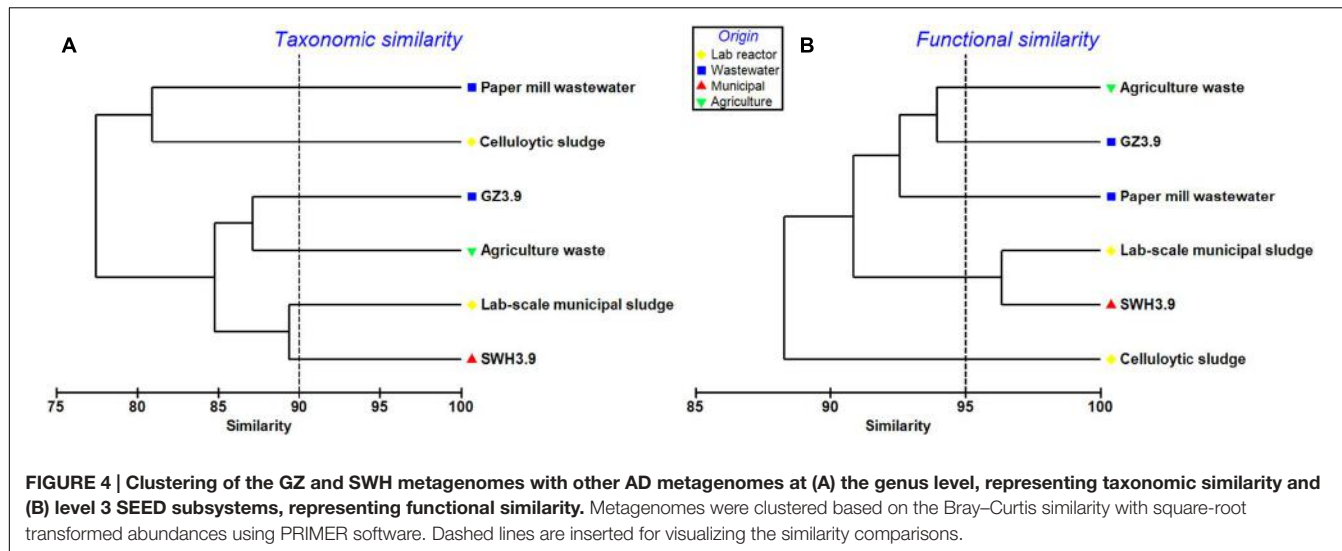


the major AD steps (Wagner and Loy, 2002; Nelson et al., 2011). Given the vast and increasing volume of high-strength industrial wastewater produced worldwide, the application of AD to wastewater is likely to grow. Therefore, it is important to thoroughly understand the microbiology involved in the anaerobic treatment of wastewater and how it differs from the more common sludge digesters. We analyzed metagenomes (i.e., covering both taxonomy and metabolic functions) from an industrial wastewater AD system and a municipal system treating sludge to reconstruct the major AD biochemical processes and examine how they differ between these two digester types.

In this study, we chose not to assemble the reads before annotation, as low-coverage sequences might be excluded by an assembler (Howe et al., 2014) and bias the taxonomic profile against rare taxa. Unlike some studies using unassembled reads (Fierer et al., 2012), here we used merged paired end reads for more reliable annotation results. However, the protein annotation rates (53.4% for GZ and 48.3% for SWH) were similar to reported rates for unmerged reads (42.7–56.1%; Fierer et al., 2012; Wirth et al., 2012). We also assembled

contigs to provide a basis for phylogenetic comparison between the metagenomes, although these were not used to generate taxonomic and functional abundances. The annotation rates in these contigs were < 68%, suggesting incomplete sequencing of genes played some role in the annotation rate but did not account for all unannotated reads. Unannotated reads could also be attributed to the high diversity of the samples (Wilkins et al., 2015a) and/or incomplete databases (Ye et al., 2012).

The presence of functional genes in an AD system should generally be correlated to the substrate it is treating. For example, a metagenome from anaerobic digestion of tannery wastewater found genes assigned to protein metabolism were the most abundant, making up about 15% of the metagenome (Wang et al., 2013). In the metagenome from the GZ digester, which treats carbohydrate-rich beverage wastewater, genes related to carbohydrate transport and metabolism were the most abundant and strongly overrepresented relative to SWH (Figure 2; Supplementary Figure S3; Hu et al., 2010). In contrast, functions related to metabolism of lipids and fatty acids were significantly overrepresented in SWH, including



the SEED subsystem for fatty acids, lipids, and isoprenoids (Figure 2), COG category for lipid transport and metabolism (Supplementary Figure S3B) and genes encoding enzymes from the cytochrome P450 family (Supplementary Figure S4). Cytochrome P450 enzymes catalyze reactions on a broad range of substrates, particularly lipid metabolites such as steroids, eicosanoids, fatty acids, and lipids (Coon et al., 1992). This functional profile of SWH suggests there was a higher lipid content in the sludge being treated there, as expected for a municipal sewerage waste stream. Similarly, the overrepresentation of SEED subsystems related to the metabolism of aromatic compounds (Figure 2) reflects the probable presence of polycyclic aromatic hydrocarbons (PAHs) in sewerage waste streams, particularly concentrated in digester sludge (Blanchard et al., 2004).

Genes encoding the cobalt-zinc-cadmium resistance protein CzcA were abundant in both metagenomes. Cobalt-zinc-cadmium resistance protein CzcA is essential for resistance against certain heavy metals (Diels et al., 1995). Its presence suggests heavy metals such as cobalt, zinc and/or cadmium, could be present in both samples. A previous study has shown that heavy metals are released with the decomposition of organic matter (Dong et al., 2013).

The taxonomic composition of the two digesters also reflected the complexity of hydrolytic functions required to process their feedstocks. The phylum *Proteobacteria* was strongly overrepresented in SWH, with the exception of the class *delta-Proteobacteria* (Figure 1B). This overrepresentation was quite evenly spread over a large number of *Proteobacteria* genera (data not shown), indicating it was not due to a few exceptional species but rather a systematic difference. Members of the *Proteobacteria* have a broad range of roles in all AD steps except for methanogenesis. In the pathway reconstruction, *Proteobacteria* genera were among the top contributors to the production of all major fermentation products except lactate and to acetogenesis in both digesters (Figure 3). Given this broad range of roles in both digesters, the overabundance of

Proteobacteria in SWH reflects the more complex range of substrates treated by that system, requiring a more diverse repertoire of functions.

Bacteria in both metagenomes were numerically dominated by reads assigned to the genus *Clostridium*, which can ferment a wide variety of carbon sources and produce VFAs and alcohols that serve as substrates for methanogenesis. A high *Clostridium* abundance has been reported in a range of anaerobic reactors (Nelson et al., 2011) including those fed with crops and a mixture of animal manure (Rademacher et al., 2012) or excess sludge (Li et al., 2013), and in our previous amplicon sequencing-based studies of the GZ and SWH digesters (Wilkins et al., 2015b; Jia et al., 2016). In this study, the class *Clostridia* was slightly overrepresented in the GZ metagenome (Figure 1). Mapping of genera to the formation of AD intermediates found that *Clostridium* spp. were the main fermenters forming four of the six major acidogenesis products (formate, acetate, butyrate, and lactate; Figure 3), consistent with their reported versatility in AD fermentation (Li et al., 2011). Members of the *Clostridiales* also have roles in initial hydrolysis (Moon et al., 2011; Dassa et al., 2014) and syntrophic acetate oxidation (SAO; Müller et al., 2013). However, it is notable that in our previous study of enrichment cultures inoculated from both digesters *Clostridium* abundance increased in tandem with the methanogen genus *Methanobacterium* (Jia et al., 2016); in this study, the class *Methanobacteriales* was likewise slightly overrepresented in GZ (Supplementary Table S4). SAO bacteria, including *Clostridium ultunense* (<0.1% in both samples; Müller et al., 2013), oxidize acetate to provide H₂ and CO₂ to syntrophic partner methanogens such as *Methanobacterium* (Zinder and Koch, 1984), and it is possible that at least some methane production from acetate in the digesters proceeds via this route. As SAO bacteria likely oxidize acetate via the reversible Wood-Ljungdahl pathway (reductive acetyl-CoA pathway; Lee and Zinder, 1988) also used in other AD processes, e.g., methanogenesis, the presence or absence of this route

cannot be determined by the presence or absence of marker genes.

As expected for a sewage waste stream, SWH contained a high abundance of human-associated pathogen genera such as *Mycobacterium* (*Mycobacterium tuberculosis*, *M. bovis* and *M. avium* accounted for ~72% of *Mycobacterium* in both samples) and *Burkholderia*, although *Mycobacterium* was also unexpectedly abundant in GZ. This high abundance of *Mycobacterium* in both digesters is especially noteworthy as they are unlikely to be important in the degradation of organic compounds under anaerobic conditions (de Oliveira et al., 2010). As removal of *Mycobacterium* at mesophilic temperatures typically requires weeks to months (Sahlstrom, 2003; El-Mashad et al., 2004), the high abundance detected in both systems suggests neither is successful in removing these potential pathogens with the retention time of the systems.

Methanomicrobiales was the most abundant archaeal order in both metagenomes (Supplementary Table S4), and contributed most of the abundant genera mapped to the methanogenesis pathway from both digesters (Figure 3; Supplementary Figure S5). The orders *Methanosarcinales* and *Methanobacterales* were also abundant, with both overrepresented in GZ (Supplementary Table S4). Our previous study using amplicon sequencing of the archaeal rRNA gene (Wilkins et al., 2015a) found that *Methanomicrobiales* was dominant in GZ but order *Methanosarcinales* in SWH, while a previous metagenomic study of SWH sludge found an overwhelming (>70%) dominance of *Methanomicrobiales*. These different results may reflect differences in methods, for example the short read length of shotgun metagenomic sequencing leading to conflation of protein sequences from the closely related orders. They could also reflect functional redundancy in the methanogenesis step of AD, i.e., maintenance of the biochemical functions over time independent of variance in taxonomic composition. Such redundancy has been proposed as a feature of higher AD steps, particularly fermentation (Werner et al., 2011), and our previous study of AD enrichment cultures has shown that similar methane yields can be obtained from systems fed with different substrates and containing diverse methanogen communities (Wilkins et al., 2015b). Detailed reconstruction of the methanogenesis pathway (Supplementary Figure S5) found that the functional potential for complete acetoclastic and hydrogenotrophic pathways were present in both metagenomes, with genes encoding enzymes involved in the acetoclastic route dominant in both samples. This agrees with our previous amplicon sequencing study (Wilkins et al., 2015a) and other previous studies that found the acetoclastic pathway tends to be dominant in methanogenic systems (Li et al., 2013; Yang et al., 2014). The time series of SWH metagenomes also suggested greater taxonomic than functional variability, with e.g., the class *Methanomicrobia* increasing 1.4-fold in relative abundance between September 2011 and March 2012 while functional abundances remained relatively constant (Supplementary Figure S7). As different microbes share similar functions (Hashsham et al., 2000), it is quite likely that the presence of functional genes, rather than particular microbial taxa, determines the

functional stability of the AD digesters. The presence of the same core functions in each digester contributed by different consortia was also illustrated by the reconstruction of the denitrification pathway, with almost non-overlapping sets of genera responsible for the same biochemical steps in each digester (Supplementary Figure S6).

The abundance of the genus *Methanosaeta* was unusually low in both digesters compared to other reported anaerobic environments, where it is often the most abundant methanogen genus (Ariesady et al., 2007; Nelson et al., 2011). Our previous amplicon-sequencing based study found the *Methanosaetaceae* to outnumber *Methanosarcinaceae* in both GZ and SWH (Wilkins et al., 2015a). Variation in the relative proportions of *Methanosaeta* and *Methanosarcina* in anaerobic digesters has been linked to operating parameters such as the frequency of substrate feeding (Conklin et al., 2006) and retention time (Ma et al., 2013), as well as biochemical factors including H₂ partial pressure and the presence of heavy metals (Yilmaz et al., 2014). Pairwise comparison of the contigs assembled from GZ and SWH found that the most similar sequences were mainly methanogens (based on NCBI nr annotation), particularly the strain *Methanosaeta concilii* GP6 (similarity >99%), indicating the two systems shared overall similar methanogen compositions.

In addition to analyzing the distribution of phylogenetic and functional genes as in previous studies (Schluter et al., 2008; Wirth et al., 2012; Wang et al., 2013) or describing the dominant pathways (Li et al., 2013), functional AD pathways were reconstructed and the relative abundances of genera from both metagenomes that may be performing these functions mapped on to these pathways. Genera associated with acidogenesis were less evenly distributed (Supplementary Table S5) than those associated with other steps. This was unexpected, as acidogenesis populations are more reliant on functional redundancy (Werner et al., 2011), while syntrophic bacteria, which are much less abundant than other functional bacteria in AD process, are sensitive to environmental change (McInerney et al., 2009; Werner et al., 2011). The more even distribution of genera in GZ (Supplementary Table S5) indicates that the community should be more functionally stable, as the presence of more parallel pathways provides resilience against fluctuations in substrate loading (Hashsham et al., 2000). This has been experimentally verified in both lab-scale (Hashsham et al., 2000) and full-scale (Werner et al., 2011) reactors, and it has been further shown that evenness rather than richness is the key factor in preserving the functional stability of an ecosystem (Wittebolle et al., 2009). In studies of anaerobic reactors with differing evenness, Werner et al. (2011) found that communities with greater evenness had higher methanogenic activity, suggesting that GZ may have higher methanogenic potential than SWH. Manipulating community evenness (e.g., by transient disturbances; Cabrol et al., 2016) may be a practical strategy for optimizing biogas production.

This study compared municipal wastewater and sludge metagenomes. Despite having different taxonomic profiles, GZ and SWH shared mostly similar potential microbial functions,

and of the major functional differences most could be related directly to the digester feedstocks. Mapping of taxa to the major metabolic pathways in AD allowed the major functional taxa in each digester to be determined, and the more even distribution of genera performing major AD functions in GZ suggested a stronger adaptive capability than in SWH (functional stability). We found the metagenome of GZ was similar to that of a production-scale biogas plant both at the phylogenetic and functional level, confirming the biogas-producing potential of industrial wastewater AD. While this study of a single high-strength industrial wastewater AD system may not be globally representative, it strongly suggests that there are major functional differences compared to the better-studied municipal sludge systems that can be directly linked to feedstock, and provides a basis for further investigation of industrial wastewater AD. Future studies should also further explore the AD microbial community with metatranscriptomic and metaproteomic analyses to better understand the metabolic functions.

REFERENCES

- Agler, M. T., Wrenn, B. A., Zinder, S. H., and Angenent, L. T. (2011). Waste to bioproduct conversion with undefined mixed cultures: the carboxylate platform. *Trends Biotechnol.* 29, 70–78. doi: 10.1016/j.tibtech.2010.11.006
- Angelidaki, I., and Ellegaard, L. (2003). Codigestion of manure and organic wastes in centralized biogas plants - Status and future trends. *Appl. Biochem. Biotechnol.* 109, 95–105. doi: 10.1385/ABAB:109:1-3:95
- Ariesady, H. D., Ito, T., and Okabe, S. (2007). Functional bacterial and archaeal community structures of major trophic groups in a full-scale anaerobic sludge digester. *Water Res.* 41, 1554–1568. doi: 10.1016/j.watres.2006.12.036
- Benson, D. A., Karsch-Mirzachi, I., Lipman, D. J., Ostell, J., and Wheeler, D. L. (2008). GenBank. *Nucleic Acids Res.* 36, D25–D30. doi: 10.1093/nar/gkm929
- Bibby, K., and Peccia, J. (2013). Identification of viral pathogen diversity in sewage sludge by metagenome analysis. *Environ. Sci. Technol.* 47, 1945–1951. doi: 10.1021/es305181x
- Blanchard, M., Teil, M. J., Ollivon, D., Legenti, L., and Chevreuil, M. (2004). Polycyclic aromatic hydrocarbons and polychlorobiphenyls in wastewaters and sewage sludges from the Paris area (France). *Environ. Res.* 95, 184–197. doi: 10.1016/j.envres.2003.07.003
- Breitbart, M., Hoare, A., Nitti, A., Siebert, J., Haynes, M., Dinsdale, E., et al. (2009). Metagenomic and stable isotopic analyses of modern freshwater microbialites in Cuatro CiEegas, Mexico. *Environ. Microbiol.* 11, 16–34. doi: 10.1111/j.1462-2920.2008.01725.x
- Cabrol, L., Poly, F., Malhautier, L., Pommier, T., Lerondelle, C., Verstraete, W., et al. (2016). Management of microbial communities through transient disturbances enhances the functional resilience of nitrifying gas-biofilters to future disturbances. *Environ. Sci. Technol.* 50, 338–348. doi: 10.1021/acs.est.5b02740
- Caspi, R., Altman, T., Billington, R., Dreher, K., Foerster, H., Fulcher, C. A., et al. (2014). The MetaCyc database of metabolic pathways and enzymes and the BioCyc collection of Pathway/Genome Databases. *Nucleic Acids Res.* 42, D459–D471. doi: 10.1093/Nar/Gkt1103
- Conklin, A., Stensel, H. D., and Ferguson, J. (2006). Growth kinetics and competition between Methanosaeta and Methanosaeta in mesophilic anaerobic digestion. *Water Environ. Res.* 78, 486–496. doi: 10.2175/106143006x95393
- Coon, M. J., Ding, X. X., Perneky, S. J., and Vaz, A. D. (1992). Cytochrome P450: progress and predictions. *FASEB J.* 6, 669–673.
- Dassa, B., Borovok, I., Ruimy-Israeli, V., Lamed, R., Flint, H. J., Duncan, S. H., et al. (2014). Rumen cellulosomics: divergent fiber-degrading strategies revealed by comparative genome-wide analysis of six ruminococcal strains. *PLoS ONE* 9:e99221. doi: 10.1371/journal.pone.0099221
- de Oliveira, L. L., Costa, R. B., Okada, D. Y., Vich, D. V., Duarte, I. C. S., Silva, E. L., et al. (2010). Anaerobic degradation of linear alkylbenzene sulfonate (LAS) in fluidized bed reactor by microbial consortia in different support materials. *Bioresour. Technol.* 101, 7687–7687. doi: 10.1016/j.biortech.2010.04.041
- Diels, L., Dong, Q., van der Lelie, D., Baeyens, W., and Mergeay, M. (1995). The czc operon of *Alcaligenes eutrophus* CH34: from resistance mechanism to the removal of heavy metals. *J. Ind. Microbiol.* 14, 142–153. doi: 10.1007/Bf01569896
- Dong, B., Liu, X. G., Dai, L. L., and Dai, X. H. (2013). Changes of heavy metal speciation during high-solid anaerobic digestion of sewage sludge. *Bioresour. Technol.* 131, 152–158. doi: 10.1016/j.biortech.2012.12.112
- El-Mashad, H. M., Zeeman, G., van Loon, W. K., Bot, G. P., and Lettinga, G. (2004). Effect of temperature and temperature fluctuation on thermophilic anaerobic digestion of cattle manure. *Bioresour. Technol.* 95, 191–201. doi: 10.1016/j.biortech.2003.07.013
- Feng, L. Y., Luo, J. Y., and Chen, Y. G. (2015). Dilemma of Sewage Sludge Treatment and Disposal in China. *Environ. Sci. Technol.* 49, 4781–4782. doi: 10.1021/acs.est.5b01455
- Ferrer, M., Golyshina, O. V., Chernikova, T. N., Khachane, A. N., Reyes-Duarte, D., Dos Santos, V. A. P. M., et al. (2005a). Novel hydrolase diversity retrieved from a metagenome library of bovine rumen microflora. *Environ. Microbiol.* 7, 1996–2010. doi: 10.1111/j.1462-2920.2005.00920.x
- Ferrer, M., Martinez-Abarca, F., and Golyshin, P. N. (2005b). Mining genomes and ‘metagenomes’ for novel catalysts. *Curr. Opin. Biotechnol.* 16, 588–593. doi: 10.1016/j.copbio.2005.09.001
- Fierer, N., Leff, J. W., Adams, B. J., Nielsen, U. N., Bates, C. T., Lauber, C. L., et al. (2012). Cross-biome metagenomic analyses of soil microbial communities and their functional attributes. *Proc. Natl. Acad. Sci. U.S.A.* 109, 21390–21395. doi: 10.1073/pnas.1215210110
- Fisher, W. D. (1958). On grouping for maximum homogeneity. *J. Am. Stat. Assoc.* 53, 789–798. doi: 10.1080/01621459.1958.10501479
- Francis, C. A., Beman, J. M., and Kuypers, M. M. (2007). New processes and players in the nitrogen cycle: the microbial ecology of anaerobic and archaeal ammonia oxidation. *ISME J.* 1, 19–27. doi: 10.1038/ismej.2007.8
- Hashsham, S. A., Fernandez, A. S., Dollhopf, S. L., Dazzo, F. B., Hickey, R. F., Tiedje, J. M., et al. (2000). Parallel processing of substrate correlates with greater functional stability in methanogenic bioreactor communities perturbed by glucose. *Appl. Environ. Microbiol.* 66, 4050–4057. doi: 10.1128/Aem.66.9.4050-4057.2000
- Howe, A. C., Jansson, J. K., Malfatti, S. A., Tringe, S. G., Tiedje, J. M., and Brown, C. T. (2014). Tackling soil diversity with the assembly of large,

AUTHOR CONTRIBUTIONS

MC analyzed data and wrote the manuscript. DW, JC, S-KN, HL, and YJ analyzed data. PL designed the experiment and wrote the manuscript.

ACKNOWLEDGMENTS

This research was supported by the Research Grants Council of Hong Kong through project 11206514. MC, HL, and YJ thank the City University of Hong Kong for their postgraduate studentships.

SUPPLEMENTARY MATERIAL

The Supplementary Material for this article can be found online at: <http://journal.frontiersin.org/article/10.3389/fmicb.2016.00778>

- complex metagenomes. *Proc. Natl. Acad. Sci. U.S.A.* 111, 4904–4909. doi: 10.1073/pnas.1402564111
- Hu, Y. F., Fu, C. Z., Yin, Y. S., Cheng, G., Lei, F., Yang, X., et al. (2010). Construction and preliminary analysis of a deep-sea sediment metagenomic fosmid library from Qiongdongnan Basin, South China Sea. *Mar. Biotechnol.* 12, 719–727. doi: 10.1007/s10126-010-9259-1
- Jensen, L. J., Julien, P., Kuhn, M., von Mering, C., Muller, J., Doerks, T., et al. (2008). eggNOG: automated construction and annotation of orthologous groups of genes. *Nucleic Acids Res.* 36, D250–D254. doi: 10.1093/nar/gkm796
- Jetten, M. S. M., Horn, S. J., and van Loosdrecht, M. C. M. (1997). Towards a more sustainable municipal wastewater treatment system. *Water Sci. Technol.* 35, 171–180. doi: 10.1016/S0273-1223(97)00195-9
- Jia, Y., Wilkins, D., Lu, H., Cai, M., and Lee, P. K. H. (2016). Long-term enrichment on cellulose or xylyan causes functional and taxonomic convergence of microbial communities from anaerobic digesters. *Appl. Environ. Microbiol.* 82, 1519–1529. doi: 10.1128/AEM.00360-15
- Kanehisa, M., and Goto, S. (2000). KEGG: kyoto encyclopedia of genes and genomes. *Nucleic Acids Res.* 28, 27–30. doi: 10.1093/nar/28.1.27
- Kent, W. J. (2002). BLAT - The BLAST-like alignment tool. *Genome Res.* 12, 656–664. doi: 10.1101/Gr.229202
- Lee, M. J., and Zinder, S. H. (1988). Carbon monoxide pathway enzyme activities in a thermophilic anaerobic bacterium grown acetogenically and in a syntrophic acetate-oxidizing coculture. *Arch. Microbiol.* 150, 513–518. doi: 10.1007/Bf00408241
- Li, A., Chu, Y. N., Wang, X. M., Ren, L. F., Yu, J., Liu, X. L., et al. (2013). A pyrosequencing-based metagenomic study of methane-producing microbial community in solid-state biogas reactor. *Biotechnol. Biofuels* 6:1. doi: 10.1186/1754-6834-6-3
- Li, Y. B., Park, S. Y., and Zhu, J. Y. (2011). Solid-state anaerobic digestion for methane production from organic waste. *Renew. Sust. Energ. Rev.* 15, 821–826. doi: 10.1016/j.rser.2010.07.042
- Lopez-Garcia, P., and Moreira, D. (2006). Selective forces for the origin of the eukaryotic nucleus. *Bioessays* 28, 525–533. doi: 10.1002/Bies.20413
- Lu, X. Y., Rao, S., Shen, Z. Y., and Lee, P. K. H. (2013). Substrate induced emergence of different active bacterial and archaeal assemblages during biomethane production. *Bioresour. Technol.* 148, 517–524. doi: 10.1016/j.biortech.2013.09.017
- Luo, G., Wang, W., and Angelidaki, I. (2013). Anaerobic digestion for simultaneous sewage sludge treatment and CO biomethanation: process performance and microbial ecology. *Environ. Sci. Technol.* 47, 10685–10693. doi: 10.1021/es401018d
- Lv, X. M., Shao, M. F., Li, C. L., Li, J., Gao, X. L., and Sun, F. Y. (2014). A comparative study of the bacterial community in denitrifying and traditional enhanced biological phosphorus removal processes. *Microbes Environ.* 29, 261–268. doi: 10.1264/jsme2.ME13132
- Ma, J. W., Zhao, B. S., Frear, C., Zhao, Q. B., Yu, L., Li, X. J., et al. (2013). Methanosaerina domination in anaerobic sequencing batch reactor at short hydraulic retention time. *Bioresour. Technol.* 137, 41–50. doi: 10.1016/j.biortech.2013.03.101
- Mackelprang, R., Waldrop, M. P., DeAngelis, K. M., David, M. M., Chavarria, K. L., Blazewicz, S. J., et al. (2011). Metagenomic analysis of a permafrost microbial community reveals a rapid response to thaw. *Nature* 480, 368–371. doi: 10.1038/nature10576
- Magrane, M., and UniProt Consortium. (2011). UniProt Knowledgebase: a hub of integrated protein data. *Database* 2011:bar009. doi: 10.1093/database/bar009
- Markowitz, V. M., Ivanova, N. N., Szeto, E., Palaniappan, K., Chu, K., Dalevi, D., et al. (2008). IMG/M: a data management and analysis system for metagenomes. *Nucleic Acids Res.* 36, D534–D538. doi: 10.1093/nar/gkm869
- Mason, O. U., Scott, N. M., Gonzalez, A., Robbins-Pianka, A., Baelum, J., Kimbrel, J., et al. (2014). Metagenomics reveals sediment microbial community response to deepwater horizon oil spill. *ISME J.* 8, 1464–1475. doi: 10.1038/ismej.2013.254
- McInerney, M. J., Sieber, J. R., and Gunsalus, R. P. (2009). Syntropy in anaerobic global carbon cycles. *Curr. Opin. Biotechnol.* 20, 623–632. doi: 10.1016/j.copbio.2009.10.001
- Meyer, F., Paarmann, D., D'Souza, M., Olson, R., Glass, E. M., Kubal, M., et al. (2008). The metagenomics RAST server - a public resource for the automatic phylogenetic and functional analysis of metagenomes. *BMC Bioinformatics* 9:386. doi: 10.1186/1471-2105-9-386
- Moon, Y. H., Iakiviak, M., Bauer, S., Mackie, R. I., and Cann, I. K. O. (2011). Biochemical analyses of multiple endoxylanases from the rumen bacterium *Ruminococcus albus* 8 and their synergistic activities with accessory hemicellulose-degrading enzymes. *Appl. Environ. Microbiol.* 77, 5157–5169. doi: 10.1128/Aem.00353-11
- Müller, B., Sun, L., and Schnurer, A. (2013). First insights into the syntrophic acetate-oxidizing bacteria - a genetic study. *Microbiologyopen* 2, 35–53. doi: 10.1002/Mbo3.50
- Müller, N., Worm, P., Schink, B., Stams, A. J. M., and Plugge, C. M. (2010). Syntrophic butyrate and propionate oxidation processes: from genomes to reaction mechanisms. *Environ. Microbiol. Rep.* 2, 489–499. doi: 10.1111/j.1758-2229.2010.00147.x
- Nelson, M. C., Morrison, M., and Yu, Z. (2011). A meta-analysis of the microbial diversity observed in anaerobic digesters. *Bioresour. Technol.* 102, 3730–3739. doi: 10.1016/j.biortech.2010.11.119
- Newcombe, R. G. (1998). Improved confidence intervals for the difference between binomial proportions based on paired data. *Stat. Med.* 17, 2635–2650. doi: 10.1002/(SICI)1097-0258(19981130)17:22<2635::AID-SIM954>3.3.CO;2-3
- Overbeek, R., Begley, T., Butler, R. M., Choudhuri, J. V., Chuang, H. Y., Cohoon, M., et al. (2005). The subsystems approach to genome annotation and its use in the project to annotate 1000 genomes. *Nucleic Acids Res.* 33, 5691–5702. doi: 10.1093/nar/gki866
- Parks, D. H., and Beiko, R. G. (2010). Identifying biologically relevant differences between metagenomic communities. *Bioinformatics* 26, 715–721. doi: 10.1093/bioinformatics/btq041
- Peng, Y., Leung, H. C., Yiu, S. M., and Chin, F. Y. (2012). IDBA-UD: a de novo assembler for single-cell and metagenomic sequencing data with highly uneven depth. *Bioinformatics* 28, 1420–1428. doi: 10.1093/bioinformatics/bts174
- Qin, J., Li, R., Raes, J., Arumugam, M., Burgdorf, K. S., Manichanh, C., et al. (2010). A human gut microbial gene catalogue established by metagenomic sequencing. *Nature* 464, 59–65. doi: 10.1038/nature08821
- Rademacher, A., Zakrzewski, M., Schluter, A., Schonberg, M., Szczepanowski, R., Goemann, A., et al. (2012). Characterization of microbial biofilms in a thermophilic biogas system by high-throughput metagenome sequencing. *FEMS Microbiol. Ecol.* 79, 785–799. doi: 10.1111/j.1574-6941.2011.01265.x
- Rajeshwari, K. V., Balakrishnan, M., Kansal, A., Lata, K., and Kishore, V. V. N. (2000). State-of-the-art of anaerobic digestion technology for industrial wastewater treatment. *Renew. Sust. Energ. Rev.* 4, 135–156. doi: 10.1016/S1364-0321(99)00014-3
- Riviere, D., Desvignes, V., Pelletier, E., Chaussonnerie, S., Guermazi, S., Weissenbach, J., et al. (2009). Towards the definition of a core of microorganisms involved in anaerobic digestion of sludge. *ISME J.* 3, 700–714. doi: 10.1038/ismej.2009.2
- Ruby, J. G., Bellare, P., and DeRisi, J. L. (2013). PRICE: software for the targeted assembly of components of (meta) genomic sequence data. *G3-Genes. Genom. Genet.* 3, 865–880. doi: 10.1534/g3.113.005967
- Sahlstrom, L. (2003). A review of survival of pathogenic bacteria in organic waste used in biogas plants. *Bioresour. Technol.* 87, 161–166. doi: 10.1016/S0960-8524(02)00168-2
- Scheer, M., Grote, A., Chang, A., Schomburg, I., Munaretto, C., Rother, M., et al. (2011). BRENDA, the enzyme information system in 2011. *Nucleic Acids Res.* 39, D670–D676. doi: 10.1093/Nar/Gkq1089
- Schluter, A., Bekel, T., Diaz, N. N., Dondrup, M., Eichenlaub, R., Gartemann, K. H., et al. (2008). The metagenome of a biogas-producing microbial community of a production-scale biogas plant fermenter analysed by the 454-pyrosequencing technology. *J. Biotechnol.* 136, 77–90. doi: 10.1016/j.biote.2008.05.008
- Smith, R. J., Jeffries, T. C., Roudnew, B., Fitch, A. J., Seymour, J. R., Delpin, M. W., et al. (2012). Metagenomic comparison of microbial communities inhabiting confined and unconfined aquifer ecosystems. *Environ. Microbiol.* 14, 240–253. doi: 10.1111/j.1462-2920.2011.02614.x
- Sousa, D. Z., Smidt, H., Alves, M. M., and Stams, A. J. M. (2009). Ecophysiology of syntrophic communities that degrade saturated and unsaturated long-chain fatty acids. *FEMS Microbiol. Ecol.* 68, 257–272. doi: 10.1111/j.1574-6941.2009.00680.x
- Storey, J. D., and Tibshirani, R. (2003). “SAM thresholding and false discovery rates for detecting differential gene expression in DNA microarrays,” in *The Analysis*

- of *Gene Expression Data*, eds G. Parmigiani, E. S. Garrett, R. A. Irizarry, and S. L. Zeger (New York, NY: Springer), 272–290.
- Tang, K., Liu, K., Jiao, N., Zhang, Y., and Chen, C. T. (2013). Functional metagenomic investigations of microbial communities in a shallow-sea hydrothermal system. *PLoS ONE* 8:e72958. doi: 10.1371/journal.pone.0072958
- Wagner, M., and Loy, A. (2002). Bacterial community composition and function in sewage treatment systems. *Curr. Opin. Biotechnol.* 13, 218–227. doi: 10.1016/s0958-1669(02)00315-4
- Wang, Z., Zhang, X. X., Huang, K., Miao, Y., Shi, P., Liu, B., et al. (2013). Metagenomic profiling of antibiotic resistance genes and mobile genetic elements in a tannery wastewater treatment plant. *PLoS ONE* 8:e76079. doi: 10.1371/journal.pone.0076079
- Weiland, P. (2003). Production and energetic use of biogas from energy crops and wastes in Germany. *Appl. Biochem. Biotechnol.* 109, 263–274. doi: 10.1385/Abab
- Werner, J. J., Knights, D., Garcia, M. L., Scalfone, N. B., Smith, S., Yarasheski, K., et al. (2011). Bacterial community structures are unique and resilient in full-scale bioenergy systems. *Proc. Natl. Acad. Sci. U.S.A.* 108, 4158–4163. doi: 10.1073/pnas.1015676108
- Wilbanks, E. G., Jaekel, U., Salman, V., Humphrey, P. T., Eisen, J. A., Facciotti, M. T., et al. (2014). Microscale sulfur cycling in the phototrophic pink berry consortia of the Sippewissett Salt Marsh. *Environ. Microbiol.* 16, 3398–3415. doi: 10.1111/1462-2920.12388
- Wilkins, D., Lu, X. Y., Shen, Z., Chen, J., and Lee, P. K. H. (2015a). Pyrosequencing of mcrA and archaeal 16S rRNA genes reveals diversity and substrate preferences of methanogen communities in anaerobic digesters. *Appl. Environ. Microbiol.* 81, 604–613. doi: 10.1128/AEM.02566-14
- Wilkins, D., Rao, S., Lu, X. Y., and Lee, P. K. H. (2015b). Effects of sludge inoculum and organic feedstock on active microbial communities and methane yield during anaerobic digestion. *Front. Microbiol.* 6:1114. doi: 10.3389/fmicb.2015.01114
- Wilmes, P., Wexler, M., and Bond, P. L. (2008). Metaproteomics provides functional insight into activated sludge wastewater treatment. *PLoS ONE* 3:e1778. doi: 10.1371/journal.pone.0001778
- Wirth, R., Kovacs, E., Maroti, G., Bagi, Z., Rakheley, G., and Kovacs, K. L. (2012). Characterization of a biogas-producing microbial community by short-read next generation DNA sequencing. *Biotechnol. Biofuels* 5:41. doi: 10.1186/1754-6834-5-41
- Wittebolle, L., Marzorati, M., Clement, L., Balloi, A., Daffonchio, D., Heylen, K., et al. (2009). Initial community evenness favours functionality under selective stress. *Nature* 458, 623–626. doi: 10.1038/Nature07840
- Wong, M. T., Zhang, D., Li, J., Hui, R. K., Tun, H. M., Brar, M. S., et al. (2013). Towards a metagenomic understanding on enhanced biomethane production from waste activated sludge after pH 10 pretreatment. *Biotechnol. Biofuels* 6:38. doi: 10.1186/1754-6834-6-38
- Yang, Y., Yu, K., Xia, Y., Lau, F. T., Tang, D. T., Fung, W. C., et al. (2014). Metagenomic analysis of sludge from full-scale anaerobic digesters operated in municipal wastewater treatment plants. *Appl. Microbiol. Biotechnol.* 98, 5709–5718. doi: 10.1007/s00253-014-5648-0
- Ye, L., Zhang, T., Wang, T., and Fang, Z. (2012). Microbial structures, functions, and metabolic pathways in wastewater treatment bioreactors revealed using high-throughput sequencing. *Environ. Sci. Technol.* 46, 13244–13252. doi: 10.1021/es303454k
- Yilmaz, V., Ince-Yilmaz, E., Yilmazel, Y. D., and Duran, M. (2014). Is aceticlastic methanogen composition in full-scale anaerobic processes related to acetate utilization capacity? *Appl. Microbiol. Biotechnol.* 98, 5217–5226. doi: 10.1007/s00253-014-5597-7
- Zinder, S. H., and Koch, M. (1984). Non-aceticlastic methanogenesis from acetate: acetate oxidation by a thermophilic syntrophic coculture. *Arch. Microbiol.* 138, 263–272. doi: 10.1007/Bf00402133

Conflict of Interest Statement: The authors declare that the research was conducted in the absence of any commercial or financial relationships that could be construed as a potential conflict of interest.

Copyright © 2016 Cai, Wilkins, Chen, Ng, Lu, Jia and Lee. This is an open-access article distributed under the terms of the Creative Commons Attribution License (CC BY). The use, distribution or reproduction in other forums is permitted, provided the original author(s) or licensor are credited and that the original publication in this journal is cited, in accordance with accepted academic practice. No use, distribution or reproduction is permitted which does not comply with these terms.



Formate-Dependent Microbial Conversion of CO₂ and the Dominant Pathways of Methanogenesis in Production Water of High-temperature Oil Reservoirs Amended with Bicarbonate

Guang-Chao Yang¹, Lei Zhou¹, Serge M. Mbadinga^{1,2}, Jin-Feng Liu¹, Shi-Zhong Yang¹, Ji-Dong Gu³ and Bo-Zhong Mu^{1,2*}

¹ State Key Laboratory of Bioreactor Engineering and Institute of Applied Chemistry, East China University of Science and Technology, Shanghai, China, ² Shanghai Collaborative Innovation Center for Biomanufacturing Technology, Shanghai, China, ³ School of Biological Sciences, The University of Hong Kong, Hong Kong, China

OPEN ACCESS

Edited by:

Fernando G. Feroso,
Instituto de la Grasa – Consejo
Superior de Investigaciones
Científicas, Spain

Reviewed by:

Uwe Strotmann,
Westfälische Hochschule, Germany
Petra Worm,
Wageningen University, Netherlands

*Correspondence:

Bo-Zhong Mu
bzmu@ecust.edu.cn

Specialty section:

This article was submitted to
Microbiotechnology, Ecotoxicology
and Bioremediation,
a section of the journal
Frontiers in Microbiology

Received: 23 January 2016

Accepted: 07 March 2016

Published: 22 March 2016

Citation:

Yang G-C, Zhou L, Mbadinga SM, Liu J-F, Yang S-Z, Gu J-D and Mu B-Z (2016) Formate-Dependent Microbial Conversion of CO₂ and the Dominant Pathways of Methanogenesis in Production Water of High-temperature Oil Reservoirs Amended with Bicarbonate. *Front. Microbiol.* 7:365.
doi: 10.3389/fmicb.2016.00365

CO₂ sequestration in deep-subsurface formations including oil reservoirs is a potential measure to reduce the CO₂ concentration in the atmosphere. However, the fate of the CO₂ and the ecological influences in carbon dioxide capture and storage (CDCS) facilities is not understood clearly. In the current study, the fate of CO₂ (in bicarbonate form; 0~90 mM) with 10 mM of formate as electron donor and carbon source was investigated with high-temperature production water from oilfield in China. The isotope data showed that bicarbonate could be reduced to methane by methanogens and major pathway of methanogenesis could be syntrophic formate oxidation coupled with CO₂ reduction and formate methanogenesis under the anaerobic conditions. The bicarbonate addition induced the shift of microbial community. Addition of bicarbonate and formate was associated with a decrease of *Methanosarcinales*, but promotion of *Methanobacteriales* in all treatments. *Thermodesulfovibrio* was the major group in all the samples and *Thermacetogenium* dominated in the high bicarbonate treatments. The results indicated that CO₂ from CDSCS could be transformed to methane and the possibility of microbial CO₂ conversion for enhanced microbial energy recovery in oil reservoirs.

Keywords: bicarbonate, oil reservoirs, stable isotope technique, CDSCS, methanogenesis, CO₂ conversion

INTRODUCTION

In recent years, increasing atmospheric CO₂ and the resulting climate problem become the focus of global issues. A total of 3.2 gigatonnes of CO₂ is released by the combustion of fossil fuels each year and has led to an increase of atmospheric CO₂ concentrations from 280 ppm in 18th century to 383 ppm in Glueck et al. (2010). Three mainly strategies to reduce CO₂ emission and building up are: reducing the CO₂ production, expanding the CO₂ utilization, and CO₂ sequestration and storage (Schrag, 2007; Yang et al., 2008). The major approaches to decrease the

CO₂ production include improvement of energy efficiency or employment of cleaner technologies. Based on energy utilization and economic input, CO₂ is chemically relatively stable and a non-attractive raw material. Carbon dioxide capture and storage (CDCS) is regarded as a potential and practical method to reduce the CO₂ emission into atmosphere. The injection of CO₂ into the oil reservoirs and geosystems may not only enhance the oil recovery (EOR) but also store about two-thirds of the CO₂ in underground systems (Mikkelsen et al., 2010; Dressel et al., 2011; Momeni et al., 2012). Injected CO₂ could be an important factor and affects the microbial metabolism and ecophysiology in storage environment (Delgado et al., 2012; Lin et al., 2013). Injected CO₂ could alter the microbial community and the methanogenic pathways (Mayumi et al., 2013) and raise the bicarbonate concentration in oil reservoirs (Kirk, 2011).

The injection of CO₂ from CDCS can be transformed into methane by microorganisms for energy recovery as value-added options, but electron donors are essential for the process (Hattori et al., 2001; De Bok et al., 2004). Formate and H₂ are known as carriers for interspecies electron transfer and CO₂ can be reduced with formate and H₂ as electron donors through CO₂-reducing microorganisms in anoxic environments (Dolfing et al., 2008). Interconversion of H₂ and CO₂ to formate by the microorganism at ambient conditions has been reported (Schuchmann and Müller, 2013). The *Thermococcus* sp. are capable of formate oxidation with H₂ production alone at high-temperature (Kim et al., 2010). Many species of microorganisms can grow on formate as a sole methanogenic substrate (Wood et al., 2003; Oren, 2014). Formate can be used by some types of methanogens with formate dehydrogenase alone for H₂ production and methane production (Lupa et al., 2008). Formate plays an important role as H₂ storage compound for CO₂ reduction in subsurface formation.

Formate is an important metabolite in anaerobic alkane oxidation in *Desulfatibacillum alkenivorans* AK-01 (Callaghan et al., 2012). Formate also plays an important role as intermediates in syntrophic butyrate or propionate oxidization (Hattori et al., 2001). Hydrogen production based on formate oxidation has been described before (Bagramyan and Trchounian, 2003; Meshulam-Simon et al., 2007). And both thermophilic and mesophilic communities with a formate-oxidizing bacterium and a hydrogenotrophic methanogen have been constructed for demonstration of syntrophic growth on formate (Dolfing et al., 2008). Formate serve as important degradation intermediate of alkanes and precursor for methanogenesis in oil reservoirs, but very little is known about formate metabolism before.

The whole oil reservoir can be regarded as an anaerobic bioreactor with variety of specialized microorganisms and has the potential for bioconversion of CO₂ (Liu et al., 2015). However, very little is known about the fate of sequestered CO₂ and the anaerobic metabolic pathway of formate in oil reservoir. In this study, the treatments were constructed with production water of high-temperature oil reservoirs amended with formate and different concentrations of C-13 labeled bicarbonate. Microbial community was analyzed based on 16S rRNA gene after incubation and high levels of methane generated.

In addition, stable isotope technique was introduced to detect the fate of injected CO₂. The objectives of this study were to provide evidence on the possibility of microbial conversion of CO₂ and metabolic pathways of formate.

MATERIALS AND METHODS

Preparation of Inoculum and Enrichment Cultures

The inoculum for the culture experiments was collected from water-flooded oilfield production water of Ba 18 block of Baolige, Huabei Oilfield in China, and cultured under anaerobic conditions at 55°C in the dark. Physicochemical characteristics of the inoculum is shown in Supplementary Table S1. About 2 mL of inoculum was transferred aseptically into a serum bottle (120 ml internal volume) with 50 ml of basal medium containing (g/L): NaCl, 0.20; MgCl₂.6H₂O, 1.20; CaCl₂.2H₂O, 0.10; NH₄Cl, 0.25; KH₂PO₄, 0.75; K₂HPO₄, 1.16; KCl, 1.30; rezusurin, 0.0001. Vitamin stock solution and trace element stock solution of 1.0 (mL/L) and Na₂S.9H₂O (0.50 g/L) were added into the medium and the final pH of the basal medium was adjusted to 7.2. The detailed composition of the vitamin stock solution and trace element stock solution was described before (Wang et al., 2012b).

¹³C-bicarbonate was introduced with a final concentration of 0, 30, 60, and 90 mM. Formate was added as the carbon source and electron donor at 10 mM. Basal medium with different concentrations of bicarbonate without added formate was used as blank. Treatments were abbreviated accordingly as S0, S30, S60, and S90 for different bicarbonate concentrations. All sets of experiments were conducted in triplicate. During the operation, the serum bottles were sealed with pure N₂ gas and removed the O₂ from the systems. All the microcosms were incubated at 55°C in the dark.

Chemical Analysis

Gas composition (CH₄, CO₂, and H₂) of headspace was measured using a Gas Chromatograph (GC112A, Shanghai Precision and Scientific Instrument, CO., Ltd, China) with a thermal conductivity detector (TCD) and a flame ionization detector (FID). The detailed method was followed as described before (Mbadinga et al., 2012). Formate and acetate were detected and quantified by Ion Chromatograph (IC DX-600, Dionex, CO., USA) with IonPac AS11-HC analytical column (4 mm × 250 mm) and ASRS 300 suppressor. The mobile phase was 2 mM of NaOH.

DNA and 16S rRNA Gene Amplification

Five mL of the culture samples were taken and concentrated by centrifugation at 12000 × g for 20 min at 4°C after 180 days cultivation. Total community DNA was extracted from the microbial biomass using the genomic DNA Kit (AxygenBiosciences, Inc., USA). Partial 16S rRNA genes of bacteria and archaea were amplified as previously described with primer 8F/805R (Zhou et al., 2013) and 340F/1000R (Gantner et al., 2011), respectively. Polymerase chain reaction (PCR) was

performed in a 25 μl reaction volume containing 12.5 μM of each primer (1 μl), 50 ng of template DNA (2 μl), 12.5 μl of 2 \times PCR master mix (LifeFeng Biotechnology, Shanghai, China) and 8.5 μl ddH₂O. PCR programs were as follows: an initial denaturation step at 95°C for 5 min, followed by 32 cycles of 94°C for 45 s, 59°C for 40 s, and 72°C for 50 s, with a final elongation step at 72°C for 10 min. Genes were amplified on a Peltier Thermal Cycler (Bio-Rad, CO., USA).

Construction of 16S rRNA Genes Libraries and Phylogenetic Analysis

Polymerase chain reaction products were cloned with a pMD 19-T simple vector kit (TaKaRa Bio, Inc., Japan) after checking by 1.8% (agarose) gel electrophoresis. Clones were randomly selected from plates and sequenced on an ABI 377 automated sequencer. The 16S rRNA sequences were checked and phylogenetic trees were generated with the protocol described before (Wang et al., 2012a). Operational taxonomic units (OTUs) were defined with the similarity of more than 97%. Phylogenetic trees of 16S rRNA genes retrieved from the original inoculum, S0, S30, S60, and S90 samples, were constructed. Sequences were performed by MEGA 5 with OTU identity of 97%. The topology of the tree was obtained with the neighbor-joining method. Bootstrap values ($n = 1000$ replicates) of $\geq 75\%$ are showed.

Data Analysis of Stable Isotope

Carbon-13 isotopic compositions of CH₄ and CO₂ were determined with isotope ratio mass spectrometer (IRMS Delta V PLUS, Thermo Scientific, CO., USA). The samples were concentrated with PreCon connector to reduce dose. The standard international delta notation for reporting isotopic value ratios were relative to the VPDB standard. The reference gas was CO₂ and $\delta^{13}\text{C}_{\text{PDB}}$ was $-23.73\text{\textperthousand}$, which was calibrated by stable isotope of carbon in charcoal black. The system was performed with ISODATNT software.

Thermodynamic Calculations

Gibbs free energy data for thermodynamic calculations with different temperatures (Table 1) were taken from (Amend and Shock, 2001). $\Delta G^{\circ}\text{T}$ is standard Gibbs free energy at temperature T and $\Delta G^{\circ'}\text{T}$ is modified with the protons from $\Delta G^{\circ}\text{T}$. The change of Gibbs free energy ($\Delta G'\text{T}$) for the reaction is calculated

with the formula: $\Delta G'_{55} = \Delta G^{\circ'}_{55} - RT\ln([R]^a/[P]^b)$, R and P are the abbreviations of reactants and products, respectively; a and b are the stoichiometric numbers of each composition.

Nucleotide Sequence Accession Numbers

The partial gene sequences for bacteria and archaea obtained from the clone libraries were submitted to GenBank database under accession numbers KR049100–KR049155 and KR017718–KR017745, respectively.

RESULTS

Methane and Hydrogen Production

Methane production increased after the initial 35 days of incubation under strictly anaerobic conditions, and an obvious lag period was observed in S90 compared with the other treatments (Figures 1A,B). The rate of methane production in S90 was about 1.95 pmol d⁻¹ ml⁻¹ during the culture of 35~80 days, while it was about 25.5, 41.4, and 39.1 pmol d⁻¹ ml⁻¹ in S0, S30, and S60, respectively. After 180 days of incubation, methane production in all the treatments reached approximately 136 $\mu\text{mol}/\text{bottle}$, corresponding to almost exhaustion of the 500 $\mu\text{mol}/\text{bottle}$ of formate introduced into the medium (Supplementary Table S2). Methane production was nearly equal to the formate consumed indicating that almost all of the methane produced was by formate reduction directly or indirectly. The ultimate methane production rate of all the samples was about 19.6 pmol d⁻¹ ml⁻¹. An obvious hydrogen production was found in S0 samples and subsequently depleted, and little hydrogen was detected in other samples amended with bicarbonate addition after 35 days and decreased with the further incubation of the cultures (Figure 1B), which showed the same trend with the S0 sample. The addition of bicarbonate decreased the amount of hydrogen production. There was no methane or hydrogen detected in all the blank treatments without added formate.

Dynamics of Microbial Community

16S rRNA clone libraries were constructed to analyze the microbial community under different bicarbonate concentrations

TABLE 1 | Gibbs free-energy changes for the feasible reactions of formate and hydrogen.

Reaction	$\Delta G^{\circ} \text{ 25}^{\circ}\text{C (kJ/mol)}$	$\Delta G^{\circ} \text{ 55}^{\circ}\text{C (kJ/mol)}$	$\Delta G^{\circ'} \text{ 55}^{\circ}\text{C (kJ/mol)}$
CO ₂ reduction			
HCO ₃ ⁻ + 4H ₂ + H ⁺ → CH ₄ + 3H ₂ O	-175.32	-168.66	-124.58
Acetate formation			
4HCOO ⁻ + H ⁺ → CH ₃ COO ⁻ + 2HCO ₃ ⁻	-139.69	-137.64	-93.66
Formate methanogenesis			
4HCOO ⁻ + H ₂ O + H ⁺ → CH ₄ + 3HCO ₃ ⁻	-170.84	-172.51	-128.53
Syntrophic formate oxidation			
HCOO ⁻ + H ₂ O → HCO ₃ ⁻ + H ₂	1.12	-0.92	-0.92

Formula: $\Delta G^{\circ'} = \Delta G^{\circ} + m \cdot 2.303RT\log 10^{-7}$ (m is the net number of protons formed in the equation) $\Delta G^{\circ}\text{T}$: standard Gibbs free energy at temperature T.

compared with the original inoculum. A total of 460 sequences were obtained and then used to analyze the archaeal composition in inoculum, S0, S30, S60, and S90 samples and 9, 5, 4, 2, and 2 OTUs were resulted with 97% similarity, respectively (**Figure 2**). All the archaeal sequences belong to *Methanomicrobiales*, *Methanobacteriales*, *Methanosarcinales*, and *Crenarchaeota*. Those affiliating with *Methanomicrobiales* and *Methanobacteriales* are CO₂-reducing methanogens while *Methanosarcinales* have a variety of methanogenic biochemical pathways. *Crenarchaeota* is known as ammonia-oxidizing bacteria (Hatzenpichler et al., 2008) and have no reported information about methanogenesis. The original inoculum contained the most varieties of archaea among all the five samples. With the addition of formate and increase in bicarbonate concentrations, the archaeal varieties decreased and only *Methanobacteriales* and *Crenarchaeota* were detected in S60 and S90. In the original inoculum,

Methanosarcinales were dominated (68.7%) with 3 OTUs (Inoculum-A-4, Inoculum-A-5, and Inoculum-A-7) and 3 OTUs (Inoculum-A-2, Inoculum-A-3 and Inoculum-A-6) with close identities to *Methanobacteriales* (22.4%), 2 OTUs (Inoculum-A-8 and Inoculum-A-9) belonged to *Methanomicrobiales* (7.5%) were also detected and OTU Inoculum-A-1 (1.4%) clustered into *Crenarchaeota*. *Methanobacteriales* (72.4%~83.8%) were dominated in all the culture treatments amended with formate. *Methanomicrobiales*, *Methanobacteriales*, *Methanosarcinales* and *Crenarchaeota* were all detected in the S0 and S30 samples, but only *Methanobacteriales* and *Crenarchaeota* were detected in the treatments (S60 and S90) with high bicarbonate concentrations.

By using bacterial gene specific primers, a total of 365 sequences were obtained and then analyzed with the 97% similarity to construct a phylogenetic tree about bacteria, and 7, 11, 10, 6, and 10 OTUs were found in the inoculum, S0, S30, S60, and S90 samples, respectively (**Figure 3**). Bacteria showed high varieties in all the five samples and most sequences belonged to *Thermotogae*, *Synergistetes*, *Acetothermia*, *Nitrospirales*, and *Firmicutes*. *Thermodesulffovibrio* belonged to *Nitrospirales* and *Clostridia* were found in all the five samples. *Thermodesulffovibrio* was dominated in the treatments (inoculum, S0, and S30) with low concentrations of bicarbonate. *Thermacetogenium*, a member of *Clostridia*, increased its presence in the treatments (S60 and S90) with high bicarbonate concentrations. *Thermoanaerobacteriaceae* was only detected in the treatments amended with bicarbonate addition (S30, S60, and S90).

Stable Carbon Isotope Analysis

Bicarbonate was added to mimic the highly buffered condition due to the injected CO₂ and stable isotope C-13 was used to identify the fate of CO₂ (bicarbonate form) in incubation with deep-subsurface fluid. The carbon isotopic compositions of methane and CO₂ were detected after incubation for 180 days. In the treatment without ¹³C-bicarbonate addition, there was no obvious ¹³CH₄ detected (**Figure 4**). But hydrogen production was detected and subsequently consumed (**Figure 1B**), indicating that H₂ were produced from formate and then used for methane production. ¹³CH₄ were detected in the treatments with ¹³C-bicarbonate addition (516.03~675.46‰; **Figure 4**) and the production rate of ¹³CH₄ increased as ¹³C-bicarbonate concentration increased, which suggested that C-13 labeled carbon dioxide (or ¹³C-bicarbonate) were reduced to ¹³CH₄ and promoted the production rate of ¹³CH₄. The ratio of labeled C-13 stayed as ¹³C-bicarbonate increased as injected ¹³C-bicarbonate concentration increased, while the amount of all detected C-13 and the percentage of labeled C-13 stayed as ¹³CO₂ or ¹³CH₄ decreased (**Table 2**). Carbon dioxide without any labeled ¹³C was detected (173.88~383.48‰) in the culture treatments, which should be produced from formate. In the treatments amended with different concentrations of ¹³C-bicarbonate, formate was oxidized to CO₂ and high concentration of CO₂ with an increasing incorporation of ¹³CO₂ and then a large fraction of ¹³CO₂ with small fraction of CO₂ were reduced to ¹³CH₄ and CH₄. (formate oxidation: HCOO⁻ + H₂O = HCO₃⁻ + H₂; CO₂ reduction: HCO₃⁻ + 4H₂ + H⁺ = CH₄ + 3H₂O). CO₂/¹³CO₂

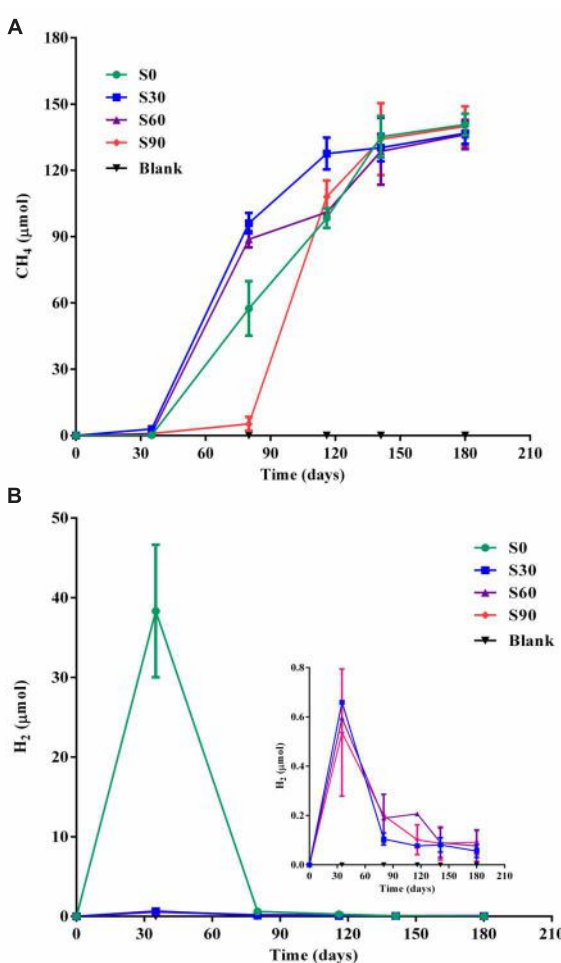


FIGURE 1 | Methane and hydrogen production in the cultures. Methane production (**A**) and hydrogen production (**B**) in serum bottle maintained under anaerobic conditions. Blank are the cultures with different concentrations of bicarbonate without added formate. S0, S30, S60, and S90 treatments were the cultures with formate and different concentrations of bicarbonate (0, 30, 60, and 90 mM, respectively).

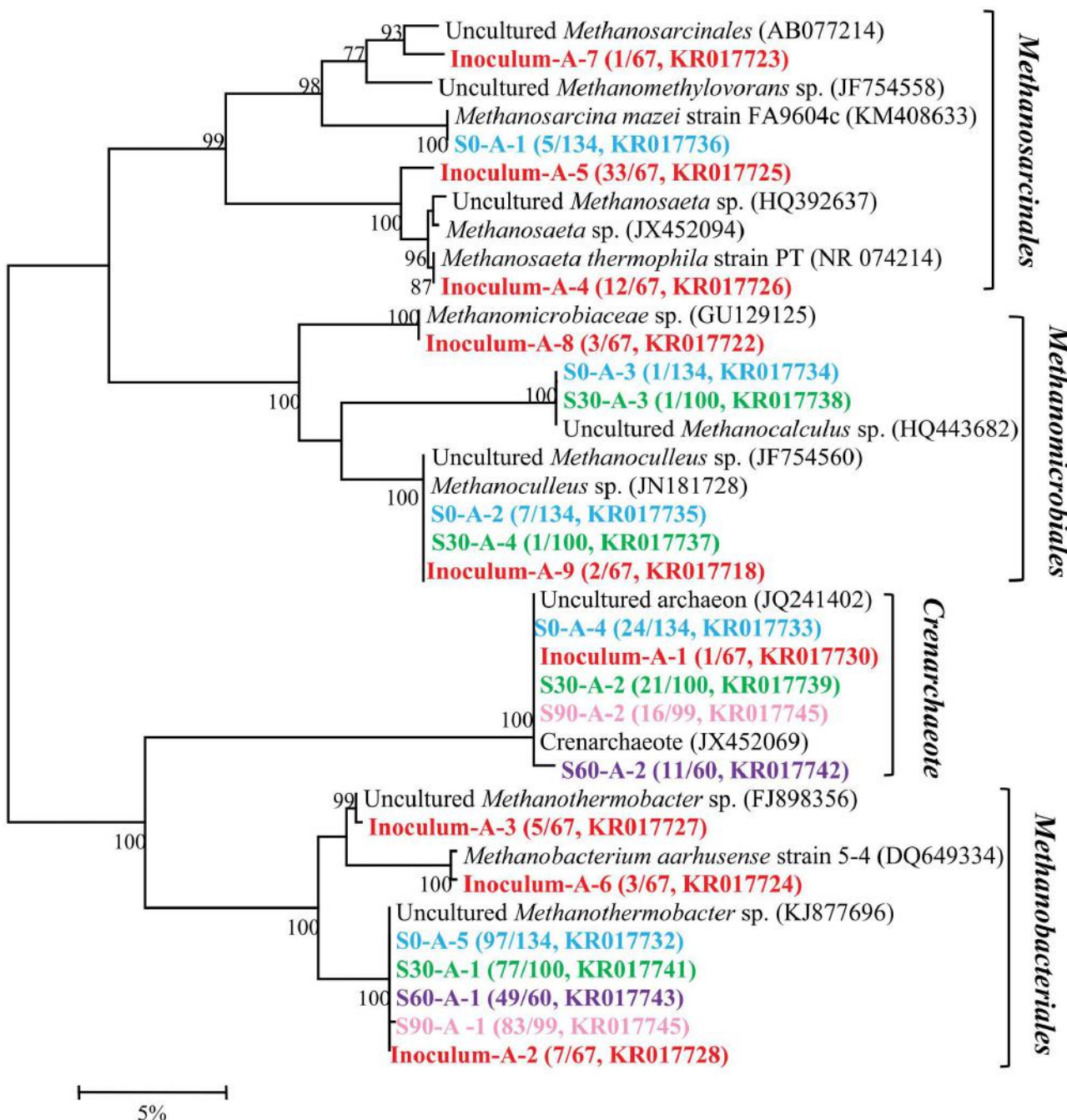
Inoculum-A: Archaea of inoculum sample**S0-A:** Archaea of 0 mM ¹³C-bicarbonate treatment (S0 sample)**S30-A:** Archaea of 30 mM ¹³C-bicarbonate treatment (S30 sample)**S60-A:** Archaea of 60 mM ¹³C-bicarbonate treatment (S60 sample)**S90-A:** Archaea of 90 mM ¹³C-bicarbonate treatment (S90 sample)

FIGURE 2 | Phylogenetic tree of archaeal genes retrieved from five samples (shown with different color). Sequences were performed by MEGA 5 with OTU identity of 97%. The topology of the tree was obtained with the neighbor-joining method. Bootstrap values ($n = 1000$ replicates) of $\geq 75\%$ are showed. Numbers in brackets are the appearance frequencies of the identical sequences in clones and the accession number.

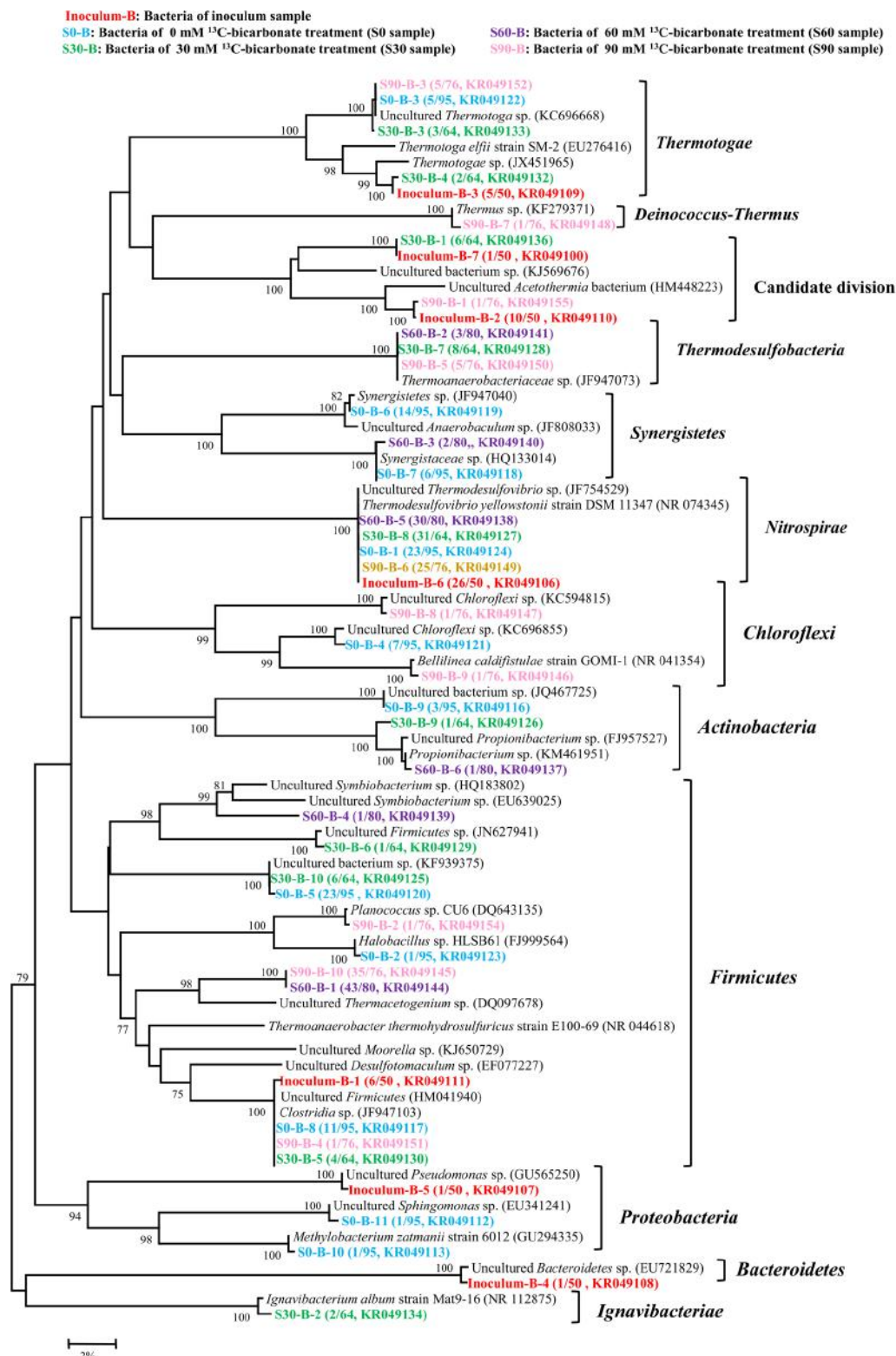


FIGURE 3 | Phylogenetic tree of bacterial genes retrieved from five samples (shown with different color). Sequences were performed by MEGA 5 with OTU identity of 97%. The topology of the tree was obtained with the neighbor-joining method. Bootstrap values ($n = 1000$ replicates) of $\geq 75\%$ are showed. Numbers in brackets are the appearance frequencies of the identical sequences in clones and the accession number.

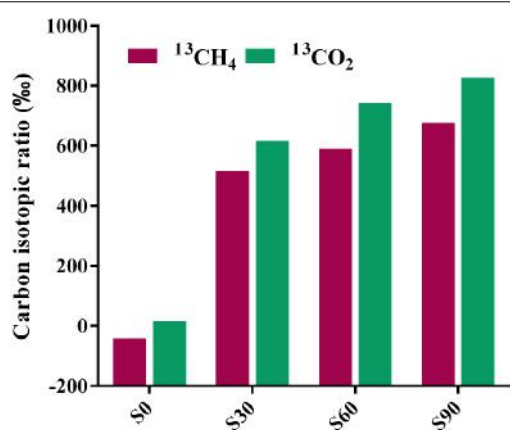


FIGURE 4 | Carbon isotopic ratios of methane and CO₂ after incubation. The relevant data are shown in Supplementary Table S3. S0, S30, S60, and S90 treatments were the cultures with formate and different concentrations of bicarbonate (0, 30, 60, and 90 mM, respectively).

also could be involved in formate methanogenesis directly by methanogens and produced CH₄/¹³CH₄.

Thermodynamics of Bicarbonate-Driven Methanogenic Reactions

Thermodynamic calculation was used to illustrate the energetically favorable metabolic pathways in the experiments with different concentrations of bicarbonate associated with microbial community. The theoretical constraints of archaea and bacteria were evaluated respectively with the data obtained in the present study with different concentration of bicarbonate. The thermodynamic calculation of different concentration of bicarbonate show the same trend. The calculations for the feasible reactions of hydrogen and formate in the sets of culture experiments amended with bicarbonate (S0, S30, S60, and S90) are as follows: CO₂ reduction, acetate formation, formate methanogenesis, and formate oxidation (Table 1). The thermodynamics are shown in Figure 5. Acetate formation, formate methanogenesis, and formate oxidation were less energetically favorable with increasing bicarbonate concentrations and CO₂ reduction became more energetically favorable. As other factors are fixed, CO₂ reduction and formate oxidation are less sensitive to the change of bicarbonate concentration than formate methanogenesis and acetate formation because one mole of bicarbonate involves in per CO₂ reduction and formate oxidation reaction. The change of Gibbs free energy ($\Delta G'_{55}$) calculated for the four reactions in all the treatments showed that all the reactions are exergonic under the experimental conditions and formate methanogenesis is the most favorable one. ΔG° 25°C of the formate oxidation is above the zero (1.12 kJ/mol) and ΔG° 55°C of the formate oxidation is only -0.92 kJ/mol, which are close to thermodynamic threshold (Figure 5 and Table 1). Both formate methanogenesis and formate oxidation are energetically favorable in the culture conditions.

DISCUSSION

Oil reservoir is an extreme environment with different conditions of temperatures, pH values, pressure, salinity, thermodynamic limits and barren habitat (Kobayashi et al., 2012; Mayer and Müller, 2014). These extreme conditions require microbes thriving in community to carry out biochemical reactions collectively. The injected CO₂ from CDCS or MEER can alter the microbial community and the metabolic pathways in deep-subsurface environments, which may dictate the fate of CO₂ (Mayumi et al., 2013; Ohtomo et al., 2013). The endogenous microorganisms in oil reservoirs can reduce CO₂ with the electron derived from the electron donors, which define the oil reservoirs as a bioreactor for CO₂ bioconversion to either fixation as acetate or as methane, a source of natural gas.

The Fate of the Injected CO₂

Our studies showed that about 136 μ mol methane produced after 180 days of incubation in each bottle and at least 516.03% was labeled in the treatments with ¹³C-bicarbonate addition, indicating that at least half of the methane produced were through the CO₂ reduction pathway for methanogenesis. At the same time, part of injected bicarbonate were presented as ¹³C-bicarbonate in culture medium and ¹³CO₂ of gas phase in headspace (Table 2). In original oil reservoir environments, residual CO₂ from EOR could be converted to methane via methanogenesis, whereas most CO₂ was dissolved in the formation fluids and appeared in gas phase after more than 30 years (Shelton et al., 2014). With the simulation reactor system in laboratory, injected CO₂ could be transformed into acetate through homoacetogenesis, but methanogenesis was not detected under the condition simulating the *in situ* pressure and temperature (Ohtomo et al., 2013). Carbon dioxide can also be converted into formate through the carbon dioxide reductase or a whole cell system (Schuchmann and Müller, 2013).

High CO₂ pressure invoke acetoclastic methanogenesis instead of syntrophic acetate oxidation coupled with CO₂-reducing methanogenesis, when acetate and oil were added as substrates (Mayumi et al., 2013). Our results showed that when formate was added as substrate and electron donors, CO₂ could be converted into methane through syntrophic formate oxidation coupled with CO₂-reducing methanogenesis and formate methanogenesis. The bio-conversion rate of CO₂ was about 19.6 pmol d⁻¹ ml⁻¹ in the treatments, and compared to original oil reservoir environments, the abundant supply of electron donor is essential to maintain and accelerate the process to take place. Naturally available H₂ or electron resources for methanogenesis can be the primary requirements to improve the conversion rate of CO₂ (Head et al., 2003; Cheng et al., 2009). And variety of enzymes (Yeates et al., 2008; Shekh et al., 2011; Alissandratos et al., 2014) and catalysts (Hull et al., 2012; Ziebart et al., 2012; Jeletić et al., 2013) can be used to convert the CO₂ into reduced compounds under *in situ* and *ex situ* experimental conditions.

TABLE 2 | The fate of injected ¹³C-bicarbonate in the experiments at 180 days of incubation.

Samples	Total- ¹³ C (μmol)	Detected- ¹³ C (μmol)	¹³ C-CH ₄ (μmol)	¹³ CO ₂ (μmol)	¹³ C-bicarbonate (μmol)
S30	1500	1383.15	68.94 (4.98%)	893.68 (64.61%)	420.53 (30.40%)
S60	3000	2390.31	78.59 (3.29%)	1253.48 (52.44%)	1058.24 (44.27%)
S90	4500	3210.23	92.84 (2.89%)	1638.02 (51.03%)	1479.37 (46.08%)

The calculations were shown in Supplementary Table S3.

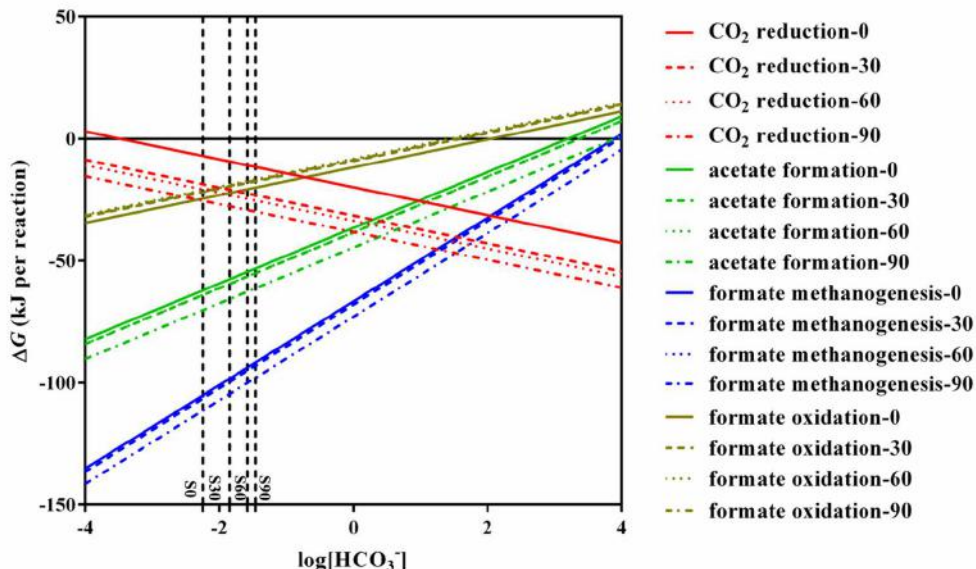


FIGURE 5 | Effects of HCO₃⁻ on change in Gibbs free energy for CO₂ reduction, acetate formation, formate methanogenesis, and formate oxidation. All lines in the figure were calculated using the conditions of S0, S30, S60, S90. The detail data were shown in Supplementary Table S2.

Methanogenic Pathway Analysis in the Experiments

Biological CO₂ fixation is a common phenomenon in biology. Six autotrophic carbon fixation pathways have been reported (Berg et al., 2010) and most key enzymes of these six biochemical pathways have been detected in oil reservoirs (Liu et al., 2015). There are three main methanogenic pathways in oil reservoirs: CO₂-reducing, acetoclastic and methylotrophic with different substrates: CO₂, acetate and methyl group containing compounds, respectively (Nazaries et al., 2013) and direct interspecies electron transfer as a new model for methanogenesis has been confirmed (Rotaru et al., 2014). In this study, formate was amended into the treatments as the carbon source and electron donor. The proposed pathways of anaerobic formate transformation and related CO₂ conversion were shown in Figure 6. Formate can be involved in CO₂ conversion and methanogenesis through many kinds of pathways.

Methane production was nearly equal to the formate consumed and consistent with stoichiometric formate oxidation reaction, indicating syntrophic formate oxidation and formate methanogenesis would be involved. Hydrogen was detected in all the samples at 35 days and decreased with the further

incubation of the cultures (Figure 1B), suggesting that hydrogen was produced and then used for the CO₂ reduction, which also indicated that syntrophic formate oxidation coupled with CO₂ reduction and formate methanogenesis would be responsible for methanogenesis. The hydrogen could be generated through syntrophic formate oxidation or as intermediate during the formate methanogenesis in the samples. The obvious hydrogen production was found in S0 treatments and little hydrogen was detected in other culture samples amended with bicarbonate addition, because a high concentration of hydrogen could not be accumulated in these treatments with the limitation of Gibbs free energy threshold ($\Delta G' = 0$, Table 1). Meanwhile, CO₂ reduction, formate oxidation, and formate methanogenesis were also below the threshold values, indicating these reactions were energetically favorable and spontaneous in the treatments. The production and subsequent consumption of hydrogen suggest that CO₂ reduction dominated in the systems.

Formate was once known as nutritional substrate but not for methanogenesis directly by methanogens (Tanner et al., 1989), but some genera of *Methanobacteriaceae*, which can use formate directly for methanogenesis were found (Oren, 2014). Methane with C-13 labeled was detected in the treatments with

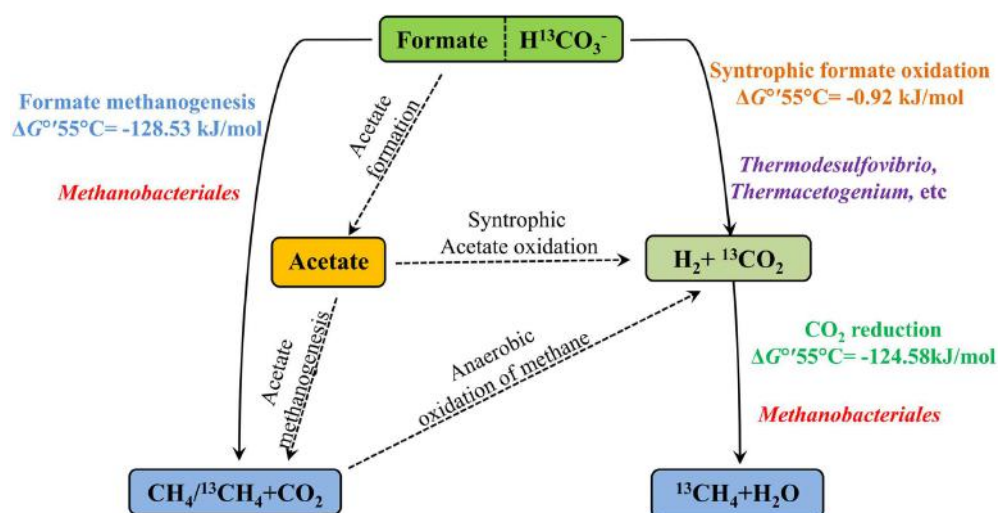


FIGURE 6 | The proposed pathways of anaerobic formate transformation and related CO₂ conversion. Solid lines mean the pathways were detected in the treatments and dotted lines mean not. ΔG°/55°C is standard Gibbs free energy at temperature 55°C and modified with protons (Table 1). Microorganisms are positioned according their probable role in the treatments.

amendment of ¹³C-bicarbonate (516.03~675.46%), suggesting that ¹³C-bicarbonate (or ¹³CO₂) was reduced to ¹³CH₄ (Figure 4), indicating the CO₂-reducing pathway was dominant in the experiments. Carbon dioxide without any labeled ¹³CO₂ was detected (173.88~383.48%) in the treatments (Figure 4), which should be produced by syntrophic formate oxidation. Formate is known as a potential energy source and important degradation intermediate in ecosystem. Based on our results, syntrophic formate oxidation coupled with CO₂ reduction and formate methanogenesis could be the possible methanogenic pathway in the experiments.

CO₂-Induced the Shift of Microbial Community

Oil reservoir is a typical anaerobic environment and the endogenous microorganisms in oil reservoir can degrade alkanes and produce methane (Mbadinga et al., 2011). In this study, the archaea in the inoculum had a high diversity and the ability to produce methane through CO₂-reducing, acetoclastic and methylotrophic methanogenic pathways (Figure 2). However, some types of archaea were not detected in the treatments with the addition of formate and increase of bicarbonate concentrations, *Methanosarcinales* disappeared in the sample amended with 30 mM of bicarbonate, and only *Methanobacteriales* and *Crenarchaeota* were detected in S60 and S90 treatments. The results indicated that *Methanomicrobiales* and *Methanosarcinales* were sensitive to the high bicarbonate concentrations. Compared to the original inoculum, *Methanobacteriales* was dominated in all the treatment cultures in the presence of formate, suggesting formate promoted the growth of the *Methanobacteriales*. *Methanobacteriales* is a kind of strict CO₂-reducing methanogens, it also possesses formate dehydrogenase and could be candidate

for formate-dependent H₂ production and methanogenesis directly (Lupa et al., 2008), which is in agreement with the mentioned methanogenic pathway.

Bicarbonate concentration showed little impact on bacterial diversity. *Thermodesulfovibrio* belonged to *Nitrospirales* was a major group in the inoculum and all the treatments (Figure 3), especially in the low concentration treatments (inoculum, S0, and S30). *Thermodesulfovibrio* is a typical sulfate-reducing bacterium and grew through the reduction of sulfate with electron donors like hydrogen and formate. *Thermodesulfovibrio* and the CO₂-reducing methanogen in co-culture experiments can produce methane syntrophically (Sekiguchi et al., 2008). In this study, *Thermodesulfovibrio* may use formate and co-work with methanogens for methane production. *Clostridia* were the most widely studied as hydrogen producer and acetogens in anaerobic environments (Drake et al., 2008; Calusinska et al., 2010), and *Thermacetogenium* belonged to *Clostridia* increased in the treatments with high bicarbonate concentrations (S60 and S90), known as a syntrophic acetate-oxidizing bacterium and acetogens (Hattori et al., 2000). However, there was no acetate accumulation (Supplementary Table S2) or acetoclastic methanogens (Figure 2) in the treatments with high bicarbonate concentrations (S60 and S90), suggesting that acetoclastic methanogenesis was not involved in the methane production of this study.

The microbial community in the experiments was capable of converting CO₂ into methane through syntrophic formate oxidation coupled with CO₂-reducing methanogenesis and formate methanogenesis. *Thermodesulfovibrio* and *Methanobacteriales* may play important role for the process in the system. The addition of bicarbonate can induce the shift of microbial community, especially in archaea.

In summary, under the microcosm study, most methane was produced by reducing the amended CO₂ through the syntrophic

formate oxidation coupled to CO₂-reducing methanogenesis and formate methanogenesis with addition of bicarbonate. The results indicated that the microbial conversion of CO₂ to methane is feasible with the microbial community in production water of high-temperature oil reservoirs. *Thermodesulfobacter* and *Methanobacteriales* may be responsible for formate utilization and CO₂ conversion. The results suggested that syntrophic formate oxidation coupled to CO₂ reduction and formate methanogenesis could be alternative methanogenic pathway and gave some knowledge on formate metabolism in subsurface environment.

AUTHOR CONTRIBUTIONS

J-DG and B-ZM designed the experiments, G-CY did the experiments, G-CY, LZ and SM carried out the microbial analysis. J-FL and S-ZY gave the suggestion for the experiments

REFERENCES

- Alissandratos, A., Kim, H. K., and Easton, C. J. (2014). Formate production through carbon dioxide hydrogenation with recombinant whole cell biocatalysts. *Bioresour. Technol.* 164, 7–11. doi: 10.1016/j.biortech.2014.04.064
- Amend, J. P., and Shock, E. L. (2001). Energetics of overall metabolic reactions of thermophilic and hyperthermophilic Archaea and Bacteria. *FEMS Microbiol. Rev.* 25, 175–243. doi: 10.1111/j.1574-6976.2001.tb00576.x
- Bagramyan, K., and Trchounian, A. (2003). Structural and functional features of formate hydrogen lyase, an enzyme of mixed-acid fermentation from *Escherichia coli*. *Biochemistry (Moscow)* 68, 1159–1170. doi: 10.1023/B:BIRY.0000009129.18714.a4
- Berg, I. A., Kockelkorn, D., Ramos-Vera, W. H., Say, R. F., Zarzycki, J., Hügler, M., et al. (2010). Autotrophic carbon fixation in archaea. *Nat. Rev. Microbiol.* 8, 447–460. doi: 10.1038/nrmicro2365
- Callaghan, A. V., Morris, B. E. L., Pereira, I. A. C., McInerney, M. J., Austin, R. N., Groves, J. T., et al. (2012). The genome sequence of *Desulfatibacillus alkenivorans* AK-01: a blueprint for anaerobic alkane oxidation. *Environ. Microbiol.* 14, 101–113. doi: 10.1111/j.1462-2920.2011.02516.x
- Calusinska, M., Happe, T., Joris, B., and Wilmutte, A. (2010). The surprising diversity of clostridial hydrogenases: a comparative genomic perspective. *Microbiology* 156, 1575–1588. doi: 10.1099/mic.0.032771–32770
- Cheng, S., Xing, D., Call, D. F., and Logan, B. E. (2009). Direct biological conversion of electrical current into methane by electromethanogenesis. *Environ. Sci. Technol.* 43, 3953–3958. doi: 10.1021/es803531g
- De Bok, F. A. M., Plugge, C. M., and Stams, A. J. M. (2004). Interspecies electron transfer in methanogenic propionate degrading consortia. *Water Res.* 38, 1368–1375. doi: 10.1016/j.watres.2003.11.028
- Delgado, A. G., Parameswaran, P., Fajardo-Williams, D., Halden, R. U., and Krajmalnik-Brown, R. (2012). Role of bicarbonate as a pH buffer and electron sink in microbial dechlorination of chloroethenes. *Microb. Cell Fact.* 11:128. doi: 10.1186/1475-2859-11-128
- Dolfing, J., Jiang, B., Henstra, A. M., Stams, A. J. M., and Plugge, C. M. (2008). Syntrophic growth on formate: a new microbial niche in anoxic environments. *Appl. Environ. Microbiol.* 74, 6126–6131. doi: 10.1128/aem.01428–1428
- Drake, H. L., Gößner, A. S., and Daniel, S. L. (2008). Old acetogens, new light. *Ann. N. Y. Acad. Sci.* 1125, 100–128. doi: 10.1196/annals.1419.016
- Dressel, B., Deel, D., Rodosta, T., Plasynski, S., Litynski, J., and Myer, L. (2011). CCS activities being performed by the U.S. DOE. *Int. J. Environ. Res. Public Health* 8, 300–320. doi: 10.3390/ijerph8020300
- Gantner, S., Andersson, A. F., Alonso-Sáez, L., and Bertilsson, S. (2011). Novel primers for 16S rRNA-based archaeal community analyses in environmental samples. *J. Microbiol. Methods* 84, 12–18. doi: 10.1016/j.mimet.2010.10.001
- Glueck, S. M., Gumus, S., Fabian, W. M. F., and Faber, K. (2010). Biocatalytic carboxylation. *Chem. Soc. Rev.* 39, 313–328. doi: 10.1039/B807875K
- Hattori, S., Kamagata, Y., Hanada, S., and Shoun, H. (2000). Thermacetogenium phaeum gen. nov., sp. nov., a strictly anaerobic, thermophilic, syntrophic acetate-oxidizing bacterium. *Int. J. Syst. Evol. Microbiol.* 50, 1601–1609. doi: 10.1099/00207713-50-4-1601
- Hattori, S., Luo, H., Shoun, H., and Kamagata, Y. (2001). Involvement of formate as an interspecies electron carrier in a syntrophic acetate-oxidizing anaerobic microorganism in coculture with methanogens. *J. Biosci. Bioeng.* 91, 294–298. doi: 10.1016/S1389-1723(01)80137-7
- Hatzenpichler, R., Lebedeva, E. V., Spieck, E., Stoecker, K., Richter, A., Daims, H., et al. (2008). A moderately thermophilic ammonia-oxidizing crenarchaeote from a hot spring. *Proc. Natl. Acad. Sci. U.S.A.* 105, 2134–2139. doi: 10.1073/pnas.0708857105
- Head, I. M., Jones, D. M., and Larter, S. R. (2003). Biological activity in the deep subsurface and the origin of heavy oil. *Nature* 426, 344–352. doi: 10.1038/nature02134
- Hull, J. F., Himeda, Y., Wang, W.-H., Hashiguchi, B., Periana, R., Szalda, D. J., et al. (2012). Reversible hydrogen storage using CO₂ and a proton-switchable iridium catalyst in aqueous media under mild temperatures and pressures. *Nat. Chem.* 4, 383–388. doi: 10.1038/nchem.1295
- Jeletic, M. S., Mock, M. T., Appel, A. M., and Linehan, J. C. (2013). A cobalt-based catalyst for the hydrogenation of CO₂ under ambient conditions. *J. Am. Chem. Soc.* 135, 11533–11536. doi: 10.1021/ja406601v
- Kim, Y. J., Lee, H. S., Kim, E. S., Bae, S. S., Lim, J. K., Matsumi, R., et al. (2010). Formate-driven growth coupled with H₂ production. *Nature* 467, 352–355. doi: 10.1038/nature09375
- Kirk, M. F. (2011). Variation in energy available to populations of subsurface anaerobes in response to geological carbon storage. *Environ. Sci. Technol.* 45, 6676–6682. doi: 10.1021/es201279e
- Kobayashi, H., Kawaguchi, H., Endo, K., Mayumi, D., Sakata, S., Ikarashi, M., et al. (2012). Analysis of methane production by microorganisms indigenous to a depleted oil reservoir for application in Microbial Enhanced Oil Recovery. *J. Biosci. Bioeng.* 113, 84–87. doi: 10.1016/j.jbbiosc.2011.09.003
- Lin, Y., Lü, F., Shao, L., and He, P. (2013). Influence of bicarbonate buffer on the methanogenic pathway during thermophilic anaerobic digestion. *Bioresour. Technol.* 137, 245–253. doi: 10.1016/j.biortech.2013.03.093
- Liu, J.-F., Sun, X.-B., Yang, G.-C., Mbadinga, S. M., Gu, J.-D., and Mu, B. (2015). Analysis of microbial communities in the oil reservoir subjected to CO₂-flooding by using functional genes as molecular biomarkers for microbial CO₂ sequestration. *Front. Microbiol.* 6:236. doi: 10.3389/fmicb.2015.00236
- Lupa, B., Hendrickson, E. L., Leigh, J. A., and Whitman, W. B. (2008). Formate-dependent H₂ production by the mesophilic methanogen *Methanococcus maripaludis*. *Appl. Environ. Microbiol.* 74, 6584–6590. doi: 10.1128/AEM.01455–1458

and results analysis. G-CY prepared the manuscript with contributions from all co-authors.

ACKNOWLEDGMENTS

This work was supported by the National Natural Science Foundation of China (Grant No. 41530318, 41273084, 41403066), the NSFC/RGC Joint Research Fund (Grant No. 41161160560) and the Fundamental Research Funds for the Central Universities of China (Grant No. WK1414029).

SUPPLEMENTARY MATERIAL

The Supplementary Material for this article can be found online at: <http://journal.frontiersin.org/article/10.3389/fmicb.2016.00365>

- Mayer, F., and Müller, V. (2014). Adaptations of anaerobic archaea to life under extreme energy limitation. *FEMS Microbiol. Rev.* 38, 449–472. doi: 10.1111/1574-6976.12043
- Mayumi, D., Dolfing, J., Sakata, S., Maeda, H., Miyagawa, Y., Ikarashi, M., et al. (2013). Carbon dioxide concentration dictates alternative methanogenic pathways in oil reservoirs. *Nat. Commun.* 4, 1998–1998. doi: 10.1038/ncomms2998
- Mbadinga, S., Li, K.-P., Zhou, L., Wang, L.-Y., Yang, S.-Z., Liu, J.-F., et al. (2012). Analysis of alkane-dependent methanogenic community derived from production water of a high-temperature petroleum reservoir. *Appl. Microbiol. Biotechnol.* 96, 531–542. doi: 10.1007/s00253-011-3828-3828
- Mbadinga, S. M., Wang, L.-Y., Zhou, L., Liu, J.-F., Gu, J.-D., and Mu, B.-Z. (2011). Microbial communities involved in anaerobic degradation of alkanes. *Int. Biodeterior. Biodegrad.* 65, 1–13. doi: 10.1016/j.ibiod.2010.11.009
- Meshulam-Simon, G., Behrens, S., Choo, A. D., and Spormann, A. M. (2007). Hydrogen metabolism in *Shewanella oneidensis* MR-1. *Appl. Environ. Microbiol.* 73, 1153–1165. doi: 10.1128/aem.01588-1586
- Mikkelsen, M., Jorgensen, M., and Krebs, F. C. (2010). The teraton challenge. A review of fixation and transformation of carbon dioxide. *Energy Environ. Sci.* 3, 43–81. doi: 10.1039/B912904A
- Momeni, A., Aghajani, M., and Zargar, G. (2012). A Simulation study of carbon dioxide sequestration in a depleted oil reservoir. *Pet. Sci. Technol.* 30, 751–765. doi: 10.1080/10916466.2010.490809
- Nazarries, L., Murrell, J. C., Millard, P., Baggs, L., and Singh, B. K. (2013). Methane, microbes and models: fundamental understanding of the soil methane cycle for future predictions. *Environ. Microbiol.* 15, 2395–2417. doi: 10.1111/1462-2920.12149
- Ohtomo, Y., Ijiri, A., Ikegawa, Y., Tsutsumi, M., Imachi, H., Uramoto, G.-I., et al. (2013). Biological CO₂ conversion to acetate in subsurface coal-sand formation using a high-pressure reactor system. *Front. Microbiol.* 4:361. doi: 10.3389/fmicb.2013.00361
- Oren, A. (2014). “The family methanobacteriaceae,” in *The Prokaryotes*, eds E. Rosenberg, E. DeLong, S. Lory, E. Stackebrandt and F. Thompson (Berlin: Springer), 165–193.
- Rotaru, A.-E., Shrestha, P. M., Liu, F., Shrestha, M., Shrestha, D., Embree, M., et al. (2014). A new model for electron flow during anaerobic digestion: direct interspecies electron transfer to *Methanosaeta* for the reduction of carbon dioxide to methane. *Energy Environ. Sci.* 7, 408–415. doi: 10.1039/C3EE42189A
- Schrag, D. P. (2007). Preparing to capture carbon. *Science* 315, 812–813. doi: 10.1126/science.1137632
- Schuchmann, K., and Müller, V. (2013). Direct and reversible hydrogenation of CO₂ to formate by a bacterial carbon dioxide reductase. *Science* 342, 1382–1385. doi: 10.1126/science.1244758
- Sekiguchi, Y., Muramatsu, M., Imachi, H., Narihiro, T., Ohashi, A., Harada, H., et al. (2008). *Thermodesulfovibrio aggregans* sp. nov. and *Thermodesulfovibrio thiophilus* sp. nov., anaerobic, thermophilic, sulfate-reducing bacteria isolated from thermophilic methanogenic sludge, and emended description of the genus *Thermodesulfovibrio*. *Int. J. Syst. Evol. Microbiol.* 58, 2541–2548. doi: 10.1099/ijsm.0.2008/000893-890
- Shekh, A. Y., Krishnamurthi, K., Mudliar, S. N., Yadav, R. R., Fulke, A. B., Devi, S. S., et al. (2011). Recent advancements in carbonic anhydrase-driven processes for CO₂ sequestration: minireview. *Crit. Rev. Environ. Sci. Technol.* 42, 1419–1440. doi: 10.1080/10643389.2011.556884
- Shelton, J. L., McIntosh, J. C., Warwick, P. D., and Yi, A. L. Z. (2014). Fate of injected CO₂ in the wilcox group, louisiana, gulf coast basin: chemical and isotopic tracers of microbial-brine-rock-CO₂ interactions. *Appl. Geochem.* 51, 155–169. doi: 10.1016/j.apgeochem.2014.09.015
- Tanner, R. S., McInerney, M. J., and Nagle, D. (1989). Formate auxotroph of *Methanobacterium thermoautotrophicum* Marburg. *J. Bacteriol.* 171, 6534–6538.
- Wang, L.-Y., Duan, R.-Y., Liu, J.-F., Yang, S.-Z., Gu, J.-D., and Mu, B.-Z. (2012a). Molecular analysis of the microbial community structures in water-flooding petroleum reservoirs with different temperatures. *Biogeosciences* 9, 4645–4659. doi: 10.5194/bg-9-4645-2012
- Wang, L.-Y., Li, W., Mbadinga, S. M., Liu, J.-F., Gu, J.-D., and Mu, B.-Z. (2012b). Methanogenic microbial community composition of oily sludge and its enrichment amended with alkanes incubated for over 500 days. *Geomicrobiol. J.* 29, 716–726. doi: 10.1080/01490451.2011.619634
- Wood, G. E., Haydock, A. K., and Leigh, J. A. (2003). Function and regulation of the formate dehydrogenase genes of the methanogenic archaeon *Methanococcus maripaludis*. *J. Bacteriol.* 185, 2548–2554. doi: 10.1128/JB.185.8.2548-2554.2003
- Yang, H., Xu, Z., Fan, M., Gupta, R., Slimane, R. B., Bland, A. E., et al. (2008). Progress in carbon dioxide separation and capture: a review. *J. Environ. Sci.* 20, 14–27. doi: 10.1016/S1001-0742(08)60002-9
- Yeates, T. O., Kerfeld, C. A., Heinhorst, S., Cannon, G. C., and Shively, J. M. (2008). Protein-based organelles in bacteria: carboxysomes and related microcompartments. *Nat. Rev. Microbiol.* 6, 681–691. doi: 10.1038/nrmicro1913
- Zhou, F., Mbadinga, S. M., Liu, J.-F., Gu, J.-D., and Mu, B.-Z. (2013). Evaluation of microbial community composition in thermophilic methane-producing incubation of production water from a high-temperature oil reservoir. *Environ. Technol.* 34, 2681–2689. doi: 10.1080/09593330.2013.786135
- Ziebart, C., Federsel, C., Anbarasan, P., Jackstell, R., Baumann, W., Spannenberg, A., et al. (2012). Well-defined iron catalyst for improved hydrogenation of carbon dioxide and bicarbonate. *J. Am. Chem. Soc.* 134, 20701–20704. doi: 10.1021/ja307924a

Conflict of Interest Statement: The authors declare that the research was conducted in the absence of any commercial or financial relationships that could be construed as a potential conflict of interest.

Copyright © 2016 Yang, Zhou, Mbadinga, Liu, Yang, Gu and Mu. This is an open-access article distributed under the terms of the Creative Commons Attribution License (CC BY). The use, distribution or reproduction in other forums is permitted, provided the original author(s) or licensor are credited and that the original publication in this journal is cited, in accordance with accepted academic practice. No use, distribution or reproduction is permitted which does not comply with these terms.



Iron, Cobalt, and Gadolinium Transport in Methanogenic Granules Measured by 3D Magnetic Resonance Imaging

Jan Bartacek^{1,2*}, Frank J. Vergeldt³, Josef Maca², Edo Gerkema³, Henk Van As³ and Piet N. L. Lens¹

¹ UNESCO-IHE, Delft, Netherlands, ² Department of Water Technology and Environmental Engineering, Institute of Chemical Technology, Prague, Czech Republic, ³ Laboratory of Biophysics and Wageningen NMR Centre, Department of Agrotechnology and Food Sciences, Wageningen University, Wageningen, Netherlands

OPEN ACCESS

Edited by:

Gavin Collins,
National University of Ireland, Galway,
Ireland

Reviewed by:

Kevin Thomas Finneran,
Clemson University, USA
Donald Jay Ferguson,
Miami University, USA

*Correspondence:

Jan Bartacek
jan.bartacek@vscht.cz

Specialty section:

This article was submitted to
Microbiotechnology, Ecotoxicology
and Bioremediation,
a section of the journal
Frontiers in Environmental Science

Received: 30 November 2015

Accepted: 22 February 2016

Published: 16 March 2016

Citation:

Bartacek J, Vergeldt FJ, Maca J, Gerkema E, Van As H and Lens PNL (2016) Iron, Cobalt, and Gadolinium Transport in Methanogenic Granules Measured by 3D Magnetic Resonance Imaging. *Front. Environ. Sci.* 4:13. doi: 10.3389/fenvs.2016.00013

Description of processes such as bioaccumulation, bioavailability and biosorption of heavy metals in biofilm matrixes requires the quantification of their transport. This study shows 3D MRI measurements of the penetration of free (Fe^{2+} , Co^{2+} and Gd^{3+}) and complexed ($[\text{FeEDTA}]^{2-}$ and $[\text{GdDTPA}]^{2-}$) metal ions in a single methanogenic granule. Interactions (sorption or precipitation) between free metals and the biofilm matrix result in extreme shortening of the spin-spin relaxation time (T_2) and a decrease of the amplitude (A_0) of the MRI signal, which hampers the quantification of the metal concentration inside the granular sludge matrix. MRI images clearly showed the presence of distinct regions (dead or living biomass, cracks, and precipitates) in the granular matrix, which influenced the metal transport. For the free metal ions, a reactive barrier was formed that moved through the granule, especially in the case of Gd^{3+} . Chelated metals penetrated faster and without reaction front. Diffusion of $[\text{GdDTPA}]^{2-}$ could be quantified, revealing the course of its transport and the uneven ($0.2\text{--}0.4 \text{ mmol}\cdot\text{L}^{-1}$) distribution of the final $[\text{GdDTPA}]^{2-}$ concentration within the granular biofilm matrix at equilibrium.

Keywords: methanogenic granular sludge, magnetic resonance microscopy, metal transport, metal diffusion, granular biofilm

INTRODUCTION

Methanogenic granules are spherical biofilms, developed spontaneously without support material in bioreactors for anaerobic wastewater treatment, such as the Upflow Anaerobic Sludge Blanket (UASB) reactor (Hulshoff Pol et al., 2004). The interactions between methanogenic granules and heavy metals have been studied mainly in relation to limitation of the microbial activity by scarcity of essential metals (Fermoso et al., 2008) or as a method for metal removal from wastewaters (Steed et al., 2000; De Lima et al., 2001). Less is known about the speciation, spatial distribution and transport of metals within a biofilm, which is nevertheless essential for any research on metal-biofilm interactions (Van Hullebusch et al., 2003; Zandvoort et al., 2006).

Knowledge of metal transport in biofilms is mainly based on mathematical models. The data for validation of these models have been obtained from indirect measurements conducted in the bulk liquid (Beyenal and Lewandowski, 2004). Thus, an experimental tool for direct measurement

of metal transport is required to confirm the validity of these models. Magnetic resonance imaging (MRI) is a non-destructive method that can be applied under *in situ* conditions to study metal transport in artificial biomatrixes (Nestle, 2002), in phototrophic biofilms (Phoenix and Holmes, 2008) and in methanogenic granules (Bartacek et al., 2009). In addition, MRI can be used to reveal the inner structure of the biofilm and to describe the transport properties (diffusivity) of the water contained in a biofilm matrix (Van As and Van Dusschoten, 1997; Lens and Hemminga, 1998; Van As and Lens, 2001).

Transport of various metals and their various chemical species has been measured using MRI in many different porous media such as sandy aquifers (Nestle et al., 2003; Moradi et al., 2008) or various biomatrixes (Donahue et al., 1994; Nestle and Kimmich, 1996; Bartacek et al., 2009). In a previous paper (Bartacek et al., 2009), we described the methodology for MRI measurements in single anaerobic granules using a mixture of Fe^{2+} and $[\text{FeEDTA}]^{2-}$. Using this MRI methodology, the present study describes transport of various metals, i.e., cobalt, iron and gadolinium, in liganded or non-liganded form in methanogenic granules. Methanogenic granules of the same origin as those used in this study were previously shown to be trace metal deficient and rather homogeneous as for their microbial composition (Fermoso et al., 2008). The aim of the MRI experiments was to describe the influence of chemical speciation on the transport of trace metals and their interaction with the granular matrix during transport. These observations were correlated with the inner structure of the granules as well.

MATERIALS AND METHODS

Source of Biomass

Mesophilic methanogenic granular sludge was obtained from a full-scale UASB reactor treating alcohol distillery wastewater at Nedalco (Bergen op Zoom, The Netherlands).

Experimental Set-Up and MRI

Single granules were fixed in a glass tube, through which demineralized or tap water was circulated to establish stable conditions. At the start of each experiment, a certain concentration of the investigated metal compound (5 mM CoCl_2 , 1 mM FeCl_2 , 2 mM $[\text{FeEDTA}]^{2-}$, 0.01 mM GdCl_3 , or 0.5 mM $[\text{GdDTPA}]^{2-}$) was introduced in the water circuit. The metal concentrations used were chosen based on the relaxivity of each metal. Subsequently, the increase of the metal concentration inside the granule was measured using the 3D Turbo Spin Echo (TSE) imaging method developed previously by Mohoric et al. (2004) with a spatial resolution of $109 \times 109 \times 218 \mu\text{m}^3$ and a temporal resolution of 11 min as presented in Bartacek et al. (2009). The 3D TSE signal was spin-lattice relaxation time (T_1) weighted applying a repetition time (T_R) of 200 ms and an echo time (T_E) of 4.53 μs (Bartacek et al., 2009).

The experiments consisted of a series (several tens to several hundreds) of TSE measurements. 3D T_2 and amplitude (A_0) maps of a single granule were acquired prior and upon termination of each experiment (T_E 1 ms, 16,384 echoes, spatial resolution identical to the TSE measurement). The iron solution

was always injected after taking several TSE images of the granule in demineralized water to document the situation at time zero. A series of 3D TSE measurements (30–400) was performed, always followed by a final 3D T_2 map measurement. 3D T_1 maps were acquired only occasionally due to their long acquisition time requirement (~ 160 min). The methodology, including calculation of the metal concentration inside the methanogenic biofilm matrix, was described previously by Bartacek et al. (2009).

MRI Imager

All MRI measurements were done at $30 (\pm 2)^\circ\text{C}$ on a 0.7 T (30.7 MHz for protons) imager consisting of a Bruker Avance console (Bruker BioSpin, Karlsruhe, Germany), a Bruker electromagnet stabilized by an external ^{19}F lock unit, a custom build solenoid RF-probe and an actively shielded gradient system with planar geometry (G_{\max} 1 T/m; Resonance Instruments Ltd, Witney, UK). The RF-probe had an inner diameter of 5 mm and was inductively coupled to avoid continuous retuning and matching of the RF-probe due to the change in loading by the iron, cobalt or gadolinium solution.

Scanning Electron Microscopy

For scanning electron microscopy (SEM), samples were fixed for 1 h in aqueous glutaraldehyde solution (2.5%), rinsed with water, and subjected to a series of ethanol washes (10, 30, 50, 70, 90, 100%; 20 min per step) before critical-point drying with carbon dioxide (CPD 020, Balzers, Liechtenstein). Samples were then fit on a brass sample holder with carbon adhesive tabs (Electron Microscopy Sciences, Hatfield, PA) and coated with carbon. An additional 5 nm platinum coating was applied by magnetron sputtering. Specimens were analyzed with a field emission scanning electron microscope (JEOL 6300 F, Tokyo, Japan) at room temperature at a working distance between 8 and 15 mm. All images were recorded digitally (Orion 6, E.L.I. sprl., Belgium) at a scan rate of 100 s (full frame) and at a size of 2528×2030 .

RESULTS

Inner Structure of Methanogenic Granules

The distribution of the amplitude (A_0) values (measure of the water density) over the methanogenic granule was homogeneous. The granules contained regions with lower A_0 (up to 30% of the average value) that always coincided with low T_1 values (lower than 0.3 s). These regions are further referred to as Type I regions in this paper. While the T_1 of the methanogenic granules typically ranged from 0.2 to 1.0 s, areas that had a T_1 comparable with free water (~ 1.2 s) were rarely detected. These areas, possibly cracks, are further referred as Type II regions in this paper.

The granules under investigation often had a distinct core surrounded by an outer layer, both composed of biomass. The core usually had slightly higher T_1 and T_2 values. Both Type I and Type II regions were located only inside the core or were associated with the core of the granules (Figure 1). Type I and Type II regions were not present in the outer layer of the granules investigated. Besides the distinct layers, also cracks and voids were occasionally observed (Figure 2D). These were

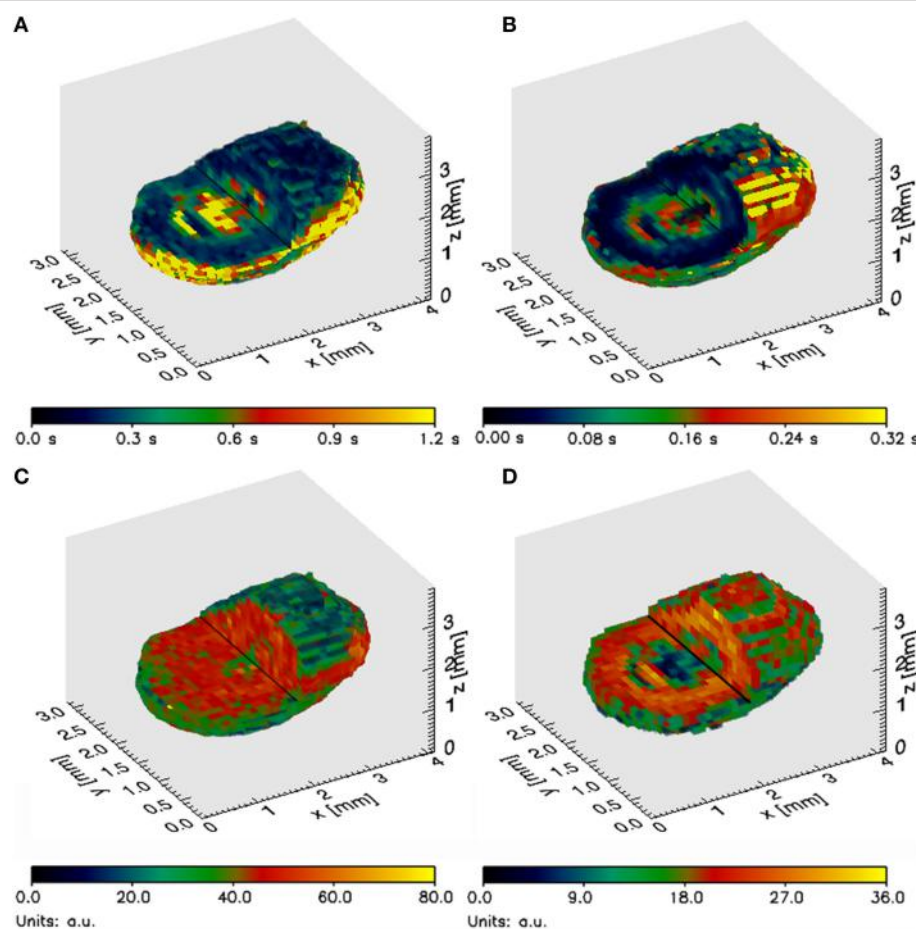


FIGURE 1 | Partial cross section of a typical methanogenic granule under investigation representing (A) 3D T_1 map, (B) 3D T_2 map, (C) 3D A_0 map and (D) 3D S map.

always localized in the core of the granules in accordance with the occurrence of Type II regions (**Figure 1**).

The core and the outer layer could also be distinguished and visualized using SEM (**Figure 2**). Although the border between the core and the outer layer was not very apparent on the picture of the whole granule (**Figure 2A**), the detailed picture of the biomass matrix inside the outer layer (**Figure 2B**) and the core (**Figure 2C**) shows clear differences. The outer layer consisted mainly of apparently intact rod-shaped cells with a limited occurrence of damaged cells (**Figure 2B**). In contrast, the core contained mostly damaged (open) cells mainly of the same morphology as the cells found in the outer layer (**Figure 2C**). The change in occurrence of the damaged cells was quite abrupt (localized by the white curve in **Figure 2A**).

Transport of Gadolinium

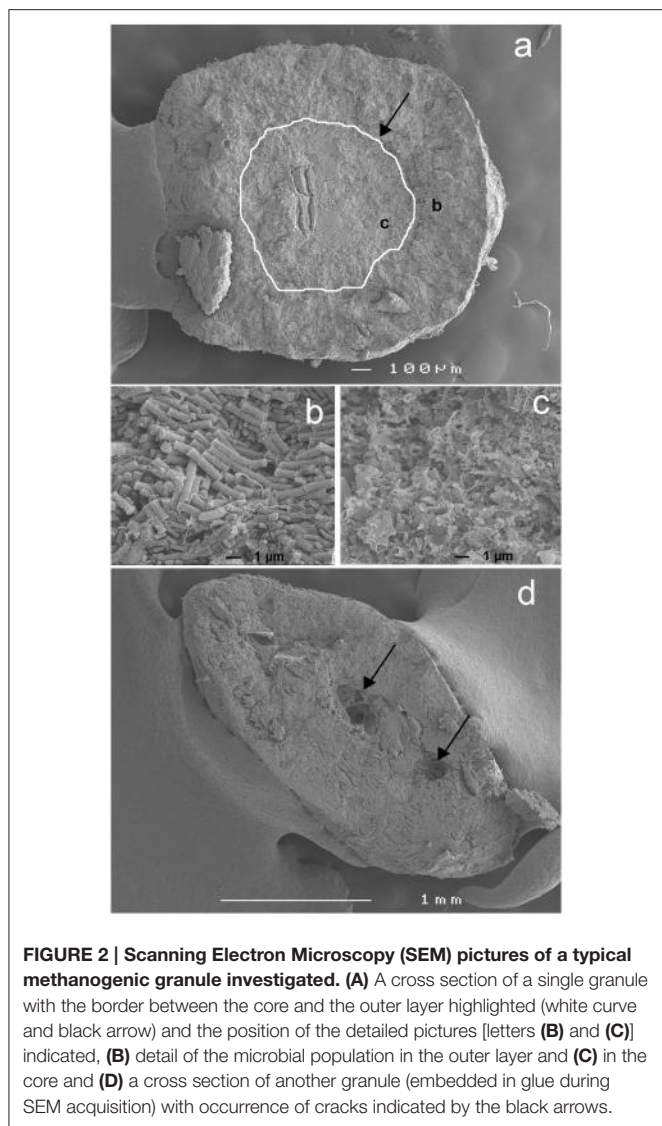
GdCl_3

A reactive barrier moving from the edge of the granule toward the core was clearly observed when the granule was exposed to $0.1 \text{ mmol} \cdot \text{L}^{-1}$ GdCl_3 (**Figure 3A**). Massive precipitation occurred causing a major decrease of

A_0 and T_2 , hampering calculations of the gadolinium concentration. Thus, the calculated concentration values illustrated in **Figure 3A** are somewhat biased, the rate of the reaction barrier movement can nevertheless be reliably observed.

$[\text{GdDTPA}]^{2-}$

The increase of the gadolinium concentration upon exposure to the $0.5 \text{ mmol} \cdot \text{L}^{-1}$ $[\text{GdDTPA}]^{2-}$ solution was much faster than with GdCl_3 (**Figure 3**). The process was as fast as the diffusion of free iron and cobalt (**Figures 5C,D**) and slightly faster than diffusion of the $\text{Fe}^{2+}/[\text{FeEDTA}]^{2-}$ mixture as reported by Bartacek et al. (2009). The final gadolinium concentration inside the granule ranged from 0.05 to $0.50 \text{ mmol} \cdot \text{L}^{-1}$ (**Figure 3B**). When averaged over the layers of uniform depth, the concentration range was 0.15 – $0.45 \text{ mmol} \cdot \text{L}^{-1}$, with the highest values in the edge (0 – $218 \mu\text{m}$) and in the center (872 – $1090 \mu\text{m}$). The decrease of both T_1 and T_2 values (**Figures 4A,B**) corresponded to this $[\text{GdDTPA}]^{2-}$ concentration increase (**Figure 4C**) and no A_0 decrease was observed (data not shown).



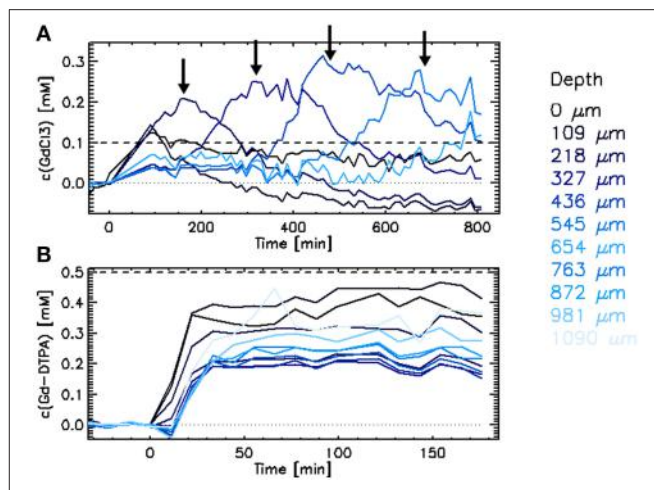
Transport of Iron

FeCl_2

Upon the injection of FeCl_2 (1 mM), the observed concentration of iron increased in the outer layers within 11 min (**Figure 5A**). The increase of the iron concentration was slightly (11–22 min) delayed in the inner layers. The fast increase was followed by a slower decrease of the calculated iron concentration, associated with the increase of the T_1 and T_2 values of the granular matrix. It can be assumed that the increase of the relaxation times was caused by changes in the biofilm matrix, e.g., dissolution of EPS, as a drop following the raise of the iron concentration inside the granule is unlikely to occur. No A_0 decrease was observed in these granules. Thus, there is no indication of iron precipitation inside the granule.

$[\text{FeEDTA}]^{2-}$

The development of the calculated iron concentration after the $[\text{FeEDTA}]^{2-}$ injection was similar to that with a FeCl_2 injection.



The main difference was that the increase in iron concentration started simultaneously in all layers of the granule (**Figure 5B**). Again, the final T_1 and T_2 values of the granular matrix were higher than those measured at the beginning of the experiment (data not shown).

Transport of Cobalt

CoCl_2

The increase of the cobalt concentration inside the granules exposed to 5 mM CoCl_2 solution was as fast as the increase of the free iron concentration inside the granules when exposed to FeCl_2 (**Figure 5**). Similarly to the FeCl_2 case, the maximum cobalt concentration was reached in all layers of the granules within 50 min upon the CoCl_2 injection. The delay in the increase of the cobalt concentration in the center of the granules indicates that a reactive barrier played a role in slowing the cobalt transport toward the center of the granule (**Figure 5D**).

The cobalt concentration inside the granule increased evenly in all directions (**Figure 6A**). The concentration values averaged over layers of specific depths (**Figure 6B**) and agreed well with the picture obtained by calculations per voxel (**Figure 6A**).

In general, the decrease in T_1 was equal or slightly larger than the values expected for 5 $\text{mmol}\cdot\text{L}^{-1}$ cobalt based on the calibration of the cobalt relaxivity in free liquid (**Figure 7A**). The final cobalt concentrations calculated inside the granule ranged from 6 to 9 $\text{mmol}\cdot\text{L}^{-1}$ (**Figure 5D**). The T_2 decrease expected based on the cobalt relaxivity calibration was minor (**Figure 7B**), not influencing the TSE signal. However, the actually measured T_2 decrease was large (theoretically corresponded to a cobalt concentration of at least 50 $\text{mmol}\cdot\text{L}^{-1}$), causing a significant decrease of the TSE signal and thus biasing calculations of the real cobalt concentration (apparent decrease in cobalt concentration). This phenomenon was accompanied by a decrease of A_0 (water density), especially in the outer layers of the granule. The decrease of A_0 contributed considerably to the apparent drop

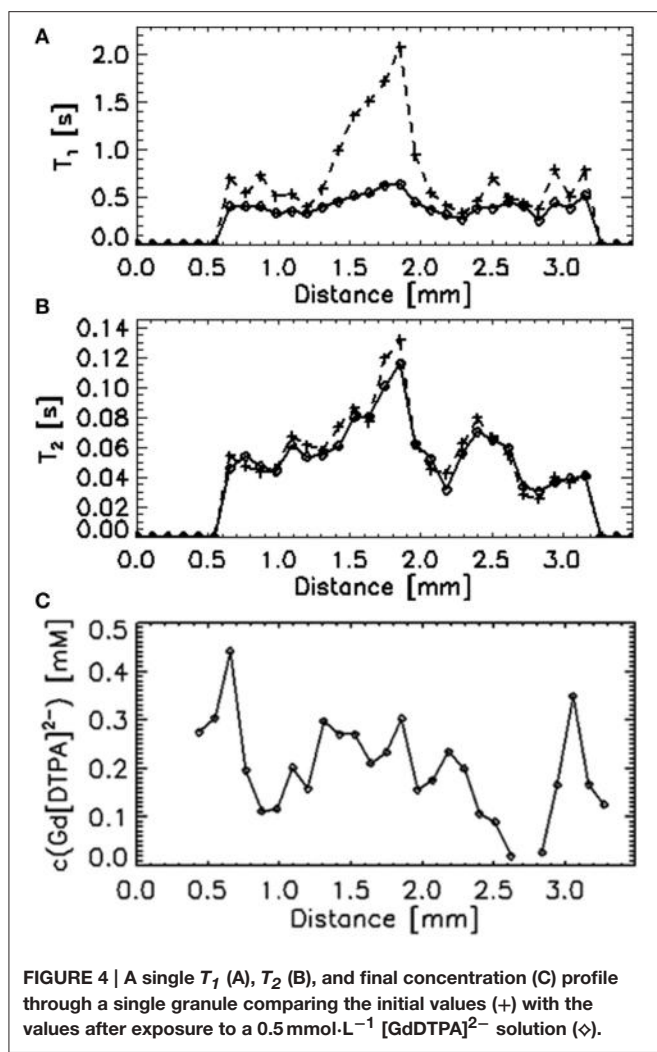


FIGURE 4 | A single T_1 (A), T_2 (B), and final concentration (C) profile through a single granule comparing the initial values (+) with the values after exposure to a $0.5 \text{ mmol}\cdot\text{L}^{-1}$ $[\text{GdDTPA}]^{2-}$ solution (\diamond).

of the calculated cobalt concentration, occurring in the 2 outer layers of the granule investigated (Figure 5D). The A_0 values were measured only at the start and upon conclusion of the experiments (the measurement took almost 2 h); hence it is impossible to describe the actual A_0 decrease in time. Knowing the A_0 values in time would allow to correct the calculated concentration values. When the final concentration value is calculated using the final values of A_0 and T_2 , the final cobalt concentrations in the outer layers are close to those calculated in the inner layers. For instance, the final cobalt concentration in the first outer layer is calculated to be $1.3 \text{ mmol}\cdot\text{L}^{-1}$ when neglecting the decrease of A_0 and T_2 in this layer. Taking the A_0 and T_2 decrease into account, the final concentration amounted to $5.2 \text{ mmol}\cdot\text{L}^{-1}$ in the same layer.

The Type II region (T_1 comparable to T_1 of the free solution) was found in the center of several granules investigated (Figure 7). The T_1 decrease in these regions agreed with the expected decrease after introduction of $5 \text{ mmol}\cdot\text{L}^{-1}$ cobalt, based on the relaxivity cobalt. An A_0 decrease was not observed. In contrast, the T_2 decrease in these regions was again larger than expected from calibration curves.

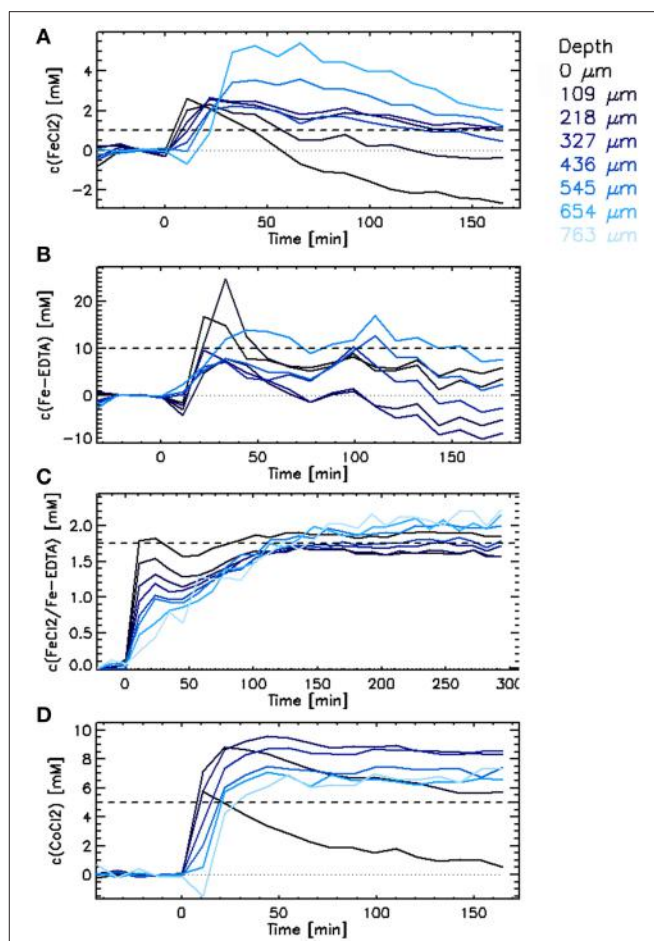


FIGURE 5 | Penetration of iron as (A) FeCl_2 , (B) $[\text{FeEDTA}]^{2-}$, and (C) $\text{FeCl}_2/[\text{FeEDTA}]^{2-}$ (0.25:1), and (D) cobalt as CoCl_2 into single methanogenic granules. Each curve depicts average values for a certain depth in the granule ranging from 0 μm (edge) to 763 μm (core). The dashed lines show the concentration of the given metal introduced into the liquid media at time zero.

DISCUSSION

Interaction of the Free Metal Ions with the Granular Biofilm Matrix

This study shows that MRI measurements can elucidate the mechanism and rate of free metal penetration in a granular matrix. As shown especially in the case of Gd^{3+} , a reaction barrier is formed and its movement can be tracked (Figure 3). Although the presence of a reaction barrier in biofilms has been anticipated in the past (Beyenal and Lewandowski, 2004), the first direct *in situ* observation of the development of the reactive barrier in wastewater treatment biofilms was shown only recently (Bartacek et al., 2012).

This study also shows that metals used for tracing transport processes in biofilms are not inert and interact with the biofilm matrix. As shown by the experiments with Fe^{2+} , Co^{2+} , and Gd^{3+} , free metal ions massively interact with the granular matrix (precipitation, sorption), causing extreme shortening of especially the T_2 value and considerable decreases in the A_0 .

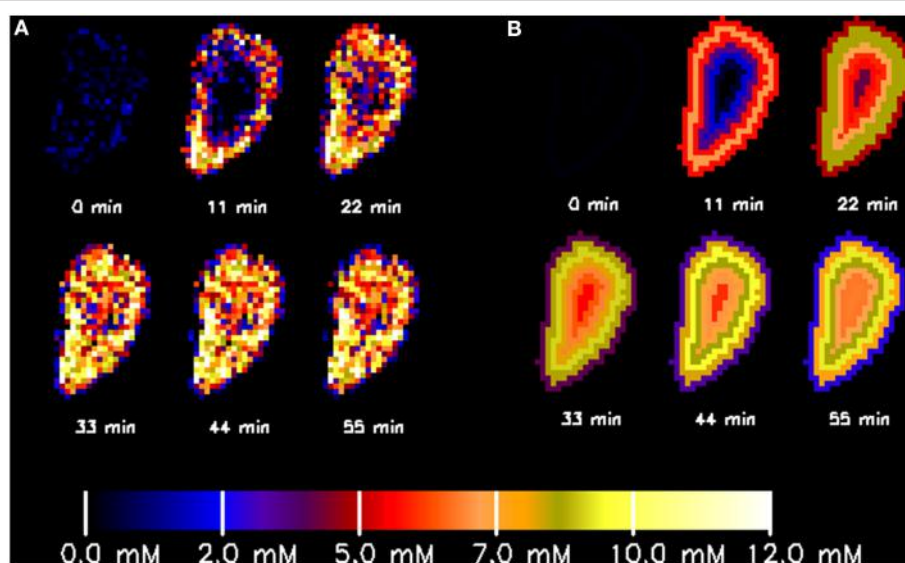


FIGURE 6 | Spatially resolved increase of cobalt concentration inside a single methanogenic granule upon injection of a $5 \text{ mmol} \cdot \text{L}^{-1}$ CoCl_2 solution at time zero as obtained by calculation at each single voxel (A) or averaged over layers of specific depths inside the granule (B).

Shortening of T_2 and decreasing of A_0 causes, respectively, T_2 weighting of the TSE signal and a decrease of the TSE signal, which in turn causes an apparent decrease of the calculated metal concentration. As long as the relations between the metal precipitation and T_1 , T_2 and A_0 changes is not quantitatively described, the exact translation of the TSE signal to the metal concentration will remain impossible.

Interaction of the Complexed Metals with the Granular Biofilm Matrix

$[\text{GdDTPA}]^{2-}$, often used as contrast agent in medical MRI (Li et al., 2007), is also an ideal example of a contrast agent for MRI studies of metal transport in a biofilm matrix (Ramanan et al., 2010). This complex did not decrease the A_0 and the T_2 decrease approximately corresponded to the values expected based on the $[\text{GdDTPA}]^{2-}$ relaxivity measured in free solution (Figure 4). The latter indicates that due to its high stability, $[\text{GdDTPA}]^{2-}$ does not disintegrate the granular matrix as shown for $[\text{FeEDTA}]^{2-}$ (Bartacek et al., 2009). However, the fact that the final concentration of gadolinium inside the granule was lower than the concentration introduced into the liquid surrounding the granule indicates that some interaction between $[\text{GdDTPA}]^{2-}$ and the granular matrix takes place. Most probably, the low $[\text{GdDTPA}]^{2-}$ concentration was caused by the Donnan effect, i.e., the presence of negatively charged EPS molecules in the granular matrix repulses the negatively charged $[\text{GdDTPA}]^{2-}$ complex. The Donnan effect probably also plays a role in the case of $[\text{FeEDTA}]^{2-}$ (Bartacek et al., 2009), but it was masked by other processes (T_2 increase in the biofilm matrix due to EDTA-biofilm interactions) in this study. The opposite outcome of the Donnan effect has been previously observed during supersaturation of alginate gels by free (positively charged) metal species (Kalis et al., 2009), but it is masked by metal precipitation in this

study (experiments with GdCl_3 , FeCl_2 , and CoCl_2). Indeed, the Donnan effect can play an important role in anaerobic granular sludge e.g., by decreasing toxicity of the negatively charged metal species such as $[\text{FeEDTA}]^{2-}$ on the one hand and increasing toxicity of the positively charged metal species such as Co^{2+} on the other hand. The lower toxicity of complexed cobalt or nickel species has been shown previously (Bartacek et al., 2008, 2010).

$[\text{FeEDTA}]^{2-}$ can increase the T_1 of the granular matrix hampering calculation of the iron concentration in the biofilm matrix (Figure 5B). This phenomenon was solved previously by Bartacek et al. (2009) by adding excess free iron achieving reliable data for iron diffusion (Figure 5C).

Implications of Metal Transport Pattern for the Deficiency of Essential Metals in Granular Sludge

Although this work did not focus on the biological activity of methanogenic biomass, it can be suggested that limitation or toxicity by different metals will be strongly affected by the transport phenomena taking place inside the granules. As shown also by Bartacek et al. (2012), trace metals tend to accumulate inside the granules when dosed as free ions. Then, the positive effect of metals supplementation lasts longer. In contrast, when dosed with organic ligands such as EDTA, the supplementation of metals causes faster and more pronounced responses. This paper further clarifies the mechanisms how are metals transported and accumulated inside the granules.

This paper also shows that supplementation of metals attached to organic ligands may cause serious degradation of the granular matrix. The negative effect of repeated CoEDTA^{2-} additions on the granular matrix was previously reported by Fermoso et al. (2008).

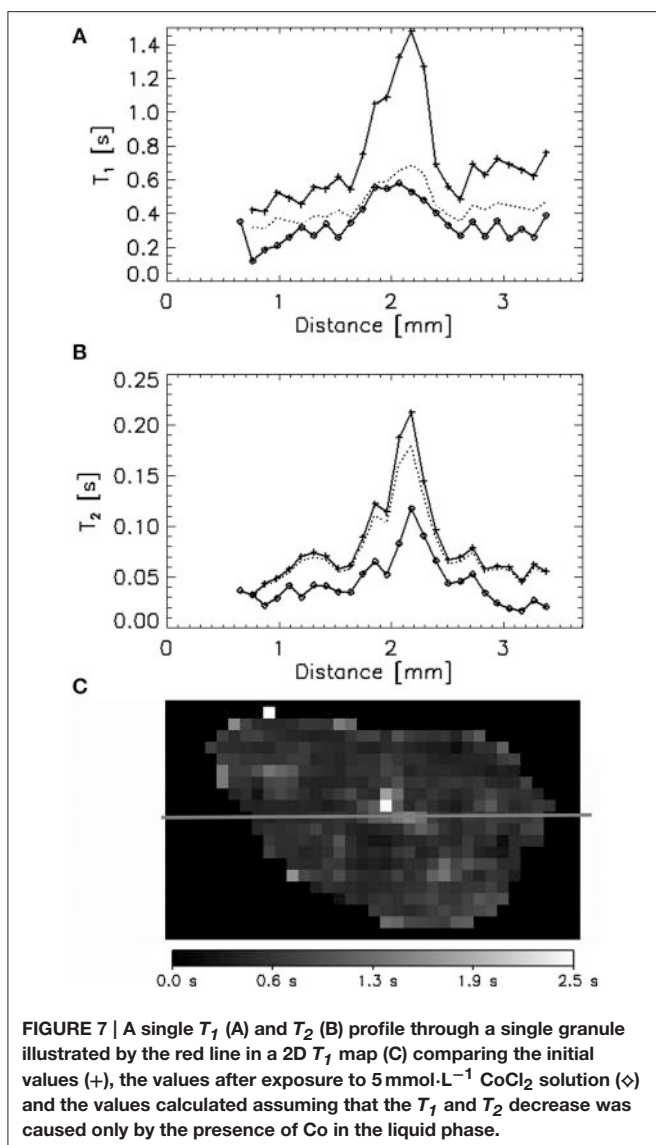


FIGURE 7 | A single T_1 (A) and T_2 (B) profile through a single granule illustrated by the red line in a 2D T_1 map (C) comparing the initial values (+), the values after exposure to $5 \text{ mmol L}^{-1} \text{ CoCl}_2$ solution (\diamond) and the values calculated assuming that the T_1 and T_2 decrease was caused only by the presence of Co in the liquid phase.

Structure of the Granular Matrix and its Influence on Metals Transport

A clearly distinguishable core was observed in most of the granules investigated, a phenomenon previously reported for other types of granular sludge (Lens et al., 1997). The core had usually a higher T_1 and T_2 (Figure 1) and the SEM observation revealed that this part of the granules was mostly composed of decaying biomass (Figure 2). As observed by Bartacek et al. (2009) and confirmed by the observation with $[\text{GdDTPA}]^{2-}$ in this study (Figure 4), the final concentration of metal complexes tend to reach the highest values in the core (except the outer layers in some cases). This can be caused by a lower amount of negatively charged EPS inside the granular core, which is mostly composed of dead biomass (Figure 2). As discussed above, the presence of EPS can cause resistance against the increase of the metal concentration.

Although microbial analysis of the granules under study was not done, it can be expected that the majority of

the methanogenic microorganisms seen in Figure 2B are of the *Methanosarcina* genus as was shown in similar granules previously (Fermoso et al., 2008). Also the morphology of the cells observed in Figure 2B supports this suggestion.

Besides the distinction between the core and the outer layers of the granules, two distinct types of regions (Type I and Type II) were observed in all cases associated with the granular core. Type I regions had a lower A_0 , T_1 and T_2 values compared to the rest of the granule, indicating that the density and mobility of water were lower in these regions. Therefore, Type I regions may indicate the presence of precipitates inside the granular matrix (Nott et al., 2001).

Type II regions were characterized by A_0 values as high as in the rest of the granules and T_1 and T_2 values similar to those measured in the liquid surrounding the granule. Considering that the granular matrix consists of approximately 95% water, the A_0 measured inside the granules (except Type I regions) can indeed be expected to be close to the A_0 values measured in the surrounding liquid. However, the T_1 and T_2 values are strongly shortened in most of the granular matrix by the presence of cell walls, EPS, precipitates, etc. (Lens et al., 1997; Gonzalez-Gil et al., 2001; Bartacek et al., 2009). Therefore, high T_1 and T_2 values may indicate the presence of cracks, such as those revealed by the SEM images (Figure 2D).

CONCLUSIONS

This study shows that the chemical speciation of a metal strongly influences the metal transport in methanogenic granules. It was shown that free metals form a reactive barrier while precipitating inside biofilm, which slows down the increase of concentration of the given metal in the center of the granule. Chelated metals penetrate the granular biofilm faster, but can be repulsed by the negatively charged organic compounds present in the biofilm matrix. This paper also shows that the metal compounds used for investigating transport properties in biofilm are not entirely inert. Thus, the interaction between the biofilm and the contrast agent may be of such a nature (e.g., precipitation of free metal ions) that might biases the quantification of metal concentrations inside the biofilm via the MRI protocol used in this study.

AUTHOR CONTRIBUTIONS

JB conducted a substantial part of the experiments, did most of data analysis, and has written the vast majority of the text. JM conducted most of the experiments and the primary data analyses. FV supported the experiments by developing experimental procedures and data acquisition for MRI. He also supported data analysis and contributed to the manuscript writing. EG supported the experimental work by operating the MRI equipment and contributed to the text in the Methods section. HVA supervised the research and guaranteed the quality as the expert on MRI. PL supervised the research and guaranteed the quality as the expert on anaerobic digestion and granular biofilm.

FUNDING

This work was supported by the European Commission via the Research Infrastructure Wageningen NMR Centre (FP6-2004-026164 Research Infrastructure Transnational Access WNMRC),

the Marie Curie Intra European Fellowship “Bioavailability of trace metals in anaerobic granular sludge reactors” (MEIF-CT-2007-041896), and the Marie Curie Reintegration Grant “Biofilms in Bioreactors for Advanced Nitrogen Removal from Wastewater” (ERG-2010-268417).

REFERENCES

- Bartacek, J., Fermoso, F. G., Baldó-Urrutia, A. M., Van Hullebusch, E. D., and Lens, P. N. L. (2008). Cobalt toxicity in anaerobic granular sludge: influence of chemical speciation. *J. Ind. Microbiol. Biotechnol.* 35, 1465–1474. doi: 10.1007/s10295-008-0448-0
- Bartacek, J., Fermoso, F. G., Catena, A. B., and Lens, P. N. L. (2010). Effect of sorption kinetics on nickel toxicity in methanogenic granular sludge. *J. Hazard. Mater.* 180, 289–296. doi: 10.1016/j.jhazmat.2010.04.029
- Bartacek, J., Fermoso, F. G., Vergeldt, F., Gerkema, E., Maca, J., Van As, H., et al. (2012). The impact of metal transport processes on bioavailability of free and complex metal ions in methanogenic granular sludge. *Water Sci. Technol.* 65, 1875–1881. doi: 10.2166/wst.2012.030
- Bartacek, J., Vergeldt, F. J., Gerkema, E., Jenicek, P., Lens, P. N. L., and Van As, H. (2009). Magnetic resonance microscopy of iron transport in methanogenic granules. *J. Magn. Reson.* 200, 303–312. doi: 10.1016/j.jmr.2009.07.013
- Beyenal, H., and Lewandowski, Z. (2004). Dynamics of lead immobilization in sulfate reducing biofilms. *Water Res.* 38, 2726–2736. doi: 10.1016/j.watres.2004.03.023
- De Lima, A. C. F., Gonçalves, M. M. M., Granato, M., and Leite, S. G. F. (2001). Anaerobic sulphate-reducing microbial process using UASB reactor for heavy metals decontamination. *Environ. Technol.* 22, 261–270. doi: 10.1080/0959332208618286
- Donahue, K. M., Burstein, D., Manning, W. J., and Gray, M. L. (1994). Studies of Gd-DTPA relaxivity and proton exchange rates in tissue. *Magn. Reson. Med.* 32, 66–76. doi: 10.1002/mrm.1910320110
- Fermoso, F. G., Bartacek, J., Chung, L. C., and Lens, P. (2008). Supplementation of cobalt to UASB reactors by pulse dosing: CoCl₂ versus CoEDTA²⁻ pulses. *Biochem. Eng. J.* 42, 111–119. doi: 10.1016/j.bej.2008.06.005
- Gonzalez-Gil, G., Lens, P. N. L., Van Aelst, A., Van As, H., Versprille, A. I., and Lettinga, G. (2001). Cluster structure of anaerobic aggregates of an expanded granular sludge bed reactor. *Appl. Environ. Microbiol.* 67, 3683–3692. doi: 10.1128/AEM.67.8.3683-3692.2001
- Hulshoff Pol, L. W., De Castro Lopes, S. I., Lettinga, G., and Lens, P. N. L. (2004). Anaerobic sludge granulation. *Water Res.* 38, 1376–1389. doi: 10.1016/j.watres.2003.12.002
- Kalis, E. J. J., Davis, T. A., Town, R. M., and Van Leeuwen, H. P. (2009). Impact of ionic strength on Cd(II) partitioning between alginate gel and aqueous media. *Environ. Sci. Technol.* 43, 1091–1096. doi: 10.1021/es802305n
- Lens, P. N. L., and Hemminga, M. A. (1998). Nuclear magnetic resonance in environmental engineering: principles and applications. *Biodegradation* 9, 393–409. doi: 10.1023/A:1008316031421
- Lens, P., Pol, L. H., Lettinga, G., and Van As, H. (1997). Use of ¹H NMR study of water transport processes in sulfidogenic granular sludge. *Water Sci. Technol.* 36, 157–163. doi: 10.1016/S0273-1223(97)00519-2
- Li, Z., Li, W., Li, X., Pei, F., Li, Y., and Lei, H. (2007). The gadolinium complexes with polyoxometalates as potential MRI contrast agents. *Magn. Reson. Imaging* 25, 412–417. doi: 10.1016/j.mri.2006.09.039
- Mohoric, A., Vergeldt, F., Gerkema, E., De Jager, A., Van Duynhoven, J., Van Dalen, G., et al. (2004). Magnetic resonance imaging of single rice kernels during cooking. *J. Magn. Reson.* 171, 157–162. doi: 10.1016/j.jmr.2004.08.013
- Moradi, A. B., Oswald, S. E., Massner, J. A., Pruessmann, K. P., Robinson, B. H., and Schulin, R. (2008). Magnetic resonance imaging methods to reveal the real-time distribution of nickel in porous media. *Eur. J. Soil Sci.* 59, 476–485. doi: 10.1111/j.1365-2389.2007.00999.x
- Nestle, N. (2002). NMR studies on heavy metal immobilization in biosorbents and mineral matrices. *Rev. Environ. Sci. Biotechnol.* 1, 215–225. doi: 10.1023/A:1021255727484
- Nestle, N., and Kimmich, R. (1996). NMR imaging of heavy metal absorption in alginate, immobilized cells, and kombu algal biosorbents. *Biotechnol. Bioeng.* 51, 538–543.
- Nestle, N., Wunderlich, A., Niessner, R., and Baumann, T. (2003). Spatial and temporal observations of adsorption and remobilization of heavy metal ions in a sandy aquifer matrix using magnetic resonance imaging. *Environ. Sci. Technol.* 37, 3972–3977. doi: 10.1021/es026250s
- Nott, K. P., Paterson-Beedle, M., Macaskie, L. E., and Hall, L. D. (2001). Visualisation of metal deposition in biofilm reactors by three-dimensional magnetic resonance imaging (MRI). *Biotechnol. Lett.* 23, 1749–1757. doi: 10.1023/A:1012492216390
- Phoenix, V. R., and Holmes, W. M. (2008). Magnetic resonance imaging of structure, diffusivity, and copper immobilization in a phototrophic biofilm. *Appl. Environ. Microbiol.* 74, 4934–4943. doi: 10.1128/AEM.02783-07
- Ramanan, B., Holmes, W. M., Sloan, W. T., and Phoenix, V. R. (2010). Application of paramagnetically tagged molecules for magnetic resonance imaging of biofilm mass transport processes. *Appl. Environ. Microbiol.* 76, 4027–4036. doi: 10.1128/AEM.03016-09
- Steed, V. S., Suidan, M. T., Gupta, M., Miyahara, T., Acheson, C. M., and Sayles, G. D. (2000). Development of a sulfate-reducing biological process to remove heavy metals from acid mine drainage. *Water Environ. Res.* 72, 530–535. doi: 10.2175/106143000X138102
- Van As, H., and Lens, P. (2001). Use of ¹H NMR to study transport processes in porous biosystems. *J. Ind. Microbiol. Biotechnol.* 26, 43. doi: 10.1038/sj.jim.7000087
- Van As, H., and Van Dusschoten, D. (1997). NMR methods for imaging of transport processes in micro-porous systems. *Geoderma* 80, 389–403. doi: 10.1016/S0016-7061(97)00062-1
- Van Hullebusch, E. D., Zandvoort, M. H., and Lens, P. N. L. (2003). Metal immobilisation by biofilms: mechanisms and analytical tools. *Rev. Environ. Sci. Biotechnol.* 2, 9–33. doi: 10.1023/B:RESB.0000022995.48330.55
- Zandvoort, M. M., Van Hullebusch, E. D., Fermoso, F. G., and Lens, P. (2006). Trace metals in anaerobic granular sludge reactors: bioavailability and dosing strategies. *Eng. Life Sci.* 6, 293–301. doi: 10.1002/elsc.200620129

Conflict of Interest Statement: The authors declare that the research was conducted in the absence of any commercial or financial relationships that could be construed as a potential conflict of interest.

Copyright © 2016 Bartacek, Vergeldt, Maca, Gerkema, Van As and Lens. This is an open-access article distributed under the terms of the Creative Commons Attribution License (CC BY). The use, distribution or reproduction in other forums is permitted, provided the original author(s) or licensor are credited and that the original publication in this journal is cited, in accordance with accepted academic practice. No use, distribution or reproduction is permitted which does not comply with these terms.



Life Cycle Environmental Impacts of Electricity from Biogas Produced by Anaerobic Digestion

Alessandra Fusi¹, Jacopo Bacenetti², Marco Fiala² and Adisa Azapagic^{1*}

¹Sustainable Industrial Systems, School of Chemical Engineering and Analytical Science, The University of Manchester, Manchester, UK, ²Dipartimento di Scienze Agrarie e Ambientali – Produzione, Territorio, Agroenergia, Università degli Studi di Milano, Milan, Italy

OPEN ACCESS

Edited by:

Gavin Collins,
National University of Ireland Galway,
Ireland

Reviewed by:

Chu-Ching Lin,
National Central University, Taiwan
Alex Oriel Godoy,
Universidad del Desarrollo, Chile

***Correspondence:**

Adisa Azapagic
adisa.azapagic@manchester.ac.uk

Specialty section:

This article was submitted to
Microbiotechnology, Ecotoxicology
and Bioremediation,
a section of the journal
*Frontiers in Bioengineering and
Biotechnology*

Received: 14 November 2015

Accepted: 23 February 2016

Published: 11 March 2016

Citation:

Fusi A, Bacenetti J, Fiala M and
Azapagic A (2016) Life Cycle
Environmental Impacts of Electricity
from Biogas Produced by Anaerobic
Digestion.
Front. Bioeng. Biotechnol. 4:26.
doi: 10.3389/fbioe.2016.00026

The aim of this study was to evaluate life cycle environmental impacts associated with the generation of electricity from biogas produced by the anaerobic digestion (AD) of agricultural products and waste. Five real plants in Italy were considered, using maize silage, slurry, and tomato waste as feedstocks and cogenerating electricity and heat; the latter is not utilized. The results suggest that maize silage and the operation of anaerobic digesters, including open storage of digestate, are the main contributors to the impacts of biogas electricity. The system that uses animal slurry is the best option, except for the marine and terrestrial ecotoxicity. The results also suggest that it is environmentally better to have smaller plants using slurry and waste rather than bigger installations, which require maize silage to operate efficiently. Electricity from biogas is environmentally more sustainable than grid electricity for seven out of 11 impacts considered. However, in comparison with natural gas, biogas electricity is worse for seven out of 11 impacts. It also has mostly higher impacts than other renewables, with a few exceptions, notably solar photovoltaics. Thus, for the AD systems and mesophilic operating conditions considered in this study, biogas electricity can help reduce greenhouse gas (GHG) emissions relative to a fossil-intensive electricity mix; however, some other impacts increase. If mitigation of climate change is the main aim, other renewables have a greater potential to reduce GHG emissions. If, in addition to this, other impacts are considered, then hydro, wind, and geothermal power are better alternatives to biogas electricity. However, utilization of heat would improve significantly its environmental sustainability, particularly global warming potential, summer smog, and the depletion of abiotic resources and the ozone layer. Further improvements can be achieved by banning open digestate storage to prevent methane emissions and regulating digestate spreading onto land to minimize emissions of ammonia and related environmental impacts.

Keywords: agricultural waste, anaerobic digestion, biogas, electricity, life cycle assessment, renewable energy

INTRODUCTION

The need to mitigate climate change and improve security of energy supply is driving a growing interest in renewable energy sources, with many world regions and countries setting ambitious targets. For example, the EU directive on the promotion of the use of energy from renewable sources (EC, 2009) sets the target of achieving a 20% share of energy from renewable resources by 2020, including biogas produced by anaerobic digestion (AD) of agricultural feedstocks.

Production of biogas is expanding rapidly in Europe. According to EurObserv'ER (2014), about 13.4 million ton oil equivalent (Mtoe) of biogas primary energy was produced in the EU during 2013, a 10% increase on the 2012 levels. Germany is the largest producer of biogas, not only in Europe but also in the world. In 2013, it had 7874 AD plants with a total installed electrical capacity of 3384 MW, which generated 27 TWh/year (EurObserv'ER, 2014; Fuchsz and Kohlheb, 2015). By comparison, the second largest world producer – China – generates just over one-quarter of that (7.6 TWh/year in 2009) (Chen et al., 2012). Italy follows closely in third place at 7.4 TWh of electricity per year produced by 1300 AD plants with a total installed capacity of 1000 MW (Brizzo, 2015). The plants are fed largely with maize grown specifically for this purpose, which in Italy occupies 10% of the total maize cultivation area (1,172,000 ha) (Casati, 2011). However, this is still only half the area in Germany (2,282,000 ha) where it covers one-third of the total maize land (Dressler et al., 2012).

The rapid expansion of biogas production in Europe is largely due to the feed-in-tariffs (FiT) schemes available in 29 countries (Whiting and Azapagic, 2014). For example, electricity generators in Italy using biogas produced in AD plants smaller than 1 MW are paid €280/MWh generated. In the UK, the subsidies are significantly lower, ranging from €130 to 210/MWh, depending on the plant size (Whiting and Azapagic, 2014). This perhaps explains why the deployment of AD was initially slower than in Italy, with only 180 AD plants installed so far, but with a further 500 projects currently under development (NNFCC, 2015). However, the FiT scheme in Italy has recently been changed, reducing the subsidy for electricity by 15–30% and introducing payments for utilization of heat and other coproducts (Ministero dello Sviluppo Economico, 2012). In the US, the growth of biogas production has also been slower than elsewhere, with only 244 AD plants currently in operation (Ebner et al., 2015); this is largely due to the absence of adequate subsidies.

Biogas produced by AD is considered to have a high saving potential with respect to greenhouse gas (GHG) emissions (EC, 2009). However, beyond that, other environmental implications of biogas production are still unclear despite quite a few life cycle assessment (LCA) studies having been carried out. This is due to several reasons. First, most previous studies of biogas have either focused on climate change or considered a limited number of impacts; for a summary, see **Table 1**. As far as the authors are aware, out of 26 studies found in the literature, only five have considered a full suite of impacts normally included in LCA studies, two of which are based in the UK (Mezzullo et al., 2013; Whiting and Azapagic, 2014), one in Argentina (Morero et al., 2015), one in Italy (Pacetti et al., 2015), and one in China (Xu et al., 2015). It is also apparent from **Table 1** that the goal, scope, life cycle impact assessment (LCIA) methodology, feedstocks, and geographical regions covered by the studies vary widely. Most studies are based in Europe with several in China and one each in Argentina, Canada, and the US. All plants have a capacity below 1 MW, with the majority being around 500 kW (where reported); some are electricity only and others combined heat and power (CHP) installations. Most studies have excluded the impacts of constructing and decommissioning the AD and

power plants. Maize is the most commonly considered feedstock, followed by animal slurry. The functional unit is largely based either on a unit of feedstock used to generate biogas or a unit of energy (biogas, heat, or electricity). Most studies have relied on secondary foreground data to estimate the impacts or used only limited primary data. However, the greatest variation among the studies is found in the number of impacts considered and the methodologies used to estimate them. The former range from 1 to 18 and the latter cover almost all known LCIA methods, including EcoIndicator 99 (Goedkoop and Spriensma, 2001), CML 2001 (Guinée et al., 2002), Impact 2002+ (Olivier et al., 2003), and ReCiPe (Goedkoop et al., 2009). These and the other differences, including the credits for coproducts, have led to very different results among the studies, making it difficult to compare them, and draw any generic conclusions on the environmental sustainability of biogas.

This study aims to make further contributions to the discussion on the environmental sustainability of biogas. The paper considers life cycle environmental impacts of electricity generation in five real AD-CHP systems using biogas produced from differing mixes of four types of feedstock. The plants are situated in Italy. The novel aspects of the work compared to previous studies include:

- estimation of impacts associated with electricity generated from biogas using different feedstocks, including dedicated maize crops, their mixture with animal slurry, and agricultural waste as well as a mixture of slurry and waste;
- use of primary data for both the feedstock production and operation of the AD-CHP systems;
- consideration of the influence of different scales of the AD-CHP systems on the environmental impacts;
- inclusion of construction and decommissioning of AD and CHP plants;
- estimation of the avoided emissions from using the digestate instead of slurry as fertilizer; and
- comparison of impacts with grid electricity, natural gas, and renewable sources of electricity.

MATERIALS AND METHODS

The environmental impacts of biogas electricity were estimated using LCA as a tool. The study was carried out in accordance with the ISO 14040/44 methodology for LCA (ISO, 2006a,b). The systems were modeled using Gabi LCA software V6.11 (Thinkstep, 2015). The CML 2001 method (Guinée et al., 2002), April 2013 update, was followed to estimate the following 11 impacts considered in this method: abiotic depletion potential of elements (ADP elements), abiotic depletion potential of fossil fuels (ADP fossil), acidification potential (AP), eutrophication potential (EP), freshwater aquatic ecotoxicity potential (FAETP), global warming potential (GWP), human toxicity potential (HTP), marine aquatic ecotoxicity potential (MAETP), ozone layer depletion potential (ODP), photochemical oxidants creation potential (POCP), also known as summer smog, and terrestrial ecotoxicity potential (TETP). For further details on the estimation of the impacts, see Supplementary Material.

TABLE 1 | LCA biogas studies available in the literature.

Reference	Country	No. of AD plants	Plant size	Feedstocks ^a	Functional unit	Foreground LCI data ^b	Capital goods	Impacts (LCIA method) ^c	Best options ^c
Jury et al. (2010)	Luxemburg	Not reported	Not reported	• 4 winter cereals • 4 summer cereals	1 MJ supplied to the natural gas grid	Secondary	Excluded	GWP and CED (impact 2002+)	Not reported
De Vries et al. (2010)	Western Europe	Not reported	Not reported	• Cattle slurry • Maize silage • Codigestion of above	1 ton of feedstock (wet)	Secondary	Excluded	GWP, AP, EP, CED, and LU (not specified)	Codigestion for GWP, EP, AP, and CED; slurry for LU
Blengini et al. (2011)	Italy	Not reported	Not reported	• Maize • Sorghum • Triticale • Miscanthus • Slurry	1 MJ of net energy (heat or electricity) delivered	Secondary	Included	6 (CML 2001)	Miscanthus for GWP, EP, and AP; maize silage for photochemical smog
Dressler et al. (2012)	Germany	1	510 kW	• Maize silage	1 kWh of electricity	Secondary	Excluded	GWP, AP, EP (CML 2001)	Not reported
Lansche and Müller (2012)	Germany	1	186 kW	• Cattle slurry • Maize silage • Grass silage • Codigestion of above	1 MJ of electricity	Primary	Excluded	GWP, AP, EP (CML 2001)	Cattle slurry
Meyer-Aurich et al. (2012)	Germany	1	500 kW	• Cattle slurry • Maize silage • Codigestion of above	1 kWh of electricity	Secondary	Excluded	GWP (IPCC, 2007)	Cattle slurry
De Vries et al. (2012)	The Netherlands	1	500 kW	• Pig slurry • Maize silage • Glycerine • Beet tails • Roadside grass • Codigestion of above	1 ton of feedstock (wet)	Secondary	Excluded	7 (ReCiPe mid-point)	Pig slurry for GWP, AP, ME, and LU; codigestion for FFD, FE, and PMF
Bacenetti et al. (2013)	Italy	3	250–999 kW	• Maize silage • Pig slurry • Codigestion of above	1 kWh of electricity	Primary	Excluded	GWP and CED (IPCC, 2007)	Pig slurry for GWP; maize silage for CED
Mezzullo et al. (2013)	UK	1	Not reported	• Cattle slurry	1 m ³ of methane	Secondary	Included	11 (Ecoindicator 99)	Not reported
Zhang et al. (2013)	China	1	Not reported	• Household waste	Household biogas (digester volume 8 m ³)	Secondary	Included	CO ₂ emissions (Not specified)	Not reported
Lijó et al. (2014a)	Italy	2	250 and 500 kW	• Animal slurry • Maize silage	1 ton of feedstock (wet)	Primary only for AD and CHP plant	Excluded	8 (ReCiPe mid-point)	Animal slurry
Lijó et al. (2014b)	Italy	1	500 kW	• Codigestion of maize and triticale silage	100 kWh of electricity	Primary only for AD and CHP plant	Excluded	8 (ReCiPe mid-point)	Maize silage

(Continued)

TABLE 1 | Continued

Reference	Country	No. of AD plants	Plant size	Feedstocks ^a	Functional unit	Foreground LCI data ^b	Capital goods	Impacts (LCIA method) ^c	Best options ^c
Rodriguez-Verde et al. (2014)	Spain	1	500 kW	<ul style="list-style-type: none"> Pig slurry Molasses Fish Biodiesel Vinassee residues 	110,000 ton/year of pig slurry	Primary and secondary	Excluded	6 (CML 2001)	Not reported
Styles et al. (2014)	UK	4	72–185 kW	<ul style="list-style-type: none"> Food waste Cattle slurry Maize and grass silage Miscanthus Codigestion of above 	1 year of farm operation	Secondary	Excluded	GWP, AP, EP, and RDP (CML 2010)	Slurry and food waste
Whiting and Azapagic (2014)	UK	1	170 kW	<ul style="list-style-type: none"> Codigestion of slurry, cheese whey, fodder beet, and maize silage 	Cogeneration of 1 MWh of heat and electricity	Primary and secondary	Included	11 (CML 2001)	Farm waste better than maize for 8 out of 11 impacts
Bacenetti and Fiala (2015)	Italy	5	100–999 kW	<ul style="list-style-type: none"> Cattle slurry Pig slurry Cereal silage Codigestion of above 	1 kWh of electricity	Tractors and equipment included; AD and CHP plant excluded	GWP (IPCC, 2007)	Feedstocks	
Ebner et al. (2015)	USA	1	Not reported	<ul style="list-style-type: none"> Codigestion of cattle slurry and food waste 	1 ton of feedstock (wet)	Secondary	Excluded	GWP (IPCC, 2007)	Not reported
Fuchsz and Kohlheb (2015)	Germany	3	600 kW	<ul style="list-style-type: none"> Maize silage Cow slurry Codigestion of above 	1 kWh of electricity	Primary only for AD plant construction	Included	GWP, AP, EP (not specified)	Maize silage for GWP; slurry for AP and EP
Ingrao et al. (2015)	Italy	1	999 kW	<ul style="list-style-type: none"> Codigestion of by-products from wheat processing and maize silage 	1 kWh of electricity	Primary	Excluded	GWP (IPCC, 2007)	Not reported
Jin et al. (2015)	China	1	Not reported	<ul style="list-style-type: none"> Food waste 	1 ton of food waste	Secondary	Excluded	5 (CML 2001)	Not reported
Lijó et al. (2015)	Italy	1	1000 kW	<ul style="list-style-type: none"> Codigestion of pig slurry and maize silage 	1 ton of feedstock (wet)	Primary only for AD and CHP plant	Excluded	8 (ReCiPe mid-point)	Not reported
Morero et al. (2015)	Argentina	2	531–573 kW	<ul style="list-style-type: none"> Agroindustrial wastes 	1 m ³ of biogas and 1 kWh of electricity	Primary and secondary	Excluded	11 (CML 2001)	Not reported
Pacetti et al. (2015)	Italy	1	Not reported	<ul style="list-style-type: none"> Maize Sorghum Wheat silage 	1 GJ of energy in the biogas	Secondary	Excluded	18 (ReCiPe mid-point)	Sorghum

(Continued)

TABLE 1 | Continued

Reference	Country	No. of AD plants	Plant size	Feedstocks ^a	Functional unit	Foreground LCI data ^b	Capital goods	Impacts (LCIA method) ^c	Best options ^c
Sidhu et al. (2015)	Canada	Not reported	Not reported	• Dairy slurry	1100 ton of dairy slurry	Primary and secondary	Excluded	7 (CML 2001)	Not reported
Xu et al. (2015)	China	Not reported	Not reported	• Food waste	1 ton of volatile solids	Secondary	Excluded	18 (ReCiPe mid-point)	Not reported
This study	Italy	5	100–999 kW	• Maize silage • Cow slurry • Codigestion of pig slurry, tomato waste, and maize silage • Codigestion of pig slurry and maize silage • Codigestion of pig slurry, maize silage, and maize ear silage	1 kWh of electricity	Primary	Included	11 (CML 2001)	Slurry for 9 out of 11 impacts; codigestion of slurry, waste, and maize sludge for marine and terrestrial ecotoxicity

^aEach bullet point represents a feedstock stream fed to the anaerobic digesters one at a time.^bLCI, life cycle inventory; Foreground data refer to the AD and CHP plants. Primary data are directly measured and/or collected as part of the study. Secondary data are from databases and literature.^cLCIA, life cycle impact assessment; AP, acidification potential; CED, cumulative energy demand; EP, eutrophication potential; FE, fresh water eutrophication; FFD, fossil fuel depletion; GWP, global warming potential; LU, land use; ME, marine eutrophication; PMf, particulate matter formation; RDP, resource depletion potential.

The next sections detail the goal of the study, the assumptions, and data used in the study.

Goal and Scope of the Study

The main goal of the study was to estimate the environmental impacts of electricity generated by different AD-CHP systems utilizing maize silage and agricultural waste. The results were compared with electricity from the grid, natural gas, and different renewables to help evaluate the environmental sustainability of biogas electricity relative to other available options.

Five real AD-CHP systems were considered using differing combinations of the following feedstocks: maize and maize ear silage; pig and cow slurry; and tomato peel and seeds (**Table 2**). The volume of the AD digesters ranged from 1650 to 2750 m³ and the installed electrical capacity of the CHP plants from 100 to 999 kW. The plants are located at farms producing the feedstocks in Lombardy in Northern Italy, where the majority of the country's biogas plants are situated (Negri et al., 2014).

As indicated in **Figure 1**, the scope of the study was from "cradle to grave," including:

- production of maize silage (where used), comprising cultivation, transport from fields to the farm (1 km), and the ensiling;
- collection of slurry and tomato waste and delivery to the AD plants;
- construction and decommissioning of AD and CHP plants;
- production of biogas in the AD plants and its treatment (filtration, dehumidification, and desulfurization);
- cogeneration of electricity and heat in the CHP plants; the heat, except that used for heating the digesters, is considered as waste as it is not used;
- storage and subsequent use of digestate as fertilizer; note that all plants but no. 2 use open storage of digestate.

Electricity distribution and consumption were excluded from the system boundary.

The functional unit was defined as "generation of 1 MWh of electricity to be fed into the grid." Although heat is cogenerated with electricity, all the impacts were allocated to the latter as the excess heat not utilized in the system is discharged as waste.

Inventory Data

Feedstock Production

The inventory data for the production of maize silage are detailed in Tables S1 and S2 in Supplementary Material. As indicated in the tables, data for field operations were collected directly from the farms. The background data were sourced from Ecoinvent (Nemecek and Kägi, 2007) and modified to match the characteristics of the machinery used for maize cultivation in Lombardy, based on information in Bodria et al. (2006). No environmental impacts were considered for tomato waste and slurry as they are waste.

Ammonia and nitrous oxide emissions as well as nitrate leachates from the application of the digestate and urea as fertilizers were estimated according to Brentrup et al. (2000). Phosphate leachates and run-offs were calculated based on Nemecek and Kägi (2007). To estimate pesticide emissions to the environment, several factors need to be considered, such

TABLE 2 | Summary of the main characteristics of the AD-CHP plants considered in the study.^a

Plant	Feedstock	Volume of AD digesters (m ³)	Dry matter content in digesters (%)	Organic loading in digesters (kg/day m ³)	Methane content in biogas (%)	Installed CHP power (kW)	Electricity generation (MWh/year)	Electricity consumption (MWh/year)	Heat generation (MWh/year)	Heat consumption by AD (MWh/year)
Plant 1	• Pig slurry • Tomato peel and seeds • Maize silage	1650	8.7	0.92	52.8	230	1945	173	2549	809
Plant 2	• Pig slurry • Maize silage	2250	10.6	1.07	52.6	300	2429	206	3184	814
Plant 3	• Pig slurry • Maize silage • Maize ear silage	2000	9.7	0.98	52.7	300	2505	276	3514	799
Plant 4	• Maize silage	2 × 2750	10.7	3.40	52.1	999	7972	717	8771	2505
Plant 5	• Cow slurry	1850	8.5	0.58	56.0	100	781	86	1095	547

^aAll data sourced directly from the farm/plant owners.

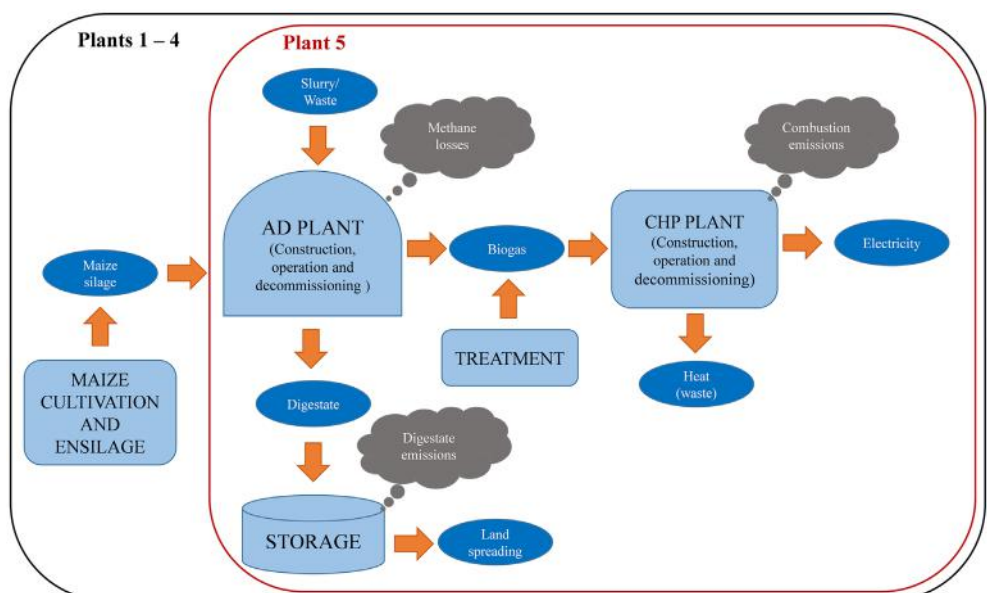


FIGURE 1 | System boundaries considered in the study. No environmental impacts are considered for the tomato waste, pig and cow slurry as they are waste. All the impacts are allocated to electricity as heat is not exported from the system.

as the way in which a pesticide is applied, the soil type, and the meteorological conditions during application (EMEP/EEA, 2013). However, considerations of these parameters is often impractical in LCA studies due to a lack of detailed data (Milà i Canals, 2007). Thus, pesticide emissions to air, water, and soil were determined in accordance with Margni et al. (2002) and Audsley (1997), assuming the following partitioning of the active pesticide components: 85% of the total amount applied remains in the soil, 5% in the plant, and 10% is emitted into the atmosphere; furthermore, 10% of the applied dose is lost as a run-off from the soil into the water. This method is also recommended for use by Curran (2012) and was applied in some other

LCA studies [e.g., Boschiero et al. (2014), Falcone et al. (2015), and Fantin et al. (2015)].

Land use change was not considered as the maize feedstock is grown on land previously used to cultivate cereals.

The transport and packaging of pesticides and fertilizers were not included in the system boundaries because of a lack of data. This is not deemed a limitation as some other studies found that their contribution was insignificant [e.g., Cellura et al. (2012)].

AD and CHP Plants

In all the AD plants evaluated in this study, the digestion takes place in continuously stirred reactors under mesophilic conditions at a

temperature of 40°C ($\pm 0.2^\circ\text{C}$), which is controlled and monitored continuously. Therefore, the digesters are operated at the top end of the temperature scale, which for mesophilic digestion ranges from 30 to 40°C (Weiland, 2010). The digesters are made from iron-reinforced concrete and have an expanded polyurethane external insulation. The biomass is fed into the digesters every 90 min in small amounts and heated using the heat generated by the adjacent CHP. As indicated in **Table 2**, the dry matter content in the digester varies from 8.5 to 10.6%, and the organic loading rate from 0.58 to 3.4 kg/day m³. The biogas composition is similar across the plants with the methane content ranging from 52 to 56% of the biogas volume.

The biogas is stored on top of the digesters in a gasometer dome with a spherical cap. Before being fed into the CHP plant, the biogas is filtered through a sand filter, dehumidified in a chiller, and then desulfurized using sodium hydroxide (NaOH). NO_x emissions are controlled by a catalytic converter. The digestate is pumped from the bottom of the digesters and stored in open tanks in all the plants except for Plant 2, where it is stored in a covered tank.

The biogas is fed into the CHP plant to generate electricity and heat. Electricity is sold to the national grid while the heat is used for heating the digesters and the excess is dissipated by fan-coolers. The electricity consumption for operating the AD plants is sourced from the national grid to ensure continuous operation during the CHP downtimes. The amount of electricity used by the system ranges from 8.5 to 11% of the total electricity generated (**Table 2**).

Detailed inventory data for the AD and CHP plants can be found in **Tables 2** and **3**. The operational data (feedstock production, consumption of electricity and heat, electricity generation) were obtained from the owners. Chemical characterization of different types of feedstock and their biogas production potentials were determined by laboratory tests (Fiala, 2012; Negri et al., 2014; Bacenetti et al., 2015) and used to calculate the biogas production by the AD plants. The emissions from the CHP plants were calculated based on NERI (2010). The useful lifetime of the AD plants was assumed to be 20 years (Nemecek and Kägi, 2007). For the CHP plants, the lifespan is shorter, between 8 and 10 years because of the high content of hydrogen sulfide (Fiala, 2012). At the end of a plant's useful lifetime, its construction materials were assumed to be landfilled, except for plastic materials, which were incinerated; the influence on the impacts of recycling is explored in a sensitivity analysis later in the paper.

The background data on the construction materials, their transport (120 km by rail and 35 km in 20–28 ton trucks) and landfilling were sourced from the Ecoinvent database v2.2 (Ecoinvent, 2010). Since the data for construction materials for the AD and CHP plants in Ecoinvent correspond to a different plant size (300 m³ for the AD and 160 kW_{el} for the CHP plants), the environmental impacts from their manufacture were estimated by scaling up or down their capacity to match the sizes of the AD and CHP plants considered in this study. This was carried out following the approach used for cost estimation in scaling up process plants (Coulson et al., 1993) but instead of costs, estimating environmental impacts as follows (Whiting and Zapagic, 2014):

$$E_2 = E_1 \cdot (C_2 / C_1)^{0.6} \quad (1)$$

where E_2 environmental impacts of the larger plant (AD or CHP); E_1 environmental impacts of the smaller plant (AD or CHP); C_2 capacity of the larger plant (volume for the AD plant and installed power for the CHP plant); C_1 capacity of the smaller plant (volume for the AD plant and installed power for the CHP plant); 0.6 scaling factor.

Digestate Use and Methane Emissions Credits

In all the plants except no. 4, the digestate is used as fertilizer on the farms, replacing pig or cow slurries applied previously as part of a traditional slurry management method (see **Figure 2**). Both digestate and the slurry from Plants 1, 3, and 5 are stored in open tanks before application, during which they emit methane. However, the emissions from digestate are lower than from slurry storage (Amon et al., 2006; Wang et al., 2014), and the AD systems were credited for the avoidance of the emissions. Note that in Plant 2, the digestate is stored in covered tanks, with no emissions of methane (IPCC, 2006); thus, the net emissions from this system are negative (**Table 3**).

At Plant 4, a closed maize cycle is practiced, whereby the digestate is used as fertilizer for the maize which is fed into the same plant (**Figure 3**). The digestate at this plant is stored in open tanks.

Alternative Electricity Sources

Grid electricity was considered here as the main alternative to electricity from biogas. This is due to the latter being fed into the national grid, displacing an equivalent amount of grid electricity. The Italian electricity mix is shown in Figure S1 in Supplementary Material. Given that the electricity mix is dominated by natural gas (53%) (IEA, 2011), biogas electricity was also compared to this

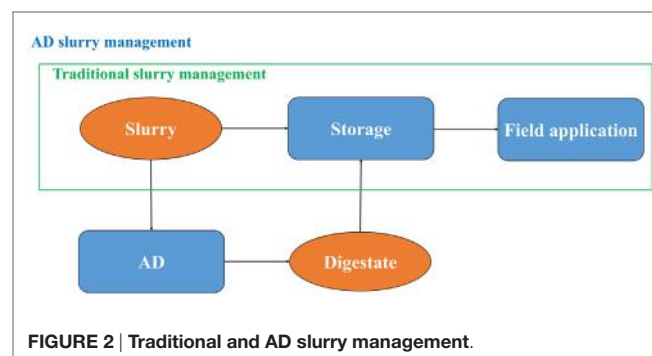


FIGURE 2 | Traditional and AD slurry management.

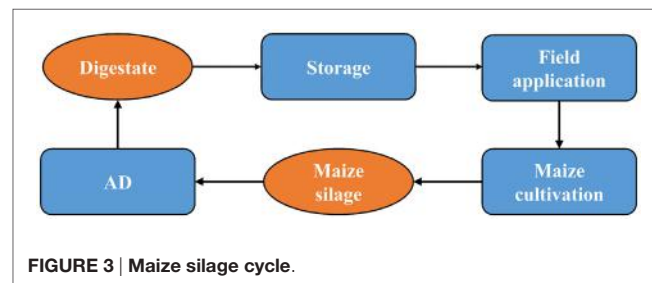


FIGURE 3 | Maize silage cycle.

TABLE 3 | Inventory data for the AD and CHP plants (expressed per megawatt hour of electricity).

	Unit	Plant 1	Plant 2	Plant 3	Plant 4	Plant 5	Data sources
AD							
Pig slurry	ton	8.4	6.0	7.3	—	—	Farm owner
Cow slurry	ton	—	—	—	—	21.0	- -
Maize silage	ton	0.9	2.25	0.8	2.45	—	- -
Tomato peel and seeds	ton	1.5	—	—	—	—	- -
Ear maize silage	ton	—	—	0.66	—	—	- -
Water	ton	0.94	0.75	—	0.23	—	- -
Sodium hydroxide	g	28.3	29.6	29.6	29.9	30.0	- -
Electricity from the grid	MWh	0.09	0.09	0.11	0.09	0.11	- -
Heat from CHP	MWh	0.42	0.34	0.32	0.38	0.70	- -
Net biogas production	Nm ³	280	278	289	252	285	Own calculations based on farm owner's data
CHP							
Electricity generated	MWh	1	1	1	1	1	- -
Heat generated	MWh	1.3	1.3	1.4	1.1	1.4	Own calculations based on farm owner's data
Emissions associated with AD							
Methane emissions from AD plant	m ³	3.8	3.8	4.0	3.4	3.9	Bacenetti et al. (2013)
Methane emissions from digestate storage	kg	8.9	0	8.9	8.9	8.9	Edelmann et al. (2011)
Credit for avoiding methane emissions from slurry storage	kg	-6.9	-6.3	-6.0	0	-32.0	Amon et al. (2006) and Wang et al. (2014)
Net emissions of methane	kg	5.9	-2.5	6.9	12.3	-19.2	Own calculations
Ammonia emissions from digestate storage	kg	0.2	0.0	0.2	0.2	0.2	Edelmann et al. (2011)
Emissions from CHP							
NO _x	g	56.1	56.1	56.1	56.1	56.1	NERI (2010)
NMVOC ^a	g	2.8	2.8	2.8	2.8	2.8	- -
CH ₄	g	120.6	120.6	120.6	120.6	120.6	- -
CO	g	86.1	86.1	86.1	86.1	86.1	- -
N ₂ O	mg	444	444	444	444	444	- -
As	mg	11	11	11	11	11	- -
Cd	mg	1	1	1	1	1	- -
Co	mg	58	58	58	58	58	- -
Cr	mg	50	50	50	50	50	- -
Cu	mg	86	86	86	86	86	- -
Hg	mg	33	33	33	33	33	- -
Mn	mg	53	53	53	53	53	- -
Ni	mg	64	64	64	64	64	- -
Pb	mg	1	1	1	1	1	- -
Sb	mg	33	33	33	33	33	- -
Se	mg	58	58	58	58	58	- -
Tl	mg	58	58	58	58	58	- -
V	mg	11	11	11	11	11	- -
Zn	mg	1097	1097	1097	1097	1097	- -

^aNon-methane volatile organic compounds.

option. Furthermore, as biogas is a renewable resource, it was also compared to the other renewables contributing to the Italian mix (see Figure S1 in Supplementary Material). The system boundary for all the alternatives was from “cradle to grave,” and all the data were sourced from Ecoinvent (2010). As for the biogas electricity, distribution and consumption of electricity were not considered.

RESULTS

The results suggest that biogas electricity generated by Plant 5 is environmentally the best option among the five plants considered (**Figure 4**), largely because it does not use maize silage as a feedstock. The exceptions to this are the MAETP and TETP for which Plant 1 is slightly better because these impacts are not affected

by maize silage (as discussed further below). Plant 1 is also the second best option for all other impacts apart from GWP and POCP, for which Plant 2 is better because of the lower methane emissions from digestate.

The differences in the impacts for Plants 2 and 4, which are fed with approximately the same amount of maize silage, are due to the differences in the digestate emissions and the capacities of the AD and CHP plants.

Despite the highest biogas production, Plant 3 is the worst option across all the impact categories because of the maize ear silage, which has impacts twice as high as maize silage owing to its lower yield (Table S2 in Supplementary Material). The exceptions to this are GWP and POCP, for which Plant 4 is worst because of the higher net methane emissions (**Table 3**).

The following sections discuss in more detail the impacts from the different plants (Figure 4) and the contributions of different life cycle stages (Figures 5A–E).

Abiotic Depletion Potential (ADP Elements and ADP Fossil)

Abiotic depletion of elements and fossil resources range from 142 to 243 mg Sb eq./MWh and from 1010 to 1570 MJ/MWh, respectively, with Plant 5 being the best and Plant 3 the worst option for both impacts.

As indicated in Figures 5A–D, the depletion of elements for Plants 1–4 is mainly due to the cultivation of maize and is associated with the materials used for agricultural machinery. For Plant 5, on the other hand, the major contributors are construction materials for the AD and CHP plants (Figure 5E); the latter is also a hotspot for Plant 1. This is due to economies of scale: they have smaller CHP plants and thus a higher consumption of resources per megawatt hour electricity generated.

As also shown in Figures 5A–D, the major contributors to fossil depletion for Plants 1–4 are the fuel used in the agricultural machinery for maize cultivation and the electricity for the AD plants. For Plant 5, the grid electricity used to operate the AD plant accounts for the majority of this impact (Figure 5E).

Acidification and Eutrophication Potentials

The estimated AP varies from 2.6 to 5.5 kg SO₂ eq./MWh and EP from 0.2 to 1.9 kg PO₄ eq./MWh. As for ADP, biogas electricity generated by Plant 5 is the best and by Plant 3 the worst option for these two impacts. For Plants 1–4, maize cultivation is responsible for the large majority of AP and EP (Figure 5A–D), whereas for Plant 5 (Figure 5E), it is the ammonia emitted during

the digestate storage as well as the emissions of acid gases and nutrients in the life cycle of the grid electricity used for AD.

Global Warming Potential (GWP₁₀₀ years)

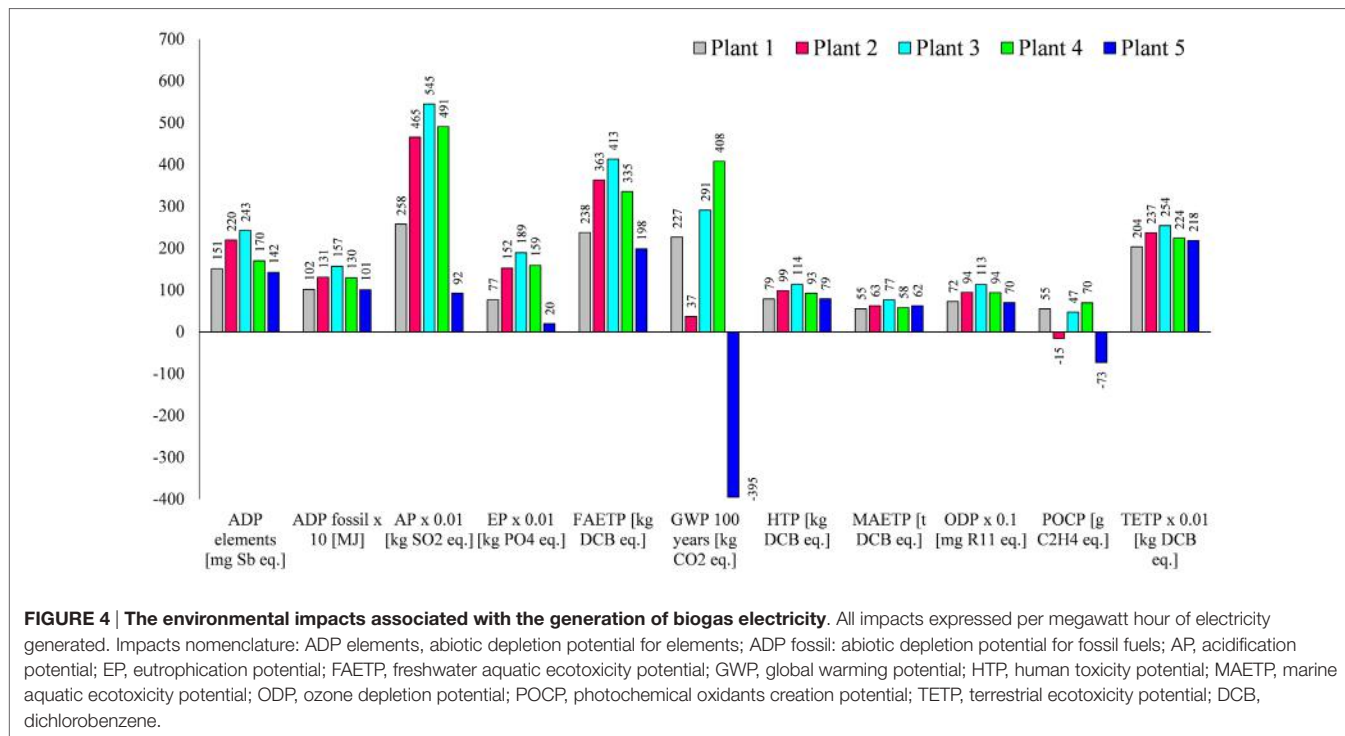
The values for GWP range from -395 to 408 kg CO₂ eq./MWh, with electricity from Plant 5 being the best option and from Plant 4 the worst. The vast majority of GWP (64%) is due to methane emissions from the digestate during its storage. For Plant 2, GWP is mainly from the maize silage (Figure 5B). The negative contributions shown in the figure are due to the methane credits for the avoidance of the traditional slurry management, as described in Section “Digestate Use and Methane Emissions Credits.” For Plant 5, the methane credits are higher than the methane emissions from the digestate, leading to a negative impact of -395 kg CO₂ eq./MWh (Figure 5E). Note that carbon dioxide emissions from biogas combustion in the CHP plant are not considered as they are biogenic in nature.

Human Toxicity Potential

This impact is lowest for electricity generated by Plants 1 and 5 [79 kg dichlorobenzene (DCB) eq./MWh] and highest for Plant 3 (114 kg DCB eq./MWh). For Plants 1–4, the main contributor is the production of maize silage and the emissions from biogas combustion, in particular chromium and thallium (see Table 3). For Plant 5, HTP is mainly affected by CHP operation, followed by AD operation and plant construction (Figure 5E).

Ecotoxicity Potentials (FAETP, MAETP, and TETP)

The lowest FAETP is estimated for Plant 1 (198 kg DCB eq./MWh) and the highest for Plant 3 (413 kg DCB eq./MWh). The



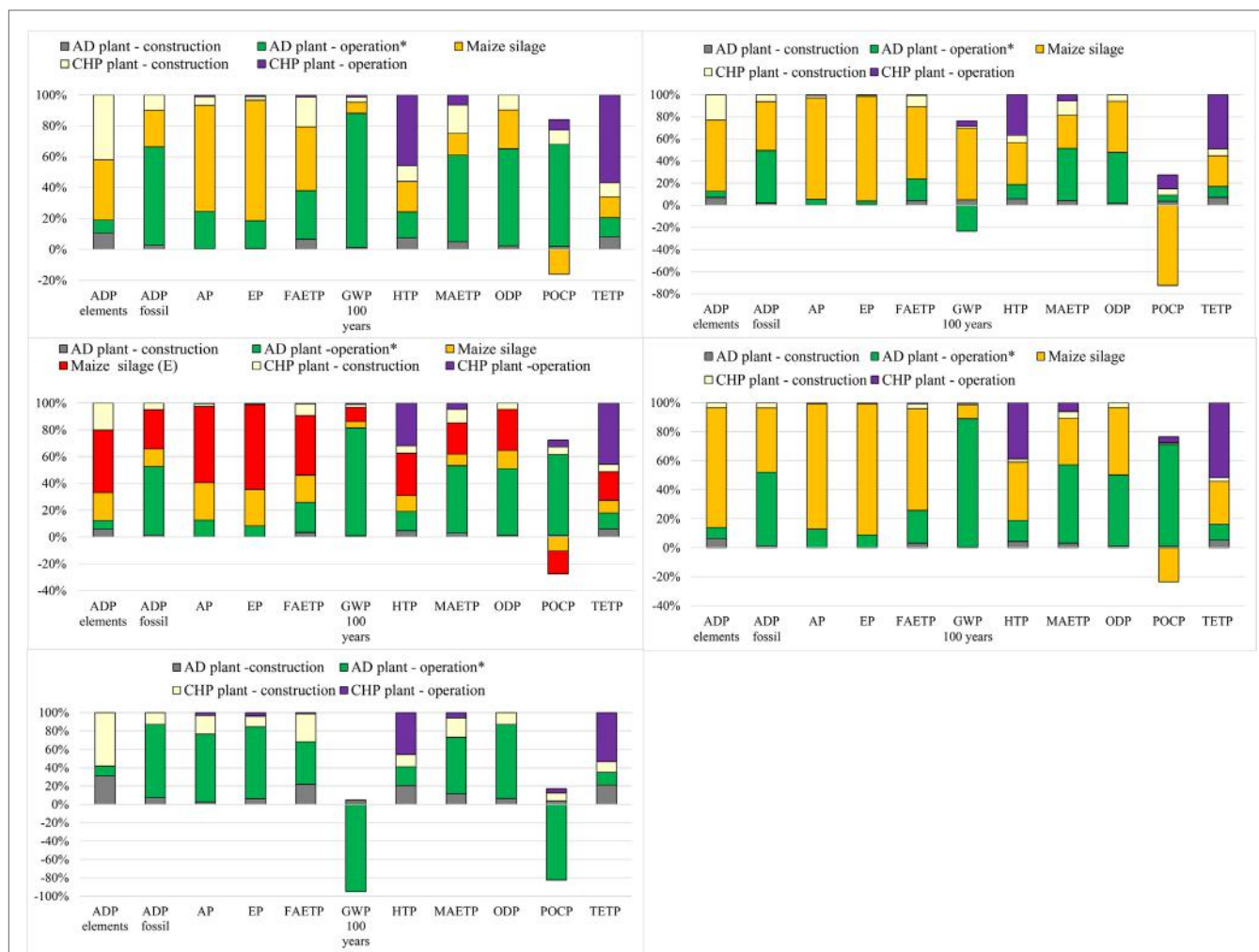


FIGURE 5 | Contribution analysis for different AD-CHP plants. (A) Plant 1 (top left); **(B)** Plant 2 (top right); **(C)** Plant 3 (middle left); **(D)** Plant 4 (middle right); **(E)** Plant 5 (bottom). AD plant – operation* includes grid electricity used for AD, methane losses during AD and emissions associated with digestate storage. Maize silage (**E**) maize ear silage. For impacts nomenclature, see figure. For the feedstocks, see **Table 2**. Negative values represent the credits for the avoidance of methane emissions by using digestate as fertilizer instead of animal slurry.

production of maize silage and the plant operation are the main contributors to this impact for Plants 1–4. This is mainly due to the emissions of pesticide used for maize cultivation (**Table 3**) and metals (nickel, beryllium, cobalt, and vanadium) emitted in the life cycle of the grid electricity. It can be noted that Plant 1 has lower MAETP and TETP, which is due to the efficiency associated with economies of scale as these impacts are mainly influenced by the plant operation (**Figures 5A,E**).

Unlike HTP, the best option for MAETP is Plant 5 at 55 ton DCB eq./MWh but, as for HTP, Plant 3 has the highest impact (77 ton DCB eq./MWh). The main hotspot is grid electricity used for AD because of the emissions of beryllium and hydrogen fluoride in the life cycle of electricity generation.

The same trend is found for TETP, with Plant 5 being the best option (2 kg DCB eq./MWh) and Plant 3 the worst (2.5 kg DCB eq./MWh). Maize silage and CHP operation are the main contributors to TETP for Plants 1–4. Like HTP, the latter is mainly

due to the emissions of chromium and thallium from biogas combustion. For Plant 5, CHP operation is the main hotspot (biogas combustion), followed by AD operation and plant construction.

Ozone Layer Depletion Potential

At 7 mg R11 eq./MWh, Plant 5 has the lowest ODP and, as for most other impacts, Plant 3 the highest (11.3 mg R11 eq./MWh). The main contributors are halons emitted in the life cycle of grid electricity used in AD (related to natural gas transportation), followed by the emissions from diesel used in the machinery during maize cultivation (Plants 1–4).

Photochemical Oxidants Creation Potential

The POCP ranges from −73 g C₂H₄ eq./MWh for Plant 5 to 70 g C₂H₄ eq./MWh for Plant 3. For Plants 1, 3, and 4, the impact is

largely due to the emissions of methane from the digestate and the methane losses from the AD plant. The negative contributions (**Figure 5**) are due to two reasons: first, according to the CML 2001 method, nitrogen oxides emitted during the cultivation of maize reduce POCP (Plants 1–4); and second, because of the methane credits (Plant 5).

Comparison with Alternative Electricity Sources

The biogas electricity is compared to electricity from the grid, natural gas, and renewables in **Figure 6** and the ranking of different options with respect to each impact is summarized in the heat map in **Figure 7**.

As can be seen in **Figure 6**, grid electricity has higher impacts than electricity from biogas for seven out of 11 categories: ADP fossil, FAETP, GWP, HTP, MAETP, ODP, and POCP. This is mainly due to the high contribution of fossil fuels in the Italian electricity mix. An exception to this is Plant 3 which has a higher HTP than the grid because of the toxic emissions in the life cycle of maize ear silage.

Electricity from the grid also has lower AP (by 10–57%) and EP (32–72%) than biogas electricity; this is due to maize cultivation which contributes significantly to these two impacts (see **Figure 5**). The exception to this is Plant 5 which has lower impacts than grid electricity (by ~60%) because it does not use maize silage.

Two further impacts are lower for grid electricity: depletion of elements and TETP. This could be explained by the greater economies of scale of the plants on the grid, which require a lower amount of resources and thus have lower toxic emissions on a life cycle basis per unit of electricity generated than the agricultural machinery and the AD-CHP plants.

Unlike grid electricity, electricity from natural gas is environmentally more sustainable than biogas for most categories, except ADP fossil, GWP, ODP, and POCP (**Figure 6**). In comparison to the renewables, biogas electricity has mostly higher impacts, with a few exceptions. For example, biogas has a lower AP than geothermal power across all the AD-CHP plants considered. Furthermore, Plant 5 has lower GWP and Plant 2 lower POCP than any other renewable option. Biogas is also better than solar PV in terms of ADP, elements, HTP, FAETP, MAETP, ODP, and

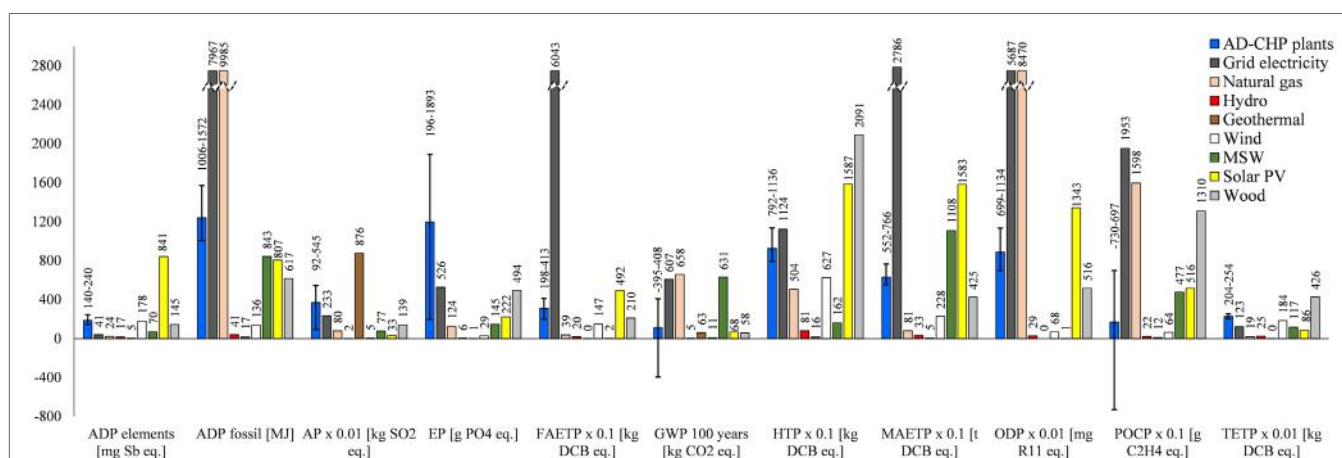


FIGURE 6 | Comparison of biogas electricity with the alternatives. All impacts expressed per megawatt hour of electricity. For the AD-CHP plants, the average results are shown, with the error bars representing the impacts ranges for different plants. For impacts nomenclature, see **Figure 5**. MSW, municipal solid waste; wood, wood chips in a CHP plant.

	Plant 1	Plant 2	Plant 3	Plant 4	Plant 5	Grid electricity	Natural gas	Hydro	Geothermal	Wind	MSW	Wood	Solar PV
ADP elements	2%	3%	2%	3%	2%	0.5%	0.3%	0.2%	0.1%	2%	1%	2%	100%
ADP fossil	10%	13%	13%	16%	10%	80%	100%	0.4%	0.2%	1%	8%	6%	8%
AP	29%	53%	56%	62%	11%	27%	9%	0.2%	100%	1%	9%	16%	4%
EP	41%	81%	84%	100%	10%	28%	7%	0.3%	0.1%	2%	8%	26%	12%
FAETP	4%	6%	6%	7%	3%	100%	1%	0.3%	0%	2%	0%	3%	8%
GWP 100 years	34%	6%	62%	44%	-60%	92%	100%	1%	10%	2%	96%	9%	10%
HTP	38%	47%	44%	54%	38%	54%	24%	4%	1%	30%	8%	100%	76%
MAETP	20%	23%	21%	27%	22%	100%	3%	1%	0.2%	8%	40%	15%	57%
ODP	9%	11%	11%	13%	8%	67%	100%	0.3%	0%	1%	0%	6%	16%
POCP	28%	-8%	36%	24%	-37%	100%	82%	1%	1%	3%	24%	67%	26%
TETP	48%	56%	53%	60%	51%	29%	5%	6%	0%	43%	27%	100%	20%

FIGURE 7 | Heat map of environmental impacts from biogas electricity and the alternatives considered in this study. The worst option is set at 100% and the others are expressed as a percentage of impact relative to the worst option. Waste, municipal solid waste; MSW, municipal solid waste; wood, wood chips in a CHP plant; solar PV, solar photovoltaics. For impacts nomenclature, see **Figure 5**.

POCP. It also has a lower MAETP than electricity from municipal solid waste and it outperforms wood for HTP, POCP, and TETP.

With a specific reference to GWP, the main driver for biogas production, Plant 5 is the best option overall, sequestering 395 kg CO₂ eq./MWh. All other plants generate higher GHG emissions than any of the renewable options considered here. The only other impact for which biogas electricity is a better option than any other is POCP, but again only for Plant 5; however, this plant has the highest TETP than any other alternative.

These results are summarized in **Figure 7**, which shows the percentage difference between the worst option and the rest of the alternatives for each impact. Overall, assuming equal importance of all the impacts, hydropower could be considered the best option and grid electricity the worst, with biogas being on average a middle-ranking option.

Comparison with Other Studies

As discussed in the Section “Introduction,” comparison of the results from different studies is not easy for the reasons outlined there. The only studies for which comparison is possible are those by Blengini et al. (2011), Dressler et al. (2012), Meyer-Aurich et al. (2012), Bacenetti et al. (2013), Whiting and Azapagic (2014), and Ingrao et al. (2015); for a summary of these studies, see **Table 1**.

As can be inferred from **Figure 8**, the results from the current study compare favorably in terms of AP, EP, GWP, and POCP, given the different assumptions, system credits, and geographical locations across the studies. However, the average GWP estimated in this work appears to be lower than in the other studies, mainly because of Plant 5 which has a negative value for this impact. Nevertheless, the impact for the AD-CHP system using pig slurry reported by Bacenetti et al. (2013) compares well with Plant 5 which uses cow slurry (−368 and −395 kg CO₂ eq./MWh, respectively). The GWP in Blengini et al. (2011) is consistent with that estimated for Plant 4, while the values found

by Dressler et al. (2012), Meyer-Aurich et al. (2012), Bacenetti et al. (2013), and Ingrao et al. (2015) agree well with the results for Plants 1 and 3. It should be noted that, unlike other studies, Meyer-Aurich et al. (2012) have considered land-use change (associated with maize cultivation), finding that it increases GWP by 20%; however, differences in other assumptions cancel out this effect and, consequently, the results still agree with those in the current study.

The comparison of the other impacts is only possible with the study by Whiting and Azapagic (2014), since the other authors did not consider them. As can be seen in **Figure 8**, the results agree for HTP but differ for ADP, FAETP, MAETP, ODP, and TETP. The reason for these differences could be due to the different updates of the CML method and Gabi software, as well as the different assumptions, credits for fertilizers, and geographical locations. On the other hand, both studies are in agreement that the contribution of the AD and CHP plants construction is significant for ADP elements and the toxicity-related impacts.

Sensitivity Analysis

Because of their significant contribution to the impacts, the following parameters are considered in the sensitivity analysis:

- (i) maize yield;
- (ii) heat utilization;
- (iii) recycling of AD and CHP construction materials; and
- (iv) covered storage of digestate in Plant 4.

The results are discussed in the following sections.

Maize Yield

To explore the effect of this parameter on the impacts, the maize yield was varied by ±15% against the baseline shown in Table S2 in Supplementary Material. The results in **Figure 9** suggest that the overall effect of maize yield on the environmental impacts is

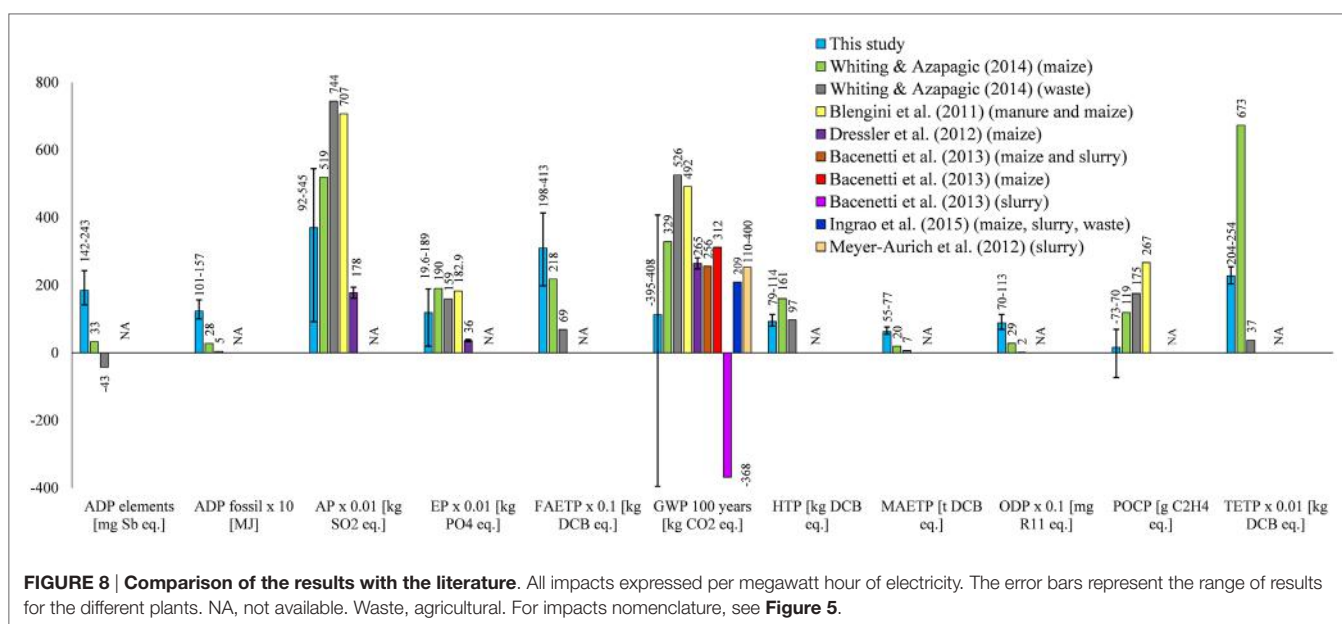


FIGURE 8 | Comparison of the results with the literature. All impacts expressed per megawatt hour of electricity. The error bars represent the range of results for the different plants. NA, not available. Waste, agricultural. For impacts nomenclature, see **Figure 5**.

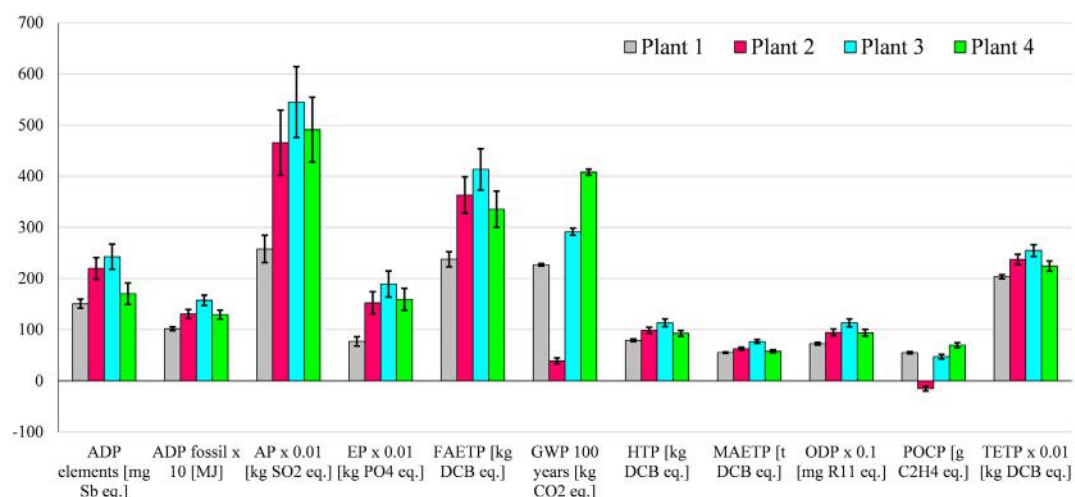


FIGURE 9 | Sensitivity analysis assuming different maize yields for biogas produced in Plants 1–4. All impacts expressed per megawatt hour of electricity. The height of the columns corresponds to the yield indicated in Table S2 in Supplementary Material. The error bars refer to the yield variation of $\pm 15\%$. For impacts nomenclature, see **Figure 5**.

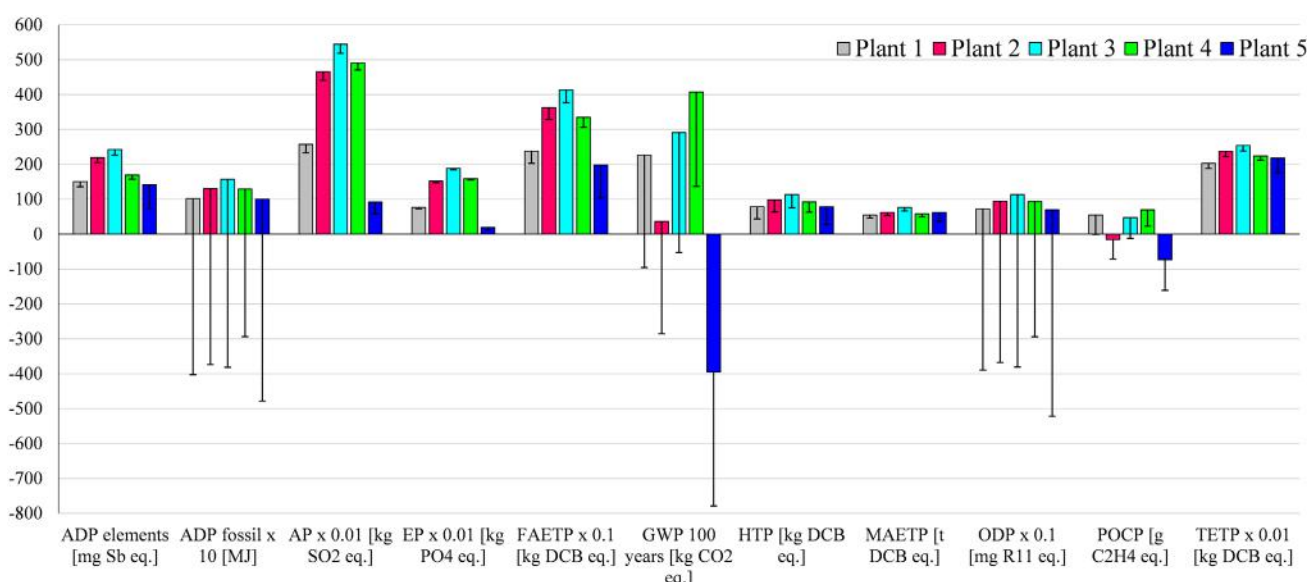


FIGURE 10 | Sensitivity analysis assuming the net heat produced is used and substitutes a gas boiler. All impacts expressed per megawatt hour of electricity. Capacity of boiler: >100 kW for Plants 1–4 and <100 kW for Plant 5. For impacts nomenclature, see **Figure 5**.

small for most impacts, except for AP and EP which change by up to 14%. This is to be expected given the high contribution of maize cultivation to these categories.

The ADP elements and FAETP results are also affected for Plant 4, varying by up to 12%, because of the change in the resource requirements for the agricultural machinery and the related toxicity of the construction materials. Despite these changes, the variation in the maize yield considered here does not affect the comparison of biogas with the alternative electricity sources discussed in Section “Comparison with Alternative Electricity Sources.”

Heat Utilization

This part of the sensitivity analysis considers a scenario in which the net heat produced by the CHP plants is used instead of being wasted. This is motivated by the introduction of subsidies for heat (see Introduction), which aim to stimulate its utilization. It was assumed that the heat generated by the CHP substitutes a gas boiler for which the AD-CHP systems were credited. The LCA data for the boiler were sourced from Ecoinvent (2010).

As indicated in **Figure 10**, if the heat were utilized all of the impacts would be reduced, some of them significantly, across the

different plants: ADP fossil would be lower by four to six times, GWP up to nine times, ODP by five to eight times, and POCP two to four times. This means that biogas electricity from all five plants would have lower impacts for these categories than any other renewable option considered here. However, there would be no change in ranking with respect to grid electricity because ADP elements, AP, EP, and TETP remain higher for biogas electricity.

Recycling of Construction Materials

As mentioned earlier, it was assumed that all the construction materials apart from plastics are landfilled after decommissioning of the plants. Since the construction of the plants has a significant contribution for some impacts, particularly for Plants 1 and 5 (Figures 5A,E), the sensitivity analysis considers if and how they would change if concrete, steel, iron, and platinum (in the CHP catalytic converter) were recycled. For these purposes,

the recycling rates for the former three materials were assumed equal to current recycling rates in Italy: 60% for concrete (UNI, 2005) and 74% for steel and iron (Fondazione per lo sviluppo sostenibile, 2012). As there are no data for platinum recycling, a recovery rate of 90% was assumed. Plastic materials were not considered for recycling as their quantity is small.

The results are presented in Figure 11 for the impacts that are affected by the recycling. The greatest reduction would be achieved for ADP elements (up to 39%) and POCP (up to 13.5%), followed by AP and FAETP (~8%); MAETP would also go down (~5%). The effect on the other impacts is small (<2%).

Covered Storage of Digestate

As discussed in Section “Results,” biogas electricity from Plant 4, which uses maize silage as the AD feedstock, has higher GWP and POCP than any other plant. Given that much of that is due to methane emissions from the open storage of digestate

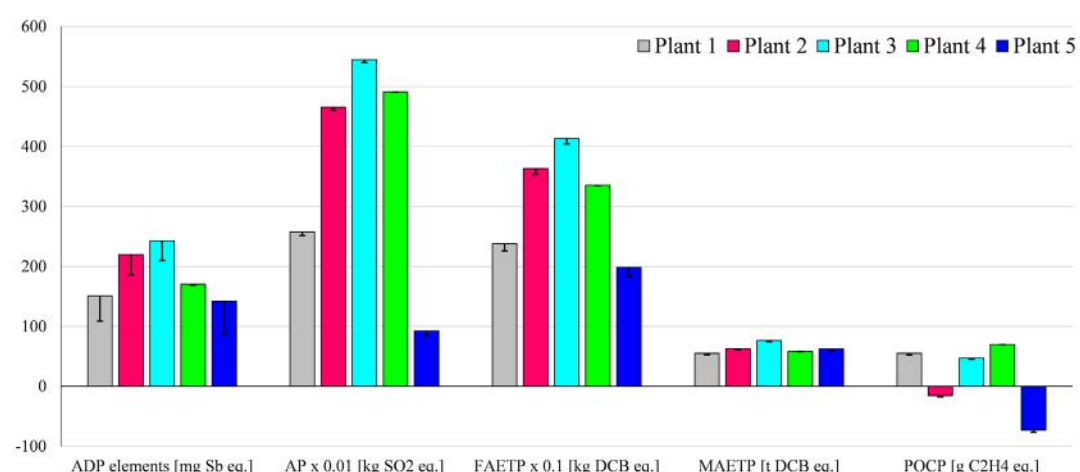


FIGURE 11 | Sensitivity analysis assuming recycling of construction materials. For impacts nomenclature, see Figure 5.

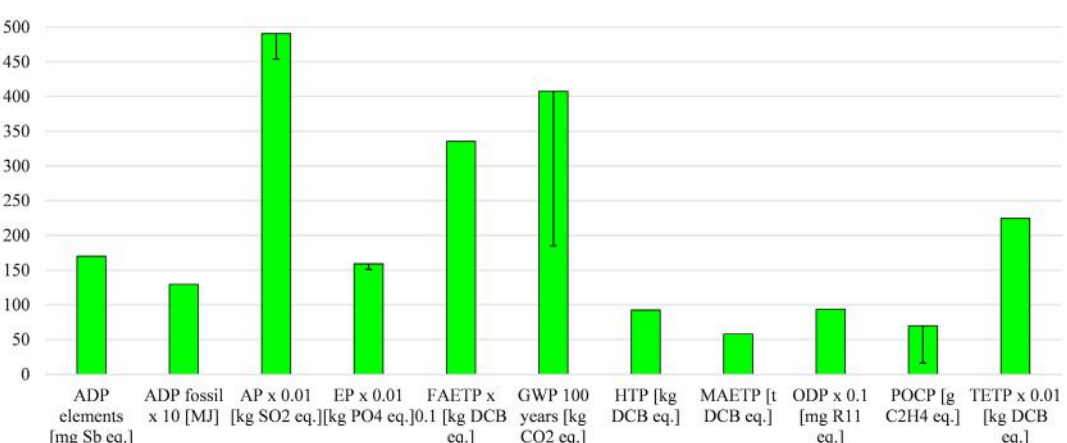


FIGURE 12 | Sensitivity analysis assuming the covered storage of digestate in Plant 4. All impacts expressed per megawatt hour of electricity. For impacts nomenclature, see Figure 5.

(**Figure 5D**), it is important to consider by how much the impacts would change if the digestate were stored in covered tanks, as in Plant 2.

The results in **Figure 12** suggest that both impacts would decrease significantly: GWP by two times and POCP threefold. In that case, Plant 4 would have lower impacts than Plant 1 and 3 but still higher than Plant 2. The AP and EP results would also be reduced, by 7 and 5%, respectively, because of the avoided ammonia emissions. This would make Plant 4 a better option than Plant 2 for these two impacts.

With respect to grid electricity, Plant 4 would have half the GWP. It would also be a better option for POCP with respect to solar PV and waste power plants.

CONCLUSION

The aim of this study was to evaluate the life cycle environmental impacts associated with generation of electricity from biogas produced by AD of agricultural products and waste. Five real AD-CHP plants situated in Italy were considered and compared to electricity from the national grid, natural gas, and different renewable technologies.

The results suggest that the main contributors to the impacts from biogas electricity are the production of the maize silage and the operation of the anaerobic digester, including open storage of digestate. Therefore, the system using animal slurry (Plant 5) is the best option among the five plants considered, except for marine and terrestrial ecotoxicity potentials for which the best system is the one utilizing slurry, agricultural waste, and a small amount of maize silage (Plant 1). The plant fed with maize ear silage (Plant 3) is the worst option because of the high impacts of the feedstock, which are almost double that of maize silage.

In reference to the size of AD-CHP plants, larger capacity does not appear to have a positive effect on environmental impacts despite the higher efficiencies typically associated with economies of scale. This is due to the larger plants requiring a high organic load to make them viable, which can only be achieved with cereal feedstocks as they have much higher biogas yield than slurry or agricultural waste. For example, a 1 MW CHP plant requires around 50 ton of maize silage per day but 400–800 ton of slurry. As this amount of slurry cannot be supplied by a single farm, it would have to be collected from different farms and transported to the plant which would not be economically and environmentally viable. Furthermore, the digester would be impractically large (20,000–40,000 m³ assuming a hydraulic retention time of 50 days) and thus expensive. Therefore, as the results of this work suggest, it is better to have smaller plants using slurry and waste rather than bigger installations: the latter may be more efficient but require cereal silage, which in turn leads to higher environmental impacts. On the other hand, smaller plants require more resources for construction per unit of electricity generated, so there are some trade-offs.

The results also suggest that utilizing the heat generated by the CHP plant would reduce all the impacts, some of them significantly (specifically depletion of fossil fuels and the ozone layer, global warming, and summer smog), making biogas electricity a

better option for these categories than any other renewable alternatives considered here. Recycling the AD and CHP construction materials would reduce the depletion of elements, acidification, freshwater, and marine toxicity as well as summer smog. The latter would also improve in addition to global warming if digestate was stored in covered tanks.

Biogas electricity is environmentally more sustainable than electricity from the grid for seven out of 11 impacts considered. This is due to the high contribution of fossil fuels in the Italian electricity mix. The remaining four impacts, for which grid electricity is a better option, are depletion of elements, acidification, eutrophication, and terrestrial ecotoxicity. Thus, biogas electricity reduces GHG emissions compared to the grid, as intended by government and the European Commission, but aggravates some other impacts.

However, in comparison with natural gas, seven out of 11 impacts are higher for electricity from biogas. It also has mostly higher impacts than the renewables, except for solar PV for which six out of 11 impacts are higher than biogas. Furthermore, biogas is a better option than geothermal power for acidification across all the feedstocks considered. If only slurry is used (Plant 5), it also has lower global warming and summer smog potentials than geothermal. Moreover, marine ecotoxicity is greater for electricity from municipal solid waste than that from biogas.

Focusing on global warming potential which drives biogas production, using slurry as a feedstock (Plant 5) is the best option across all the electricity options considered here, sequestering 395 kg CO₂ eq./MWh. All the other biogas systems generate higher greenhouse emissions than any of the renewable options considered here. The only other impact for which biogas electricity is a better option than any other is summer smog, but only for the slurry feedstock; however, it also has higher terrestrial ecotoxicity than any other electricity alternative.

In summary, biogas electricity can help reduce GHG emissions relative to fossil-intensive grid electricity such as that of Italy; however, some other impacts are increased. On the other hand, if mitigation of climate change is the main aim, then other renewables have a greater potential to reduce GHG emissions. If, in addition to this, other impacts are considered, then hydro, wind, and geothermal power are better alternatives to biogas. However, if the subsidies for heat utilization are successful, the environmental sustainability of biogas electricity would improve significantly, particularly for global warming, summer smog, and depletion of the ozone layer and abiotic resources. Further policy changes should include a ban on open digestate storage to prevent methane emissions and regulation on digestate spreading on land to minimize emissions of ammonia and related environmental impacts.

Finally, it should be noted that the results obtained in this study correspond to mesophilic digestion at 40°C and may differ from the results for other operating conditions. Furthermore, the analysis did not consider other environmental aspects, such as habitat destruction and biodiversity loss, as they are outside the scope of LCA. These and other impacts could be evaluated in future research alongside economic costs and social impacts as part of a broader sustainability assessment.

AUTHOR CONTRIBUTIONS

AA and MF conceived and supervised the work; JB collected the data; AF carried out the LCA study; AA, AF, and JB wrote the paper.

ACKNOWLEDGMENTS

This work was funded by the UK Engineering and Physical Sciences Research Council (EPSRC), grant no. EP/K011820/1. This funding is gratefully acknowledged. The authors are also

REFERENCES

- Amon, B., Kryvoruchko, V., Amon, T., and Zechmeister-Boltenstern, S. (2006). Methane, nitrous oxide and ammonia emissions during storage and after application of dairy cattle slurry and influence of slurry treatment. *Agric. Ecosyst. Environ.* 112, 153–162. doi:10.1016/j.agee.2005.08.030
- Audsley, E. (1997). *Harmonization of Environmental Life Cycle Assessment for Agriculture*. European Commission DG VI Agriculture. Silsoe: Silsoe Research Institute.
- Bacenetti, J., Duca, D., Fusi, A., Negri, M., and Fiala, M. (2015). Mitigation strategies in the agro-food sector: the anaerobic digestion of tomato puree by-products. An Italian case study. *Sci. Total Environ.* 526, 88–97. doi:10.1016/j.scitotenv.2015.04.069
- Bacenetti, J., and Fiala, M. (2015). Carbon footprint of electricity from anaerobic digestion plants in Italy. *Environ. Eng. Manag. J.* 14, 1495–1502.
- Bacenetti, J., Negri, M., Fiala, M., and Gonzalez Garcia, S. (2013). Anaerobic digestion of different feedstock: impact on energetic and environmental balances of biogas process. *Sci. Total Environ.* 46, 541–551. doi:10.1016/j.scitotenv.2013.06.058
- Bengini, G. A., Brizio, E., Cibrario, M., and Genon, G. (2011). LCA of bioenergy chains in Piedmont (Italy): a case study to support public decision makers towards sustainability. *Resour. Conserv. Recycl.* 57, 36–47. doi:10.1016/j.resconrec.2011.10.003
- Bodria, L., Pellizzi, G., and Piccarolo, P. (2006). *Il trattore e le macchine operatrici*. Bologna: Ed. Edagricole.
- Boschiero, M., Kelderer, M., and Zerbe, S. (2014). “Handling agricultural residues in LCAs – a case study on woodchips from apple orchards in South Tyrol,” in *Proceedings Convegno della Rete Italiana LCA*, Florence.
- Brentrup, F., Küsters, J., Lammel, J., and Kuhlmann, H. (2000). Methods to estimate on-field nitrogen emissions from crop production as an input to LCA studies in the agricultural sector. *Int. J. Life Cycle Assess.* 5, 349–357. doi:10.1007/BF02978670
- Brizzo, F. (2015). Biogas: l’Italia è terzo produttore al mondo dopo Germania e Cina. *La Stampa*. Available at: www.lastampa.it/2015/02/01/scienza/ambiente/focus/biogas-litalia-terzo-produttore-al-mondo-dopo-germania-e-cina-OS-jLZIsghgUmMloNF7mxIN/pagina.html
- Casati, D. (2011). Le superfici possono ricominciare a salire. *Terra e Vita* 35, 40–46.
- Cellura, M., Ardente, F., and Longo, S. (2012). From the LCA of food products to the environmental assessment of protected crops districts: a case-study in the south of Italy. *J. Environ. Manag.* 93, 194–208. doi:10.1016/j.jenvman.2011.08.019
- Chen, S., Chen, B., and Song, D. (2012). Life-cycle energy production and emissions mitigation by comprehensive biogas-digestate utilization. *Bioresour. Technol.* 114, 357–64. doi:10.1016/j.biortech.2012.03.084
- Coulson, J. M., Richardson, J. F., and Sinnott, R. K. (1993). *Chemical Engineering*. Oxford: Butterworth-Heinemann.
- Curran, A. M. (2012). *Life Cycle Assessment Handbook: A Guide for Environmentally Sustainable Products*. New Jersey: John Wiley & Sons and Scrivener Publishing.
- De Vries, J. W., Corré, W. J., and Dooren, H. J. (2010). *Environmental Assessment of Untreated Manure Use, Manure Digestion and Co-Digestion with Silage Maize*. Wageningen: Wageningen UR Livestock Research.
- De Vries, J. W., Vinken, T. M. W. J., Hamelin, L., and De Boer, I. J. M. (2012). Comparing environmental consequences of anaerobic mono- and co-digestion of pig manure to produce bio-energy e a life cycle perspective. *Bioresour. Technol.* 125, 239–248. doi:10.1016/j.biortech.2012.08.124
- Dressler, D., Loewen, A., and Nelles, M. (2012). Life cycle assessment of the supply and use of bioenergy: impact of regional factors on biogas production. *Int. J. Life Cycle Assess.* 17, 1104–1115. doi:10.1007/s11367-012-0424-9
- Ebner, J. H., Rodrigo, A., Labatut, R. A., Rankin, M. J., Pronto, J. L., Gooch, C. A., et al. (2015). Lifecycle greenhouse gas analysis of an anaerobic codigestion facility. *Environ. Sci. Technol.* 49, 199–208. doi:10.1021/acs.est.5b01331
- EC. (2009). *Directive 2009/28/EC, Promotion of the Use of Energy from Renewable Sources*. Luxembourg: Office for Official Publications of the European Communities.
- Ecoinvent. (2010). *Ecoinvent Database v2.2*. Zurich; Lausanne: Ecoinvent.
- Edelmann, W., Schleiss, K., Engeli, H., and Baier, U. (2011). *Ökobilanz der stromgewinnung aus landwirtschaftlichem Biogas*. Bundesamt für Energie. Available at: <http://www.halfin.ch/Biogas/Dokumente/oekobilanz%20landwirtschaft.pdf>
- EMEP/EEA. (2013). *Agriculture Other (Use of Pesticides and Limestone)*. Air Pollutant Emission Inventory Guidebook 2013. Technical Report, No. 12/2013. Copenhagen: European Environment Agency.
- EurObserv'ER. (2014). *EurObserv'ER – Etat des énergies renouvelables en Europe Observ'ER*. Paris. Available at: http://www.energies-renouvelables.org/observ'er/stat_baro/barobilan/barobilan14_FR.pdf
- Falcone, G., Strano, A., Stillitano, T., De Luca, A., Iofrida, N., and Gulisano, G. (2015). Integrated sustainability appraisal of wine-growing management systems through LCA and LCC methodologies. *Chem. Eng. Trans.* 44, 223–228. doi:10.3303/CET1544038
- Fantin, V., Rondini, I., Righi, S., Pasteris, A., Coatti, F., Passerini, F., et al. (2015). “Environmental assessment of wheat and maize production in an Italian farmers cooperative,” in *Proceedings International Conference LCA for Feeding the Planet and Energy for Life*, Stresa.
- Fiala, M. (2012). *Energia da biomasse*. Santarcangelo di Romagna: Maggioli Editore.
- Fondazione per lo sviluppo sostenibile. (2012). *Approfondimenti settoriali dedicati alle singole filiere del riciclo e recupero*. Available at: <http://www.fondazionesvilupposostenibile.org/>
- Fuchs, M., and Kohlheb, N. (2015). Comparison of the environmental effects of manure- and crop-based agricultural biogas plants using life cycle analysis. *J. Clean. Prod.* 86, 60–66. doi:10.1016/j.jclepro.2014.08.058
- Goedkoop, M., and Spriensma, R. (2001). *The Eco-Indicator 99: A Damage Oriented Method for Life Cycle Assessment. Methodology Report*, 3rd Edn. Amersfoort: Pré Consultants.
- Goedkoop, M. J., Heijungs, R., Huijbregts, M., De Schryver, A., Struijs, J., and Van Zelm, R. (2009). *ReCiPe 2008, A Life Cycle Impact Assessment Method Which Comprises Harmonised Category Indicators at the Midpoint and the Endpoint Level, 1st ed. Report I: Characterisation*. Available at: www.cia-recipe.net
- Guinée, J. B., Gorreé, M., Heijungs, R., Huppes, G., Kleijn, R., Koning, A., et al. (2002). *Handbook on Life Cycle Assessment. Operational Guide to the ISO Standards. I: LCA in Perspective. II: Guide. III: Operational Annex. IV: Scientific Background*. Dordrecht: Kluwer Academic Publishers, 692.
- IEA (International Energy Agency). (2011). *OECD – Electricity and Heat Generation. Electricity Information Statistics (Database)*. Available at: <http://www.oecd-ilibrary.org/energy/>
- Ingrao, C., Rana, R., Tricase, C., and Lombardi, M. (2015). Application of carbon footprint to an agro-biogas supply chain in Southern Italy. *Appl. Energy* 149, 75–88. doi:10.1016/j.apenergy.2015.03.111
- IPCC. (2006). *Agriculture, Forestry and Other Land Use: IPCC Guidelines for National Greenhouse Gas Inventories*. Cambridge: Cambridge University Press.

grateful to the editor and the reviewers for their comments that helped to improve the paper. We would also like to thank Dr. Laurence Stamford and Ellen Gleeson at the University of Manchester for proofreading the manuscript and Dr. Martyn Jones, also at Manchester, for his assistance with the figures.

SUPPLEMENTARY MATERIAL

The Supplementary Material for this article can be found online at <http://journal.frontiersin.org/article/10.3389/fbioe.2016.00026>

- IPCC. (2007). *Climate Change 2007: The Physical Science Basis. Contribution of Working Group I to the Fourth Assessment Report of the Intergovernmental Panel on Climate Change*. Cambridge: Cambridge University Press.
- ISO. (2006a). *ISO 14040. Environmental Management – Life Cycle Assessment – Principles and Framework*. Geneva: International Organization for Standardization.
- ISO. (2006b). *ISO 14044. Environmental Management – Life Cycle Assessment – Requirements and Guidelines*. Geneva: International Organization for Standardization.
- Jin, Y., Chen, T., Chen, X., and Yu, Z. (2015). Life-cycle assessment of energy consumption and environmental impact of an integrated food waste-based biogas plant. *Appl. Energy* 151, 227–236. doi:10.1016/j.apenergy.2015.04.058
- Jury, C., Benetto, E., Koster, D., Schmitt, B., and Welfring, J. (2010). Life cycle assessment of biogas production by monofermentation of energy crops and injection into the natural gas grid. *Biomass Bioenergy* 34, 54–66. doi:10.1016/j.biombioe.2009.09.011
- Lansche, J., and Müller, J. (2012). Life cycle assessment of energy generation of biogas fed combined heat and power plants: environmental impact of different agricultural substrates. *Eng. Life Sci.* 12, 313–320. doi:10.1002/elsc.201100061
- Lijó, L., González-García, S., Bacenetti, J., Fiala, M., Feijoo, G., Lema, J. M., et al. (2014a). Life cycle assessment of electricity production in Italy from anaerobic co-digestion of pig slurry and energy crops. *Renew. Energy* 68, 625–635. doi:10.1016/j.renene.2014.03.005
- Lijó, L., González-García, S., Bacenetti, J., Fiala, M., Feijoo, G., and Moreira, M. T. (2014b). Assuring the sustainable production of biogas from anaerobic mono-digestion. *J. Clean. Prod.* 72, 23–34. doi:10.1016/j.jclepro.2014.03.022
- Lijó, L., González-García, S., Bacenetti, J., Negri, M., Fiala, M., Feijoo, G., et al. (2015). Environmental assessment of farm-scaled anaerobic co-digestion for bioenergy production. *Waste Manage.* 41, 50–59. doi:10.1016/j.wasman.2015.03.043
- Margni, M., Rossier, D., Crettaz, P., and Jolliet, O. (2002). Life cycle impact assessment of pesticides on human health and ecosystems. *Agric. Ecosyst. Environ.* 93, 379–392. doi:10.1016/S0167-8809(01)00336-X
- Meyer-Aurich, A., Schattauer, A., Hellebrand, H. J., Klauss, H., Plöchl, M., and Berga, W. (2012). Impact of uncertainties on greenhouse gas mitigation potential of biogas production from agricultural resources. *Renew. Energy* 37, 277–284. doi:10.1016/j.renene.2011.06.030
- Mezzullo, W., Manus, M., and Hammond, G. (2013). Life cycle assessment of a small-scale anaerobic digestion plant from cattle waste. *Appl. Energy* 102, 657–664. doi:10.1016/j.apenergy.2012.08.008
- Milà i Canals, L. (2007). *LCA Methodology and Modelling Considerations for Vegetable Production and Consumption. Working Paper 02/07*. Guildford: Centre for Environmental Strategy (CES), University of Surrey.
- Ministero dello Sviluppo Economico. (2012). *Decreto ministeriale 6 luglio 2012 – Incentivi per energia da fonti rinnovabili elettriche non fotovoltaiche*. Roma: Gazzetta Ufficiale della Repubblica Italiana.
- Morero, B., Groppelli, E., and Campanella, E. A. (2015). Life cycle assessment of biomethane use in Argentina. *Bioresour. Technol.* 182, 208–216. doi:10.1016/j.biortech.2015.01.077
- Negri, M., Bacenetti, J., Brambilla, M., Manfredini, A., Cantore, C., and Bocchi, S. (2014). Biomethane production from different crop systems of cereals in Northern Italy. *Biomass Bioenergy* 63, 321–329. doi:10.1016/j.biombioe.2014.01.041
- Nemecek, T., and Kägi, T. (2007). *Life Cycle Inventories of Agricultural Production Systems. Ecoinvent Report Version 2.0*, Vol. 15. Zurich: Swiss Centre for LCI, ART.
- NERI. (2010). *Emissions from Decentralized CHP Plants*. 113. Available at: <http://www2.dmu.dk/pub/FR786.pdf>
- NNFCC. (2015). *Anaerobic Digestion Deployment in the UK*. NNFCC. Available at: www.nnfcc.co.uk/tools/nnfcc-report-anaerobic-digestion-deployment-in-the-uk#sthash.pBZjWiVU.dpuf
- Olivier, J., Margni, M., Charles, R., Humbert, S., Payet, J., Rebitzer, G., et al. (2003). IMPACT 2002+: a new life cycle impact assessment methodology. *Int. J. Life Cycle Assess.* 8, 324–330. doi:10.1007/BF02978505
- Pacetti, T., Lombardi, L., and Federici, G. (2015). Water-energy nexus: a case of biogas production from energy crops evaluated by water footprint and life cycle assessment (LCA) methods. *J. Clean. Prod.* 101, 278–291. doi:10.1016/j.jclepro.2015.03.084
- Rodriguez-Verde, I., Regueiro, L., Carballa, M., Hospido, A., and Lema, J. M. (2014). Assessing anaerobic co-digestion of pig manure with agroindustrial wastes: the link between environmental impacts and operational parameters. *Sci. Total Environ.* 497, 475–483. doi:10.1016/j.scitotenv.2014.07.127
- Siduo, Z., Xiaotao, T. B., and Clift, R. (2015). Life cycle analysis of a biogas-centred integrated dairy farm-greenhouse system in British Columbia. *Process Saf. Environ. Prot.* 93, 18–30. doi:10.1016/j.psep.2014.02.017
- Styles, D., Gibbons, J., Williams, A. P., Stichnothe, H., Chadwick, D. R., and Healey, J. R. (2014). Cattle feed or bioenergy? Consequential life cycle assessment of biogas feedstock options on dairy farms. *Glob. Change Biol. Bioenergy* 7, 1034–1049. doi:10.1111/gcbb.12189
- Thinkstep. (2015). *Gabi Software-System and Database for Life Cycle Engineering*. Stuttgart: Thinkstep.
- UNI. (2005). *UNI 8520-1: 2005 Aggregati per calcestruzzo – Istruzioni complementari per l'applicazione della EN 12620 – Parte 1: Designazione e criteri di conformità*. Available at: www.uni.com/index.php
- Wang, Y., Dong, H., Liu, C., and Xin, H. (2014). Comparison of air emissions from raw liquid pig manure and biogas digester effluent storages. *Trans. ASABE* 57, 635–645. doi:10.13031/trans.57.10292
- Weiland, P. (2010). Biogas production: current state and perspectives. *Appl. Microbiol. Biotechnol.* 85, 849–860. doi:10.1007/s00253-009-2246-7
- Whiting, A., and Azapagic, A. (2014). Life cycle environmental impacts of generating electricity and heat from biogas produced by anaerobic digestion. *Energy* 70, 181–193. doi:10.1016/j.energy.2014.03.103
- Xu, C., Shi, W., Hong, J., Zhang, F., and Chen, W. (2015). Life cycle assessment of food waste-based biogas generation. *Renew. Sustain. Energy Rev.* 49, 169–177. doi:10.1016/j.rser.2015.04.164
- Zhang, L. X., Wang, C. B., and Song, B. (2013). Carbon emission reduction potential of a typical household biogas system in rural China. *J. Clean. Prod.* 47, 415–421. doi:10.1016/j.jclepro.2012.06.021

Conflict of Interest Statement: The authors declare that the research was conducted in the absence of any commercial or financial relationships that could be construed as a potential conflict of interest.

Copyright © 2016 Fusi, Bacenetti, Fiala and Azapagic. This is an open-access article distributed under the terms of the Creative Commons Attribution License (CC BY). The use, distribution or reproduction in other forums is permitted, provided the original author(s) or licensor are credited and that the original publication in this journal is cited, in accordance with accepted academic practice. No use, distribution or reproduction is permitted which does not comply with these terms.



Biological Phosphorus Removal During High-Rate, Low-Temperature, Anaerobic Digestion of Wastewater

Ciara Keating^{1*}, Jason P. Chin², Dermot Hughes¹, Panagiotis Manesiotis³, Denise Cysneiros^{1†}, Therese Mahony¹, Cindy J. Smith¹, John W. McGrath² and Vincent O'Flaherty^{1*}

¹ Microbial Ecology Laboratory, Microbiology, School of Natural Sciences and Ryan Institute, National University of Ireland Galway, Ireland, ² School of Biological Sciences and the Institute for Global Food Security, The Queen's University of Belfast, Belfast, UK, ³ School of Chemistry and Chemical Engineering, The Queen's University of Belfast, Belfast, UK

OPEN ACCESS

Edited by:

Cynthia Carlile-Marquet,
University of Birmingham, UK

Reviewed by:

Boonfei Tan,
Singapore-MIT Alliance for Research
and Technology, Singapore
Jimmy Roussel,
University of Birmingham, UK

*Correspondence:

Vincent O'Flaherty
vincent.oflaherty@nuigalway.ie;
Ciara Keating
ci.keating1@gmail.com

†Present address:

Denise Cysneiros,
Future Biogas, 10-12 Frederick
Sanger Road, Guildford, GU2 7YD,
UK

Specialty section:

This article was submitted to
Microbiotechnology, Ecotoxicology
and Bioremediation,
a section of the journal
Frontiers in Microbiology

Received: 15 November 2015

Accepted: 12 February 2016

Published: 03 March 2016

Citation:

Keating C, Chin JP, Hughes D,
Manesiotis P, Cysneiros D, Mahony T,
Smith CJ, McGrath JW
and O'Flaherty V (2016) Biological
Phosphorus Removal During
High-Rate, Low-Temperature,
Anaerobic Digestion of Wastewater.
Front. Microbiol. 7:226.
doi: 10.3389/fmicb.2016.00226

We report, for the first time, extensive biologically mediated phosphate removal from wastewater during high-rate anaerobic digestion (AD). A hybrid sludge bed/fixed-film (packed pumice stone) reactor was employed for low-temperature (12°C) anaerobic treatment of synthetic sewage wastewater. Successful phosphate removal from the wastewater (up to 78% of influent phosphate) was observed, mediated by biofilms in the reactor. Scanning electron microscopy and energy dispersive X-ray analysis revealed the accumulation of elemental phosphorus (~2%) within the sludge bed and fixed-film biofilms. 4', 6-diamidino-2-phenylindole (DAPI) staining indicated phosphorus accumulation was biological in nature and mediated through the formation of intracellular inorganic polyphosphate (polyP) granules within these biofilms. DAPI staining further indicated that polyP accumulation was rarely associated with free cells. Efficient and consistent chemical oxygen demand (COD) removal was recorded, throughout the 732-day trial, at applied organic loading rates between 0.4 and 1.5 kg COD m⁻³ d⁻¹ and hydraulic retention times of 8–24 h, while phosphate removal efficiency ranged from 28 to 78% on average per phase. Analysis of protein hydrolysis kinetics and the methanogenic activity profiles of the biomass revealed the development, at 12°C, of active hydrolytic and methanogenic populations. Temporal microbial changes were monitored using Illumina MiSeq analysis of bacterial and archaeal 16S rRNA gene sequences. The dominant bacterial phyla present in the biomass at the conclusion of the trial were the Proteobacteria and Firmicutes and the dominant archaeal genus was *Methanosaeta*. *Trichococcus* and *Flavobacterium* populations, previously associated with low temperature protein degradation, developed in the reactor biomass. The presence of previously characterized polyphosphate accumulating organisms (PAOs) such as *Rhodocyclus*, *Chromatiales*, *Actinobacter*, and *Acinetobacter* was recorded at low numbers. However, it is unknown as yet if these were responsible for the luxury polyP uptake observed in this system. The possibility of efficient phosphate removal and recovery from wastewater during AD would represent a major advance in the scope for widespread application of anaerobic wastewater treatment technologies.

Keywords: sewage, LtAD, microbial ecology and physiology, phosphate removal, hybrid reactor, psychrophilic

INTRODUCTION

High-rate anaerobic digestion (AD) wastewater treatment technologies provide low-cost and effective removal of pollutants, with many advantages over other catalytic processes, combined with the recovery of energy in the form of methane. Despite many instances of its successful application, a drawback associated with AD wastewater treatment has been the inability to achieve acceptable – even moderate – levels of inorganic nutrient, in particular phosphate (P), removal that would avoid the need for extensive aerobic biological or chemical post-treatment (McGrath and Quinn, 2003; Caravelli et al., 2012; Hauduc et al., 2015).

Phosphate recovery and re-use from various sources is urgently needed to address an imminent P availability crisis. The current practice of mining rock-P (an exhaustible resource) for agricultural use is unsustainable. Wastewater streams offer an important opportunity to recover and recycle P, thus helping to close the P cycle. Indeed, up to 30% of world demand for P could theoretically be satisfied by its recovery from domestic waste streams alone (Gilbert, 2009). To date, the well-established Enhanced Biological Phosphate Removal (EBPR) systems have been applied for P removal from wastewaters. EBPR is based upon the exposure of activated sludge to alternating anaerobic and aerobic phases: P removal across the system is achieved via the intracellular accumulation of polyphosphate (polyP) by specialized group (or groups) of microorganisms. However, in reality these systems can demonstrate variability in performance, as polyP uptake is dependent on a number of operational and microbiological conditions that remain to be fully elucidated (McGrath and Quinn, 2003; Zeng et al., 2013; Yu et al., 2014; Motlagh et al., 2015). To date, biological P removal and recovery during AD wastewater treatment had not been reported. Despite this, luxury polyP uptake has been observed in strictly anaerobic archaeal species (Rudnick et al., 1990; Smirnov et al., 2002; Auernik et al., 2008; Toso et al., 2011; Orell et al., 2012) indicating the possibility for application of polyP synthesis as a means for P removal under anaerobic conditions. The potential for efficient removal and recovery of P during AD of dilute wastewaters was significantly advanced by Hughes et al. (2011) using a novel hybrid bioreactor system incorporating a fixed-film section of packed pumice stone. Despite this advance, the precise mechanism of phosphate removal and the role of the microbial consortia within the system remain to be ascertained.

Sewage wastewater is an important source of P into the environment, which if not intercepted, can lead to eutrophication of receiving water bodies (Khan et al., 2011; Barca et al., 2012; Wang and Pei, 2013). Sewage is generally treated in developed countries using aerobic biological systems, such as the activated sludge process, although these do not rank well in terms of sustainability criteria due, for example, to the high levels of energy required for aeration. Anaerobic treatment technologies have been successfully implemented for low-strength domestic sewage, but mainly in tropical/warm temperature regions (Smith et al., 2012). In temperate climates, the requirement to heat wastewaters to facilitate mesophilic operation would negate any

energy savings gained. Low temperature (psychrophilic) AD allows for the economically efficient application of AD to low-strength wastewaters in temperate regions (McKeown et al., 2012). A reduction in hydrolysis rates corresponding with the accumulation of biodegradable solids in high-rate reactor systems operated at short hydraulic retention times (HRTs), however, may preclude low-temperature anaerobic treatment opportunities. The capacity for, and the extent of, the development of efficient hydrolytic biomass remain largely unexplored. It is known and well-studied, however, that increased methanogenic and acetogenic activity can develop during low-temperature AD, driven both by shifts in the microbial community and the development of psychrotolerance in organisms, such as *Methanosaeta* (McKeown et al., 2012; Zhang et al., 2012; Gunnigle et al., 2015). Some recent studies (Regueiro et al., 2014; Gunnigle et al., 2015) indicate that the Bacteroidetes and Proteobacteria phyla may be important in the case of a low-temperature shock. However, limited information is available on the bacterial community during prolonged low-temperature operation. Moreover, the roles played by the diverse bacterial species responsible for hydrolysis and acidification is only understood at a very basic level in AD generally. The capacity for enhanced hydrolysis, acidification and methanogenesis at low temperatures could underpin successful operation of future high-rate AD sewage treatment systems in temperate regions.

Our hypotheses were that high levels of P removal during AD would be achievable during high-rate treatment of synthetic sewage at low-temperature, in conjunction with highly efficient, low-temperature methanogenic biodegradation of the solid, colloidal and soluble fractions of a sewage wastewater: (i) at loading rates $>1 \text{ kg total COD m}^{-3} \text{ day}^{-1}$; (ii) while producing an effluent quality of $<125 \text{ mg total COD l}^{-1}$; (iii) with microbial community development resulting in increased hydrolytic, acidogenic, and methanogenic activity at low-temperatures. Our aim was to test these hypotheses in a laboratory-scale bioreactor system.

MATERIALS AND METHODS

Reactor Design, Set-Up, and Operation

This study employed a glass laboratory-scale hybrid sludge bed/fixed-film (packed pumice stone) reactor (2.8 l working volume) as described by Hughes et al. (2011). The reactor was seeded with 20 g VSS l^{-1} of seed biomass [obtained through a sludge-screening step (Keating et al., 2012)]. The substrate used was a synthetic sewage based wastewater (SYNTHESE) from Aiyuk and Verstraete (2004) at 500 mg l^{-1} COD_{Tot} outlined in **Table 1**. The reactor was operated at 12°C in a trial of 732 days. The trial was divided into five phases, each involving a different applied HRT and organic loading rate (OLR; **Table 2**) with Phase 4B marking a change in the fixed-film filter unit.

Performance Analyses

Reactor effluent was sampled on a daily basis and combined into a weekly composite sample for total COD (COD_{Tot}),

TABLE 1 | Composition of 500 mg l⁻¹ COD_{Tot} SYNTHES (Aiyuk and Verstraete, 2004).

Chemical components	Food ingredients	Trace metals
Urea (100 mg l ⁻¹)	Starch (131.2 mg l ⁻¹)	Cr(NO ₃) ₃ ·9H ₂ O (0.9 mg l ⁻¹)
NH ₄ Cl (12.5 mg l ⁻¹)	Milk powder (125 mg l ⁻¹)	CuCl ₂ ·2H ₂ O (0.6 mg l ⁻¹)
Na-Acetate-3H ₂ O (140.6 mg l ⁻¹)	Dried yeast (56.2 mg l ⁻¹)	MnSO ₄ ·H ₂ O (0.1 mg l ⁻¹)
Peptone (18.7 mg l ⁻¹)	Soy Oil (31.2 mg l ⁻¹)	NiSO ₄ ·6H ₂ O (0.3 mg l ⁻¹)
MgHPO ₄ ·3H ₂ O (31.2 mg l ⁻¹)		PbCl ₂ (0.1 mg l ⁻¹)
K ₂ HPO ₄ ·3H ₂ O (25 mg l ⁻¹)		ZnCl ₂ (0.3 mg l ⁻¹)
FeSO ₄ ·7H ₂ O (6.2 mg l ⁻¹)		
CaCl ₂ (6.2 mg l ⁻¹)		

soluble COD (COD_{Sol}), suspended COD (COD_{Sus}), and colloidal COD (COD_{Col}) determinations according to Standard Methods (APHA and AWWA, 2005). Protein and polysaccharide concentrations in the effluent were determined by the Lowry method (Lowry et al., 1951) and the DuBois method (DuBois et al., 1956), respectively. For the measurement of total phosphorus (expressed as PO₄³⁻) samples were passed through a 0.45 µm filter prior to analysis using the molybdatevanadate Test 'N Tube™ method (Hach Lange, UK). The concentration of volatile fatty acids (VFAs) in the effluent was determined by chromatographic analysis in a Varian Saturn 2000 GC/MS system (Varian Inc., Walnut Creek, CA, USA). Biogas analysis was performed by gas chromatography (Varian Inc., Walnut Creek, CA, USA) according to standard methods (APHA and AWWA, 2005).

Biomass Characterization

Maximum Specific Methanogenic Activity (SMA) Testing

To evaluate changes in sludge hydrolytic and methanogenic capabilities the seed biomass and reactor biomass at HRT changes

(36, 24, 12, and 8 h) were screened using the maximum specific methanogenic activity (SMA) testing method employing the pressure transducer technique as described previously (Colleran et al., 1992; Coates et al., 1996). Briefly, the test involved the measurement of the increase in biogas pressure over time following the addition of soluble substrates; propionate (30 mM), butyrate (15 mM), ethanol (30 mM), and acetate (30 mM) or of the decrease in pressure following the addition of 1 atm of H₂/CO₂ (80:20). Controls included vials without substrate addition and the addition of N₂/CO₂ (80:20) at 1 atm as a gaseous control. Tests were carried out in triplicate at 37 and 12°C. Biogas analysis was performed as described previously. Results were expressed as ml CH₄ g VSS⁻¹ day⁻¹.

Protein Degradation Assays for the Determination of *k*, *V_{max}*, *A_{max}*, and *K_m*

The maximum specific activity (*A_{max}*), the maximum initial velocity (*V_{max}*), the apparent half-saturation constant (*K_m*) and the first-order hydrolysis constant of the seed inoculum and reactor biomass were evaluated on a protein source (solubilized skimmed milk powder). These rates were determined using substrate depletion assays, which were set up similarly to the SMA test described above. Tests were performed in triplicate at 12 and 37°C using 2 g VSS l⁻¹ with 2 g COD/vial of protein. The bottles were sampled at regular intervals, protein concentration was measured in the samples and a substrate depletion curve was plotted. The concentration of protein was determined using the Lowry method (Lowry et al., 1951). The kinetic parameters described above were calculated as described by Bialek et al. (2013).

Scanning Electron Microscopy (SEM) and Energy Dispersive X-Ray (EDX)

Scanning electron microscopy (SEM) was used to assess the structure of unused pumice stone, washed pumice stone and colonized stones and biomass from the filter, at the end of the trial. Samples were fixed by incubating in 2.5% Glutaraldehyde stock (containing 50% Glutaraldehyde, 4% Sucrose, and 0.1 M Sodium Phosphate Tribasic buffer) at 4°C overnight. Following this, a series of ethanol washes (50, 70 and 90%) were set up in individual microporous specimen cups (Canemco & Marivac,

TABLE 2 | Reactor operation phases and associated operational conditions.

PHASE DAYS	Start-Up* 1–35	1 36–105	2 106–209	3 210–307	4A 308–487	4B 487–638	5 639–732
HRT ⁱ	36	36	24	18	12	12	8
TEMP ⁱⁱ	12	12	12	12	12	12	12
OLR ⁱⁱⁱ	0.3	0.3	0.5	0.6	1	1	1.5
VLR ^{iv}	0.67	0.67	1.00	1.33	2	2	3
SLR ^v	0.03	0.03	0.05	0.10	0.16	0.16	0.23
SLR ^{vi}	0.02	0.02	0.03	0.05	0.08	0.08	0.11
UV ^{vii}	2.5	2.5	2.5	2.5	2.5	2.5	2.5

ⁱHydraulic retention time (h); ⁱⁱTemperature (°C); ⁱⁱⁱOrganic loading rate (kg COD m⁻³ d⁻¹*); ^{iv}Volumetric loading rate (m³ Wastewater m⁻³ Reactor d⁻¹); ^vSludge loading rate based on granular sludge bed VSS estimated at each phase (kg COD kg [VSS]⁻¹ d⁻¹)*; ^{vi}Sludge loading rate (m³ Wastewater kg [VSS]⁻¹ d⁻¹); ^{vii}Up-flow velocity (m h⁻¹). *Values calculated based on influent concentration of 500 mg l⁻¹ COD_{Tot}.

Canton de Gore, QC, Canada). Samples were then placed in each cup (50, 70, and 90, respectively) for 10 min each at room temperature. Samples were then mounted on aluminum slabs with a carbon tab (Agar Scientific, Essex, UK), incubated for 2 min at 37°C and then incubated at room temperature in sealed petri dishes with blue silica desiccants. Once the samples were dehydrated they were coated with a thin layer of gold and viewed using a SEM (Model S-4700, Hitachi, Japan). EDX was used to provide elemental composition of the samples. SEM and EDX were carried out at the National Centre for Biomedical Engineering Science (NCBES) at NUI, Galway.

DAPI (4',6-Diamidino-2-Phenylindole)

4',6-Diamidino-2-phenylindole staining was performed on granular biomass and biomass from the fixed-film filter. One hundred microliters of cells (granular biomass and free-cells suspension) were centrifuged at 18K × g for 10 min. The supernatant was discarded and the pellet resuspended in 100 µl of DAPI (50 µg/ml containing 150 mM KCl and 10 mM HEPES-KOH buffer pH7). The samples were incubated overnight at 4°C. The samples were then centrifuged and the pellet washed twice with reverse-osmosis water. The pellet was then resuspended in 100–200 µl of water. Ten microliters was spotted onto a slide and viewed under the microscope following air-drying. Samples were viewed using a Leica DMR microscope, a Prior L200S light source, an Olympus DP73 camera and Olympus cellSens software, with a filter cube which had an emission filter of 340–380 nm and a long-pass suppression filter of 450 nm.

Molecular Characterization

DNA/RNA Co-Extraction from Biomass

Genomic DNA and RNA was extracted from granular biomass samples taken from R1 on Days 0 (Inoc), 105 (Phase 1), 209 (Phase 2), 301 (Phase 3), 361 (Phase 4A.a), 429 (Phase 4A.b), 454 (Phase 4A.c), 534 (Phase 4B.a), 596 (Phase 4B.b), and at end of the trial (Phase 5-Day 732). Biomass was sampled from the fixed-film filter at two points: – mid-trial (Day 230) and at the end of the trial (Day 732). Samples were flash frozen in liquid nitrogen and stored at -80°C prior to the extraction procedure. The nucleic acids were co-extracted by a modification of a phenol extraction method (Griffiths et al., 2000). Granular biomass (1 g) was crushed to a powder in a liquid nitrogen cooled mortar (BelArt) and 0.25 g of this powder was added into a sterile lysing matrix E tube (Fischer Scientific) prior to adding 250 µl of 1% cetyl trimethylammonium bromide (CTAB) extraction buffer, 250 µl 0.1 M Na₃PO₄ (pH 8) extraction buffer and 250 µl of phenol-chloroform-isoamyl alcohol (25:24:1; pH 8). Microbial cells in the samples were lysed by bead beating for 10 min at 3.2K × g in a Vortex-Genie2™ (Scientific Industries Inc.) Phase separation was achieved by centrifugation at 13.3K × g for 10 min at 4°C. The clear aqueous supernatant was transferred into a sterile Phase Lock Gel™ tube (Fischer Scientific) with equal volume of chloroform isoamyl alcohol (24:1). Phase separation was achieved by centrifugation at 13.3K × g for 10 min at 4°C. The supernatant was transferred into fresh RNase free tubes and total nucleic acids (TNA) were precipitated by using 2.5 vol of ice-cold ethanol (100%) and 1/10 vol of 3 M sodium acetate (pH 5.2)

added to the extract, incubated on ice for 30 min and centrifuged (13.3K × g) at 4°C for 20 min. TNA were resuspended in 50 µl of diethylpyrocarbonate (DEPC) water. The integrity of each sample was assessed using agarose gel electrophoresis and quantified using a Qubit v2.0 fluorometer (Life Technologies, Darmstadt, Germany). Samples were then stored at -80°C prior to use in downstream applications. RNA was prepared by treating the TNAs with TurboDNase (Invitrogen) according to the manufacturer's instructions. RNA was confirmed DNA free by 16S rRNA PCR of a range of RNA dilutions. Reverse transcription was then carried out using 10 µl of DNA free RNA sample, 100 µM random hexamer primers (Invitrogen), 1 µl DEPC water following the SuperScript™ III (Invitrogen) protocol according to manufacturer's instructions. DNA and cDNA were purified with the QIAquick PCR Purification Kit (Qiagen, Germany).

Quantitative-Polymerase Chain Reaction (qPCR)

Quantitative-Polymerase Chain Reaction was carried out for Archaeal and Bacterial domains using DNA and cDNA generated from granular biomass and filter biomass extracted from R1. The primers 1369F and 1492R and Taqman probe TM1389F were used for bacterial analysis (Suzuki et al., 2000). The primers 787F and 1059R and Taqman probe 915F were used for archaeal analysis (Yu et al., 2005). Quantitative standard curves were constructed using standard plasmids containing the full-length 16S rRNA gene sequence from the representative bacterial strain (*Escherichia coli*) and representative archaeal strain (*Methanoscincus bakeri*). The plasmids were extracted using a Plasmid Extraction kit (BIOLINE). A PCR reaction was then carried out using the primer pairs described above. This product was cleaned using QIAQuick PCR Clean Up kit (Qiagen, Crawley, UK) according to manufacturers instructions. To construct the RT-PCR cDNA standard curves were produced from cDNA prior *in vitro* transcription of the target mRNA by using the MEGAshortscript T7 kit (Ambion) as described by Smith et al. (2006). The concentration of all standards was measured in duplicate using a Qubit system (Invitrogen) and converted into copy concentration. A 10-fold serial dilution series (10⁹–10¹ copies ml⁻¹) was generated for each standard solution and analyzed by real-time PCR, in duplicate, with its corresponding primer and probe set. The dynamic range of each standard curve was determined based on the linear regression *r*² value of >0.98.

Quantitative real-time PCR was performed using a LightCycler 480 (Roche, Manheim, Germany). Each 25 µl reaction mixture was prepared using the LightCycler TaqMan Master Kit (Roche; 2 µl of template, 4 µl PCR-grade water, 10 µl of 2X reaction solution, 500 nM of each primer and 200 nM of probe). PCR amplification and detection was carried out as described previously (Smith et al., 2006). The volume-based concentrations (copies l⁻¹) were converted to per g biomass.

Illumina MiSeq Analysis

Terminal Restriction Fragment Length Polymorphism (TRFLP) was used as a screening step to select samples to send for

16S amplicon sequencing. TRFLP peaks were analyzed in Peakscanner (Life Technologies™). Fragments with peak height of less than 0.5% were regarded as background noise. The resulting TRFLP profiles were aligned using the web-based program T-Align with a confidence interval of 0.5 (Smith et al., 2005). The produced consensus files were then input into the software Primer 6 (PRIMER-E, Plymouth, UK) for subsequent statistical analysis. Cluster analysis, dendograms and MDS plots of the TRFLP data were constructed using the UPGMA algorithm in Primer software beta version 6 (PRIMER-E, Plymouth, UK) after a square root transformation was applied to the matrix. This analysis allowed the identification of samples deemed interesting to aid in the selection of samples to analyze for total and active bacterial and archaeal community compositions through the construction of 16S Illumina MiSeq library generation.

From this analysis DNA and cDNA from Day 0 (Inoc), Days 105 (Phase 1), 301 (Phase 3), 454 (Phase 4A.c), 732 (End), and the filter upon take-down (FE) samples were used for 16S amplicon sequencing. The 16S rRNA gene V4 variable region was amplified using the ‘universal’ (for the co-amplification of archaeal and bacterial sequences) primer set 515F (5'-GTGCCAGCMGCCGCGTAA-3') and 806R (5'-GGACTACHVGGGTWTCT-AAT-3') -Caporaso et al. (2012) with barcodes for multiplexing on the forward primer. The PCR conditions included an initial denaturation step at 94°C for 3 min, followed by 28 cycles of denaturation at 94°C for 30 s, annealing at 53°C for 40 s, and extension at 72°C for 1 min, with a final elongation step at 72°C for 5 min using HotStarTaq Plus Master Mix Kit (Qiagen, USA) for the reaction. Amplicons were then pooled in equal proportions and purified using calibrated Ampure XP beads (Beckman Coulter). The combined and purified product was prepared using the Illumina TruSeq DNA library protocol. DNA amplification and sequencing was performed at MR DNA Molecular Research Laboratory (www.mrdnalab.com; Shallowater, TX, USA) using the MiSeq reagent kit V3 (2 × 250 bp) for paired-end reads on a Solexa MiSeq machine following the manufacturer’s guidelines.

A total of 1,173489 raw 16S rRNA V4 sequences were obtained by Illumina paired end sequencing from the 12 samples. Sequence data were processed using a proprietary analysis pipeline (MR DNA, Shallowater, TX, USA; Dowd et al., 2008). This analysis involved the processing of the forward single-end read by removing barcodes, primers, sequences <200 bp, sequences with ambiguous base calls and sequences with homopolymers exceeding 6 bp. Sequences were further denoised, operational taxonomic units (OTUs) generated and chimeras removed using UCHIME (Edgar et al., 2011). 17,449 chimeric sequences were identified and removed from the samples. OTUs were defined after singleton sequences were removed, clustering at 3% divergence (97% similarity) using UCLUST (Dowd et al., 2008; Edgar, 2010). After quality processing, raw reads were reduced to 593,321 reads (Inoc DNA 70,432/cDNA 52,580, Phase 1 DNA 37,491/cDNA 58,858, Phase 3 DNA 37,491/cDNA 21,118, Phase 4A.c DNA 37,491/cDNA 79,698, End DNA 57, 225/cDNA 43,583, FE DNA 35,058/cDNA 49,801). Final OTUs were taxonomically classified using BLASTn against a curated GreenGenes database (DeSantis et al., 2006). In total 9,215 OTUs were identified, affiliated to 46 bacterial phyla and two archaeal classes. Raw sequences were submitted to the SRA database under the bioproject submission number PRJNA307661.

RESULTS AND DISCUSSION

Phosphate Removal During AD Wastewater Treatment

Phosphate removal from the wastewater, significantly in excess of microbial growth requirements [1.5–2% of sludge dry weight (Schlegel and Zaborosch, 1993; Blackall et al., 2002)] was achieved during this trial (Table 3). P removal upon start-up (~35 days) was initially high (68%) but decreased during Phase 1 (Table 3). P removal efficiency increased considerably during Phases 2 (to 69%) and 3 (~78%). Following a reduction of the applied HRT to 12 h during Phase 4, P concentrations increased in the effluent (Table 3). After the filter was changed (Phase 4B), effluent P values increased with an average removal efficiency of 48%. P

TABLE 3 | Average Phosphate concentration (in mg l⁻¹) and average Phosphate, COD_{Tot}, COD_{Sus}, COD_{Col}, COD_{Sol}, Carbohydrate, Protein, and removal efficiency (RE) (%) in reactor effluent and the VFA:COD ratio for the five phases of reactor operation.

Parameter	Startup	Phase 1	Phase 2	Phase 3	Phase 4A	Phase 4B	Phase 5
Phosphate conc.	13	21.5	10.5	7.6	15.2	19.5	25
RE*Phosphate	61	36	69	78	55	43	28
RE*COD Total	22	80	84	78	74	77	70
RE*COD Suspended	0	47	60	65	37	44	36
RE*COD Colloidal	17	64	37	29	13	16	0
RE*COD Soluble	91	81	87	77	75	79	74
RE*Carbohydrate	85	98	99	85	95	84	17
RE*Protein	94	100	97	99	100	100	100
VFA:COD ratio	0.05	0.10	0.14	0.25	0.26	0.35	—
Theoretical CH ₄ potential ⁺ (l d ⁻¹)	0.07	0.26	0.41	0.51	0.73	0.75	1.03

⁺Methane potential calculated stoichiometrically, considering that all COD_{totalremoved} was converted into methane and that 1 g of COD_{totalremoved} would produce 350 ml of methane under standard temperature and pressure conditions (McCarty, 1964). The results were presented in liters per day based on the total loading of 1 day (g COD d⁻¹).

removal decreased further to 28% during Phase 5 corresponding to an increase in the OLR to $1.5 \text{ kg COD m}^{-3} \text{ d}^{-1}$. P removal was at its optimum during Phase 3 (OLR of $0.6 \text{ kg COD m}^{-3} \text{ d}^{-1}$).

We hypothesize that P removal in the system was biological in nature, mediated by biofilms within the reactor and the fixed-film unit rather than due to chemical precipitation (Hughes et al., 2011). Such high levels of P removal have, to date, only been associated with low-temperature AD systems (Hughes et al., 2011) and it is not known whether it could be achieved at higher temperatures or with more concentrated wastewaters. It appeared that P uptake required a period of acclimation after initial high rates during the start-up period, or perhaps a period of development associated with the colonization of biofilms within the system as evidenced by increased removal efficiency after Phase 1 (Table 3). It was noted that the presence of *Rhodococcus* (a previously characterized PAO) had increased at this point from 0.7% in the inoculum to 4.2% in Phase 1 (based on cDNA analysis). SEM and EDX analysis carried out on sludge granules, unused pumice stone, washed pumice stone and biomass from the filter at the end of the trial demonstrated $\sim 2\%$ elemental phosphorus in the biomass and colonized stones (Figure 1). These samples also demonstrated a 2% increase in calcium (Figure 1). Recent research has indicated the formation of calcium phosphate granules as a new phosphorus product during the treatment of black water (Tervahauta et al., 2014). Some calcium phosphate forms may have partially solubilized at allowing interaction with the microbial biofilm, however, calcium phosphate would be largely insoluble at lower temperatures. Most significantly, DAPI staining from biomass taken from the initial inoculum and from throughout the trial indicated biological P accumulation was occurring owing to the presence

of polyP granules in the sludge bed and filter biofilms (Figure 2). The presence of polyP was confirmed by an enzymatic assay with ppx. PolyP was most notably observed in the biomass taken from the filter mid-trial (Figures 2A,B). Furthermore, phosphate removal decreased following the change of filter material (Table 3; Figure 3), this may be indicative of the loss of biomass associated with P-uptake. PolyP granules were strongly associated with large biofilm particles with free cells infrequently showing evidence of polyP. Thus, it appears that specifically, the biofilms on and within the filter materials were fundamental to P uptake. It is possible, however, that some calcium phosphate precipitation could be occurring in parallel to biological phosphorus accumulation through polyP uptake.

Pumice, the filter material employed in fixed-film section of the bioreactor, is not a new material to wastewater treatment and chemical adsorption of P in this material has also been demonstrated (Onar and Öztürk, 1993). It is the biological interaction with the material, however, which promotes efficient P removal and recovery greatly in excess of that possible through adsorption onto pumice alone (Hughes et al., 2011). It is not yet known whether the nature of the matrix material could play a role in promoting P uptake and removal via polyP formation. Indeed there is very little prior literature to provide clues as to the basis for the observed phenomenon. A study by Wang et al. (2006) described P uptake in the anaerobic phase of an EBPR reactor system. The authors hypothesized that uptake was biological in nature; but dismissed polyP accumulation as the route to P removal. The possibility of polyP uptake by anaerobic bacteria and archaea should not be readily overlooked, however. PolyP is a “key” evolutionary molecule (Kulaev and Kulakovskaya, 2000) and, as such,

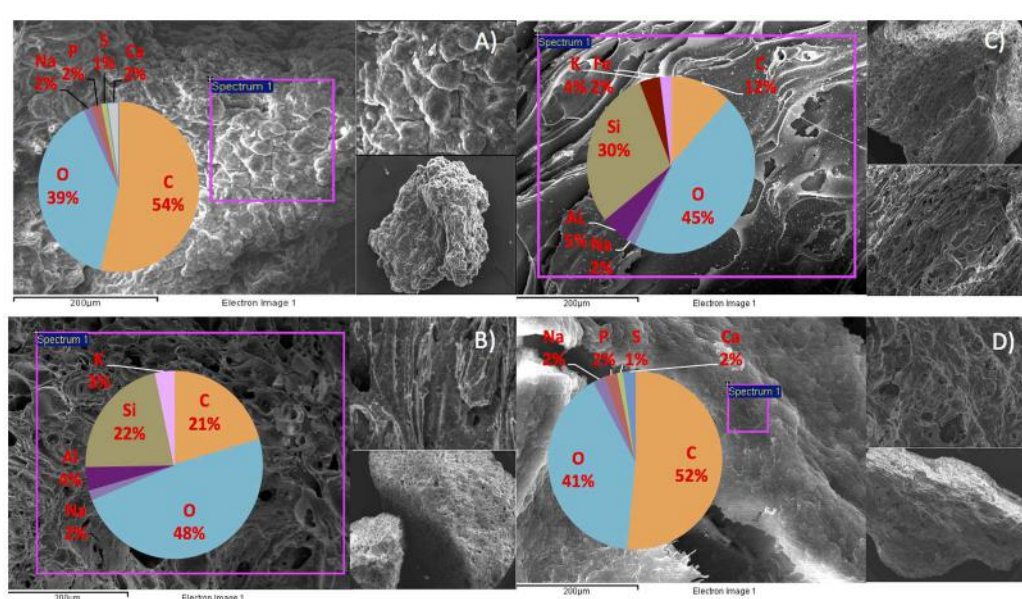


FIGURE 1 | SEM/EDX images and element composition of reactor contents at the end of the trial (A) sludge granule, (B) unused pumice stone, (C) washed pumice stone and (D) biomass on the pumice stone.

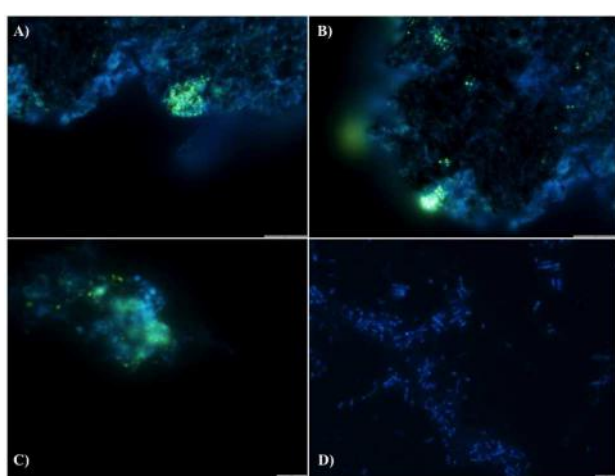


FIGURE 2 | DAPI stained images for the detection of polyphosphate (evidenced by yellow fluorescence) in reactor biomass from (A) Filter Mid-Trial, (B) Filter Mid-Trial, (C) Day 532 and (D) free cells from the filter from the end of the trial.

is found in living cells across the Bacteria and Eukarya domains (Kulaev and Kulakovskaya, 2000; Benzerara et al., 2014; Sahdeo Prasad, 2014; Kulakovskaya et al., 2015; Zhang et al., 2015). Additionally, several authors have described polyP uptake in a variety of Archaeal species (Rudnick et al., 1990; Smirnov et al., 2002; Auernik et al., 2008; Orell et al., 2012). Moreover, P removal rates continued to decrease corresponding to increases in the OLRs applied. This may indicate that carbon limitation may have been important for polyP uptake,

which has been noted in known PAOs (Deinema et al., 1980). Thus, the capacity and environmental triggers for polyP formation, sufficient to facilitate biotechnological exploitation, under anaerobic methanogenic conditions warrant further investigation. Additionally, linking these parameters to the microbial populations underpinning luxury polyP uptake could provide a significant advance in biotechnological opportunities for P removal. The identification of the exact speciation of the phosphate within the system is the focus of ongoing research efforts.

In this study, we determined the biological activity profile and microbial community structure of the bioreactor system in order to provide a clearer indication of the environment in which P removal was encouraged.

The Treatment Performance of the Hybrid Reactor

In addition to significant P removal, this system demonstrated efficient and stable process performance throughout continuous operation over 732 days at 12°C with effluent COD concentrations mostly within marine discharge limits for Ireland (125 mg COD_{Tot} l⁻¹; Figure 3). COD_{Sol} removal efficiency was stable and efficient throughout all phases of the trial. COD_{Tot} and COD_{Sus} removal efficiency values exceeded those reported in similar low-temperature sewage systems (Chu et al., 2005; Gao et al., 2011) and were comparable to results observed in an anaerobic membrane bioreactor treating domestic wastewater (Smith et al., 2013). C3–C6 VFAs were generally not detectable, while acetic acid was detected only during brief transient periods (data not shown). Effluent concentrations of COD_{Tot} and COD_{Sus} were initially high (>250 mg l⁻¹) due to

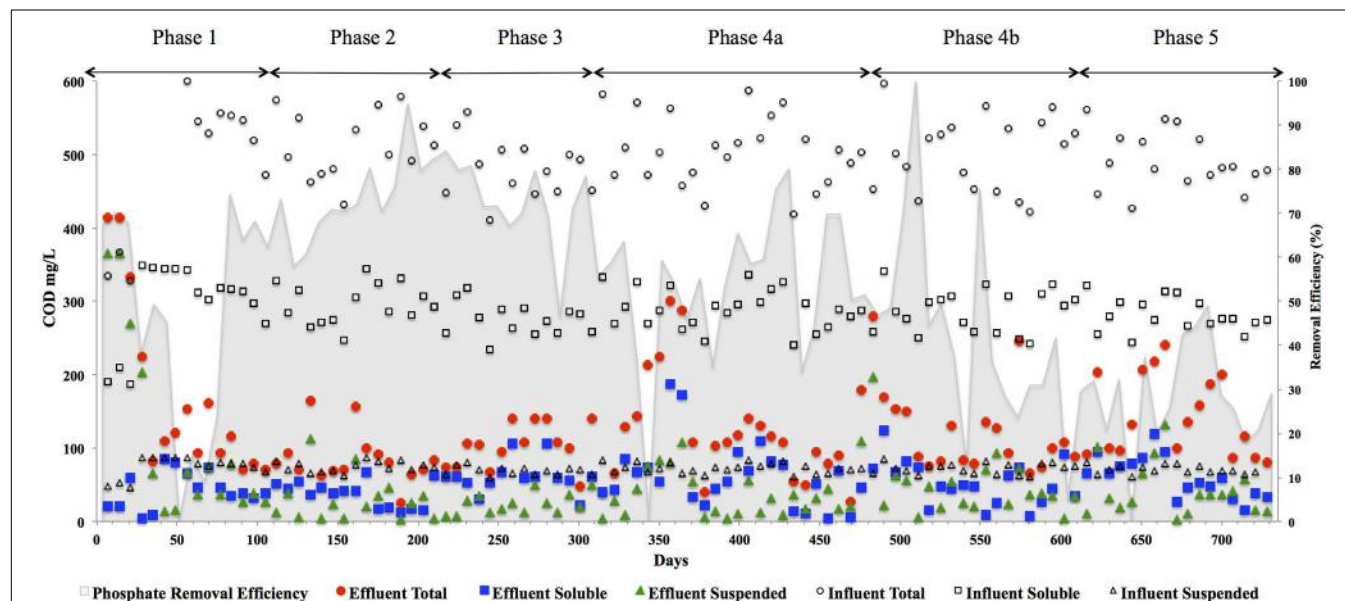


FIGURE 3 | COD_{total}, COD_{soluble}, COD_{suspended}, and COD_{colloidal} concentrations in (mg l⁻¹) in the reactor effluent for the five phases of reactor operation. Effluent Total (●), Effluent Soluble (■), Effluent Suspended (▲), Influent Total (○), Influent Soluble (□), Influent Suspended (△), and Influent Colloidal (◊) and phosphate removal (%) [based on an average influent concentration of 34 mg l⁻¹] in shading on secondary axis.

biomass washout upon commencement of the trial, the start-up phase was short, however, lasting 35 days (**Figure 3**). Increases in the applied OLR led to transient decreases in COD removal although, in concentration terms, the increases in effluent concentrations were minimal. Phase 3 was associated with a drop in the average COD_{Tot} and COD_{Sol} removal efficiencies but an increase in P removal (**Table 3**). Specific features included a decrease in the average carbohydrate removal efficiency from 99 to 85%, the appearance of acetic acid in the effluent (data not shown; at low levels, up to 24 mg l⁻¹) and an increased VFA:COD ratio (**Table 3**) from 0.14 (Phase 2) to 0.25 (Phase 3). These data indicated that both hydrolysis and methanogenesis were not functioning as well in Phase 3, although P removal was at its highest in this phase (78%). Phase 4 was divided into Phase 4A (prior to a change in the filter matrix on day 487) and Phase 4B (after the filter change). A decrease in COD_{Tot} and COD_{Sus} removal efficiencies along with evidence of filter clogging merited the replacement of the filter matrix with new pumice stone. The filter change resulted in increased overall COD removal efficiency during Phase 4B, particularly with respect to the removal of solids (**Table 3**). Particulates have been shown to comprise 85% of the COD_{Tot} in domestic sewage (Aiyuk and Verstraete, 2004; Lew et al., 2009). Our data support the idea that particulates were physically entrapped in the filter section of the reactor, allowing them to be subsequently degraded. Moreover, no accumulation of solids was observed in the granular bed section of reactor. During the fifth and final phase of operation, the average COD_{Tot}, COD_{Sus}, and COD_{Sol} removal efficiencies were 70, 36, and 74%, respectively (**Table 3**). The reduced performance of the reactor with respect to the degradation of particulate COD during Phase 5 indicated that a 8 h HRT was too short for complete degradation or retention of complex substrates. Another possibility for reduced performance may be related to the volumetric loading rate applied, which may not have allowed for the retention of particulates. Moreover, the sludge loading rate was much greater in this final phase than in Phase 4A (**Table 1**).

The quality of the biogas generally ranged between 50 and 60% throughout the trial. Methane yields were consistent with methanogenic activity but lower than the theoretical methane yield (**Table 3**). As no solids accumulation was observed in the system it is estimated that a large proportion of the methane generated was dissolved in the reactor effluent. This is unsurprising as the recovery of methane from low-temperature systems is a known difficulty. The solubility of methane in the effluent increases with decreasing temperature (Bandara et al., 2012). Several studies have demonstrated this effect. For example, Matsuura et al. (2015) found solubility increased in UASB effluent by a factor of 1.4 when decreasing from 25 to 10°C, while as much as 50% of the methane generated in an AnMBR was dissolved in the reactor effluent at 15°C (Smith et al., 2011). Substantial methane oversaturation been demonstrated in anaerobic effluents (Hartley and Lant, 2006; Souza et al., 2011), owing to liquid-gas mass transfer limitations (Pauss et al., 1990). This is compounded further when the wastewater stream to be treated is relatively low-strength (Bandara et al., 2011; Smith et al., 2012).

Hydrolytic Capabilities of the Biomass

The seed biomass had negligible methanogenic activity at 12°C, but increased in activity after the first phase of operation (**Table 4**). Greater activity at mesophilic temperatures, recorded throughout the trial, suggested the development of a low temperature tolerant methanogenic community, rather than a truly psychrophilic one. All assays, at both mesophilic and psychrophilic temperatures, revealed higher SMA for hydrogenotrophic methanogenesis, indicating a preference toward this route as seen previously (McHugh et al., 2006; McKeown et al., 2009; Ryan et al., 2010). The SMA on propionate at 12°C increased during the trial, indicating that an important degradation pathway was via propionate. At the end of Phase 3, the SMA, at 37°C, no activity was detectable against acetate, which may explain the accumulation of acetate in the reactor effluent during Phase 3. By the end of the trial, the biomass SMA on the direct methanogenic substrates H₂/CO₂ and acetate had increased (**Table 4**).

The hybrid system degraded protein during all phases of the trial, however, with removal efficiencies between 97 and 100% (**Table 3**). This was surprising since proteins are considered to be harder to degrade than carbohydrates under anaerobic conditions, especially at cold temperatures (Aiyuk and Verstraete, 2004; Bialek et al., 2013). This result suggests that an active and efficient psychrophilic, or psychrotolerant, proteolytic group developed in the reactor. To elucidate the hydrolytic capacity of the microbial biomass, particularly with respect to protein degradation, tests using skimmed milk as a protein source were performed and various kinetic parameters (A_{max} , K_m , and k) were calculated. The half-saturation constant K_m was higher at 12°C than at 37°C throughout the trial (**Table 4**) indicating that microorganisms with lower substrate affinity predominated at the lower temperature, which is in agreement with a previous report (Banik et al., 1998). By the end of Phase 1, the K_m at 37 and 12°C had doubled compared to the K_m of the seed biomass, again an indication of a decrease in the substrate affinity, presumably as a response to the adaptation to cold temperatures (**Table 4**). At the end of Phase 2, the K_m decreased slightly at 37°C and decreased by 44% at 12°C suggesting that proteolytic bacteria with higher substrate affinity started to dominate in the consortium at this stage as a response to the low concentration of protein in the influent. From the end of Phase 3 until the end of the trial, the K_m decreased slightly and stabilized at both temperatures indicating further acclimatization of proteolytic bacteria with higher substrate affinity (**Table 4**).

The initial A_{max} (maximum specific activity; g Protein⁻¹ d⁻¹) was twice as large at 37°C (74 g COD g protein⁻¹ d⁻¹) than at 12°C (35 g protein⁻¹ d⁻¹), while k (first-order hydrolysis constant) was approximately seven times higher at 37°C than at 12°C (**Table 4**). By the end of the trial, A_{max} and k were 4.5- and 2-times higher, respectively, at 12°C than at 37°C, indicating the emergence of a psychrophilic proteolytic consortium rather than a psychrotolerant one. This is in agreement with the high protein removal levels achieved by the reactor throughout the trial.

TABLE 4 | Specific Methanogenic Activity (SMA) of reactor sludge throughout the trial at 37 and 12°C in ml Methane (CH_4) g [VSS] $^{-1}$ d $^{-1}$.

	Prop*	But ⁺	Ethanol	Acetate	H ₂ /CO ₂	A _{max} ^a	K _m ^b	K ^c
Seed 37°C	61 ⁽²¹⁾	31 ⁽⁷⁾	52 ⁽¹⁷⁾	80 ⁽²⁰⁾	125 ⁽³²⁾	74 ⁽²²⁾	0.8 ⁽⁰⁾	4 ^(2.6)
Seed 12°C	2 ⁽¹⁾	1 ⁽¹⁾	7 ⁽²⁾	3 ⁽¹⁾	4 ^(0.2)	35 ⁽²⁰⁾	2.7 ^(0.2)	0.6 ⁽⁰⁾
P 1 37°C	70 ⁽⁷⁾	199 ⁽²⁷⁾	492 ⁽⁸²⁾	272 ⁽¹⁵⁸⁾	587 ⁽²⁷⁶⁾	40 ⁽¹⁾	1.9 ^(0.1)	4.5 ^(0.2)
P 1 12°C	7 ⁽⁶⁾	24 ⁽¹¹⁾	7 ⁽⁶⁾	12 ⁽¹¹⁾	21 ⁽⁴⁾	58 ⁽¹¹⁾	4.2 ^(2.5)	1.3 ^(0.4)
P 3 37°C	70 ^(0.5)	273 ⁽⁹⁾	197 ⁽⁷⁷⁾	ND	56.5 ^(0.4)	67 ⁽²⁷⁾	0.9 ⁽⁰⁾	0.1 ⁽⁰⁾
P 3 12°C	10 ⁽¹³⁾	10 ^(0.3)	25 ⁽³⁾	ND	19 ⁽¹⁾	188 ⁽¹¹²⁾	1.3 ⁽⁰⁾	4.2 ^(2.6)
End 37°C	26 ⁽¹⁴⁾	44 ⁽²⁸⁾	284 ⁽¹³⁵⁾	176 ⁽²³⁾	319 ⁽³⁶⁾	34 ⁽¹⁰⁾	0.9 ⁽⁰⁾	1.7 ^(0.3)
End 12°C	20 ⁽¹¹⁾	13 ⁽³⁸⁾	36 ⁽³²⁾	9 ⁽⁴⁾	16 ⁽¹⁰⁾	155 ⁽³⁶⁾	1.2 ^(0.1)	3.8 ^(0.5)

*Propionate; ⁺butyrate; ND, no detectable activity found. ^aMaximum substrate utilizing rate g COD g protein $^{-1}$ d $^{-1}$. ^bApparent half-saturation constant g protein l $^{-1}$.

^cHydrolysis rate constant d $^{-1}$ based on hydrolysis kinetic assays from protein depletion assays from reactor biomass throughout the trial at 37 and 12°C. Values are the mean across triplicate vials with standard deviation in brackets.

Molecular Characterization of the Microbial Community

Quantitative PCR (qPCR)

Archaeal gene and transcripts abundances in this study are greater than those reported by previous authors (Town et al., 2014), indicating a highly active archaeal population within this system. Temporally, archaeal transcript numbers decreased during Phase 3 (and again during Phase 4), a reduction of approximately three orders of magnitude compared to the numbers in the seed biomass. These datapoints (Phase 3, Phase 4A.a, and Phase 4A.b) immediately preceded transient deteriorations in reactor performance (Figure 3), and an increase in effluent acetate concentrations (data not shown). The reduction also corresponded with no detectable acetoclastic activity and greatly reduced hydrogenotrophic activity in biomass sampled during Phase 3 (Table 4). Bacterial copy numbers also decreased at this stage (~2 log) compared to the seed (Figure 4), which perhaps reflected the reduced hydrolytic capacity of the biomass sampled during Phase 3 (Table 4). By the end of the trial, the archaeal copy numbers were the highest recorded (6.66×10^{13} copies g $^{-1}$) and the bacterial numbers had also increased by two orders of magnitude (Figure 4), which coincided with increases in the hydrolytic and methanogenic activity of the biomass (Table 4); and efficient COD removal at an OLR of 1.5 kg m $^{-3}$ d $^{-1}$ (Table 3).

Next Generation Sequencing

In total, 593,231 16S rRNA gene sequences >200 bp were obtained from 12 biomass samples. In total 9,215 OTUs were identified, affiliated to 46 bacterial phyla and two archaeal classes.

Bacterial populations

A variety of putatively fermentative and hydrolytic species were identified in the reactor. The bacterial community structure in low temperature systems has previously been indicated to be similar to that in mesophilic settings, with fermentative members of the Bacteroidetes and syntrophic members of the Proteobacteria being predominant (O'Reilly et al., 2010).

The abundance of Proteobacteria increased during the trial and this was the most abundant bacterial phylum at a cDNA-level in the sludge bed and filter unit biomass, being comprised

mainly of Delta, Gamma, and Beta-Proteobacteria, although Alpha and Epsilon Proteobacterial classes were also present. The phylum Proteobacteria contains a diverse consortium of species, including members isolated from low temperature environments. They are also common throughout anaerobic digestors, including mesophilic (Nelson et al., 2011) and low-temperature systems (O'Reilly et al., 2010; Bialek et al., 2012). Proteobacteria are capable of growth on a range of organic substrates (Yamada et al., 2005). Many species are associated with acetogenesis (Werner et al., 2011). The relative abundance of the phylum Firmicutes also increased dramatically during Phases 3 and 4 (Figure 5A) and they were the second most abundant bacterial phylum (~27%) at the end of the trial. The most dominant classes of Firmicutes were the Bacilli and Clostridia (mainly Lactobacillales; Figure 5B). Psychrophilic species belonging to the class Clostridia have been isolated and identified from diverse environments (Prevost et al., 2013) and the appearance of such species in the reactor could have contributed to the development of a psychrophilic proteolytic activity, as demonstrated in the protein degradation tests (Table 4). The Bacteroidetes were an abundant phylum in the reactor. They increased from relatively low starting levels (ca. 10%) to reach a relatively stable level of 20–30% of the biomass. The major classes present were the Bacteroidia, Sphingobacteria, and Flavobacteria. Bacteroidetes, like the Firmicutes, play important roles in the degradation of complex organic compounds. *Flavobacterium* species have been shown to degrade protein and to possess psychrophilic proteases (Zhang et al., 2011). The Chloroflexi were also present at high levels (6–12%) throughout the trial. The *Anaerolineaceae* were the dominant representative of the Chloroflexi phylum in this trial and are thought to play an important role in granulation (Yamada et al., 2005). Other phyla present included the Actinobacteria (1–7%), Fusobacteria, Acidobacteria, Caldibacteria, Nitrospirae, OP8, OP9, Synergistetes, and Planctomycetes. The analysis revealed the emergence from the initial inoculum, of a small proportion of polyP-accumulating organisms (PAOs), such as *Rhodococcus* (4% Phase 1 cDNA, negligible at the end of the trial) and *Acinetobacter* (from ~2% from Phase 3), in granular and filter biomass.

Archaeal populations

The phylum Euryarchaeota represented a large majority of the sequences identified from the biomass. A clear perturbation

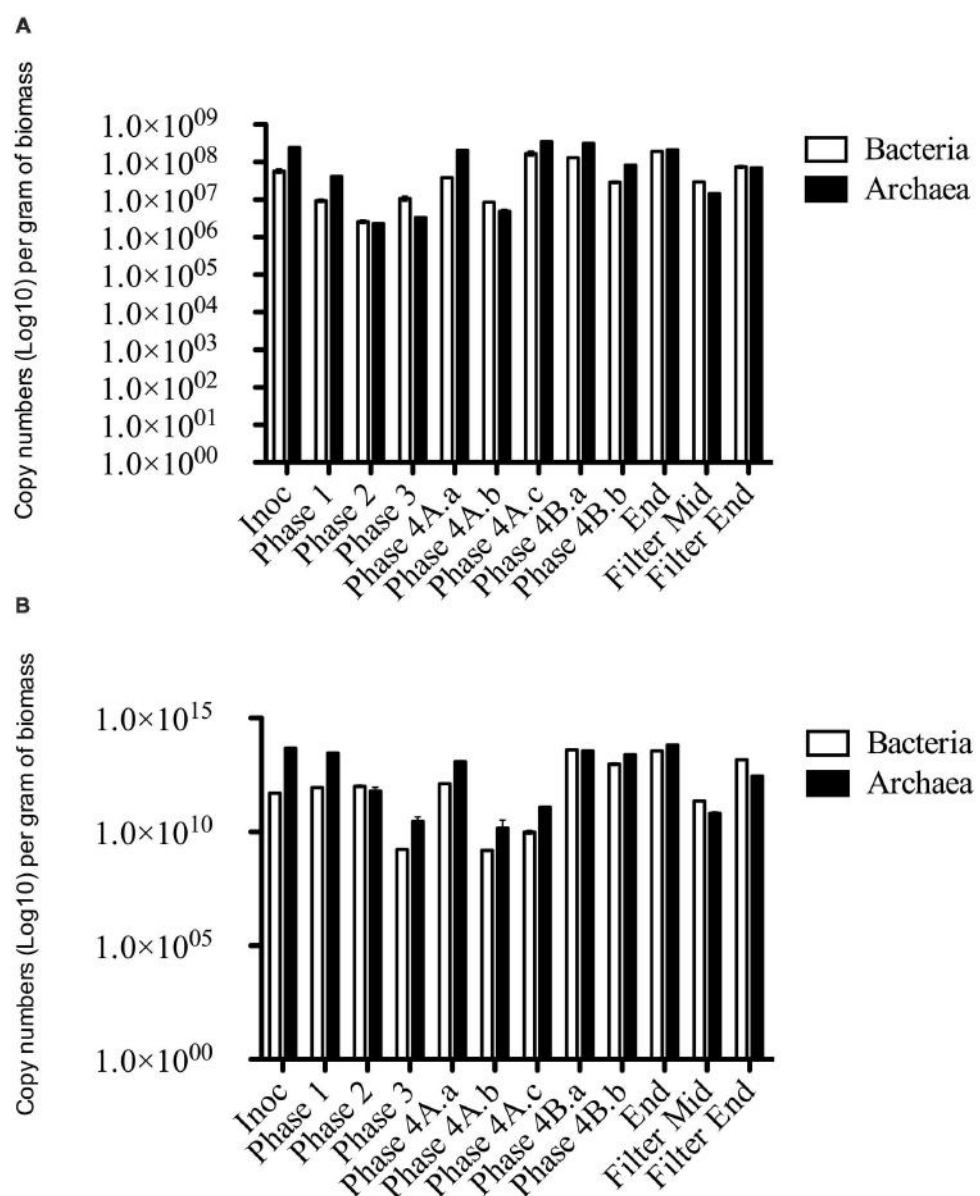
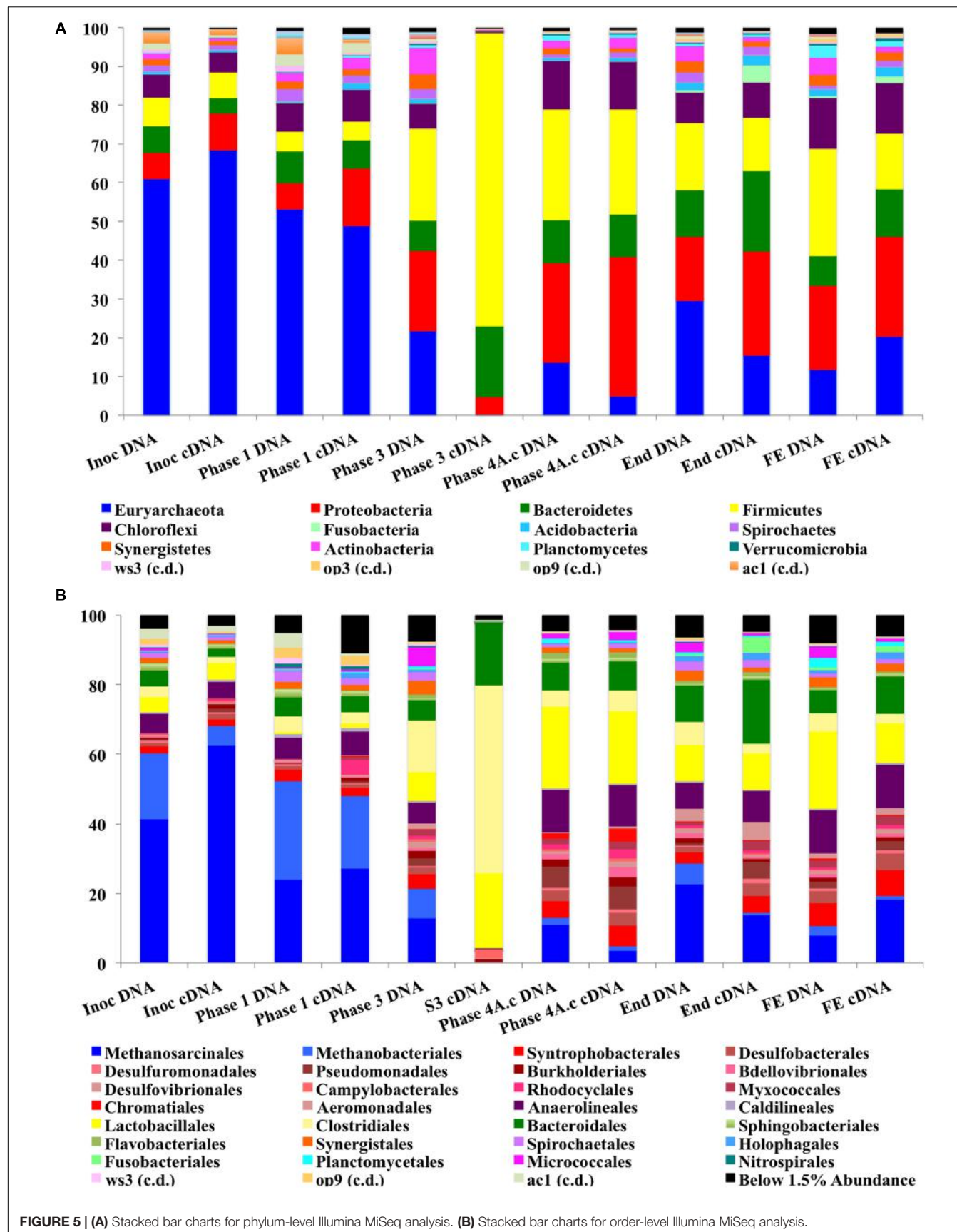


FIGURE 4 | qPCR data of Bacterial and Archaeal copy numbers (log scale) for (A) DNA and (B) cDNA from biomass samples throughout the trial.

was observed at the end of Phase 3, most notably observed in the cDNA sample (Phase 3; Day 301; **Figure 5A**). While the NGS data cannot be directly compared to the qPCR results, the qPCR data did indicate a ~3 log reduction in archaeal 16S rRNA gene copy numbers in this phase (**Figure 4**). The perturbation coincided with the deterioration of methanogenesis in the reactor, represented by an increase in the effluent VFA:COD ratio; no detectable acetoclastic- and greatly reduced hydrogenotrophic-SMA. Furthermore, an increase in acetic acid concentrations was observed with values reaching 24 mg l⁻¹ (data not shown).

The Methanosaetales dominated the archaeal community (55–75% of the population on a DNA basis and 68–88% on a

cDNA basis; **Figure 5B**). The genus *Methanosaeta* was the sole representative of the group. The dominance of *Methanosaeta* was not surprising since they have been found to dominate the methanogenic community in reactors during steady state conditions when acetate concentrations were low (Raskin et al., 1995). Although Methanosaetaceae dominated the consortium in the reactor, a decrease in the relative abundance of this group was observed at the end of Phase 1 (**Figure 5B**). At the same time, the proportion of the hydrogenotrophic orders Methanobacteriales and Methanomicrobiales increased, indicating the importance of methanogenesis via H₂/CO₂ in the reactor. The SMA data presented earlier supports this view, as do previous reports (McKeown et al., 2009;



O'Reilly et al., 2010). The increase in hydrogenotrophic methanogens and reduced acetotrophic methanogenesis, without acetate accumulation, may have been as a result of syntrophic acetate oxidation (Schnürer et al., 1996) whereby acetate is converted to hydrogen and CO₂ by homoacetogenic bacteria. The increase in Firmicutes in the next sampling point (Figure 5A), which include homoacetogenic species, may be linked to the disturbance seen as both aceto clastic and hydrogenotrophic methanogens decreased. Higher effluent acetate concentrations were seen at this point indicating that the homoacetogenic bacteria may have been generating acetate as the sole end product from H₂CO₂ or multicarbon compounds and thus, may have outcompeted the hydrogenotrophic methanogens. Homoacetogens have been reported to adapt to low temperature better than hydrogenotrophic methanogens (Kotsyurbenko et al., 2001). A drawback associated with the SMA method carried out is that this method does not account for homoacetogenic activity.

The NGS and SMA indicated a distinct disturbance to the archaeal community within the system during Phase 3. While the qPCR data supported this finding (with a decrease in archaeal numbers during Phase 3) the abundance data indicated that the archaeal community was quantitatively dominant for the majority of the trial. In fact, qPCR of Phase 3 cDNA indicated archaeal numbers were higher than bacterial numbers. qPCR has the advantage of being quantitative, specific and highly sensitive (Suzuki et al., 2000; Yu et al., 2005; Ritalahti et al., 2006). Thus, while there was a disturbance to the archaeal community they were still numerically abundant and active. There are inherent limitations to the interpretation and integration of the qPCR and sequencing data. The sequencing analysis, however, could be used to retrospectively target the microbial groups found through the development of specific primer sets.

CONCLUSION

We propose here a potentially important method for sequestration of phosphorus using luxury polyP uptake under anaerobic conditions previously not described in the literature. These findings support the idea that modified AD systems could provide the basis for significant recovery and reuse of phosphorus from wastewaters, a significant advance in AD

REFERENCES

- Aiyuk, S., and Verstraete, W. (2004). Sedimentological evolution in an UASB treating SYNTHES, a new representative synthetic sewage, at low loading rates. *Bioresour. Technol.* 93, 269–278. doi: 10.1016/j.biortech.2003.11.006
- APHA and AWWA (2005). "Aggregate organic constituents," in *Standard Methods for the Examination of Water and Wastewater*, 20th Edn, eds L. S. Clesceri, A. E. Greenberg, A. D. Eaton, (Washington, DC: American Public Health Association).
- Auerlik, K. S., Cooper, C. R., and Kelly, R. M. (2008). Life in hot acid: pathway analyses in extremely thermoacidophilic archaea. *Curr. Opin. Biotechnol.* 19, 445–453. doi: 10.1016/j.copbio.2008.08.001
- Bandara, W. M., Kindaichi, T., Satoh, H., Sasakawa, M., Nakahara, Y., Takahashi, M., and Okabe, S. (2011). Removal of residual dissolved methane gas in an upflow anaerobic sludge blanket reactor treating low-strength wastewater at low temperature with degassing membrane. *Water Res.* 45, 3533–3540. doi: 10.1016/j.watres.2011.04.030
- Banik, G. C., Viraraghavan, T., and Dague, R. R. (1998). Low temperature effects on anaerobic microbial kinetic parameters. *Environ. Technol.* 19, 503–512. doi: 10.1080/0959331908616706
- Barca, C., Gérante, C., Meyer, D., Chazarenc, F., and Andrès, Y. (2012). Phosphate removal from synthetic and real wastewater using steel slags produced in Europe. *Water Res.* 46, 2376–2384. doi: 10.1016/j.watres.2012.02.012
- Benzerara, K., Skouri-Panet, F., Li, J., Ferard, C., Gugger, M., Laurent, T., et al. (2014). Intracellular Ca-carbonate biominerization is widespread treatment technologies. However, the precise environmental and biological triggers that might promote the process of anaerobic P removal further; the exact role of the microbial biomass and the pumice filter unit; the mechanisms and conditions for anaerobic polyP formation and to what extent AD with P recovery can be developed toward a full-scale technological solution, remain to be elucidated. These questions should be a focus for on-going research efforts.

AUTHOR CONTRIBUTIONS

CK operated the reactor, processed all samples, generated all data, and interpreted all data. She also prepared the first draft of the manuscript and contributed to the further drafting and the finalized draft. JC and PM performed the ppx assays, the DAPI analysis on biomass throughout the trial and subsequently trained CK in the DAPI analysis. DC contributed to the design of the hydrolysis experiments and trained CK in the calculations. CS supported the design and interpretation of the microbial ecology experiments. DH designed the reactor system, contributed to the experimental design and drafting and editing of the manuscript. VOF and TM contributed to the interpretation of the reactor trial and the drafting and editing of the manuscript. JM was supervisor to the work with polyP. VO was the primary supervisor of the work.

FUNDING

This work was supported by the Science Foundation Ireland Charles Parsons Award (06_CP_E006), Investigator Programme Grant (14/IA/2371), Science Foundation Ireland (14/IA/2371), and the Irish Environmental Protection Agency (2014-W-LS-7). CJS is supported by Science Foundation Ireland Starting Investigator-COFUND fellowship (11/SIRG/B2159).

ACKNOWLEDGMENT

The authors wish to thank Aoife Duff and Eoin Gunnigle for the provision of culture strains.

- in cyanobacteria. *Proc. Natl. Acad. Sci. U.S.A.* 111, 10933–10938. doi: 10.1073/pnas.1403510111
- Bialek, K., Cysneiros, D., and O'Flaherty, V. (2013). Low-Temperature (10[[−3920]]C) anaerobic digestion of dilute dairy wastewater in an EGSB bioreactor: microbial community structure, population dynamics, and kinetics of methanogenic populations. *Archaea* 2013, 1–10. doi: 10.1155/2013/346171
- Bialek, K., Kumar, A., Mahony, T., Lens, P. N. L., and O' Flaherty, V. (2012). Microbial community structure and dynamics in anaerobic fluidized-bed and granular sludge-bed reactors: influence of operational temperature and reactor configuration. *Microbial. Biotechnol.* 5, 738–752. doi: 10.1111/j.1751-7915.2012.00364.x
- Blackall, L. L., Crocetti, G. R., Saunders, A. M., and Bond, P. L. (2002). A review and update of the microbiology of enhanced biological phosphorus removal in wastewater treatment plants. *Antonie Van Leeuwenhoek* 81, 681–691. doi: 10.1023/A:1020538429009
- Caporaso, J. G., Lauber, C. L., Walters, W. A., Berg-Lyons, D., Huntley, J., Fierer, N., et al. (2012). Ultra-high-throughput microbial community analysis on the Illumina HiSeq and MiSeq platforms. *ISME J.* 6, 1621–1624. doi: 10.1038/ismej.2012.8
- Caravelli, A. H., De Gregorio, C., and Zaritzky, N. E. (2012). Chemical Engineering Journal. *Chem. Eng. J.* 209, 469–477. doi: 10.1016/j.cej.2012.08.039
- Chu, L. B., Yang, F. L., and Zhang, X. W. (2005). Anaerobic treatment of domestic wastewater in a membrane-coupled expanded granular sludge bed (EGSB) reactor under moderate to low temperature. *Process Biochem.* 40, 1063–1070. doi: 10.1016/j.procbio.2004.03.010
- Coates, J. D., Coughlan, M. F., and Colleran, E. (1996). Simple method for the measurement of the hydrogenotrophic methanogenic activity of anaerobic sludges. *J. Microbiol. Methods* 26, 237–246. doi: 10.1016/0167-7012(96)00915-3
- Colleran, E., Concannon, F., and Golden, T. (1992). Use of methanogenic activity tests to characterize anaerobic sludges, screen for anaerobic biodegradability and determine toxicity thresholds against individual anaerobic tropic groups and species. *Water Sci. Technol.* 25, 31–40.
- Deinema, M. H., Habets, L. H. A., Scholten, J., Turkstra, E., and Webers, H. A. M. (1980). The accumulation of polyphosphate in *Acinetobacter* spp. *FEMS Microbiol. Lett.* 9, 275–279. doi: 10.1111/j.1574-6968.1980.tb05652.x
- DeSantis, T. Z., Hugenholtz, P., Larsen, N., Rojas, M., Brodie, E. L., Keller, K., et al. (2006). Greengenes, a chimera-checked 16S rRNA gene database and workbench compatible with ARB. *Appl. Environ. Microbiol.* 72, 5069–5072. doi: 10.1128/AEM.03006-05
- Dowd, S. E., Callaway, T. R., Wolcott, R. D., Sun, Y., McKeehan, T., Hagevoort, R. G., et al. (2008). Evaluation of the bacterial diversity in the feces of cattle using 16S rDNA bacterial tag-encoded FLX amplicon pyrosequencing (bTEFAP). *BMC Microbiol.* 8:125. doi: 10.1186/1471-2180-8-125
- DuBois, M., Gilles, K. A., Hamilton, J. K., Rebers, P. A., and Smith, F. (1956). Colorimetric method for determination of sugars and related substances. *Anal. Chem.* 28, 350–356. doi: 10.1021/ac60111a017
- Edgar, R. C. (2010). Search and clustering orders of magnitude faster than BLAST. *Bioinformatics* 26, 2460–2461. doi: 10.1093/bioinformatics/btq461
- Edgar, R. C., Haas, B. J., Clemente, J. C., Quince, C., and Knight, R. (2011). UCHIME improves sensitivity and speed of chimera detection. *Bioinformatics* 27, 2194–2200. doi: 10.1093/bioinformatics/btr381
- Gao, D.-W., Tao, Y., An, R., Fu, Y., and Ren, N. -Q. (2011). Fate of organic carbon in UAFB treating raw sewage: impact of moderate to low temperature. *Bioresour. Technol.* 102, 2248–2254. doi: 10.1016/j.biortech.2010.10.029
- Gilbert, N. (2009). Environment: the disappearing nutrient. *Nature* 461, 716–718. doi: 10.1038/461716a
- Griffiths, R. I., Whiteley, A. S., O'Donnell, A. G., and Bailey, M. J. (2000). Rapid method for coextraction of DNA and RNA from natural environments for analysis of ribosomal DNA- and rRNA-based microbial community composition. *Appl. Environ. Microbiol.* 66, 5488–5491. doi: 10.1128/AEM.66.12.5488-5491.2000
- Gunnigle, E., Siggins, A., Botting, C. H., Fuszard, M., O'Flaherty, V., and Abram, F. (2015). Low-temperature anaerobic digestion is associated with differential methanogenic protein expression. *FEMS Microbiol. Lett.* 362:fmv059. doi: 10.1093/femsle/fmv059
- Hartley, K., and Lant, P. (2006). Eliminating non-renewable CO₂ emissions from sewage treatment: an anaerobic migrating bed reactor pilot plant study. *Biotechnol. Bioeng.* 95, 384–398. doi: 10.1002/bit.20929
- Hauduc, H., Takács, I., Smith, S., Szabo, A., Murthy, S., Daigger, G. T., et al. (2015). *ScienceDirect. Water Res.* 73, 157–170. doi: 10.1016/j.watres.2014.12.053
- Hughes, D., Enright, A.-M., Mahony, T., and O'Flaherty, V. (2011). *Novel Anaerobic Sewage Treatment and Bioenergy Production: High-Rate Anaerobic Digestion as a Core Technology for Sustainable Treatment of Municipal and Low-Strength Industrial Wastewaters.* EPA STRIVE Report Series No. 64. Johnstown Castle: Environmental Protection Agency.
- Keating, C., Cysneiros, D., Mahony, T., and O' Flaherty, V. (2012). The hydrolysis and biogas production of complex cellulosic substrates using three anaerobic biomass sources. *Water Sci. Technol.* 67:293. doi: 10.2166/wst.2012.543
- Khan, A. A., Gaur, R. Z., Tyagi, V. K., Khursheed, A., Lew, B., Mehrotra, I., et al. (2011). Resources, conservation and recycling. *Resour. Conserv. Recycl.* 55, 1232–1251.
- Kotsyurbenko, O. R., Glagolev, M. V., Nozhevnikova, A. N., and Conrad, R. (2001). Competition between homoacetogenic bacteria and methanogenic archaea for hydrogen at low temperature. *FEMS Microbiol. Ecol.* 38, 153–159. doi: 10.1016/S0168-6496(01)00179-9
- Kulaev, I., and Kulakovskaya, T. (2000). Polyphosphate and phosphate pump. *Annu. Rev. Microbiol.* 54, 709–734. doi: 10.1146/annurev.micro.54.1.709
- Kulakovskaya, T. V., Lichko, L. P., and Ryazanova, L. P. (2015). Diversity of phosphorus reserves in microorganisms. *Biochem. Moscow* 79, 1602–1614. doi: 10.1134/S0006297914130100
- Lew, B., Tarre, S., Beliavski, M., and Green, M. (2009). Bioresource technology. *Bioresour. Technol.* 100, 6155–6162. doi: 10.1016/j.biortech.2009.06.073
- Lowry, O. C., Rosebrough, N., and Farr, A. (1951). Protein measurement with the Folin phenol reagent. *J. Biol. Chem.* 193, 265–275.
- Matsuura, N., Hatamoto, M., Sumino, H., Syutsubo, K., Yamaguchi, T., and Ohashi, A. (2015). Recovery and biological oxidation of dissolved methane in effluent from UASB treatment of municipal sewage using a two-stage closed downflow hanging sponge system. *J. Environ. Manage.* 151, 200–209. doi: 10.1016/j.jenvman.2014.12.026
- McCarty, P. L. (1964). Anaerobic waste treatment fundamentals. *Public Works* 95, 107–112.
- McGrath, J. W., and Quinn, J. P. (2003). Microbial phosphate removal and polyphosphate production from wastewaters. *Adv. Appl. Microbiol.* 52, 75–100. doi: 10.1016/S0065-2164(03)01003-7
- McHugh, S., Collins, G., and O'Flaherty, V. (2006). Long-term, high-rate anaerobic biological treatment of whey wastewaters at psychrophilic temperatures. *Bioresour. Technol.* 97, 1669–1678. doi: 10.1016/j.biortech.2005.07.020
- McKeown, R. M., Hughes, D., Collins, G., Mahony, T., and O'Flaherty, V. (2012). Low-temperature anaerobic digestion for wastewater treatment. *Curr. Opin. Biotechnol.* 23, 444–451. doi: 10.1016/j.copbio.2011.11.025
- McKeown, R. M., Scully, C., Enright, A. -M., Chinalia, F. A., Lee, C., Mahony, T., et al. (2009). Psychrophilic methanogenic community development during long-term cultivation of anaerobic granular biofilms. *ISME J.* 3, 1231–1242. doi: 10.1038/ismej.2009.67
- Motlagh, A. M., Bhattacharjee, A. S., and Goel, R. (2015). *ScienceDirect. Water Res.* 81, 1–14. doi: 10.1016/j.watres.2015.04.023
- Nelson, M. C., Morrison, M., and Yu, Z. (2011). Bioresource technology. *Bioresour. Technol.* 102, 3730–3739. doi: 10.1016/j.biortech.2010.11.119
- Onar, A. N., and Öztürk, B. (1993). Adsorption of phosphate onto pumice powder. *Environ. Technol.* 14, 1081–1087. doi: 10.1080/09593339309385385
- O'Reilly, J., Lee, C., Chinalia, F., Collins, G., Mahony, T., and O'Flaherty, V. (2010). Microbial community dynamics associated with biomass granulation in low-temperature (15 [[−3920]]C) anaerobic wastewater treatment bioreactors. *Bioresour. Technol.* 101, 6336–6344. doi: 10.1016/j.biortech.2010.03.049
- Orell, A., Navarro, C. A., Rivero, M., Aguilar, J. S., and Jerez, C. A. (2012). Inorganic polyphosphates in extremophiles and their possible functions. *Extremophiles* 16, 573–583. doi: 10.1007/s00792-012-0457-9
- Pauss, A., Andre, G., Perrier, M., and Guiot, S. R. (1990). Liquid-to-Gas mass transfer in anaerobic processes: inevitable transfer limitations of methane and hydrogen in the biomethanation process. *Appl. Environ. Microbiol.* 56, 1636–1644.
- Prevost, S., Cayol, J.-L., Zuber, F., Tholozan, J.-L., and Remize, F. (2013). Characterization of clostridial species and sulfite-reducing anaerobes isolated from foie gras with respect to microbial quality and safety. *Food Control* 32, 222–227. doi: 10.1016/j.foodcont.2012.11.030

- Raskin, L., Zheng, D., Griffin, M. E., Stroot, P. G., and Misra, P. (1995). Characterization of microbial communities in anaerobic bioreactors using molecular probes. *Antonie Van Leeuwenhoek* 68, 297–308. doi: 10.1007/BF00874140
- Regueiro, L., Carballa, M., and Lema, J. M. (2014). Outlining microbial community dynamics during temperature drop and subsequent recovery period in anaerobic co-digestion systems. *J. Biotechnol.* 192, 179–186. doi: 10.1016/j.biotech.2014.10.007
- Ritalahti, K. M., Amos, B. K., Sung, Y., Wu, Q., Koenigsberg, S. S., and Löffler, F. E. (2006). Quantitative PCR targeting 16S rRNA and reductive dehalogenase genes simultaneously monitors multiple Dehalococcoides strains. *Appl. Environ. Microbiol.* 72, 2765–2774. doi: 10.1128/AEM.72.4.2765-2774.2006
- Rudnick, H., Hendrich, S., Pilatus, U., and Blotevogel, K. -H. (1990). Phosphate accumulation and the occurrence of polyphosphates and cyclic 2,3-diphosphoglycerate in *Methanosarcina frisia*. *Arch. Microbiol.* 154, 584–588. doi: 10.1007/BF00248840
- Ryan, P., Forbes, C., McHugh, S., O'Reilly, C., Fleming, G. T. A., and Colleran, E. (2010). Enrichment of acetogenic bacteria in high rate anaerobic reactors under mesophilic and thermophilic conditions. *Water Res.* 44, 4261–4269. doi: 10.1016/j.watres.2010.05.033
- Sahdeo Prasad, A. K. T. (2014). Drug discovery inspired by mother nature for cancer therapy. *Biochem. Physiol.* 4:e128. doi: 10.4172/2168-9652.1000e128
- Schlegel, H. G., and Zaborosch, C. (1993). *General Microbiology*. Cambridge: Cambridge University Press.
- Schnürer, A., Schink, B., and Svensson, B. H. (1996). *Clostridium ultunense* sp. nov., a mesophilic bacterium oxidizing acetate in syntrophic association with a hydrogenotrophic methanogenic bacterium. *Int. J. Syst. Bacteriol.* 46, 1145–1152. doi: 10.1099/00207713-46-4-1145
- Smirnov, A. V., Kulakovskaya, T. V., and Kulaev, I. S. (2002). Phosphate accumulation by an extremely halophilic archae *Halobacterium salinarium*. *Process Biochem.* 37, 643–649. doi: 10.1016/S0032-9592(01)00250-3
- Smith, A. L., Dorner, H., Love, N. G., Skerlos, S. J., and Raskin, L. (2011). “Role of membrane biofilm in psychrophilic anaerobic membrane bioreactor for domestic wastewater treatment,” in *Proceeding of the 84th Annual Water Environment Federation Technical Exhibition and Conference*, Los Angeles, CA.
- Smith, A. L., Skerlos, S. J., and Raskin, L. (2013). Psychrophilic anaerobic membrane bioreactor treatment of domestic wastewater. *Water Res.* 47, 1655–1665. doi: 10.1016/j.watres.2012.12.028
- Smith, A. L., Stadler, L. B., Love, N. G., Skerlos, S. J., and Raskin, L. (2012). Perspectives on anaerobic membrane bioreactor treatment of domestic wastewater: a critical review. *Bioresour. Technol.* 122, 149–159. doi: 10.1016/j.biortech.2012.04.055
- Smith, C. J., Danilowicz, B. S., Clear, A. K., Costello, F. J., Wilson, B., and Meijer, W. G. (2005). T-Align, a web-based tool for comparison of multiple terminal restriction fragment length polymorphism profiles. *FEMS Microbiol. Ecol.* 54, 375–380. doi: 10.1016/j.femsec.2005.05.002
- Smith, C. J., Nedwell, D. B., Dong, L. F., and Osborn, A. M. (2006). Evaluation of quantitative polymerase chain reaction-based approaches for determining gene copy and gene transcript numbers in environmental samples. *Environ. Microbiol.* 8, 804–815. doi: 10.1111/j.1462-2920.2005.00963.x
- Souza, C. L., Chernicharo, C. A. L., and Aquino, S. F. (2011). Quantification of dissolved methane in UASB reactors treating domestic wastewater under different operating conditions. *Water Sci. Technol.* 64, 2259–2267. doi: 10.2166/wst.2011.695
- Suzuki, M. T., Taylor, L. T., and DeLong, E. F. (2000). Quantitative analysis of small-subunit rRNA genes in mixed microbial populations via 5'-nuclease assays. *Appl. Environ. Microbiol.* 66, 4605–4614. doi: 10.1128/AEM.66.11.4605-4614.2000
- Tervahauta, T., Bryant, I. M., Leal, L. H., Buisman, C. J., and Zeeman, G. (2014). Improved energy recovery by anaerobic grey water sludge treatment with black water. *Water* 6, 2436–2448. doi: 10.3390/w6082436
- Toso, D. B., Henstra, A. M., Gunsalus, R. P., and Zhou, Z. H. (2011). Structural, mass and elemental analyses of storage granules in methanogenic archaeal cells. *Environ. Microbiol.* 13, 2587–2599. doi: 10.1111/j.1462-2920.2011.02531.x
- Town, J. R., Links, M. G., Fonstad, T. A., and Dumonceaux, T. J. (2014). B Molecular characterization of anaerobic digester microbial communities identifies microorganisms that correlate to reactor performance. *Bioresour. Technol.* 151, 249–257. doi: 10.1016/j.biortech.2013.10.070
- Wang, C., and Pei, Y. (2013). Separation and purification technology. *Separat. Purif. Technol.* 117, 83–88. doi: 10.1016/j.seppur.2013.04.003
- Wang, X., Ji, M., Wang, J. F., Liu, Z., and Yang, Z. Y. (2006). Anaerobic uptake of phosphate in an anaerobic-aerobic granular sludge sequencing batch reactor. *Water Sci. Technol.* 53:63. doi: 10.2166/wst.2006.266
- Werner, J. J., Knights, D., Garcia, M. L., Scalfone, N. B., Smith, S., Yarasheski, K., et al. (2011). Bacterial community structures are unique and resilient in full-scale bioenergy systems. *Proc. Natl. Acad. Sci. U.S.A.* 108, 4158–4163. doi: 10.1073/pnas.1015676108
- Yamada, T., Sekiguchi, Y., Imachi, H., Kamagata, Y., Ohashi, A., and Harada, H. (2005). Diversity, localization, and physiological properties of filamentous microbes belonging to chloroflexi subphylum I in mesophilic and thermophilic methanogenic sludge granules. *Appl. Environ. Microbiol.* 71, 7493–7503. doi: 10.1128/AEM.71.11.7493-7503.2005
- Yu, S., Sun, P., Zheng, W., Chen, L., Zheng, X., Han, J., et al. (2014). Bioresource technology. *Bioresour. Technol.* 171, 80–87. doi: 10.1016/j.biortech.2014.08.057
- Yu, Y., Lee, C., Kim, J., and Hwang, S. (2005). Group-specific primer and probe sets to detect methanogenic communities using quantitative real-time polymerase chain reaction. *Biotechnol. Bioeng.* 89, 670–679. doi: 10.1002/bit.20347
- Zeng, W., Li, B., Yang, Y., Wang, X., Li, L., and Peng, Y. (2013). Impact of nitrite on aerobic phosphorus uptake by poly-phosphate accumulating organisms in enhanced biological phosphorus removal sludges. *Bioprocess Biosyst. Eng.* 37, 277–287. doi: 10.1007/s00449-013-0993-4
- Zhang, F., Blasius, L. C., Karolin, J. O., Powell, R. J., Geddes, C. D., and Hill, R. T. (2015). Phosphorus sequestration in the form of polyphosphate by microbial symbionts in marine sponges. *Proc. Natl. Acad. Sci. U.S.A.* 112, 4381–4386. doi: 10.1073/pnas.1423768112
- Zhang, L., Hendrickx, T. L., Kampman, C., Zeeman, G., Temmink, H., Li, W., et al. (2012). The effect of sludge recirculation rate on a UASB-digester treating domestic sewage at 15[–3920]°C. *Water Sci. Technol.* 66, 2597–2603. doi: 10.2166/wst.2012.487
- Zhang, S. C., Sun, M., Li, T., Wang, Q. H., Hao, J. H., Han, Y., et al. (2011). Structure analysis of a new psychrophilic marine protease. *PLoS ONE.* 6:e26939. doi: 10.1371/journal.pone.0026939

Conflict of Interest Statement: The authors declare that the research was conducted in the absence of any commercial or financial relationships that could be construed as a potential conflict of interest.

Copyright © 2016 Keating, Chin, Hughes, Manesiotti, Cysneiros, Mahony, Smith, McGrath and O’Flaherty. This is an open-access article distributed under the terms of the Creative Commons Attribution License (CC BY). The use, distribution or reproduction in other forums is permitted, provided the original author(s) or licensor are credited and that the original publication in this journal is cited, in accordance with accepted academic practice. No use, distribution or reproduction is permitted which does not comply with these terms.



Enhanced Anaerobic Digestion of Food Waste by Supplementing Trace Elements: Role of Selenium (VI) and Iron (II)

Javkhlan Ariunbaatar^{1*}, Giovanni Esposito¹, Daniel H. Yeh² and Piet N. L. Lens³

¹ Department of Civil and Mechanical Engineering, University of Cassino and Southern Lazio, Cassino, Italy, ² Department of Civil and Environmental Engineering, University of South Florida, Tampa, FL, USA, ³ UNESCO-IHE Institute for Water Education, Delft, Netherlands

OPEN ACCESS

Edited by:

Prayad Pokethitiyook,
Mahidol University, Thailand

Reviewed by:

Sabine Kleinsteuber,
Helmholtz Centre for Environmental
Research, Germany
Guy Robert Lanza,
State University of New York, USA

*Correspondence:

Javkhlan Ariunbaatar
javkhlan.ariunbaatar@gmail.com

Specialty section:

This article was submitted to
Microbiotechnology, Ecotoxicology
and Bioremediation,
a section of the journal
Frontiers in Environmental Science

Received: 24 November 2015

Accepted: 28 January 2016

Published: 18 February 2016

Citation:

Ariunbaatar J, Esposito G, Yeh DH
and Lens PNL (2016) Enhanced
Anaerobic Digestion of Food Waste by
Supplementing Trace Elements: Role
of Selenium (VI) and Iron (II).
Front. Environ. Sci. 4:8.
doi: 10.3389/fenvs.2016.00008

This paper discusses the potential to enhance the anaerobic digestion of food waste FW by supplementing trace elements (Fe, Co, Ni, Zn, Mn, Cu, Se, and Mo) individually as well as in cocktails. A series of batch experiments on the biomethane potential of synthetic food waste were performed with low (FW-A) and high (FW-B) trace element background concentrations prepared in, respectively, Delft (The Netherlands) and Tampa (Florida, USA). The most effective trace elements for FW-A were Fe with an increase of 39.2 ($\pm 0.6\%$) of biomethane production, followed by Se (34.1 $\pm 5.6\%$ increase), Ni (26.4 $\pm 0.2\%$ increase) and Co (23.8 $\pm 0.2\%$ increase). For FW-B supplementing these trace elements did not result in enhancement of the biomethane production, except for Se. FW-B had a Se concentration of 1.3 (± 0.5) $\mu\text{g/gTS}$, while it was below the detection limit for FW-A. Regardless of the FW source, Se resulted in 30–35% increase of biomethane production at a concentration range of 25–50 $\mu\text{g/L}$ (0.32–0.63 μM). Volatile fatty acids analysis revealed that TE supplementation enhances their consumption, thus yielding a higher biomethane production. Moreover, additional experiments on sulfide inhibition showed the enhancing effects of trace elements on the anaerobic digestion of food waste were not related with sulfide toxicity, but with the enzymatic reactions and/or microbial biomass aggregation.

Keywords: anaerobic digestion, food waste, trace element requirement, sulfide inhibition, selenium, iron

INTRODUCTION

Food waste (FW) is the largest fraction of municipal solid waste, and it was estimated that 1.3 billion tons of food is wasted every year (FAO, 2011). At present the most common FW stabilization technology is still landfilling. Landfilling is strongly discouraged by legislations such as the EU Directives on Landfill (1999/31/EC) and the Waste Framework (2006/12/EC), as it utilizes huge land areas and contributes to further environmental impacts including soil and groundwater pollution, greenhouse gases emissions (Ariunbaatar et al., 2014). Besides the environmental issues associated with FW, it is worth mentioning that 250 km³ of water and 28% of the world's agricultural area is used for the production of the 1.3 billion tons of FW (Parfit et al., 2010). It is thus important to recover and/or recycle waste to endorse responsible usage of natural resources. Therefore, anaerobic digestion (AD) of FW has become an important research field, as it couples

waste stabilization to the production of energy as well as fertilizer (Zhang et al., 2011; Ariunbaatar et al., 2014).

FW contains easily biodegradable solids and a high water content, thus it serves as a perfect substrate for AD. Nevertheless, previous studies have shown that regardless of the inoculum origin, a prolonged operation of AD on FW, even at low organic loading rates, could suffer from instability due to the increased inhibition by volatile fatty acids (VFA), ammonia and/or sulfide (Demirel and Scherer, 2011; Zhang et al., 2015). This instability is often linked with the lack of micronutrients or trace elements (TE; Demirel and Scherer, 2011; Banks et al., 2012; Zhang et al., 2015). The effects of TE to recover anaerobic digesters from failure have been studied extensively (Zhang et al., 2015). Supplementing TE does not only prevent and/or recover an inhibition; it can also enhance the AD process and yield a higher biomethane production.

To understand the roles of TE in an anaerobic system, the biochemical reaction and the anaerobic food web have always been the core of the research. It is well known that in anaerobic processes, TE generally act as: (1) micronutrients for various enzymatic reactions as co-factors; (2) promoters of microbial aggregation, which leads to an enhanced activity of the anaerobic microbes in case of syntrophy; (3) agents binding carriers-proteins and/or nutrients such as phosphates; (4) help to overcome sulfide toxicity through metal sulfide precipitation; (5) at higher concentrations TE can become toxicants to the microbial biomass (Takashima and Speece, 1989; Oleszkiewicz and Sharma, 1990; De Vrieze et al., 2013). These various effects of the TE depend on the environmental conditions, the background concentrations, bioavailability, and microbial uptake. Bioavailability of TE is often correlated with their speciation, which is the distribution of an element amongst different chemical species in a system (Worms et al., 2006; Ortner et al., 2015).

Various concentrations of different TE have been studied for the AD of FW. For instance, Zhang et al. (2011) used supplements of trace metals (Fe, Co, Mo, and Ni) to stabilize a single-stage reactor treating FW, and concluded that Fe was the most effective metal for a stable AD of FW. Similarly, De Vrieze et al. (2013) obtained a higher methane production from co-digestion of FW with an iron-rich activated sludge. Banks et al. (2012) found that adding Se and Co could recover a FW digester suffering from a propionic acid accumulation due to elevated ammonium concentrations. Facchin et al. (2013) achieved a 45–65% higher methane production yield from FW with supplementation of TE (Co, Mo, Ni, Se, and W) cocktail, and stressed the importance of Se and Mo for the biomethane production. Qiang et al. (2012) studied the requirements of Fe, Co, Ni for high-solid FW digestion ($6.3 \text{ kgCOD/m}^3 \cdot \text{d}$); and calculated the theoretical values of Fe, Co, and Ni per gram of chemical oxygen demand (COD) of the FW to be 200.0, 6.0, and 5.7 mg/kgCOD, respectively. Nevertheless, none of the studies carried out a systematic experiment on the trace element benchmark concentrations for an enhancement or an inhibition of the biomethane production from FW.

This research aims at investigating the concentration range of the TE for an inhibition or enhancement for a typical

FW prepared in Delft (The Netherlands). A series of batch experiments on the biomethane potential (BMP) of a synthetic FW was conducted by supplementing cocktails of TE including cobalt, nickel, copper, manganese, iron, zinc, selenium, and molybdenum. The first set of BMP tests focused on the optimum concentrations of the TE supplementation for an enhancement of the BMP. The next set of experiments was carried out to determine the different effects of the TE individually or in groups. A follow-up experiment on the most important TE was conducted with FW prepared in Tampa (USA) using the same inoculum and experimental conditions. An additional experiment on hydrogen sulfide inhibition was conducted to elaborate the potential role of TE in alleviating hydrogen sulfide toxicity in the anaerobic process.

MATERIALS AND METHODS

Substrate and Inoculum

FW composition varies on many factors such as the region, season, culture, economic income, and demographics. To reduce experimental bias, the substrate used for this research was synthetically generated based on an average compositional analysis of FW in the EU, as it was used in previous research (Ariunbaatar et al., 2014, 2015). It contained 79% fruits and vegetables, 5% pasta and rice, 6% bread and bakery, 8% meat and fish, 2% dairy product (Ariunbaatar et al., 2014, 2015). A fresh substrate was prepared for each set of experiment using food bought from local supermarkets in Delft, The Netherlands (Albert Heijn) and Tampa, USA (Walmart). Although the same ingredients were used, the synthetic FW-A (prepared in Delft, The Netherlands) and FW-B (prepared in Tampa, USA) had differences in the TE background concentrations.

For all experiments, the same digestate from a full-scale mesophilic AD plant located in Capaccio-Salerno (Italy) was used as inoculum. The plant treats the buffalo dung together with the milk whey and sewage sludge generated from the mozzarella producing industry. It was used previously in studies of Ariunbaatar et al. (2014, 2015) and Liotta et al. (2015).

Biomethane Potential Tests

The biomethane potential (BMP) test of FW was conducted in duplicate serum bottles as described by Ariunbaatar et al. (2014, 2015). The substrate to inoculum ratio was 0.5 gVS/gVS. Prior to starting the BMP test in an incubator controlled at mesophilic condition ($35 \pm 2^\circ\text{C}$), all BMP test bottles were flushed with nitrogen (or helium) gas to ensure anaerobic conditions. To maintain the initial total alkalinity (3.5–4.0 gCaCO₃/L) of the inoculum, sodium bicarbonate (NaHCO₃) was added to each bottle. The daily biomethane production was measured with the liquid displacement method using sodium hydroxide (120 g/L) to absorb the carbon dioxide. The BMP test was continued for 20 days, as most (80–85%) of the organics are converted to biomethane and the AD process reaches a plateau (Ariunbaatar et al., 2014, 2015). The normalized specific biomethane production (SBP) was calculated using the

TABLE 1 | Trace elements groups used in this research.

TE category	Oxidation state	Group number*	TE tested
Metals	TE (II)	1	Co; Ni
		2	Co; Ni; Fe
		3	Co; Ni; Fe; Zn
		4	Co; Ni; Fe; Zn; Mn; Cu
Transition metals and/or metalloids	TE (VI)	–	Se; Mo

*Group number refer to TE mixture.

net cumulative biomethane production (after deducting the biomethane production of the blank, i.e., the inoculum without substrate) and the initial VS added.

The first set of experiments was carried out to determine the concentration ranges for inhibition or enhancement of the AD process by adding a cocktail solution of TE. A stock solution of each TE ($\text{NiCl}_2 \cdot 6\text{H}_2\text{O}$, $\text{CuCl}_2 \cdot 2\text{H}_2\text{O}$, $\text{MnCl}_2 \cdot 2\text{H}_2\text{O}$, $\text{FeCl}_2 \cdot 4\text{H}_2\text{O}$, $\text{CoCl}_2 \cdot 6\text{H}_2\text{O}$, ZnCl_2 , Na_2SeO_4 , Na_2MoO_4) was prepared. A cocktail solution containing all the TE was added to the bottles in eight different concentrations (5, 10, 50, 100, 500 $\mu\text{g/L}$, and 1, 3, 10 mg/L). After determining the optimum enhancement concentration, a second set of experiments was carried out focusing on the different effects of the TE by grouping them based on their elemental category and/or their oxidation state as shown in **Table 1**. The effects of supplementing four different groups of TE (II): (1) Co, Ni; (2) Co, Ni, Fe; (3) Co, Ni, Fe, Zn; and (4) Co, Ni, Fe, Zn, Mn, and Cu were studied (**Table 1**). The effect of TE, which resulted in the highest BMP was also tested individually.

Different concentrations of sodium sulfide (corresponding to 50, 75, 150, 250, and 500 mg $\text{H}_2\text{S}/\text{L}$) were added in the serum bottles to perform the batch experiment on the hydrogen sulfide inhibition of the BMP tests of FW.

Analytical Methods

Total solids (TS) and volatile solids (VS) were conducted in triplicates according to the standard methods¹, and the ashes were preserved with 1% nitric acid. Total TE concentration was analyzed in ash samples by Thermo-Scientific ICP-MS. The minimum detection limit for the ICP-MS method was 2 $\mu\text{g/L}$, and the final values were converted to $\mu\text{g/gTS}$ for comparison with the literature. Hydrogen sulfide and volatile fatty acids (VFA) samples were taken every 4 days from the liquid fraction. Hydrogen sulfide concentrations were measured with Hach test kits following the manufacturer's guidelines (HACH, Loveland, Colorado, USA). The VFA samples were prepared in 2% formic acid and analyzed by gas chromatography (Varian 430-GC) equipped with a Nukol Supelco FID column, using helium as a carrier gas as described by Mussoline et al. (2013).

¹APHA, Standard Methods for the Examination of Water and Wastewater 21st Edn. ISBN: 0875530478.

TABLE 2 | Concentration of TE in the FW and inoculum.

	Buffalo manure ($\mu\text{g/gTS}$)	FW-A ($\mu\text{g/gTS}$)	FW-B ($\mu\text{g/gTS}$)
Fe	682.72 \pm 28.78	213.91 \pm 24.50	510.93 \pm 7.34
Ni	4.93 \pm 0.05	3.97 \pm 1.32	11.25 \pm 0.95
Mn	107.78 \pm 26.88	52.12 \pm 5.10	20.33 \pm 5.86
Co	1.35 \pm 0.45	0.73 \pm 0.07	2.73 \pm 0.08
Cu	28.72 \pm 22.07	3.97 \pm 0.66	22.27 \pm 4.65
Zn	214.42 \pm 137.72	239.07 \pm 33.77	361.34 \pm 4.27
Se	4.81 \pm 0.06	BDL	1.34 \pm 0.45
Mo	7.32 \pm 2.41	1.99 \pm 0.66	10.67 \pm 5.70
W	<0.03	N/A	0.43 \pm 0.02

BDL, below detection limit; N/A, not analyzed.

RESULTS

Characterization of Substrate and Inoculum

The TS and VS concentrations of the synthetic FW were 24.1 (± 0.4)% and 21.9 (± 0.1)%, respectively, whereas the inoculum contained 2.5 (± 0.5)% of TS and 1.5 (± 0.4)% of VS. **Table 2** shows the concentrations of the TE in the FW and inoculum. Interestingly FW-B (prepared in USA) had a much higher concentration of all TE, except for manganese (Mn), regardless that the same ingredients were used for the FW preparation. It is also interesting to note that selenium (Se) was not detected in FW-A, but was present at 1.3 (± 0.5) $\mu\text{g/gTS}$ in FW-B (**Table 2**).

Effect of TE Concentration on AD of FW-A

The control (with no TE addition) of FW-A had a net SBP of 421.2 (± 14.6) $\text{mlCH}_4/\text{gVS}_{\text{added}}$. **Table 3** shows the cocktail solution concentration and its enhancing or inhibiting effects on the net SBP of FW-A. It can be seen that supplementing a TE cocktail solution of 5–500 $\mu\text{g/L}$ to the BMP test bottles yielded an enhancement of the AD process, while higher concentrations resulted in an inhibition of the AD process (**Table 3A**).

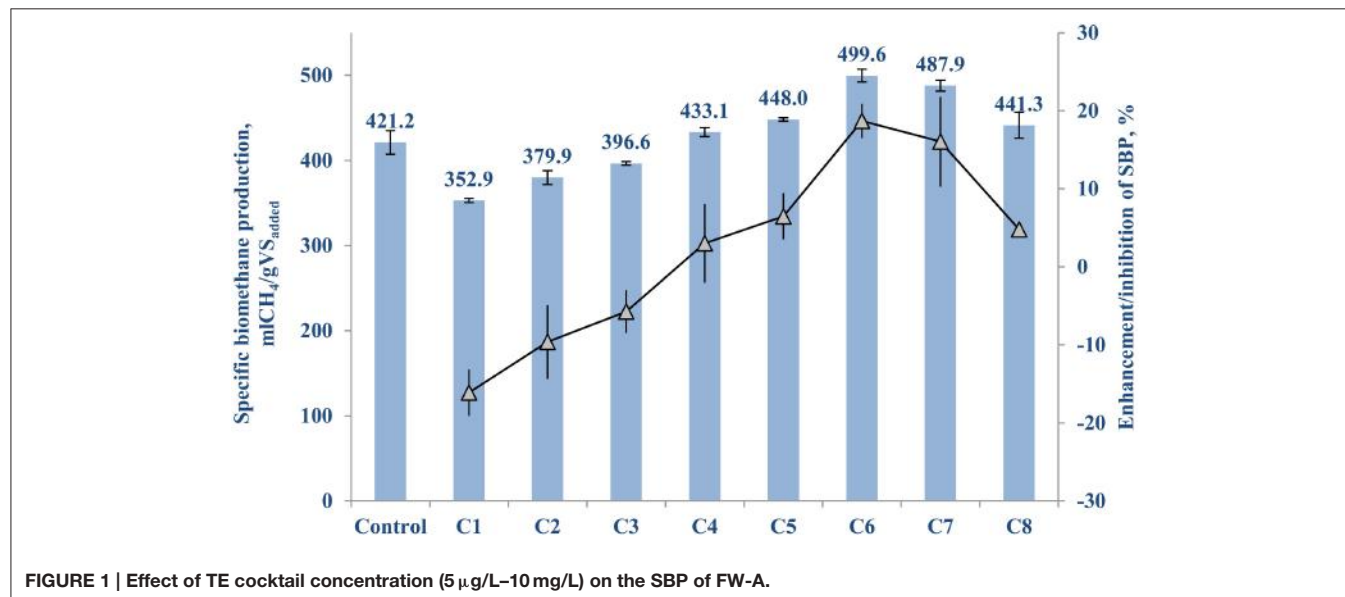
Figure 1 shows the highest SBP results of 499.6 (± 8.0) $\text{mlCH}_4/\text{gVS}_{\text{added}}$ and 489.9 (± 7.3) $\text{mlCH}_4/\text{gVS}_{\text{added}}$ were achieved with a supplementation of 50 and 10 $\mu\text{g/L}$ of TE cocktails, respectively, which are 18.7 (± 2.2)% and 16.0 (± 5.8)% higher than the control. Hence, the optimum TE supplementation concentration range is between 10 and 50 $\mu\text{g/L}$ for this particular type of inoculum and FW (**Table 3A** and **Figure 1**).

Table 3B shows the concentrations of the individual TE for the second set of experiment. **Figure 2** illustrates the highest enhancement was achieved with the second (Co, Ni, Fe) and third (Co, Ni, Fe, Zn) cocktail solutions, with a SBP of 481.3 (± 10.1) $\text{mlCH}_4/\text{gVS}_{\text{added}}$ and 472.4 (± 8.0) $\text{mlCH}_4/\text{gVS}_{\text{added}}$, respectively. The increase of SBP by the first and fourth groups of TE was almost similar with negligible differences (459.9 \pm 8.9 and 462.8 \pm 12.4 $\text{mlCH}_4/\text{gVS}_{\text{added}}$), which implies the cobalt, nickel, iron and zinc cocktail had a more positive effect than manganese and copper addition. Hence, the next set of experiments was

TABLE 3 | Effect of TE concentrations on the net SBP of FW-A: (A) First set of experiment; and (B) Second set of experiment.

(A)										
Cocktail solution	Concentration	Individual TE ($\mu\text{g/L}$)	Ni (μM)	Cu (μM)	Mn (μM)	Fe (μM)	Co (μM)	Zn (μM)	Se (μM)	Mo (μM)
C1	10 mg/L	1250	21.29	20	23	22	21	19	16	13
C2	3 mg/L	375	6.39	5.86	6.82	6.70	6.36	5.73	4.75	3.91
C3	1 mg/L	125	2.13	1.95	2.27	2.23	2.12	1.91	1.58	1.30
C4	500 $\mu\text{g/L}$	62.5	1.06	0.98	1.14	1.12	1.06	0.96	0.79	0.65
C5	100 $\mu\text{g/L}$	12.5	0.21	0.20	0.23	0.22	0.21	0.19	0.16	0.13
C6	50 $\mu\text{g/L}$	6.25	0.11	0.10	0.11	0.11	0.11	0.10	0.08	0.07
C7	10 $\mu\text{g/L}$	1.25	0.02	0.02	0.02	0.02	0.02	0.02	0.02	0.01
C8	5 $\mu\text{g/L}$	0.625	0.01	0.01	0.01	0.01	0.01	0.01	0.01	0.01

(B)		TE in the cocktail solution	Concentrations of individual TE (μM)							
Group number	Ni	Co	Fe	Zn	Cu	Mn	Se	Mo		
1	Co; Ni	0.43	0.42	–	–	–	–	–	–	
2	Co; Ni; Fe	0.28	0.28	0.30	–	–	–	–	–	
3	Co; Ni; Fe; Zn	0.21	0.21	0.22	0.19	–	–	–	–	
4	Co; Ni; Fe; Zn; Mn; Cu	0.14	0.14	0.15	0.13	0.13	0.15	–	–	
–	Se; Mo	–	–	–	–	–	0.32	0.26		

**FIGURE 1 | Effect of TE cocktail concentration (5 $\mu\text{g/L}$ –10 mg/L) on the SBP of FW-A.**

carried out to determine the individual effect of this third group of TE on the BMP of FW, i.e., Co (II), Ni (II), Fe (II), and Zn (II).

Figure 3A shows the cumulative biomethane production curves of the BMP bottles supplied with 50 $\mu\text{g/L}$ solutions of Fe (0.89 μM), Zn (0.76 μM), Ni (0.85 μM), and Co (0.85 μM) each. Each of them yielded at least a 18% higher biomethane production than the control. **Figure 3B** shows the Fe (II) supplementation yielded a remarkable 39.2 (± 0.6)% higher SBP, followed by nickel and cobalt with a 23–26% increase.

Another set of experiments was carried out supplementing TE with oxidation state of six, i.e., transition metals [Mo (VI)] or

metalloid [Se (VI)] as a cocktail (**Table 1**) as well as individually (**Figure 4**). Adding only Se (VI) to the bottles yielded a notable SBP increase of 34.1 (± 5.6)% (**Figure 4B**), whereas Mo (VI) had an inhibitory effect (data not presented). Supplementing a cocktail of TE (VI) had a relatively poor SBP increase of 9.5 (± 1.3)%, which can be attributed mostly to the Se (VI) effect.

Se (VI) and Fe (II) supplementation resulted in the highest ($>30\%$) enhancement of the BMP of FW-A (**Figures 3, 4**), thus the detailed VFA analysis of these samples was studied. **Figure 5** shows the samples with the Fe (II) and Se (VI) supplementation had much lower acetic, propionic, iso-butyric and butyric acids

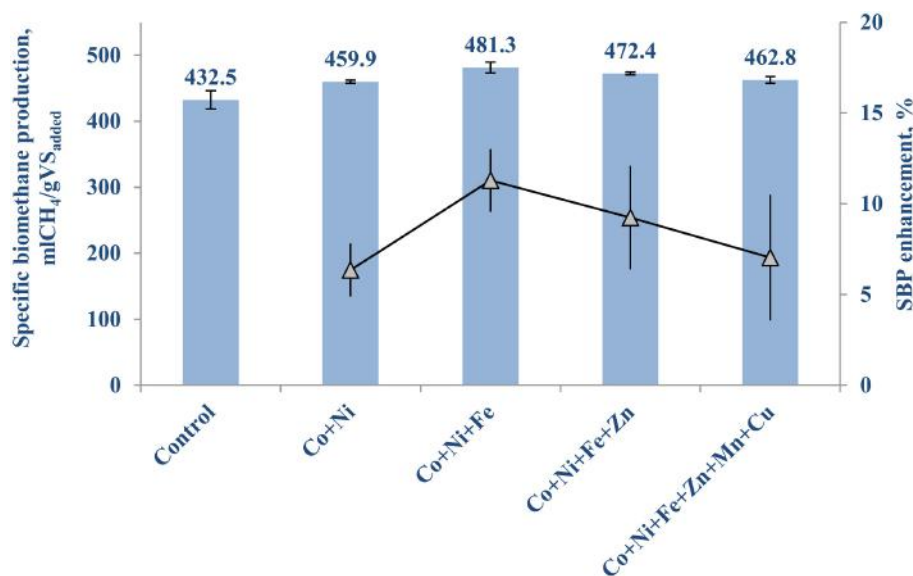


FIGURE 2 | Effect of TE (II) on the SBP of FW-A.

concentrations as compared to the control. On the first day of the BMP test, both iron, and selenium supplemented bottles had a similar (442.9 and 465.1 mg/L) acetic acid concentration, which is twice as less as the concentration in the control (893.2 mg/L). On day 5, the acetic acid concentration decreased to 148.7 mg/L in the BMP test with iron supplementation, whereas it increased to 562.7 mg/L in the bottle with selenium supplementation. The acetic acid concentration gradually decreased in all the BMP test bottles with time (Figure 5). The propionic acid concentration in the control was higher (279.3 mg/L) as compared to the propionic acid concentration in the iron (173.5 mg/L) and selenium (112.1 mg/L) supplemented bottles. It should also be stressed that throughout the experiment the propionic acid concentration was much lower in the selenium supplemented incubations.

Effect of TE Supplementation on FW-B

The net SBP of the FW-B was $412.5 (\pm 12.0)$ $\text{mlCH}_4/\text{gVS}_{\text{added}}$, which is comparable with the SBP obtained with FW in EU. Surprisingly, supplementation of TE did not yield any enhancement of the biomethane production (data not presented). Only the case of Se (VI) addition of $10\text{--}20 \mu\text{g/L}$ ($0.13\text{--}0.25 \mu\text{M}$) yielded a $30.1 (\pm 2.4)\%$ increase of biomethane production (Figure 6).

Hydrogen Sulfide Inhibition on FW-B

Figure 7 shows the sulfide inhibition of the AD of FW-B starts around 50 mg/L, resulting in $5.13 (\pm 2.76)\%$ less SBP. Based on the SBP results and the hydrogen sulfide concentrations, the IC_{50} was calculated as 215 mg/L at pH of 6.4–8.0. The maximal hydrogen sulfide concentration obtained in all the tested scenarios with TE as well as the control for FW-B, was less than 15 mg/L in the system throughout the experiment.

DISCUSSION

Importance of TE Supplementation on AD of FW

This study showed that the background TE concentration of FW determines the enhancement of the BMP of FW (Table 4). The net SBP of FW-A and FW-B were $421.2 (\pm 14.6)$ $\text{mlCH}_4/\text{gVS}_{\text{added}}$ and $412.5 (\pm 12.0)$ $\text{mlCH}_4/\text{gVS}_{\text{added}}$, respectively, which is in a good agreement with the literature (Banks et al., 2012; De Vrieze et al., 2013; Ariunbaatar et al., 2014, 2015). The effect of TE addition had nevertheless a different effect on FW-A and FW-B, due to their different TE background concentration (Table 2).

The importance of the trace metals Fe, Ni, Co and the metalloid Se was very clear for FW-A with low TE concentration, while only Se addition had enhancing effect on FW-B with high TE background concentration (Table 4). Similarly Lindorfer et al. (2012) reported that samples from exclusive digestion of FW and food production wastes from single sources in Germany and Austria showed a low concentration of several TE, including Cu, Ni, Zn, Co, Mn, Mo, Se, and W.

Hydrogen sulfide, produced by degradation of sulfur containing amino acids or dissimilarity sulfate reduction using sulfate present in the initial substrate, is highly toxic to microorganisms, as it forms an inactive protein, metal complexation, and interferes with key metabolic enzymes in the cells (Karhadkar et al., 1987; Zandvoort et al., 2006; Chen et al., 2014). Therefore, the experiment on sulfide inhibition was conducted (Figure 7) and the calculated IC_{50} was in the range of the reported values of 125–250 mg/L (Koster et al., 1986; Oleszkiewicz et al., 1989; Chen et al., 2008). However, no difference in the hydrogen sulfide concentration was observed between the control and the TE supplemented incubations (50 $\mu\text{g/L}$). The hydrogen sulfide concentrations (15 mg/L) that

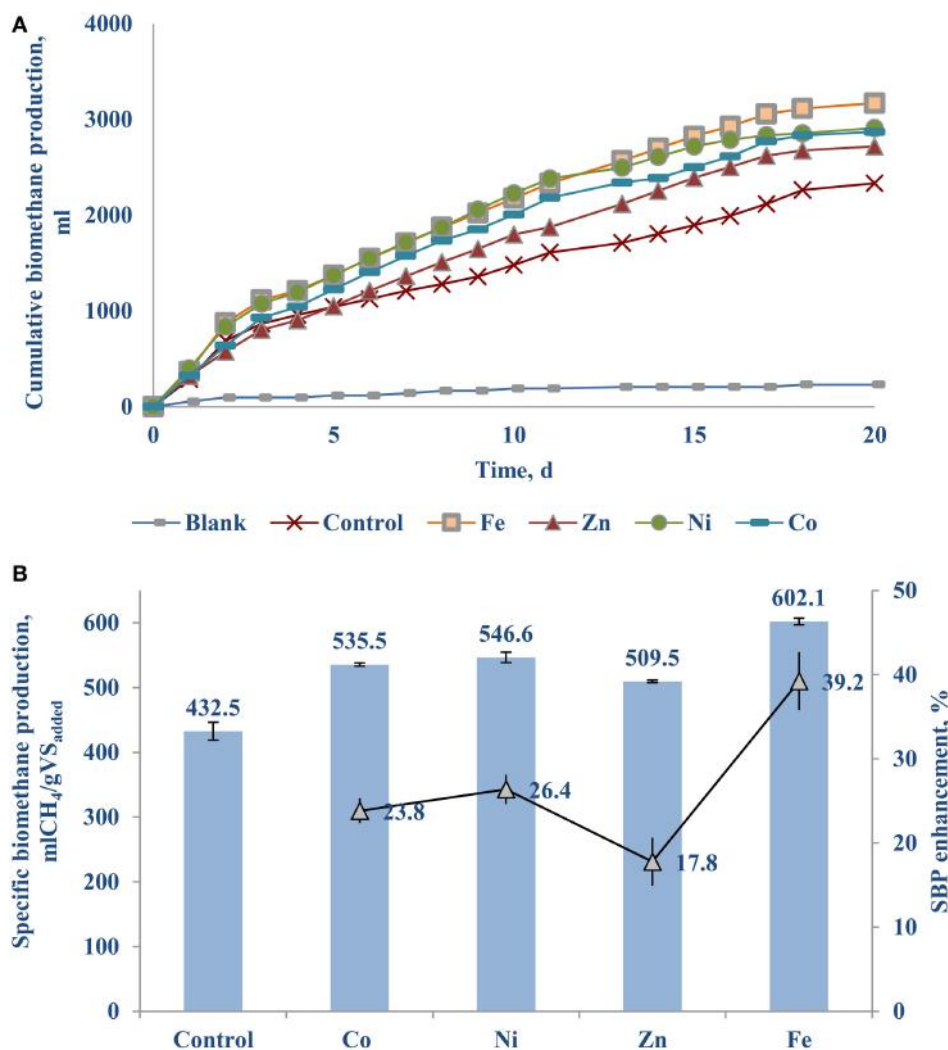


FIGURE 3 | The individual effect of Fe, Zn, Ni, and Co on the BMP of FW-A: (A) Cumulative methane curves; and (B) SBP.

developed in the BMP tests were much lower than the inhibitory level (**Figure 7**) throughout the experiment, suggesting that there was no hydrogen sulfide inhibition in the AD of FW. Ortner et al. (2014) also observed no sulfide inhibition with AD treating slaughterhouse waste. Hence, the enhanced SBP due to addition of TE was not related with sulfide, but rather with the enzymatic reactions (physiological contribution; Oleszkiewicz and Sharma, 1990; Glass and Orphan, 2012; Thanh et al., 2015) and/or the aggregation of microbial biomass promoting interspecies electron transfer (Oleszkiewicz and Sharma, 1990; Thanh et al., 2015).

Roles of Fe (II) and Se (VI) on the AD of FW

This study elucidated the most important TE (II) were Fe > Ni > Co for the AD of FW-A (**Figures 2, 3**). It corresponds with the order of the most commonly found TE concentrations (Fe >> Zn ≥ Ni > Co = Mo > Cu) in methanogenic archaea (Takashima and Speece, 1989). The performance of the AD process fed with

FW can indeed be enhanced by supplementing Fe (II) (Qiang et al., 2012, 2013; De Vrieze et al., 2013).

Regardless of the biochemical pathways to produce methane, almost every metalloenzyme involved in the methanogenesis contains Fe (Glass and Orphan, 2012), whereas Co and Ni are contained only in some of the essential metalloenzymes such as CO dehydrogenase, acetyl-CoA decarbonylase, methyl-H4SPT:HS-CoM methyl-transferase, methyl-CoM reductase (Oleszkiewicz and Sharma, 1990; Zandvoort et al., 2006; Pobeheim et al., 2011; Glass and Orphan, 2012; Nordell et al., 2016). Besides, the crucial roles of Fe in metalloenzymes, high concentrations of Fe supplementation are an important factor for other TE speciation and solubility, particularly for Ni and Co (Shakeri Yekta et al., 2014). Therefore, supplementing Fe (0.89 μM for FW-A) resulted in the stimulation of the overall microbial activities and thus a quick consumption of VFA (**Figure 5**) and an increased SBP (**Figure 3**). Nevertheless, addition of Fe for FW-B

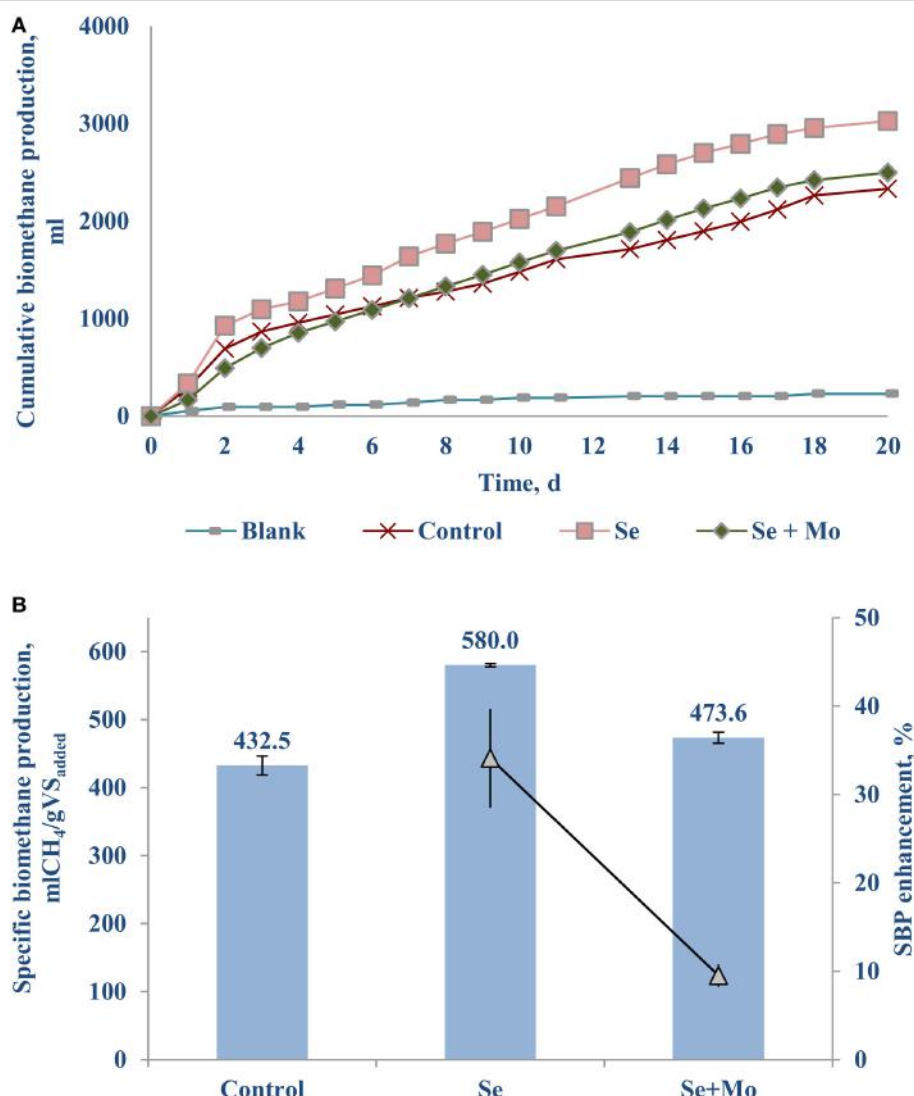


FIGURE 4 | Effect of TE (VI) on the SBP of FW-A: (A) Cumulative methane curves; and (B) SBP.

did not result in enhancement or inhibition of the AD process. Interestingly, the total concentration of Fe in FW-B (**Table 1**) is almost similar to the inhibitory level of the FW-A (**Table 3**), which indicates only some of the Fe in FW-B was bioavailable.

Selenium was not detected in FW-A, and was present only in low concentrations in FW-B (**Table 1**). This study showed that Se (VI) of the AD of FW is as important as Fe (II) for the AD of FW. The crucial roles of Se (VI) have been stressed by several recent studies (Banks et al., 2012; Facchin et al., 2013; Yirong et al., 2015; Zhang et al., 2015). Supplementing Se (VI) reduced both the acetic and propionic acid concentrations in the batch incubation, thus enhancing the biomethane production by more than 30% (**Figures 4–6**). It indicates that Se is involved in common hydrogenases (Oleszkiewicz and Sharma, 1990), provides co-enzymes necessary for propionate oxidation and

syntrophic hydrogenotrophic methanogenesis (Banks et al., 2012; Yirong et al., 2015). Besides, selenocysteine (Sec) has been recognized as the 21st amino acid, and a constituent of at least 25 proteins, named selenoproteins, present in all living systems from Archaea, Bacteria, and Eukarya (Nanchariah and Lens, 2015). Thus, lack of Se can slow down the AD process. The biochemical role of Se in stimulating AD of FW should be further studied using expression of the hydrogenases as a function of TE concentration as done by Worm et al. (2009).

The optimal Se concentration for AD of FW was determined in the range of 25–50 µg/L (0.32–0.64 µM). Se was not detected in FW-A, whereas it was 1.34 (±0.45) µg/gTS in FW-B. Thus, less Se supplementation was required for the AD of FW-B to achieve the same enhancement of the biomethane production (**Tables 1, 4, Figures 4, 6**). This indicates the lack of Se in local food can

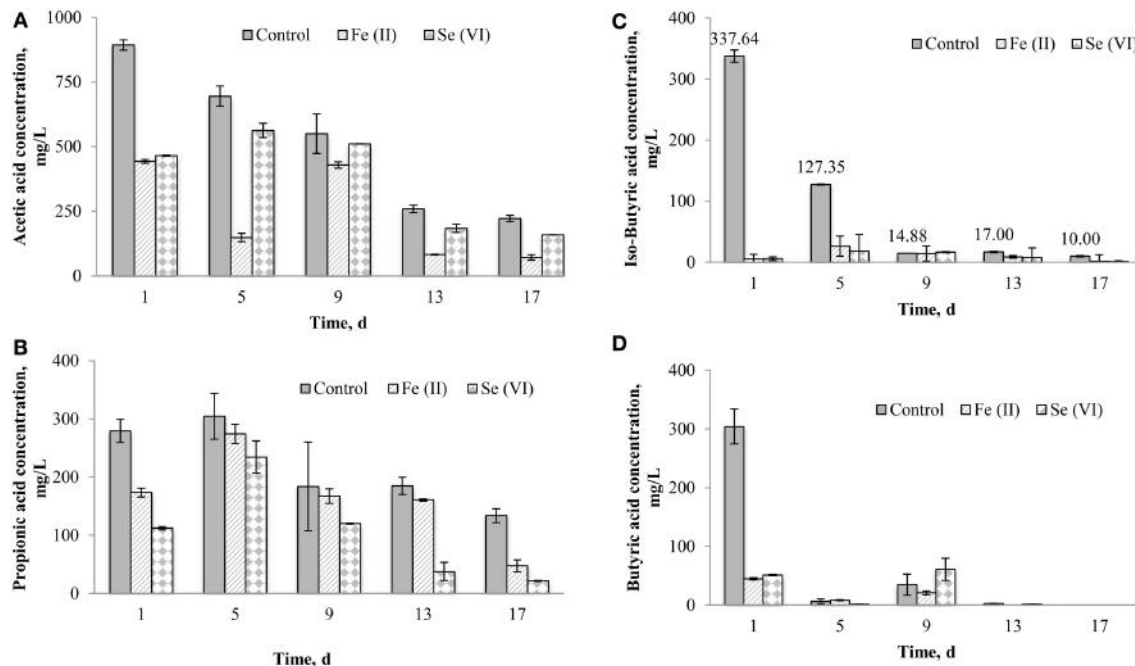


FIGURE 5 | Effect of Se (VI) and Fe (II) supplementation on the VFA production during the AD of FW-A: (A) Acetic acid; (B) Propionic acid; (C) Iso-butyric acid; and (D) Butyric acid.

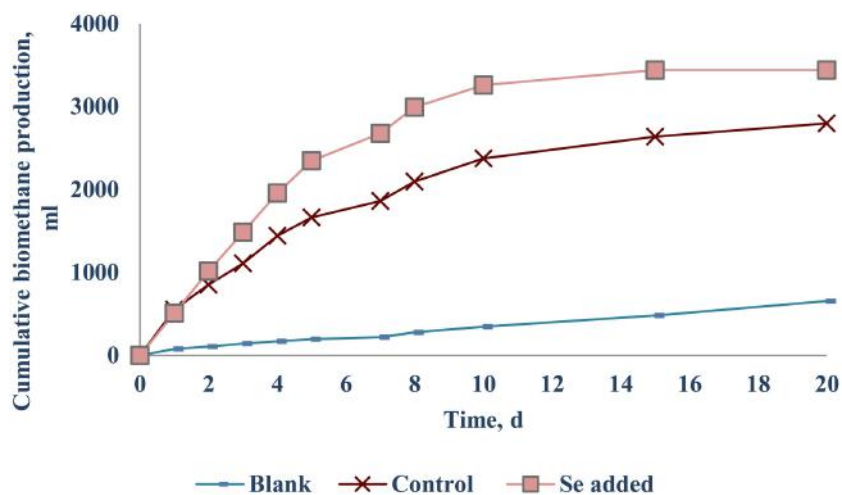


FIGURE 6 | Effect of Se (VI) addition on FW-B.

result in poor or deteriorated AD. It could be attributed to the Se bioavailability in agricultural soils to bio-uptake by plants and organisms, which dictates the entrance of Se in terrestrial Se food chain (Winkel et al., 2011), and Se fertilization might be needed.

Even though TE speciation and bioavailability was not studied, this research showed their important implication. Bioavailability depends on physical, biological, and chemical factors that are highly complex and interdependent processes (Worms et al.,

2006; Glass and Orphan, 2012). For instance, sometimes even if TE are taken up in the cell, their effects may be reduced by complexation inside the cytosol, compartmentalization, and efflux or by modification of the extracellular TE speciation (Worms et al., 2006; Glass and Orphan, 2012). In general, TE transport across the cell membrane is rate limiting and the overall process can be simplified to a thermodynamic equilibrium among the TE species. Further laboratory as well as mathematical modeling research is required on TE speciation and TE effects on

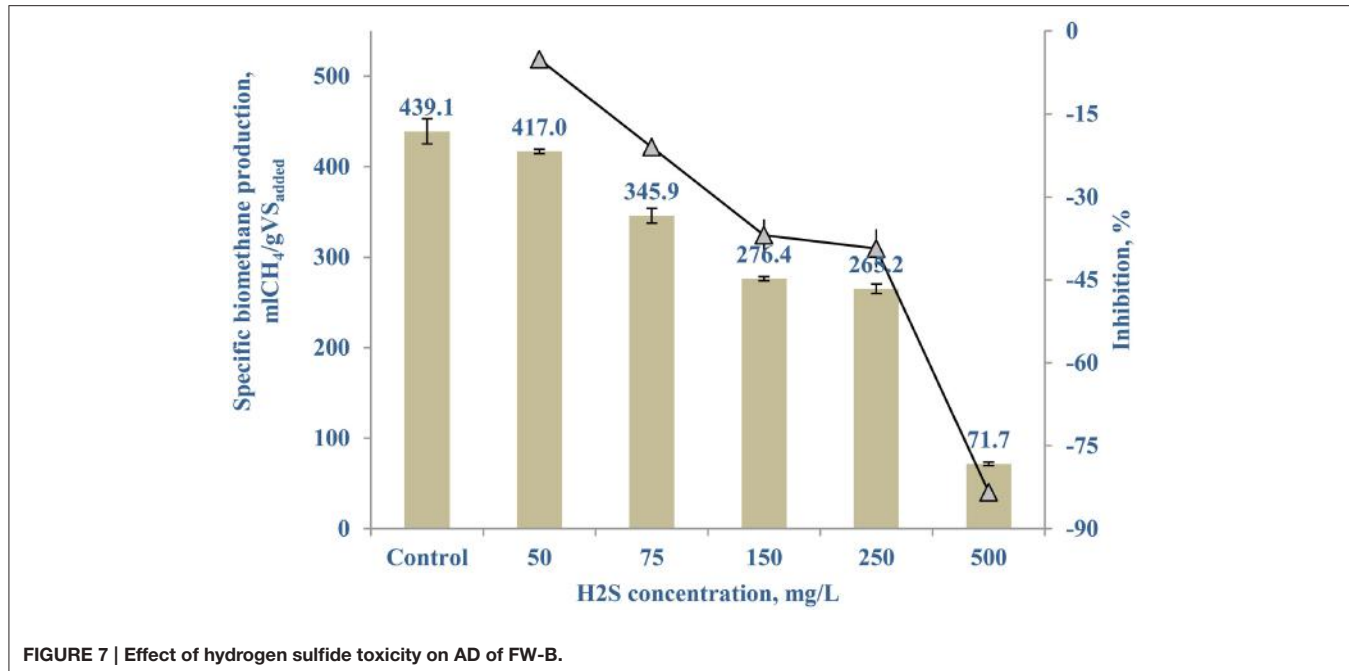


FIGURE 7 | Effect of hydrogen sulfide toxicity on AD of FW-B.

TABLE 4 | Enhanced AD of FW by supplementing TE.

TE Concentrations	Experimental conditions	Enhanced AD process	References
Fe (50 µg/L = 0.8 µM)	Mesophilic (35 ± 2°C) batch	39% higher biomethane production from FW-A, while no effect on FW-B	This study
Se (25–50 µg/L = 0.32–0.64 µM depending on the initial concentration in the FW)	Mesophilic (35 ± 2°C) batch	30–35% higher biomethane production from both FW-A and FW-B	This study
Cocktail of Se (0.2 mg/L), Fe (5 mg/L), Co (1 mg/L) and Ni (1 mg/L)	Mesophilic (35°C) continuous (OLR = 1–4 gVS/L.d)	Recovered from VFA accumulation at 5 gVS/L.d	Zhang et al., 2015
Cocktail containing 0.1 mg/L of Al, B, Co, Cu, Fe, Mn, Ni, Zn, Mo, Se, and W	Thermophilic (55°C) continuous (OLR = 1–4 gVS/L.d)	Delayed VFA accumulation by 88 days	Yirong et al., 2015
Cocktail of Se (0.16 µg/g) and Co (0.22 µg/g)	Mesophilic (36–37°C) semi-continuous (OLR = 1.6–5 gVS/L.d)	Organic loading could be increased from 2 gVS/L.d to 5 gVS/L.d with no ammonia inhibition	Banks et al., 2012
Cocktail containing 1 mg/L Co, Ni, Fe	Mesophilic continuous (OLR = 1.9–6.3 gCOD/L.d)	Delayed digester failure due to VFA accumulation	Qiang et al., 2012
	Mesophilic batch	7.5–7.8 times faster fermentation process as compared to control	
Cocktail of Se (1.8 mg/L), W (0.8 mg/L) and Co (0.06 mg/L)	Mesophilic (37°C) continuous (OLR = 2.5–3 gVS/L.d)	7–15% increase of biomethane production	Feng et al., 2010

the AD process and how to use this to implement process control of TE supplementation.

CONCLUSIONS

The supplementation of trace elements increased the biomethane potential of a FW with low trace elements concentration: the most effective elements were Fe with an increase of 39.2 ($\pm 0.6\%$)

of biomethane production of the FW from Europe, followed by Se ($34.1 \pm 5.6\%$ increase), Ni ($26.4 \pm 0.2\%$ increase), and Co ($23.8 \pm 0.2\%$ increase). The same experiments did not result in an increased biomethane production when FW with an elevated background concentration of trace elements was used, except for Se supplementation. Addition of 10 µg/L Se (0.13 µM) to the incubation of FW with background concentration (making the total Se

concentration $\sim 50 \mu\text{g/L} = 0.63 \mu\text{M}$) resulted in a 30% increased biomethane production. Sulfide inhibition was not observed at the prevailing concentrations, and hence the enhancing effect of trace elements is at the enzymatic or biomass stimulating level.

AUTHOR CONTRIBUTIONS

JA is the corresponding author and main researcher. GE is project leader and main supervisor. DY is the project collaborating partner and co-supervisor. PL is the project initiator and

co-supervisor. GE, DY and PL have all contributed in finalizing the manuscript.

ACKNOWLEDGMENTS

This research was supported by the Erasmus Mundus Joint Doctoral Program ETeCoS³ (Environmental Technologies for Contaminated Solids, Soils and Sediments) [EU grant agreement FPA no. 2010-0009]; and the Partnerships for International Research and Education (PIRE) project 298 [National Science Foundation (USA) under Grant Number 1243510].

REFERENCES

- Ariunbaatar, J., Panico, A., Frunzo, L., Esposito, G., Lens, P. N., and Pirozzi, F. (2014). Enhanced anaerobic digestion of food waste by thermal and ozonation pretreatment methods. *Environ. Manage.* 46, 142–149. doi: 10.1016/j.jenvman.2014.07.042
- Ariunbaatar, J., Panico, A., Yeh, D. H., Pirozzi, F., Lens, P. N., and Esposito, G. (2015). Enhanced mesophilic anaerobic digestion of food waste by thermal pretreatment: Substrate versus digestate heating. *Waste Manag.* 46, 176–181. doi: 10.1016/j.wasman.2015.07.045
- Banks, C. J., Zhang, Y., Jiang, Y., and Heaven, S. (2012). Trace element requirements for stable food waste digestion at elevated ammonia concentrations. *Bioresource Technol.* 104, 127–135. doi: 10.1016/j.biortech.2011.10.068
- Chen, Y., Cheng, J. J., and Creamer, K. S. (2008). Inhibition of anaerobic digestion process: a review. *Bioresource Technol.* 99, 4044–4064. doi: 10.1016/j.biortech.2007.01.057
- Chen, J. L., Ortiz, R., Steele, T. W., and Stuckey, D. C. (2014). Toxicants inhibiting anaerobic digestion: a review. *Biotechnol. Adv.* 32, 1523–1534. doi: 10.1016/j.biotechadv.2014.10.005
- Demirel, B., and Scherer, P. (2011). Trace element requirements of agricultural biogas digesters during biological conversion of renewable biomass to methane. *Biomass Bioenerg.* 35, 992–998. doi: 10.1016/j.biombioe.2010.12.022
- De Vrieze, J., De Lathouwer, L., Verstraete, W., and Boon, N. (2013). High-rate iron-rich activated sludge as stabilizing agent for the anaerobic digestion of kitchen waste. *Water Res.* 47, 3732–3741. doi: 10.1016/j.watres.2013.04.020
- Facchini, V., Cavinato, C., Fatone, F., Pavan, P., Cecchi, F., and Bolzonella, D. (2013). Effect of trace element supplementation on the mesophilic anaerobic digestion of food waste in batch trials: the influence of inoculum origin. *Biochem. Eng. J.* 70, 71–77. doi: 10.1016/j.bej.2012.10.004
- FAO (2011). *Global Food Losses and Food Waste Study Conducted for the International Congress*. Rome.
- Feng, X. M., Karlsson, A., Svensson, B. H., and Bertilsson, S. (2010). Impact of trace element addition on biogas production from food industrial waste-linking process to microbial communities. *FEMS Microbiol. Ecol.* 74, 226–240. doi: 10.1111/j.1574-6941.2010.00932.x
- Glass, J. B., and Orphan, V. J. (2012). Trace metal requirements for microbial enzymes involved in the production and consumption of methane and nitrous oxide. *Front. Microbiol.* 3:61. doi: 10.3389/fmicb.2012.00061
- Karhadkar, P. P., Audic, J. M., Faup, G. M., and Khanna, P. (1987). Sulfide and sulfate inhibition of methanogenesis. *Water Res.* 21, 1061–1066. doi: 10.1016/0043-1354(87)90027-3
- Koster, I. W., Rinzema, A., De Vegt, A. L., and Lettinga, G. (1986). Sulfide inhibition of the methanogenic activity of granular sludge at various pH-levels. *Water Res.* 20, 1561–1567. doi: 10.1016/0043-1354(86)90121-1
- Lindorfer, H., Ramhold, D., and Frauzy, B. (2012). Nutrient and trace element supply in anaerobic digestion plants and effect of trace element application. *Water Sci. Technol.* 66, 1923–1929. doi: 10.2166/wst.2012.399
- Liotta, F., Esposito, G., Fabbricino, M., van Hullebusch, E. D., Lens, P. N., Pirozzi, F., et al. (2015). Methane and VFA production in anaerobic digestion of rice straw under dry, semi-dry and wet conditions during start-up phase. *Environ. Technol.* doi: 10.1080/09593330.2015.1074288. [Epub ahead of print].
- Mussoline, W., Esposito, G., Lens, P., Spagni, A., and Giordano, A. (2013). Enhanced methane production from rice straw co-digested with anaerobic sludge from pulp and paper mill treatment process. *Bioresource Technol.* 148, 135–143. doi: 10.1016/j.biortech.2013.08.107
- Nanchariah, Y. V., and Lens, P. N. (2015). Selenium biomobilization for biotechnological applications. *Trends Biotechnol.* 33, 323–330. doi: 10.1016/j.tibtech.2015.03.004
- Nordell, E., Nilsson, B., Paledal, S. N., Karisalmi, K., and Moestedt, J. (2016). Co-digestion of manure and industrial waste—The effects of trace element addition. *Waste Manag.* 47, 21–27. doi: 10.1016/j.wasman.2015.02.032
- Oleszkiewicz, J. A., and Sharma, V. K. (1990). Stimulation and inhibition of anaerobic processes by heavy metals—a review. *Biol. Waste* 31, 45–67. doi: 10.1016/0269-7483(90)90043-r
- Oleszkiewicz, J. A., Marsteller, T., and McCartney, D. M. (1989). Effects of pH on sulfide toxicity to anaerobic processes. *Environ. Technol.* 10, 815–822. doi: 10.1080/09593338909384801
- Ortner, M., Rameder, M., Rachbauer, L., Bochmann, G., and Fuchs, W. (2015). Bioavailability of essential trace elements and their impact on anaerobic digestion of slaughterhouse waste. *Biochem. Eng. J.* 99, 107–113. doi: 10.1016/j.bej.2015.03.021
- Ortner, M., Leitzinger, K., Skupien, S., Bochmann, G., and Fuchs, W. (2014). Efficient anaerobic mono-digestion of N-rich slaughterhouse waste: influence of ammonia, temperature and trace elements. *Bioresource Technol.* 174, 222–232. doi: 10.1016/j.biortech.2014.10.023
- Parfitt, J., Bartherl, M., and Macnaughton, S. (2010). Food waste within food supply chains: quantification and potential for change to 2050. *Philos. Trans. R. Soc. Lond. B. Biol. Sci.* 365, 3065–3081. doi: 10.1098/rstb.2010.0126
- Pobbeheim, H., Munk, B., Lindorfer, H., and Guebitz, G. M. (2011). Impact of nickel and cobalt on biogas production and process stability during semi-continuous anaerobic fermentation of a model substrate for maize silage. *Water Res.* 45, 781–787. doi: 10.1016/j.watres.2010.09.001
- Qiang, H., Lang, D. L., and Li, Y. Y. (2012). High-solid mesophilic methane fermentation of food waste with an emphasis on Iron, Cobalt, and Nickel requirements. *Bioresource Technol.* 103, 21–27. doi: 10.1016/j.biortech.2011.09.036
- Qiang, H., Niu, Q., Chi, Y., and Li, Y. (2013). Trace metals requirements for continuous thermophilic methane fermentation of high-solid food waste. *Chem. Eng. J.* 222, 330–336. doi: 10.1016/j.cej.2013.02.076
- Shakeri Yekta, S., Lindmark, A., Skjellberg, U., Danielsson, Å., and Svensson, B. H. (2014). Importance of reduced sulfur for the equilibrium chemistry and kinetics of Fe (II), Co (II) and Ni (II) supplemented to semi-continuous stirred tank biogas reactors fed with stillage. *J. Hazard. Mater.* 269, 83–88. doi: 10.1016/j.jhazmat.2014.01.051
- Takashima, M., and Speece, R. E. (1989). Mineral nutrient requirements for high-rate methane fermentation of acetate at low SRT. *Water Pollut. Control Fed.* 61, 1645–1650.
- Thanh, P. M., Ketheesan, B., Yan, Z., and Stuckey, D. (2015). Trace metal speciation and bioavailability in anaerobic digestion: a review. *Biotechnol. Adv.* doi: 10.1016/j.biotechadv.2015.12.006. [Epub ahead of print].

- Winkel, L. H., Johnson, C. A., Lenz, M., Grundl, T., Leupin, O. X., Amini, M., et al. (2011). Environmental selenium research: from microscopic processes to global understanding. *Environ. Sci. Technol.* 46, 571–579. doi: 10.1021/es203434d
- Worms, I., Simon, D. F., Hassler, C. S., and Wilkinson, K. J. (2006). Bioavailability of trace metals to aquatic microorganisms: importance of chemical, biological and physical processes on biouptake. *Biochimie* 88, 1721–1731. doi: 10.1016/j.biochi.2006.09.008
- Worm, P., Fermoso, F. G., Lens, P. N., and Plugge, C. M. (2009). Decreased activity of a propionate degrading community in a UASB reactor fed with synthetic medium without molybdenum, tungsten and selenium. *Enzyme. Microb. Tech.* 45, 139–145. doi: 10.1016/j.enzmictec.2009.02.001
- Yirong, C., Heaven, S., and Banks, C. J. (2015). Effect of a trace element addition strategy on volatile fatty acid accumulation in thermophilic anaerobic digestion of food waste. *Waste Biomass Valorizat.* 6, 1–12. doi: 10.1007/s12649-014-9327-2
- Zandvoort, M. H., van Hullebusch, E. D., Gieteling, J., and Lens, P. N. (2006). Granular sludge in full-scale anaerobic bioreactors: trace element content and deficiencies. *Enzyme. Microb. Tech.* 39, 337–346. doi: 10.1016/j.enzmictec.2006.03.034
- Zhang, L., Lee, Y. W., and Jahng, D. (2011). Anaerobic co-digestion of food waste and piggery wastewater: focusing on the role of trace elements. *Bioresource Technol.* 102, 5048–5059. doi: 10.1016/j.biortech.2011.01.082
- Zhang, W., Wu, S., Guo, J., Zhou, J., and Dong, R. (2015). Performance and kinetic evaluation of semi-continuously fed anaerobic digesters treating food waste: role of trace elements. *Bioresource Technol.* 178, 297–305. doi: 10.1016/j.biortech.2014.08.046

Conflict of Interest Statement: The authors declare that the research was conducted in the absence of any commercial or financial relationships that could be construed as a potential conflict of interest.

Copyright © 2016 Ariunbaatar, Esposito, Yeh and Lens. This is an open-access article distributed under the terms of the Creative Commons Attribution License (CC BY). The use, distribution or reproduction in other forums is permitted, provided the original author(s) or licensor are credited and that the original publication in this journal is cited, in accordance with accepted academic practice. No use, distribution or reproduction is permitted which does not comply with these terms.



Substrate Type and Free Ammonia Determine Bacterial Community Structure in Full-Scale Mesophilic Anaerobic Digesters Treating Cattle or Swine Manure

OPEN ACCESS

Edited by:

Eric D. Van Hullebusch,
University Paris-Est, France

Reviewed by:

Daniel Puyol,

University Rey Juan Carlos, Spain

Seung Gu Shin,

Pohang University of Science and Technology, South Korea

Gavin Collins,

National University of Ireland, Galway,
Ireland

*Correspondence:

Xiangzhen Li
lixz@cib.ac.cn

[†]These authors have contributed equally to this work.

Specialty section:

This article was submitted to
Microbiotechnology, Ecotoxicology and Bioremediation,
a section of the journal
Frontiers in Microbiology

Received: 10 June 2015

Accepted: 16 November 2015

Published: 30 November 2015

Citation:

Li J, Rui J, Yao M, Zhang S, Yan X, Wang Y, Yan Z and Li X (2015) Substrate Type and Free Ammonia Determine Bacterial Community Structure in Full-Scale Mesophilic Anaerobic Digesters Treating Cattle or Swine Manure. *Front. Microbiol.* 6:1337.
doi: 10.3389/fmicb.2015.01337

Jiabao Li^{1,2†}, Junpeng Rui^{1,2†}, Minjie Yao^{1,2}, Shiheng Zhang^{1,2}, Xuefeng Yan^{1,2}, Yuanpeng Wang³, Zhiying Yan^{1,2} and Xiangzhen Li^{1,2*}

¹ Key Laboratory of Environmental and Applied Microbiology, Chengdu Institute of Biology, Chinese Academy of Sciences, Sichuan, China, ² Environmental Microbiology Key Laboratory of Sichuan Province, Chengdu Institute of Biology, Chinese Academy of Sciences, Sichuan, China, ³ Department of Chemical and Biochemical Engineering, College of Chemistry and Chemical Engineering, Xiamen University, Fujian, China

The microbial-mediated anaerobic digestion (AD) process represents an efficient biological process for the treatment of organic waste along with biogas harvest. Currently, the key factors structuring bacterial communities and the potential core and unique bacterial populations in manure anaerobic digesters are not completely elucidated yet. In this study, we collected sludge samples from 20 full-scale anaerobic digesters treating cattle or swine manure, and investigated the variations of bacterial community compositions using high-throughput 16S rRNA amplicon sequencing. Clustering and correlation analysis suggested that substrate type and free ammonia (FA) play key roles in determining the bacterial community structure. The COD: NH₄⁺-N (C:N) ratio of substrate and FA were the most important available operational parameters correlating to the bacterial communities in cattle and swine manure digesters, respectively. The bacterial populations in all of the digesters were dominated by phylum Firmicutes, followed by Bacteroidetes, Proteobacteria and Chloroflexi. Increased FA content selected Firmicutes, suggesting that they probably play more important roles under high FA content. Syntrophic metabolism by Proteobacteria, Chloroflexi, Synergistetes and Planctomycetes are likely inhibited when FA content is high. Despite the different manure substrates, operational conditions and geographical locations of digesters, core bacterial communities were identified. The core communities were best characterized by phylum Firmicutes, wherein *Clostridium* predominated overwhelmingly. Substrate-unique and abundant communities may reflect the properties of manure substrate and operational conditions. These findings extend our current understanding of the bacterial assembly in full-scale manure anaerobic digesters.

Keywords: anaerobic digester, animal manure, bacterial community, free ammonia, core community

INTRODUCTION

Anaerobic digestion (AD) represents an efficient process for the treatment of various kinds of organic waste along with biogas production (Alvarado et al., 2014). The biological process involves four sequential steps: substrate hydrolysis, fermentation, acetogenesis and methanogenesis, which requires the cooperation of bacteria and archaea (Ali Shah et al., 2014). Archaea, especially methanogens, are key players during methanogenesis, thus attracting much attention. However, bacterial populations are essential in anaerobic digesters treating insoluble organic materials, such as animal manure, since the hydrolysis step is often the bottleneck of AD process due to the nature of complex and recalcitrant substrates (Werner et al., 2011; St-Pierre and Wright, 2014; Carballa et al., 2015). In addition, bacteria also take charge of the critical syntrophic metabolism coupled to methanogenesis (Morris et al., 2013), so that stable performance can be achieved during the AD processes.

Multiple factors including digester design, substrate and operational conditions influence microbial community structures (Lin et al., 2013; Town et al., 2014). Substrate is recognized as a key factor affecting fermentation efficiency, as well as the microbial community composition (Zhang et al., 2013; Ziganshin et al., 2013). Cluster analysis of the bacterial and archaeal communities shows that reactors treating similar substrates group together (Sundberg et al., 2013). It is postulated that substrate type determines the observed differences in phylogenetic structure based on a meta-analysis of 16S rRNA gene sequences retrieved from 79 digesters treating various substrates (Zhang et al., 2014). Nonetheless, microbial populations in anaerobic manure digesters can display high variations even at the digestion of a common core substrate (St-Pierre and Wright, 2014).

Operational conditions including temperature and ammonia content could impact bacterial community structure. It is reported that bacterial communities clustered based on factors rather than the input materials in lab-scale thermophilic digesters (Town et al., 2014). That is probably because high temperature imposes much stronger influences than other operational conditions on the communities (Ziganshin et al., 2013). Animal manure is widely used as substrate in anaerobic digesters, which often contains high free ammonia (FA) due to high protein content (Deublein and Steinhauser, 2008; Riviere et al., 2009). FA has an inhibiting or even toxic effect on prokaryotic communities because it may passively diffuse into cells, causing proton imbalance and potassium deficiency (Sprott and Patel, 1986; Chen et al., 2008). FA also inhibits pH sensitive species (Chen et al., 2008). Syntrophic acetate oxidization (SAO) performed by SAO bacteria is observed to become important under high ammonia content (Schnurer et al., 1999; Schnurer and Nordberg, 2008). Therefore, the selectivity of ammonia to different microbial populations could be the mechanism structuring prokaryotic communities in anaerobic digesters treating animal manure.

In anaerobic digesters, core communities [represented by operational taxonomic units (OTUs)] are commonly found in different digesters with relative high abundances (Riviere et al.,

2009; Saunders et al., 2015). In addition, core communities of anaerobic digesters were found within microbial populations that are capable of performing substrate hydrolysis, fermentation and syntrophic metabolism (St-Pierre and Wright, 2014; Rui et al., 2015). They may vary depending on different substrate (Riviere et al., 2009; Nelson et al., 2011; St-Pierre and Wright, 2014). Therefore, the elucidation of core and unique communities among different full-scale anaerobic digesters might be useful to indicate important traits of AD process, and to identify putatively important organisms for microbial management in AD (Saunders et al., 2015). Previously, core and unique OTUs were identified in 7 different full-scale anaerobic digesters with the clone library method (Riviere et al., 2009). Three anaerobic digesters shared 132 core OTUs (St-Pierre and Wright, 2014). However, information is still limited due to limited samples of full-scale biogas reactors. Core and unique OTUs can be better determined by using more independently-operated full-scale anaerobic digesters and high-throughput methods (Saunders et al., 2015). In China, there are 3717 large-scale (digester volume >500 m³) and 18,853 medium-scale (digester volume of 50–500 m³) biogas plants that have been established by the end of 2009 (Jiang et al., 2011). Of these, swine and cattle manure are two most popular substrates. Few studies have been conducted to identify the potential core and unique bacterial populations, as well as the factors driving the assembly of the bacterial communities, among multiple full-scale anaerobic digesters treating animal manure.

In this study, we collected 20 sludge samples from independently-operated full-scale anaerobic digesters at different geographical locations across China. The objectives were to identify: (i) important factors shaping the bacterial communities, and (ii) the potential core and unique bacterial populations in digesters treating cattle and swine manure.

MATERIALS AND METHODS

Sample Description and Operational Parameters

From August to October, 2012, 20 sludge samples (at least 400 ml each) were collected from digesters located from the northeast to the southwest of China (Table S1), including 8 cattle manure digesters (c1–c8) and 12 swine manure digesters (s9–s20). Autoclaved anaerobic flasks were filled with sludge samples that discharged from the sampling valve, and transported to the laboratory on ice immediately. Most digesters were built at livestock breeding plants for the treatment of animal manure. Operational parameters, e.g., digester type and volume, substrate type, sludge retention time (SRT), biogas production and digestion temperature, were directly obtained from the plant operators. Chemical properties of sludge, including pH, chemical oxygen demand (COD), ionized-ammonia (NH₄⁺-N), and phosphate, were measured according to the method described previously (Li et al., 2014; Shen et al., 2014). Free ammonia (FA) was calculated based on the total ammonia, pH and temperature values (Rajagopal et al., 2013).

Among the 20 sampling digesters, continuous stirred-tank reactors (CSTRs) were used by 18 digesters, and upflow solid reactors (USRs) were used by the rest 2 digesters (c6 and s9). Operational parameters varied, with SRT ranging between 15 and 30 days, digester volume between 60 and 10,000 m³, biogas production between 0.13 and 1.0 m³ m⁻³ d⁻¹, digester temperature between 25 and 36.5 °C, sludge pH between 6.50 and 7.75, COD between 314.70 and 7243.80 mg l⁻¹, NH₄⁺-N between 89.24 and 3474.14 mg l⁻¹, FA between 1.34 and 149.23 mg l⁻¹, and phosphate between 2.97 and 92.39 mg l⁻¹.

DNA Extraction and 16S rRNA Gene Amplicon Sequencing

Genomic DNA was extracted according to the method of Rademacher et al. (2012). The concentrations and quality of DNA were checked using a NanoDrop 2000 spectrophotometer. For 16S rRNA gene amplicon sequencing, the primers 515F (5'-GTGYCAGCMGCCGCGTA- 3') and 806R (5'-GGACTACHVGGGTWTCTAAT -3') were used to amplify V4-V5 region of the 16S rRNA gene. The forward and reverse primers had modifications introduced at 5' ends to contain the MiSeq sequencing adaptor sequences. The 10-mer barcode sequence was added between the adaptor and reverse primer sequences. An aliquot of 10 ng of purified DNA from each sample was used as a template for PCR amplification in 25 µl reaction mixture. The following conditions were used: denaturation at 94°C for 3 min, followed by 30 cycles of denaturation at 94°C for 30 s, annealing at 55°C for 1 min and extension at 72°C for 1 min, with a final extension at 72°C for 5 min. Triplicate PCR reactions were performed per sample and pooled. The PCR products were purified using Gel Extraction kit (Omega bio-tek). Equal molar of PCR product from each sample was pooled together. Sequencing library was constructed using Truseq DNA Library Prep kits according to the manufacturer's instruction and sequenced by Illumina MiSeq platform using MiSeq Reagent Kit v2.

Sequence Data Analysis

The raw sequences were sorted based on the unique sample barcodes, trimmed for sequence quality using the QIIME pipeline (Caporaso et al., 2010). Chimera sequences were removed using the Uchime algorithm (Edgar et al., 2011). Each sample was rarefied to an equal sequencing number of 11,080 (the fewest number of sequences in a single sample). The sequences were clustered by the complete-linkage clustering method incorporated in the QIIME pipeline (Caporaso et al., 2010). Operational taxonomic units (OTUs) were picked at 97% identity using cd-hit in the QIIME pipeline. Singleton sequences were filtered out. Shannon's diversity index, Chao1 estimator of richness and the observed OTUs number were calculated at 97% sequence identity in the Ribosomal Database Project (RDP) pipeline (<http://pyro.cme.msu.edu/>). A phylogenetic affiliation of each representative sequence was analyzed by RDP Classifier at a confidence threshold of 80% (Wang et al., 2007).

After reprocessing, potential core, substrate-unique and shared communities (represented by specific OTUs) were identified. Core OTUs were distributed in all the digesters, while

substrate-unique OTUs only existed in more than 80% of cattle or swine manure digesters. Shared OTUs were distributed in more than 80% of all digesters and excluded the core OTUs. Based on the abundance-based differences, shared OTUs were further categorized into three types: cattle-abundant (higher relative abundance in cattle manure digesters), swine-abundant (higher relative abundance in swine manure digesters), and both-equal OTUs (equal abundance in both cattle and swine digesters).

Statistical Analysis

The overall differences in the bacterial community structures were evaluated by principal coordinates analysis (PCoA) based on Bray-Curtis distances using the relative abundances of OTUs without singletons as the input data. Three nonparametric multivariate permutation tests, including multiple response permutation procedure (MRPP), permutational multivariate analysis of variance (Adonis), and analysis of similarity (ANOSIM), were performed to assess the significance of the difference in the structures of bacterial communities between the two types of digesters (Deng et al., 2012). Using a set of OTUs without singletons, Canonical correspondence analysis (CCA) was performed to discern the correlations between the bacterial communities and the operational parameters. FA, pH, NH₄⁺-N, COD, C:N were selected by the R function *bioenv* as the most significant parameters. The above analyses were carried out with the Vegan package in R (Dixon, 2003). Pearson's correlation analysis was conducted to examine the correlations between the community composition and the operational parameters with SPSS Statistics 21.0.

Nucleotide Sequence Accession Numbers

The original sequencing data are available at the European Nucleotide Archive by accession No. PRJEB6969 (<http://www.ebi.ac.uk/ena/data/view/PRJEB6969>).

RESULTS

Diversity and Structure of Bacterial Communities

The variations of bacterial community composition within 20 full-scale anaerobic digesters were characterized using barcoded amplicons resulting in 429,907 chimera-free reads and further 4629 OTUs at a cutoff of 97% similarity. The 744 OTUs had an average relative abundance of more than 0.01%. The bacterial diversity indices varied across all the samples (Table S2). Correlation analysis showed significant and negative relationships between Shannon's index, the observed number of OTUs and free ammonia (FA), sludge pH and NH₄⁺-N (Table 1). Other parameters including biogas production, C:N, digester volume, temperature, SRT, COD, and phosphate did not show any significant correlations with the diversity indices.

Two potential clusters were observed by means of PCoA analysis of the bacterial communities (Figure 1A). Cluster 1 contained 8 samples exclusively from cattle manure digesters; Cluster 2 consisted of 12 samples originating from swine manure digesters. Approximately, PCo1 and PCo2 explained 45% of the

total variations in the bacterial community structure among the digesters. The significant difference between the two potential clusters was verified with three nonparametric multivariate permutation tests (Adonis, $F = 5.85$, $P = 0.001$; ANOSIM, $R = 0.77$, $p = 0.001$; MRPP, $\delta = 0.64$, $P = 0.001$). The results indicated that substrate type was likely to segregate bacterial communities in these anaerobic digesters. In addition, the segregation of bacterial communities within each cluster was also observed, suggesting that other parameters also contributed to the variations in the bacterial communities.

TABLE 1 | Pearson's correlation between operational parameters and bacterial diversity indices of all samples^a.

Diversity indices	pH	NH ₄ ⁺ -N	FA
Chao1 richness	-0.44	-0.37	-0.35
Observed OTUs	-0.62**	-0.67**	-0.52*
Shannon's index	-0.56**	-0.57**	-0.62**

^aFA, free ammonia.

** $P < 0.01$, * $P < 0.05$. Only operational parameters with significant relationships with any of the three indices were listed.

Bacterial Community Composition

Roughly, 99% of total reads were annotated at phylum level, 93% at order level, and 45.5% at genus level. In all the 20 digesters, the phylum Firmicutes (57.79%) was dominated, followed by Bacteroidetes, Proteobacteria and Chloroflexi (Figure 2 and Table S3). Above taxa constituted 85.6% of total reads. Other phyla were relatively low in the relative abundance in most digesters (Figure 2 and Table S3). All the phyla shared high degree of variations in the relative abundances in different samples. Notably, Firmicutes overwhelmingly dominated in one cattle manure digester and five swine manure digesters (Table S3). However, Chloroflexi predominated in digester c7 (23.88%), followed by Spirochaetes and Acidobacteria.

At the genus level, most abundant genera (relative abundance $>0.30\%$) were affiliated to phylum Firmicutes, e.g., *Clostridium sensu stricto*, *Clostridium XI*, *Syntrophomonas*, *Clostridium III*, and *Pelotomaculum* (Figure 3 and Table S3). Other abundant genera were also included, such as *Smithella*, *Syntrophorhabdus* in phylum Proteobacteria, and *Corynebacterium* in phylum Actinobacteria. The 19 genera accounted for 40.4% of total genera reads. Despite the dominance of these genera, high variations in the relative abundance were

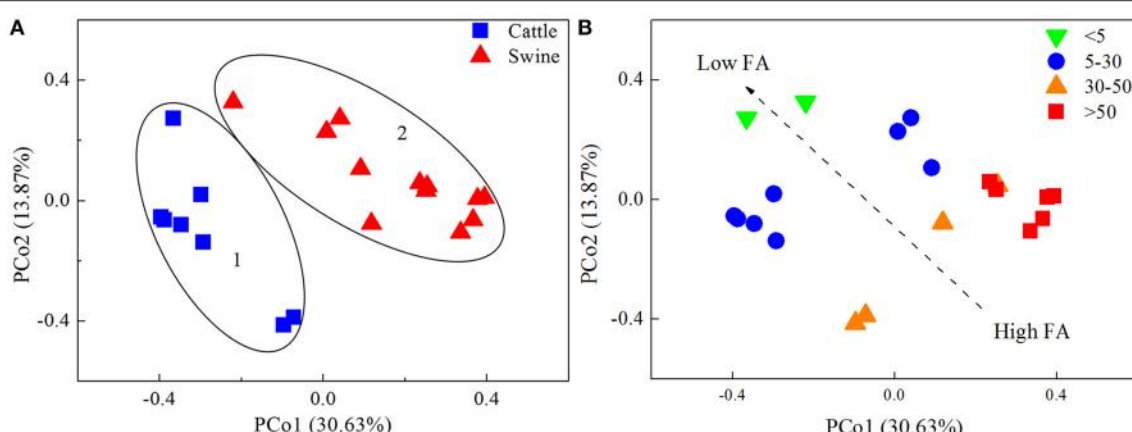


FIGURE 1 | The principal coordinates analysis (PCoA) plots of the bacterial communities in 20 independently-operated full-scale anaerobic digesters. Bray-Curtis distance was used for the PCoA analysis. Plots were ranked by (A) substrate type, and (B) free ammonia content (FA, mg l⁻¹).

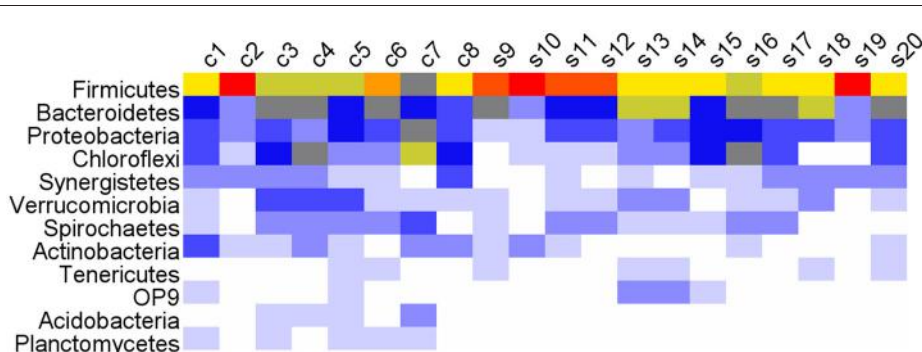
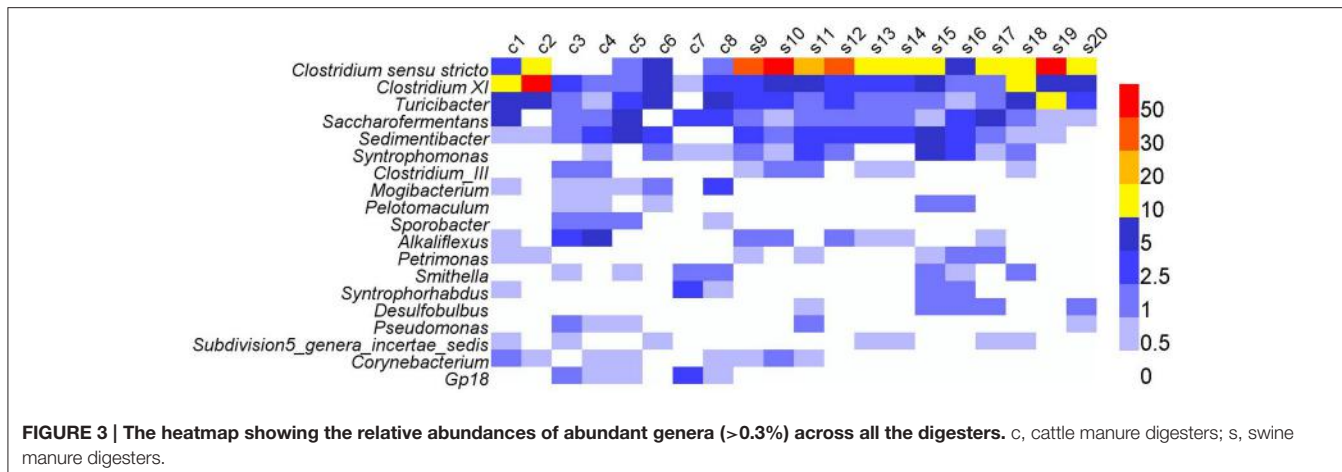


FIGURE 2 | The heatmap showing the relative abundances of various phyla (>0.1%) across all the digesters. c, cattle manure digesters; s, swine manure digesters.



observed in different samples, e.g., *Clostridium sensu stricto* varied between 0.14 and 56.75%, and *Clostridium XI* between 0.89 and 52.15% (Table S3).

Potential Core, Substrate-Unique, and Shared Communities

Based on the occurrence and the relative abundances of OTUs in all the samples, we defined three major groups.

Core OTUs

OTUs distributing in all the 20 digesters were defined as core OTUs. This study identified 25 core OTUs that made up 3.36% of 744 abundant bacterial OTUs, but accounted for 34.4% of total reads (Table S4). The core OTUs were primarily affiliated to genera *Clostridium sensu stricto*, *Clostridium XI*, *Turicibacter*, *Saccharofermentans*, *Sedimentibacter*, *Syntrophomonas* in phylum Firmicutes, order Bacteroidales of phyla Bacteroidetes, genus *Acinetobacter* in phylum Proteobacteria, family Anaerolineaceae in phylum Chloroflexi, genus *Subdivision5_genera_incertae_sedis* in phylum Verrucomicrobia and genus *Corynebacterium* in phylum Actinobacteria. The relative abundances of most core OTUs were higher than 0.5% (Table S4).

Substrate-Unique OTUs

Substrate-unique OTUs were defined as those merely distributed in more than 80% of cattle or swine manure digesters. Nineteen and twenty OTUs were detected only in cattle and swine manure digesters, consisting of 5.62 and 3.29% of their respective total reads (Table S4). These OTUs were mainly distributed in phylum Firmicutes, and also in phylum Actinobacteria in Cluster 1, and phylum Bacteroidetes in Cluster 2. However, most of them were unclassified at the genus level.

Shared OTUs

Shared OTUs were defined as those found in more than 80% of each type of digesters, but excluding the core OTUs. The identified 108 shared OTUs made up 21.49% of total reads, and can be further binned into three groups: cattle-abundant, swine-abundant and both-equal OTUs. There were 14 and 9 OTUs as

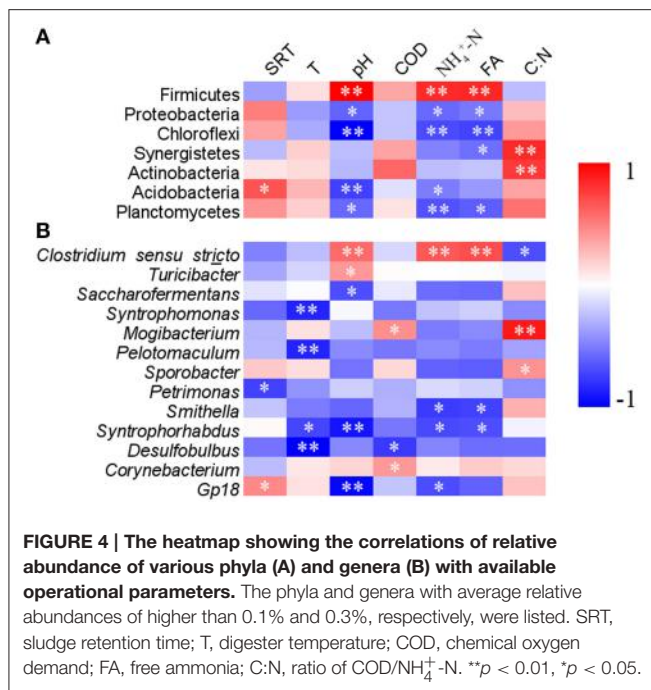
cattle- and swine-abundant OTUs, respectively (Table S4). Swine-abundant OTUs were all represented by phylum Firmicutes. Differently, cattle-abundant OTUs included phyla Firmicutes, Synergistetes, Bacteroidetes, Chloroflexi and Actinobacteria.

Relationships between Bacterial Community Compositions and Available Operational Parameters

Correlation analysis of the bacterial community compositions with most available operational parameters showed that biogas production, temperature, COD and phosphate did not significantly correlate to the relative abundances of any dominant phyla (Table S5). However, FA positively correlated with the relative abundance of phylum Firmicutes, and negatively correlated to Proteobacteria, Chloroflexi, Synergistetes, and Planctomycetes (Figure 4A). Sludge pH and NH_4^+ -N usually showed same correlation patterns with these phyla as those of FA. Sludge pH and SRT were also significantly correlated with the relative abundance of Acidobacteria. C:N was positively correlated with the relative abundances of phyla Synergistetes and Actinobacteria ($p < 0.01$).

At the genus level, sludge pH, FA, and NH_4^+ -N were observed to correlate with 27, 24, and 24 genera, respectively (Table S6). Other operational parameters showed less correlation with the various genera. As the dominant genus, *Clostridium sensu stricto* was positively correlated with NH_4^+ -N and FA ($p < 0.01$), whereas *Smithella* and *Syntrophorhabdus* were negatively correlated with above two parameters (Figure 4B). Additionally, significantly positive correlations with sludge pH were observed for *Clostridium sensu stricto* and *Turicibacter*, but negative correlations between pH and *Saccharofermentans* and *Syntrophorhabdus*.

At the OTU level, NH_4^+ -N, FA, C:N, and pH were the four most dominant available parameters that were correlated with 39, 35, 30, and 25 OTUs, respectively, in all digesters (Table S7). Cattle-abundant and unique OTUs were exclusively and positively correlated with C:N and COD ($p < 0.05$; Table 2), while swine-abundant and unique OTUs were significantly



correlated with FA and NH₄⁺-N. These results were further corroborated with CCA analysis (Figure 5).

DISCUSSION

Although our studied digesters were operated under different operational conditions, substrate types and geographical locations, potential core and unique OTUs were identified. Further, substrate type and free ammonia (FA) were revealed as the most dominant factors differentiating bacterial communities in these digesters.

In this study, the observed clustering of the samples from different full-scale digesters could be attributed to substrate type. This is consistent with findings that substrate shapes microbial community structure in AD systems (Sundberg et al., 2013; Wagner et al., 2013; Ziganshin et al., 2013; Zhang et al., 2014). A wide variety of components in manure can be utilized to produce biogas in AD systems, e.g., protein, cellulose and lipid. Though the feedstock in both types of digesters is animal manure, different chemical natures and microbial communities in manure inoculum could contribute to the variations of community structure in the AD systems. Indeed, swine manure is a kind of protein-rich organic substrate (Hansen et al., 1998), while cattle manure is often composed of cellulose-rich material since the feedstock is mainly silage with high C:N (ASABE, 2005). In this study, cattle manure digesters did show significantly higher C:N compared to swine manure digesters ($p < 0.05$, data not shown).

Nevertheless, substrate type could not explain the observed segregation of the bacterial communities within both cluster members. A previous study also reported high variations of microbial populations in anaerobic manure digesters at the digestion of a common core substrate (St-Pierre and Wright,

2014). Operational parameters may cause such variations. In this study, correlation analysis revealed that pH, FA, and NH₄⁺-N were all significantly correlated with Shannon's diversity and the observed number of OTUs. However, further analysis revealed that sludge pH did not affect the clustering in both Cluster 1 and Cluster 2 samples. Rather, NH₄⁺-N and FA were highly related to the clustering of the samples (Figure 1B). FA is very toxic to methanogenic community (Chen et al., 2008). We also observed that the responses of different bacterial taxa to FA were not the same. Thus, the selection of different prokaryotic taxa by free ammonia is likely an important mechanism shaping prokaryotic community structure in manure AD systems.

Excessive FA is detrimental to AD process because high FA content not only changes pH in the digesters, but also causes proton imbalance and potassium deficiency in microbial cells (Sprott and Patel, 1986; Chen et al., 2008). In this study, though the sludge pH was neutral in these digesters, FA content highly varied, and more than 50 mg l⁻¹ was detected in several swine manure digesters (s9, s10, s11, s12, s14, and s19). However, the FA content in the swine manure digesters is less likely to cause acute ammonia inhibition (Rajagopal et al., 2013). Alternatively, it may select specific bacterial populations that can better tolerate higher FA. For example, members of phylum Firmicutes, especially *Clostridium sensu stricto*, showed a positive correlation with FA (Figure 4 and Table S6). Firmicutes are ubiquitously involved in substrate hydrolysis, fermentation and acetogenesis (Nelson et al., 2011; De Vrieze et al., 2015). Several known species which are capable of syntrophic acetate oxidation (SAO) at elevated total ammonia concentrations are affiliated to this phylum (Schnurer et al., 1996; Westerholm et al., 2010; Sieber et al., 2012). Therefore, Firmicutes probably play more essential roles under high free ammonia content.

In contrast, many populations affiliated to Proteobacteria, Chloroflexi, Synergistetes, and Planctomycetes showed negative correlations with FA ($p < 0.05$; Figure 4A, Table S6), suggesting that they may be inhibited by high FA content. Many Synergistetes and Chloroflexi members are able to perform syntrophic metabolism in association with hydrogenotrophic methanogens during AD process (Sekiguchi et al., 2003; Yamada et al., 2006; Sieber et al., 2012). Dominant genera *Smithella* and *Syntrophorhabdus* in phylum Proteobacteria are able to convert propionate and aromatic compounds into acetate by syntrophic association with hydrogenotrophic methanogens (de Bok et al., 2001; Qiu et al., 2008). In this study, they were less represented in digesters with high FA content. In addition, other syntrophic microbes, e.g., *Pelotomaculum*, *Syntrophomonas*, and *Desulfobulbus* showed decreased trends, even though such changes were not significant at $p = 0.05$. The overall results indicated that syntrophic metabolism by these microbes are likely inhibited when FA content is high.

High FA content is also known to trigger the metabolic shift toward SAO (Schnurer et al., 1999; Schnurer and Nordberg, 2008). A limited number of mesophilic syntrophic acetate oxidizers have been isolated, e.g., *Clostridium ultunense* (Schnurer et al., 1996), *Syntrophacetkus schinkii* (Westerholm et al., 2010), and *Tepidanaerobacter acetatoxydans* (Westerholm

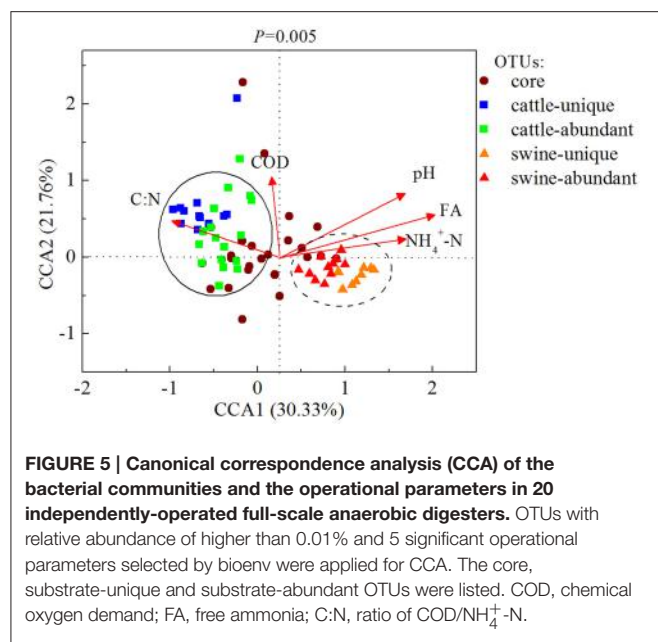
TABLE 2 | Pearson's correlation of substrate-unique and abundant OTUs with operational parameters^a.

	OTU ID	pH	COD	NH ₄ ⁺ -N	FA	Phosphate	C:N	Taxa rank
Cattle-unique	1334						0.46*	Lachnospiraceae
	1390		0.51*				0.91**	Clostridiales
	4218		0.55*				0.95**	Clostridiales
	4402		0.46*				0.82**	Lachnospiraceae
	5948		0.54*				0.82**	Lachnospiraceae
	8380		0.54*				0.79**	Lachnospiraceae
	9822						0.76**	Coriobacterineae
	10378		0.53*				0.92**	Clostridia
	11301						0.52*	Clostridiales
	12256		0.5*				0.89**	Clostridiales
	14799		0.49*				0.90**	Coriobacterineae
Cattle-abundant	532	-0.53*		-0.45*			0.55*	Sporobacter
	4023		0.53*					Corynebacterineae
	5640						0.52*	Bacteria
	5752		0.46*				0.63**	Planococcaceae
	6375			-0.46*			0.77**	Firmicutes
	7332		0.5*				0.55*	Corynebacterineae
	7857						0.65**	Bacteria
	8408		0.56**				0.72**	<i>Clostridium sensu stricto</i>
	8614	-0.57**						Anaerovorax
	11860	-0.45*		-0.49*	-0.49*		0.56**	Ruminococcaceae
Swine-unique	1558	0.47*		0.92**	0.90**			Firmicutes
	3161			0.63**	0.62**	0.55*		Clostridiales
	7786			0.65**	0.70**			<i>Lactobacillus</i>
	9568			0.55*	0.49*			Bacteria
	11072			0.78**	0.84**			Firmicutes
	13212	0.52*			0.54*			<i>Clostridium sensu stricto</i>
	13626			0.55*	0.49*			Clostridiaceae 1
	14200			0.73**	0.76**			Bacteroidetes
	15022			0.56*	0.56**			<i>Lactobacillus</i>
	1099	0.48*		0.79**	0.80**			Syntrophomonadaceae
Swine-abundant	1351			0.45*	0.56**			Lachnospiraceae
	2441					0.45*		Clostridiales
	4394	0.56**					-0.48*	<i>Clostridium XI</i>
	5383			0.54*				Clostridiales
	8677			0.63**	0.52*			Bacteria
	13608	0.46*		0.57**	0.61**			<i>Clostridium sensu stricto</i>

^aCOD, chemical oxygen demand. FA, free ammonia. C:N, ratio of COD/NH₄⁺-N. **P < 0.01, *P < 0.05. Only significant relationships were listed.

et al., 2011). However, we did not observe the emergence of these species in most digesters, possibly suggesting that SAO is not a dominant pathway. This is likely caused by the fact that FA content (1.34–149.23 mg l⁻¹) in our studied digesters did not reach the ammonia inhibition threshold (Hansen et al., 1998), and thus characterized SAO species were not observed. Alternatively, some uncharacterized heterogeneous SAO bacteria are possibly responsible for SAO in reactors with increased ammonia content (Werner et al., 2014). Further simultaneously in-depth studies of methanogenic and bacterial communities and their interactions are warranted.

The core communities play critical roles in AD processes and the concept might be useful to identify putatively important organisms for microbial management in AD (Saunders et al., 2015). The core bacterial communities were defined as those commonly found in anaerobic digesters, and six core OTUs were identified within phyla Chloroflexi, Betaproteobacteria, Bacteroidetes, and Synergistetes (Riviere et al., 2009). In line with St-Pierre and Wright (2014), we identified different core OTUs mainly distributed in phylum Firmicutes. This is probably due to different substrates used in anaerobic digesters, which support differential microbial populations in the engineered



AD systems (Zhang et al., 2014). Indeed, phylum Chloroflexi may predominate in digesters treating municipal wastewater or sewage sludge (Riviere et al., 2009; Nelson et al., 2011; Sundberg et al., 2013), while Firmicutes are dominant in most manure digesters or co-digesters of mixed substrates (Liu et al., 2009; Sundberg et al., 2013; St-Pierre and Wright, 2014). As a result, *Clostridium* in phylum Firmicutes, which contains various genes encoding cellulose and hemicellulose-digesting enzymes for the degradation of complex plant fibers (Deublein and Steinhauser, 2008; Zhu et al., 2011), gained dominance in the core OTUs of these digesters. Other core OTUs mainly included genera *Turicibacter*, *Sedimentibacter*, *Saccharofermentans*, and *Syntrophomonas*. These bacterial populations were recognized as important players in substrate hydrolysis, fermentation, acetogenesis, and syntrophic metabolism (Bossard et al., 2002; Chen et al., 2010; Vanwonterghem et al., 2014). Due to the combined high abundances of core communities in all the digesters, they may be targets for manipulation of microbial activities to achieve an efficient performance and stability in manure anaerobic digesters.

Substrate-unique and abundant OTUs were identified, while a majority of these OTUs were unclassified at genus level. Substrate-unique and abundant OTUs may reflect the variations

of manure quality, and the differences in the digestive tracts of rumen and non-rumen animals. This is supported by the fact that cattle-unique and abundant OTUs were exclusively and positively correlated with C:N and COD ($p < 0.05$), while swine-unique and abundant OTUs positively correlated with FA and NH₄⁺-N ($p < 0.05$). The C:N and FA strongly select unique bacterial populations that can be well adapted in these anaerobic digesters.

Our findings are based on mesophilic digesters treating cattle and swine manure. When adding more digester samples with different substrates or operational parameters, such as chicken manure and high temperature, the revealed key factors shaping bacterial community structure may change. If one environmental factor outcompetes other factors, it may decouple the relationships between microbial communities and other factors (Rui et al., 2015). Indeed, temperature is recognized as a key factor to shift microbial community structure in AD systems (Sundberg et al., 2013; De Vrieze et al., 2015).

Overall, our study revealed that substrate and free ammonia play key roles in determining the bacterial community structure. The selection of different prokaryotic taxa by substrates and free ammonia is likely an important mechanism shaping prokaryotic community structure in manure AD systems. Core communities may be responsible for the central function in AD systems, while substrate-unique and abundant communities may reflect the selection effects largely exerted by substrate quality and operational conditions. These findings provide further understanding of the bacterial assembly in full-scale manure anaerobic digesters.

ACKNOWLEDGMENTS

This work was supported by 973 project (No. 2013CB733502), National Key Technology Support Program (2014BAD02B04) and the National Natural Science Foundation of China (41271260). We thank Anna Doloman for the help on manuscript improvement.

SUPPLEMENTARY MATERIAL

The Supplementary Material for this article can be found online at: <http://journal.frontiersin.org/article/10.3389/fmicb.2015.01337>

REFERENCES

- ASABE (2005). *Manure Production and Characteristics*. ASABE Standard D384.2.
- Ali Shah, F., Mahmood, Q., Maroof Shah, M., Pervez, A., and Ahmad Asad, S. (2014). Microbial ecology of anaerobic digesters: the key players of anaerobiosis. *Sci. World J.* 2014:183752. doi: 10.1155/2014/183752
- Alvarado, A., Montanez-Hernandez, L. E., Palacio-Molina, S. L., Oropeza-Navarro, R., Luevanos-Escareno, M. P., and Balagurusamy, N. (2014). Microbial trophic

- interactions and mcrA gene expression in monitoring of anaerobic digesters. *Front. Microbiol.* 5:597. doi: 10.3389/fmicb.2014.00597
- Bossard, P. P., Zbinden, R., and Altweig, M. (2002). *Turicibacter sanguinis* gen. nov., sp. nov., a novel anaerobic, Gram-positive bacterium. *Int. J. Syst. Evol. Microbiol.* 52(Pt 4), 1263–1266. doi: 10.1099/00207713-52-4-1263
- Caporaso, J. G., Kuczynski, J., Stombaugh, J., Bittinger, K., Bushman, F. D., Costello, E. K., et al. (2010). QIIME allows analysis of high-throughput community sequencing data. *Nat. Methods* 7, 335–336. doi: 10.1038/nmeth.f.303

- Carballa, M., Regueiro, L., and Lema, J. M. (2015). Microbial management of anaerobic digestion: exploiting the microbiome-functionality nexus. *Curr. Opin. Biotechnol.* 33, 103–111. doi: 10.1016/j.copbio.2015.01.008
- Chen, S., Niu, L., and Zhang, Y. (2010). *Saccharofermentans acetigenes* gen. nov., sp. nov., an anaerobic bacterium isolated from sludge treating brewery wastewater. *Int. J. Syst. Evol. Microbiol.* 60(Pt 12), 2735–2738. doi: 10.1099/ijss.0.017590-0
- Chen, Y., Cheng, J. J., and Creamer, K. S. (2008). Inhibition of anaerobic digestion process: a review. *Bioresour. Technol.* 99, 4044–4064. doi: 10.1016/j.biortech.2007.01.057
- de Bok, F. A., Stams, A. J., Dijkema, C., and Boone, D. R. (2001). Pathway of propionate oxidation by a syntrophic culture of *Smithella propionica* and *Methanospirillum hungatei*. *Appl. Environ. Microbiol.* 67, 1800–1804. doi: 10.1128/AEM.67.4.1800-1804.2001
- Deng, Y., He, Z., Xu, M., Qin, Y., Van Nostrand, J. D., Wu, L., et al. (2012). Elevated carbon dioxide alters the structure of soil microbial communities. *Appl. Environ. Microbiol.* 78, 2991–2995. doi: 10.1128/AEM.06924-11
- Deublein, D., and Steinhauser, A. (2008). *Biogas from Waste and Renewable Resources: An Introduction*. Weinheim: Wiley-VCH Verlag GmbH & Co., KGaA.
- De Vrieze, J., Saunders, A. M., He, Y., Fang, J., Nielsen, P. H., Verstraete, W., et al. (2015). Ammonia and temperature determine potential clustering in the anaerobic digestion microbiome. *Water Res.* 75, 312–323. doi: 10.1016/j.watres.2015.02.025
- Dixon, P. (2003). VEGAN, a package of R functions for community ecology. *J. Veg. Sci.* 14, 927–930. doi: 10.1111/j.1654-1103.2003.tb02228.x
- Edgar, R. C., Haas, B. J., Clemente, J. C., Quince, C., and Knight, R. (2011). UCHIME improves sensitivity and speed of chimer detection. *Bioinformatics* 27, 2194–2200. doi: 10.1093/bioinformatics/btr381
- Hansen, K. H., Angelidaki, I., and Ahring, B. K. (1998). Anaerobic digestion of swine manure: inhibition by ammonia. *Water Res.* 32, 5–12. doi: 10.1016/S0043-1354(97)00201-7
- Jiang, X. Y., Sommer, S. G., and Christensen, K. V. (2011). A review of the biogas industry in China. *Energy Policy* 39, 6073–6081. doi: 10.1016/j.enpol.2011.07.007
- Li, J. B., Rui, J. P., Pei, Z. J., Sun, X. R., Zhang, S. H., Yan, Z. Y., et al. (2014). Straw- and slurry-associated prokaryotic communities differ during co-fermentation of straw and swine manure. *Appl. Microbiol. Biotechnol.* 98, 4771–4780. doi: 10.1007/s00253-014-5629-3
- Lin, L., Wan, C., Liu, X., Lee, D. J., Lei, Z., Zhang, Y., et al. (2013). Effect of initial pH on mesophilic hydrolysis and acidification of swine manure. *Bioresour. Technol.* 136, 302–308. doi: 10.1016/j.biortech.2013.02.106
- Liu, F. H., Wang, S. B., Zhang, J. S., Zhang, J., Yan, X., Zhou, H. K., et al. (2009). The structure of the bacterial and archaeal community in a biogas digester as revealed by denaturing gradient gel electrophoresis and 16S rDNA sequencing analysis. *J. Appl. Microbiol.* 106, 952–966. doi: 10.1111/j.1365-2672.2008.04064.x
- Morris, B. E., Henneberger, R., Huber, H., and Moissl-Eichinger, C. (2013). Microbial syntrophy: interaction for the common good. *FEMS Microbiol. Rev.* 37, 384–406. doi: 10.1111/1574-6976.12019
- Nelson, M. C., Morrison, M., and Yu, Z. (2011). A meta-analysis of the microbial diversity observed in anaerobic digesters. *Bioresour. Technol.* 102, 3730–3739. doi: 10.1016/j.biortech.2010.11.119
- Qiu, Y. L., Hanada, S., Ohashi, A., Harada, H., Kamagata, Y., and Sekiguchi, Y. (2008). *Syntrophorhabdus aromaticivorans* gen. nov., sp. nov., the first cultured anaerobe capable of degrading phenol to acetate in obligate syntrophic associations with a hydrogenotrophic methanogen. *Appl. Environ. Microb.* 74, 2051–2058. doi: 10.1128/AEM.02378-07
- Rademacher, A., Zakrzewski, M., Schluter, A., Schonberg, M., Szczepanowski, R., Goesmann, A., et al. (2012). Characterization of microbial biofilms in a thermophilic biogas system by high-throughput metagenome sequencing. *FEMS Microbiol. Ecol.* 79, 785–799. doi: 10.1111/j.1574-6941.2011.01265.x
- Rajagopal, R., Masse, D. I., and Singh, G. (2013). A critical review on inhibition of anaerobic digestion process by excess ammonia. *Bioresour. Technol.* 143, 632–641. doi: 10.1016/j.biortech.2013.06.030
- Riviere, D., Desvignes, V., Pelletier, E., Chaussonnerie, S., Guermazi, S., Weissenbach, J., et al. (2009). Towards the definition of a core of microorganisms involved in anaerobic digestion of sludge. *ISME J.* 3, 700–714. doi: 10.1038/ismej.2009.2
- Rui, J., Li, J., Zhang, S., Yan, X., Wang, Y., and Li, X. (2015). The core populations and co-occurrence patterns of prokaryotic communities in household biogas digesters. *Biotechnol. Biofuels* 8, 158. doi: 10.1186/s13068-015-0339-3
- Saunders, A. M., Albertsen, M., Vollertsen, J., and Nielsen, P. H. (2015). The activated sludge ecosystem contains a core community of abundant organisms. *ISME J.* 1–10. doi: 10.1038/ismej.2015.117. Available online at: <http://www.nature.com/ismej/journal/vaop/ncurrent/full/ismej2015117a.html>
- Schnurer, A., and Nordberg, A. (2008). Ammonia, a selective agent for methane production by syntrophic acetate oxidation at mesophilic temperature. *Water Sci. Technol.* 57, 735–740. doi: 10.2166/wst.2008.097
- Schnurer, A., Schink, B., and Svensson, B. H. (1996). *Clostridium ultunense* sp. nov., a mesophilic bacterium oxidizing acetate in syntrophic association with a hydrogenotrophic methanogenic bacterium. *Int. J. Syst. Bacteriol.* 46, 1145–1152. doi: 10.1099/00207713-46-4-1145
- Schnurer, A., Zellner, G., and Svensson, B. H. (1999). Mesophilic syntrophic acetate oxidation during methane formation in biogas reactors. *FEMS Microbiol. Ecol.* 29, 249–261. doi: 10.1016/S0168-6496(99)00016-1
- Sekiguchi, Y., Yamada, T., Hanada, S., Ohashi, A., Harada, H., and Kamagata, Y. (2003). *Anaerolinea thermophila* gen. nov., sp. nov. and *Caldilinea aerophila* gen. nov., sp. nov., novel filamentous thermophiles that represent a previously uncultured lineage of the domain Bacteria at the subphylum level. *Int. J. Syst. Evol. Microbiol.* 53(Pt 6), 1843–1851. doi: 10.1099/ijss.0.02699-0
- Shen, L., Hu, H. Y., Ji, H. F., Cai, J. Y., He, N., Li, Q. B., et al. (2014). Production of poly(hydroxybutyrate–hydroxyvalerate) from waste organics by the two-stage process: focus on the intermediate volatile fatty acids. *Bioresour. Technol.* 166, 194–200. doi: 10.1016/j.biortech.2014.05.038
- Sieber, J. R., McInerney, M. J., and Gunsalus, R. P. (2012). Genomic insights into syntropy: the paradigm for anaerobic metabolic cooperation. *Annu. Rev. Microbiol.* 66, 429–452. doi: 10.1146/annurev-micro-090110-102844
- Sprott, G. D., and Patel, G. B. (1986). Ammonia toxicity in pure cultures of methanogenic bacteria. *Syst. Appl. Microbiol.* 7, 358–363. doi: 10.1016/S0723-2020(86)80044-0
- St-Pierre, B., and Wright, A. D. (2014). Comparative metagenomic analysis of bacterial populations in three full-scale mesophilic anaerobic manure digesters. *Appl. Microbiol. Biotechnol.* 98, 2709–2717. doi: 10.1007/s00253-013-5220-3
- Sundberg, C., Al-Soud, W. A., Larsson, M., Alm, E., Shakeri Yekta, S., Svensson, B. H., et al. (2013). 454-pyrosequencing analyses of bacterial and archaeal richness in 21 full-scale biogas digesters. *FEMS Microbiol. Ecol.* 85, 612–626. doi: 10.1111/1574-6941.12148
- Town, J. R., Links, M. G., Fonstad, T. A., and Dumonceaux, T. J. (2014). Molecular characterization of anaerobic digester microbial communities identifies microorganisms that correlate to reactor performance. *Bioresour. Technol.* 151, 249–257. doi: 10.1016/j.biortech.2013.10.070
- Vanwonterghem, I., Jensen, P. D., Dennis, P. G., Hugenholtz, P., Rabaey, K., and Tyson, G. W. (2014). Deterministic processes guide long-term synchronised population dynamics in replicate anaerobic digesters. *ISME J.* 8, 2015–2028. doi: 10.1038/ismej.2014.50
- Wagner, A. O., Lins, P., Malin, C., Reitschuler, C., and Illmer, P. (2013). Impact of protein-, lipid- and cellulose-containing complex substrates on biogas production and microbial communities in batch experiments. *Sci. Total Environ.* 458–460, 256–266. doi: 10.1016/j.scitotenv.2013.04.034
- Wang, Q., Garrity, G. M., Tiedje, J. M., and Cole, J. R. (2007). Naive Bayesian classifier for rapid assignment of rRNA sequences into the new bacterial taxonomy. *Appl. Environ. Microbiol.* 73, 5261–5267. doi: 10.1128/AEM.0062-07
- Werner, J. J., Garcia, M. L., Perkins, S. D., Yarasheski, K. E., Smith, S. R., Muegge, B. D., et al. (2014). Microbial community dynamics and stability during an ammonia-induced shift to syntrophic acetate oxidation. *Appl. Environ. Microbiol.* 80, 3375–3383. doi: 10.1128/AEM.00166-14
- Werner, J. J., Knights, D., Garcia, M. L., Scalfone, N. B., Smith, S., Yarasheski, K., et al. (2011). Bacterial community structures are unique and resilient in full-scale bioenergy systems. *Proc. Natl. Acad. Sci. U.S.A.* 108, 4158–4163. doi: 10.1073/pnas.1015676108

- Westerholm, M., Roos, S., and Schnürer, A. (2010). *Syntrophaceticus schinkii* gen. nov., sp. nov., an anaerobic, syntrophic acetate-oxidizing bacterium isolated from a mesophilic anaerobic filter. *FEMS Microbiol. Lett.* 309, 100–104. doi: 10.1111/j.1574-6968.2010.02023.x
- Westerholm, M., Roos, S., and Schnürer, A. (2011). *Tepidanaerobacter acetatoxydans* sp. nov., an anaerobic, syntrophic acetate-oxidizing bacterium isolated from two ammonium-enriched mesophilic methanogenic processes. *Syst. Appl. Microbiol.* 34, 260–266. doi: 10.1016/j.syapm.2010.11.018
- Yamada, T., Sekiguchi, Y., Hanada, S., Imachi, H., Ohashi, A., Harada, H., et al. (2006). *Anaerolinea thermolimosa* sp. nov., *Levilinea saccharolytica* gen. nov., sp. nov. and *Leptolinea tardivitalis* gen. nov., sp. nov., novel filamentous anaerobes, and description of the new classes *Anaerolineae classis* nov. and *Caldilineae classis* nov. in the bacterial phylum Chloroflexi. *Int. J. Syst. Evol. Microbiol.* 56(Pt 6), 1331–1340. doi: 10.1099/ijts.0.64169-0
- Zhang, T., Liu, L., Song, Z., Ren, G., Feng, Y., Han, X., et al. (2013). Biogas production by co-digestion of goat manure with three crop residues. *PLoS ONE* 8:e66845. doi: 10.1371/journal.pone.0066845
- Zhang, W., Werner, J. J., Agler, M. T., and Angenent, L. T. (2014). Substrate type drives variation in reactor microbiomes of anaerobic digesters. *Bioresour. Technol.* 151, 397–401. doi: 10.1016/j.biortech.2013.10.004
- Zhu, L., Wu, Q., Dai, J., Zhang, S., and Wei, F. (2011). Evidence of cellulose metabolism by the giant panda gut microbiome. *Proc. Natl. Acad. Sci. U.S.A.* 108, 17714–17719. doi: 10.1073/pnas.1017956108
- Ziganshin, A. M., Liebetrau, J., Proter, J., and Kleinstreuber, S. (2013). Microbial community structure and dynamics during anaerobic digestion of various agricultural waste materials. *Appl. Microbiol. Biotechnol.* 97, 5161–5174. doi: 10.1007/s00253-013-4867-0

Conflict of Interest Statement: The authors declare that the research was conducted in the absence of any commercial or financial relationships that could be construed as a potential conflict of interest.

Copyright © 2015 Li, Rui, Yao, Zhang, Yan, Wang, Yan and Li. This is an open-access article distributed under the terms of the Creative Commons Attribution License (CC BY). The use, distribution or reproduction in other forums is permitted, provided the original author(s) or licensor are credited and that the original publication in this journal is cited, in accordance with accepted academic practice. No use, distribution or reproduction is permitted which does not comply with these terms.



Effects of sludge inoculum and organic feedstock on active microbial communities and methane yield during anaerobic digestion

David Wilkins, Subramanya Rao, Xiaoying Lu[†] and Patrick K. H. Lee*

School of Energy and Environment, City University of Hong Kong, Kowloon Tong, Hong Kong

OPEN ACCESS

Edited by:

Giovanni Esposito,
University of Cassino and Southern Lazio, Italy

Reviewed by:

Seung Gu Shin,
Pohang University of Science and Technology, South Korea
Zhongtang Yu,
The Ohio State University, USA

***Correspondence:**

Patrick K. H. Lee
patrick.kh.lee@cityu.edu.hk

†Present address:

Xiaoying Lu,
Faculty of Science and Technology, Technological and Higher Education Institute of Hong Kong, Tsing Yi, Hong Kong

Specialty section:

This article was submitted to
Microbiotechnology, Ecotoxicology and Bioremediation,
a section of the journal
Frontiers in Microbiology

Received: 25 June 2015

Accepted: 28 September 2015

Published: 13 October 2015

Citation:

Wilkins D, Rao S, Lu X and Lee PKH (2015) Effects of sludge inoculum and organic feedstock on active microbial communities and methane yield during anaerobic digestion.
Front. Microbiol. 6:1114.
doi: 10.3389/fmicb.2015.01114

Anaerobic digestion (AD) is a widespread microbial technology used to treat organic waste and recover energy in the form of methane ("biogas"). While most AD systems have been designed to treat a single input, mixtures of digester sludge and solid organic waste are emerging as a means to improve efficiency and methane yield. We examined laboratory anaerobic cultures of AD sludge from two sources amended with food waste, xylose, and xylan at mesophilic temperatures, and with cellulose at meso- and thermophilic temperatures, to determine whether and how the inoculum and substrate affect biogas yield and community composition. All substrate and inoculum combinations yielded methane, with food waste most productive by mass. Pyrosequencing of transcribed bacterial and archaeal 16S rRNA showed that community composition varied across substrates and inocula, with differing ratios of hydrogenotrophic/acetoclastic methanogenic archaea associated with syntrophic partners. While communities did not cluster by either inoculum or substrate, additional sequencing of the bacterial 16S rRNA gene in the source sludge revealed that the bacterial communities were influenced by their inoculum. These results suggest that complete and efficient AD systems could potentially be assembled from different microbial inocula and consist of taxonomically diverse communities that nevertheless perform similar functions.

Keywords: anaerobic digestion, biogas, methanogenesis, pyrosequencing

INTRODUCTION

Microbial anaerobic digestion (AD) of wastewater and sewage allows the recovery of energy in the form of biogas (methane) while simultaneously reducing the concentration of organic substrates and displacing pathogens. This makes it a valuable component of both municipal and industrial wastewater treatment, as on-site energy consumption can be offset by biogas production. While the use of AD to treat wastewater and sewage streams is well-established, it is increasingly considered a viable method for the treatment of solid organic wastes including food waste and the organic components of municipal solid waste (MSW; Zhang et al., 2007; Khalid et al., 2011). These materials would otherwise go to landfill, where microbially mediated aerobic or anaerobic decomposition would release carbon dioxide and methane to the atmosphere, or to incineration with similar consequences. Capturing energy in the form of biogas while simultaneously reducing greenhouse gas emissions thus makes AD an attractive alternative to traditional solid waste management practices (Khalid et al., 2011).

Digestion of sewage sludge amended with food waste can result in higher methane production than from either substrate digested separately (Kim et al., 2003; Sosnowski et al., 2003; Iacovidou et al., 2012), although the improvement is conditional on the mixing ratio and reactor conditions (Heo et al., 2003; Zhang et al., 2008). Lignocellulosic biomass including agricultural by-products (e.g., rice straw, corn stover) and domestic “green waste” (e.g., lawn clippings) are also attractive solid waste amendment candidates due to their high availability, low cost and the environmental impact of alternative disposal methods (Li et al., 2011). However, these materials require pre-treatment with a method such as steam pre-treatment (Chandra et al., 2007), acid hydrolysis or alkali treatment (Galbe and Zacchi, 2007) to separate the cellulose, hemicellulose, and lignin components which are covalently linked and thus recalcitrant to microbial catalysis. These methods typically yield some combination of cellulose, glucose, and xylose/xylan as the major bacterially available components following hydrolysis (Öhgren et al., 2005; Chandra et al., 2007; Galbe and Zacchi, 2007).

Despite the importance and widespread use of AD, the composition of AD microbial communities is poorly understood (Rivière et al., 2009; Narihiro et al., 2015) and major methanogen groups regularly detected in AD reactors remain uncharacterized (Narihiro et al., 2009; Nelson et al., 2011). All known methanogens are of the phylum *Euryarchaeota*, which comprises six established orders (*Methanobacteriales*, *Methanocellales*, *Methanococcales*, *Methanomicrobiales*, *Methanopyrales*, and *Methanosarcinales*) and one proposed order (*Methanomassiliicoccaceae*; Borrel et al., 2013). In AD reactors, the hydrogenotrophic *Methanobacteriales* and *Methanomicrobiales* and acetoclastic/hydrogenotrophic *Methanosarcinales* are typically dominant (Nettmann et al., 2008; Rastogi et al., 2008; Zhu et al., 2008; Nelson et al., 2011; Wilkins et al., 2015). The uncultured ArcI/Arc I/WSA2 group is also routinely detected at high abundance in AD communities (Chouari et al., 2005b; Rivière et al., 2009; Nelson et al., 2011; Wilkins et al., 2015). The bacterial component of AD communities is typically dominated by the phyla *Chloroflexi*, *Proteobacteria*, *Firmicutes*, and *Bacteroidetes* (Rivière et al., 2009; Nelson et al., 2011). With the exception of *Chloroflexi*, the functional role of which is still being actively investigated, genera detected from the remaining three major phyla are associated with all steps of the AD process excluding methanogenesis (Nelson et al., 2011); functional assessment of the role of bacterial groups in AD therefore benefits from classification to the family level or finer. Notably, a meta-analysis of AD 16S rRNA gene surveys found over 50% of *Bacteroidetes* sequences could not be classified beyond phylum (Nelson et al., 2011). The effects of substrate and inoculum source are also poorly explored. While meta-analyses of AD microbial communities have found that they cluster by substrate (Regueiro et al., 2013; Zhang et al., 2014), it is not clear whether diverse and substrate-specific communities can be enriched from a common source by substrate amendment. A more complete understanding of the microbial communities associated with the digestion of wastewater sludge amended with organic solids is critical to improving the efficiency of this method.

This study aimed to characterize the relative importance and effect of both sludge inoculum and organic waste substrate on the active archaeal and bacterial community composition and methane yields from AD. We sought to determine whether or not the source inoculum continues to have a large effect on community composition and methane production following medium-term enrichment, and if so whether this effect is mediated by the organic waste substrate. Two sludge types (from industrial wastewater and sewage) were incubated with food waste as well as cellulose, xylose, and xylan representing pre-treated lignocellulosic organic matter. Previous studies aimed at characterizing the community composition of AD sludge or wastewater (Chouari et al., 2005a; Rivière et al., 2009; Nelson et al., 2011; Zhang et al., 2014) or of cultures inoculated from AD sources (Wagner et al., 2013; Narihiro et al., 2015) have used clone library or pyrotag sequencing of the 16S rRNA or other marker genes. While this method is able to give an overview of the cells present in the system, it does not differentiate between active (i.e., metabolizing and dividing) and dormant cells. In systems such as AD where sludge and wastewater are recycled and cells may have long residence times, and particularly in closed laboratory cultures, this may exaggerate the importance of inactive populations. In contrast, reverse transcription and sequencing of transcribed small-subunit rRNA provides a more accurate reflection of the metabolically active microbial population. By targeting transcribed rRNA molecules rather than rRNA genes, this study was thus able to reveal the active archaeal and bacterial populations in different digestion scenarios. We also examined the effects of meso- and thermophilic temperatures on the digestion of cellulose.

MATERIALS AND METHODS

Sample Collection

Two sludge samples were obtained for this study. The first was taken from an Upflow Anaerobic Sludge Blanket (UASB) digester treating sugar wastewater from a beverage factory in Guangzhou, China (“GZ”). The second was taken from mesophilic anaerobic digester in the Shek Wu Hui sewage treatment plant in Hong Kong (“SWH”). Operating conditions and physicochemical properties for these digesters have been previously reported (Wilkins et al., 2015). Triplicate 1 L samples were collected simultaneously from the midsection of each digester and mixed thoroughly. The samples were incubated at 35°C and used as inocula within 72 h.

Batch Culture

A series of batch culture experiments were carried out to identify the major active taxa involved in the digestion of various substrates. Sludge samples (50 mL) from the two digesters were centrifuged at 1,500 × g for 2 min, then resuspended in 100 mL of 0.2 M phosphate buffer (pH 7.2) made anaerobic by purging it with ultra-high purity (99.999%) N₂ gas. Food waste was collected from the university canteen and blended into slurry with a food processor. The volatile solids composition of the food waste was determined by the standard method

given in Rice et al. (2012). Cellulose (type 101, highly purified fibers), xylan (from beechwood), and xylose (purity \geq 99%) were purchased from Sigma-Aldrich (St. Louis, MO, USA). Duplicate batch cultures were set up in 160 mL serum bottles each with 5 g volatile solids/L of food waste or 5 g/L of cellulose, xylan, or xylose as the sole carbon source. Controls with no added substrate were also prepared. Serum bottles were sealed with butyl rubber stoppers and purged with ultra-high purity N₂ gas for 10 min to ensure completely anaerobic conditions. The serum bottles were incubated at 35°C (i.e., similar to the mesophilic operating temperature of the sampled AD systems) without shaking. To investigate the effect of temperature, additional duplicate cellulose cultures were incubated at 55°C (thermophilic) without shaking. Incubations proceeded for 69–87 days and samples for chemical analysis were collected every 7–10 days.

To determine the total methane production of each culture, headspace gas was collected from each culture and methane concentration measured by gas chromatograph (GC; GC-2010 Plus, Shimadzu, Kyoto, Japan) with a flame ionization detector. The injector and detector temperatures were isothermal at 30 and 200°C, respectively, and the GC was programmed to maintain 35°C for 8 min. Helium (3 mL/min) was used as the carrier gas in a Rt-QS-BOND column (Restek Corporation, Bellefonte, PA, USA). The volume of headspace gas was measured every 3–10 days by syringe at ambient temperature and pressure, and the total volume of methane produced was calculated. Volatile fatty acids (VFAs) concentrations were determined by a high-performance liquid chromatograph fitted with an Aminex HPX-87H column (Bio-Rad, Hercules, CA, USA) and photodiode array detector (Waters, Milford, MA, USA).

454 Pyrosequencing and Operational Taxonomic Unit (OTU) Formation

Nucleic acid extraction, reverse transcription, PCR amplification and sequencing were performed as previously described (Lu et al., 2013). Briefly, 1 mL from each duplicate culture was collected and pooled at the midpoint of growth, as determined by linearly increasing methane concentration. Samples were immediately centrifuged at 13,800 \times g for 6 min at 4°C, and the cell pellet stored at –80°C until RNA extraction (less than 1 week). Total RNA was extracted with the RNeasy Mini Kit (Qiagen, Valencia, CA, USA) following the manufacturer's protocol, with additional mechanical lysis by vortexing for 10 min with 100 mg of 100 μ g-diameter zirconia/silica beads (Biospec Products, Bartlesville, OK, USA), and DNA contamination was removed with the RNase-free DNase kit (Qiagen, Valencia, CA, USA) following the manufacturer's protocol. 2 μ L of total RNA from each sample was reverse transcribed to complementary DNA (cDNA) with the SuperScript III First Strand Synthesis System (Invitrogen, Carlsbad, CA, USA), following the manufacturer's protocol with random hexamer priming. Template- and enzyme-free negative control reactions were performed in parallel.

From the sludge inocula, genomic DNA (gDNA) was extracted from two pooled replicate 250 mg samples with the PowerSoil DNA Extraction Kit (MoBio Laboratories, Carlsbad, CA, USA),

following the manufacturer's protocol with additional mechanical lysis as above. Sludge inoculum gDNA was used for bacterial community analysis only; the archaeal community composition has been previously reported (Wilkins et al., 2015). DNA concentration and purity was assessed with a NanoDrop 2000 UV-Vis Spectrophotometer (NanoDrop Products, Wilmington, DE, USA).

The transcribed bacterial V1–V3 and archaeal V1–V2 16S rRNA regions were amplified from template cDNA and gDNA (bacterial only) with the 27F/534R (Wu et al., 2010) and A2Fa/A571R (Kan et al., 2011) primer pairs respectively, with PCR ingredients and conditions per the cited studies for 30 amplification cycles in triplicate reactions. To enable multiplexed 454 pyrosequencing, barcode sequences were incorporated between the adaptors and forward primers (Hamady et al., 2008). Amplicons were pooled and purified with the Agencourt AMPure XP kit (Beckman Coulter, Pasadena, IN, USA), then quantified with the Quant-iT Broad-Range DNA Assay kit (Life Technologies, Grand Island, NY, USA). Equimolar concentrations from each sample were sequenced by BGI (Hong Kong sequencing facility) on a 454 GS FLX Titanium platform (Roche, Branchburg, NJ, USA). Pyrosequencing reads generated for this study have been deposited in the NCBI Sequence Read Archive under project # PRJNA275176.

Operational taxonomic units (OTUs) were generated for each domain separately following the UPARSE pipeline (Edgar, 2013), with culture cDNA and sludge inoculum gDNA samples pooled to aid direct taxonomic comparison. Demultiplexed reads were filtered to a maximum expected error of one error per read and trimmed to a uniform length of 122 bp using the “fastq_filter” command of USEARCH (version 7.0.109; Edgar, 2010). This length was selected to maximize sequence length while reducing the expected error rate to less than one error per read. Reads shorter than 122 bp were removed. Dereplicated reads were clustered using the “cluster_ots” command of USEARCH with the default radius of 0.03 (97% sequence similarity). Reads were assigned to OTUs using the “usearch_global” command of USEARCH. Each OTU was assigned a taxonomic lineage using the QIIME (version 1.8.0; Caporaso et al., 2010b) script “assign_taxonomy.py,” with the Greengenes (version 13_5; DeSantis et al., 2006) 97% similar 16S rRNA core reference set and taxonomy as reference. Due to the short sequence length, only taxonomic assignments to the genus level were considered. OTU representative sequences were aligned with PyNAST (Caporaso et al., 2010a) using the QIIME script “parallel_align_seqs_pynast.py” against the aligned Greengenes core reference set, and a tree built with FastTree (Price et al., 2010) using the QIIME script “make_phylogeny.py.” Chimeric OTU representative sequences were identified using the USEARCH command “uchime_ref” and the “Gold” database (<http://drive5.com/uchime/gold.fa>, retrieved 27 October 2014). Reads matching any of the following conditions were removed from downstream analysis: failed to cluster with at least one other read (singleton or failed to be assigned to OTU); belonged to OTU identified as chimeric; belonged to OTU with representative sequence that failed to align with PyNAST.

Alpha and Beta Diversity

Inoculum DNA samples were excluded from all diversity analyses except for the construction of rarefaction curves, as differences in copy number between the DNA and RNA molecules would make direct comparison unreliable. Rarefaction curves were constructed to compare sample richness and assess whether richness was sampled to exhaustion. For each domain, 20 depths were selected at even intervals between one and the maximum sample read count for that domain. Each sample was randomly subsampled to each depth 10 times using the “rrarefy” function from the R package vegan (Oksanen et al., 2015), and the average OTU count at each depth calculated. To allow direct comparison of sample diversity, samples within each domain (excluding inoculum DNA samples) were randomly rarefied 10 times to the read count of the most depauperate sample in that domain. The number of OTUs, Chao1 richness estimator and abundance-based coverage estimator (ACE) were then calculated for each sample using the “estimateR” function from vegan and averaged. For each domain, the weighted UniFrac distance (Lozupone and Knight, 2005) between samples (excluding inoculum DNA samples) was calculated and the distances visualized with principal coordinates analysis (PCoA). To test if there were significant differences between the communities from different digesters and incubated with different substrates, analysis of similarities (ANOSIM) tests were performed using the “anosim” function from the vegan package. To test the hypothesis that the culture bacterial communities would be affected by the composition of the sludge inoculum, the combined culture (RNA) and inoculum (gDNA) OTU table was randomly subsampled to the depth of the most depauperate

sample using “rrarefy” and the unweighted UniFrac distance calculated. The unweighted distance was selected in this case to minimize potential biases in copy number while comparing OTUs generated from both genomic and transcribed rRNA. The UniFrac distances between each culture sample and its source inoculum were compared to the distances between culture samples and the non-source inoculum, and statistical significance determined with the non-parametric Mann–Whitney test.

RESULTS

Sequencing and OTU Formation

A total of 40,596 archaeal and 51,766 bacterial (including inoculum gDNA) 16S rRNA reads were obtained. Following read quality control, 34,595 archaeal and 39,550 bacterial reads were retained. Following OTU formation and quality control, 327 archaeal and 679 bacterial OTUs were formed comprising 28,020 and 24,802 reads respectively.

Because the bacterial and archaeal communities were assessed with different primer pairs and sequencing targets, richness and diversity comparisons were performed between samples and groups of samples but not between domains. No sample reached a richness plateau under rarefaction (Supplementary Figure S1), suggesting the OTU richness was not sampled to exhaustion. However, in both digesters and for both microbial domains, the rarefaction curve for the 55°C cellulose samples fell far below those for all other incubation conditions, suggesting these cultures had unusually low richness. When the samples were rarefied to equal depth (Table 1), 55°C cellulose samples were

TABLE 1 | List of cultures prepared for this study, methane and volatile fatty acid (VFA) production, and details on OTU formation and alpha diversity.

Digester	Condition	Methane (mL/g) (SD) ^a	Acetate (mM) (SD) ^b	Butyrate (mM) (SD) ^b	Propionate (mM) (SD) ^b	Domain	Reads ^c	OTUs ^d	Chao1 ^d	ACE ^d
GZ	Cellulose	481.5 (71)	0 (0)	0 (0)	0 (0)	Archaea	2,479	148	192	204
	Cellulose (55°C)	315 (24)	0.39 (0.01)	3.2 (0.07)	1.7 (0.42)	Bacteria	1,707	144	230	241
	Food waste	583.5 (6.4)	0 (0)	0 (0)	0 (0)	Archaea	3,438	45	54	57
	Xylan	296 (16)	0 (0)	0 (0)	0 (0)	Bacteria	2,365	29	39	47
	Xylose	264 (47)	0 (0)	0 (0)	0 (0)	Archaea	3,672	132	200	192
						Bacteria	2,008	156	239	250
SWH	Cellulose	489.5 (77)	1.3 (0.01)	4.3 (0.52)	0 (0)	Archaea	3,045	74	110	113
	Cellulose (55°C)	410 (28)	0.86 (0)	3.4 (0.2)	0.82 (0.23)	Bacteria	3,506	59	94	106
	Food waste	576 (31)	1.6 (0.13)	7.9 (0.21)	0.4 (0.14)	Archaea	2,318	34	36	36
	Xylan	381 (25)	0 (0)	0 (0)	0 (0)	Bacteria	837	23	29	25
	Xylose	276 (28)	0 (0)	0 (0)	0 (0)	Archaea	2,434	60	73	76
						Bacteria	2,995	63	102	105

^aAverage of replicate measurements of total production. ^bAverage of replicate measurements of final accumulated concentration. ^cQuality-controlled reads contributing to the final OTU table. ^dAveraged over 10 rounds of random subsampling to the depth of the most depauperate sample within each domain.

consistently the least rich in both OTU count and estimated richness (Chao1 and ACE). In samples inoculated from the GZ digester, samples amended with other substrates had similar observed and estimated richness within each domain (130–148 archaeal OTUs, 123–156 bacterial). However, SWH sludge amended with xylan had substantially higher observed and estimated richness (145 archaeal and 172 bacterial OTUs) than other SWH samples.

Taxonomic Composition

Operational taxonomic units identified in this study were generally well-taxonomically classified, with 155 GZ archaea OTUs (66% of reads), 170 SWH archaea OTUs (74%), 105 GZ bacteria OTUs (37%), and 122 SWH bacteria OTUs (61%) classified to at least the genus level. At the phylum level, the archaeal community was consistently dominated by the *Euryarchaeota* (relative abundance 87–100%), with 0–1.2% *Crenarchaeota* and 0–11% unclassified. The two methanogenic orders *Methanomicrobiales* and *Methanosarcinales* dominated all cultures at the order level (Figure 1), with most containing at least 10–30% of each order.

All GZ incubations included a relatively high abundance of *Methanolica* (23–93%), while *Methanolica* was only abundant in the SWH xylan incubation (22%; Table 2). *Methanosaeta* were also quite abundant in GZ incubations (0–37%), with the major exception being cellulose at 55°C (0%). In contrast,

Methanoculleus was present in GZ incubations at ≤0.16% but in SWH at 1.5–84%. *Methanosaeta* were present in SWH at 0.043–68% but in GZ at 0.058–24%.

Among the bacteria, the phyla *Firmicutes* (7.3–93%), *Chloroflexi* (0.12–65%), *Proteobacteria* (0–41%), and *Synergistetes* (0–54%) were most abundant (Figure 1). The sludge inocula bacterial communities from each digester were likewise dominated by the *Chloroflexi* (GZ) and *Chloroflexi/Firmicutes/Proteobacteria* (SWH), typical for AD sludge (Nelson et al., 2011). OTUs of the genus *Clostridium* (0.12–73%) were ubiquitous and abundant in all cultures but the SWH 55°C cellulose (0.12%), and were not abundant in the inoculum sludge (GZ 0.94%, SWH 0.57%). As with the archaeal genera, the 55°C cellulose samples contained a high abundance of genera particular to those samples. *Anaerobaculum*, while found in only two samples, comprised 54% of the SWH 55°C cellulose community. *Thermacetogenium*, likewise found in only two samples, was nevertheless 8.8% of the GZ 55°C cellulose community. Both of these idiosyncratic genera were absent from the sludge inocula (Table 3).

Effect of Inoculum Source and Organic Waste Substrate

On average, the enrichment bacterial communities resembled their respective source inoculum more closely (smaller unweighted UniFrac distance) than the other inoculum (Mann–Whitney $p = 0.01$, Figure 2). However, there was no statistically significant clustering of culture communities by either source digester or substrate (ANOSIM, all $p \geq 0.05$; Figure 3). Because no significant community-level differences were identified for these two factors, we did not examine individual taxa for significant differences.

In the GZ cultures, the measured VFA (acetate, propionate, and butyrate) were only detected for cellulose amended cultures at 55°C, while in the SWH cultures they were detected for cultures amended with food waste, cellulose, and cellulose at 55°C (Table 1). Butyrate was the major VFA to accumulate in the cultures, reaching its highest concentration (7.9 mM) in the SWH food waste culture, which also had moderate concentrations of acetate and propionate (Table 1). By contrast, all three measured VFAs were below the detection threshold in the GZ food waste culture.

Food waste amendment resulted in the highest total methane productivity in batch cultures from both inoculum sources, with yield consistently varying in the order food waste > cellulose > cellulose (55°C) > xylan > xylose (Table 1). Methane yields for the same substrate but different inocula were within 1 standard deviation of each other, with the exception of cellulose (55°C) and xylan; in both cases the yield from the SWH culture was higher (Table 1). Negligible (<10 mL total) methane was produced from the control (without substrate) cultures.

DISCUSSION

This study aimed to characterize the microbial communities involved in digestion of waste substrates including food waste

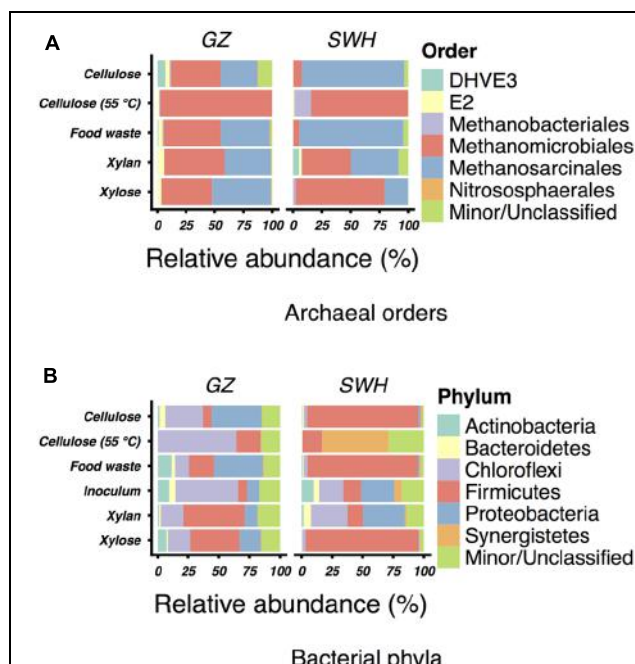


FIGURE 1 | Relative abundances of (A) archaeal orders in the enrichment cultures and (B) bacterial phyla in the cultures and sludge inocula. For each, the six most abundant taxa (excluding unclassified OTUs) by mean relative abundance across all samples are shown. All less abundant and unclassified taxa are grouped in “Minor/Unclassified.” Abundances are for the complete (non-normalized) read set for each sample. Note that the Greengenes taxonomy includes some candidate and uncultured divisions.

TABLE 2 | Relative abundances of the most abundant archaeal genera detected in this study.

Genus	GZ						SWH				
	Cellulose	Cellulose (55°C)	Food waste	Xylan	Xylose	Cellulose	Cellulose (55°C)	Food waste	Xylan	Xylose	
<i>Methanoculleus</i>	0.16	0.058	—	—	—	5.1	84	3.5	1.5	61	
<i>Methanosarcina</i>	0.4	0.058	0.84	0.52	24	55	0.043	68	1.1	13	
<i>Methanothermobacter</i>	0.04	0.058	—	—	—	—	8.2	—	—	—	
<i>Methanolinea</i>	23	93	25	32	24	0.36	—	0.62	22	4.8	
<i>Methanoaeta</i>	29	—	37	24	5.4	0.56	—	0.041	28	7.2	
<i>Methanobacterium</i>	0.16	0.76	0.16	0.12	0.099	0.033	—	0.082	—	2.2	

All genera with a relative abundance of at least 1% in one sample are included. Genera are given in descending order of their mean relative abundance across all samples. A dash indicates that no OTUs associated with the genus were detected. Note that the Greengenes taxonomy includes some candidate and uncultured divisions.

as well as lignocellulosic pre-treatment products. By reverse transcribing and sequencing 16S rRNA transcripts rather than the 16S rRNA gene (as is more typical in microbial community studies of the AD process (Nelson et al., 2011)), we were able to examine the active microbial populations. This is especially useful in closed systems such as laboratory cultures where cells from the inocula may persist despite being metabolically inactive (Lu et al., 2013), helping to reveal active members of complex communities that may otherwise be obscured in DNA-based surveys (Brettar et al., 2012).

Methanogen Composition

Our previous study of the GZ and SWH sludge archaeal communities found on the basis of sequencing the methanogen-specific methyl coenzyme M reductase (*mcrA*) gene that the GZ sludge was *Methanomicrobiales*-dominated while SWH was *Methanosarcinales*-dominated (Wilkins et al., 2015). This study confirmed the high abundance of the *Methanomicrobiales* and *Methanosarcinales* (Figure 1), although the lack of a single dominant order in cultures inoculated from the same source suggests that substrate amendment disrupted any initial numerical advantage. Previous 16S rRNA gene sequencing of GZ and SWH sludge also revealed a substantial population of the uncultured ArcI/WSA2 group (Wilkins et al., 2015). The uncultured ArcI/WSA2 group of *Euryarchaeota*, frequently reported at high abundance in 16S rRNA gene-based AD community surveys (Chouari et al., 2005b; Rivière et al., 2009; Nelson et al., 2011; Wilkins et al., 2015), was conspicuous for its near-absence in this study, found at only 0–0.9% relative abundance across all samples. As this study targeted rRNA transcripts from active populations, it is possible that WSA2 were present but inactive. However, the WSA2 group are believed to be active methanogens, having been observed to grow in culture on formate and H₂/CO₂ (Chouari et al., 2005a) and possibly compete with *Methanoaeta* for acetate (Rivière et al., 2009). It is thus more likely that they are not a major component, active or otherwise, of the cultures.

Effect of Inoculum Source and Organic Waste Substrate

Although the enrichment cultures' bacterial communities were significantly more similar to their inoculum than to the other

sludge sample, there was no significant clustering of communities by inoculum source or by substrate. While this may in part be attributable to the small sample size, it does suggest that inoculum source is not the major factor structuring the enriched communities. Despite these differences, all combinations of inoculum source and substrate resulted in methane-yielding communities.

As previously reported (Lu et al., 2013), food waste amendment resulted in the highest methane productivity in batch cultures from both inoculum sources, with yield consistently varying in the order food waste > cellulose > cellulose (55°C) > xylan > xylose (Table 1). The probable mechanism for the improved methane productivity of food waste-amended sewage sludge is that it reduces the protein concentration relative to carbohydrates and lipids, which are more labile under microbial hydrolysis, thereby increasing the microbial growth rate and the overall hydrolytic efficiency of the AD system (Iacovidou et al., 2012); the initial hydrolysis step is likely rate-limiting in the digestion of sewage sludge. Additionally, food waste may contain a higher proportion of available organic substrates than indicated by volatile solids analysis, for example in the form of VFAs or alcohols.

The SWH food waste-amended culture was also notable for its high accumulation of VFA, particularly butyrate (Table 1). In addition to fermentation from glucose, butyrate (and longer carboxylates) can be produced in AD systems by chain elongation of ethanol or lactate with acetate via the reverse β oxidation pathway, found in many AD bacteria (Spirito et al., 2014) including *Clostridium* sp. (Seedorf et al., 2008). This may account for the high accumulation of butyrate relative to acetate, which would be consumed, and to propionate, which can also be elongated by this route (Spirito et al., 2014). However, it is noteworthy that a similar accumulation pattern was observed in both 55°C cellulose cultures (Table 1); as the chain elongation pathway has been reported to be suppressed at this temperature in AD reactors (Spirito et al., 2014), it is unlikely that the butyrate was produced in these cultures by the same route. Rapid initial acidification and VFA production is typical in complex organic waste digestion, but is usually followed by acetogenic uptake and consequent buffering (Sosnowski et al., 2008). VFA accumulation may therefore indicate that VFA production is outstripping acetogenesis and potentially hindering digestion efficiency with the consequent pH decrease (Siegert and Banks,

TABLE 3 | Relative abundances of the most abundant bacterial genera detected in this study.

Genus	GZ			SWH		
	Inoculum	Cellulose	Cellulose (55°C)	Inoculum	Cellulose	Cellulose (55°C)
<i>Anaerobaculum</i>	—	—	—	—	—	—
<i>Geobacter</i>	2.7	19	—	5.0	6.8	—
<i>Thermacetogenium</i>	—	—	8.8	—	—	0.36
<i>Clostridium</i>	0.94	2.4	8.5	5.6	22	0.57
<i>Coprothermobacter</i>	—	—	—	—	—	—
<i>Desulfobivrio</i>	0.085	2.6	—	2.4	—	0.8
<i>Limnohabitans</i>	—	—	—	—	1.1	—
T78	0.26	—	—	—	—	—
vadinCA02	—	—	—	—	10	2.1
SHD-231	0.17	—	—	—	0.35	4.4
<i>Ethanologenys</i>	2.0	—	—	0.15	—	0.43
<i>Pelotomaculum</i>	0.43	0.18	—	0.2	0.22	3.0
<i>Rhodobacter</i>	—	—	—	—	—	—
<i>Syntrophobacter</i>	2.0	13	—	12	3.0	4.6
<i>Syntrophomonas</i>	1.8	0.94	—	1.5	8.0	0.73
<i>Kosmotoga</i>	0.77	1.1	0.3	0.6	2.6	3.7
<i>Syntrophus</i>	0.34	1.0	—	3.2	0.27	0.44
<i>Treponema</i>	0.43	0.059	—	0.2	0.32	—

All genera with a relative abundance of at least 1% in one sample are included. Genera are given in descending order of their mean relative abundance across all samples. A dash indicates that no OTUs associated with the genus were detected. Note that the Greengenes taxonomy includes some candidate and uncultured divisions.

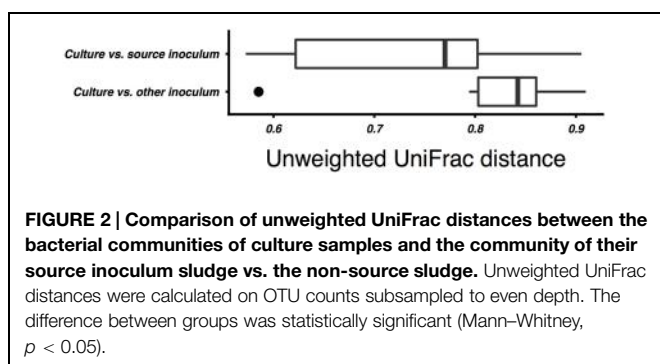


FIGURE 2 | Comparison of unweighted UniFrac distances between the bacterial communities of culture samples and the community of their source inoculum sludge vs. the non-source sludge. Unweighted UniFrac distances were calculated on OTU counts subsampled to even depth. The difference between groups was statistically significant (Mann–Whitney, $p < 0.05$).

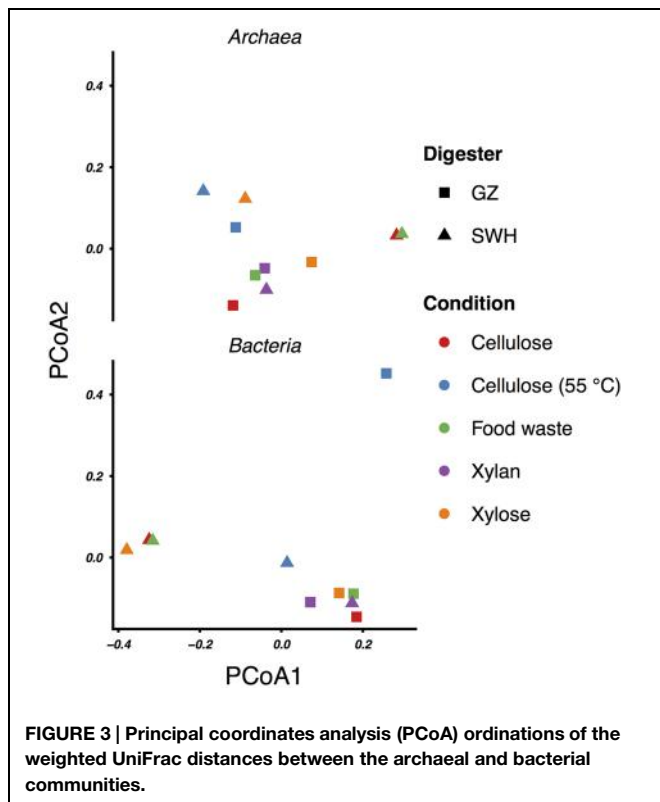


FIGURE 3 | Principal coordinates analysis (PCoA) ordinations of the weighted UniFrac distances between the archaeal and bacterial communities.

2005; Iacovidou et al., 2012). In this case, however, the high butyrate concentrations do not seem to have hindered the efficiency of the SWH food waste culture, which had comparable methane production to the GZ culture ($\sim 580 \text{ mL/g}$) despite the striking difference in VFA concentration.

The bacterial community in the SWH food waste culture was dominated by the genus *Clostridium* (54%), which was present but at much lower abundance in the GZ culture (5.6%). The dominant *Clostridium* OTU in the SWH food waste sample, OTU 1873 (52%; Supplementary Table S1), was not classified to the species level. Regardless, *Clostridium* species are common components of AD communities (Nelson et al., 2011) able to hydrolyze a diverse range of organic compounds, and produce metabolites including butyrate, acetate, and propionate (Tracy et al., 2012). The high abundance of *Clostridium* in the SWH food waste culture relative to VFA-consuming acetogens such as

Syntrophobacter (GZ: 12%, SWH: 0.27%) and *Syntrophomonas* (GZ: 1.5%, SWH: 2%; Appels et al., 2008) thus suggests that *Clostridium*-driven VFA production was indeed proceeding faster than uptake in that sample. This may reflect differences in the inoculum microbial community, although *Clostridium* was quite abundant in other GZ cultures (e.g., 43% in GZ, 3.1% in SWH xylan cultures) and OTU 1873 was not detected in the SWH sludge inoculum (Supplementary Table S1). It may rather reflect the differing waste streams treated by the two source digesters, with the sugar-rich beverage factory waste stream treated by the GZ digester providing a higher concentration of labile carbohydrates for hydrolysis and/or fermentation.

Cellulose was the second most efficient organic substrate, with the mesophilic (35°C) culture outperforming the thermophilic (55°C ; Table 1). Temperature affects several aspects of AD performance, including the microbial growth rate, inhibition of certain community members, enzyme kinetics and the solubility of organic substrates and intermediate compounds (Appels et al., 2008). As both source digesters were operated at mesophilic temperatures, it is likely that the sludge inocula communities were adapted to mesophilic conditions. The most obvious effect of thermophilic growth on the microbial community was the much lower bacterial and archaeal richness relative to the mesophilic cultures (Table 1), although this did not result in a convergence of the community profiles (Figure 3). Of the archaea, the GZ thermophilic cellulose community was dominated by the genus *Methanolinea* (93%) while the SWH culture was dominated by *Methanoculleus* (84%), neither of which were major components of AD sludge from either digester (Wilkins et al., 2015). Both the recently described genus *Methanolinea* (Imachi et al., 2008) and members of the *Methanoculleus* (Barret et al., 2013) perform methanogenesis via the hydrogenotrophic pathway, which can be coupled with syntrophic bacterial oxidation of VFAs to H_2/CO_2 . The bacterial communities were also dominated by a small number of OTUs. GZ was dominated by two OTUs from the poorly described phylum *Chloroflexi*, OTU 5 (family *Anaerolineaceae*, 45%) and OTU 9 (class *Anaerolineae*, 20%). The *Chloroflexi* are frequently found in high abundance in AD communities (Björnsson et al., 2002; Nelson et al., 2011). While their role in AD systems remains poorly described (Rivièvre et al., 2009; Narihiro et al., 2015), isolates from AD reactors have been found to grow fermentatively (Yamada and Sekiguchi, 2009 and references therein) and some exhibit faster growth when co-cultivated with hydrogenotrophic methanogens (Yamada et al., 2005, 2007), suggesting a syntrophic or “semi-syntrophic” (Yamada and Sekiguchi, 2009) role. Similarly, OTU 10 (genus *Anaerobaculum*) comprised 53% of all bacteria in the SWH sample and belongs to a group (the *Synergistetes*) also identified as a “core” taxon in AD communities (Rivièvre et al., 2009) but with an unknown role (Narihiro et al., 2015), although some *Synergistetes* have been shown to utilize acetate and are likely syntrophically coupled with hydrogenotrophic methanogens (Ito et al., 2011). If it is assumed that these dominant bacteria are indeed syntrophic partners of the hydrogenotrophic methanogens found in both cultures, these low-richness communities represent assembly of

phylogenetically distant OTUs to perform nevertheless similar roles in the AD process, and resulting in similar methane productivity (**Table 1**). Given that all of these OTUs were undetected or present at <1% in the respective source digester's sludge inoculum (Supplementary Table S1), it is likely that they were inactive and/or at very low abundance in the inoculum and increased in abundance due to cellulose amendment and adaptation to thermophilic growth.

While the mesophilic (35°C) cellulose cultures were overall richer than the thermophilic (**Table 1**), these communities were also dominated by a relatively small number of OTUs in the SWH culture, although the GZ culture was relatively diverse. While the genera *Methanosaeta* (29%) and *Methanolinea* (23%) comprised the majority of the GZ archaea, these genera were each represented by a number of OTUs, and several OTUs classified only to the family *Methanoregulaceae* were also present at 1–10% (Supplementary Table S1). By contrast, the archaeal community in the SWH mesophilic cellulose culture was dominated by two OTUs classified to the order *Methanosarcinales*, OTU 3 (43%) and OTU 4 (30%). Overall, the SWH methanogen community was dominated by the acetoclastic order *Methanosarcinales*, while the GZ culture contained a more even mix of *Methanosarcinales* and hydrogenotrophic *Methanomicrobiales*, a similar compositional pattern to that observed for food waste (**Figure 1**) and consistent with the overall similarities between the mesophilic cellulose and food waste communities for each digester (**Figure 3**). This again suggests that the composition of the sludge inoculum within a digestion culture has a large effect on the relative contribution of the acetoclastic and hydrogenotrophic pathways in the active community, even with the substrate composition held constant. This is consistent with the demonstrated similarity of culture bacterial communities to their respective sludge inocula (**Figure 2**).

Cultures amended with xylan, the least efficient methane producers (**Table 1**) as previously reported (Lu et al., 2013), and with xylose also had similar archaeal and bacterial communities within each sludge source (with the exception of SWH bacteria; **Figures 1** and **3**). For both substrates and source digesters, the methanogen community contained substantial populations of both *Methanosarcinales* and *Methanomicrobiales* while the bacterial communities were dominated by the *Firmicutes*, *Chloroflexi* and *Proteobacteria* (**Figure 1**). The SWH xylan cultures were notable for their unusually high observed and estimated total richness (**Table 1**). This cannot be attributed to noise introduced during PCR or sequencing, as it was independently observed in the (separately sequenced) archaeal and bacterial communities and as the number of unique OTUs in this sample was not unusually high, indicating that they were simply enriched in OTUs also found in other samples. Compared to simpler and monomeric substrates (e.g., xylose), xylan also requires a large set of enzymes (xylanases) for complete hydrolysis (Pérez et al., 2002) and consequently produces a broad range of fermentation substrates. The higher richness may therefore reflect the presence in the SWH sludge inoculum of taxa able to utilize xylan and its hydrolysis products, which were subsequently enriched.

While AD of xylose to methane has been little studied, Temudo et al. (2008) examined biomass production from anaerobic sludge inocula grown on either glucose or xylose as the sole carbon source. They reported that xylose resulted in 20% lower biomass yield than glucose, and suggested that the higher ATP requirement for xylose active transport in bacteria resulted in a lower net energetic yield for xylose than glucose per mole of substrate (Temudo et al., 2008) assuming that xylose transport in the relevant species is effected by high-affinity ABC transporters, while glucose transport proceeds mainly via an ATP-independent route such as the phosphotransferase system (PTS). As at least some anaerobic bacteria possess ATP-independent uptake systems for cellobiose (Kajikawa and Masaki, 1999), the major hydrolysis product of cellulose [e.g., when hydrolyzed by extracellular cellulosomes such as that produced by *Clostridium thermocellum* (Bégum and Lemaire, 1996)], cellulose may enjoy a similar energetic advantage over xylose that would account for the difference in methane yield.

This study aimed to characterize the effects of differences in sludge inocula and organic substrate on the microbial communities associated with AD and their methane yield. Narihiro et al. (2015) reported a similar investigation in which anaerobic digester sludge and swine manure were amended with a range of intermediate AD substrates including acetate and fatty acids, and found that the resulting enriched bacterial and archaeal communities clustered significantly by substrate, with acetate-amended communities clustering further by inoculum source. Similarly, a meta-analysis of 16S rRNA gene clones from AD reactors (Zhang et al., 2014) and denaturing gradient gel electrophoresis analysis of organic waste AD reactors (Regueiro et al., 2013) found that communities clustered by substrate. In this study, however, while there were some similarities by inoculum source and substrate in the active community taxonomic compositions (e.g., the presence or absence of certain genera; **Tables 2** and **3**), ANOSIM did not support a statistically significant grouping of either the archaeal or bacterial communities by source digester or growth substrate although bacterial communities were on average more similar to their source inoculum sludge than to the non-source sludge (**Figure 2**). Given that methane yields were relatively consistent across substrates (**Table 1**), this suggests that microbial communities assembled from different inocula to perform similar digestion tasks may have similar efficiency despite differing composition. We plan to confirm these results with a larger set of source inocula, which will also provide additional statistical power to test clustering of the communities by inoculum source and substrate. Additional experiments are also needed to better characterize the microbial communities, including by sequencing the active populations in the initial inoculum and comparing the active to dormant populations by parallel sequencing of 16S rRNA genes, and by culturing in a continuous flow system using pre-treated lignocellulosic matter as a substrate to better simulate a practical reactor. Tag pyrosequencing of the methanogen-specific *mcrA* gene (Wilkins et al., 2015) would also be useful to better characterize the as yet uncultivated fraction of the methanogen population.

AUTHOR CONTRIBUTIONS

DW and SR analyzed data and wrote the manuscript; XL performed laboratory work; PL designed the experiment and wrote the manuscript.

ACKNOWLEDGMENTS

This research was supported by the Research Grants Council of Hong Kong through projects # 116111 and # 11206514.

REFERENCES

- Appels, L., Baeyens, J., Degrève, J., and Dewil, R. (2008). Principles and potential of the anaerobic digestion of waste-activated sludge. *Prog. Energy Combust. Sci.* 34, 755–781. doi: 10.1016/j.pecs.2008.06.002
- Barret, M., Gagnon, N., Kalmokoff, M. L., Topp, E., Verastegui, Y., Brooks, S. P. J., et al. (2013). Identification of *Methanoculleus* spp. as active methanogens during anoxic incubations of swine manure storage tank samples. *Appl. Environ. Microbiol.* 79, 424–433. doi: 10.1128/AEM.02268-12
- Bégum, P., and Lemaire, M. (1996). The cellulosome: an exacellular, multiprotein complex specialized in cellulose degradation. *Crit. Rev. Biochem. Mol. Biol.* 31, 201–236. doi: 10.3109/10409239609106584
- Björnsson, L., Hugenholtz, P., Tyson, G. W., and Blackall, L. L. (2002). Filamentous Chloroflexi (green non-sulfur bacteria) are abundant in wastewater treatment processes with biological nutrient removal. *J. Gen. Microbiol.* 148, 2309–2318. doi: 10.1016/S0958-1669(00)00204-4
- Borrel, G., O'Toole, P. W., Harris, H. M. B., Peyret, P., Brugère, J. F., and Gribaldo, S. (2013). Phylogenomic data support a seventh order of methylotrophic methanogens and provide insights into the evolution of methanogenesis. *Genome Biol. Evol.* 5, 1769–1780. doi: 10.1093/gbe/evt128
- Brettar, I., Christen, R., and Höfle, M. G. (2012). Analysis of bacterial core communities in the central Baltic by comparative RNA-DNA-based fingerprinting provides links to structure-function relationships. *ISME J.* 6, 195–212. doi: 10.1038/ismej.2011.80
- Caporaso, J. G., Bittinger, K., Bushman, F. D., DeSantis, T. Z., Andersen, G. L., and Knight, R. (2010a). PyNAST: a flexible tool for aligning sequences to a template alignment. *Bioinformatics* 26, 266–267. doi: 10.1093/bioinformatics/btp636
- Caporaso, J. G., Kuczynski, J., Stombaugh, J., Bittinger, K., Bushman, F. D., Costello, E. K., et al. (2010b). QIIME allows analysis of high-throughput community sequencing data. *Nat. Methods* 7, 335–336. doi: 10.1038/nmeth.f.303
- Chandra, R. P., Bura, R., Mabee, W. E., Berlin, A., Pan, X., and Saddler, J. N. (2007). “Substrate pretreatment: the key to effective enzymatic hydrolysis of lignocellulosics?,” in *Advances in Biochemical Engineering/Biotechnology*, eds T. Schepers and L. Olsson (Berlin: Springer), 67–93.
- Chouari, R., Le Paslier, D., Daegelen, P., Ginestet, P., Weissenbach, J., and Sghir, A. (2005a). Novel predominant archaeal and bacterial groups revealed by molecular analysis of an anaerobic sludge digester. *Environ. Microbiol.* 7, 1104–1115. doi: 10.1111/j.1462-2920.2005.00795.x
- Chouari, R., Le Paslier, D., Dauga, C., Daegelen, P., Weissenbach, J., and Sghir, A. (2005b). Novel major bacterial candidate division within a municipal anaerobic sludge digester. *Appl. Environ. Microbiol.* 71, 2145–2153. doi: 10.1128/AEM.71.4.2145-2153.2005
- DeSantis, T. Z., Hugenholtz, P., Larsen, N., Rojas, M., Brodie, E. L., Keller, K., et al. (2006). Greengenes, a chimera-checked 16S rRNA gene database and workbench compatible with ARB. *Appl. Environ. Microbiol.* 72, 5069–5072. doi: 10.1128/AEM.03006-05
- Edgar, R. C. (2010). Search and clustering orders of magnitude faster than BLAST. *Bioinformatics* 26, 2460–2461. doi: 10.1093/bioinformatics/btq461
- Edgar, R. C. (2013). UPARSE: highly accurate OTU sequences from microbial amplicon reads. *Nat. Methods* 10, 996–998. doi: 10.1038/nmeth.2604
- The funding sources had no role in the design, execution, or publication of the research, and no conflict of interest is declared. We thank the plant operators for their assistance with sampling.
- Galbe, M., and Zacchi, G. (2007). “Pretreatment of lignocellulosic materials for efficient bioethanol production,” in *Biofuels*, ed. L. Olsson (Berlin: Springer), 41–65.
- Hamady, M., Walker, J. J., Harris, J. K., Gold, N. J., and Knight, R. (2008). Error-correcting barcoded primers for pyrosequencing hundreds of samples in multiplex. *Nat. Methods* 5, 235–237. doi: 10.1038/nmeth.1184
- Heo, N. H., Park, S. C., Lee, J. S., Kang, H., and Park, D. H. (2003). “Single-stage anaerobic codigestion for mixture wastes of simulated Korean food waste and waste activated sludge,” in *Biotechnology for Fuels and Chemicals*, eds B. H. Davison, J. W. Lee, M. Finkelstein, and J. D. McMillan (Totowa, NJ: Humana Press), 567–579.
- Iacovidou, E., Ohandja, D.-G., and Voulvoulis, N. (2012). Food waste co-digestion with sewage sludge—realising its potential in the UK. *J. Environ. Manage.* 112, 267–274. doi: 10.1016/j.jenvman.2012.07.029
- Imachi, H., Sakai, S., Sekiguchi, Y., Hanada, S., Kamagata, Y., Ohashi, A., et al. (2008). *Methanolinea tarda* gen. nov., sp. nov., a methane-producing archaeon isolated from a methanogenic digester sludge. *Int. J. Syst. Evol. Microbiol.* 58, 294–301. doi: 10.1099/ijss.0.65394-0
- Ito, T., Yoshiguchi, K., Arieyadi, H. D., and Okabe, S. (2011). Identification of a novel acetate-utilizing bacterium belonging to Synergistes group 4 in anaerobic digester sludge. *ISME J.* 5, 1844–1856. doi: 10.1038/ismej.2011.59
- Kajikawa, H., and Masaki, S. (1999). Cellobiose transport by mixed ruminal bacteria from a cow. *Appl. Environ. Microbiol.* 65, 2565–2569. doi: 10.1007/s002849900321
- Kan, J., Clingenpeel, S., Macur, R. E., Inskeep, W. P., Lovalvo, D., Varley, J., et al. (2011). Archaea in Yellowstone Lake. *ISME J.* 5, 1784–1795. doi: 10.1038/ismej.2011.56
- Khalid, A., Arshad, M., Anjum, M., Mahmood, T., and Dawson, L. (2011). The anaerobic digestion of solid organic waste. *Waste Manage.* 31, 1737–1744. doi: 10.1016/j.wasman.2011.03.021
- Kim, H. W., Han, S. K., and Shin, H. S. (2003). The optimisation of food waste addition as a co-substrate in anaerobic digestion of sewage sludge. *Waste Manage. Res.* 21, 515–526. doi: 10.1177/0734242X0302100604
- Li, Y., Park, S. Y., and Zhu, J. (2011). Solid-state anaerobic digestion for methane production from organic waste. *Renew. Sustain. Energy Rev.* 15, 821–826. doi: 10.1016/j.rser.2010.07.042
- Lozupone, C., and Knight, R. (2005). UniFrac: a new phylogenetic method for comparing microbial communities. *Appl. Environ. Microbiol.* 71, 8228–8235. doi: 10.1128/AEM.71.12.8228-8235.2005
- Lu, X., Rao, S., Shen, Z., and Lee, P. K. H. (2013). Substrate induced emergence of different active bacterial and archaeal assemblages during biomethane production. *Bioresour. Technol.* 148, 517–524. doi: 10.1016/j.biortech.2013.09.017
- Narihiro, T., Nobu, M. K., Kim, N.-K., Kamagata, Y., and Liu, W.-T. (2015). The nexus of syntrophy-associated microbiota in anaerobic digestion revealed by long-term enrichment and community survey. *Environ. Microbiol.* 17, 1707–1720. doi: 10.1111/1462-2920.12616
- Narihiro, T., Terada, T., Ohashi, A., Wu, J.-H., Liu, W.-T., Araki, N., et al. (2009). Quantitative detection of culturable methanogenic archaea abundance in anaerobic treatment systems using the sequence-specific rRNA cleavage method. *ISME J.* 3, 522–535. doi: 10.1038/ismej.2009.4

- Nelson, M. C., Morrison, M., and Yu, Z. (2011). A meta-analysis of the microbial diversity observed in anaerobic digesters. *Bioresour. Technol.* 102, 3730–3739. doi: 10.1016/j.biortech.2010.11.119
- Nettmann, E., Bergmann, I., Mundt, K., Linke, B., and Klocke, M. (2008). Archaea diversity within a commercial biogas plant utilizing herbal biomass determined by 16S rDNA and mcrA analysis. *J. Appl. Microbiol.* 105, 1835–1850. doi: 10.1111/j.1365-2672.2008.03949.x
- Öhgren, K., Galbe, M., and Zacchi, G. (2005). Optimization of steam pretreatment of SO₂-impregnated corn stover for fuel ethanol production. *Appl. Biochem. Biotechnol.* 124, 1055–1068. doi: 10.1385/ABAB
- Oksanen, J., Blanchet, F. G., Kindt, R., Legendre, P., Minchin, P. R., O'Hara, R. B., et al. (2015). *Vegan: Community Ecology Package. R Package Version 2.2-1*. Available at: <http://CRAN.R-project.org/package=vegan>
- Pérez, J., Muñoz-Dorado, J., de la Rubia, T., and Martínez, J. (2002). Biodegradation and biological treatments of cellulose, hemicellulose and lignin: an overview. *Int. Microbiol.* 5, 53–63. doi: 10.1007/s10123-002-0062-3
- Price, M. N., Dehal, P. S., and Arkin, A. P. (2010). FastTree 2 – approximately maximum-likelihood trees for large alignments. *PLoS ONE* 5:e9490. doi: 10.1371/journal.pone.0009490.s003
- Rastogi, G., Ranade, D. R., Yeole, T. Y., Patole, M. S., and Shouche, Y. S. (2008). Investigation of methanogen population structure in biogas reactor by molecular characterization of methyl-coenzyme M reductase A (mcrA) genes. *Bioresour. Technol.* 99, 5317–5326. doi: 10.1016/j.biortech.2007.11.024
- Regueiro, L., Veiga, P., Figueiroa, M., Lema, J. M., and Carballa, M. (2013). Influence of transitional states on the microbial ecology of anaerobic digesters treating solid wastes. *Appl. Microbiol. Biotechnol.* 98, 2015–2027. doi: 10.1007/s00253-013-5378-8
- Rice, E. W., Baird, R. B., Eaton, A. D., and Clesceri, L. S. (2012). *Standard Methods for the Examination of Water and Wastewater*, 22nd Edn. New York, NY: American Public Health Association, American Water Works Association, Water Environment Federation.
- Rivière, D., Desvignes, V., Pelletier, E., Chaussonnerie, S., Guermazi, S., Weissenbach, J., et al. (2009). Towards the definition of a core of microorganisms involved in anaerobic digestion of sludge. *ISME J.* 3, 700–714. doi: 10.1038/ismej.2009.2
- Seedorf, H., Fricke, W. F., Veith, B., Brüggemann, H., Liesegang, H., Strittmatter, A., et al. (2008). The genome of *Clostridium kluyveri*, a strict anaerobe with unique metabolic features. *Proc. Natl. Acad. Sci. U.S.A.* 105, 2128–2133. doi: 10.1007/s12155-014-9486-9
- Siegert, I., and Banks, C. (2005). The effect of volatile fatty acid additions on the anaerobic digestion of cellulose and glucose in batch reactors. *Process Biochem.* 40, 3412–3418. doi: 10.1016/j.procbio.2005.01.025
- Sosnowski, P., Klepacz-Smolka, A., Kaczorek, K., and Ledakowicz, S. (2008). Kinetic investigations of methane co-fermentation of sewage sludge and organic fraction of municipal solid wastes. *Bioresour. Technol.* 99, 5731–5737. doi: 10.1016/j.biortech.2007.10.019
- Sosnowski, P., Wieczorek, A., and Ledakowicz, S. (2003). Anaerobic co-digestion of sewage sludge and organic fraction of municipal solid wastes. *Adv. Environ. Res.* 7, 609–616. doi: 10.1016/S1093-0191(02)00049-7
- Spirito, C. M., Richter, H., Rabaey, K., Stams, A. J., and Angenent, L. T. (2014). Chain elongation in anaerobic reactor microbiomes to recover resources from waste. *Curr. Opin. Biotechnol.* 27, 115–122. doi: 10.1016/j.copbio.2014.01.003
- Temudo, M. F., Mato, T., Kleerebezem, R., and van Loosdrecht, M. C. M. (2008). Xylose anaerobic conversion by open-mixed cultures. *Appl. Microbiol. Biotechnol.* 82, 231–239. doi: 10.1007/s00253-008-1749-y
- Tracy, B. P., Jones, S. W., Fast, A. G., Indurthi, D. C., and Papoutsakis, E. T. (2012). Clostridia: the importance of their exceptional substrate and metabolite diversity for biofuel and biorefinery applications. *Curr. Opin. Biotechnol.* 23, 364–381. doi: 10.1016/j.copbio.2011.10.008
- Wagner, A. O., Lins, P., Malin, C., Reitschuler, C., and Illmer, P. (2013). Impact of protein-, lipid- and cellulose-containing complex substrates on biogas production and microbial communities in batch experiments. *Sci. Total Environ.* 458, 256–266. doi: 10.1016/j.scitotenv.2013.04.034
- Wilkins, D., Lu, X.-Y., Shen, Z., Chen, J., and Lee, P. K. H. (2015). Pyrosequencing of mcrA and archaeal 16S rRNA genes reveals diversity and substrate preferences of methanogen communities in anaerobic digesters. *Appl. Environ. Microbiol.* 81, 604–613. doi: 10.1128/AEM.02566-14
- Wu, G. D., Lewis, J. D., Hoffmann, C., Chen, Y.-Y., Knight, R., Bittinger, K., et al. (2010). Sampling and pyrosequencing methods for characterizing bacterial communities in the human gut using 16S sequence tags. *BMC Microbiol.* 10:206. doi: 10.1186/1471-2180-10-206
- Yamada, T., Imachi, H., Ohashi, A., Harada, H., Hanada, S., Kamagata, Y., et al. (2007). *Bellilinea caldifistulae* gen. nov., sp. nov. and *Longilinea arvoryzae* gen. nov., sp. nov., strictly anaerobic, filamentous bacteria of the phylum Chloroflexi isolated from methanogenic propionate-degrading consortia. *Int. J. Syst. Evol. Microbiol.* 57, 2299–2306. doi: 10.1099/ijss.0.65098-0
- Yamada, T., and Sekiguchi, Y. (2009). Cultivation of uncultured *Chloroflexi* subphyla: significance and ecophysiology of formerly uncultured *Chloroflexi* Subphylum I with natural and biotechnological relevance. *Microbes Environ.* 24, 205–216. doi: 10.1264/jsme2.ME091515
- Yamada, T., Sekiguchi, Y., Imachi, H., Kamagata, Y., Ohashi, A., and Harada, H. (2005). Diversity, localization, and physiological properties of filamentous microbes belonging to *Chloroflexi* subphylum I in mesophilic and thermophilic methanogenic sludge granules. *Appl. Environ. Microbiol.* 71, 7493–7503. doi: 10.1128/AEM.71.11.7493-7503.2005
- Zhang, P., Zeng, G., Zhang, G., Li, Y., and Zhang, B. (2008). Anaerobic co-digestion of biosolids and organic fraction of municipal solid waste by sequencing batch process. *Fuel Process. Technol.* 89, 485–489. doi: 10.1016/j.fuproc.2007.11.013
- Zhang, R., El-Mashad, H. M., Hartman, K., Wang, F., Liu, G., Choate, C., et al. (2007). Characterization of food waste as feedstock for anaerobic digestion. *Bioresour. Technol.* 98, 929–935. doi: 10.1016/j.biortech.2006.02.039
- Zhang, W., Werner, J. J., Agler, M. T., and Angenent, L. T. (2014). Substrate type drives variation in reactor microbiomes of anaerobic digesters. *Bioresour. Technol.* 151, 397–401. doi: 10.1016/j.biortech.2013.10.004
- Zhu, H., Parker, W., Basnar, R., Proracki, A., Falletta, P., Béland, M., et al. (2008). Biohydrogen production by anaerobic co-digestion of municipal food waste and sewage sludges. *Int. J. Hydrogen Energy* 33, 3651–3659. doi: 10.1016/j.ijhydene.2008.04.040

Conflict of Interest Statement: The authors declare that the research was conducted in the absence of any commercial or financial relationships that could be construed as a potential conflict of interest.

Copyright © 2015 Wilkins, Rao, Lu and Lee. This is an open-access article distributed under the terms of the Creative Commons Attribution License (CC BY). The use, distribution or reproduction in other forums is permitted, provided the original author(s) or licensor are credited and that the original publication in this journal is cited, in accordance with accepted academic practice. No use, distribution or reproduction is permitted which does not comply with these terms.

Advantages of publishing in Frontiers



OPEN ACCESS

Articles are free to read for greatest visibility and readership



FAST PUBLICATION

Around 90 days from submission to decision



HIGH QUALITY PEER-REVIEW

Rigorous, collaborative, and constructive peer-review



TRANSPARENT PEER-REVIEW

Editors and reviewers acknowledged by name on published articles



REPRODUCIBILITY OF RESEARCH

Support open data and methods to enhance research reproducibility



DIGITAL PUBLISHING

Articles designed for optimal readership across devices



FOLLOW US
@frontiersin



IMPACT METRICS

Advanced article metrics track visibility across digital media



EXTENSIVE PROMOTION

Marketing and promotion of impactful research



LOOP RESEARCH NETWORK

Our network increases your article's readership